Analysis of *Staphylococcus aureus* Virulence Determinants

By:

John Connolly BSc
(University of Liverpool)

A thesis submitted for the degree of Doctor of Philosophy
September 2015

The University of Sheffield
Faculty of Science
Department of Molecular Biology & Biotechnology

Summary

The success of the pathogen *Staphylococcus aureus* lies in its array of virulence determinants, which enable pathogenesis. The recent identification of novel *S. aureus* virulence determinants led to the hypothesis that there are more to be found.

In silico analysis of the *S. aureus* genome identified three staphylococcal superantigen-like proteins (SSL12, SSL13 & SSL14), incorrectly annotated in the genome database as hypothetical proteins. Production of recombinant SSL12, 13 & 14 proteins gave a low yield of soluble protein, which precluded biochemical analysis. A genetic approach was taken and a triple gene deletion mutant constructed. No role for the 3 SSLs was found in an *in vivo* infection model, or in *in vitro* phagocytosis assays. However, a subtle reduction in growth in human blood, associated with the cellular component of blood was seen when compared with the wild-type.

A genome-wide library of 1,920 strains each with a separate gene disrupted by a transposon (Tn) insertion was screened on human blood agar. Both the purine (*purA* and *purB*) and tetrahydrofolate (THF; *pabA*) synthesis pathways were found to be important for growth on human blood, but, in the case of the *pabA* disrupted strain, not on human plasma. THF is a single carbon donor/acceptor in many *S. aureus* biosynthesis pathways, and its synthesis is the target of sulphonamide antibiotics. The human blood phenotype for *pabA* was linked to dTTP synthesis, which is formed via a THF-dependent pathway, or a THF-independent pathway requiring the enzyme Tdk. As the *pabA* mutant can grow on human plasma it was hypothesised that Tdk is inhibited by a factor in the cellular component of blood, which leads to a requirement for dTTP. This suggests that the activity of sulphonamide drugs is the result of inhibition of THF coupled with the inhibition of Tdk by an as yet unknown factor present in human blood.

This thesis is dedicate to my wife
for her love and patience

Acknowledgements

I would like to thank my supervisors, Professor Simon Foster and Professor Moira Whyte for their support, guidance and encouragement throughout my PhD. I would like to thank the staff at The Royal Hallamshire Hospital, including Dr David Sammut, Dr Jennifer Carling-Wright and Vanessa Singleton for their help with phlebotomy. Particular thanks go to Dr Lynne Prince for her patient assistance with all things neutrophil related. I would like to thank all members past and present from the Foster lab including Jorge, Stephane, Felix, Alex, Beatriz, Kasia, Kathrine, Amy and Richard. I would also like to show my gratitude to the blood donors for making this work possible. Several people from the lab have aided me in accomplishing this work, including the fish people, Tomasz Prajsnar, Alex Williams and Gaz McVicker. I would like to acknowledge the very talented Dr Emma Johnson for technical advice and assistance.

I would like to express particular thanks to my mum for her support, encouragement and love. This work would not have been possible without you and our walks together. I would also like to thank my dad and my brothers for their love and support. Separate thanks go to Phil for igniting my interest in science, something I will be forever grateful for. Thanks go to my aunt Bet, for her love and support and for her understanding when my visits were so rare. Special thanks go to my wife, Jacqueline, for her support and love and also for putting up with me throughout the writing of this thesis and in general. Lastly, a special dedication goes to my amazing kids for your patience when I have been too busy to pay you as much attention as I would have liked.

This work was funded by The University of Sheffield.

Abbreviations

6-His	Hexahistidine
ABC	ATP binding cassette
ADC	4-amino-4-deoxychorismate
AFS	Ammonium ferrous sulphate
AG	Adenine and guanine
AICAIR	5-amino-1-(5-phospho-D-ribosyl)imidazole-4-carboxamide
AIP	Autoinducing peptide
AIR	5-amino-1-(5-phospho-β-D-ribosyl)imidazole
Amp	Ampicillin
AMPs	Antimicrobial peptides
APC	Antigen presenting cell
APS	Ammonium persulphate
attB	Attachement site in the bacterial genome
attP	Attachment site in the phage genome
BCIP	5-bromo-5-chloro-3-indolyl phosphate
BHI	Brain heart infusion
BLAST	Basic local alignment search tool
bp	Base pair
CA	Community acquired
CAIR	5-amino-1-(5-phospho-D-ribosyl)imidazole-4-carboxylate
Cat	Chloramphenicol
CDM	Chemically defined media
CDS	Coding sequence
CFU	Colony forming unit
CIP	Calf intestinal alkaline phosphatase
CNS	Coagulase negative staphylococci
CPS	Coagulase positive staphylococci
CVS	Coagulase variable staphylococci
DF	Downstream fragment
DHF	Dihydrofolate
DIG	Digoxigenin
DMF	*N*,*N*-dimethylformamide
DMSO	Dimethyl sulphoxide
dpf	Days post fertilisation
EB	Elution buffer
ECM	Extracellular matrix
EDTA	Ethylenediamine tetra-acetic acid
Ery	Erythromycin
ETs	Enterotoxins
FA	Folic acid
Fab	Fragment antigen binding
FAICAIR	5-formamido-1-(5-phospho-D-ribosyl)-imidazole-4-carboxamide
FBS	Foetal bovine serum
Fc	Fragment crystallisable
FGAM	2-(formamido)-N^1-(5-phospho-β-D-ribosyl)acetamidine
FGAR	N^2-formyl-N^1-(5-phospho-β-D-ribosyl)glycinamide
FSc	Forward scatter
GAR	N^1-(5-phospho-β-D-ribosyl)glycinamide
HBSS	Hanks balance salts solution

hpi	Hours post infection
IL-8	Interleukin 8
IMP	Inosine monophosphate
IPTG	Isopropyl β-D-1-thiogalactopyranoside
IVET	*In vitro* expression technology
Kan	Kanamycin
LB	Luria-Bertani
LWT	London wild-type
M	Molar
MCS	Multiple cloning site
Met	Methionine
MHC	Major histocompatibility complex
MIC	Minimum inhibitory concentration
MOI	Multiplicity of infection
MRSA	Methicillin resistant *Staphylococcus aureus*
MSA	Multiple sequence alignment
MSCRAMM	Microbial surface components recognising adhesive matrix molecules
N^5-CAIR	N^5-carboxyaminoimidazole ribonucleotide
NARSA	Network on Antimicrobial Resistance in *Staphylococcus aureus*
NCBI	National Centre for Biotechnology Information
Neo	Neomycin
NETs	Neutrophil extracellular traps
NGS	Next-generation sequencing
Nr	Non-redundant
NTML	Nebraska transposon mutagenesis library
OD_{600}	Optical density at 600 nm
ORF	Open reading frame
PAMPs	Pathogen associated molecular patterns
PATRIC	Pathosystems Resource Integration Centre
PBS	Phosphate buffered saline
PCR	Polymerase chain reaction
PFU	Plaque forming units
PI	Phagocytic index
PK	Proteinase K
PPP	Platelet poor plasma
(p)ppGpp	Guanosine tetraphosphate; Guanosine pentaphosphate
PRA	5-phospho-β-D-ribosylamine
PRP	Platelet rich plasma
PRPP	5-phospho-β-D-ribose 1-diphosphate
PRR	Pattern recognition receptors
psi	Pounds per square inch
RBC	Red blood cell
rpm	Revolutions per minute
SAF	*Staphylococcus aureus* factor
SAgs	Superantigens
SAICAIR	5'-phosphoribosyl-4-(*N*-succinocarboxamide)-5-aminoimidazole
SCOTS	Selective capture of transcribed sequences
SCVs	Small colony variants
SDS-PAGE	Sodium dodecyl polyacrylamide gel electrophoresis
SNPs	Single nucleotide polymorphism
Spec	Spectinomycin

SS	Signal sequence
SSLs	Staphylococcal superantigen-like protein
STM	Signature-tagged mutagenesis
TAE	Tris/acetate/EDTA
TCA	Tricarboxylic acid cycle
TCR	T-cell receptor
TCS	Two-component system
TEMED	*N*,*N*,*N*'*N*'-tetramethyl-ethylenediamine
Tet	Tetracycline
THF	Tetrahydrofolate
TLR	Toll-like receptor
TMP	Trimethoprim
Tn	Transposon
TNFα	Tumour necrosis factor alpha
TSS	Toxic shock syndrome
UF	Upstream fragment
UV	Ultraviolet
v/v	Volume for volume
VF	Virulence factor
$VitB_5$	Vitamin B_5
w/v	Weight for volume
Φ	Phage
σ	Sigma factor

Table of Contents

List of Figures

List of Tables

CHAPTER 1

INTRODUCTION

1.1 The staphylococci

Staphylococci are Gram positive bacteria, forming irregular grape-like clusters first noted by Ogston (1881) when defining their importance in bacteraemia. Since the work of Ogston, 49 named staphylococci species have been identified and recorded on the NCBI Taxonomy database (Federhen, 2012). There are a further 2,881 unnamed staphylococci records, many, if not all of which, may belong to the 49 named species, though some may be identified as new *Staphylococcus sp*. Of the 49 named species, 40 fall into the category of coagulase negative staphylococci (CNS), 7 are coagulase positive staphylococci (CPS) and 2 are coagulase variable staphylococci (CVS).

Although CNS are commonly found in clinical samples, they were considered contaminants, due to their abundance on human skin (Kloos & Bannerman, 1994). Approximately half of the recognised staphylococci are known to inhabit the human body, with particular strains showing specificity for defined regions of the body (Longauerova, 2006; Piette & Verschraegen, 2009). *S. epidermidis* and *S. hominis* are the most abundant staphylococci on the trunk and limbs respectively (Gemmell, 1986), *S. capitis* on the head and *S. auricularis* on the external ear (von Eiff *et al*., 2002). A heightened recognition of the importance of CNS in nosocomial infections has come about through the increased use of indwelling devices. CNS are now known to be responsible for several diseases, including pneumonia, endocarditis and osteomyelitis and are the most common cause of venous catheter-related bacteraemia, 50-70% of cases are caused by *S. epidermidis* (Casey *et al*., 2007; von Eiff *et al*., 2002).

The bacteria are able to resist the low pH and high osmolarity of the skin and possess extracellular enzymes including fatty acid modifying enzyme (FAME) and other virulence factors, including adhesins, phenol soluble modulins (PSMs) and some strains produce haemolysin (Longauerova, 2006). Biofilm formation allows growth of CNS bacteria on indwelling devices, after initial adhesin-mediated attachment (Piette & Verschraegen, 2009). Treatment of CNS infections is problematic due to the prevalence of antibiotic resistance (von Eiff *et al*., 2002). As the CNS are permanent residents of

the skin surface, there is a selective pressure to evolve mechanisms to overcome exposure to antibiotics.

1.2 *Staphylococcus aureus*

The species name *aureus* was chosen by Rosenbach in 1884 due to the golden pigmentation of *Staphylococcus aureus* colonies (*aureus* meaning golden in Latin), compared with other, non-pigmented, staphylococci (Liu *et al*., 2005). *S. aureus* lives as a permanent resident in the anterior nares of ~20% of the population and is a transient coloniser of a further ~60%, also living in the axillae, vagina and the surface of damaged skin. Colonised patients are at greater risk of infection; however carriers appear to have a reduced risk of mortality (Claassen *et al*., 2005; Holtfreter *et al*., 2009; Wertheim *et al*., 2004). Risk factors for infection include type I diabetes, surgery and the use of intravenous drugs. *S. aureus* causes a spectrum of diseases, from relatively mild skin rashes, to more serious diseases such as endocarditis and systemic infections such as septicaemia and toxic shock syndrome (Foster, 2005; Lowy, 1998; Visai *et al*., 2009).

1.2.1 *S. aureus* as a public health issue

The development of resistance to commonly used antibiotics has led to difficulties in treating *S. aureus* infection. Resistance to methicillin was seen in *S. aureus* shortly after its introduction in 1961, giving rise to Methicillin Resistant *S. aureus* (MRSA; François *et al*., 2010). More recently resistance has been seen to vancomycin, one of the few remaining effective antibiotics used in the treatment of *S. aureus* (Jousselin *et al*., 2013). MRSA in particular has developed into a serious public health concern as a major cause of nosocomial infection (Foster, 2005; Lowy, 1998; Mekontso-Dessap *et al*., 2005). As with other staphylococci, the use of indwelling devices, for instance intravenous catheters, increases the risk of *S. aureus* infection, as they become coated with serum and fibrinogen, which can be adhered to by *S. aureus* surface proteins such as clumping factor A (ClfA; Lowy, 1998).

An emerging problem is the occurrence of community-acquired MRSA (CA-MRSA). The occurrence of CA-MRSA has caused alarm as it appears to affect healthy and non-

immune compromised individuals (Tseng *et al*., 2009). CA-MRSA strains encode antibiotic resistance on the staphylococcal cassette chromosome (SCC*mec*). The SCC*mec* often encodes the regulatory phenol soluble modulin, *psm-mec* (Fechter *et al*., 2014). The emergence of this strain may be the result of horizontal gene transfer of the SCC*mec* accompanied by the PVL toxin (Foster, 2005; Lowy, 1998).

Relative to *S. aureus*, the CNS armoury of virulence factors is poor (Longauerova, 2006). Genomic comparison of *S. aureus* and *S. epidermidis*, the most common cause of CNS-associated infection, shows that *S. aureus* encodes a large number of virulence factors, such as cytotoxins, not found in *S. epidermidis* (Gill et al., 2005). This suggests that the enhanced virulence of *S. aureus* compared to *S. epidermidis*, and other CNS, is the result of these additional virulence determinants.

1.3 Virulence determinants and their genetic control

A successful *S. aureus* infection relies on the pathogen's ability to colonise the initial infection site, adapt to the stresses of the host environment, acquire nutrients for growth, resist host defences and spread to other sites in the host when the nutrient levels in the original foci of infection are exhausted. To accomplish these stages of infection, *S. aureus* expresses multiple virulence factors from different categories, depending on the stage of infection (Cheung *et al*., 2004; Lowy, 1998). In the initial stage of infection the relatively low numbers of bacteria must attach to host tissues and replicate. *S. aureus* expresses multiple adhesins with specificity to host components of the extracellular matrix allowing firm binding (Foster & Höök, 1998). At this stage the bacteria must fend off host immune factors that are present at the site of infection and prevent the ingress of additional factors to the site of infection, by producing cell wall-associated or secreted immune evasion proteins (Foster, 2005). Once the bacterial load has increased, nutrient levels concomitantly decrease and the necessity for immune evasion components is less pressing than the requirement for nutrients. At this stage degradative enzymes and toxins are produced to allow deeper penetration of tissues and access to nutrients whilst adhesin expression is curtailed to allow detachment and spread (George & Muir, 2007). Some of the virulence factors that accomplish this are shown in Figure 1.1.

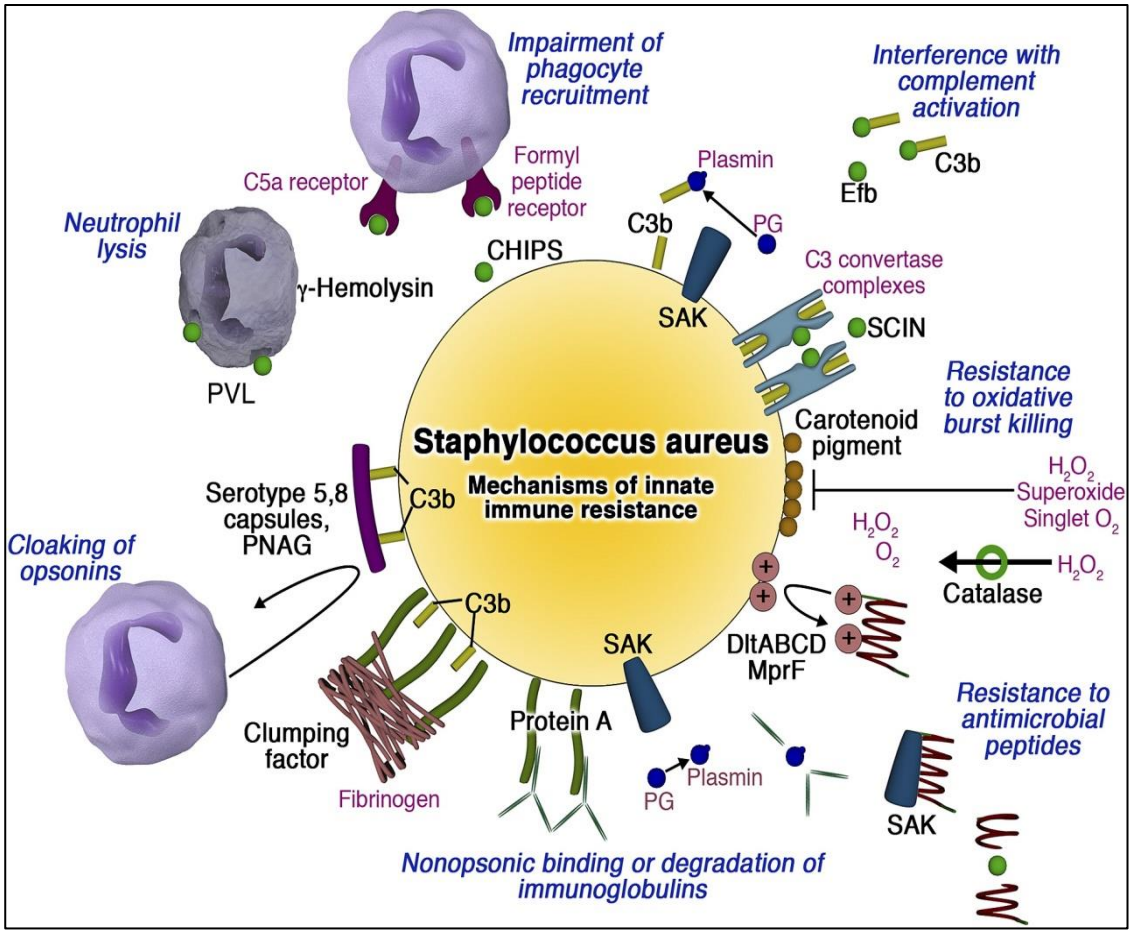

Figure 1.1 Representative virulence determinants of *S. aureus*.

Pink components are those of the host, black are *S. aureus* expressed factors. Adapted from (Nizet, 2007).

Clearly specific virulence factors are required at specific times during infection. The bacteria control gene expression in response to environmental signals recognised by a complex network of proteins, which trigger the appropriate gene expression. These regulators can themselves be classed as virulence factors, as disruption of virulence factor regulation has been shown to have detrimental effects on *S. aureus* pathogenicity. *S. aureus* has 16 two-component systems (TCS), multiple DNA binding proteins (e.g. the SarA family) and approximately 250 non-coding RNAs (ncRNAs) that control gene expression allowing adaptation to the changing environment of the host (Bronner *et al*., 2004). Not all of these systems are devoted to expression of virulence genes. Some of these regulators and their effects on virulence factor expression are shown in Table 1.1. A complete discussion of all regulatory components and all virulence factors known to be expressed by *S. aureus* is beyond the scope of this work. Discussion of the major virulence regulatory components and many of their corresponding virulence determinants follows.

1.3.1 Regulation of virulence early in infection

1.3.1.1 The Fur and SaeRS regulators

Upon entering the human host, whether orally or via an accidental/surgical wound or the site of an indwelling device, *S. aureus* encounters a hostile nutrient limiting environment. Humans have evolved mechanisms to sequester Fe from body tissues, due to its toxicity and requirement by pathogens (Johnson *et al*., 2011). *S. aureus* exploits the low Fe concentration upon entering the host environment, by using it as a trigger for gene expression. The Fur protein downregulates gene expression, by binding directly to a promoter region, known as the fur-box blocking transcription (Cassat & Skaar, 2012). In a low Fe environment, fur-box binding is alleviated, allowing expression of genes required for Fe acquisition. The genes controlled by Fur include the *isd* system, used for the acquisition of Fe from host proteins, including haemoglobin and haptoglobin and Fe chelating siderophores (Hammer & Skaar, 2011). Furthermore, this response has been shown to be important for nasal colonisation, as IsdA is required for binding the nasal epithelium in the Fe limited nares (Clarke *et al*., 2004).

Table 1.1 Major virulence factor regulators of *S. aureus* and representatives of the genes they control.

Regulators arrayed along the top row, controlled virulence factor in column 1. + = upregulated. - = downregulated.

Name	Gene	*agr*	*sae*	*graRS*	*arlRS*	σ^B	*codY*	*fur*	*rsp*	*sarA*	*sarR*	*sarT*	*rot*	*sarS*	*mgrA*	Ref*
Adhesins																
Autolysin	*aaa*	-	+	+												1, 2
Autolysin	*atl*	-	+	+												1, 2
Bone sialoprotein-binding protein	*bbp*				+	+										3, 4
Clumping factor A	*clfA*	-				+			-							3, 5, 6
Clumping factor B	*clfB*					+							+			7, 8
Coagulase	*coa*	-	+	+		+	+	+		+			+			2, 3, 9, 10, 11, 12, 13
Collagen-binding protein	*cna*									-						14
Extracellular adherence protein	*eap/ map*		+					+	+							5, 11, 15
Extracellular matrix-binding protein	*ebh*				+										-	16, 17
Extracellular fibrinogen-binding protein	*efb*							+								13
Elastin-binding protein	*ebps*			-		+										2, 3
Extracellular matrix protein-binding protein	*emp*		+					+	+							5, 11, 15
Fibronectin binding protein A&B	*fnbpAB*	-	+			+	+		-	+						3, 5, 6, 10, 11, 12
Iron-regulated surface determinant A&B	*isdAB*	-	+					-								6, 13, 15
Surface protein G	*sasG*	-					+		-							5, 6, 12
Immunoglobulin-binding protein	*sbi*	-	+					+								13, 15, 18
Serine-aspartate repeat-containing proteins	*sdrCDE*	-		+	+				-	+			+		+	2, 4, 5, 6, 17, 19, 20
Protein A	*spa*	-	+					+	-	-			+	+	-	5, 6, 9, 10, 11, 13, 14, 17
von Willebrand factor-binding protein	*vWbp*					+										3
Degradative Enzymes																
Enolase	*eno*			-												2
Hyaluronate lyase	*hysA*	+					-			-						14, 21, 22
Lipases	*lip, geh*	+		+		-		-	+				-		+	2, 3, 5, 10, 13, 17

Table 1.1 continued

Name	Gene	*agr*	*sae*	*graRS*	*arlRS*	σ^B	*codY*	*fur*	*rsp*	*sarA*	*sarR*	*sarT*	*rot*	*sarS*	*mgrA*	Ref*
Nuclease	*nuc*	+	+		+	-									+	3, 4, 10, 17
Proteases	-	+			-	-			+	-			-		+	2, 3, 5, 10, 17
Staphylokinase	*sak*	+				-									+	3, 10, 17
Nutrient Acquisition																
Iron-regulated surface determinants	*isd*							-								23
siderophores	-							-					+			15, 20
Immune Evasion																
capsule	-	+			+/-	+				+					+/-	2, 3, 4, 10, 12, 17, 24
Chemotaxis inhibitory protein	*chp*		+					+								13, 25
Ribitol/D-alanine substituting operon	*dltABCD*	-		+									+			2, 20, 26
Phosphatidyl-glycerol lysyltransferase	*mprF*			+												26
FPRL1 inhibitor	*flr*							+					+			8, 13
Staphylococcal complement inhibitor	*scnA scnB*		+					+								13, 25
Staphylococcal superantigen-like proteins	*ssl11*	-	+					+					+			13, 27
	ssl10							+							+	13, 17
	ssl9	-	+					+					+			13, 27
	ssl8	-	+					+							+	11, 13, 14
	ssl7	-	+					+					+			13, 27
	ssl6							+								13
	ssl5	-	+													11
	ssl4							+								13
	ssl3							+								13
	ssl2							+								13
	ssl1	-	+					+					+			13, 27
Stress Resistance																
O-acetyltransferase	*oatA*			-												2
Fatty acid modifying enzyme (FAME)	-	+								+						14
Catalase	*katA*						-	+								12, 28

Table 1.1 continued

Name	Gene	*agr*	*sae*	*graRS*	*arlRS*	σ^B	*codY*	*fur*	*rsp*	*sarA*	*sarR*	*sarT*	*rot*	*sarS*	*mgrA*	Ref*
Toxins																
enterotoxins	-	+						+	+	+						5, 13, 14
Toxic shock syndrome toxin-1	*tst*	+								+						14
exfoliative toxins	-	+														10
α-haemolysin	*hla*	+	+			-		-		+		-	-	-		3, 10, 13, 14
β-haemolysin	*hlb*	+	+		-				+	+			-			4, 5, 10, 14
δ-haemolysin	*hld*	+	+		+					+		-		+		4, 10, 14
γ-haemolysin	*hlg*	+		+	-	-				+			-		+	2, 3, 4, 10, 17, 29
Leukotoxins	*lukE*	+			-					+			-		+	4, 8, 13, 17, 29
	lukD	+			-				+	+			-		+	4, 8, 13, 17, 29
	lukA/G												-			8
	lukB/H												-			8
	pvl	+					-			+			-			10, 29, 30
Phenol soluble modulins	*psm*	+					-									12, 18

* Table information was gathered from the following publications: 1. Heilmann *et al*., (2005); 2. Herbert *et al*., (2007); 3. Bischoff *et al*., (2004); 4. Liang *et al*., (2005); 5. Lei *et al*., (2011); 6. Ythier *et al*., (2012); 7. Hempel *et al*., (2010); 8. Mootz *et al*., (2015); 9. Hart *et al*., (1993); 10. Novick, (2003a); 11. Pantrangi *et al*., (2010); 12. Pohl *et al*., (2009); 13. Torres *et al*., (2010); 14. Arvidson & Tegmark, (2001); 15. Johnson *et al*., (2011); 16. Walker *et al*., (2013); 17. Luong *et al*., (2006); 18. Fechter *et al*., (2014); 19. Cheung *et al*., (2004); 20. Said-Salim *et al*., (2003); 21. Hart *et al*., (2013); 22. Ibberson *et al*., (2014); 23. Mazmanian *et al*., (2003); 24. Goerke *et al*., (2005); 25. Sun *et al*., (2010); 26. Joo & Otto, (2015); 27. Benson *et al*., (2011); 28. Horsburgh *et al*., (2001); 29. Bronner *et al*., (2004); 30. Montgomery *et al*., (2012).

Table 1.1 shows that along with the *isd* operon, Fur negatively regulates α-haemolysin (*hla*) transcription in high Fe conditions. Hla is a homoheptameric leukotoxin that interacts with epithelial cells, lymphocytes, monocytes, eosinophils and red blood cells, leading to pore formation and necrosis (Prince *et al*., 2012; Vandenesch *et al*., 2012). As the majority of the body's Fe is housed in RBCs, the Fe-regulated expression of Hla early in infection is an important aspect of Fe acquisition (Hammer & Skaar, 2011). A large number of adhesins and immune evasion proteins are positively regulated by Fur (Table 1.1). In the *fur* mutant strains, the level of transcript for the adhesins and immune evasion proteins is reduced. Whether Fur controls expression of these genes directly or indirectly is uncertain. However, (Johnson *et al*., 2011) demonstrated that Fur directly upregulates the *saeRS* TCS in low Fe growth conditions. As the *sae* system is a known positive regulator of adhesins and immune evasion proteins (Table 1.1) it is possible that reduced expression of *sae* results in the reduced adhesin and immune evasion protein levels in the *fur* deletion mutant.

The *sae* TCS consists of the *saeS* sensor and the *saeR* regulator, known to be most active during the exponential phase of growth, though what the sensor responds to is as yet unknown (Benson *et al*., 2012; Bronner *et al*., 2004). SaeR has been shown to positively regulate purine synthesis and amino acid transport and metabolism genes in the mid-exponential and early stationary phase of growth (Voyich *et al*., 2009). The importance of the *sae* system to pathogenicity is dependent on the type of infection. An *saeRS* mutant is non-virulent in a murine sepsis model of infection. However, no difference was seen between the *S. aureus* wild type and the *S. aureus saeRS* mutant in an abscess model (Voyich *et al*., 2009). Voyich *et al.* hypothesise that the quorum sensing system *agr* is likely more crucial for abscess formation, as a quorum is likely to be reached rapidly at the site of infection, resulting in toxin and degradative enzyme secretion. This demonstrates the dependence of *S. aureus* on multiple regulatory systems, which make it such a versatile pathogen.

1.3.1.2 Repressor of toxins (*rot*) and other *sar* family members

The *rot* gene is a member of the 11 member *sar* family of transcription regulators (*sarA*, *sarR*, *sarS*, *sarT*, *sarU*, *rot*, *sarX*, *mgrA*, *sarZ*, *sarV* and *sarY*). The *sarA* gene was the first *sar* gene discovered and each of the other 10 are homologous to *sarA*

(Cheung *et al*., 2008). The complex interactions between the *sar* family members, and between the *sar* family and *agr*, is shown in Table 1.2. The complexity of *sar* regulation can be seen by looking at the activity of a single member, using Table 1.2. If SarR activity is repressed it triggers late stage infection gene expression mediated by SarA. SarA promotes *agr* expression and represses SarT and SarV expression. Downregulation of the SarT activity derepresses SarT-dependent downregulation of *agr* and *sarU*, another positive regulator of *agr*, thereby indirectly enhancing the *agr* upregulation by SarA. Inhibition of SarV expression (also inhibited by MgrA, another positive regulator of *agr*) regulates autolytic activity, thereby influencing the level of cell wall degradation and growth (Manna *et al*., 2004). This suggests that SarR is active early during infection, preventing SarA mediated upregulation of *agr* activated genes.

An important regulator is the *sar* family transcription regulator repressor of toxins (*rot*), associated with biofilm-related disease (Mootz *et al*., 2015). The *rot* protein binds to the promoters of *S. aureus* protease genes, inhibiting their expression, thereby allowing biofilm formation. Analysis of biofilm detachment from a polycarbonate surface has demonstrated that *agr* mediated expression of proteases is required for the dissolution of biofilm (Boles & Horswill, 2008). Therefore, the repression of proteases by *rot* promotes stable biofilm formation. As shown in Table 1.1 *rot* has dual functions being inhibitory to secreted proteases and extracellular toxins, while promoting expression of immune evasion proteins and adhesins, which are required for the establishment of infection.

1.4 Virulence factors associated with early infection

1.4.1 Adhesins

To colonise and persist within its host, *S. aureus* expresses microbial surface components recognising adhesive matrix molecules (MSCRAMMs). Members of the MSCRAMM family allow colonisation of wounds (Foster & Höök, 1998), skin surface (Coates *et al*., 2014), the nares (Schaffer *et al*., 2006), indwelling devices (Hartford *et al*., 1997) and tissues within the body associated with specific diseases, such as healthy aortic tissue resulting in endocarditis (Hienz *et al*., 1996).

Table 1.2 Interaction between *sar* family regulators and the *agr* system.

	Sar Family Regulators†											*agr*	References*
	sarA	***sarR***	***sarT***	***rot***	***sarS***	***mgrA***	***sarU***	***sarX***	***sarZ***	***sarV***	***sarY***		
sarA		-				+							1, 2, 3
sarT	-											-	3
rot												-	4, 5, 6
sarS					+	-						-	1, 2, 3, 4
mgrA					+			+				+	4, 7
sarU			-										3
sarX						+						-	8
sarV	-					-							3
agr	+		-			+	+	-	+				5, 8, 9, 10, 11

* Table information was gathered from the following publications: 1. Bischoff *et al*., (2004); 2. Luong *et al.,* (2006); 3. Cheung *et al.,* (2004); 4. Herbert *et al*., (2007); 5. Liang *et al*., (2005); 6. Geisinger *et al*, (2006); 7. Ingavale *et al*., (2003); 8. Manna & Cheung, (2003); 9. Hart *et al.,* (1993); 10. Bronner *et al.*, (2004); 11. Thoendel *et al*., (2011); 12. Johnson *et al*., (2011); 13. Said-Salim *et al*., (2003).

† Regulatory proteins arrayed along the top row, positively or negatively regulate those regulatory proteins in the first column.

The functions of adhesins have been determined by *in vitro* binding assays using purified protein and the comparison of whole bacteria deficient in a particular adherence protein with the wild type strain. One problem with using purified protein is that unless the protein is expressed along with the posttranslational modification machinery then the effects of posttranslational modifications are not accounted for. Isogenic mutants are also used to assess the importance of a particular adhesin gene to the pathogenicity of *S. aureus*, using *in vivo* models. These analyses can be problematic due to the high level of redundant function of *S. aureus* adhesins, for instance the extracellular matrix (ECM) components fibrinogen and fibronectin are bound by the autolysins Aaa and Atl (Heilmann *et al*., 2005; Hirschhausen *et al*., 2010), the extracellular adherence protein, Eap/Map (Haggar *et al*., 2003), extracellular fibrinogen-binding protein, Efb (Cheng *et al*., 2014; Lee *et al*., 2004), extracellular matrix protein-binding protein, Emp (Hussain *et al*., 2001) and the fibronectin binding protein, FnbpAB (Flock *et al*., 1987; Wann *et al*., 2000). These proteins also bind other ECM components and have other roles in infection. This redundancy may well be artefactual and a result of the methods employed to study *S. aureus* adhesins, or it may be due to differential expression of adhesins or an evolutionary manifestation of their importance to pathogenicity.

1.4.1.1 Roles of adhesins in disease and colonisation

Several *S. aureus* adhesins are known to be associated with specific diseases and sites in the host, based on the tissues they promote binding to and *in vivo* analyses. The collagen-binding protein, Cna promotes binding to the cornea promoting the inflammatory eye disease keratitis (Rhem *et al*., 2000) and is also associated with infective endocarditis by binding to undamaged aortic valves (Hienz *et al*., 1996). The adhesin von Willebrand binding protein, vWbp, binds to the ECM component von Willebrand factor and has coagulase activity (Bjerketorp *et al*., 2004). The importance of vWbp coagulase activity for bacteraemia and abscess formation has been demonstrated by analysis of a single *vwbp* mutant and a double mutant with the coagulase gene, *coa*. The Efb protein is important for postoperative wound recovery as it inhibits platelet aggregation at the wound site, which is important for plugging the wound and releasing mediators, such as growth factors, to promote wound healing (Shannon & Flock, 2004; Shannon *et al*., 2005). The plasmin sensitive, Pls, protein found in MRSA strains promotes binding to keratinocytes (Huesca *et al*., 2002), inhibits

fibronectin and immunoglobulin G (IgG) binding, and promotes invasion of endothelial cells (Hussain *et al*., 2009). Pls has been shown to play an important role in the development of sepsis and septic arthritis, using an isogenic *pls* mutant (Josefsson *et al*., 2005). Surface protein G, SasG, promotes adhesion to desquamated nasal epithelial cells important for colonisation of the nares (Corrigan *et al*., 2007). Bacterial biofilm formation is important for indwelling device associated infections. SasG promotes the intercellular aggregation step of biofilm formation (Geoghegan *et al*., 2010; Kuroda *et al*., 2008). In addition to SasG, clumping factor B, ClfB and Fe regulated surface determinant A, IsdA promote colonisation of the nares by binding to nasal cells (Clarke *et al*., 2009; Corrigan *et al*., 2009) and both proteins bind loricrin and cytokeratin-10, components of the nasal epithelium (Clarke *et al*., 2009; Mulcahy *et al*., 2012; O'Brien *et al*., 2002).

1.4.1.2 Adhesins as immune evasion proteins

Several adhesins of *S. aureus* have roles in immune evasion. The bone sialoprotein inhibits classical pathway complement opsonisation by binding to classical pathway regulators C4BP & factor H (the complement system is discussed in more detail in the next section; Hair *et al*., 2013). Eap promotes internalisation by fibroblasts, thereby making the bacteria undetectable to host immunity (Haggar *et al*., 2003). Another protein that uses this method of immune evasion is the serine-rich adhesin for platelets, SraP. This glycosylated cell wall protein mediates binding to human platelets (Siboo *et al*., 2005), adhesion and uptake by epithelial cells (Yang *et al*., 2014). Efb and its homologue Ehb bind the C3b and C3d complement fragments inhibiting complement activation and B-cell activation respectively (Lee *et al*., 2004; Ricklin *et al*., 2008). FnbpA uses bound fibronectin to interact with α5β1 integrins on the surface of epithelial cells promoting phagocytosis and intracellular evasion of immunity (Edwards *et al*., 2011).

The staphylococcal immunoglobulin-binding protein, Sbi, and protein A, Spa, are similar in sequence and function. Both proteins bind to the Fc region of IgG, presenting it to immune cells in the incorrect orientation, thereby blocking opsonophagocytosis (Atkins *et al*., 2008). In addition to two IgG binding domains, Sbi has two C3 binding domains. When bound to C3 on the surface of *S. aureus* complement activation is

inhibited; when bound away from the surface this activates the alternative pathway leading to futile consumption of C3 (Burman *et al*., 2008). The Spa adhesin binds keratinocytes, but it can also bind the Fab domain of IgG and IgM leading to massive upregulation of B-cell activity and B-cell apoptosis (Falugi *et al*., 2013).

The complement protein C3b opsonises *S. aureus*, promoting recognition and phagocytosis by macrophages and neutrophils. Clumping factor A, ClfA, binds the complement regulator, factor I, promoting cleavage of the C3b opsonin to the non-opsonin iC3b (Hair *et al*., 2008). ClfA is also involved in camouflaging *S. aureus*, preventing recognition by host immunity. This is done by coating the surface of the bacteria with fibrinogen, leading to false recognition of self by the immune response (Higgins *et al*., 2006).

1.4.2 Immune evasion

The presence of components of the immune system throughout the animal kingdom, from porifera to humans, reflects our common evolutionary heritage. The evolution of the immune system is estimated to have begun 600 million years ago with the first multicellular animals, leading to the complex protective systems seen today (Cooper & Herrin, 2010; Reddick & Alto, 2014). This evolution has led to innate and adaptive responses to infection both consisting of cellular and molecular components. Cells including neutrophils, macrophages and monocytes and molecules including antimicrobial peptides (AMPs) and complement proteins belong to the innate immune system (Janeway, 2001). Interaction between the innate and adaptive arms of immunity is clear, as many of the cells and molecules of the innate system require immunoglobulins (a product of adaptive immune B-cells) for their full function (Iwasaki & Medzhitov, 2010; Parcina *et al*., 2008). At the early stages of infection, *S. aureus* secretes a battery of proteins to evade innate immune factors by preventing recognition by host immunity, killing by host proteins such as complement and AMPs and migration of the primary innate cellular response to *S. aureus*, the neutrophil, to the site of infection.

The first obstacles to *S. aureus* are pattern recognition receptors (PRRs), AMPs and complement. PRRs recognise pathogen associated molecular patterns (PAMPs), such as

peptidoglycan, lipoteichoic acid and lipoproteins. The 10 member Toll-like receptor (TLR) family of human PRRs were the first to be discovered (initially found in the fruit fly *Drosophila melanogaster*) and are the most studied (Medzhitov *et al*., 1997). NOD-like receptors, P-type lectin receptors and RIG-I-like receptors also have important roles in mediating the human immune response to PAMPs. Lipoprotein recognition by TLR2/TLR6 complex on the surface of keratinocytes, epithelial cells and macrophages triggers an intracellular signalling cascade, leading to expression and secretion of specific cytokines and AMPs into the surrounding milieu (Iwasaki & Medzhitov, 2010; van Kessel *et al*., 2014). Askarian *et al*., (2014) reported a new immune evasion protein named TirS, which blocks the signalling cascade triggered by lipoprotein recognition by TLR2. Bardoel *et al*., (2012) and Yokoyama *et al*., (2012) showed using fluorescently labelled staphylococcal superantigen-like protein 3 (SSL3) and competition assays between TLR2 and monoclonal antibodies that SSL3 is a ligand of TLR2 and upon binding it inhibits neutrophil and macrophage activation and interleukin production.

AMPs are found on the skin and tissues at all times and are expressed in response to PRR activation. AMPs are immune regulators promoting wound healing, neutrophil activity and have a direct killing effect on pathogens, by formation of pores at the bacterial cell surface. The positive charge of AMPs is exploited by *S. aureus* using two systems, 1. The *dltABCD* operon substitutes the ribitol component of teichoic acids with positively charged D-alanine. 2. The MprF protein adds a lysine residue to the lipids on the intracellular surface, and then aids flipping of the phospholipid presenting the positively charged lysine on the extracellular surface. The activity of the *dlt* operon and MprF give *S. aureus* a net positive charge leading to electrostatic repulsion of AMPs (Fedtke, 2004; Peschel *et al*., 1999; Weidenmaier *et al*., 2005). The regulatory mechanisms that control this activity are discussed in section 1.7.1.

The main functions of the complement system against *S. aureus* are opsonisation, activation and attraction of neutrophils to the site of infection. The activation of the complement system on the surface of *S. aureus* is initiated via the classical, lectin or the alternative pathways, leading to production of the C3 convertase. The C3 convertase complex cleaves complement protein C3 producing the neutrophil chemoattractant C3a and the opsonin C3b. When the concentration of C3b reaches a threshold level, the C3

convertase dissociates to form the C5 convertase and C5 is cleaved to give C5a, another neutrophil chemoattractant, and C5b (Foster, 2005; Walport, 2001a, 2001b).

S. aureus lessens the impact of the complement system via the release of several proteins. Host plasmin formation leads to direct Efb/Sbi-dependent plasmin cleavage of IgG (required for classical pathway complement activation) and the C3b opsonin. Efb also binds to C3b, preventing opsonisation (Koch *et al*., 2012; Kwieciński *et al*., 2010). The staphylococcal complement inhibitor (SCIN) proteins, discovered relatively recently, are members of the *S. aureus* complement evasion arsenal. They bind directly to the C3 convertase, stabilising the complex. For their function the C3 convertases need to dissociate, by stabilising them SCIN inhibits activation of complement via all pathways (Rooijakkers *et al*., 2006).

Neutrophils are found primarily in blood. They function by phagocytosis of *S. aureus* and killing by an array of toxic intracellular components (including reactive oxygen intermediates and AMPs; Rigby & DeLeo, 2012). Their chemotaxis from blood to the site of infection is important for clearance of *S. aureus* (Bestebroer *et al*., 2007; Li *et al*., 2002). They are directed to the site of infection by chemoattractants, including C5a, C3a, formylated peptides and interleukin-8 (IL-8). The neutrophils move freely through the blood, but upon infection P-selectin and E-selectin are translocated from endothelial Weibel-Palade bodies to the surface of the endothelium, proximal to the site of infection. P-selectin glycoprotein ligand 1 (PSGL-1) expressed on the neutrophil surface binds to these selectins providing a weak attachment and the force imparted by the flowing blood breaks the attachment and the neutrophil roles along the lumen surface maintaining a weak attachment to the selectins. At the site of infection, IL-8 is presented on the surface of the endothelia on heparin sulphate proteoglycans. Neutrophil receptors recognise IL-8 and promote integrin expression, including Mac-1, LFA-1 and VLA-4, which interact with the endothelial receptors ICAM-1, ICAM-2 and VCAM-1 to give stable attachment to the endothelial surface. Transendothelial migration of neutrophils is mediated via interaction with ECM components, such as fibrinogen and fibronectin, between the cells of the endothelium and expression of proteases by the neutrophils to weaken the bonding between cells. The cells then migrate to the focus of infection along the concentration gradient of chemoattractants (Chavakis *et al*., 2007; Rigby & DeLeo, 2012; Spaan *et al*., 2013).

The formyl peptide receptor inhibitory protein, FLIPr and FLIPr-like proteins, SSL5, Eap and CHIPS are secreted by *S. aureus* inhibiting neutrophil migration to the site of infection. SSL5 binds to PSGL-1 on the neutrophil, inhibiting neutrophil rolling at the lumen surface (Bestebroer *et al*., 2007). Eap binds to ICAM-1 expressed by endothelial cells, blocking recognition by neutrophils expressing Map-1 and LFA-1, preventing stable adherence of neutrophils to the lumen surface (Haggar *et al*., 2004). CHIPS competes with C5a and formylated peptides for binding to their respective chemotaxis receptors on the neutrophil surface (Rooijakkers *et al*., 2006). The FLIPr protein expressed by *S. aureus* also inhibits formylated peptide chemoattraction of neutrophils (Prat *et al*., 2009).

1.5 Regulation of virulence determinants late in infection

As an infection progresses and bacterial load increases, the acquisition of nutrients becomes a limiting factor. One method bacteria employ to overcome this is to dramatically reduce their metabolic rate and "wait out the storm". Amino acid starvation leads to production of the alarmones ppGpp and pppGpp, triggering the stringent response. This production is triggered by an increase in uncharged tRNAs binding to the ribosome, leading to synthesis of the alarmones by the ribosome associated RelA/SpoT homologue proteins (Stenz *et al*., 2011). The alarmones downregulate growth related gene expression and upregulate genes for amino acid biosynthesis and stress tolerance (Gaca *et al*., 2015; Stenz *et al*., 2011).

The importance of nucleotide biosynthesis enzymes to pathogenesis attests to the low level of nucleotides in human blood (Brown & Stocker, 1987; O'Callaghan *et al*., 1988; Samant *et al*., 2008). The purine pathway genes *purQ*, *purL*, *purF*, *purM* and *purN* and pyrimidine synthesis genes *pyrC*, *pyrAA*, *pyrF* and *pyrE* are positively regulated by the *cvfC* operon, a four gene operon *cvfC*1-4. The *thyA* gene required for thymidylate synthesis in thymidine limited conditions is upregulated by CvfC3. Loss of *thyA* has been implicated in a reduction in *hla* expression, suggesting a role for *thyA* in upregulation of *hla* (Ikuo *et al*., 2010). The ability to acquire nutrients from the host, such as nucleotides and amino acids is important for bacterial growth. The *cvfC* operon demonstrates coordinated upregulation of biosynthesis genes, of particular importance

in the low nutrients environment of the host, with virulence genes required for the destructive acquisition of nutrients.

1.5.1 Destructive acquisition of nutrients

Control of gene expression using quorum sensing methods allows bacteria to limit the production of certain proteins to a time when they are required. The accessory gene regulator (*agr*) is a quorum sensing TCS of *S. aureus* (Figure 1.2). It is controlled from two promoters P2 and P3, leading to transcription of RNAII and RNAIII respectively (George & Muir, 2007; Novick *et al*., 1993). RNAII is transcribed constitutively at a low level and is translated to give the AgrABCD proteins (George & Muir, 2007). The membrane protein AgrB interacts with AgrD at the membrane, proteolytically cleaving AgrD to give an autoinducer peptide (AIP), which targets the transmembrane receptor histidine kinase AgrC (Bronner *et al*., 2004; Ji *et al*., 1995). The AIP is continuously processed and secreted leading to changes in gene expression when a threshold level, parallel with bacterial numbers, is reached. Binding of AIP to AgrC causes autophosphorylation of AgrC, which activates AgrA promoting increased transcription of RNAII from P2 and transcription of the *agr* effector molecule RNAIII from the P3 promoter.

The AgrA protein directly promotes transcription of phenol soluble modulins (PSMs; Thoendel *et al*., 2011). However, the complex 514 base RNAIII molecule is the primary regulatory molecule of the *agr* system. The effect of RNAIII on virulence factor expression is shown in Table 1.1; downregulating expression of adhesins and immune evasion proteins and upregulating expression of toxins and degradative enzymes. This regulation is carried out directly at the transcriptional and translational level and indirectly through inhibition of *rot* by binding to *rot* mRNA preventing recognition by the ribosome (George & Muir, 2007).

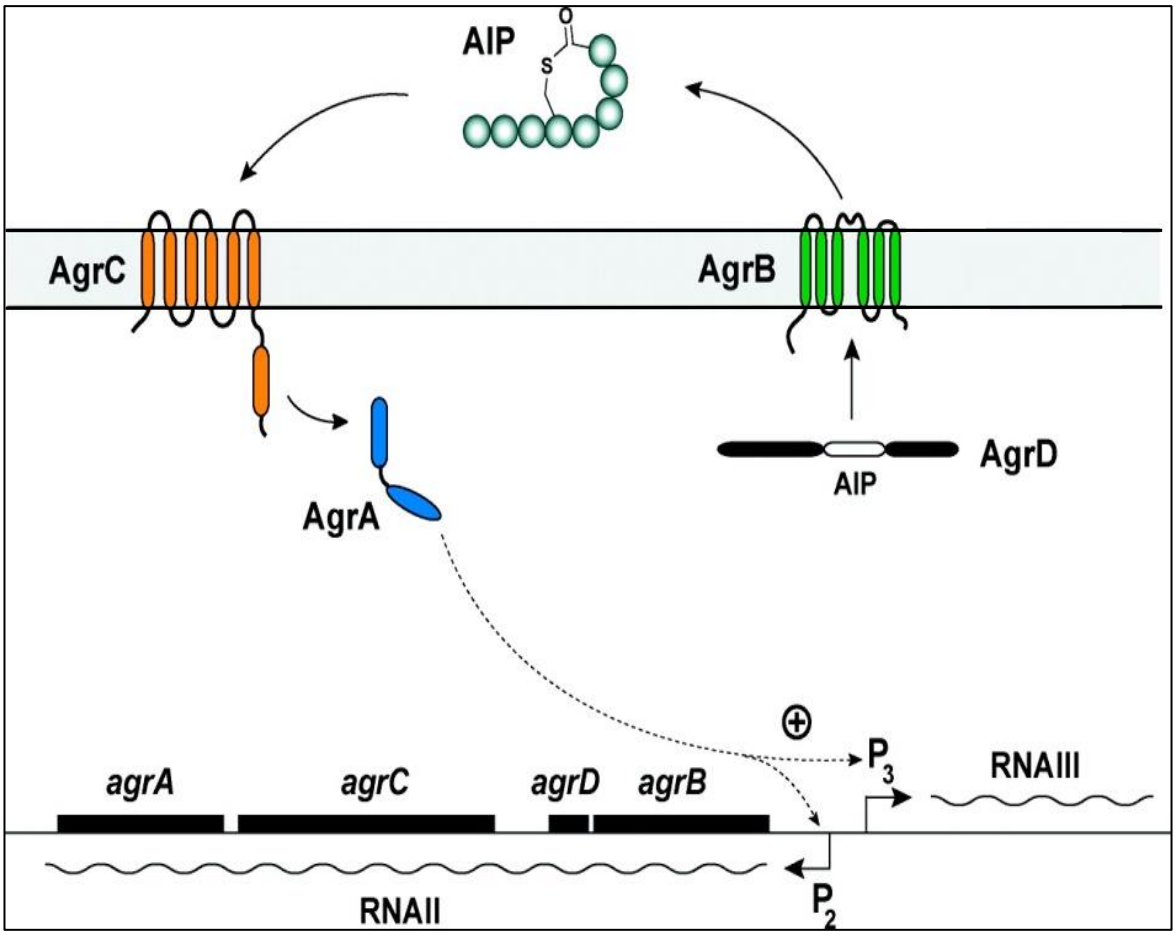

Figure 1.2 The accessory gene regulator (*agr*) system of *S. aureus*.

The autoinducing peptide (AIP) is constitutively secreted by *S. aureus*. This is enabled by constitutive expression of RNAII, producing the AgrABCD proteins. AgrD is proteolytically cleaved by the membrane protein AgrB releasing the AIP. At a threshold level, AIP is recognised by the sensor protein AgrC, leading to phosphorylation of AgrA. Phosphorylated AgrA can then positively regulate RNAII and RNAIII transcription.

Image modified from (Thoendel *et al*., 2011).

The *agr* system allows for coordinated gene expression at high cell density when nutrient levels are low. At this stage evasion of host immunity is not as pressing as the need for nutrients, furthermore, at the later stage of infection, secretion of proteins such as the SSLs to prevent movement of neutrophils to the site of infection is a less suitable response, as neutrophils are likely to have reached the infection and be present in high numbers. The liberation of toxins by high numbers of bacteria also provides a substantial counterattack against the immune response. The need at this stage is to liberate nutrients from surrounding tissues and spread to new sites of infection. Another benefit of controlling toxin production during the early stages is that high levels of some toxins are required before they are fully functional. Indeed low levels of the PSMs of *S. aureus* have been shown to promote activation and migration of neutrophils to the site of infection, and lysis of neutrophils at high concentrations (Berube *et al*., 2014; Kretschmer *et al*., 2010).

If a quorum is not reached before the depletion of available nutrients, the CodY protein allows *S. aureus* to recognise and respond to the low nutrient availability. CodY represses its target genes by binding to their promoters, binding more effectively when bound to isoleucine or GTP. Decreasing nutrients and energy levels, isoleucine and GTP levels, respectively, leads to derepression of the CodY target genes. The *sarA* and *agr* promoters are CodY targets, preventing their transcription when nutrient levels are high enough to maintain the growing *S. aureus* population (Pohl *et al*., 2009; Stenz *et al*., 2011).

1.5.2 Alternative sigma factor B (σ^B)

Sigma factors bind to the core polymerase allowing recognition of specific promoter elements. The RsbW protein complexes with σ^B preventing interaction with the polymerase, during exponential growth phase. Dephosphorylation of RsbV by RsbU in response to environmental stress leads to displacement of σ^B from RsbW, forming an RsbW/RsbV complex, allowing σ^B interaction with the polymerase (Bronner *et al*., 2004; Novick, 2003a). σ^B activates adhesins and genes required for aggregation and biofilm formation.

Expression of toxins and degradative enzymes, controlled by *agr*, leads to destruction of host tissues and acute infection. *S. aureus* is also the cause of prolonged chronic infections, requiring long-term treatment. *S. aureus* is able to persist within the host intracellularly, inside phagocytic cells, such as macrophages and a range of "non-professional phagocytes" including epithelial and endothelial cells (Olivier *et al*., 2009; Clement *et al*., 2005). This persistence is enabled by switching from an aggressive phenotype, to a near inactive resistant state. The sigma factor σ^B associated with resistance to environmental stresses, mediates this switch by downregulating the *agr* system (Tuchscherr *et al*., 2015). This offers an alternative response to low nutrient levels that can be exploited by *S. aureus*.

1.6 Virulence factors associated with late infection

1.6.1 Degradative enzymes

The proteases are important degradative enzymes, as they not only degrade ECM components, such as collagen and fibrinogen, allowing deeper penetration of tissues and release of peptides and amino acids that can be assimilated (Ohbayashi *et al*., 2011; Shaw *et al*., 2004), but they also degrade the *S. aureus* surface adhesins, allowing for migration of the pathogen. Kolar *et al*., (2013) compared the growth and pathogenicity of MRSA USA300 Lac with the same strain deficient in its 10 secreted protease genes. The strains showed identical growth in defined and rich media, but the protease mutant demonstrated significantly reduced starvation survival in a peptide based media and reduced growth in pig serum, suggesting a role for nutrient acquisition in serum. In murine models of systemic infection and abscess formation the protease mutant CFU was significantly reduced compared to the wild type. However, the mortality outcome of systemic infections was significantly higher for the protease mutant. This was determined to be due to greater levels of toxins produced by the protease mutant, suggesting that protease activity plays a role in regulating toxin production and disease severity, by degrading secreted toxins. Adhesins were also found at higher levels in the protease mutant, supporting the role of proteases in cleaving adhesins from the bacterial surface.

Table 1.1 shows that the nuclease gene, *nuc*, is upregulated by both the *agr* and *sae* system. Degradation of nucleic acids to nucleotides is important throughout infection,

supporting the evidence for poor availability of nucleotides in the human host. Nuclease is required for the degradation of neutrophil extracellular traps (NETs; Berends *et al*., 2010). NETs are made up of the contents of neutrophils, the DNA, AMPs and histone proteins, ejected from the neutrophil trapping the bacteria (Berends *et al*., 2010; Schilcher *et al*., 2014). Nuclease has been shown to be an important virulence factor associated with NET-dependant clearance of respiratory tract infections (Berends *et al*., 2010).

Staphylokinase, Sak, activates the host protease plasmin from its inactive form, plasminogen. Binding of fibrin or staphylococcal enolase, Eno, to Sak/plasmin complexes maintains this active state by preventing plasmin inhibition by the host α2-antiplasmin (Mölkänen *et al*., 2002). The active plasmin can then attack ECM components and clotting factors, releasing nutrients and promoting the spread of infection, while inhibiting wound healing. Sak also binds to the AMP, α-defensin, which reduces plasmin formation, but blocks the antimicrobial effects of α-defensin (Jin *et al*., 2004).

Hyaluronate lyase, HysA, cleaves the carbohydrate hyaluronic acid, an integral part of the ECM. This activity is important for virulence in an *in vivo* murine model of pulmonary infection (Ibberson *et al*., 2014). Isogenic mutants of the lipase genes, *lip1* and *lip2* are less able to form biofilms, have reduced CFU in the liver, spleen and kidneys of intraperitoneally infected mice and are less able to form abscesses (Hu *et al*., 2012). Lipase also inhibits phagocytosis and phagocytic killing of *S. aureus* by neutrophils *in vitro* (Rollof *et al*., 1988).

1.6.2 Secreted toxins

S. aureus secretes a large number of toxins, which are essential for virulence. This large variety of toxins allows for the range of *S. aureus* toxin-derived diseases, from mild skin infections to life-threatening systemic infections. The secreted toxins of *S. aureus* can be placed into five categories: Exfoliative toxins; enterotoxins, including the toxic shock syndrome toxin, TSST-1; the haemolysins; two-component leukotoxins and the phenol soluble modulins (PSMs).

1.6.2.1 Exfoliative toxins

The exfoliative toxins (ETs) are the cause of staphylococcal scalded skin syndrome (SSSS), a disease discovered by Gottfried Ritter von Rittershain in 1878 (Bukowski *et al*., 2010). Localised blistering caused by ETs is referred to as bullous impetigo, which is then referred to as Ritter's disease or SSSS when the large, fluid filled blisters cover large areas of the body. The blisters are easily damaged; leading to sloughing off of the surface skin layers, which if untreated or not treated correctly can lead to secondary infections (Ladhani, 2003). The disease is most common in infants, with a low mortality rate of < 5%. Adults suffering from immune suppression, HIV, chronic alcoholism, renal failure or cancer are susceptible to SSSS, with a high mortality rate of 59%, of which the underlying disease is a factor (Manders, 1998).

SSSS is caused by *S. aureus* secretion of the exfoliative toxins (ETA, ETB and ETD). Associating *S. aureus* with this disease proved difficult, as blisters are usually aseptic, as upon secretion of the toxins, they are transported throughout the body in the blood where they reach the skin surface away from the foci of infection. This spread is controlled by anti-toxin antibodies, explaining the frequency of infant infections, as infants are less likely to have been exposed to ET toxin antigens (Ladhani, 2003; Rogolsky, 1979). The toxins are serine proteases, but unlike others they have a very specific target. The ETs have been referred to as molecular scissors, cutting the bond between surface layer skin cells, the keratinocytes, by cleaving a specific site in desmoglein-1 (Dsg1), a protein bridge between the cells of the epidermis that maintains intercellular adhesion (Hanakawa *et al*., 2002; Ladhani, 2003). This cleavage only affects the surface epidermal layers, as in addition to Dsg1, the deeper dermal layers have Dsg3, which compensates for the disruption of Dsg1 (Hanakawa *et al*., 2002).

1.6.2.2 Enterotoxins/superantigens

1.6.2.2.1 Food poisoning

There are 19 staphylococcal enterotoxins (SEs; SEA-SEE & SEG-SER – SEF is now known as TSST-1) and several variants known as SE-like or SEl proteins, which have either no role in food poisoning, or have no demonstrated role (Lina *et al*., 2004; Murray, 2005). The SE genes are found on mobile genetic elements including plasmids,

staphylococcal pathogenicity islands and prophages potentiating their spread between *S. aureus* strains (Novick, 2003b). SEB, SEC and SED are upregulated by the *agr* system and SEH, SER and SEL are expressed post-exponentially, but the role of *agr* in their regulation has not been defined (Schelin *et al*., 2011). The most common cause of staphylococcal food poisoning is SEA, with symptoms including vomiting, diarrhoea, abdominal pain and nausea (Argudín *et al*., 2010; Schelin *et al*., 2011). The enterotoxins cause vomiting and diarrhoea by stimulating the vagus nerve and triggering the diarrhoea and vomiting response (Murray, 2005).

1.6.2.2.2 Toxic shock syndrome

All SEs and SE-like proteins are superantigens (SAgs) that can massively overstimulate T-cell proliferation and the release of pro-inflammatory cytokines leading to the rare, acute disease, toxic shock syndrome (TSS). Symptoms of TSS include fever, rash, shock and multiple organ failure (Argudín *et al*., 2010; Ortega *et al*., 2010). The toxic shock syndrome toxin 1 (TSST-1) is in a separate group from the SEs and SEls (Ortega *et al*., 2010). It has no emetic properties, but is the primary cause of menstrual TSS, associated with tampon use (Murray, 2005). Non-menstrual TSS occurs in association with a separate staphylococcal infection; it is caused by SEs, including TSST-1 and can lead to fatal complications in the treatment of the associated infection (Ellis *et al*., 2003; Iandolo, 1989).

A normal antigen will be processed by an antigen presenting cell (APC) and displayed on the cell surface in the peptide binding groove of the major histocompatibility complex (MHC). The antigen will be recognised by the T-cell receptors (TCRs) of 0.01-0.1% of T-cells, prompting their proliferation and release of immune mediating cytokines (Janeway, 2001; Manders, 1998). Staphylococcal SAgs do not require processing and bind directly to MHC class II on the surface of APCs, outside the peptide binding groove, on the outside of the MHC/II molecule (Dellabona *et al*., 1990). This allows SAgs to activate T-cells that have a TCR containing a Vβ segment, stimulating proliferation and release of toxic levels of cytokines from 5 – 30% of T-cells (i.e. those that have the Vβ segment; Manders, 1998). It is this subversion of the adaptive immune response that leads to TSS.

The diseases TSS and SSSS rely on the expression of SEs and ETs, respectively. The remaining toxins to be discussed are not associated with a specific disease, but have specific activities that contribute to the virulence of *S. aureus*.

1.6.2.3 Haemolysins

The haemolysins are so named due to their ability to lyse red blood cells (RBCs). This function is likely important for the acquisition of Fe, as ~80% of the body's Fe is associated with haemoglobin, while most of the remaining is associated as cofactors in other metaloproteins, or chelated by Fe storage proteins (Hammer & Skaar, 2011). As shown in Table 1.1, the alpha, beta and delta haemolysin genes (*hla*, *hlb* and *hld*, respectively) are expressed throughout infection, likely due to a need for Fe. However, *hla* mRNA translation to Hla is controlled by RNAIII, the *agr* effector molecule, and *hld* is encoded centrally on the RNAIII molecule, so *hld* expression must only be at a low level early in infection (Arvidson & Tegmark, 2001; Bronner *et al*., 2004). This may allow for low level expression of Hla for the acquisition of Fe, which increases as the need for Fe increases with bacterial load. The fourth haemolysin γ-haemolysin (Hlg) is a two-component leukotoxin and will be discussed in the next section.

Hla is a homoheptameric leukotoxin that interacts with the ADAM10 receptor on the surface of endothelial cells. This interaction promotes disruption of the vascular endothelial barrier by inhibiting production of the intercellular adherence protein cadherin (Gouaux *et al*., 1994; Powers *et al*., 2012). Hla also promotes pro-inflammatory IL-1β, IL-18 production in monocytes by promoting formation of the NLRP3 inflammasome complex, a host signalling complex involved in regulating inflammatory cytokine production. This is followed by necrosis of monocytes in an NLRP3-dependent pyronecrosis, releasing the tissue damaging contents of monocytes (Craven *et al*., 2009).

Hlb is a sphingomyelinase that cleaves the sphingomyelin in cell membranes making them permeable. The level of sphingomyelin in the membrane of different cell types determines their susceptibility to Hlb. Hlb is more active on sheep RBCs than human, but is a potent necrotic toxin of human monocytes (Walev *et al*., 1996). This toxin also has a role in immune evasion, by inhibiting production of IL-8 by endothelial cells,

reducing neutrophil chemotaxis to the site of infection, which may play an important role early in infection, suggesting a possible reason for its early expression (Tajima *et al*., 2009).

Hld is now recognised as the phenol soluble modulin, PSM-δ. Hld and Hlb synergistically promote escape from the phagosome, by Hld interaction with ceramide. Ceramide is one of the products of sphingomyelin cleavage by Hlb and so Hlb activity is required before Hld can function (Giese *et al*., 2011). Hld also causes mast cell degranulation and release of immune stimulating molecules (Nakamura *et al*., 2013).

1.6.2.4 Two-component leukotoxins

The leukotoxins are a family of *S. aureus* secreted toxins. They target leukocytes and red blood cells and are important virulence factors. The toxins consist of an F component and an S component, or two S components in the case of γ-haemolysin. Individually the F and S components cannot form pores, but together form hetero-oligomeric pores on their target cell surface. Panton-Valentine leukocidin (PVL) is associated with CA-MRSA strains. Initial confusion over its role in pathogenesis was the result of its specificity for human and rabbit neutrophils, as studies in murine models showed no difference in pathogenicity between isogenic PVL mutants with the wild-type (Bubeck Wardenburg *et al*., 2008; Voyich *et al*., 2006). The toxin effectively lyses human and rabbit neutrophils and stimulates the release of pro-inflammatory cytokines IL-1β and IL-18 by monocytes (Holzinger *et al*., 2012; Loffler *et al*., 2010). Hlg consists of two S components HlgAC and one F component HlgB, giving two active toxins AB and CB. Both toxins are active against RBCs, neutrophils, macrophages and monocytes (Dalla Serra *et al*., 2005).

The most recently discovered leukotoxin is LukGH, also known as LukAB. This toxin targets monocytes, macrophages, and dendritic cells and has a potent necrotic effect on human neutrophils (Dumont *et al*., 2011; Ventura *et al*., 2010). LukAB/GH kills neutrophils extracellularly and intracellularly effecting escape after phagocytosis (DuMont *et al*., 2013). The toxin also promotes NET formation, which can lead to damage to host tissues (Malachowa *et al*., 2013). The LukED toxin is cytotoxic to T-cells, macrophages and dendritic cells expressing the CCR5 HIV receptor and a murine

model negative for CCR5 expression is more resistant to *S. aureus* challenge (Alonzo III *et al*., 2012). The toxin also targets neutrophils and monocytes via the CXCR1 and CXCR2 receptors leading to their lysis (Reyes-Robles *et al*., 2013).The LukMF toxin is commonly associated with strains of *S. aureus* causing bovine mastitis. This leukotoxin is the most active of the leukotoxins against bovine neutrophils (Barrio *et al*., 2006; Rainard *et al*., 2003).

1.6.2.5 Phenol soluble modulins (PSMs)

The small peptide toxins, phenol soluble modulins (PSMs), include *hld*, discussed above, the alpha-type PSMα1-4, the beta-type PSMβ1-2 and PSM-mec. PSMs are cytolytic and have also been linked to regulatory roles in the expression of *hla* (PSMα) and downregulation of *agr* (PSM-mec; Berube *et al*., 2014). PSMs promote the migration of neutrophils to the site of infection and it has been hypothesised that once an infection is well established, PSMs are upregulated under the control of *agr*, and attract neutrophils, which are then effectively lysed by high levels of PSM and other toxins leading to tissue damage by release of the toxic neutrophil contents (Kretschmer *et al*., 2010; Kretschmer *et al*., 2012). However, the chemotaxis and extracellular killing activity of PSMs is inhibited by human serum, suggesting that PSMs may well only have a role as intracellular toxins, an activity demonstrated in osteoblasts (Rasigade *et al*., 2013).

1.7 Regulators associated with specific environmental stimuli

1.7.1 The *graRS* TCS

Positively charged AMPs secreted by a variety of cells and released by platelets are found in host tissues, within the phagolysosome and on the skin surface (Weidenmaier *et al*., 2005). AMPs, such as defensins, cathelicidins, lysozyme and thrombocidins attack the cell wall of *S. aureus*, leading to death of the pathogen (Fedtke, 2004; Kraus *et al*., 2008). The cationic AMPs are attracted to the anionic charge of the bacterial cell wall, imparted by negatively charged cell wall molecules such as phospholipids, peptidoglycan and wall teichoic acid (Fedtke, 2004; Kraus *et al*., 2008). The TCS *graRS* allows *S. aureus* to respond to the presence of AMPs, triggering expression of the *dltABCD* operon and *mprF*, discussed above.

Biofilms enhance antibiotic and immune resistance of individual bacteria within the biofilm. Ion chelation by sodium citrate is employed for anticoagulation in catheter locks. Shanks *et al.*, (2008) showed that the *graRS* system is stimulated by low levels of sodium citrate, leading to VraFG-dependent biofilm formation. This biofilm formation was also dependent on SarA mediated expression of *fnbpAB*. Citrate is an intermediate of the TCA cycle and other intermediates (isocitrate, fumarate, malate and oxaloacetate) also stimulate biofilm formation (Shanks *et al*., 2008).

1.7.2 The *srrAB* TCS

The *srrAB* TCS downregulates toxin production in anaerobic and microaerobic conditions (Bronner *et al*., 2004). It downregulates the *agr* system and is itself downregulated by *agr* (Novick, 2003a; Pragman *et al*., 2004). The *srrAB* TCS is required for resistance to $NO^{\cdot}$ released by the host. $NO^{\cdot}$ levels are high on the skin and nares, making resistance important for survival in these host niches. Resistance is achieved by production of the flavohaemoglobin, Hmp. The *hmp* gene is under the control of SrrAB, along with genes required for anaerobic respiration and repair of oxidative damage. Hypoxic conditions within the biofilm result in activation of *srrAB* and this inactivation is essential for biofilm formation (Kinkel *et al*., 2013).

The polysaccharide intercellular adhesin (PIA) is produced from the *icaABCD* locus. PIA promotes aggregation of *S. aureus* and biofilm formation and is commonly associated with cystic fibrosis *S. aureus* infections. Transcription from the *ica* locus is inhibited in aerobic conditions by IcaR. The anaerobic millieu associated with cystic fibrosis infections, leads to phosphoylation of SrrA by SrrB, which then binds the *icaA* promoter, between the IcaR binding site and the *icaA* gene, leading to transcription and biofilm formation (Ulrich *et al*., 2007).

As discussed in section 1.6.2.2.2 toxic shock syndrome is associated with the use of tampons. The *srr* system has been implicated in tampon-associated toxic shock syndrome. SrrA inhibits TSST-1 in anaerobic conditions and it has been proposed that insertion of a tampon into the normally anaerobic vagina leads to temporary aeration and expression of the TSST-1 toxin (Yarwood *et al*., 2001).

1.8 Methods in analysis of virulence factors

1.8.1 Characterisation of individual virulence factors *in vitro* and *in vivo*

A frequently used method for the analysis of virulence factors is the disruption or deletion of a potential virulence factor encoding gene, followed by observation of the resulting phenotype. For an *in vitro* study, this may involve analysis of growth in the absence of a specific nutrient, or growth on tissue culture or specific host cell type. Alternatively, the protein product of the putative virulence factor can be overexpressed and purified and then its structural properties and function can be analysed in isolation. An important problem of *in vitro* analyses is that they do not mimic the host environment well. Inside the host a virulence factor may be released at low concentrations, or expressed only at certain times during infection in order to function correctly, while a relatively large amount of purified protein may be used *in vitro* over extended periods (Cross, 2008; Smith, 1998). This may lead to spurious conclusions as to the activity of the virulence factor, such as binding ligands that would not be bound within the host at the lower *in vivo* concentration and lower exposure times. In the majority of *in vitro* experiments the media used, including rich media, defined media and minimal media is the single source of nutrients throughout the experiment (Quinn *et al*., 1997; Smith, 1998). This does not reflect the conditions *in vivo*, where access to nutrients is changing over the course of infection, which alters the growth rate and gene expression of the bacteria.

Complementing *in vitro* analyses with *in vivo* studies overcomes many of the above problems. Strains with a disrupted gene for a putative virulence factor can be used to infect animal models and the outcome of infection assessed. The strain will then encounter all the changes in nutrient availability and host immune factors that are missing from many *in vitro* studies. Putative virulence factor genes from a known pathogen can be inserted into avirulent or poorly virulent species and the effect can then be assessed *in vivo*. RNA interference (RNAi) can be used to knock-down the expression of pathogen and host gene products, to identify pathogen gene products required for virulence and host products required to fight infection (Burrack & Higgins, 2007). Problems of inoculum size and the site at which the bacteria are inoculated arise with *in vivo* studies. A balance has to be found between too high a dose and too low a dose. Too high and the defences of the subject animals are immediately overcome, too

low and all subject animals recover; in both cases little is learnt. Interestingly the required CFU varies between infection routes, for example direct injection into the bloodstream may require a higher CFU than intraperitoneal infection due to the immediate availability of host defence cells in the blood (Cross, 2008). The category of virulence factor also determines the site of infection for an *in vivo* model. Infection by skin scrape is better suited to analysis of tissue degrading enzymes, whereas intraperitoneal infection may be better suited for analysis of virulence factors associated with liver abscess formation.

The *S. aureus* 8325 genome contains 2,755 genes, according to the Patric database. Of these 2,755, there are 645 hypothetical genes, which have no function assigned to them. The remaining 2,110 contain all genes with known or predicted functions, including genes encoding virulence factors. However, some of these genes may well be incorrectly assigned and non-virulence factors may indeed be virulence factors. To assess all of these genes individually by *in vitro* and *in vivo* methods would be costly and slow and only provide full information for one strain of one species, wasting resources and time that could be spent using a more directed approach. Methods have been developed to narrow the focus of analyses to a subset of genes that have the potential to be important for pathogenicity.

1.8.2 Identification of virulence factors by *in silico* analysis

Advances in genome sequencing technologies have led to whole genome sequencing of multiple pathogenic species and strains (Buermans & Dunnen, 2014; van Dijk *et al*., 2014). Bioinformatics can be used to compare the genomes of known pathogens to identify shared virulence factors and compare the host genome with that of the pathogen to identify proteins that may interact with the host. Furthermore, whole genomes can be searched for known promoter elements to identify genes controlled by regulators known to be important for virulence factor expression (Burrack & Higgins, 2007). Available genome sequences also allow for ordered transposon mutagenesis libraries of individual strains, which can be used to assess the importance of non-essential genes to the virulence of a pathogen (Fey *et al*., 2013). Bioinformatics is a powerful approach that can be used to identify potential targets in order to direct work in the laboratory, allowing for a more focused approach to characterise virulence factors.

1.8.3 Selective capture of transcribed sequences (SCOTS)

Selective capture of transcribed sequences (SCOTS) was developed by (Graham & Clark-Curtiss, 1999). The SCOTS method allows comparison of transcribed genes *in vivo* with transcribed genes *in vitro* (see Figure 1.3). Total RNA is extracted and converted to cDNA, then bacterial cDNA (limited to 200-500bp) is captured by hybridisation to biotinylated bacterial DNA. The most common cDNA will be ribosomal DNA (rDNA), so the biotinylated rDNA site is blocked by an initial round of hybridisation with plasmid DNA encoding rDNA. Subtractive hybridisation between linkered cDNA from *in vitro* or *in vivo* growth, leaves enriched *in vitro* cDNA demonstrating down-regulation *in vivo,* or enriched *in vivo* cDNA, demonstrating upregulation *in vivo* (Wang *et al*., 2014). SCOTS can be used to determine gene expression changes *in vitro* using cell cultures (Graham & Clark-Curtiss, 1999) and from tissues recovered from *in vivo* animal models (Baltes & Gerlach, 2004). This method can identify genes positively or negatively regulated, but says nothing of the function of the genes.

1.8.4 *In vivo* expression technology (IVET)

The success of *S. aureus* and other pathogens results from their ability to respond to a change in their environment by appropriate gene expression. IVET offers a means of tracking the change in expression by comparison of growth in different environments. The basis of the IVET method was introduced by Osbourn *et al*., (1987) and further developed by Mahan *et al*., (1993) who coined the name IVET. The IVET method and modifications to the method are shown diagrammatically in Figure 1.4.

The first use of IVET took advantage of a *purA* mutant strain's rapid clearance from the host. A promoterless *purA lacZY* fusion, was inserted into a suicide vector and random genomic fragments (known as gene x) were inserted upstream. Transformation of the vectors into the *purA* mutant was then carried out, leading to homologous recombination and formation of a merodiploid strain library. Those strains expressing gene x *in vivo* were able to grow due to expression of *purA* downstream of gene x, those that were not did not survive. To separate those genes expressed only *in vivo* from those expressed at all times, after collection of the bacteria from host tissues, *lacZY* activity

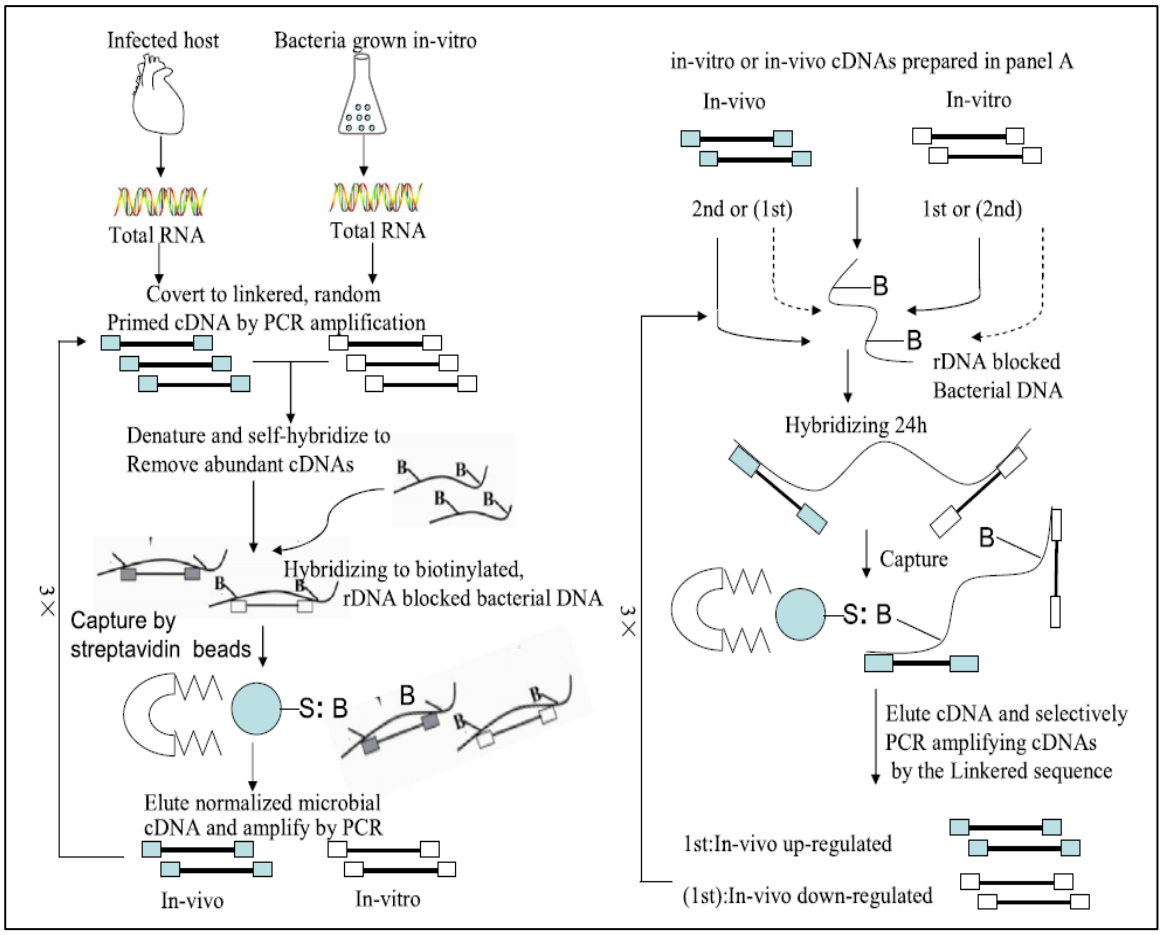

Figure 1.3 Representation of the selective capture of transcribed sequences (SCOTS) methodology.

Total RNA from *in vitro* and *in vivo* growth is extracted and reverse transcribed to linkered cDNA. Bacterial cDNA is extracted (barring ribosomal cDNA) by hybridisation to fragmented biotinylated bacterial genomic DNA, pre-hybridised with rDNA, and isolated with streptavidin-coated magnetic beads. Primer binding sites on the linker DNA are then used to amplify the cDNA and any remaining rDNA is removed, by further rounds of hybridisation to rDNA-blocked bacterial genomic DNA. The cDNA from *in vitro* growth is then hybridised to fragmented biotinylated bacterial genomic, followed by hybridisation of cDNA from *in vivo* growth, or vice versa, to enrich either *in vivo* transcribed cDNA or *in vitro* transcribed cDNA.

Image modified from Wang *et al.*, (2014).

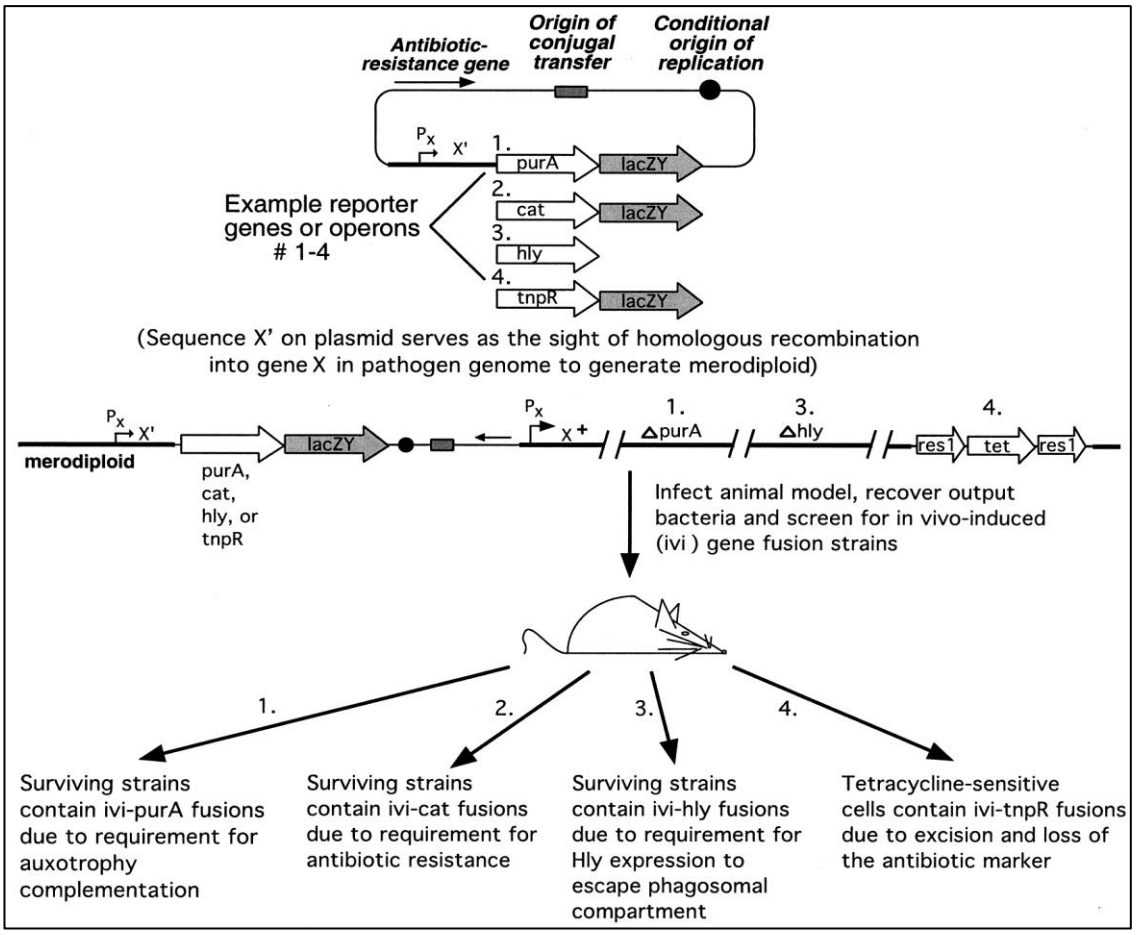

Figure 1.4 Representation of the *in vivo* expression technology (IVET) methodology.

Bacterial genome fragments are inserted upstream of a specific reporter gene within a vector. The vector is integrated into the genome of the pathogen, producing a library of strains each with a different genomic fragment upstream of the reporter. The strain library is then used to infect a model organism. The reporter is required to complement an existing auxotrophy in the bacteria, an antibiotic resistance marker or to perform a specific function. Those fragments that do not stimulate expression from the reporter promoter *in vivo*, will not be represented, due to loss of their host bacteria. The successful strains are then assessed for the exclusivity of their expression *in vivo*, by *in vitro* analysis of LacZY activity. Those strains that do not have LacZY activity *in vitro* are expressed only *in vivo*.

Image modified from (Angelichio & Camilli, 2002).

was measured by growth on indicator media, those showing no *lacZY* activity are only expressed *in vivo* (Angelichio & Camilli, 2002). Other reporter genes used as alternatives to *purA* include *purEK*, *panB* and *thyA* (Rediers *et al*., 2005).

Pathogens are required to alter their pattern of gene expression to respond to the change in their environment over the course of infection. At the early stages, colonisation and resistance to host immunity are required to establish infection. In later stages, changes in metabolism are required to respond to reduction in nutrient levels and expression of toxins and degradative enzymes are required to spread to other sites within the host. A *purA* auxotroph will likely not reach these later stages before clearance by host immunity; therefore, important virulence determinants required at these stages will not be detected. Alternatives to *purA* include the use of an antibiotic resistance gene, which allows analysis of expression at later stages of infection, by delaying antibiotic treatment of infected animals until an infection is well established (Angelichio & Camilli, 2002; Darwin, 2005).

The *hla* gene of *Listeria monocytogenes* is required for escape from within the phagosome. Using *hla* as an alternative to *purA*, allows analysis of intracellular and intraphagosomal gene expression in *L. monocytogenes*. Other genes with known functions have been used in this way (Angelichio & Camilli, 2002; Rediers *et al*., 2005).

RIVET is a recombination-based IVET that uses a resolvase gene, in place of *purA*, to excise an antibiotic cassette previously inserted into the genome. As only low levels of resolvase are required for activity, RIVET can detect *in vivo* expressed genes required only for short periods during infection (Angelichio & Camilli, 2002).

The IVET method has limitations that affect its results, leading to false positives and false negatives. IVET does not take into account gene products that are expressed both *in vitro* and *in vivo*, but may be only active *in vivo* due to posttranslational modification. Gene expression will vary under different *in vitro* conditions; therefore, a gene may be upregulated *in vivo* and downregulated in one *in vitro* condition, but not in another (Rediers *et al*., 2005).

1.8.5 Signature-tagged mutagenesis (STM)

Signature-tagged mutagenesis (STM) allows analysis of multiple genes within a single host, to identify those genes required by the pathogen for survival in the host. STM was developed by Hensel *et al*., (1995) and the method is shown diagrammatically in Figure 1.5. The basic STM method relies on variable tags, with identical flanking regions, allowing PCR of all the variable regions in a single reaction. A pool of tags are made and inserted into transposons (Tn). The Tn pool is then transformed into the pathogen of interest, giving a pool of strains with a Tn, containing a unique tag, inserted into an individual gene. Genomic DNA is extracted from the pool before infection (input pool) and from animals infected with the pool (output pool) and the tags are amplified for both pools. Input and output tags are then hybridised to DNA from the Tn mutant library. DNA that hybridises to probes from the input pool, but not the output pool is deemed likely to be important for virulence.

As with IVET and SCOTS, there are drawbacks in the use of STM. A problem affecting STM results is the specificity of some virulence factors for a particular host. An example of this is the PVL toxin, which kills human and rabbit neutrophils, but not mouse neutrophils (Loffler *et al*., 2010). Therefore, STM would not detect the *pvl* gene in a mouse model. This can be overcome for some virulence factors, by using a variety of hosts, which also has the benefit of identifying genes that are central to the pathogenicity of a species (Shea *et al*., 2000). It is unlikely that STM would highlight the importance of PVL, as it is a secreted toxin, and the STM methodology is limited in that the benefits of secreted proteins by different members of the pool of strains will be enjoyed by all strains. Essential genes cannot be assessed by STM, as Tn disruption of an essential gene means that that strain cannot grow and will not be represented in the input pool (Autret & Charbit, 2005).

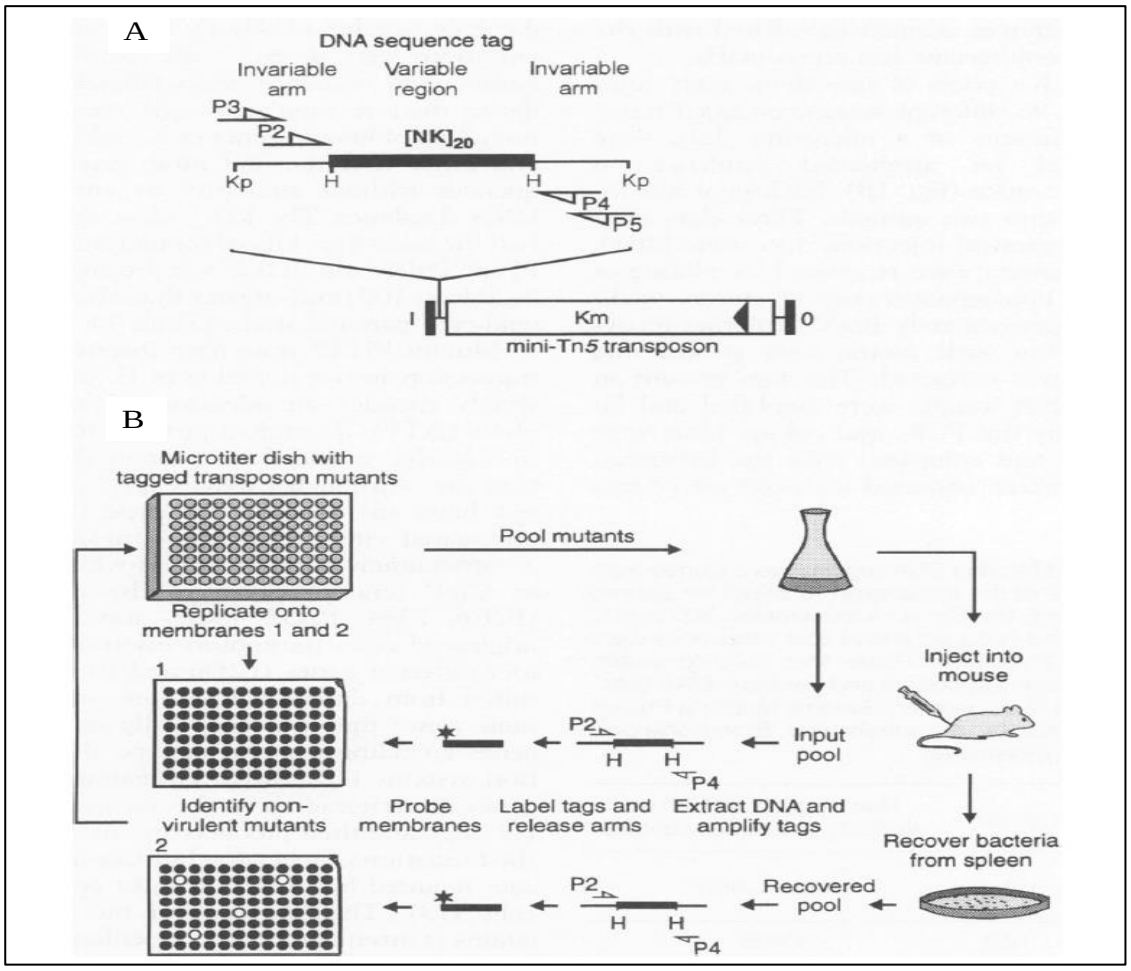

Figure 1.5 Representation of the signature-tagged mutagenesis (STM) methodology.

A. DNA tags, with a variable central sequence flanked by invariable sequences are inserted into transposons (Tn). The tagged Tn are then used to create a bacterial strain library, each strain with a Tn inserted at a specific gene, containing a unique tag.

B. Strains from a 96-well plate are pooled and then used to infect a model organism. Prior to infection, genomic DNA is extracted from the pool to give the input pool. Genomic DNA is then extracted from the host organism to give the output pool. The tags are amplified from primer binding sites within the invariable regions, labelled and the invariable tags removed. The input pool is hybridised to the Tn DNA from the 96-well plate. Those tags that hybridise from the input pool, but not the output pool are considered potentially required for virulence.

Image modified from (Hensel *et al*., 1995).

Each of the methods outlined in section 1.8.2-1.8.5 have limitations, but all provide targets for the more in-depth studies of isogenic mutants and functional assays. The potential targets that are frequently found by *in vivo* expression methods were assessed by Rediers *et al.*, (2005), who found that a large proportion of the genes belong to those classes involved in nutrient acquisition and biosynthesis. These include Fe and other metal ion scavenging systems; upregulation of transporters for uptake of amino acids and sugars; amino acid synthesis and catabolism; protein synthesis and degradation; stress resistance genes, such as acid tolerance and osmotic stress; secretion, virulence factors and nucleic acid metabolism components. Purine biosynthesis is a particularly prevalent finding in STM screens, reflecting the low purine availability in the host (Shea *et al*., 2000). A third of genes shown to be required *in vivo* have no known function, demonstrating that there are a large number of potential virulence associated genes that are yet to be characterised.

1.8.6 *S. aureus* specific problems associated with STM and IVET

Work done in this laboratory by Prasjnar *et al.*, (2012) highlights a *S. aureus* specific problem with expression technologies, relating to the dynamics of *S. aureus* infections. The observation that in a zebrafish model of systemic infection bacterial numbers remain static for the first 24hr post infection, and are then either cleared or grow to approximately 10^6 per larvae, resulting in the death of the host, suggested a niche was available to avoid host clearance during this initial period.

Using a mix of two isogenic strains, expressing different antibiotic resistance markers, a population bottleneck was seen in which low numbers of the starting inoculum contribute to the bacterial load seen at the end of infection. This resulted in skew towards one strain or the other found in larvae at the end of infection, and not the equal numbers of each strain at the end of infection, if the contribution of both was equal. Furthermore, isogenic strains with a different fluorescent label demonstrated that abscesses within zebrafish embryos were caused by a very low number of bacteria, if not a single bacterium, as many abscesses showed only a single fluorescent marker. A selective advantage of one strain over another was ruled out by passage of bacteria back through the host, leading to loss of the bias seen in the previous passage through the

host. This clearly demonstrated a niche were a small number of bacteria survive and go on to seed infection.

The bottleneck effect is not associated only with zebrafish, and has been shown in a murine model of systemic infection (McVicker *et al*., 2014). Mice were intravenously infected with a 1:1:1 ratio of *S. aureus* strains, which were isogenic, apart from the presence of different antibiotic resistance cassettes. The numbers of bacteria in the kidneys, liver, spleen, heart and lungs was then measured during infection. At the early stage of infection no clonal bias was seen and bacterial numbers remained steady (similarly to the early stages of a zebrafish infection) and confined mainly to the liver and spleen. A high degree of clonal bias was seen later in infection when bacterial numbers increased in the kidneys. After 2 days, only one or two of the three strains (more frequently just one strain) were found in the majority of kidneys assessed. This clonal bias was also seen in the liver, spleen, heart and lungs at later stages of the infection (72 h).

A limited number of strains in the mixed population would survive *in vivo* and this would not be due to the expression of required genes, but rather to the stochastic clonal expansion process outlined above. This demonstrates the limitations of *in vivo* analysis of gene expression and mixed mutant analyses using *S. aureus* strain libraries.

1.9 Rationale and objectives

The success of *S. aureus* as a pathogen is dependent on colonisation of the host, evasion of host defences, liberation and synthesis of nutrients, stress tolerance and the ability to spread through the host. These activities are enabled by an array of virulence factors controlled by a complex system of regulators, themselves classed as virulence determinants. The recent addition of the new leukotoxin, LukAB/GH (Dumont *et al*., 2011; Ventura *et al*., 2010), to the armoury of *S. aureus* virulence factors raises the possibility that there may be further proteins, either with or without known functions that play important roles in pathogenesis. Two methods were used to address this, a bioinformatics analysis of the *S. aureus* genome (Chapter 3) and screening an ordered library of transposon mutants, the Nebraska transposon mutagenesis library (Chapter 4).

Attempts were then made to characterise the putative virulence determinants found and identify their role in *S. aureus* pathogenicity (Chapter 3 & Chapter 5).

CHAPTER 2

MATERIALS AND METHODS

2.1 Media

All media was prepared using distilled H_2O and autoclaved at 121^{o}C at 15psi, unless otherwise stated

2.1.1 Baird-Parker agar

Baird-Parker Agar Base (Oxoid)	63 g l^{-1}
Egg Yolk Emulsion (VWR)	50 ml l^{-1}

Once cooled to 50^{o}C after autoclaving, egg yolk emulsion was added.

2.1.2 Brain heart infusion (BHI)

BHI (Oxoid)	37 g l^{-1}

For BHI agar 1.5% (w/v) agar No. 1 (Oxoid) was added.

2.1.3 Blood and blood component agar

2.1.3.1 Preparation of blood components

2.1.3.1.1 Human blood collection

A 21 gauge needle was used to obtain venous blood from healthy volunteers, with their informed consent, at the Royal Hallamshire Hospital. The South Sheffield Ethics Committee approved the protocol for phlebotomy. Blood was collected in 50 ml Falcon tubes containing the anticoagulant sodium citrate, to give a concentration of 0.4% (w/v) for a full 50 ml Falcon tube. Tubes were gently rotated to ensure that the anticoagulant was incorporated evenly throughout the blood. Anticoagulant was added to all samples unless stated. Blood that was not used on the day of collection was discarded.

2.1.3.1.2 Human plasma preparation

Blood samples collected as in section 2.1.3.1.1 were centrifuged at 270 g for 20 min in 50 ml Falcon tubes. This gave two phases, a lower cell rich phase and an upper platelet rich phase. The upper phase was collected and either used directly as platelet rich plasma (PRP), or centrifuged at 1155 g for 40 min to give platelet poor plasma (PPP), by removal of clotting factors. Plasma was stored at -20^{o}C.

2.1.3.1.3 Human serum preparation

Human serum was either purchased from Millipore or prepared from blood donated as in section 2.1.3.1.1. Blood was collected without anticoagulant and stored at 4^{o}C for 6 h to allow clotting. Once clotted, the blood was centrifuged at 5,000 rpm and the serum was carefully collected from the top of the pelleted clot. Serum was stored at -20^{o}C.

2.1.3.1.4 Non-human blood products

Non-human animal blood was purchased from TCS Biosciences Ltd. Non-human animal sera were purchased from Sigma-Aldrich. Blood was stored at 4^{o}C and sera were stored at -20^{o}C.

2.1.3.2 Serum or plasma agar (50%)

3% (w/v) agar No. 1 (Oxoid)	30 g l^{-1}

Once the agar cooled to 55^{o}C an equal volume of agar was added to serum or plasma, pre-warmed to 37^{o}C, to give 50% (v/v) serum or 50% (v/v) plasma agar.

2.1.3.3 Human or non-human blood agar (30%)

2% (w/v) agar No. 1 (Oxoid)	20 g l^{-1}

Once cooled to 50^{o}C, agar was added to human or non-human blood, pre-warmed to 37^{o}C, to give a final concentration of 30% (v/v) blood agar.

2.1.3.4 RBC homogenate agar (30%)

Red blood cells (RBCs) were collected as a by-product of neutrophil preparation (section 2.18.1). RBCs were thawed on ice, then vortexed and an equal volume of platelet poor plasma was added, restoring an equivalent RBC concentration to whole blood. Plates were then prepared with the RBC homogenate, as in section 2.1.3.3.

2.1.3.5 Sheep blood agar (5%)

Columbia agar (Sigma-Aldrich) 42 g l^{-1}

Once cooled to 50^{o}C, sheep blood was added to a final concentration of 5% (v/v).

2.1.4 Chemically defined media (CDM)

Chemically defined media (CDM) was developed by Hussain *et al*., (1991). The media was prepared from 5 separately prepared solutions in the following ratio: 7 (solution 1) : 1 (solution 2) : 0.5 (solution 3) : 0.1 (solution 4) : 1 (solution 5). Solution 1, 3 and 4 were merged before autoclaving, and then cooled. Solution 2 was filter sterilised using a 0.2 µm pore filter and added to cooled solutions 1, 3 and 4. Solution 5 was autoclaved separately and added to solutions 1-4 when cooled.

For CDM agar 1.5% (w/v) agar No. 1 (Oxoid) was added to solutions 1, 3 and 4 before autoclaving.

Divalent cations were removed from all glassware by acid washing overnight with 0.1M HCl and autoclaved prior to CDM preparation.

2.1.4.1 CDM Solution 1

Table 2.1 CDM solution 1 ingredients.

Chemical	Weight	Chemical	Weight
$Na_2HPO_4.2H_2O$	7 g	L-Lysine	0.1 g
KH_2PO_4	3 g	L-Leucine	0.15 g
L-Aspartic Acid	0.15 g	L-Methionine	0.1 g
L-Alanine	0.1 g	L-Phenylalanine	0.1 g
L-Arginine	0.1 g	L-Proline	0.15 g
L-Cysteine	0.05 g	L-Serine	0.1 g
Glycine	0.1 g	L-Threonine	0.15 g
L-Glutamic Acid	0.15 g	L-Tryptophan	0.1 g
L-Histidine	0.1 g	L-Tyrosine	0.1 g
L-Isoleucine	0.15 g	L-Valine	0.15 g

Dissolved in 700 ml of distilled water adjusted to pH 7.2

2.1.4.2 CDM Solution 2 (1000x)

Table 2.2 CDM solution 2 ingredients.

Chemical	Weight	Chemical	Weight
Biotin (fridge)	0.02 g	Pyridoxal	0.8 g
Nicotinic Acid	0.4 g	Pyridoxamine di-HCl	0.8 g
D-Pantothenic Acid	0.4 g	Riboflavin	0.4 g
Thiamine HCL	0.4 g		

Dissolved in 140 ml of distilled water. Opaque yellow colour when mixed that becomes clear yellow upon filtration

2.1.4.3 CDM Solution 3

Table 2.3 CDM solution 3 ingredients.

Chemical	Weight	Chemical	Weight
Adenine Sulphate	0.02 g	Guanine HCl	0.02 g

Dissolved in 50 ml of 0.1M HCl

2.1.4.4 CDM Solution 4

Table 2.4 CDM solution 4 ingredients.

Chemical	Weight	Chemical	Weight
$CaCl_2.H_2O$	0.01 g	$(NH_4)_2Fe(SO_4)_2.H_2O$	0.006 g

Dissolved in 10 ml of 0.1M HCl

2.1.4.5 CDM Solution 5

Table 2.5 CDM solution 5 ingredients.

Chemical	Weight	Chemical	Weight
Glucose	10 g	$MgSO_4.7H_2O$	0.5 g

Dissolved in 100 ml of distilled water

2.1.5 Luria-Bertani media (LB)

Tryptone (Oxoid)	10 g l^{-1}
Yeast extract (Oxoid)	5 g l^{-1}
NaCl	7 g l^{-1}

For LB agar 1.5% (w/v) agar No. 1 (Oxoid) was added.

2.1.6 LK media

Tryptone (Oxoid)	10 g l^{-1}
Yeast extract (Oxoid)	5 g l^{-1}
KCl	7 g l^{-1}

For LK top agar 1.5% (w/v) agar No. 1 (Oxoid) was added.
For LK bottom agar 0.7% (w/v) agar No. 1 (Oxoid) was added.

2.1.7 RPMI-1640 media

RPMI-1640 was purchased from Sigma-Aldrich and stored in 50 ml aliquots, at 4^{o}C. Before use, foetal calf serum (Sigma-Aldrich) was added to 10% (v/v).

2.1.8 Tryptic soy broth

Tryptic soya broth (Oxoid) 30 g l^{-1}

2.2 Antibiotics

Table 2.6 Antibiotics used in this study.

Antibiotic	Stock concentration (mg ml^{-1})	*S. aureus* working concentration (µg ml^{-1})	*E. coli* working concentration (µg ml^{-1})	Solvent
Ampicillin (Amp)	100	-	100	dH_2O
Chloramphenicol (Cat)	30	30	-	100% (v/v) ethanol
Erythromycin (Ery)	5	5	-	100% (v/v) ethanol
Kanamycin (Kan)	50	50	50	dH_2O
Lincomycin (Lin)	25	25	-	50% (v/v) ethanol
Neomycin (Neo)	50	50	-	dH_2O
Spectinomycin (Spec)	100	-	100	dH_2O
Tetracycline (Tet)	5	5	-	100% (v/v) ethanol
Trimethoprim (TMP)	50	1000-0.122	-	100% (v/v) DMSO

2.3 Bacterial strains, plasmids and bacteriophage

2.3.1 Maintenance, storage and culture of bacteria

Bacterial strains used in this study are given in Table 2.7 and 2.8.

2.3.2 *S. aureus* strains

S. aureus strains used in this study are given in Table 2.7. Strains were inoculated onto BHI agar, containing a selective antibiotic where required, from -80°C Microbank stock vials (Pro-lab Diagnostics). Plates were placed at 4°C for short-term storage. Microbank vials were used for long-term storage at -80°C. For standard growth, 1 colony was used to inoculate 5 ml of BHI in a 25 ml Universal tube, with or without antibiotic. Cultures

were then grown overnight at 37°C aerobically at 250 rpm on a rotary shaker. The overnight culture was then used to inoculate 50 ml of fresh pre-warmed media in a sterile 250 ml conical flask at an OD_{600} of 0.05-0.01. Strains were then grown to exponential or stationary phase at 37°C aerobically at 250 rpm on a rotary shaker.

Table 2.7 *S. aureus* strains used in this study. Ery^R, erythromycin resistance; Kan^R, kanamycin resistance; Lin^R, lincomycin resistance; Tet^R, tetracycline resistance.

Strain	Relevant genotype/markers	Source/reference
SH1000	Functional *rsbU*+ derivative of 8325-4	(Horsburgh *et al*., 2002)
RN4220	Restriction negative, modification positive strain	(Kreiswirth *et al*., 1983)
SJF4276	USA300 JE2. USA300 LAC strain cured of plasmids p01 and p03	(Fey *et al*., 2013)
NewHG	Functional *sae* derivative of Newman	(Mainiero *et al*., 2010)
Newman	Constitutively active *sae* strain	(Duthie & Lorenz, 1952)
SJF3661	Newman Δ*lukAB* (unmarked deletion)	Victor J. Torres (Dumont *et al*., 2011)
JC001	NewHG $ssl13^-$ $ssl14^-$ $ssl15^-$ Kan^R	This study
JC002	JC001, pJC001 inserted at lipase – $ssl13^+$ $ssl14^+$ $ssl15^+$ Kan^R Tet^R	This study
JC003	JC001, pKasbar inserted at lipase Kan^R Tet^R	This study
JC004	NewHG, pJC001 inserted at lipase Tet^R	This study
JC005	NewHG, pKasbar inserted at lipase Tet^R	This study
NE27-SH	(SH1000) *nos*::Tn *bursa aurealis* Ery^R Lin^R	This study
NE92-SH	(SH1000) *qoxA*::Tn *bursa aurealis* Ery^R Lin^R	This study
NE95-SH	(SH1000) *agrB*::Tn *bursa aurealis* Ery^R Lin^R	This study
NE229-SH	(SH1000) Hypothetical protein SAOUHSC_02152 disrupted by Tn *bursa aurealis* Ery^R Lin^R	This study
NE460-SH	(SH1000) *atl*::Tn *bursa aurealis* Ery^R Lin^R	This study
NE522-SH	(SH1000) *purB*::Tn *bursa aurealis* Ery^R Lin^R	This study
NE529-SH	(SH1000) *purA*::Tn *bursa aurealis* Ery^R Lin^R	This study
NE573-SH	(SH1000) *ribBA*::Tn *bursa aurealis* Ery^R Lin^R	This study
NE594-SH	(SH1000) *gltA*::Tn *bursa aurealis* Ery^R Lin^R	This study
NE635-SH	(SH1000) *ribE*::Tn *bursa aurealis* Ery^R Lin^R	This study
NE821-SH	(SH1000) *pabA*::Tn *bursa aurealis* Ery^R Lin^R	This study
NE873-SH	(SH1000) *agrC*::Tn *bursa aurealis* Ery^R Lin^R	This study

Table 2.7 continued

Strain	Relevant genotype/markers	Source/reference
NE896-SH	(SH1000) Hypothetical protein SAOUHSC_00938 disrupted by Tn *bursa aurealis* Ery^R Lin^R	This study
NE912-SH	(SH1000) *clpP*::Tn *bursa aurealis* Ery^R Lin^R	This study
NE1048-SH	(SH1000) *pyrP*::Tn *bursa aurealis* Ery^R Lin^R	This study
NE1253-SH	(SH1000) *murQ*::Tn *bursa aurealis* Ery^R Lin^R	This study
NE1267-SH	(SH1000) *pemK*::Tn *bursa aurealis* Ery^R Lin^R	This study
NE1296-SH	(SH1000) *saeS*::Tn *bursa aurealis* Ery^R Lin^R	This study
NE1299-SH	(SH1000) *yjbK*::Tn *bursa aurealis* Ery^R Lin^R	This study
NE1304-SH	(SH1000) *araC*::Tn *bursa aurealis* Ery^R Lin^R	This study
NE1315-SH	(SH1000) *mecA*::Tn *bursa aurealis* Ery^R Lin^R	This study
NE1354-SH	(SH1000) *hla*::Tn *bursa aurealis* Ery^R Lin^R	This study
NE1391-SH	(SH1000) *odhB*::Tn *bursa aurealis* Ery^R Lin^R	This study
NE1434-SH	(SH1000) *cyoE*::Tn *bursa aurealis* Ery^R Lin^R	This study
NE1509-SH	(SH1000) *bmrA*::Tn *bursa aurealis* Ery^R Lin^R	This study
NE1532-SH	(SH1000) *agrA*::Tn *bursa aurealis* Ery^R Lin^R	This study
NE1536-SH	(SH1000) *gcvH*::Tn *bursa aurealis* Ery^R Lin^R	This study
NE1604-SH	(SH1000) Unnamed ABC transporter SAOUHSC_02763 disrupted by Tn *bursa aurealis* Ery^R Lin^R	This study
NE1622-SH	(SH1000) *saeR*::Tn *bursa aurealis* Ery^R Lin^R	This study
NE1775-SH	(SH1000) *lipA*::Tn *bursa aurealis* Ery^R Lin^R	This study
NE1908-SH	(SH1000) *ybhF_2*::Tn *bursa aurealis* Ery^R Lin^R	This study
NE27-USA	(USA300) *nos*::Tn *bursa aurealis* Ery^R Lin^R	This study
NE92-USA	(USA300) *qoxA*::Tn *bursa aurealis* Ery^R Lin^R	This study
NE95-USA	(USA300) *agrB*::Tn *bursa aurealis* Ery^R Lin^R	This study
NE229-USA	(USA300) Hypothetical protein SAUSA300_1119 disrupted by Tn *bursa aurealis* Ery^R Lin^R	This study
NE460-USA	(USA300) *atl*::Tn *bursa aurealis* Ery^R Lin^R	This study
NE522-USA	(USA300) *purB*::Tn *bursa aurealis* Ery^R Lin^R	This study
NE529-USA	(USA300) *purA*::Tn *bursa aurealis* Ery^R Lin^R	This study
NE573-USA	(USA300) *ribBA*::Tn *bursa aurealis* Ery^R Lin^R	This study
NE594-USA	(USA300) *gltA*::Tn *bursa aurealis* Ery^R Lin^R	This study
NE635-USA	(USA300) *ribE*::Tn *bursa aurealis* Ery^R Lin^R	This study
NE821-USA	(USA300) *pabA*::Tn *bursa aurealis* Ery^R Lin^R	This study
NE873-USA	(USA300) *agrC*::Tn *bursa aurealis* Ery^R Lin^R	This study
NE896-USA	(USA300) Hypothetical protein SAUSA300_0903 disrupted by Tn *bursa aurealis* Ery^R Lin^R	This study

Table 2.7 continued

Strain	Relevant genotype/markers	Source/reference
NE912-USA	(USA300) *clpP*::Tn *bursa aurealis* Ery^R Lin^R	This study
NE1048-USA	(USA300) *pyrP*::Tn *bursa aurealis* Ery^R Lin^R	This study
NE1253-USA	(USA300) *murQ*::Tn *bursa aurealis* Ery^R Lin^R	This study
NE1267-USA	(USA300) *pemK*::Tn *bursa aurealis* Ery^R Lin^R	This study
NE1296-USA	(USA300) *saeS*::Tn *bursa aurealis* Ery^R Lin^R	This study
NE1299-USA	(USA300) *yjbK*::Tn *bursa aurealis* Ery^R Lin^R	This study
NE1304-USA	(USA300) *araC*::Tn *bursa aurealis* Ery^R Lin^R	This study
NE1315-USA	(USA300) *mecA*::Tn *bursa aurealis* Ery^R Lin^R	This study
NE1354-USA	(USA300) *hla*::Tn *bursa aurealis* Ery^R Lin^R	This study
NE1391-USA	(USA300) *odhB*::Tn *bursa aurealis* Ery^R Lin^R	This study
NE1434-USA	(USA300) *cyoE*::Tn *bursa aurealis* Ery^R Lin^R	This study
NE1509-USA	(USA300) *bmrA*::Tn *bursa aurealis* Ery^R Lin^R	This study
NE1532-USA	(USA300) *agrA*::Tn *bursa aurealis* Ery^R Lin^R	This study
NE1536-USA	(USA300) *gcvH*::Tn *bursa aurealis* Ery^R Lin^R	This study
NE1604-USA	(USA300) Unnamed ABC transporter SAUSA300_2407 disrupted by Tn *bursa aurealis* Ery^R Lin^R	This study
NE1622-USA	(USA300) *saeR*::Tn *bursa aurealis* Ery^R Lin^R	This study
NE1775-USA	(USA300) *lipA*::Tn *bursa aurealis* Ery^R Lin^R	This study
NE1908-USA	(USA300) *ybhF_2*::Tn *bursa aurealis* Ery^R Lin^R	This study
JC006	JE2-*pabA*, pJC002 inserted at lipase – $pabA^+$ Ery^R Lin^R Tet^R	This study
JC007	JE2-*pabA*, pKasbar inserted at lipase Ery^R Lin^R Tet^R	This study
JC008	JE2, pJC002 inserted at lipase – $pabA^+$ Ery^R Lin^R Tet^R	This study
JC009	JE2, pKasbar inserted at lipase Ery^R Lin^R Tet^R	This study
JC010	SH-*pabA*, pJC002 inserted at lipase – $pabA^+$ Ery^R Lin^R Tet^R	This study
JC011	SH-*pabA*, pKasbar inserted at lipase Ery^R Lin^R Tet^R	This study
JC012	SH1000, pJC002 inserted at lipase – $pabA^+$ Ery^R Lin^R Tet^R	This study
JC013	SH1000, pKasbar inserted at lipase Ery^R Lin^R Tet^R	This study

2.3.3 *E. coli* strains

The standard growth and storage conditions of *E. coli* strains was that of *S. aureus* (section 2.3.2), but LB media was used alternatively to BHI. All *E. coli* strains from this study are listed in Table 2.8.

Table 2.8 *E. coli* strains used in this study.

Strain	Relevant genotype/Markers	Source
TOP10	F- *mcr Δ* (*mrr-hsdRMS-mcrBC*) Φ 80 *lacZ ΔM15 ΔlacX74 recA1 deoR araD139 Δ*(*ara-leu*) *7697 galK rpsL* (Str^R) *endA1 nupG*	Invitrogen
BL21 (DE3)	F^- *ompT hsdS*B (r_B^- m_B^-) *gal dcm lacY1* (DE3)	Novagen

2.3.4 Plasmids

Plasmids used in this study were purified using QIAGEN kits (section 2.11.4) and stored at -20°C in elution buffer or nuclease free sdH_2O.

Table 2.9 Plasmids used in this study.

Plasmid	Relevant genotype/Markers	Source
pET-21d	His6-tag overexpression vector; Amp^R	Novagen
pKASBAR	Hybrid vector of pCL84 and pUC18 for integration into *S. aureus* lipase gene (*geh*), *attP*; Tet^R (*S. aureus*), $Spec^R$ (*E. coli*)	K. Wacnik and B. Salamaga, unpublished
pGM073	pKASBAR derivative with improved MCS containing *ezrA-psmOrange; attP*, Tet^R (*S. aureus*), Amp^R (*E. coli*)	G. McVicker, unpublished
pGL485	Cat^R derivative of *E. coli-S. aureus* shuttle vector pMJ8426, containing *E. coli lacI* gene under the control of a constitutive promoter; $Spec^R$ (*E. coli*), Cat^R (*S. aureus*) , Kan^R	J. Garcia-Lara, unpublished
pOB1	*Streptococcus faecalis* derived shuttle vector; Amp^R (*E. coli*), Ery^R (*S. aureus*)	(Oliver *et al*., 1977)
pOB_UF_Kan_DF	*ssl12*, *ssl13*, *ssl14* deletion construct derived from pOB1; Amp^R, Ery^R, Kan^R	This study
pJC001	pGM073 containing *ssl12*, *ssl13* and *ssl14* and upstream control elements; Tet^R	This study
pJC002	pGM073 containing the *pab* operon, *pabA*, *pabB* and *pabC* and upstream control elements; Tet^R	This study
pSSL12	pET21d containing *ssl12* gene, Amp^R	This study
pSSL13	pET21d containing *ssl13* gene, Amp^R	This study
pSSL14	pET21d containing *ssl14* gene, Amp^R	This study

2.3.5 Bacteriophage

The bacteriophage Φ11 was used in this study for the transduction of genetic material between strains (Mani *et al*., 1993). Φ11 is a 45kb, temperate-transducing phage of serological group B, requiring Ca^{2+} to establish infection (Novick, 1991).

2.4 Enzymes and chemicals

The chemicals used in this study were analytical grade, purchased from Fisher Scientific, Roche or Sigma-Aldrich. Restriction enzymes, T4 DNA ligase, dNTPs and their corresponding buffers were all purchased from New England Biolabs or Promega and stored at -20°C. Storage and concentration of stock solutions is given in Table 2.10

Table 2.10 Maintenance of stock chemicals used in this study.

Stock solution	Storage temperature	Concentration	Solvent
Lysostaphin	-20°C	5 mg ml^{-1}	20 mM sodium acetate
Lysozyme	-20°C	10 mg ml^{-1}	dH_2O
Isopropyl β-D-1-thiogalactopyranoside (IPTG)	-20°C	1M	dH_2O

2.5 Buffers and stock solutions

All buffers and stocks solutions used in this work were prepared with dH_2O and autoclaved if required, then stored at room temperature or 4°C, unless stated otherwise. Methods for the preparation of buffers and stock solutions can be found in Sambrook & Russell, (2001), unless otherwise stated.

2.5.1 Amino acid stock solutions

Stock solutions of the amino acids glycine, methionine and serine, at 100x the working concentration of CDM (Table 2.1) were prepared and autoclaved.

Glycine 14.29 g l^{-1}

L-Methionine 14.29 g l^{-1}

L-Serine 14.29 g l^{-1}

Stock solutions were used to supplement CDM media minus the above amino acids, as required.

2.5.2 DNA loading buffer (6x)

Bromophenol blue	0.25% (w/v)
Xylene cyanol FF	0.25% (w/v)
Glycerol	30% (v/v)

2.5.3 Phosphate buffered saline (PBS)

NaCl	8 g l^{-1}
Na_2HPO_4	1.4 g l^{-1}
KCl	0.2 g l^{-1}
KH_2PO_4	0.2 g l^{-1}

The pH was adjusted to 7.4 using NaOH.

2.5.4 TAE (50x)

Trisma base	242 g l^{-1}
Glacial acetic acid	0.57 % (v/v)
Na_2EDTA pH 8.0	0.05M

The buffer was diluted 1:50 with dH_2O before use.

2.5.5 Recombinant protein refolding buffers

2.5.5.1 L-Arginine base refolding buffer (880 mM)

L-Arginine 1M	300 ml
Tris-HCl pH 7.5 1M	18.76 ml
NaCl 5M	1.43 ml
KCl 1M	300 µl
dH_2O	19.51 ml

Volumes of each component were adjusted depending on volume of buffer required.

2.5.5.2 50 mM L-Arginine, L-Glutamic acid base refolding buffer (50 mM)

L-Arginine 112 mM	150 ml
L-Glutamic acid 112 mM	150 ml
Tris-HCl pH 7.5 1M	18.76 ml
NaCl 5M	1.43 ml
KCl 1M	300 µl
dH_2O	19.51 ml

Volumes of each component were adjusted depending on volume of buffer required.

2.5.6 E3 solution (10x)

NaCl	50 mM
KCl	1.7 mM
$CaCl_2$	3.3 mM
$MgSO_4$	3.3 mM

Methylene blue was added to a final concentration of 0.00005% (w/v) to prevent fungal growth (Nusslein-Volhard & Dahm, 2002). The 10x solution was diluted to 1x using sdH_2O.

2.5.7 Methylcellulose

E3 solution minus methylene blue was used to dissolve methylcellulose to a concentration of 3% (w/v). Repeated freezing and thawing was done to aid methylcellulose solubility. Aliquots of 10 ml in sterile syringes were sored long-term at -20^{o}C. For use and short-term storage, methylcellulose syringes were kept at 28.5^{o}C.

2.5.8 HiTrap™ column buffers

2.5.8.1 START buffer

$NaPO_4$	0.1M
NaCl	0.5M
sdH_2O	to 1 l

8M urea or 6M guanidine was added for insoluble protein purification.

2.5.8.2 Elution buffer

START buffer containing:

Imidazole	0.5M

2.5.9 Phage buffer

$MgSO_4$	1 mM
$CaCl_2$	4 mM
Tris-HCl pH 7.8	50 mM
NaCl	0.6% (w/v)
Gelatin	0.1% (w/v)

2.5.10 QIAGEN buffers

2.5.10.1 QIAGEN Buffer P1

Tris-HCl pH 8	50 mM
EDTA	10 mM
RNase A	100 µg ml^{-1}

2.5.10.2 QIAGEN Buffer P2

NaOH	200 mM
SDS	1 % (w/v)

2.5.10.3 QIAGEN Buffer P3

Potassium acetate pH 5.5	3.0M

2.5.10.4 QIAGEN Buffer EB

Tris-HCl pH 8.5	10 mM

2.5.10.5 QIAGEN Buffer N3, QG, PB and PE

Supplied with the QIAquick kit; details of solution contents not provided.

2.5.11 SDS-PAGE solutions

2.5.11.1 SDS-PAGE reservoir buffer (10x)

Glycine	144 g l^{-1}
Tris base	30.3 g l^{-1}
SDS	10 g l^{-1}

The buffer was diluted to 1:10 with dH_2O before use.

2.5.11.2 SDS-PAGE loading buffer (2x)

Tris-HCl pH 6.8	0.62M
SDS	10 % (w/v)
Glycerol	20 % (v/v)
Bromophenol blue	0.1 % (w/v)

Fresh 10 % (v/v) β-mercaptoethanol was added to the buffer prior to use.

2.5.11.3 Coomassie Blue staining solution

Coomassie blue	0.1 % (w/v)
Methanol	5 % (v/v)

Glacial acetic acid	10 % (v/v)

2.5.11.4 Destain solution

Methanol	5 % (v/v)
Glacial acetic acid	10 % (v/v)

2.5.12 Southern blotting buffers and solutions

2.5.12.1 Depurination solution

HCl	250 mM

2.5.12.2 Denaturing buffer

NaOH	0.5M
NaCl	1.5M

2.5.12.3 Neutralising buffer

Tris-HCl (pH 7.5)	0.5M
NaCl	3M

2.5.12.4 SSC (20x)

NaCl	3M
Tri-sodium citrate·$2H_2O$	300 mM

1M NaOH was used to adjust to pH 7. All other SSC concentrations were prepared from 20x, by dilution with sdH_2O.

2.5.12.5 Pre-hybridisation solution

SSC	5×
Blocking reagent (Roche)	1% (w/v)

N-lauroylsarcosine, Na salt	0.1% (w/v)
SDS	0.02% (w/v)

2.5.12.6 Hybridisation solution

Digoxigenin-labelled probes were added to pre-hybridisation solution (section 2.5.12.5) to 5-25 ng ml^{-1}.

2.5.12.7 Wash solution (2x)

SSC	2×
SDS	0.1% (w/v)

2.5.12.8 Wash solution (0.5x)

SSC	0.5×
SDS	0.1% (w/v)

2.5.12.9 Maleic acid buffer

Maleic acid	0.1M
NaCl	0.15M

The pH was adjusted to 7.5 with solid NaOH.

2.5.12.10 Washing buffer

Maleic acid buffer containing 3% (v/v) Tween 20.

2.5.12.11 Blocking solution

Maleic acid buffer containing 1% (w/v) blocking reagent (Roche), dissolved by heating and stored at -20^{o}C.

2.5.12.12 Antibody solution

Blocking solution containing 0.2 µl ml^{-1} Anti-digoxigenin-AP conjugate (Roche).

2.5.12.13 Detection buffer

Tris-HCl (pH 9.5)	100 mM
NaCl	100 mM
$MgCl_2 \cdot 6H_2O$	50 mM

The pH was adjusted to 7.5 using 1M NaOH.

2.5.12.14 TE buffer

Tris-HCl	1 mM
EDTA	0.1 mM

The pH was adjusted to 7.5 using 1M HCl before autoclaving.

2.6 Determining bacterial cell density

2.6.1 Spectrophotometric measurement (OD_{600})

Spectrophotometric measurements at 600 nm (OD_{600}) were used to quantify bacterial yield. A Jenway 6100 spectrophotometer or a Biochrom WPA Biowave DNA spectrophotometer were used to measure OD_{600}. Samples were diluted 1:10 with fresh media when necessary to reduce concentration to a measurable level.

2.6.2 Direct cell counts (CFU)

The bacterial CFU was determined using the method devised by Miles *et al*., (1938). Samples were serially diluted 1:10 and 10 µl drops from each dilution applied to the surface of well dried agar plates. Plates were incubated overnight at 37°C and the dilution producing visible colonies was used to determine CFU.

2.7 Centrifugation

The following centrifuges were used for harvesting cells or precipitated material:

i. Eppendorf microfuge 5415D; max volume of 2 ml, max speed of 13,200 rpm (10,000 x g).

ii. Sigma centrifuge 4K15C; max volume of 50 ml, max speed of 5,100 rpm (5525 x g).

iii. Jouan centrifuge JAC50.10; max volume of 50 ml, max speed of 13,000 rpm (10,000 x g).

iv. Avanti™ J25I (Beckman); max volumes and speeds depend on the rotor.
JA-20; max volume of 50 ml, max speed of 20,000 rpm (48,384 x g).
JA-10.5; max volume of 500 ml, max speed of 10,000 rpm (18,480 x g).

v. Falcon 6/300R (Sanyo); max volume of 750 ml, max speed 5,600 rpm (7,047 x g).

2.8 Growth curves

Strains were streaked from Microbank vials onto BHI plates containing suitable antibiotics (section 2.3.1). A single colony was used to inoculate 5 ml BHI (no antibiotics) in a sterile 25 ml Universal tube, which was incubated overnight at 37°C, aerated by shaking at 250 rpm on a rotary shaker. The overnight culture was used to inoculate 50 ml of pre-warmed BHI (no antibiotics), from the same batch as the overnight culture, to an OD_{600} of 0.01. For non-CDM growth experiments triplicate cultures were grown at 37°C in a Grant OLS 200 water-bath with shaking equivalent to 250 rpm. Growth was monitored by OD_{600} (section 2.6.1) or direct cell counts (section 2.6.2) until stationary phase. For CDM experiments triplicate cultures were grown at 37°C on a rotary shaker at 250rpm. Growth was monitored by OD_{600} (section 2.6.1) over 24-48 h.

2.9 Transformation techniques

2.9.1 Transformation of *E. coli*

2.9.1.1 Preparation of *E. coli* electrocompetent cells

E. coli Top10 or *E. coli* BL21 was streaked onto LB agar and incubated at 37°C overnight. A single colony was used to inoculate 5 ml of LB in a 25 ml sterile Universal, which was incubated at 37°C, aerated on a rotary shaker at 250 rpm. 400 ml of pre-warmed LB was inoculated using the pre-culture to an OD_{600} of 0.05, and incubated at 37°C, aerated on a rotary shaker at 250 rpm until an OD_{600} of 0.5-0.7 was reached. The culture was gently rotated by hand in ice-slurry for 15 min to cool, at which point the cells were harvested by centrifugation in 4x100 ml aliquots at 5,100 rpm, at 4°C for 10 min. Cells were washed 3 times with 25 ml of ice-cold sdH_2O, then merged into one tube. After centrifugation at 5,100 rpm, at 4°C for 10 min the pellet was resuspended in 10% (v/v) ice-cold glycerol. Cells were divided into 50 µl aliquots, snap frozen in liquid nitrogen and stored at -80°C.

2.9.1.2 Transformation of *E. coli* electrocompetent cells

50 µl aliquots of electrocompetent *E. coli* were thawed on ice and 5 µl (approximately 1ng) of plasmid DNA was added. The sample was transferred to a 1 mm pre-chilled (Bio-Rad) electroporation cuvette. A Gene Pulser system set at 200 Ω, 1.75 kV and 25 µF was then used to electroporate the cells. 400 µl of room-temperature LB was immediately added to the cuvettes to recover the bacteria and transferred to 37°C for 60 min. 100 µl of cells were then spread on LB agar plates containing the selective antibiotic and incubated at 37°C for 24 h.

2.9.2 Transformation of *S. aureus*

2.9.2.1 Preparation of *S. aureus* electrocompetent cells

S. aureus RN4220 was streaked onto BHI agar and incubated overnight at 37°C. A single colony was used to inoculate 400 ml of BHI, which was grown for 10-12 h at 37°C, aerated on a rotary shaker at 250 rpm. The culture was then used to inoculate 400 ml of pre-warmed BHI to an OD_{600} of 0.1. This culture was grown for 60-90 min at

37°C, shaking at 250 rpm to give and OD_{600} of 0.4-0.6. Cells were harvested by centrifugation of 5,100 rpm at room temperature for 10 min in 4x100 ml aliquots. Cells were washed 3 times with 25 ml sdH_2O, then merged into one tube. The pellet was resuspended in 20 ml 10% (v/v) glycerol and centrifuged for 10 min at 5,100 rpm. The pellet was resuspended in 10 ml 10% (v/v) glycerol and incubated at room temperature for 30 min. Centrifugation at 5,100 rpm at room temperature for 10 min was again used to harvest the cells. Cells were then resuspended in 500 µl 10% (v/v) glycerol. Cells were split into 50 µl aliquots and used immediately for transformation.

2.9.2.2 Transformation of *S. aureus* by electroporation

To each 50 µl aliquot of *S. aureus* RN4220 prepared in section 2.9.2.1, approximately 1 µg of plasmid DNA was added. The sample was transferred to a 1 mm (Bio-Rad) electroporation cuvette. A Gene Pulser system set at 100 Ω, 2.3 kV and 25 µF was then used to electroporate the cells. Cells were recovered by immediate addition of 1 ml BHI and incubation at 37oC for 3 h, at 250 rpm on a rotary shaker. Cells were spread on BHI agar plates, with selective antibiotic, in 200 µl aliquots and incubated for 48 h at 37°C.

2.10 Phage techniques

2.10.1 Preparation of phage lysates

A single colony of donor strain was used to inoculate 5 ml of BHI containing appropriate antibiotics and grown overnight at 37°C. Using the overnight culture, 5 ml of BHI was inoculated to a starting OD_{600} of 0.2 in a sterile 25 ml Universal tube. 5 ml of phage buffer and 100 µl of stock phage lysate (Φ11) were added and the mixture incubated stationary at 25°C for 4-6 h. Once cleared, the lysate was filter sterilised through a 0.2 µm pore syringe filter and stored at 4°C. This method allowed for the production of lysates with titres of approximately 10^{10} plaque forming units (PFU) per ml.

2.10.2 Determination of phage titres

A single colony of *S. aureus* SH1000 was used to inoculate 5 ml of BHI, which was grown to an OD_{600} of 0.5-0.7 at 37°C, shaking at 250 rpm. Phage lysate was serially diluted in phage buffer, by addition of 100 µl aliquots to 900 µl aliquots of phage buffer

and 100 µl of each dilution added to 400 µl of *S. aureus* SH1000 culture with 50 µl of 1M $CaCl_2$. The samples were then incubated stationary at room temperature for 10 min, and then 5 ml of LK top agar was added to each sample. The mixtures were then poured over LK bottom agar plates, overlaying the bottom agar, and were incubated for 48 h are 37°C. Plaques were then counted and multiplied by the dilution factor; a range of $10^7 – 10^{10}$ confirmed a successful lysate.

2.10.3 Phage transduction

The recipient strain was grown overnight in 50 ml of LK and the cells were harvested by centrifugation at 5,100 rpm for 10 min. The pellet was resuspended in 1 ml of LK and 500 µl of cells was added to 500 µl of phage lysate and 1 ml of LK containing 10 mM $CaCl_2$ in a 25 ml Universal tube. A second Universal tube containing 500 µl of cells, 1 ml of LK containing 10 mM $CaCl_2$, but no phage, was used as a control. The samples were incubated stationary for 25 min at 37°C, then for a further 15 min at 37°C shaking at 250 rpm. Immediately after incubation, 1 ml of ice-cold 0.02M sodium citrate was added and the mixtures were placed on ice for 5 min. Cells were harvested by centrifugation at 5,100 rpm, at 4°C for 10 min. The pellet was resuspended in ice-cold 0.02M sodium citrate and incubated on ice for 45 min. 100 µl and 200 µl aliquots were spread onto LK agar plates containing 0.05% (w/v) sodium citrate, plus selective antibiotic. Once dry, the plates were incubated at 37°C for 24-72 h. Colonies that formed were patched onto BHI agar containing the appropriate antibiotic, to determine that colonies had the correct resistance profile.

2.11 DNA purification techniques

2.11.1 Gel extraction (Qiaquick)

DNA was separated on a 1% (w/v) TAE agarose gel, stained with ethidium bromide. A sterile scalpel blade was used to excise the required band, visualised on a UV transilluminator. Purification of DNA from the agarose gel slice was carried out using the QIAGEN QIAquick gel extraction kit. After weighing the gel slice, 3x gel slice volume of buffer QG were added. The gel slice was incubated at 60°C for 10-15 min with frequent gentle mixing, until the gel was completely dissolved. If the dissolved gel solution had an orange colour, the pH was above 7.5. 10 µl of 3M sodium acetate pH 5

was added to lower the pH below 7.5 to allow binding to the silica membrane. After addition of 1 gel volume of isopropanol, the sample was applied to the QIAquick spin column and centrifuged at 13,000 rpm for 1 min, allowing binding of the DNA to the membrane and loss of dissolved gel. The column was washed by passing 500 µl of buffer QG through the column, by centrifugation at 13,000 rpm for 1 min. The column was washed again with 750 µl of buffer PE, passed through the column by centrifugation at 13,000 rpm for 1min. Residual ethanol was removed from the column by a further centrifugation step at 13,000 rpm for 1 min. The column was placed in a microcentrifuge tube and 50 µl of buffer EB was pipetted directly onto the centre of the column. After incubation for 1 min, the DNA was eluted by centrifugation at 13,000 rpm for 1min. The sample was stored at -20^{o}C.

2.11.2 PCR purification (Qiaquick)

DNA fragments from PCR and enzymatic reactions were purified with the QIAGEN QIAquick PCR purification kit. DNA samples were diluted 5x with buffer PB. The sample was then placed into a QIAquick spin column and centrifuged at 13,000 rpm for 1 min. The flow through was discarded and the sample washed in 750 µl of buffer PE, centrifuged again at 13,000 rpm for 1 min and the column transferred to a microcentrifuge tube. The DNA was eluted by addition of 50 µl buffer EB, followed by centrifugation at 13,000 rpm. The sample was stored at -20^{o}C.

2.11.3 Genomic DNA preparation

The QIAGEN DNeasy^{TM} blood and tissue kit was used to purify *S. aureus* genomic DNA. 1 ml of overnight culture was centrifuged for 10 min at 13,000 rpm. The pellet was washed with 1 ml sdH_2O and centrifuged at 13,000 rpm for 10 min. The cells were then resuspended in 180 µl of sdH_2O and 10 µg ml^{-1} lysostaphin was added and samples were incubated for 1 h at 37^{o}C. The DNA could then be purified using the manufacturer's instructions supplied with the DNeasy blood and tissue kit. Samples were stored at -20^{o}C.

2.11.4 Plasmid preparation

The QIAGEN QIAprep™ Spin column kit was used for purification of plasmids from *E. coli*. 3 ml of overnight culture of *E. coli* was centrifuged at 10,000 rpm for 1 min, to harvest the cells. The pellet was resuspended in 250 µl buffer P1 containing RNase A. Addition of buffer P2 to lyse the cells was followed by inverting the tube 4-6 times to ensure complete lysis. Within 5 min of starting the lysis reaction, 350 µl of neutralising buffer N3 was added and the tube was again inverted 4-6 times. The mixture was centrifuged at 13,000 rpm for 10 min to remove cellular debris, chromosomal DNA, precipitated protein and SDS. The supernatant was transferred to a QIAprep spin column and centrifuged for 1 min at 13,000 rpm. After discarding the flow-through, the column was washed with 750 µl buffer PE and centrifuged at 13,000 rpm for 1 min. To remove any remaining ethanol from the column, the column was centrifuged again at 13,000 rpm for 1 min. The column was placed into a microcentrifuge tube and the plasmid DNA was eluted by pipetting 50 µl of EB buffer onto the centre of the column, and after 1 min incubation at room temperature, centrifuging the column for 1 min at 13,000 rpm. The samples were stored at -20^{o}C.

2.11.5 Ethanol precipitation of DNA

To enhance precipitation and aid in visualisation of the DNA pellet, 1 µl of glycogen (Roche) was added to DNA samples. 3M sodium acetate pH 5.2 was added to the purified DNA sample and 3x the sample volume of ice-cold ethanol was also added. The samples were then incubated at -20^{o}C overnight to allow precipitation. Precipitated DNA was recovered by centrifugation for 15 min at 13,000 rpm at 4^{o}C and the pellet was washed twice, without resuspension in 70% (v/v) ethanol. After air drying to remove any residual ethanol, the pellet was resuspended in buffer EB.

2.12 *In vitro* DNA manipulation techniques

2.12.1 Polymerase chain reaction (PCR) techniques

2.12.1.1 Primer design

The primers designed for this study are given in Table 2.11. They are short

oligonucleotides (20-43 nucleotides) and their design was based on the genomes of *S. aureus* strains 8325-4, USA300 FPR3757 and Newman and the plasmid pGM073. Restriction enzyme sites were included at the 5' end when required for cloning. Efficient digestion at restriction sites was permitted by addition of 6 bases (A or T) at the 5' end of the cut site. Primers were designed using the NCBI Primer-BLAST tool (http://www.ncbi.nlm.nih.gov/tools/primer-blast/). This tool allows the user to set the melting temperature of the primer to within a certain range. The tool also predicts non-specific binding of the primers to sites outside the target site of the *S. aureus* genome and to sites within other available genomes, including *Homo sapiens*. The primers were manufactured by Eurofins MWG operon (http://www.eurofinsdna.com) and stored at −20°C in sdH_2O as 100 μM stock solutions or as 10 μM working solutions.

Table 2.11 Primers used in this study.

Primer	Sequence (5'-3')	Application
01124-F	ATAATACCATGGCTATGTTATTACTATTA GGTACTGTATTACCTCAAAATC	Amplification of each individual *ssl* for insertion into the pET21d overexpression plasmid Also used to sequence the inserts
01124-R	ATAATACTCGAGATCAAAGAGGACGTCA ACAGTTATTT	
01125-F	ATAATACCATGGCTATGTTGTTACTATTA GGTACAGCATCTACACAA	
01125-R	ATAATACTCGAGGTTTGATTTTTCGAGGA TAACTTCAA	
01127-F	ATAATACCATGGCTATGTTGTTACTTTTA GAAACTACATCAACACAA	
01127-R	ATAATACTCGAGGTTAGATTTTTCGAGTA TGACTTCAATTT	
FU	CGGGCGGTACCATTTGTTGACCTATTTTC GTATCAGC	Construction of the *ssl* deletion construct
RU	CGGCCGTCGACAAATCTCCTTTGCGTGAA TTACC	
FD	CGGCGGTCGACTGACTTATACTTCATGCA CTTTAATTCC	
RD	CGGGCGCATGCATGATGAGTGATTATTTT AAGAATATGTTTT	
KanF	GGCGGGTCGACCAGCGAACCATTTGAGG	
KanR	GGGGCGTCGACAATTCCTCGTAGGCGCTC GG	
isdA-F	GATTATGAAATATCTATGACATAGG	Amplify *isdA*, used as a control to confirm *S. aureus* DNA.
isdA-R	GTTATACGAAAATAGATGTGCTAG	
tripF	ATAATAGGGCCCGCACATCGCGTTCTTGT AGA	Amplify the *ssl* triplet for

Table 2.11 continued

Primer	Sequence (5'-3')	Application
tripR	ATAATACCTCAGCTTGGGGAGTGACAACGAAAT	**(cont.)** complementation
Tset1F	GCACATCGCGTTCTTGTAGA	Sequencing primers for the *ssl* triplet
Tset1R	TGCGGCTGAGTGTAATATTTGAT	
Tset2F	TCAAATATTACACTCAGCCGCA	
Tset2R	GGAAATTGTGTAGATGCTGTACCT	
Tset3F	AGGTACAGCATCTACACAATTTCC	
Tset3R	TCAGAGGAATCATGATACGAGGA	
Tset4F	CGCAAATACTATATTGACTTCGCTC	
Tset4R	CTTGGGGAGTGACAACGAAAT	
pGM-F	CGAGTCAGTGAGCGAGGAAG	Amplify the pGM073 plasmid from either side of the insertion site. Confirms successful integration of plasmid backbone or construct
pGM-R	GTATCTGCCCTTTTTCTGCCC	
pab-F	ATAATAGGGCCCATTGTACTGTCTTGACCACCACT	Cloning primers for the *pab* operon
pab-R	ATAATACTCGAGATACGTATACAAGAATTAACAACAGCA	
pab1-F	CCACCACTAAAGACAACGATGG	Sequencing primers for the *pab* operon
pab1-R	TGCACACCAAAAACCGGAAA	
pab2-F	TGACGGAGCGACTTTTCCAA	
pab2-R	GCCACTCTGTGATATTCTCCCT	
pab3-F	CCGATGAAAGGGACAATGCC	
pab3-R	CCTTGCCGTCCTCTGAAGTT	
pab4-F	ACGACAGAACGAAAGCATTTAGC	
pab4-R	ACGTATACAAGAATTAACAACAGCA	
NE27F	TCATTCCAATAACTTTCAGCCA	Each of the primers in this section was used to determine the presence of the Tn *bursa aurealis*, inserted in a specific gene in the strain corresponding to
NE27R	AAGTGATTTGCTAAGCGTGT	
NE92F	CTTCTTTCACCCATTTGTCGT	
NE92R	TTGCTTCTATTATTTGGCACACT	
NE95F	CCATCACATCTCTGTGATCTAGT	
NE95R	TGG GCA AAT GGC TCT TTG AT	
NE213F	GGCCGAAAAAGATTGGTGGC	
NE213R	CGTCCTGGATAGCCTTCAGC	

Table 2.11 continued

Primer	Sequence (5'-3')	Application
NE229F	CCGATATGATTATACAAGGGGCA	**(cont.)** the NE number given in the primer name.
NE229R	TCTTTCCAAAACGAACCATCA	
NE460F	TGTTGTAAACCACATCGCCT	
NE460R	ACATGCATTTGTTGATGGGG	
NE522F	ATGTTTGCGTTGATACAGGC	
NE522R	TCGAGTATACATACGATAGGAGT	
NE529F	TGCATTATGGTCTCGATATTGGT	
NE529R	TTGCGCACCTTCGAAAAGTA	
NE573F	TGTTCCGAAATCTGTAGGCA	
NE573R	AGTACATTTAGAAACAGACGTTTTG	
NE594F	CCTTTCAGAGAACCTACGGC	
NE594R	TCATAAAGAAACAGTAAAGGGGA	
NE635F	TCCACAGTAATAGACCCTTGC	
NE635R	GGAACTTTGCTAGTTGAGGC	
NE821F	ATGGCATTGATAAGCCCGTT	
NE821R	TGCTGTAATCTTTAAGCAATTTGG	
NE873F	AGAGCCATTTGCCCAATTCA	
NE873R	AAGTAAGCAGTAAGATAGTCGAAA	
NE896F	AAAACGAGAGAAGGGGCTTG	
NE896R	CGG ACA TCC TAT GCT AAG AAA	
NE912F	CGACATTGCGGGATTCTCTG	
NE912R	CCTTGAGCACCACCTAATGG	
NE1048F	ACTTGTCACACTTTTTGTCTCT	
NE1048R	GCATCAAATTTCACAATCCCCA	
NE1253F	ACGCTTAGTGCACATGACAA	
NE1253R	AACTTTTCCGACACCAACCA	
NE1267F	AGCTTTTTATCTTCTGTGCTAAGT	
NE1267R	AGTTAGATTGCTTTTAGCATTAGGA	
NE1296F	CTCATGATCCTTAGTGATTATACCA	
NE1296R	TGTAAATGGTCACGAAGTCCC	
NE1299F	TCGAACTCTAACTCATAATCCGT	
NE1299R	ACGAGCATTTGTCCTACTTCA	
NE1304F	TCCAAATTTTGCTTACTATCTTTCT	
NE1304R	CACAGTCTATGAACACCGGA	
NE1315F	AAGTGCTTTAATGCTTTAACTGT	
NE1315R	TGACTTCTTGATCAACATGACTAT	
NE1354F	CGAAGTCTGGTGAAAACCCT	

Table 2.11 continued

Primer	Sequence (5'-3')	Application
NE1354R	TGAATCCTGTCGCTAATGCC	
NE1391F	TTCGTAATCATGTCGTCGCC	
NE1391R	ACG TAG GGG ATA GCG TAG AA	
NE1434F	CTTAATTCCGGCTTTTGCGG	
NE1434R	TGTGTTGCCCATTTTGTTTGA	
NE1509F	ACGCTCAGTTTTATGGGAGC	
NE1509R	TGTTCAAATGACAATACACCGTC	
NE1532F	TCATTTGCGAAGACGATCCA	
NE1532R	CCGATGCATAGCAGTGTTCT	
NE1536F	AGTTGAATAGCATCTAGCCTTATG	
NE1536R	CGGTTATATGCTTTTTGCTCCTT	
NE1604F	ACGTGGCAGCTTGAATATCAT	
NE1604R	ACAAGGGACACGTGAATCAG	
NE1622F	CCCCATACAGTTGTGATGGTAT	
NE1622R	GTCACTCATTGTTAAAACAGATTTC	
NE1775F	ATGCCTAATTGGGAACCTGG	
NE1775R	AACTTGCCAGATACCTCTGC	
NE1908F	CGGGTTATCCATCGAATTTGC	
NE1908R	GGTGTTGGTAAAACAACCGT	

2.12.1.2 PCR amplification

2.12.1.2.1 *Taq* polymerase

Taq polymerase (Promega) was used for standard PCR amplification when product accuracy was not required. The following components were added to 0.5 ml thin-walled PCR tubes

Template DNA	100 - 500 ng
Forward primer	300 nM*
Reverse primer	300 nM*
10x *Taq* PCR buffer (Promega)	10 µl
$MgC1_2$	1.5 - 4.5 mM*
dNTPs	0.2 mM*
Taq DNA polymerase	0.5 µl (2.5 Units)
dH_2O	to 100 µl

*final concentration

Amplifications were carried out using a TC-3000 (Techne) PCR machine. The lid was preheated to 105°C for 4 min, and the following thermal cycling program was used:

1 cycle Initial denaturation	95°C 5 min
30 cycles Denaturation	95°C 30 s
Annealing	56-60°C 30 s – 1 min
Extension	72°C 1 min kb^{-1} + 10%
1 cycle Final extension	72°C 5 min

The reaction products were stored at −20°C.

2.12.1.2.2 Phusion polymerase

For amplifications requiring 3'-5' proofreading activity, the high fidelity Phusion polymerase (New England Biolabs) was used. The following master mix was prepared on ice:

Template DNA	10-250 ng
5x Phusion HF buffer	10 µl
10 mM dNTPs	1 µl
10 µM forward primer	2.5 µl
10 µM reverse primer	2.5 µl
Phusion polymerase	0.5 µl
Nuclease free H_2O	to 50 µl

The TC-3000 (Techne) PCR machine was used, as in section 2.12.1.2.1. The lid was preheated to 105°C for 4 min, and the following thermal cycling program was used:

1 cycle Initial denaturation	98°C 30 s
30 cycles Denaturation	98°C 10 s
Annealing	56-60°C 10-30 s
Extension	72°C 30 s kb^{-1}
1 cycle Final extension	72°C 5 min

The reaction products were stored at -20^{o}C.

2.12.1.3 *E. coli* colony PCR

Taq polymerase reaction components were added to PCR tubes (as in section 2.12.1.2.1) minus template DNA. A single colony was then patched onto an agar plate using a sterile pipette tip, and added to the reaction mix. The PCR reaction was that used in section 2.12.1.2.1.

2.12.2 Restriction endonuclease digestion

Restriction enzymes were purchased from Promega, or New England Biolabs and restriction digestion of DNA was carried out according to the manufacturer's instructions. Digestions were performed at 37^{o}C for 1-2 h, depending on the enzyme used. Once digestion was complete, the enzymes were immediately deactivated at 70^{o}C. The QIAquick gel extraction kit (section 2.11.1) was used to remove the restriction enzymes and buffers.

2.12.3 Alkaline phosphatase treatment of vector DNA

To significantly reduce self-ligation of digested vector DNA, calf intestinal alkaline phosphatase (CIP) was used to remove the 5' PO_4 group from digested vector DNA. CIP was added to the digestion reaction mixture, after DNA digestion and inactivation of the restriction enzyme, following the manufacturer's instructions. Incubation at 70^{o}C for 30 min was used to deactivate CIP. The QIAquick gel extraction kit (section 2.11.1) was used to remove the CIP and buffers.

2.12.4 DNA ligation

Appropriate restriction enzymes were used to digest vector DNA and insert DNA. Vector and insert were then ligated, at different ratios of vector to insert. Reactions were performed in a 10 µl volume with 1 µl of 10x T4 DNA ligase buffer and 1 µl of 3 U µl^{-1} T4 DNA ligase (Promega). The reactions were incubated overnight at 15^{o}C. Ethanol precipitation (Section 2.11.4) was used to purify the ligations, which were then used to

transform electrocompetent cells. A ligation reaction was also prepared without insert DNA, as a negative control.

2.12.5 Agarose gel electrophoresis

Separation of DNA samples was normally carried out in a 1% (w/v) agarose gel in 1x TAE buffer. A 0.8% (w/v) agarose gel was used for Southern blotting experiments. Horizontal submerged gels were poured and run using horizontal electrophoresis tanks (Life Technologies, Scie-Plas). 4-10 µl of ethidium bromide (10 mg ml^{-1}; BioRad or Fisher Scientific), was added to molten gel to enable DNA visualisation by UV transilliuminator.

One fifth the sample volume of 6x DNA loading buffer was added and samples were loaded into the wells of the agarose gel. Gels were run for 40-70 min at 120 V at room temperature. Once run the gels were visualised and photographed using an UVi Tec Digital camera and UVi Doc Gel documentation system. DNA fragment size was assessed by electrophoresis of 5 µl of DNA ladder (Fisher Scientific) in a neighbouring well to the sample.

2.12.6 Plasmid sequencing

Plasmid insert DNA sequences were determined by the Core Genetics Service, University of Sheffield, using the primers listed in Table 2.11. Sequencing traces were analysed using Finch TV software (Geospiza). Alternatively, the GATC Biotech DNA sequencing service was used (https://www.gatc-biotech.com/en/index.html). The sequence accuracy was assessed using the Geneious software package (Biomatters Ltd.).

2.13 Southern blotting

All buffers used for Southern blotting are given in section 2.5.12.

2.13.1 Labelling of DNA probes with digoxigenin

The Southern hybridisation probe was labelled with digoxigenin (DIG) using the DNA labelling and detection kit (Roche). DNA template (approximately 3 µg in a 5 µl volume) was denatured by boiling for 10 min and chilled on ice for a further 10 min. Added to the denatured probe template were 2 µl of 10x hexanucleotide mixture and 2 µl of 10x dNTP labelling mixture. The volume was adjusted to 20 µl with sdH_2O and 1 µl of Klenow polymerase was added. The reaction was incubated for 20 h and terminated by addition of 200 mM EDTA pH 8.0. The labelled probe was purified using the QIAquick PCR purification kit (section 2.11.2) and stored at -20^{o}C.

2.13.2 Quantification of DIG-labelled DNA probes

Probe concentration was quantified by comparison to DIG labelled control DNA (Roche). Control DNA was diluted and 1 µl of each dilution (from 1:20 to 1:2,000,000) were spotted onto positively charged, nylon membranes (Roche). The DNA was fixed to the membrane (see section 2.13.4) and detected immunologically using anti-DIG antibody solution. Spot intensities of the probe could then be compared with the known concentration of the control DNA.

2.13.3 Membrane blotting

Digested genomic DNA was separated by 0.8% (w/v) gel electrophoresis, as in section 2.12.5, without ethidium bromide. DIG labelled DNA ladder (Roche) was electrophoresed in one lane, to allow assessment of band sizes. The gel was soaked in Southern depurination solution for 10 min, in order to nick large DNA molecules aiding transfer of DNA during blotting. After washing in dH_2O, the gel was soaked 2 times in Southern denaturing solution for 15 min. The gel was then neutralised by soaking 2 times in Southern neutralising solution for 15 min. The DNA was transferred from the gel to the surface of a Roche positively charged, nylon membrane (Figure 2.1).

Capillary transfer was used to blot the nylon membrane with gel DNA. 1-3 pieces of Whatman paper were soaked in 20x SSC and placed on a bridge resting in a reservoir of 20x SSC. The gel was placed on the Whatman paper, ensuring no air bubbles between

the gel and the paper. Before placing the gel on the Whatman paper, the edges of the bridge, covered by the Whatman paper, were covered by thin strips of Parafilm, so that when the gel is laid on the Whatman paper, the edges of the gel are on top of the Parafilm. This prevents the 20x SSC from being drawn up the outsides of the gel, ensuring that it passes through the middle of the gel, where the DNA is found. One dry piece of Whatman paper was laid over the gel and a stack of paper towels, a glass or plastic plate and a 500 g weight was placed on top. The DNA was allowed to transfer overnight at room temperature.

2.13.4 Fixing the DNA to the membrane

Roche positively charged nylon membranes were used for all Southern procedures. Once DNA was transferred to the membrane it was fixed with a UV crosslinker (Amersham Life Sciences RPN 2500), 70 mJ cm^{2-1} for 15 s.

2.13.5 Pre-hybridisation and hybridisation

Before probing of membranes with DIG-labelled probes, the membranes were pre-hybridised for 1 h at 68^{o}C in pre-hybridisation solution (20 ml per 100 cm^2 of membrane). The membrane was then hybridised with 5-25 ng ml^{-1} probe in hybridisation solution, overnight at 68^{o}C. The membrane was washed twice in 2x wash solution for 5 min at room temperature to remove unbound probe. The membrane was then washed twice in 0.5x wash solution for 15 min at 68^{o}C.

2.13.6 Colorimetric detection of DIG-labelled DNA

The hybridised and stringency washed membrane was then gently agitated for 1 min in washing buffer. The membrane was then blocked for 30 min by gentle agitation in blocking solution and then transferred to antibody solution containing 1:5000 dilution of stock anti-DIG antibody (Roche) for 30 min. The membrane was then washed twice by gentle agitation in washing buffer for 15 min. The membrane was gently agitated in detection buffer for 2 min, then transferred to 10 ml of colour substrate solution containing 66 µl nitro-blue tetrazolium at 50 mg ml^{-1} in 70% (v/v) DMF and 33 µl BCIP at 50 mg ml^{-1}. The colour was developed in the dark, and then the membrane was

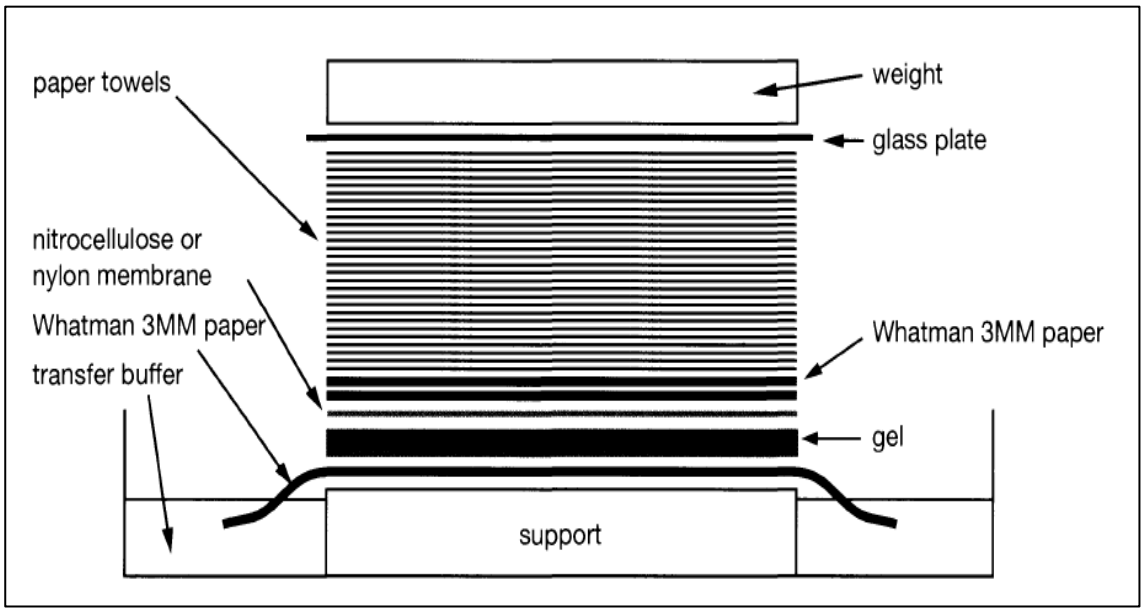

Figure 2.1 Capillary transfer of DNA to nylon membranes.

Imaged reproduced from Sambrook & Russell, (2001)

washed in 1x TE buffer to stop the reaction. The membrane was dried and stored in the dark.

2.14 Protein analysis

2.14.1 SDS-PAGE

Resolving gels were prepared using the following components. Ammonium persulphate (APS) and *N*,*N*,*N*'*N*'-tetramethyl-ethylenediamine (TEMED) were added immediately prior to pouring, to avoid gel formation before pouring:

11 % (w/v) resolving gel

dH_2O	3.5 ml
1.5M Tris-HCl (pH8.8)	2.5 ml
10 % (w/v) SDS	100 µl
30 % (w/v) Acrylamide/Bis (37.5:1,BioRad)	4 ml
10 % (w/v) APS	100 µl
TEMED	20 µl

The above components were loaded into gel casting apparatus (Bio-Rad Mini-Protean II gel slabs). A layer of isopropanol was pipetted onto the top of the gel, to isolate the gel from the air and remove any bubble that may have formed. Once the gel had set the isopropanol was drained and the top of the gel washed with dH_2O. Components of the stacking gel were then mixed and poured on top as follows:

dH_2O	2.5 ml
0.5M Tris-HCl (pH 6.8)	0.62 ml
10 % (w/v) SDS	50 µl
30 % (w/v) Acrylamide/Bis (37.5:1BioRad)	0.83 µl
10 % (w/v) APS	50 µl
TEMED	5 µl

Wells were formed in the gel by inserting a Bio-Rad plastic comb, which also isolated the stacking gel from the air. Once the gel had formed it was transferred to a Protean II

protein gel running tank (Bio-Rad) and submerged in 1x SDS-PAGE reservoir buffer (section 2.5.11.1). The comb was removed and samples of 5-20 µl in SDS-PAGE loading buffer (section 2.5.11.2) were loaded into the wells. Molecular weight markers of known sizes were also loaded to determine the size of sample bands. The proteins were separated by electrophoresis at 150 V until the dye front had migrated to the base of the plate.

2.14.2 Coomassie staining

Gels were placed in Coomassie Blue stain (section 2.5.11.3) for 30 min, to allow protein staining. Stain was removed from the gel by submersion in destain solution (section 2.5.11.4) overnight. The gel was then washed in dH_2O.

2.14.3 Drying gels

The washed gel was placed between two sheets of DryEase mini cellophane (Invitrogen), pre-soaked in Gel-Dry^{TM} Drying solution (Invitrogen). A mini-gel drying frame and base (Novex) was used to hold the gel and sheets, to allow drying at room temperature. Images of the gels were taken once dried.

2.15 Recombinant protein production

2.15.1 Expression of recombinant proteins in *E. coli* BL21

A single colony of *E. coli* BL21, containing pET21d with the required insert was used to inoculate 5 ml of LB containing 100 µg ml^{-1} Amp, in a sterile Universal tube. After overnight incubation, shaking at 250 rpm at 37^{o}C, the culture was used to inoculate either 100 ml or 2 l of LB to an OD_{600} of 0.05, which was incubated at 37^{o}C, shaking at 250rpm, until an OD_{600} of 0.4-0.6 was reached. At this point 1 ml of sample was removed, to give an uninduced sample (see section 2.15.2) and 1 mM IPTG was added to induce protein expression. The culture was re-incubated for a further 3 h, as above. 2x 1 ml samples were removed to give two induced samples (see section 2.15.2). Cells were harvested by centrifugation at 5,100 rpm for 10 min at 4^{o}C, and the pellet retained and stored at -20^{o}C.

2.15.2 Analysis of recombinant protein solubility

Uninduced and induced cells were harvested by centrifugation at 13,000 rpm for 5 min at room temperature and the supernatant discarded. The uninduced sample was resuspended in 100 µl SDS loading buffer and one of the two induced samples was resuspended in 250 µl SDS loading buffer. The samples were boiled for 5 min and centrifuged at 13,000 rpm to remove any insoluble material. Samples were compared by SDS-PAGE to determine overexpression of recombinant protein. To assess the solubility of the recombinant protein, the second induced sample was resuspended in 250 µl of START buffer (section 2.5.8.1) with lysozyme 1 mg ml^{-1}. After incubation at room temperature for 1 h, the sample was sonicated 3 times for 10 s (Sanyo Soniprep 150). Soluble and insoluble material was separated by centrifugation at 13,000 rpm for 10 min. Soluble protein, found in the supernatant, was transferred to a separate microfuge tube and 250 µl SDS loading buffer was added. The insoluble material in the pellet was resuspended in 250 µl START buffer containing 8M urea. After addition of 250 µl of SDS loading buffer, both samples were boiled for 5 min and centrifuged at 13,000 rpm for 3 min and assessed by SDS-PAGE.

2.15.3 Separation of soluble and insoluble material

The sample pellet produced in section 2.15.1 was thawed and resuspended in 5 ml or 50 ml of START buffer minus urea. To weaken the cells, the sample was freeze-thawed 3 times, by freezing at -80^{o}C and thawing on ice. The cells were broken by sonication 10 times for 10 s (Sanyo Soniprep 150) and then centrifuged at 10,000 rpm for 25 min at 4^{o}C. For soluble recombinant protein, the supernatant was filtered into another tube through a 0.45 µm pore filter and stored at 4^{o}C. If the recombinant protein was insoluble, then the pellet was resuspended completely in 5 ml or 50 ml START buffer containing 8M urea or 6M guanidine and incubated overnight at 4^{o}C. To remove any insoluble material and unbroken cells, the sample was centrifuged at 10,000 rpm for 25 min at 4^{o}C and passed through a 0.45 µm pore filter and stored at 4^{o}C.

2.15.4 Protein purification using HiTrap™ column

A 5 ml HiTrap™ affinity column (GE Healthcare) and Bio-Rad Econo Gradient system

was employed to purify recombinant protein. The HiTrap™ column was washed with 15 ml dH_2O, and then charged with 20 ml of 50 mM $NiSO_4$. Excess Ni^{2+} ion was removed by washing the column with a further 15 ml of dH_2O. Tubing and pumps of the Econo Gradient system were flushed with START buffer (START buffer, plus 8M urea or 6M guanidine for insoluble protein) at a flow rate of 1.5 ml min^{-1}. The $NiSO_4$ charged column was attached to the Econo Gradient system and equilibrated with 5 ml of START buffer. The systems spectrophotometer was zeroed, and then the supernatant containing the His6-tagged protein was passed through the column at a flow rate of 1 ml min^{-1}. Unbound protein was washed through the column with 5% (v/v) elution buffer until the absorbance returned to zero. Elution of the bound His6-tagged protein was achieved by gradually increasing the elution buffer gradient from 5-100% (v/v) at a flow rate of 1 ml min^{-1}, while 1 ml elution fractions were collected. Fractions were analysed by SDS-PAGE to determine which fractions contained the recombinant protein. Those that contained protein were pooled and stored at -20^oC. The HiTrap™ column was washed with 10 ml 50 mM EDTA to remove $NiSO_4$, followed by 10 ml dH_2O and 10 ml of 20% (v/v) ethanol, and stored at 4^oC.

2.15.5 Protein dialysis

2.15.5.1 Preparation of dialysis membrane

Size 2 dialysis membrane tubing (Medicell International Ltd.) was used for protein dialysis. Prior to use, tubing was boiled in 2 mM EDTA for 20 min and washed in dH_2O. The boiled tubing was placed in 50% (v/v) ethanol and stored long-term at 4^oC.

2.15.5.2 Dialysis of recombinant protein

Fractions eluted in section 2.15.4, solubilised in either 8M urea or 6M guanidine were placed in dialysis tubing and dialysed in PBS with decreasing concentrations of urea or guanidine, unless stated otherwise. For urea solubilised recombinant protein, starting dialysis was carried out at 4^oC for 12 h in PBS plus 8M urea. Buffer was then replaced with fresh PBS containing 6M urea and dialysis was continued for 12 h at 4^oC. This was repeated with urea concentrations of 4M, 3M, 2M, 1M, 0.5M and 0M. Similarly for 6M guanidine solubilised samples, starting dialysis was carried out at 4^oC for 12 h in PBS buffer plus 6M guanidine. PBS buffer was replaced with reducing guanidine

concentration of 4M, 3M, 2M, 1M, 0.5M and 0M every 12 h. After dialysis was complete, samples were transferred to Falcon tubes and 10% (v/v) glycerol was added. The presence or absence of protein was determined by SDS-PAGE.

2.16 Protein refolding by drip dilution

L-Arginine base refolding buffer (880 mM; section 2.5.5.1), or L-Arginine, L-Glutamic acid base refolding buffer (50 mM; section 2.5.5.2) was poured into a sterile 500 ml Pyrex beaker, at 20x the volume of insoluble protein eluted in the presence of urea or guanidine (section 2.15.4; i.e for 5 ml of eluted protein, 100 ml of refolding buffer was used). The insoluble protein was dripped into the buffer by pipette, at a rate of approximately 1 ml min^{-1}. The protein was then allowed to refold overnight at 4^{o}C. The solution was added to 50 ml Falcon tubes and centrifuged for 20 min at 5,100rpm, at 4^{o}C to remove any insoluble material. The sample was then passed through a 0.2 µm pore filter and then concentrated using an Amicron Ultra Centrifugal filter. Concentrated samples were analysed by SDS-PAGE.

2.17 Determining minimum inhibitory concentration (MIC)

The sulphonamide trimethoprim (TMP) was added to 10 ml of media in a 25 ml Universal tube, to a concentration of 1 mg ml^{-1}. This was then serially diluted 1:1 to a TMP concentration of 0.122 µg ml^{-1}. *S. aureus* USA300 JE2 was then added to each dilution to an OD_{600} of 0.05. Samples were incubated at 37^{o}C overnight with shaking at 250rpm. The OD_{600} of each sample was then recorded.

2.18 Flow cytometry analysis of neutrophil necrosis

2.18.1 Neutrophil preparation

Neutrophils were routinely purified by technicians and researchers at the Royal Hallamshire Hospital. Neutrophils were requested before preparation and provided if enough were collected from the donor. The following method was used to prepare neutrophils of a purity consistently >95%.

Blood was collected and the cellular phase pelleted and platelet poor plasma (PPP)

prepared as in sections 2.1.3.1.1 and 2.1.3.1.2. From the cellular phase, the red blood cells were sedimented out from the leukocytes with 6 ml 6% (w/v) dextran (Sigma-Aldrich) and 0.9% (w/v) saline to a final volume of 50 ml. After 20 min, an interface forms between the red blood cells (lower phase) and the leukocytes (upper phase). The leukocytes were carefully removed and centrifuged at 185 g for 6 min and the lower red blood cell phase was either discarded or stored at -20^{o}C. The soft leukocyte pellet was resuspended in 1 ml of PPP and carefully layered over a discontinuous plasma-Percoll gradient (Amersham Pharmacia Biotech). The plasma Percoll gradient consisted of a lower layer of 51% (v/v) Percoll and 49% (v/v) PPP and an upper layer of 42% (v/v) Percoll and 58% (v/v) PPP. The neutrophils were separated through the gradient at 225 g for 11 min. The central band of neutrophils were isolated and resuspended in 10 ml PPP and 30 ml Hanks Balance salts solution (HBSS) without Ca^{2+} and Mg^{2+}. A 10 µl aliquot was used to determine cell count using a haemocytometer. The cells were washed twice in 10 ml PPP and 30 ml Hanks Balance salts solution by centrifugation at 420 g for 6 min, to remove any residual Percoll. The neutrophil pellet was then resuspended in RPMI-1640 with 10% (v/v) foetal calf serum (Sigma-Aldrich) to give a cell density of $5x10^{6}$ neutrophils ml^{-1}. Cell count was repeated to confirm neutrophil numbers.

2.18.2 Bacterial supernatant

Supernatants were prepared and used on the same day, unless otherwise stated. A single colony of bacteria was used to inoculate 20 ml of RPMI-1640 with 10% (v/v) foetal calf serum (Sigma-Aldrich) in a 250 ml conical flask and incubated for 24 h at 37^{o}C shaking at 250rpm. Cells were removed by centrifugation for 10 min at 5,100 rpm and the supernatant was passed through a 0.2 µm pore filter.

2.18.3 Neutrophil necrosis by *S. aureus* supernatant

All neutrophil necrosis experiments were done in 96-well polyvinyl chloride Falcon Flexiwell plates (BD Biosciences) to minimise neutrophil adhesion to the well surface. Neutrophils were added to wells in 50 µl volumes containing approximately $2.5x10^{5}$ cells. An equal volume of neat or diluted supernatant was added to the 50 µl neutrophil suspensions in duplicate, to give a total well volume of 100 µl. 50 µl of fresh RPMI-

1640 with 10% (v/v) foetal calf serum was added to two wells containing 50 µl neutrophil suspensions, providing a control for baseline neutrophil death. The samples were then incubated at 37^{o}C for 30 min – 3 h, as required, to allow for neutrophil necrosis.

2.18.4 Flow cytometric analysis of necrosis

Immediately after incubation the neutrophils were pelleted by centrifugation at 400 g for 2 min to remove bacterial supernatant and resuspended in PBS. Neutrophil necrosis was assessed by addition of 1:10000, final concentration, of the DNA intercalating vital dye To-Pro-3 (Invitrogen) to the neutrophils. Samples were analysed using a dual laser FACSCalibur flow cytometer (BD Biosciences). Neutrophil events were gated according for forward scatter (FSc) and side scatter (SSc), and fluorescence was measured using the FL4 channel, specific to the emission wavelength produced by To-Pro-3, when bound to DNA. Up to 10,000 events were counted and analysed using the FlowJo^{TM} (TreeStar) cytometry analysis software.

2.18.5 Quantification of absolute neutrophil number

CountBright^{TM} absolute counting beads (Invitrogen) were used to determine absolute neutrophil numbers. CountBright^{TM} beads are microspheres that fluoresce intensely at a wide range of wavelengths, allowing analysis by flow cytometry. The concentration of microspheres is known per ml of supplied solution. After neutrophil recovery and addition of To-Pro-3 (section 2.18.4), and immediately prior to flow cytometry analysis, 50 µl of beads were added to the sample. As the concentration is known, the absolute number of beads in each sample is known. The beads were appropriately gated and bead fluorescence was measured using a different channel to FL4 (that used to measure To-Pro-3 fluorescence). The ratio of bead events to neutrophil events was then multiplied by the absolute number of beads, to give absolute neutrophil numbers in the sample.

2.19 Phagocytic index (PI) determination

2.19.1 Co-culture of neutrophils and *S. aureus*

Neutrophils were prepared as in section 2.18.1 and 50 µl aliquots containing 2.5x10^{5}

were added to the wells of 96-well plates. *S. aureus* was grown in 10 ml of RPMI-1640 with 10% (v/v) foetal calf serum, overnight at 37^{o}C, with shaking at 250rpm. Cultures were diluted to an OD_{600} of 1 in RPMI-1640 with 10% foetal calf serum, and then 12.5 µl of this diluted culture was added to neutrophil containing wells, in triplicate, to give an MOI of 10. The 96-well plates were then incubated for 30 min at 37^{o}C to allow for phagocytosis.

2.19.2 Neutrophil fixation and PI calculation

To determine the phagocytic index (PI) the contents of wells, prepared in section 2.19.1, were cytocentrifuged onto microscope slides and visualised by light microscopy. Cells were added to chambers and spun at 300 g for 3 min using a Shandon Cytspin 3 (Thermo Scientific). Cells were fixed to the slides with 100% methanol and stained with Quick-Diff stains (Gentaur). Slides were mounted with DPX (Fisher Scientific) and cover slips were applied. Neutrophils were observed using a Zeiss Axioplan microscope using the 100x oil immersion lens. The PI was calculated according to the following formula: phagocytic index = (total number of engulfed bacteria/total number of counted neutrophils) × (number of neutrophils containing engulfed cells/total number of counted neutrophils) × 100.

2.20 Whole human blood growth assay

Whole human blood was collected, as in section 2.1.3.1.1. The blood was transferred to microcentrifuge tubes in 1.25 ml aliquots. A culture of *S. aureus* wild-type and a culture of *S. aureus* mutant strain, grown overnight in RPMI-1640 with 10% (v/v) foetal calf serum, at 37^{o}C, shaking at 250rpm, were diluted to a CFU of $2x10^{4}$ ml^{-1}. 62.5 µl of diluted culture was added to each 1.25 ml of whole human blood to give an estimated starting CFU of 1000. A 100 µl aliquot of the sample was removed to determine the actual CFU, as in section 2.6.2. Samples were then incubated for 3 h at 37^{o}C with gentle agitation. A 100 µl sample was then removed to determine the end-point CFU, as in section 2.6.2. The difference in growth between mutant strains and wild-type strains could then be determined. Statistical analyses were done using Prism version 6.0 (Graphpad). Significance was assumed at a *p*-value below 0.05.

2.21 Human plasma growth assay

The human plasma growth assay was done exactly as that of the whole human blood assay (section 2.20), however, human plasma was used instead to human blood.

2.22 Screening the Nebraska transposon mutagenesis library (NTML) on solid media

The NTML consisted of twenty 96-well microtiter plates each containing *S. aureus* JE2 strains with a different Tn disrupted gene. Plates were thawed on ice and the wells of each microtiter plate were inoculated onto solid media using a 96-pin replicator (Boekel Industries). Plates were incubated at 37^{o}C for varied incubation times, dependent on the contents of the solid media.

2.23 Zebrafish embryo assay techniques

2.23.1 Zebrafish strain

All zebrafish experiments performed in this study were done with London Wild-Type (LWT) zebrafish.

2.23.2 Zebrafish husbandry

All adult zebrafish were kept in a continuous recirculating closed aquarium system at 28^{o}C, with a day/night cycle of 14/10 h. Embryos were kept in E3 medium at 28.5^{o}C. Zebrafish were maintained under a Project Licence awarded to the University of Sheffield by the UK Home Office. Zebrafish embryos used in this study were not protected under the Animals (Scientific Procedures) Act, as the embryos used were younger than 5 dpf.

2.23.3 Zebrafish anaesthesia

A stock solution of 0.4% (w/v) tricaine (Sigma) was prepared in 20 mM Tris-HCl, pH 7 and stored at -20^{o}C. Tricaine was added to E3 solution containing zebrafish embryos to a final concentration of 0.02% (w/v), 10 min before injection.

2.23.4 Microinjection of *S. aureus* into zebrafish embryos

S. aureus was grown at 37^{o}C in 50 ml BHI to an OD_{600} of approximately 1, and then centrifuged at 5,100 rpm for 10 min to harvest the cells. The pellet was resuspended in 4 ml of sterile PBS and serially diluted to a CFU of $1.2x10^{9}$ CFU ml^{-1}, then confirmed by plating on solid media. Anaesthetised embryos were embedded in 3% (w/v) methylcellulose on the surface of microscope slides. An electrode puller was used to obtain a fine injection tip from non-filament glass capillaries, allowing injection of 1 nl of bacterial suspension, of known concentration, into the bloodstream of embryos. To confirm the concentration, 1 nl was also injected into 100 µl PBS, and plated after serial dilution on BHI agar. Injections were performed using a pneumatic micropump (World Precision Instruments), a micromanipulator (WPI) and a dissecting microscope. The injected embryos were then placed into separate wells of a 96-well microtitre dish.

2.23.5 Assessment of zebrafish embryo mortality post-infection

Mortality was assessed several times a day, up to 120 hpi. Cessation of heart beat indicated mortality, and dead fish were removed and recorded.

2.23.6 Determination of *S. aureus* growth *in vivo*

To determine bacterial numbers over the course of infection, 5 embryos, each in 100 µl of E3 solution, were transferred to separate microcentrifuge tubes, and then mechanically homogenised using a micropestle (Eppendorf). Serial dilution of the homogenates, followed by plating onto BHI agar was used to determine bacterial numbers within zebrafish at each time-point sampled.

2.23.7 Statistical analysis

Survival curves were compared using the log rank (Mantel-Cox) test. Analyses were done using Prism version 6.0 (Graphpad). Significance was assumed at a *p*-value below 0.05.

CHAPTER 3

THE SEARCH FOR NOVEL STAPHYLOCOCCAL VIRULENCE FACTORS

3.1 Introduction

As outlined in Chapter 1, *S. aureus* encodes an array of virulence factors required for colonisation, survival and spread through the host. The genomic revolution has allowed for the utilisation of information from other species to potentially allow identification of novel virulence determinants of *S. aureus*.

The first complete genome sequence for a living organism was determined in 1995 for the bacterium *Haemophilus influenzae* (Fleischmann *et al*., 1995). There are now 3,316 bacterial, 179 eukaryotic and 202 archaeal genome sequences available on the Genome database of the European Bioinformatics Institute (http://www.ebi.ac.uk/genomes/bacteria.html). In addition to this genomic information, sequence data from viral genomes, organelles, vector sequences, metagenomics and non-metagenomics studies has led to near exponential growth of DNA sequence data stored on freely available databases. For instance, the GenBank database, made available by the National Centre for Biotechnology Information (NCBI) in 1983, started with 606 DNA sequences (translated to protein sequences) totalling 680,338 DNA bases. The database now contains $>1.85x10^8$ DNA sequences (coding sequences translated to protein) totalling $>1.93x10^{11}$ DNA bases (Burks *et al*., 1985). The development of Next-generation sequencing (NGS) technologies over the last 10-15 years has been the vanguard for the expansion of biological sequence data. NGS has allowed for a rapid decrease in cost and time associated with the sequencing of large genomes (Morey *et al*., 2013). The varied uses of NGS, beyond the sequencing of genomes, and some of the commonly used NGS technologies are reviewed by Koboldt *et al*., (2013) and Morey *et al*., (2013). Databases dedicated to protein sequence data such as UniProt (created from the merger of Swiss-Prot, TrEMBL and PIR databases), which contains $>5x10^4$ protein sequences, are available with sequence information derived experimentally or more commonly from prediction based on the available DNA sequence data. Other sequence databases exist for specific kinds of data such as the protein domain databases Pfam (Finn *et al*., 2014) and CDD (Marchler-Bauer *et al*., 2015). A host of bioinformatics databases housing non-sequence information also exist. Extracting information germane to an organism's

phenotype from this wealth of data requires the use of computers. This has led to bioinformatics, a discipline at the boundary between computer science and biology.

Bioinformatics can be applied to many forms of biological information, not just sequencing data. In general, bioinformatics analysis of biological sequence data can only be used for hypothesis generation, later to be corroborated or contradicted in the laboratory (Tang *et al*., 1998). Once a genome has been sequenced, the coordinates of potential protein coding sequences (CDSs) are determined using programs such as GLIMMER (Salzberg *et al*., 1998) and rbsfinder (Suzek *et al*., 2001), which identify sequence characteristics of CDSs, including start codons and promoter elements with an appropriate number of downstream codons. Once the CDSs were identified, Baba *et al*. (2002) used a protein BLAST search of the NCBI non-redundant (nr) protein sequence database to identify homologous genes to the CDSs of *S. aureus* MW2, thereby assigning function based on homology. This can lead to errors, as a protein may be homologous, but not share the same function and the nr database annotation may be incorrect. It has been suggested that ~30% of functional annotation is erroneous (Devos & Valencia, 2001; Koskinen *et al*., 2015). The process does allow for rapid and accurate classification of the majority of CDSs, but as of 2000, an estimated 30% of all CDSs from sequenced genomes were classed as hypothetical or unknown function genes (Weinstock, 2000), which increased to 40-50% by 2006 (Sivashankari & Shanmughavel, 2006). This demonstrates a substantial lack of knowledge of the proteins required for bacterial survival in their different environments.

One use of genomic data is to compare genomes from related strains with different virulence characteristics. The genome of the hospital-acquired methicillin-resistant *S. aureus* (MRSA252) was compared to the community-acquired methicillin susceptible *S. aureus* (MSSA476; Holden *et al*., 2004). The methicillin resistance gene *mecA* is found, along with important virulence determinants, on the pathogenicity island SCC*mec* at a specific site on MRSA strain genomes (Fechter *et al*., 2014). The MSSA476 genome contains an SCC*mec*-like element (SCC*far*), at the same site, with a fusidic acid resistance gene, rather than *mecA*. The hospital acquired strain MRSA252 has a greater number of antibiotic resistance genes, associated with transposons. This increased resistance profile of MRSA252 may be the result of the selective pressure to acquire resistance genes in a hospital environment. BLASTN comparison of the MRSA252,

MSSA476 and N315 genomes was used to identify regions outside of the core genome of these strains. Spread throughout the genome of MRSA252, in small genomic islets and larger regions were a large number of metabolic and transport associated genes, not found in the other two strains. It was hypothesised that these metabolic genes may benefit MRSA252 survival in the varied and often harsh hospital environment (Holden *et al*., 2004). Many of the differences between MRSA252 and MSSA476 were related to mobile genetic elements and insertion sequences. This analysis demonstrated the importance of horizontal gene transfer in the evolution of *S. aureus*.

The aim of the following chapter was initially to identify a potential toxin (here named *Staphylococcus aureus* Factor - SAF) with potent neutrophil killing effects, identified in *S. aureus* strains SH1000 and Newman supernatant by Dr Sadia Anwar. The scope was then widened to search the *S. aureus* genome for any novel toxins or virulence factors.

Results 3.2

Dr Anwar used a candidate approach to determine whether one of the known toxins of *S. aureus* was responsible for the dramatic neutrophil necrosis phenotype. Phenol soluble modulins (PSMs) and Panton-Valentine leukocidin (PVL) were ruled out as the potential cause, as *S. aureus* SH1000 does not encode them. The haemolysins and LukED were considered potential candidates. Dr Anwar developed a flow cytometry assay to measure neutrophil cell necrosis, the details of which are given in Chapter 2.18. Using this assay, *hla*, *hlb*, *hld*, *hlg* and *lukED* were ruled out as the cause of the neutrophil necrosis phenotype. This suggested that a novel toxin was responsible for the observed phenotype. Furthermore, activity was lost in boiled supernatant, suggesting that SAF is a protein.

3.2.1 Is SAF an *S. aureus* leukotoxin?

The lysis of neutrophils is the function of several characterised leukotoxins secreted by *S. aureus*, none of which are responsible for the phenotype, as determined by Dr Anwar. This suggested that if none of the known leukotoxins secreted by *S. aureus* are responsible for the necrotic phenotype, then it is caused by an as yet unknown secreted toxin. To determine this, two databases were constructed using the BLAST+ suite of

programs that allow database construction and execution of local Basic Local Alignment (BLAST) searches (Altschul *et al*., 1990; Camacho *et al*., 2009).

3.2.1.1 Construction of the *S. aureus* leukotoxin database

Construction of the database is shown diagrammatically in Figure 3.1A. Database 1 consisted of *S. aureus* toxins returned by a search of the NCBI Protein database using the following search term:

((leukotox* OR leukocid*) OR (leucotox* OR leucocid*)) AND (*Staphylococcus aureus*[Organism])

This search returned 34,323 protein sequences. A Perl program was written allowing for the removal of sequences with 100% identity (Appendix 3.1). Amongst these sequences were a large number annotated as non-toxins, hypothetical proteins or probable toxins, which were removed using shell commands and Excel. This left 693 *S. aureus* toxins from the haemolysin and two-component leukotoxin classes, which were used to construct the database.

3.2.1.2 Construction of the non-*S. aureus* leukotoxin database

Construction of the database is shown diagrammatically in Figure 3.1B. Database 2 consisted of toxins returned with the following query of the NCBI Protein database:

((leukotox* OR leukocid*) OR (leucotox* OR leucocid*)) NOT (Staphylococcus aureus[Organism])

This returned 2,380 protein sequences. procedure procedure identical to that used in section 3.2.1.1 was implemented for the removal of non-toxin sequences, based on their annotation. This reduced the number of sequences from 2,380 to 396 from 30 different species, none of which were *S. aureus*. As in Database 1, the sequences were from the haemolysin and two-component leukotoxin classes.

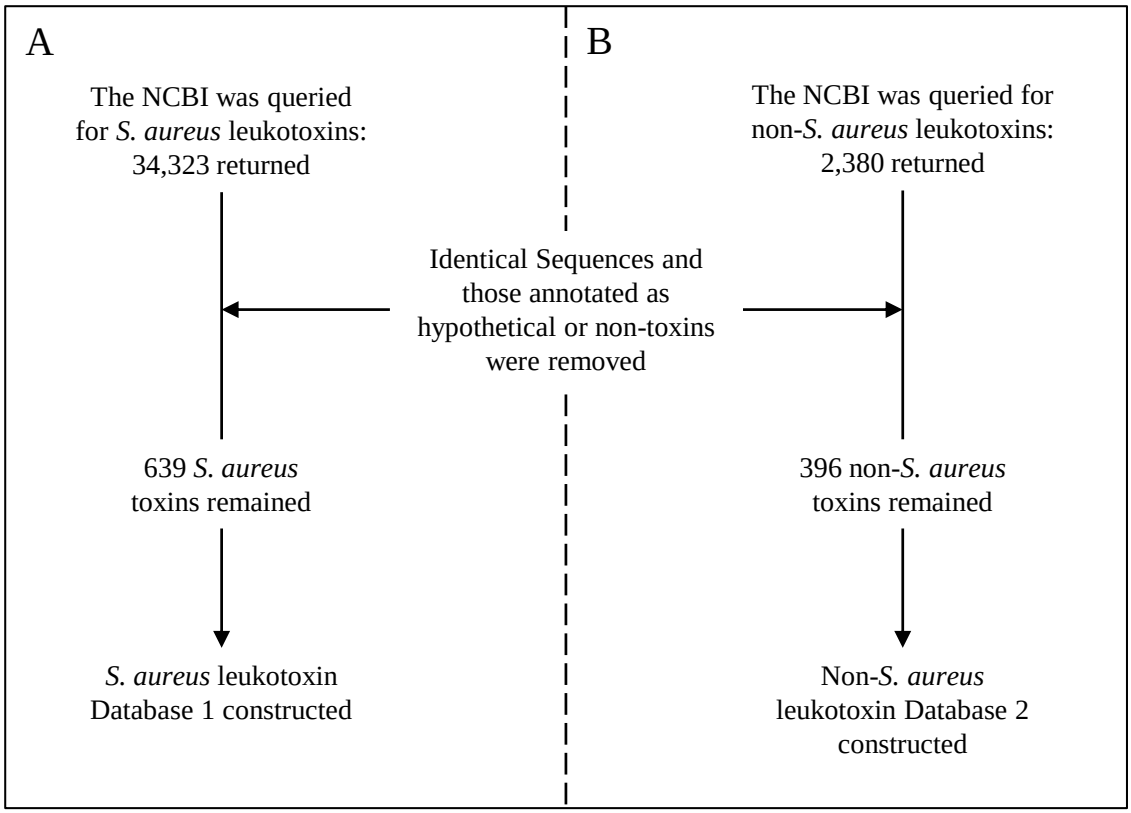

Figure 3.1 Construction of the *S. aureus* (A) and non-*S. aureus* (B) leukotoxin databases, shown diagrammatically.

3.2.1.3 Homology search of the 645 *S. aureus* hypothetical proteins

The homology search of the hypothetical proteins of *S. aureus* 8325 follows the scheme of the flow diagram in Figure 3.2. The *S. aureus* 8325 hypothetical proteins were downloaded from the Pathosystems Resource Integration Centre (PATRIC). According to PATRIC there are 645 hypothetical proteins within the genome of *S. aureus*. A Protein BLAST search, using a low expectation value of 10^{-10}, was used to determine homology between the 645 hypothetical proteins and the leukotoxin sequences of Database 1 and Database 2. No hits were returned for any of the hypothetical sequences in BLAST runs against either database. This suggests that SAF is either not present amongst the hypothetical proteins of *S. aureus*, or that SAF is present, but is not one of the toxin types found in Database 1 or 2. Another possibility is that SAF is a leukotoxin, but is so distantly related that it cannot be found using such a low e-value. If SAF is not a protein, then finding it by comparing protein sequences would be impossible.

3.2.2 Characterisation of SAF

For the following flow cytometry assays, the method designed by Dr Anwar was used (Chapter 2.18; shown diagrammatically in Figure 3.3). Briefly, supernatants were prepared from RPMI-1640 + 10% (v/v) FBS cultures as outlined in Chapter 2.18.2. Supernatants were either used neat or diluted as required and duplicate or triplicate 50 µl aliquots of supernatant were added to 50 µl of neutrophils in a 96-well plate. Neutrophil numbers were approximately 5 x 10^6 per ml. 50 µl of treated or untreated media was added to the same number of neutrophils to give a baseline death without *S. aureus* supernatant products. The 96-well plate was then incubated at 37^{o}C for 0.5-3 h. The vital dye To-Pro-3 was used to determine the level of neutrophil necrosis, as it penetrates cells that have lost their membrane integrity and fluoresces red on binding to DNA (Dockrell *et al*., 2003; Van Hooijdonk *et al*., 1994). The contents of each well was transferred to test tubes for flow cytometry analysis using a dual laser FACSCalibur flow cytometer (BD Biosciences). To-Pro-3 and 50 µl of Countbright™ beads were added to the samples just before the analysis. Countbright™ beads allow for quantification of absolute neutrophil number within a sample (see Chapter 2.18.5 for detailed information).

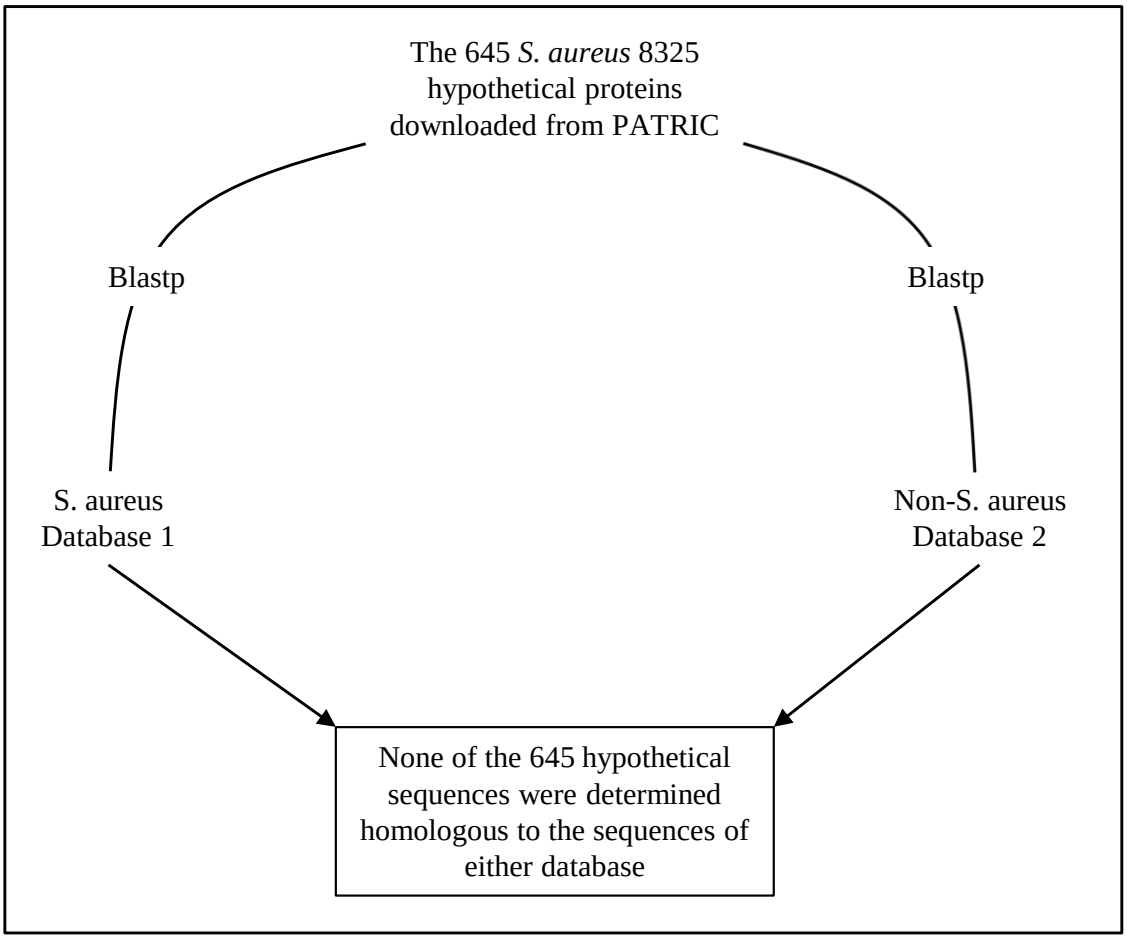

Figure 3.2 Homology search for SAF shown diagrammatically.

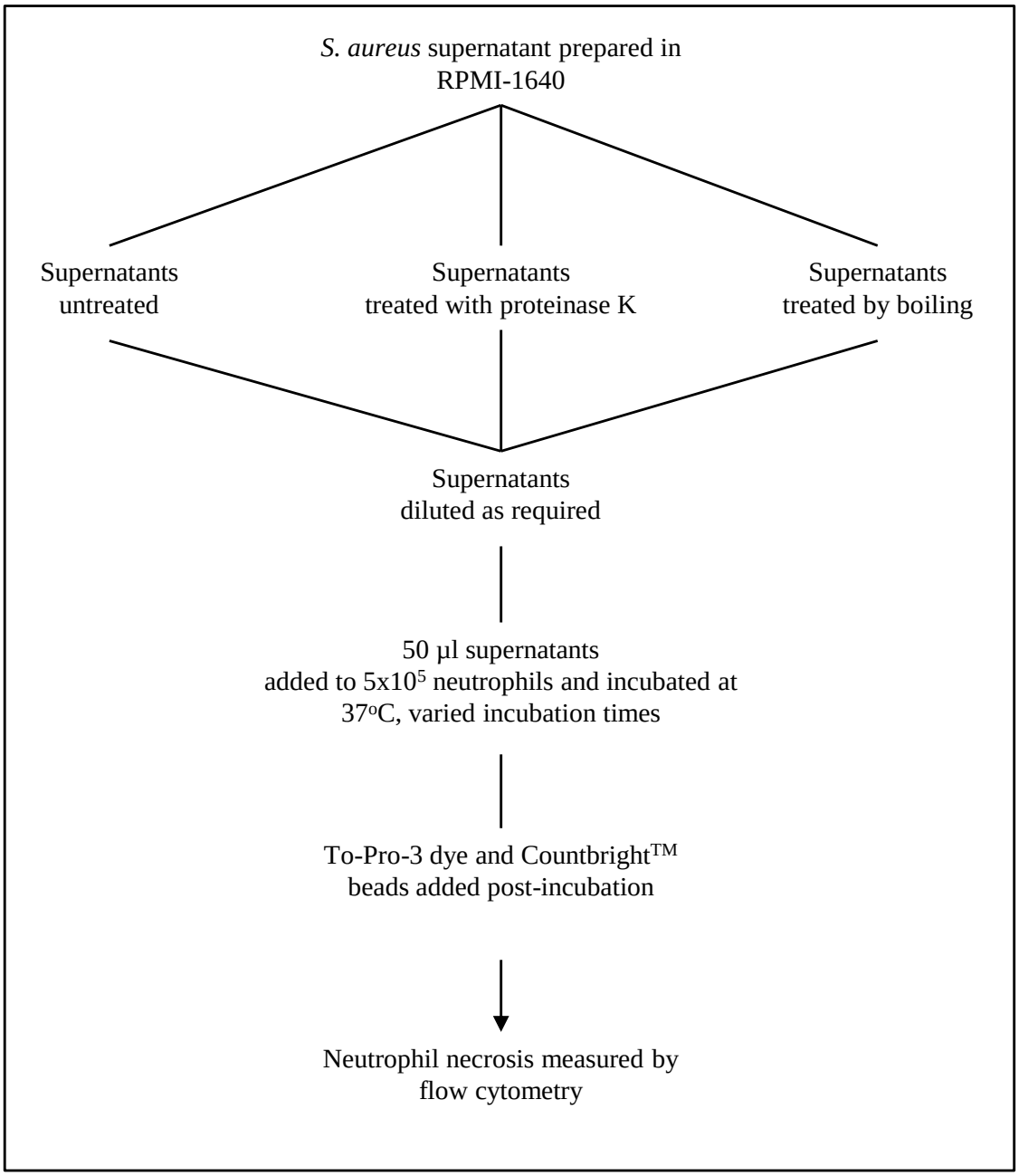

Figure 3.3 Flow cytometry assay of neutrophil necrosis, shown diagrammatically.

RPMI-1640 media was treated in parallel to supernatants, providing controls.

3.2.2.1 Confirmation that SAF is a protein

Before further attempts to identify SAF, it was essential to confirm that SAF is a protein. Dr Anwar has previously shown that boiled supernatant loses SAF activity, suggesting that SAF is a protein. To confirm that SAF is a protein, aliquots of the same overnight supernatant were either boiled or treated with proteinase K (PK) to destroy any protein activity. The treated supernatants were then compared to an untreated supernatant aliquot from the same batch, using the flow cytometry assay outlined in section 3.2.2. Figure 3.4A clearly shows that neutrophil killing activity remains in untreated supernatant and this effect is dose dependent. Neutrophil numbers are reduced relative to the media control and a large proportion of those neutrophils that remain have lost membrane integrity demonstrated by the high To-Pro-3 emission. SAF activity is lost from PK treated supernatant, as no difference is seen between media and neat supernatant (Figure 3.4B). However, PK appears to promote death of neutrophils, as the overall neutrophil numbers are reduced from that seen in untreated media and, as the supernatant is diluted, neutrophil numbers increase over the PK treated media control. Furthermore, the To-Pro-3 activity in the control and neat supernatant was high relative to the diluted supernatant, demonstrating reduced cell membrane integrity of neutrophils incubated in conditions with higher PK levels. As shown by Dr Anwar, boiling of supernatant destroys the neutrophil killing activity of *S. aureus* supernatant (Figure 3.4C).

Figure 3.4 shows the effect of untreated, boiled and proteinase K treated supernatant on neutrophil necrosis, from a single replicate. However, during this work, publication of two research articles changed the direction of the project. Ventura *et al*. (2010) analysed the cell surface proteins of *S. aureus* USA300/LAC and found two proteins to be particularly abundant on the surface and extracellularly, encoded by SAUSA300_1974 and SAUSA300_1975. These genes are predicted by similarity to encode the LukF and LukS proteins of an as yet uncharacterised two-component leukotoxin, which the group named LukF-G LukS-H (LukGH). These genes were not among the 645 hypothetical proteins used above (3.2.1), as their annotation reflects their recognition as potential leukotoxins. The strain used encodes PVL, but using Δ*pvl*, Δ*lukH* and Δ*pvl*/*lukH* strains, the group found that LukGH is a potent leukotoxin of neutrophils that acts synergistically with PVL. Furthermore, it was found that surface associated LukGH

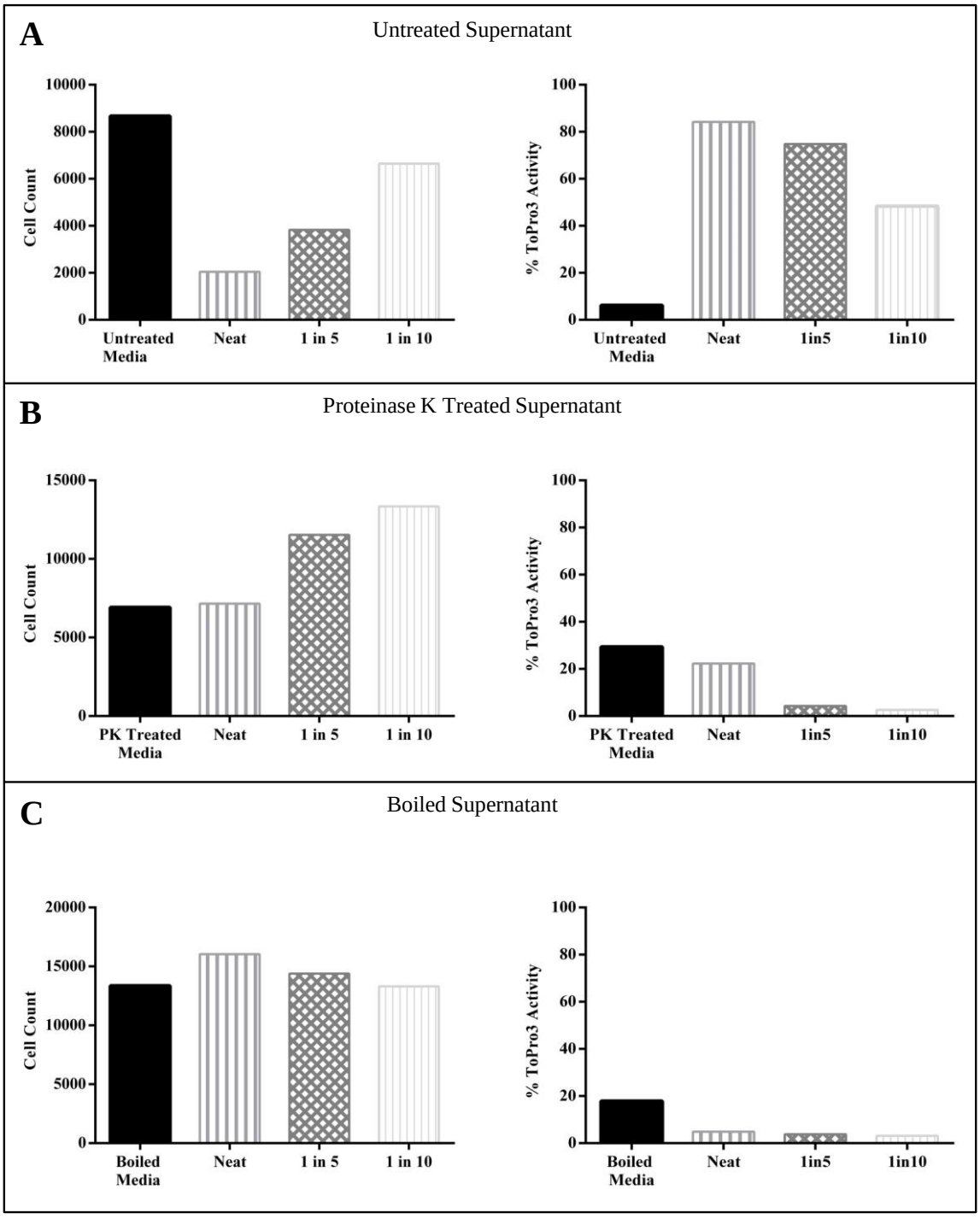

Figure 3.4 Flow cytometry analysis of neutrophil killing by *S. aureus* supernatant.

A. Untreated supernatant.

B. Proteinase K treated supernatant.

C. Boiled supernatant.

Data shown is from a single replicate.

may promote intracellular neutrophil lysis upon phagocytosis. Soon after, Dumont *et al*. (2011) reported their finding that LukGH (named LukAB in their study) was primarily responsible for neutrophil lysis in the *S. aureus* Newman background and that isogenic *lukED*, *hlg* and *hla* mutants retained this phenotype. This was particularly interesting as the neutrophil killing phenotype observed for SAF was shown in *S. aureus* Newman. The group also found that LukAB was important for killing monocytes, macrophages and dendritic cells and has a role in *S. aureus* survival *in vivo*. Since confirming that LukAB/GH is a leukotoxin, aspects of its neutrophil killing mechanism have been characterised and its importance in intracellular killing confirmed (Badarau *et al*., 2015; DuMont *et al*., 2013a, 2013b).

3.2.2.2 Growth curve of *S. aureus* Newman *lukAB*

To compare SAF activity in the wild-type *S. aureus* Newman and *S. aureus* Newman Δ*lukAB*, the mutant strain was requested from Professor Victor Torres, University of New York and kindly supplied. It was essential to compare the growth characteristics of wild-type and mutant, so that supernatants from the same phase of growth could be compared by flow cytometry assay. Growth assays were done as in Chapter 2.8. A single colony of each strain was inoculated into 5 ml of bovine serum and incubated overnight at 37^{o}C. Each overnight was then used to inoculate 3 x 50 ml of pre-warmed bovine serum in 250 ml conical flasks. An initial sample and hourly samples were taken to assess growth by optical density at 600nm (OD_{600}; Figure 3.5A) and by colony forming unit (CFU; Figure 3.5B). Figure 3.5 show that the pattern of growth is the same for both strains. Both show no lag when added to pre-warmed media and reach the plateau phase at the same time. For this reason, preparation of supernatants from overnight cultures was considered appropriate for comparison of SAF activity using the two strains.

3.2.2.3 Is SAF LukAB?

The effect of culture supernatant of the wild-type and ΔlukAB on neutrophils was analysed by flow cytometry using the method outlined in section 3.2.2. Supernatants from each strain were used fresh, as it had been previously shown that SAF is unstable over time (results not shown).

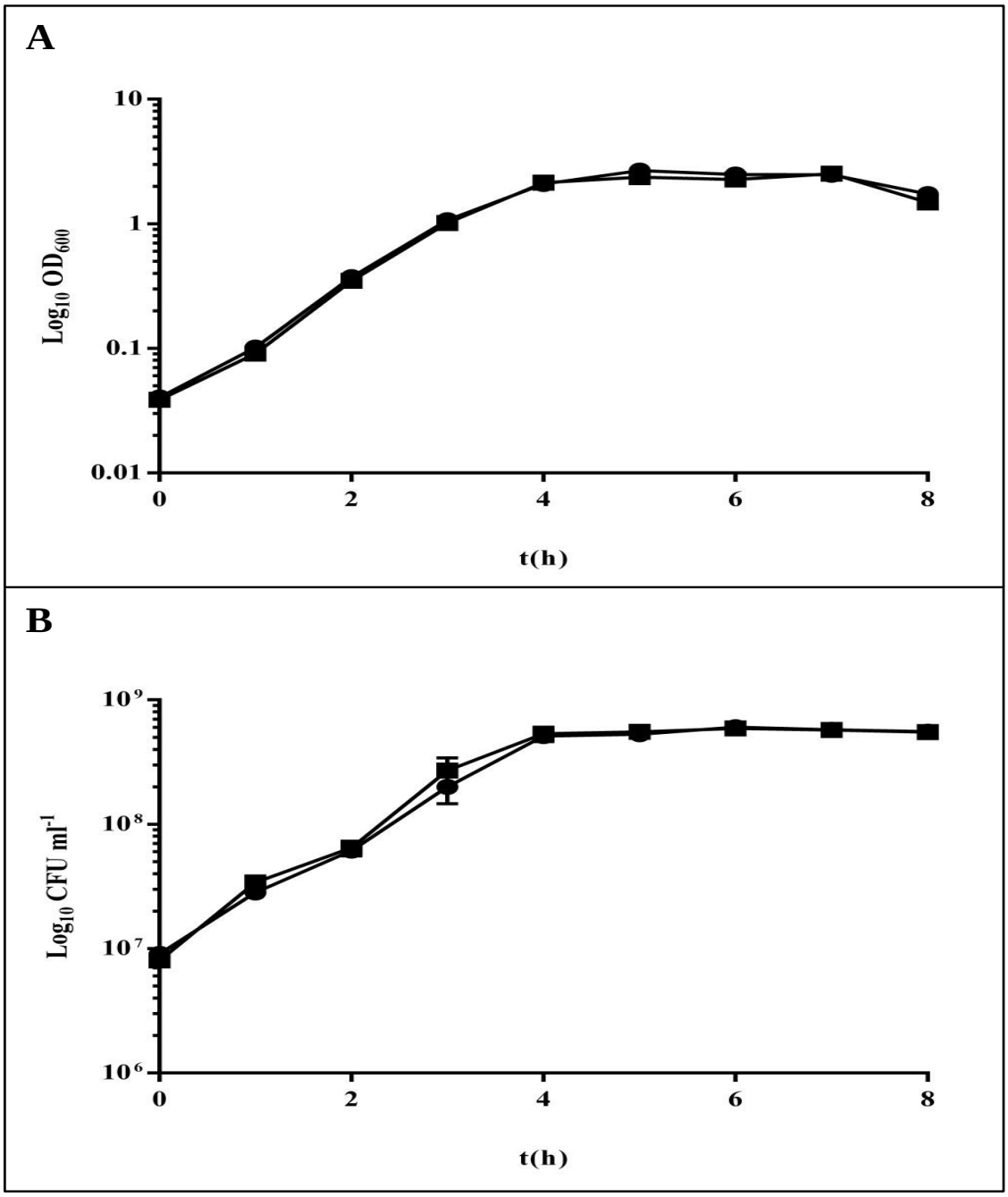

Figure 3.5 The role of *lukAB* in the growth of *S. aureus*.

● = *S. aureus* Newman; ■ = *S. aureus* Newman *lukAB.*

CFU and OD_{600} readings for *S. aureus* Newman and *S. aureus* Newman *lukAB* are not significantly different (CFU p=0.93, OD_{600} p=0.86).

The results clearly show that LukAB is responsible for the necrosis phenotype attributed to SAF (Figure 3.6).

3.2.3 Analysis of the *S. aureus* genome for further novel toxins

With the discovery that SAF is LukAB/GH a decision to switch the focus of the project was made. The discovery of this toxin raised the possibility that other as yet undiscovered toxins may exist in the *S. aureus* genome and if so, could the method employed in section 3.2.1 be extended and applied to all toxins and could other bioinfromatics methods be developed to identify potential novel toxins from the *S. aureus* genome? An NCBI Protein BLAST was carried-out, using the same stringent e-value as the local BLAST from section 3.2.1, using the LukA/G and LukB/H protein sequence. This was to confirm that if the sequence had been amongst the hypothetical proteins it would have hit against known leukotoxins. Both sequences returned alignments aerolysins, γ-haemolysins and leukotoxins ED. This suggested that the methodology used in section 3.2.1 is sound.

3.2.3.1 Construction of a database of known virulence factors

Unlike the list of toxins used in the search for SAF, the goal of this list was not to find a toxin with a specific function (neutrophil killing in the case of SAF), but rather to find any novel toxin expressed by *S. aureus*. The list of toxins required was larger than that created in section 3.2.1, as it was required to contain a greater diversity of toxins. The database was again created using the methodology outlined in Figure 3.1 and the BLAST+ programs. The toxin sequences were downloaded from the NCBI Protein database using the following query:

“toxin OR *toxin OR haemolysin OR hemolysin OR leukocidin OR "phenol soluble modulin" OR *cidin OR porin OR cytolysin OR lysin* OR *lysin”

This query returned 138,811 protein sequences from a diverse species background, from which the BLAST database was constructed.

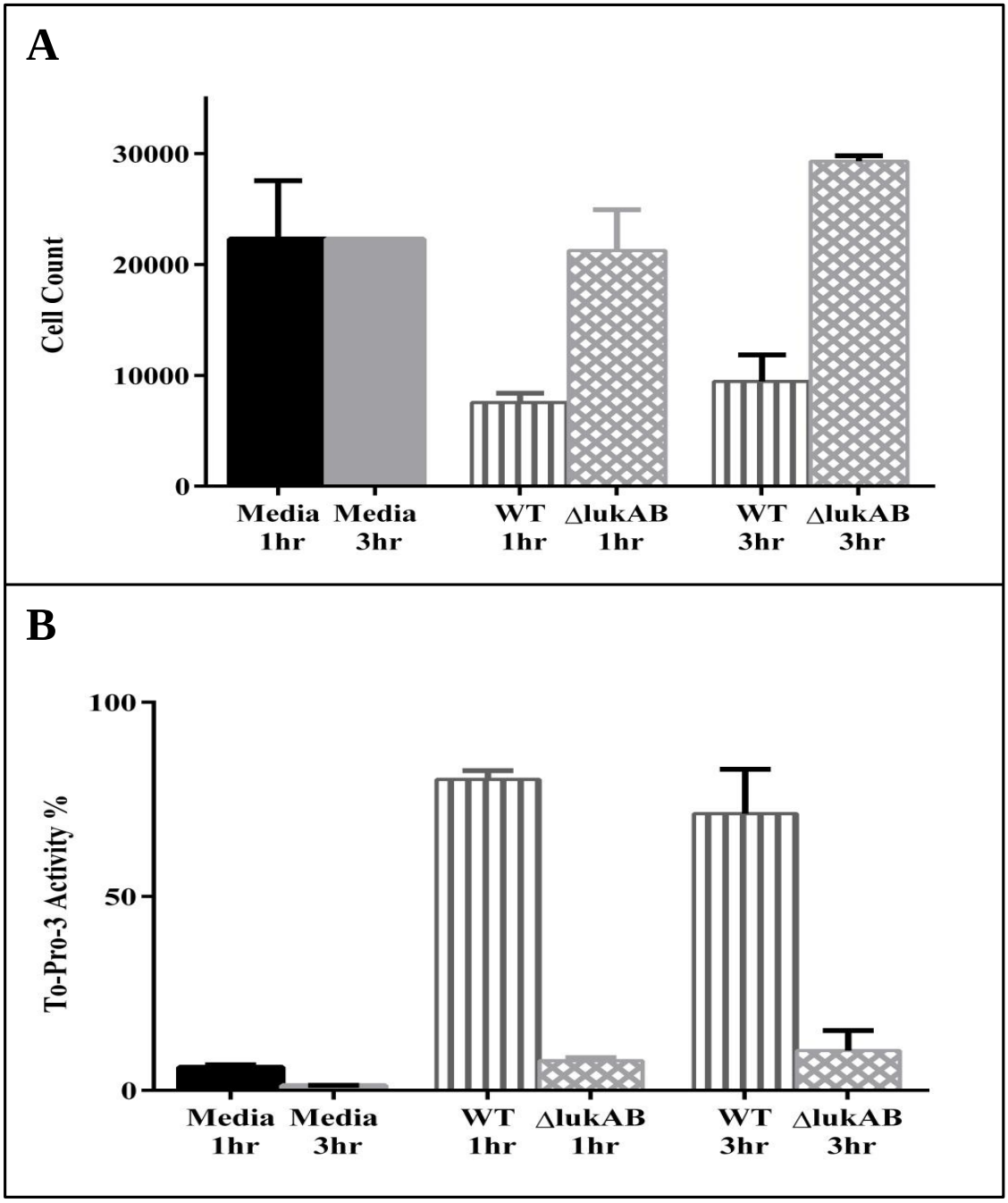

Figure 3.6 The role of LukAB in neutrophil necrosis.

A. Neutrophil survival is significantly increased when incubated with *lukAB* mutant culture supernatant compared to the wild-type culture supernatant, $p < 0.05$ at 1 h and 3 h.

B. To-Pro-3 activity is significantly increased for neutrophils incubated with wild-type supernatant compared to lukAB mutant supernatant, $p < 0.001$ at 1 h and 3 h.

3.2.3.2 BLAST search of the 138,811 sequence database

The homology search of the hypothetical proteins of *S. aureus* 8325 follows the scheme of the flow diagram in Figure 3.7. Execution of BLAST runs was done using a custom Python script (Appendix 3.2a) that could be more easily changed and implemented than using the command line. The XML output file was then parsed using a custom Python script (Appendix 3.2b) to give tab-delimited query annotation, the annotation of the sequence hit by the query and the e-value. A higher e-value of 10^{-7} was used, compared to the e-value of 10^{-10} used in section 3.2.1.3, to allow alignment of more distantly related sequences. However, this e-value is still low in order to minimise false positive results. A BLAST search of the full 138,811 sequence database with the 645 hypothetical proteins of *S. aureus* returned 98 results. Based on the annotation of the database sequences, 55% of the results were alignments to database sequences annotated as hypothetical/unnamed protein sequences and 41% of alignments were with non-toxin sequences. Four of the 645 hypothetical proteins aligned with database sequences annotated as toxins (Table 3.1).

Three of the hypothetical proteins in Table 3.1 are potentially exotoxins. They may also be Staphylococcal superantigen-like proteins (SSLs), which are immune evasion proteins (see Chapter 1). Although immune evasion proteins were not the target of the search, they were still considered interesting to this study. Figure 3.7 shows that the majority of database hits were to hypothetical or non-toxin sequences within the 138,811 database. This demonstrated that the database did not consist of just toxin sequences. It was hypothesised that potential toxins may have been concealed by the large amount of non-toxin and hypothetical protein sequences within the 138,811 sequence database. It was decided that trimming the database of the majority of non-toxin sequences, by removing redundant sequences, may reveal toxins amongst the 645 hypothetical proteins.

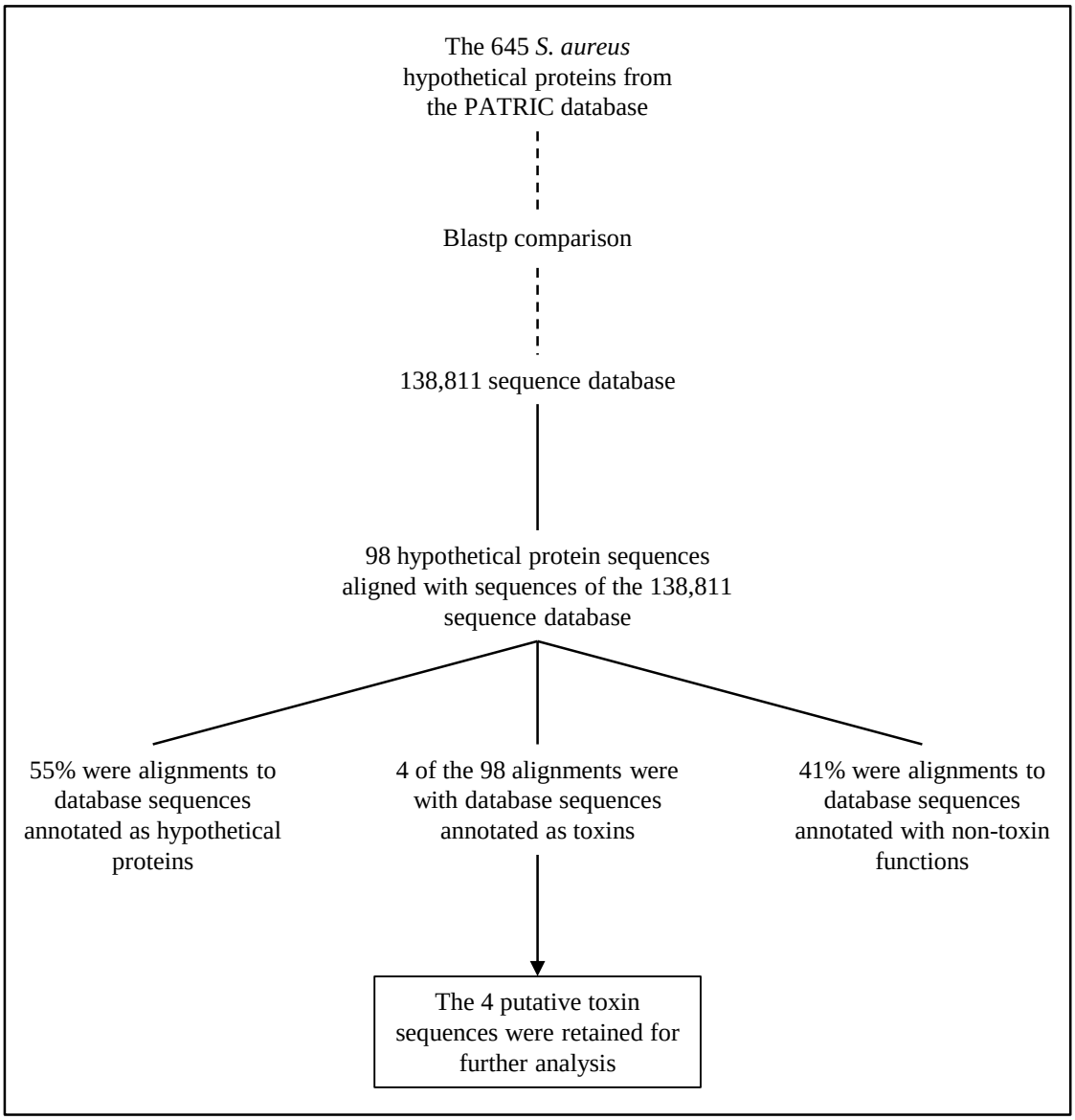

Figure 3.7 Homology search of the 138,811 sequences database for novel toxins within the 645 *S. aureus* hypothetical proteins, shown diagrammatically.

Table 3.1 Hypothetical proteins that aligned with virulence factors.

Hypothetical Protein Query ID	PATRIC ID	Number of Hits	Most Common Database Hit
SAOUHSC_01124	VBIStaAur99865_1032	426	Superantigen-like Proteins/Exotoxin
SAOUHSC_01125	VBIStaAur99865_1033	500	Superantigen-like Protein/Exotoxins
SAOUHSC_01127	VBIStaAur99865_1034	500	Superantigen-like Protein/Exotoxins
SAOUHSC_01438	VBIStaAur99865_1314	9	Conserved virulence factor C

3.2.3.3 Removing redundancy with CD-HIT and Perl

Removal of redundant sequences should result in loss of a large number of hypothetical and non-toxin sequences. It will also result in loss of toxin sequences; however, there should not be a loss in the diversity of sequences, only in quantity. Therefore, sequences that are homologous to toxin sequences may become more visible in the BLAST output. Two methods were used to remove redundant sequences, 1. The custom Perl script written in section 3.2.1.1 was used (see Appendix 3.1 for program and description). This reduced the 138,811 sequences to 53,032 protein sequences and 2. The CD-HIT online server, which reduced the number of database sequences to 50,048. CD-HIT is available to run locally or online and functions by clustering sequences based on a specified similarity (100% in this case). A single sequence from each cluster is then returned (Li *et al*., 2001). Although the goal of the two programs was the same, the results differed, but not considerably. In order to avoid missing potential toxins in the BLAST search, it was decided that the prudent choice would be to use the larger of the two databases – i.e. the database trimmed using the Perl script.

3.2.3.4 BLAST of the 53,032 sequence database

The homology search of the hypothetical proteins of *S. aureus* 8325 follows the scheme of the flow diagram in Figure 3.8. The same parameters and custom scripts to those used in 3.2.3.2 were used to run the BLAST search of the non-redundant database. The search returned 48 alignments with significant hits to the database. Although this is considerably fewer than the 98 returned in section 3.2.3.2, only 6% of the results were alignments between *S. aureus* hypothetical proteins and database sequences annotated as hypothetical/unnamed proteins. However, 90% of results were alignments with database sequences annotated as non-toxin sequences. An additional toxin/immune evasion protein was found using this database (Table 3.2). This sequence did hit exotoxins and SSLs in the full database search, however, the majority of alignments in the output were to hypothetical proteins. Reducing the number of hypothetical protein improved the quality of the output, but the majority of results were alignments between hypothetical proteins and non-toxins, based on annotation. The hypothetical protein that aligned with conserved virulence factor C (Table 3.1) was not found, but is still included in Table 3.2 as it was found by the prior method.

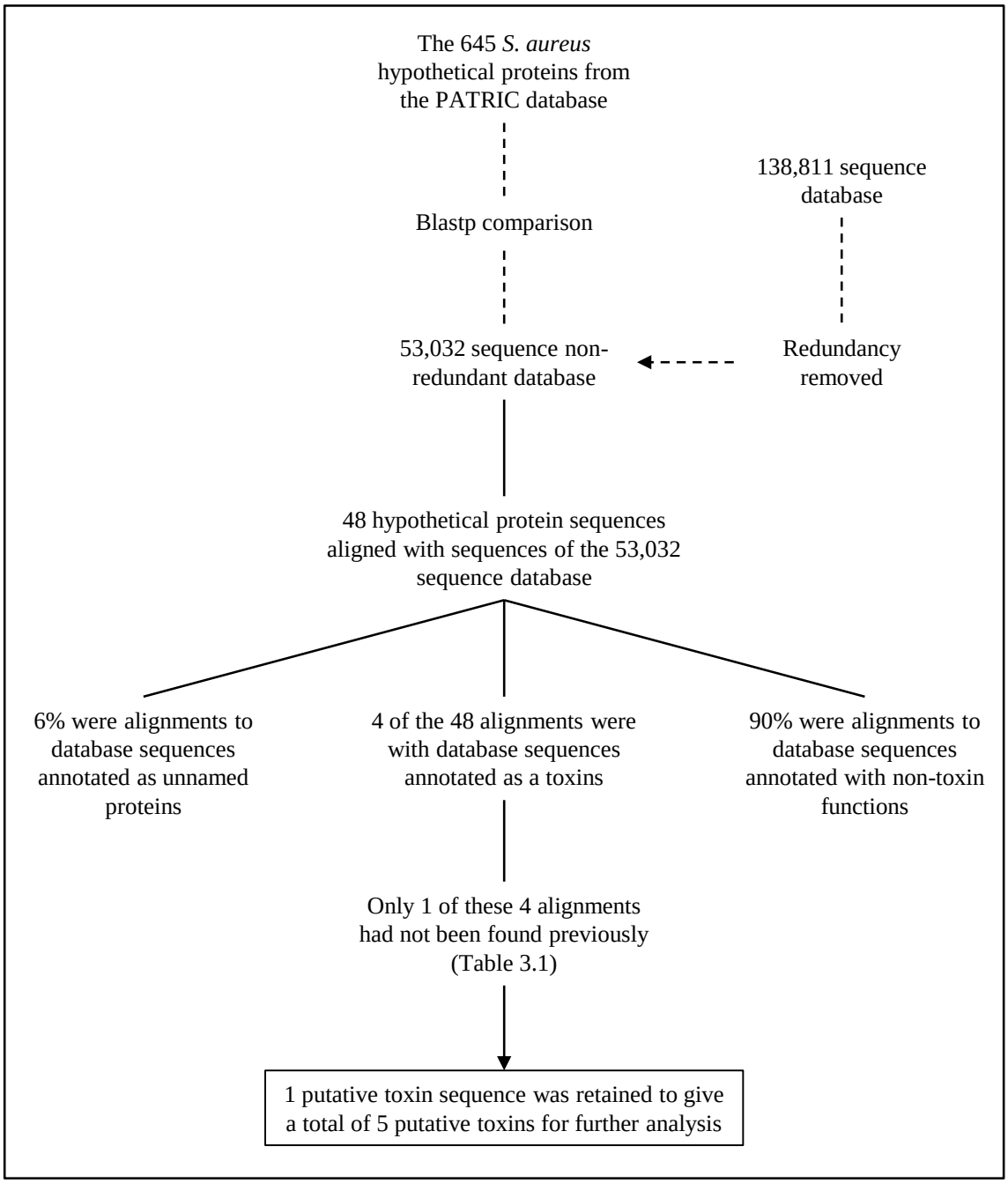

Figure 3.8 Homology search of the 53,032 sequences non-redundant database for novel toxins within the *S. aureus* hypothetical proteins, shown diagrammatically.

Table 3.2 Hypothetical proteins that aligned with virulence factors.

Hypothetical Protein Query ID	PATRIC ID	Number of Hits	Most Common Hit Name
SAOUHSC_00354*	VBIStaAur99865_0324	6	superantigen-like protein/Exotoxin
SAOUHSC_01124	VBIStaAur99865_1032	52	superantigen-like protein/exotoxin
SAOUHSC_01125	VBIStaAur99865_1033	90	superantigen-like protein/exotoxin
SAOUHSC_01127	VBIStaAur99865_1034	81	superantigen-like protein/exotoxin
SAOUHSC_01438	VBIStaAur99865_1314	6	Conserved virulence factor C

* Additional sequence found by homology search of the 53,032 sequence database

The possibility that further toxins are present among the 645 hypothetical proteins, but clouded out by database sequences annotated as non-toxins still exists when using the non-redundant database.

3.2.3.5 Removal of all non-virulence factor sequences from the non-redundant database

For most virulence factors, and all *S. aureus* toxins, to perform their function they must be secreted and attached to the *S. aureus* cell surface or released into the extracellular environment. *S. aureus* uses several secretion systems to translocate proteins across the cell wall (Bartlett & Hulten, 2010; Hecker *et al*., 2010; Sibbald *et al*., 2006). To allow proteins to be targeted to the secretion pathway, secreted proteins have an N-terminal signal sequence, which is a short sequence motif that is removed during translocation. Therefore, secreted virulence factor sequences can be separated from non-secreted non-virulence factors present in the non-redundant database, based on the presence or absence of a signal sequence. The signal sequence prediction program SignalP uses a hidden Markov model to predict Gram-negative, Gram-positive and eukaryotic signal sequences and sequence cleavage site (Bendtsen *et al*., 2004). A custom Perl program was written to trim the non-redundant database sequences to their first 100 amino acids (Appendix 3.3). These trimmed sequences were then uploaded on to the SignalP 3.0 server and only those sequences predicted to contain a signal sequence were retained. Excel, one-line shell commands and Perl scripts were then used to remove any further non-virulence factor sequences (based on their annotation), to give a database (herein named the VF database) of 860 sequences all with annotation corresponding to a virulence function. This database could now be used to search the hypothetical and known protein sequences of *S. aureus* for potential novel VFs.

3.2.3.6 Analysis of all *S. aureus* protein sequences using the VF database

The reason for comparing the hypothetical protein sequences of *S. aureus* to the VF database is clear. If one of the hypothetical proteins is a VF, it may be homologous to a known VF, the sequence of which may be present in the VF database. A BLAST search would align the two sequences and the hypothetical protein could then be studied further in the laboratory. The known function protein sequences of *S. aureus* were

compared with the VF database for two reasons; firstly the known protein sequences were used as a control. The purpose of the VF database is to allow selective extraction of potential VFs from a list of protein sequences using the BLAST algorithm, therefore a BLAST using the sequences with known function should extract the known VFs of *S. aureus*. Secondly, it is possible that proteins have been incorrectly assigned to roles that are not virulence related. Therefore, if a protein from the sequences with assigned function aligns to a VF in the database, it may be incorrectly annotated. Available information on any such sequences should be checked before they are added to the list of sequences for further study (Table 3.2).

3.2.3.6.1 BLAST search of the VF database using the 645 hypothetical proteins

The BLAST search using the hypothetical sequences as queries was repeated for the VF database, using the same parameters as prior searches. No new VFs were discovered using the VF database and all sequences (barring conserved virulence factor C) in Table 3.2 were present in the result.

3.2.3.6.2 BLAST search of the VF database using the 2,110 *S. aureus* known function sequences

The BLAST search of the VF database using the 2,110 assigned function sequences of *S. aureus* as the query returned 29 results. Of these, 11 were known *S. aureus* toxins and 18 were virulence factors involved in colonisation and immune evasion, all of which are described in Table 3.3.

Before attempts to characterise the sequences in Table 3.2, further bioinformatics analyses were made to identify novel VFs from the hypothetical proteins of *S. aureus*.

Table 3.3 All protein sequences returned by BLAST query of the VF database with the known sequences of *S. aureus* 8325.

Known Protein Query ID	PATRIC ID	Name of Known Protein	Number of Hits	Most Common Hit Name	Reference
Toxins and Virulence Factors					
SAOUHSC_00988	VBIStaAur99865_0908	Exfoliative Toxin B	6	exfoliative toxin	(Amagai *et al*., 2002)
SAOUHSC_01121	VBIStaAur99865_1029	α-Haemolysin Precursor	133	Haemolysins, leukotoxins	(Prince *et al*., 2012)
SAOUHSC_02163	VBIStaAur99865_1962	β-Haemolysin	4	beta-haemolysin	(Tajima *et al*., 2009)
SAOUHSC_02708	VBIStaAur99865_2451	γ-Haemolysin Component A	132	Leukotoxins and haemolysins	(Sugawara-Tomita *et al*., 2002)
SAOUHSC_02710	VBIStaAur99865_2454	γ-Haemolysin Component B	132	Leukotoxins and haemolysins	
SAOUHSC_02709	VBIStaAur99865_2453	γ-Haemolysin Component C	133	Leukotoxins and haemolysins	
SAOUHSC_01954	VBIStaAur99865_1779	Leukotoxin LukD	132	Leukotoxins and haemolysins	(Reyes-Robles *et al*., 2013)
SAOUHSC_01955	VBIStaAur99865_1780	Leukotoxin LukE	132	Leukotoxins and haemolysins	
SAOUHSC_02241	VBIStaAur99865_2035	Leukocidin LukF-PV (LukA/G)	134	Primarily leukotoxins. Small number of α-haemolysins	(Holzinger *et al*., 2012)
SAOUHSC_02243	VBIStaAur99865_2036	Leukocidin LukS-PV (LukB/H)	132	Primarily leukotoxins. Small number of α-haemolysins	
SAOUHSC_02971	VBIStaAur99865_2680	Aureolysin	4	lambda toxin	(Laarman *et al*., 2011)
SAOUHSC_00383	VBIStaAur99865_0353	Staphylococcal superantigen-like 1	161	Exotoxins, superantigen-like proteins & superantigens	(Patel *et al*., 2010)
SAOUHSC_00384	VBIStaAur99865_0354	Staphylococcal superantigen-like 2	126	Exotoxins, superantigen-like proteins & superantigens	
SAOUHSC_00386	VBIStaAur99865_0355	Staphylococcal superantigen-like 3	127	Exotoxins, superantigen-like proteins & superantigens	
SAOUHSC_00389	VBIStaAur99865_0357	Staphylococcal superantigen-like 4	126	Exotoxins, superantigen-like proteins & superantigens	
SAOUHSC_00390	VBIStaAur99865_0358	Staphylococcal superantigen-like 5	144	Exotoxins, superantigen-like proteins & superantigens	
SAOUHSC_00391	VBIStaAur99865_0359	Staphylococcal superantigen-like 6	126	Exotoxins, superantigen-like proteins & superantigens	
SAOUHSC_00392	VBIStaAur99865_0360	Staphylococcal superantigen-like 7	142	Exotoxins, superantigen-like proteins & superantigens	

Table 3.3 continued

Known Protein Query ID	PATRIC ID	Name of Known Protein	Number of Hits	Most Common Hit Name	Reference
SAOUHSC_00393	VBIStaAur99865_0361	Staphylococcal superantigen-like 8	162	Exotoxins, superantigen-like proteins & superantigens	
SAOUHSC_00394	VBIStaAur99865_0362	Staphylococcal superantigen-like 9	136	Exotoxins, superantigen-like proteins & superantigens	
SAOUHSC_00395	VBIStaAur99865_0363	Staphylococcal superantigen-like 10	146	Exotoxins, superantigen-like proteins & superantigens	
SAOUHSC_00399	VBIStaAur99865_0367	Staphylococcal superantigen-like 11	131	Exotoxins, superantigen-like proteins & superantigens	
SAOUHSC_02706	VBIStaAur99865_2450	IgG-Binding Protein SBI	35	protein A	(Burman *et al*., 2008)
SAOUHSC_00069	VBIStaAur99865_0059	Protein A, von Willebrand Factor Binding Protein Spa	14	protein A	(Atkins *et al*., 2008)
SAOUHSC_02169	VBIStaAur99865_1967	CHIPS	1	CHIPS	(Rooijakkers *et al*., 2006)
SAOUHSC_01936	VBIStaAur99865_1763	Serine Protease SplE	3	exfoliative toxin	(Popowicz *et al*., 2006; Reed *et al*., 2001)
SAOUHSC_01939	VBIStaAur99865_1765	Serine Protease SplC	6	exfoliative toxin	
SAOUHSC_01941	VBIStaAur99865_1766	Serine Protease SplB	6	exfoliative toxin	
SAOUHSC_01942	VBIStaAur99865_1767	Serine Protease SplA	6	exfoliative toxin	

3.2.3.7 CD-HIT clustering method

Sequence alignments below 25-30% are at a level of similarity known as “the twilight zone” and homology inferred between sequences below this level of similarity is tenuous in the absence of other data. The clustering method of CD-HIT was exploited to cluster the VF database sequences with the 71 hypothetical sequences with signal sequences at 30% identity. The hypothesis being that hypothetical proteins with homology to VFs will be found in clusters with VF sequences and those that are not homologous, will be in their own cluster, or cluster with other hypothetical protein sequences. The CD-HIT program was downloaded and run locally. Alpha-haemolysin was again used as a control sequence. Only two clusters of interest were produced using this method. Cluster 1 was the control cluster, containing 51 sequences, the control sequence and 50 sequences that were a mix of haemolysins, leukotoxins and cytotoxins. The remaining cluster consisted of 3 of the putative exotoxins/SSLs (SAOUHSC_01124, SAOUHSC_01125 & SAOUHSC_01127; see Table 3.2) and 30 exotoxin or SSL sequences. The fourth putative SSL SAOUHSC_00354 was not present in the cluster. This method added no new VFs to Table 3.2, however, it did show that the putative SSLs (in particular SAOUHSC_01124-5-7) are worth further study.

3.2.3.8 Construction of a Non-redundant (Nr) Bacterial Database

The concern with the database constructed in section 3.2.3.5 was that it may not have been complete and all VF varieties were not in it. The sequences in the database were initially found using a search only for toxins; so, many VFs may not be represented in the database. Furthermore, many toxin types may not have been returned by the original search. To construct a database containing all varieties of VF, a database containing all varieties of bacterial sequence was constructed and reduced to a smaller size to remove redundancy and maintain diversity by clustering to 90% with CD-HIT. All hypothetical, unknown, unnamed, uncharacterised and putative sequences were also removed from the database. Sequences < 5 amino acids and > 5,500 amino acids were removed with merged and modified command line Perl programs located at the following URL (http://archive.sysbio.harvard.edu/csb/resources/computational/scriptome/UNIX/Tools/

Change.html). Two different methods were employed to create this database, the successful methodology employed to construct the database is outline in Figure 3.9A.

3.2.3.8.1 Query of Nr Bacterial Database with the 645 hypothetical protein sequences of *S. aureus*

The homology search of the hypothetical proteins of *S. aureus* 8325 follows the scheme of the flow diagram in Figure 3.9B. The BLAST search was done using the same parameters used in section 3.2.3.2. Of the 645 hypothetical proteins, 408 successfully aligned with the Nr Bacterial Database. Those that aligned to VFs, based on annotation, are shown in Table 3.4. 98% of hypothetical proteins aligned with non-VF sequences, based on database sequence annotation. The 4 Exotoxin/SSL sequences in Table 3.2 all aligned and two additional hypothetical protein sequences were added that aligned with Nr Bacterial database sequences annotated as the staphylococcal complement inhibitor (SCIN) and the formyl peptide receptor-like 1 inhibitory protein (FLIPr-like). These immune evasion proteins interact with IgG and complement/complement receptors inhibiting complement activation and chemotaxis (Prat *et al*., 2009; Rooijakkers *et al*., 2006).

3.2.3.8.2 Query of bacterial database using 2,110 known function protein sequences

The purpose of searching the bacterial database with the known function sequences of *S. aureus* is as a control. If the database possessed the expected sequence diversity, then it was expected that many known virulence factors would be returned by the search. The same methodology used in Figure 3.9B was applied to the 2,110 *S. aureus* sequences annotated with a known function. As expected, a large number of the results returned by the search were between known function proteins, not related to virulence, and their corresponding protein in the database (95.8% of the 2,045 results). The remaining 4.2% were alignments between known virulence factor sequences and their corresponding sequence (Table 3.5).

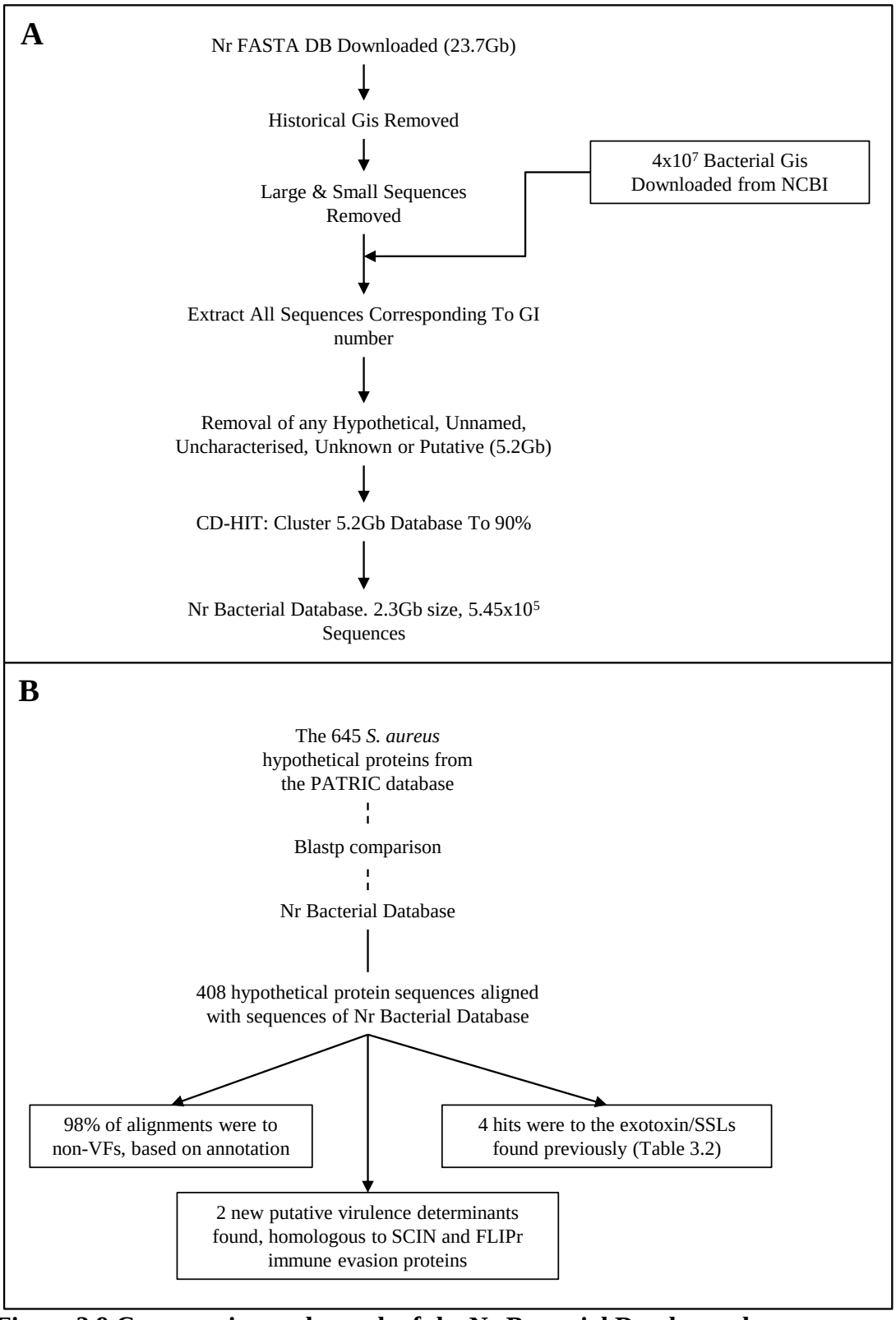

Figure 3.9 Construction and search of the Nr Bacterial Database, shown diagrammatically.

For scripts used for constructing the non-redundant bacterial sequence database see Appendix 3.4. The clustering program CD-HIT was run on the University of Sheffield Iceberg High Performance Computer Resource.

Table 3.4 Hypothetical proteins that aligned with virulence factors of the non-redundant bacterial sequence database.

Query ID	PATRIC ID	Number of Hits	Most Common Hit Name
SAOUHSC_00191	VBIStaAur99865_0178	16	Complement Inhibitor SCIN
SAOUHSC_01112	VBIStaAur99865_1019	43	formyl peptide receptor-like 1 inhibitory protein
SAOUHSC_00354	VBIStaAur99865_0324	37	Exotoxins/SSLs
SAOUHSC_01124	VBIStaAur99865_1032	110	Exotoxins/SSLs
SAOUHSC_01125	VBIStaAur99865_1033	110	Exotoxins/SSLs
SAOUHSC_01127	VBIStaAur99865_1034	110	Exotoxins/SSLs

Table 3.5 NCBI BLAST of known sequences against the Nr Bacterial database.

Known *S. aureus* Queries	Total Number of Hits	Bacterial Database Sequence Aligned With
Adhesins		
ClfAB, FnbpAB, Emp, Efb, SagG, Map/Eap, vWbp, Sbi	1962	ClfAB, FnbpAB, Emp, Efb, SagG, Map/Eap, vWbp, Sbi
Regulatory Proteins		
SarAS, SaeRS, ArlS, AgrBD, Rot	585	SarAS, SaeRS, ArlS, AgrBD, Rot
Enzymes		
Coa, HysA, Eno, SbcCC, Nuc, Sak	1118	Coa, HysA, Eno, SbcCC, Nuc, Sak
Nutrient Acquisition		
SirABC, SbnA, SbnC-I, IsdAB, IsdD-I, MntH, Ferredoxin, Iron Transport Protein	2250	SirABC, SbnA, SbnC-I, IsdAB, IsdD-I, MntH, Ferredoxin, Iron Transport Protein
Immune Evasion Proteins		
Spa*, OatA, KatA, Sod, Chp, 16 x Capsule Synthesis Proteins	2035	Spa*, OatA, KatA, Sod, Chp
Toxins		
11 x Exotoxin, Hla, Enterotoxin, LukED, Hlb, LukGH/AB, Hld, HlgABC	1997	11 x Exotoxin, Hla, Enterotoxin, LukED, Hlb, LukGH/AB, Hld, HlgABC

* Spa is also an adhesin

3.2.4 Identifying the putative virulence factors

Interestingly, FLIPr-like and SCIN proteins were not found amongst the known function proteins in the results of the BLAST search against the bacterial database (Table 3.5). This suggested that their annotation is outdated and so they were found in the hypothetical proteins search of the bacterial database (Table 3.4). This would rule them out for further study, as their functions are already well known. The SCIN protein sequence of the Nr Bacterial database was hit by the hypothetical protein with the ID SAOHSC_00191. The NCBI Protein database was queried with this ID and identical sequences to the result were requested. The first identical sequence in the list returned was the SCIN protein from *S. aureus* strain 21236. To confirm their identity both sequences were compared with bl2Seq (Figure 3.10A). The bl2Seq result demonstrated that SAOUHSC_00191 is SCIN and is incorrectly categorised as a hypothetical protein in the PATRIC database (the source of the hypothetical protein sequences).

A similar search would have been carried-out for the hypothetical protein SAOUHSC_01112, which aligned with the FLIPr-like protein in the Nr Bacterial database, but it proved unnecessary. A search of the UniProt database with the ID SAOUHSC_01112 returned the result shown in Figure 3.10B. This showed that the hypothetical protein annotation was, similarly to SCIN, out of date on the PATRIC website. The protein was in fact the FPRL1 inhibitory protein, which has the short name FLIPr.

FLIPr and SCIN were ruled out as subjects for further study, as they are both well characterised proteins with known roles in *S. aureus* virulence (Prat *et al*., 2009; Rooijakkers *et al*., 2006).

The hypothetical protein SAOUHSC_01438 aligns with the conserved virulence factor C (CvfC; see Table 3.3). The *cvfABC* operon has been shown to be a virulence factor in silkworm and mouse models of infection. Loss of *cvfABC* results in reduced expression of α-haemolysin concomitant with downregulation of RNAII, thereby reducing transcription RNAIII, the primary regulator of *agr* controlled genes. This demonstrated that the *cfvABC* operon has a role in positive control of the *agr* system (Kaito *et al*., 2005). SAOUHSC_01438 is a protein of 83 amino acids and aligns with the first 82

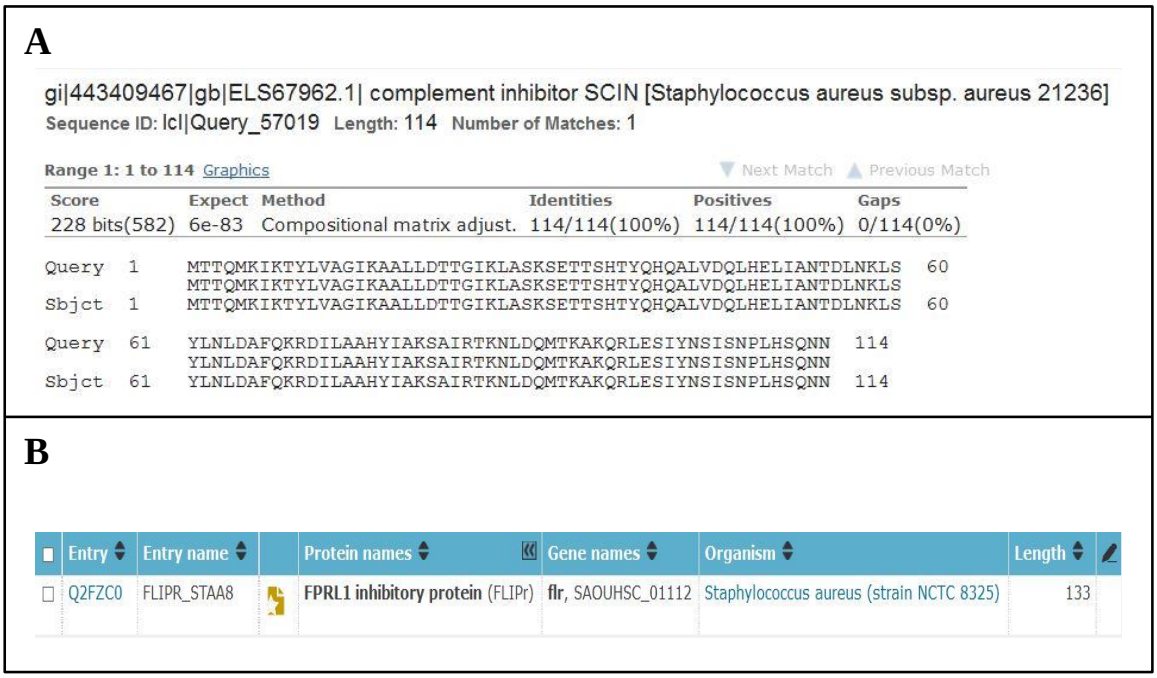

Figure 3.10 Confirmation that hypothetical proteins SAOUHSC_00191 and SAOUHSC_01112 are known function proteins.

amino acid residues of the 374 amino acid CvfC protein from *S. aureus* N315. This suggested that SAOUHSC_01438 is a short single domain protein and that domain is present at the N-terminal of CvfC.

The CvfC protein sequence from *S. aureus* N315 and SAOUHSC_01438 were both used to search the Protein Family database (PFam). This database searches a protein sequence and highlights domains within the sequence. The N-terminal of CvfC contains a NifU domain and a downstream Virulence Factor domain and HEAT domain. The single domain encoded by the SAOUHSC_01438 protein sequence is also a NifU domain. Information on this domain at the EBI's Interpro website (http://www.ebi.ac.uk /interpro/) states that NifU domains are required for the formation of FeS clusters and the maturation of FeS proteins. Iron sulphur clusters are important cofactors in electron transfer and energy production (Pandelia *et al*., 2011). SAOUHSC_01438 was ruled out of any further study, as its similarity to a domain that is not directly associated with virulence does not justify inclusion. Furthermore, it is likely that it is not a secreted protein, as it was only found when the full list of VFs was searched in section 3.2.3.2. It was also not present in the results when the redundancy was removed from the list and when only signal sequence containing proteins were used.

3.2.4.1 Are the remaining hypothetical proteins exotoxins or SSLs?

The SSL protein cluster was discovered by Williams *et al.*, (2000) and initially named the staphylococcal enterotoxin cluster (set cluster; Lina *et al*., 2004). Eleven SSL genes are clustered on the genomic island √Saα (Smyth *et al*., 2007). The number of SSLs vary between strains from 7 – 11 and there is clear homology between the 11 genes (Bestebroer *et al*., 2007; Langley *et al*., 2005). This cluster is found in all strains of *S. aureus* so far tested, including isolates from 49 humans, 8 cows, 2 chickens and 2 sheep. Although the SSL cluster is found in all isolates, there is significant variation in gene number and sequence identity (Fitzgerald *et al*., 2003). Solved structures of SSL proteins show structural homology to CHIPS protein (Bestebroer *et al*., 2009). Furthermore, structures of SSL5 and SSL7 show considerable similarity to superantigens, however the MHC II binding site, used to trigger T-cell proliferation, has been lost and they do not stimulate T-cells (Arcus *et al*., 2002; Chung *et al*., 2007; Smyth *et al*., 2007). The SSL proteins contain a domain shared with superantigens, the

β-grasp domain, which is linked to an N-terminal β-barrel oligonucleotide/ oligosaccharide-binding fold (OB-fold; Arcus *et al*., 2002; Itoh *et al*., 2010b; Williams *et al*., 2000). As discussed in Chapter 1, the SSLs have varied roles in immune evasion by *S. aureus*.

Patel *et al*., 2010 reported that there are 14 SSL genes, eleven in a cluster (SSL1-SSL11) and a further triplet approximately 700kb downstream (SSL12-SSL14). The relative positioning of the hypothetical sequence triplet to the known cluster of SSLs is the same as that described by Patel *et al*. Furthermore, SAOUHSC_00354 is found in close proximity to the known cluster of eleven SSLs (~23kb upstream of the SSL cluster; Figure 3.11). To confirm that SAOUHSC_01124-5-7 and SAOUHSC_00354 are SSLs, it was decided to search for identical proteins using the identical proteins option provided by the NCBI protein database. This was unnecessary for SAOUHSC_01124-5-7 as entry of their protein IDs into the NCBI Protein database returned the updated annotation, which states that these proteins are recognised staphylococcal superantigen-like proteins (SSL12, 13 & 14).

SAOUHSC_00354 was found to be identical to the following sequences classes: enterotoxins, beta-grasp domain containing proteins, hypothetical proteins, exotoxins and SSLs. The nomenclature history for the SSLs suggests that the enterotoxins and beta-grasp domain containing proteins are in fact SSLs (Lina *et al*., 2004).

Dr Suzan Rooijakkers (University Medical School Utrecht) was contacted as an expert on SSLs. She explained that the group was working with SAOUHSC_00354 and was attempting overexpression of the protein in *Lactococcus lactis*, as *E. coli* overexpression produced very little protein. The group had also found that this SSL binds to neutrophils. Given past experience with LukAB, it was important not to duplicate efforts and so it was decided to move forward with SSL12, 13 & 14 only, as their role in pathogenesis had not been determined.

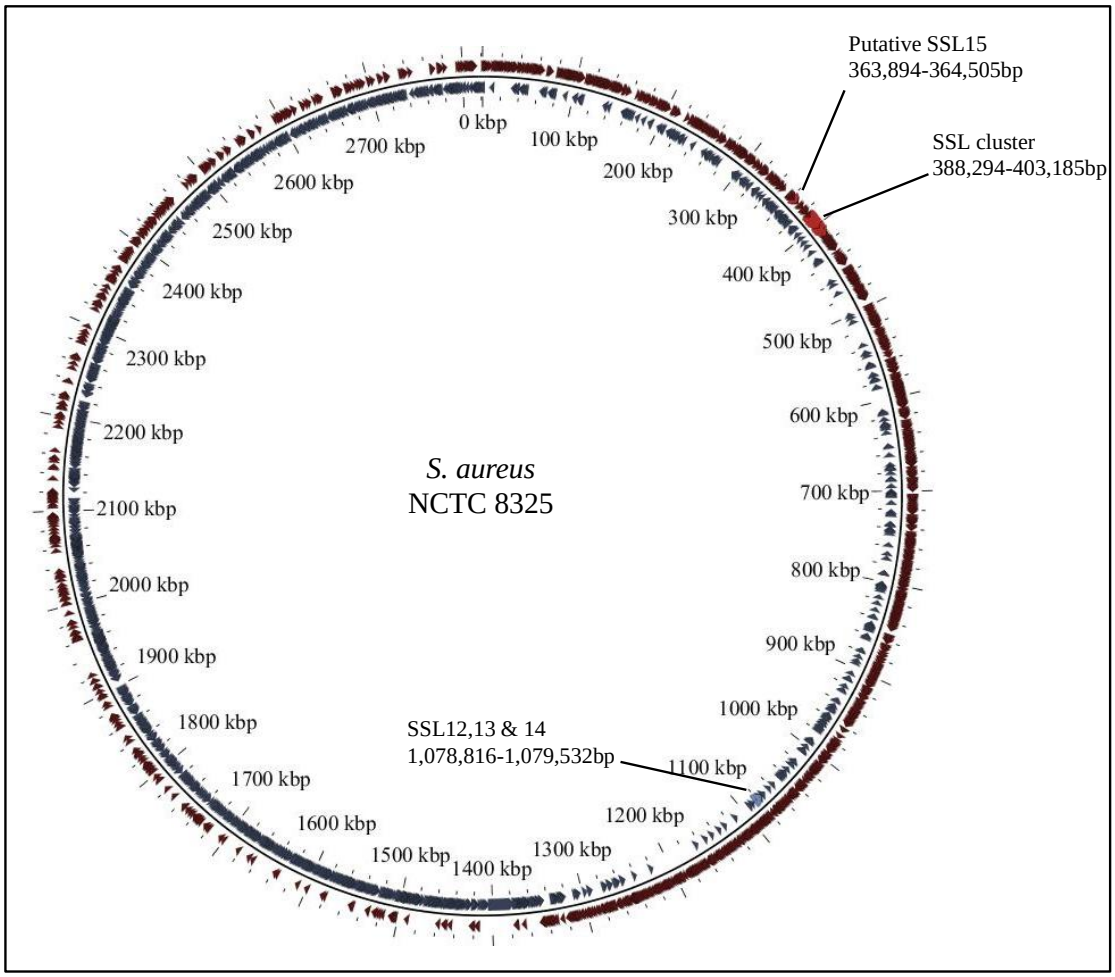

Figure 3.11 Position of SSLs on the *S. aureus* 8325 genome.

The cluster of 11 SSLs and the putative SSL15 are on the positive strand of the genome in relatively close proximity, ~23kb.

SSL12, 13 & 14 are on the negative strand approximately 700kb downstream of the SSL cluster.

3.2.5 Characterisation of SSL12, SSL13 & SSL14

3.2.5.1 The pET21d protein expression system

In order to determine the activity of SSL12, 13 & 14 recombinant protein was produced using the pET21d system. The effectiveness of the pET21d protein overexpression system relies on two things, the T7 polymerase induced by IPTG in *E. coli* strain BL21 and the pET21d plasmid encoding a T7 polymerase controlled promoter. The T7 polymerase is extremely active and can produce rRNA levels of target mRNA within three hours of activity from its promoter (Studier & Moffatt, 1986). The open reading frame (ORF) of a target gene can be inserted into the pET21d plasmid downstream of the T7 promoter and transformed into *E. coli* Top10. Transformation is confirmed by ampicillin resistance. The plasmid is then transformed into *E. coli* BL21, an *E. coli* strain containing a lysogenic phage with the T7 polymerase under the control of the IPTG inducible *lacUV5* promoter, and IPTG can be used to induce expression of the target protein. As *E. coli* does not encode T7 specific promoters, the T7 polymerase only acts on that encoded in the plasmid and the expression can be to such a high level that it makes up > 50% of the total cell protein (Studier & Moffatt, 1986). To allow recovery of the target protein, downstream of the target ORF the plasmid encodes a 6-His tag, followed by a T7 transcription termination signal. The 6-His tag allows for purification of the protein using a nickel-affinity chromatography column.

3.2.5.2 SSL12, SSL13 & SSL14 pET21d plasmid constructs

Construction of the SSL pET21d plasmids is shown in Figure 3.12. As discussed in section 3.2.3.5, secreted proteins encode an N-terminal signal sequence that is recognised by the secretion system. This signal peptide is cleaved during secretion to give the mature protein. Therefore, the forward primers were designed so as to remove the signal sequences of SSL12-13-14 (for primer sequences see Chapter 2.12.1.1). NcoI and XhoI were designed into the forward and reverse primer allowing their restriction, to insert into the multiple cloning site (MCS) within the pET21d plasmid cut with the same enzymes (Chapter 2.12.2). As the primers were designed downstream of the ORF start codon, an ATG codon was inserted into the forward primer, and two residues were inserted upstream of the ATG, between the restriction site and start codon to keep the ORF in frame. The PCR product sizes were confirmed by 1% (w/v) gel electrophoresis

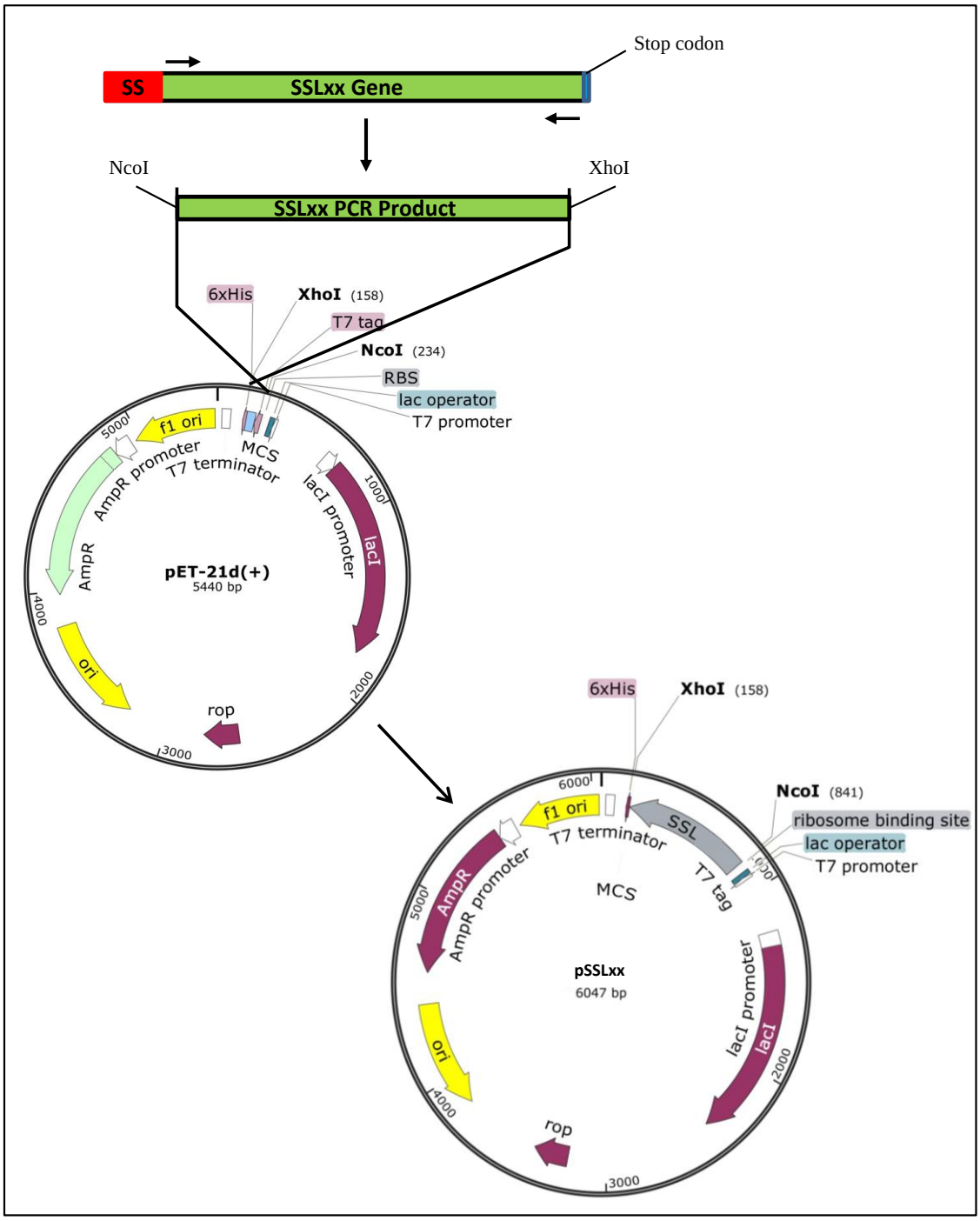

Figure 3.12 Representative construction of the pSSL plasmids.

The red box in the gene represents the signal sequence (SS). The thin blue region of the gene is the stop codon. Stop codon and SS absent from the PCR product. All steps were done in duplicate and repeated for each SSL gene to give pSSL12, pSSL13 and pSSL14.

(Chapter 2.12.5) and gel extracted with the QIAquick Gel Extraction kit (Chapter 2.11.1). Plasmid and primer DNA was then cut with NcoI and XhoI restriction enzymes and purified by gel extraction again, using the QIAquick Gel Extraction kit. The cut PCR products were ligated into cut pET21d and ethanol precipitated (Chapter 2.12.4 & Chapter 2.11.5 respectively). The ligation product was then transformed into *E. coli* Top10 (Chapter 2.9.1.2). The entire process was completed in duplicate to allow for any PCR errors.

To confirm the success of construction, plasmid DNA was extracted from the *E. coli* Top10 using the QIAprep Spin Mini kit (Chapter 2.11.4). Extracted plasmid DNA was digested with NcoI and XhoI and expected fragments were confirmed by gel electrophoresis (Figure 3.13). Plasmid inserts were sequenced at the Core Genomic Facility, University of Sheffield (for sequencing primers see Chapter 2.12.1.1) to confirm the correct sequence (see Appendix 3.5 for sequence data). One sequence from each duplicate was correct. This recombinant plasmid was transformed into *E. coli* BL21 from *E. coli* Top10 (Chapter 2.9.1.2).

3.2.5.3 Protein overexpression of SSL12, 13 & 14 in *E. coli* BL21

Cultures of *E. coli* BL21 containing each plasmid were prepared and protein expression was carried out (Chapter 2.15.1). Expression was induced for 4 h at 37^{o}C in mid-exponential cultures by addition of IPTG. Samples were taken before and after IPTG addition to assess the level of expression. To determine if the proteins were soluble or insoluble, samples were taken after IPTG induction. Cells were disrupted in both samples and centrifuged, the supernatant contained any soluble protein and the pellet contained the insoluble protein. To determine solubility, samples were assessed by electrophoresis on an 11% (w/v) SDS-PAGE gel, which was stained with Coomassie Blue (Chapter 2.14.1 and Chapter 2.14.2, respectively). Protein was found to be overexpressed in IPTG induced samples and found in the insoluble fraction for all SSLs (Figure 3.14).

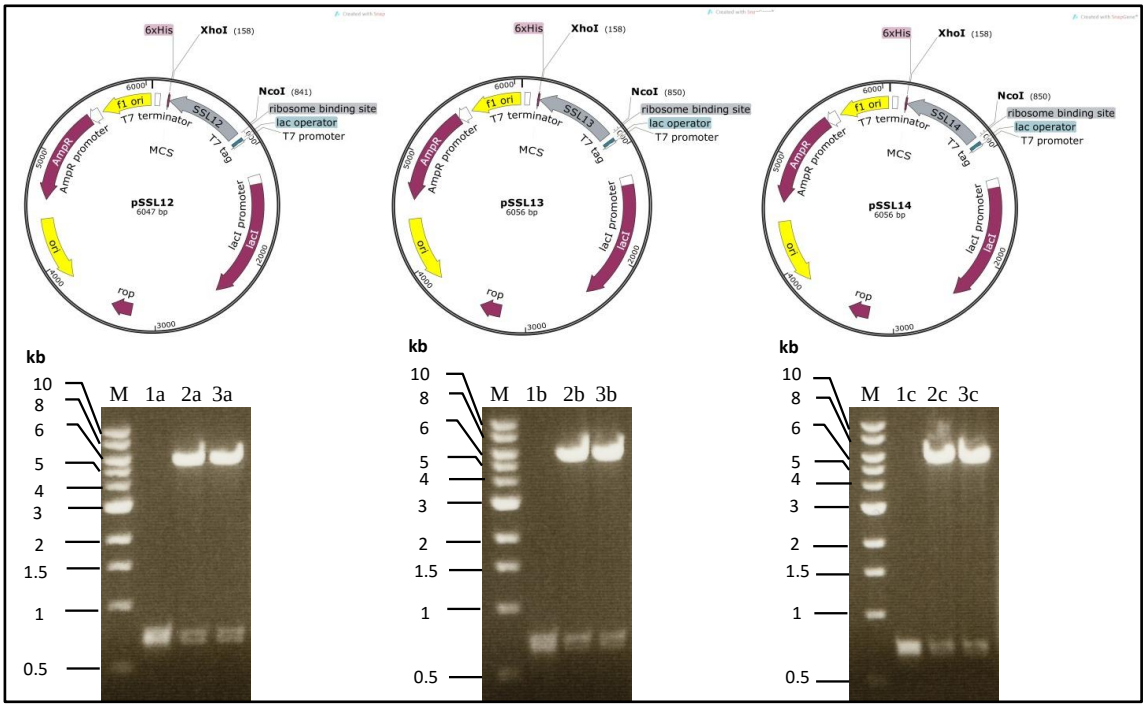

Figure 3.13 Confirmation of correct construct insert sizes for recombinant SSL production.

DNA fragments were separated by 1% (w/v) agarose gel electrophoresis. Standards (M) of sizes shown are in each panel.

Lanes 1a, 1b and 1c are PCR products for SSL12, SSL13 and SSL14 respectively. Lanes 2a/3a, 2b/3b and 2c/3c are digested construct from each duplicate.
Expected bands of ~700bp for the insert and 5,440bp for pET21d are shown.

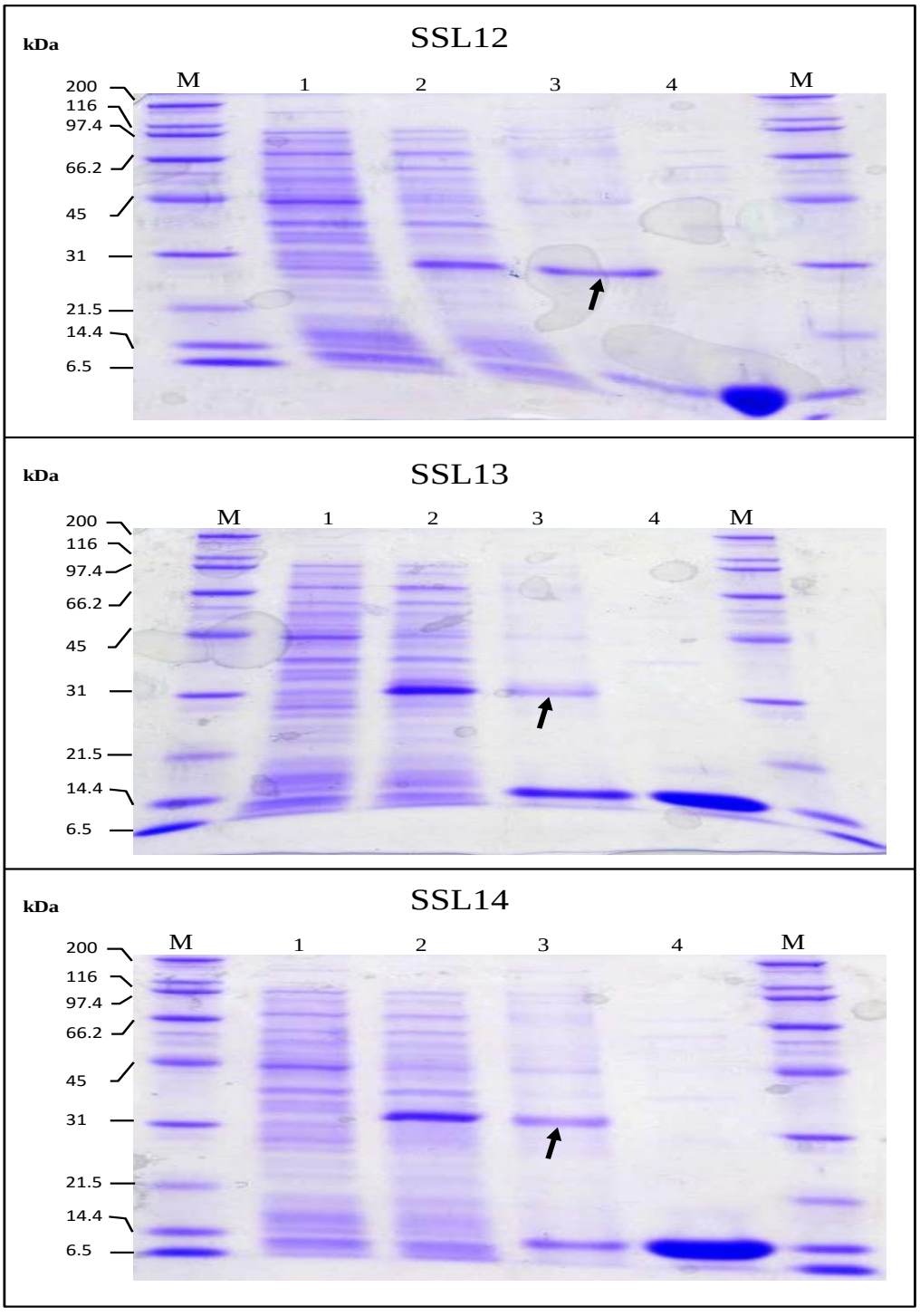

Figure 3.14 Overexpression and solubility of SSL12, 13 & 14.

Protein samples were separated by 11% (w/v) SDS-PAGE. Markers (M) of sizes shown are present on each gel.

Lane 1. Uninduced sample.

Lane 2. Induced sample.

Lane 3. Insoluble protein (arrows indicate protein).

Lane 4. Soluble protein (no overexpressed protein was found in the soluble fractions).

3.2.5.4 Effect of induction temperature and induction time on solubility

Soluble protein is required to characterise the activity of the SSLs (e.g. binding assays with immune molecules or cells etc.). For this reason attempts were made to induce production of soluble protein. As discussed in section 3.2.5.3, cultures of *E. coli* BL21 expressing SSL12, 13 or 14 were grown to mid-exponential at 37^{o}C, at which point IPTG was added to induce protein expression and the cultures were grown for another 4 h at 37^{o}C. 37^{o}C is the standard temperature for growth of *E. coli*. The assumption made from the results in section 3.2.5.3 was that as *E. coli* grows at this temperature it produces too high a level of SSL protein from the T7 promoter, and as it is rapidly translated it forms aggregates leading to insoluble protein. The hypothesis was that if the growth temperature was reduced to 30^{o}C and 25^{o}C then growth would slow and production of protein would become more manageable for the bacteria. An additional time point of 18 h was used allowing for slowing production of protein and the experiment was carried-out in 250 ml conical flasks using 100 ml culture volume (Figure 3.15). Soluble protein, at equivalent levels to the expressed insoluble protein, was found to be produced at 30^{o}C after 4 h IPTG induction (Figure 3.15B, lane 4).

3.2.5.5 Overexpression of the SSLs at 30^{o}C in a 3 litre culture

A large amount of protein was required to fully characterise the SSL proteins. Soluble protein was found to be produced at 30^{o}C; however, the majority of protein even at this temperature was in the insoluble fraction (Figure 3.12, lanes 3&5). Therefore, the overexpression of SSLs was scaled up to 3 litre cultures grown at 30^{o}C in order to provide enough material for protein characterisation. However, none of the 3 litre cultures produced soluble protein (Figure 3.16, lane 4).

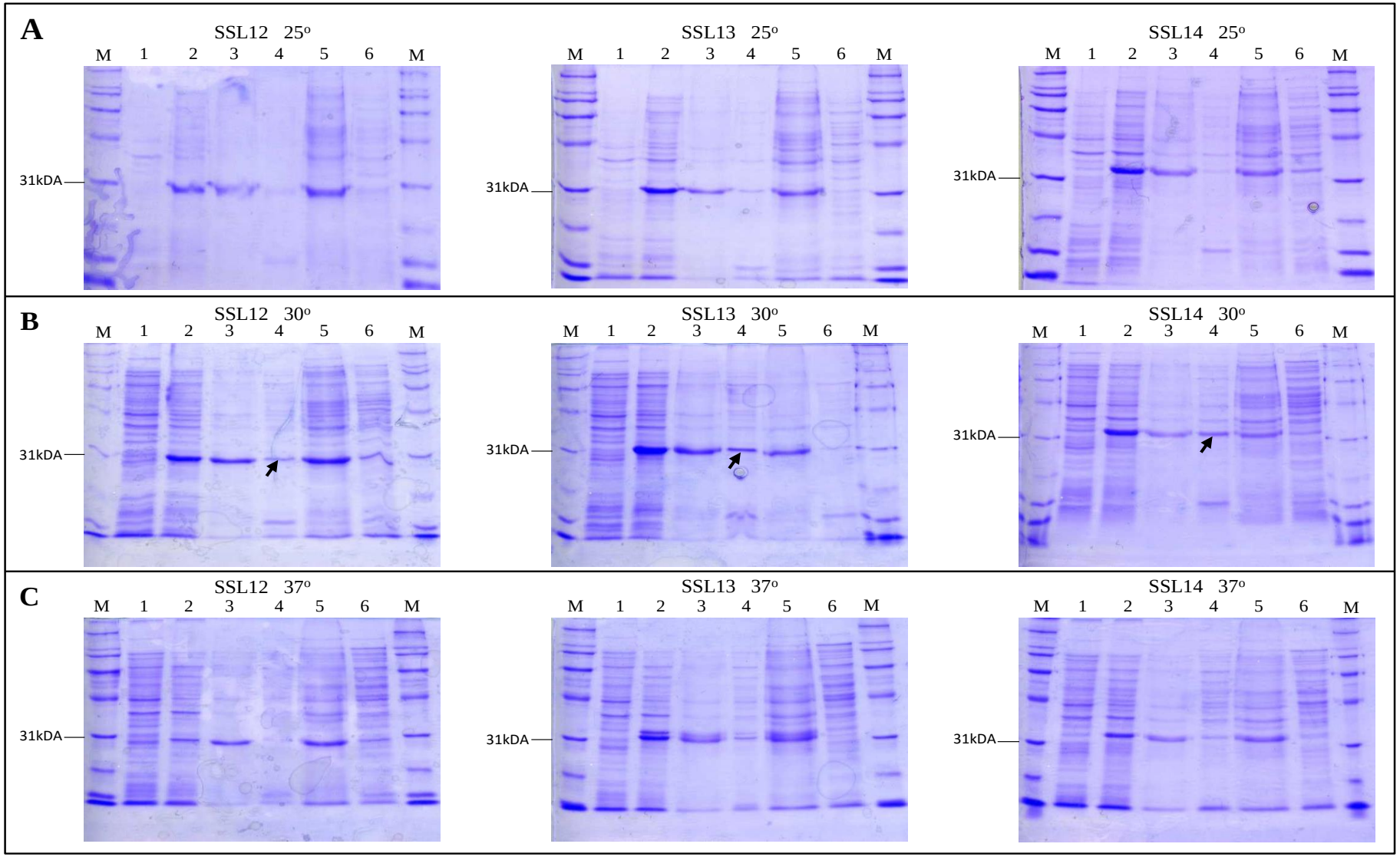
A
SSL12 25º
M 1 2 3 4 5 6 M
31kDA
SSL13 25º
M 1 2 3 4 5 6 M
31kDA
SSL14 25º
M 1 2 3 4 5 6 M
31kDA
B
SSL12 30º
M 1 2 3 4 5 6 M
31kDA
SSL13 30º
M 1 2 3 4 5 6 M
31kDA
SSL14 30º
M 1 2 3 4 5 6 M
31kDA
C
SSL12 37º
M 1 2 3 4 5 6 M
31kDA
SSL13 37º
M 1 2 3 4 5 6 M
31kDA
SSL14 37º
M 1 2 3 4 5 6 M
31kDA

Figure 3.15 Effect of temperature on SSL solubility.

Protein samples were separated by 11% (w/v) SDS-PAGE. Markers (M) with relevant size shown are present on each gel.

Arrows indicate soluble protein bands at 30^{o}C.

A. IPTG induction at 25^{o}C.

B. IPTG induction at 30^{o}C.

C. IPTG induction at 37^{o}C.

Lane 1. Uninduced samples.

Lane 2. Induced sample.

Lane 3. Insoluble protein produced after 4 h induction.

Lane 4. Soluble protein produced after 4 h induction.

Lane 5. Insoluble protein produced after 18 h induction.

Lane 6. Soluble protein produced after 18 h induction.

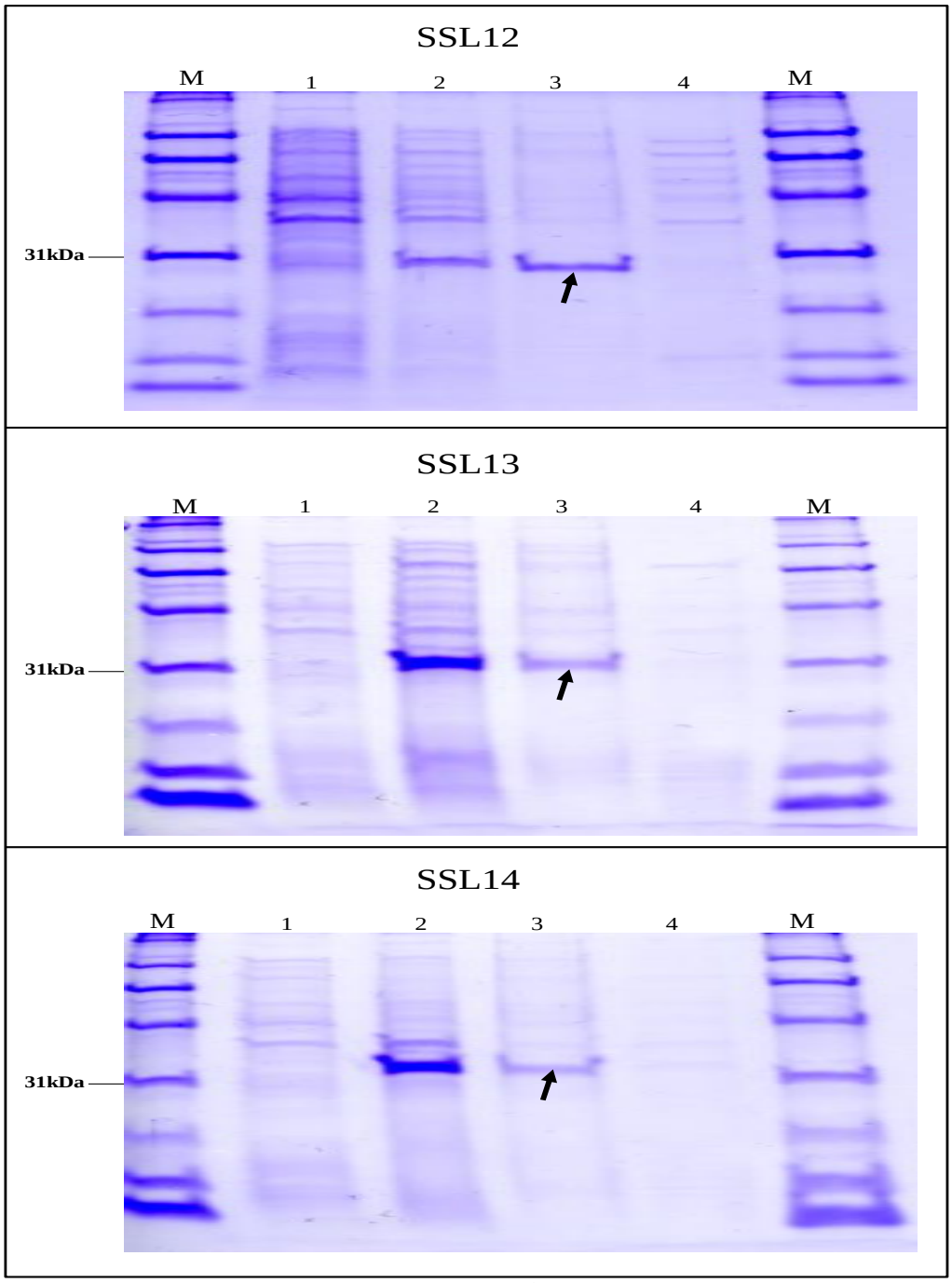

Figure 3.16 Overexpression of SSLs at 30^{o}C using a higher culture volume.
Protein samples were separated by 11% (w/v) SDS-PAGE. Markers (M) with relevant size shown are present on each gel.

Lane 1. Uninduced sample.

Lane 2. Induced sample.

Lane 3. Insoluble protein (arrows indicate protein).

Lane 4. Soluble protein (no overexpressed protein was found in the soluble fractions).

3.2.5.6 Overexpression of the SSLs at 30°C in 4 x 250 ml cultures

Expression of soluble protein at 30°C was successful using 250 ml conical flask and 100 ml of culture (section 3.2.4.4). However, the volume was not enough for characterisation and since large volume cultures did not produce soluble protein, attempts were made to produce enough protein for characterisation using multiple small cultures. Protein overexpression was done using the same condition as in section 3.2.4.4, but with multiple conical flasks and only 4 h IPTG induction. Inconsistent expression of soluble protein was seen and in lanes that do show soluble protein it is only a small amount when compared to the insoluble protein (Figure 3.17). Therefore it was concluded that this method does not provide a consistent source of soluble SSL protein.

3.2.5.7 Purification of insoluble SSL12, 13 & 14 protein in the presence of 8M urea

Insoluble SSL protein, from a 100 ml culture induced with IPTG, was purified by nickel affinity chromatography using a nickel charged HiTrap™ column (Chapter 2.15.4). Charging the column with nickel facilitates the interaction of the column with the C-terminal 6-His tag added to the recombinant protein. For affinity chromatography to work, the protein must be soluble, therefore 8M urea was added to all buffers, which increases the capacity for solubilisation of protein by H_2O (Bennion & Daggett, 2003). The protein was passed through the column in START buffer. Unbound protein was then removed from the column by passing elution buffer containing 5% (w/v) imidazole through the column. Gradually increasing imidazole concentration over a 1 h time period allowed for elution of the recombinant protein. Elutions were collected every minute in 1 ml aliquots and the presence of protein was confirmed by 11% (w/v) SDS-PAGE (Figure 3.18). Those elutions containing protein were pooled to give a stock of SSL12, SSL13 and SSL14. The approximate volume of eluted protein varied from 5-9 ml.

3.2.5.8 Refolding of protein samples by stepwise dialysis

Dialysis of protein samples to gradually reduce the concentration of urea in samples was used to refold the insoluble proteins into a soluble form (Chapter 2.15.5.2). Initially

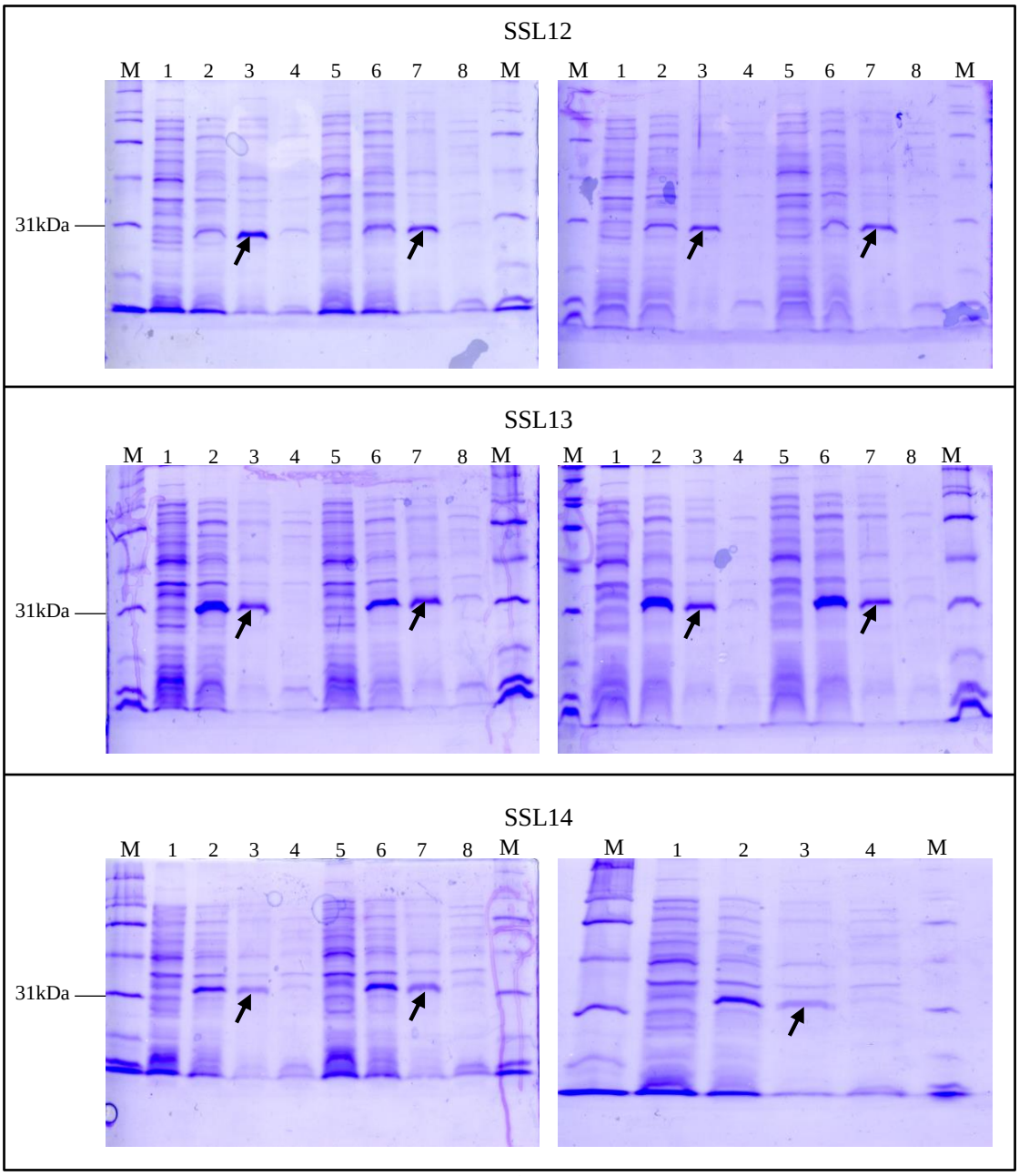

Figure 3.17 Overexpression of SSLs at 30^{o}C using multiple low volume cultures. Protein samples were separated by 11% (w/v) SDS-PAGE. Markers (M) with relevant size shown are present on each gel.

Lanes 1&5. Uninduced sample.

Lanes 2&6. Induced sample.

Lanes 3&7. Insoluble protein (arrows indicate protein).

Lanes 4&8. Soluble protein (no overexpressed protein or low level overexpressed protein was found in the soluble fractions).

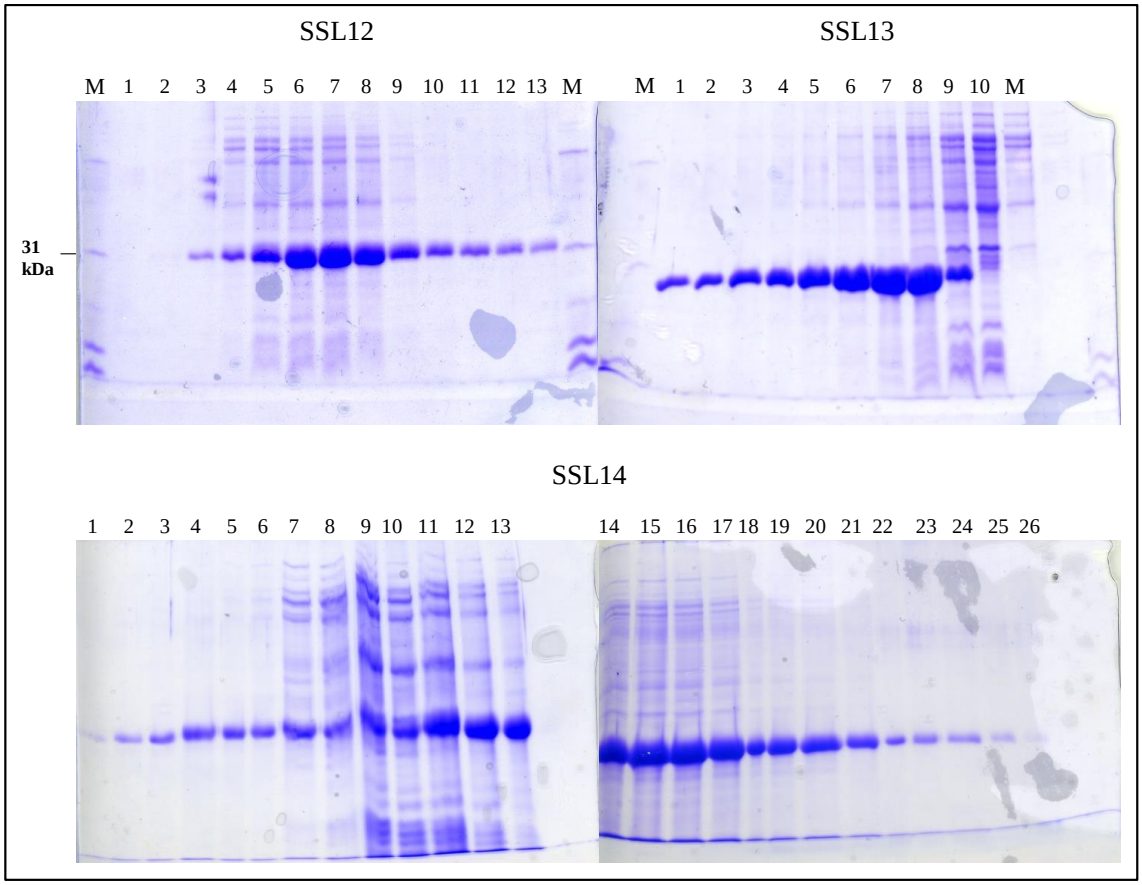

Figure 3.18 Purification of urea solubilised SSL protein and elution into separate 1 ml samples.

Protein samples were separated by 11% (w/v) SDS-PAGE. Markers (M) with relevant size shown.

Each lane contains 10 µl from 1 ml elution samples.

Samples from lanes containing protein were retained and pooled:

SSL12 lanes 5-9, pooled volume = ~5 ml.

SSL13 lanes 3-8, pooled volume = ~6 ml.

SSL14 lanes 12-20, pooled volume = ~9 ml.

PBS + 8M urea was used as the buffer and the aim was to remove the urea using the following sequence every 12 h: 6M, 4M, 3M, 2M, 1M, 0.5M, 0M urea. However, the protein precipitated at 3M urea concentration.

An alternative means of solubilising insoluble protein is 6M guanidine. SSL13 was again overexpressed and purified using guanidine rather than urea. Dialysis using decreasing concentrations of guanidine was used starting at 4M. However, again at 3M guanidine the protein precipitated.

3.2.5.9 Refolding protein by dilution in the presence of L-Arg

Dilution is an alternative method of protein renaturation to dialysis. Whereas in dialysis the sample is kept separate from the buffer by dialysis tubing (Chapter 2.15.5.1), in the dilution method the sample is added directly to the buffer to allow refolding, then concentrated (Chapter 2.16). An initial attempt was made using H_2O as the buffer. No soluble protein was found after dilution or after concentration of the diluted sample (data not shown).

L-Arg as an additive to dilution buffers was shown to enhance refolding of Sak protein fragments (He *et al*., 2008). Using an L-Arg Base Refolding Buffer containing 880 mM L-Arg (Chapter 2.5.5.1), 1 ml of pooled SSL12, SSL13 and SSL14 elutions (eluted from the HiTrap™ column as in section 3.2.5.7; Figure 3.18) were diluted 20-fold by slowly dripping the samples into refolding buffer. Only 1 ml of the total pooled elution samples was diluted, to prevent loss of the full 5-9 ml of eluted protein (Figure 3.18). Samples were then concentrated using an Amicron Ultra Centrifugal Filter. After centrifugation to remove any insoluble material, the concentrated samples were analysed by electrophoresis of 10 µl using an 11% (w/v) SDS-PAGE gel (Figure 3.19A). Soluble protein was found for each SSL.

As the method produced soluble protein it was repeated by dilution of 1 ml of eluted protein sample or 3 ml of eluted protein sample, collected as in section 3.2.5.7. This was done to determine if a higher soluble protein concentration could be achieved, without causing aggregation upon concentration with the Amicron filter. Concentrated samples were analysed by electrophoresis of 10 µl of each concentrated sample on an 11% (w/v)

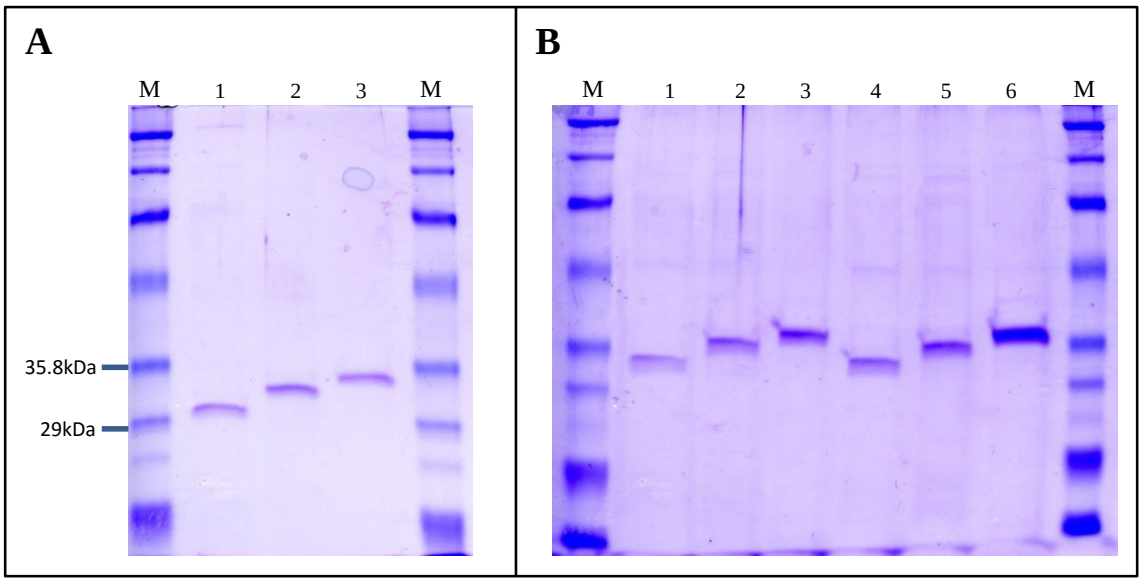

Figure 3.19 Solubilisation of recombinant SSL protein using 880 mM L-Arg.

Protein samples were separated by 11% (w/v) SDS-PAGE. Markers (M) with relevant size shown are present on each gel.

A. Each lane contains 10 µl (80% of total) of soluble protein sample, produced by dilution refolding of 1 ml of HiTrap™ eluted protein in 880 mM L-Arg buffer.
Lane 1 = SSL12, lane 2 = SSL13, lane 3 = SSL14.

B. Lanes 1-3 contain 10 µl (80% of total) of soluble protein sample, produced by dilution refolding of 1 ml of HiTrap™ eluted protein in 880 mM L-Arg buffer.
Lanes 4-6 contain 10 µl (80% of total) of soluble protein sample, produced by dilution refolding of 3 ml of HiTrap™ eluted protein in 880 mM L-Arg buffer.
Lane 1&4 = SSL12, lane 2&5 = SSL13, lane 3&6 = SSL14.

SDS-PAGE gel (Figure 3.19B). A low volume of protein was collected for each sample, the majority of which was loaded onto the SDS-PAGE gel. For this reason, difference in soluble protein yield could only be determined from the appearance of bands on the SDS-PAGE gel. It is clear from the image (Figure 3.19B) that dilution of 3 ml of eluted protein sample (lanes 4-6) produced more soluble protein than dilution of 1 ml of eluted protein sample (lanes 1-3). This demonstrated that higher concentrations of soluble protein could be acquired by dilution of higher volumes of the protein eluted from HiTrap™ columns.

The problem with using L-Arg is that the concentration of L-Arg is very high and may interfere with downstream SSL characterisation experiments (i.e. the purpose of purifying the SSLs). To that end, the above experiment was repeated using 10-fold less L-Arg (Figure 3.20). Considerably less protein was recovered in a soluble form at this L-Arg concentration.

3.2.5.10 Refolding protein by dilution in the presence of L-Arg and L-Glu

L-Arg and L-Glu have also been shown to enhance the performance of purification buffers and enhance the stability of the protein during storage (Golovanov *et al*., 2004). Enhanced refolding is thought to be due to the L-Arg/L-Glu crowding hydrophobic regions of the protein, allowing time for the proteins to fold in such a way that the hydrophobic residues are housed within the hydrophobic core of the protein. Golovanov used 50 mM L-Arg and 50 mM L-Glu in their buffers, therefore the same concentration was added to the Base Refolding Buffer (Chapter 2.5.5.2).

Each SSL protein was overexpressed in a 1.5 litre culture volume. The insoluble protein was solubilised with 8M urea and purified by Nickel-affinity chromatography, in the presence of urea as in section 3.2.5.7. Approximately 7 ml of each SSL was eluted from the HiTrap™ columns, as in Figure 3.18. The full 7 ml of each eluted SSL protein was drip-diluted 20-fold into 50 mM L-Arg and L-Glu buffer. Samples were stored at 4^{o}C to allow refolding overnight, followed by concentration of the diluted samples using an Amicon Ultra centrifugal filter. Residual insoluble protein was removed by centrifugation. 10 µl of the 7 ml elution sample, 10 µl of the 20-fold diluted sample and 10 µl of the concentrated samples were analysed for each SSL protein by

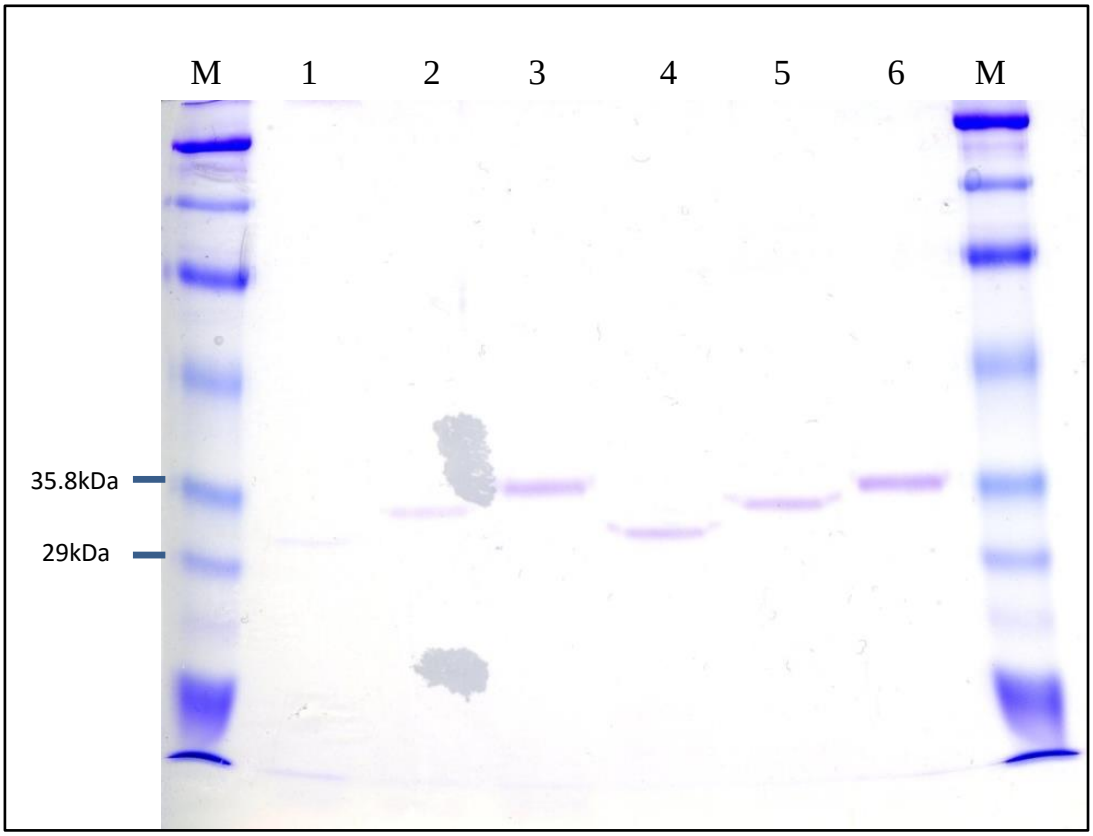

Figure 3.20 Solubilisation of recombinant SSL protein using 88 mM L-Arg.

Protein samples were separated by 11% (w/v) SDS-PAGE. Markers (M) with relevant size shown are present on each gel.

Lanes 1-3 contain 10 µl (80% of total) of soluble protein sample, produced by dilution refolding of 1 ml of HiTrap™ eluted protein in 88 mM L-Arg buffer.
Lanes 4-6 contain 10 µl (80% of total) of soluble protein sample, produced by dilution refolding of 3 ml of HiTrap™ eluted protein in 88 mM L-Arg buffer.
Lane 1&4 = SSL12, lane 2&5 = SSL13, lane 3&6 = SSL14.

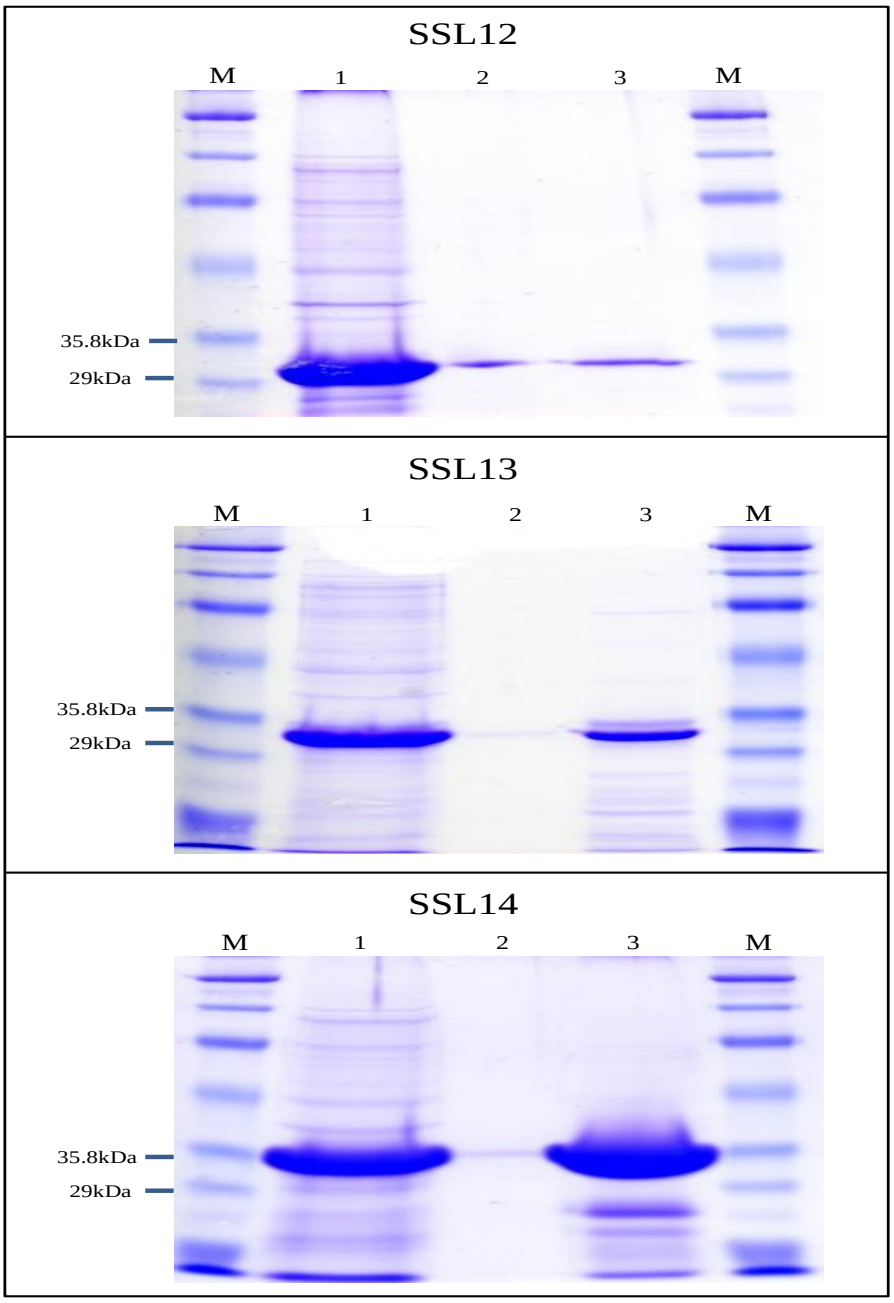

Figure 3.21 Solubilisation of recombinant SSL protein using L-Arg and L-Glu. Protein samples were separated by 11% (w/v) SDS-PAGE. Markers (M) with relevant size shown are present on each gel.

Lane 1. 10 µl of urea solubilised SSL protein taken from the pooled HiTrap™ elution samples.

Lane 2. 10 µl of soluble SSL protein from the pooled HiTrap™ elution samples after 20-fold dilution in L-Arg/L-Glu refolding buffer.

Lane 3. 10 µl (80% of total) of soluble SSL protein after Amicron concentration of the diluted sample.

electrophoresis on an 11% (w/v) SDS-PAGE gel (Figure 3.21). From the protein in Figure 3.21 (lane 3) for each SSL it is clear that the method of protein folding works and works most efficiently for SSL14. However, from a 1.5 litre culture, between 10 and 12 µl of purified protein was produced. Indeed the volume was so low that the majority of it was used to prepare the SDS-PAGE gels in Figure 3.21, preventing quantification of protein yield. Therefore, it was decided that an alternative method of SSL characterisation was required.

3.2.5.11 Construction of the SSL triplet deletion plasmid

In order to determine a role for the SSLs in host pathogen interaction a triplet mutant was created. The deletion plasmid construction method is shown diagrammatically in Figure 3.22. A 1.2kb fragment immediately upstream of the SSL triplet (UF) was amplified by PCR using primers FU and RU (for PCR method and primers see Chapter 2.12.1.2 and Chapter 2.12.1.1, respectively). The FU primer encodes a KpnI restriction site and RU encodes a SalI restriction site. The plasmid pOB encoding erythromycin resistance was used as the deletion vector. The plasmid and upstream fragment were digested with KpnI and SalI (Chapter 2.12.2) and ligated together (Chapter 2.12.4). Ligations were ethanol precipitated (Chapter 2.11.5) and transformed into *E. coli* Top10 (Chapter 2.9.1.1), giving plasmid pOB-UF. Plasmid DNA was extracted using the QIAprep Spin Mini kit (Chapter 2.11.4) and digested with KpnI and SalI and the presence of the UF fragment was confirmed by 1% (w/v) gel electrophoresis (Chapter 2.12.5; Figure 3.23A). The 1.2kb fragment immediately downstream of the SSL triplet (DF) was then amplified using primers FD and RD, encoding a SalI cut site in FD and a SphI cut site in RD. Plasmid pOB-UF and downstream fragment were digested with SalI and SphI and ligated as above. The precipitated ligation product was used to transform *E. coli* Top10, giving pOB-UF-DF. Plasmid DNA was extracted using the QIAprep Spin Mini kit and digested with SphI and SalI and the presence of the DF fragment was confirmed by 1% (w/v) gel electrophoresis (Figure 3.23B).

The kanamycin resistance cassette from the plasmid pGL485 (Liew *et al*., 2011) was amplified with primers KanF and KanR (Chapter 2.12.1.1), both encoding a SalI restriction site. The Kan^R cassette was spliced in between the UF and DF fragments, by

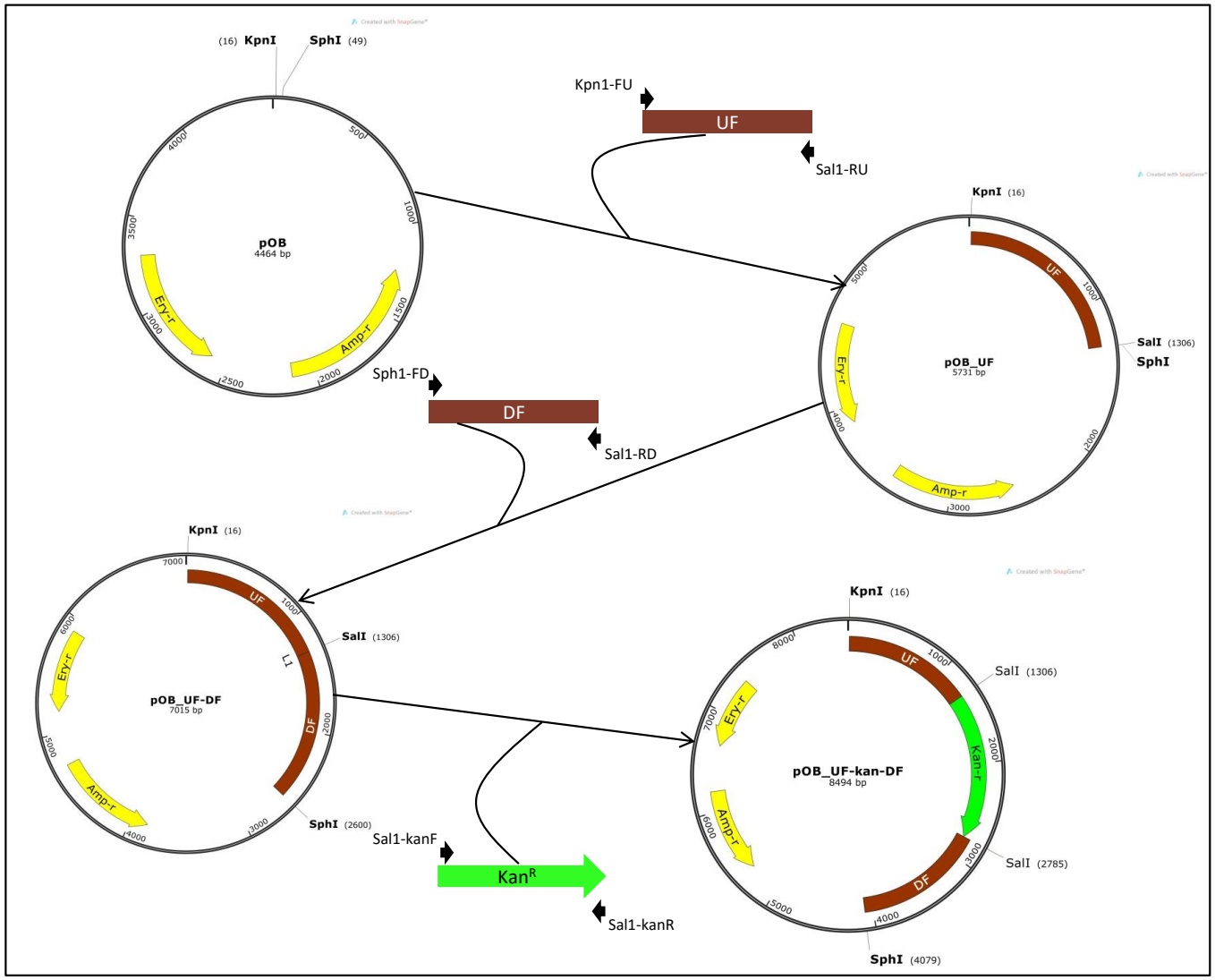

Figure 3.22 Construction of the SSL deletion plasmid.

UF = 1.2kb PCR fragment amplified from immediately upstream of the SSL triplet. DF = 1.2kb PCR fragment amplified from immediately downstream of the SSL triplet. The Kan^R cassette was amplified from pGL485. Primer FU, RU, FD, RD, KanF, KanR encode the restriction sites required to insert the fragments into the pOB plasmid.

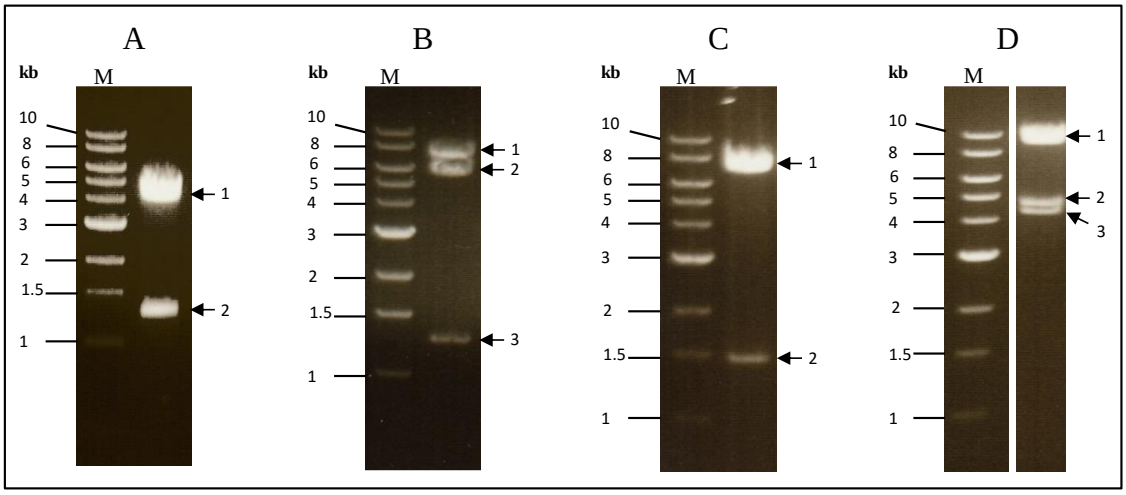

Figure 3.23 Confirmation of successful construction of the SSL deletion plasmid.

DNA fragments were separated by 1% (w/v) agarose gel electrophoresis. Standards (M) of sizes shown are in each panel.

A. pOB-UF digested with KpnI and SalI.

Arrow 1. Digested plasmid, 4,464 bp.

Arrow 2. UF fragment 1,288 bp.

B. pOB-UF-DF digested with SphI and SalI.

Arrow 1. Undigested plasmid, 7,036 bp.

Arrow 2. Digested plasmid, 5,752 bp.

Arrow 3. DF fragment 1,284 bp.

C. pOB-UF-Kan-DF digested with SalI.

Arrow 1. Digested plasmid, 7,036 bp.

Arrow 2. Kan cassette 1,473 bp.

D. pOB-UF-Kan-DF digested with KpnI & SphI.

Arrow 1. Undigested plasmid, 8,509 bp.

Arrow 2. Digested plasmid, 4,464.

Arrow 3. Full insert 4,045 bp.

digesting the amplified cassette and pOB-UF-DF with SalI and ligating as in Chapter 2.12.4. The ligation product was used to transform *E. coli* Top10 to give the pOB-UF-Kan-DF deletion construct. The successful integration of Kan^R was confirmed by 1% (w/v) gel electrophoresis of the purified plasmid digested with SalI (Figure 3.23C). The plasmid DNA was digested separately with KpnI and SphI to confirm the presence of the full insert (Figure 3.23D). For primer sequences see Chapter 2.12.1.1.

3.2.5.12 Deletion of the SSL triplet from *S. aureus* NewHG

The method of deletion is shown diagrammatically in Figure 3.24. The pOB-UF-Kan-DF plasmid was extracted from *E. coli* Top10 and used to transform electrocompetent RN4220 (Chapter 2.9.2.2). RN4220 is a restriction negative modification positive strain of *S. aureus*. Single crossover homologous recombination occurs between the upstream or downstream region of the RN4220 copy of the triplet and the upstream or downstream copy on the pOB-UF-Kan-DF plasmid. The plasmid is incorporated into the RN4220 genome, conveying resistance to kanamycin and erythromycin (Figure 3.24A). The merodiploid can then be resolved by phage transduction using Φ11 bacteriophage (Chapter 2.10.3). Successful resolvant transductants will be kanamycin resistant, due to the Kan^R cassette replacing the SSLs and erythromycin sensitive, due to loss of the plasmid insertion. PCR (Chapter 2.12.1.2; Figure 3.24B) and Southern hybridisation (Chapter 2.13) were used to confirm successful SSL deletion. For the PCR analysis five sets of primers were used: 01124-F and 01124-R, a positive control to confirm the presence of SSL12 in the wild-type DNA, also confirms the absence of SSL12 in NewHGΔSSL DNA, 01125-F and 01125-R; 01127-F and 01127-R, confirm the absence of SSL13 and 14, respectively, in NewHGΔSSL DNA, isdA-F and isdA-R used as a positive control for *S. aureus* genomic DNA, Kan-F and Kan-R confirm the presence of the Kan^R cassette in NewHGΔSSL. Amplification products of expected sizes were found (Figure 3.25A). For primer sequences see Chapter 2.12.1.1. The Southern hybridisation analysis is shown in Figure 3.25B, C & D, genomic DNA of the correct sizes for SSL deletion were probed.

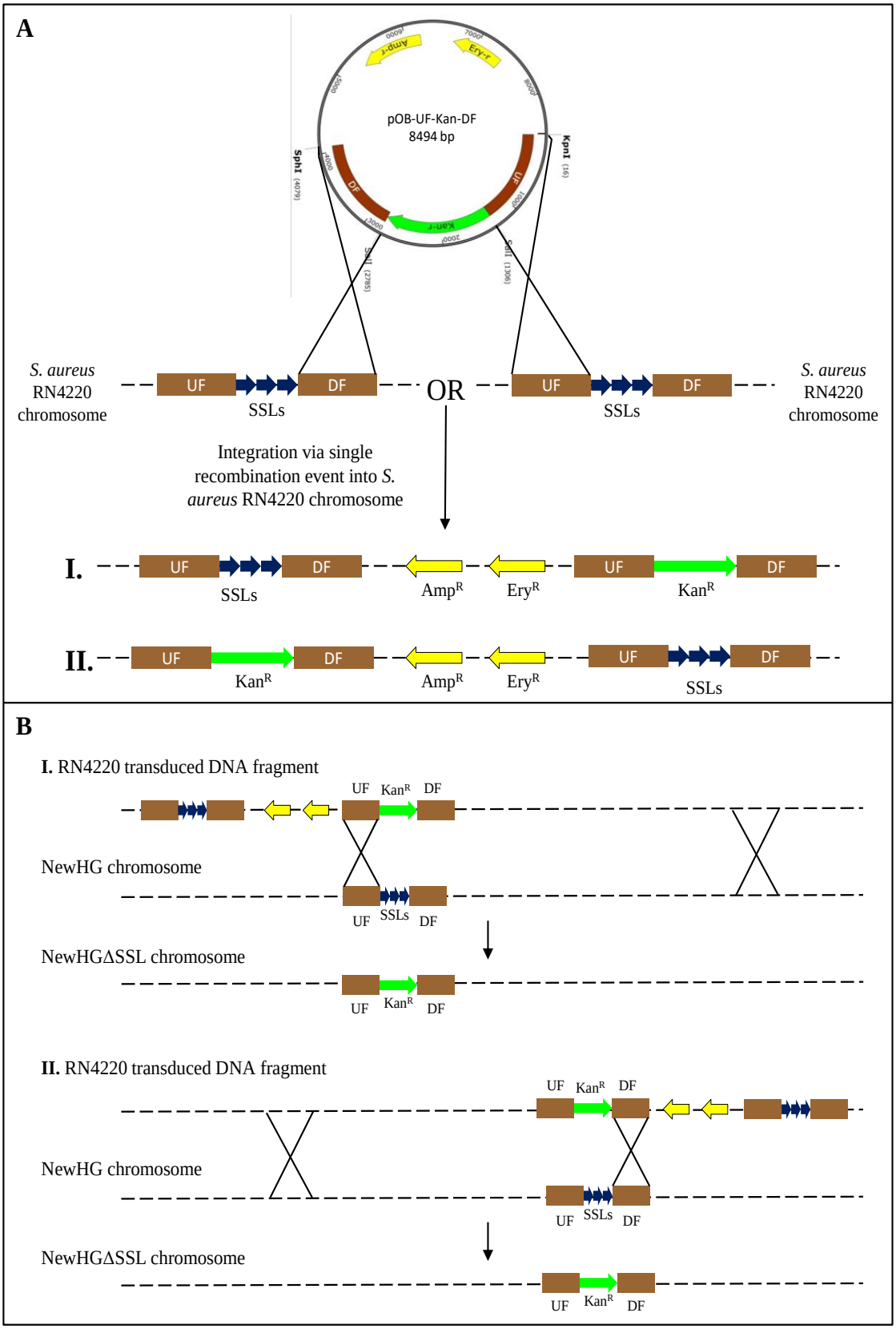
A
pOB-UF-Kan-DF
8494 bp
Amp-r
Ery-r
Kan-r
UF
DF
KpnI (16)
SphI (4076)
SalI (2785)
SbfI (1306)
S. aureus RN4220 chromosome
UF
DF
SSLs
OR
UF
DF
SSLs
S. aureus RN4220 chromosome
Integration via single recombination event into S. aureus RN4220 chromosome
I.
UF
DF
SSLs
AmpR
EryR
UF
DF
KanR
II.
UF
DF
KanR
AmpR
EryR
UF
DF
SSLs
B
I. RN4220 transduced DNA fragment
UF KanR DF
NewHG chromosome
UF SSLs DF
NewHGΔSSL chromosome
UF KanR DF
II. RN4220 transduced DNA fragment
UF KanR DF
NewHG chromosome
UF SSLs DF
NewHGΔSSL chromosome
UF KanR DF

Figure 3.24 Deletion of the SSL triplet shown diagrammatically.

A. Integration of the pOB-UF-Kan-DF plasmid into the *S. aureus* RN4220. Integration can occur either via single crossover events between the UF or the DF fragments of the pOB-UF-Kan-DF plasmid and the UF or DF fragments of the RN4220 genome.

B. Deletion of the SSL triplet by double crossover between either of the two possible integrations transduced into *S. aureus* NewHG. This results in loss of the Ery^R plasmid.

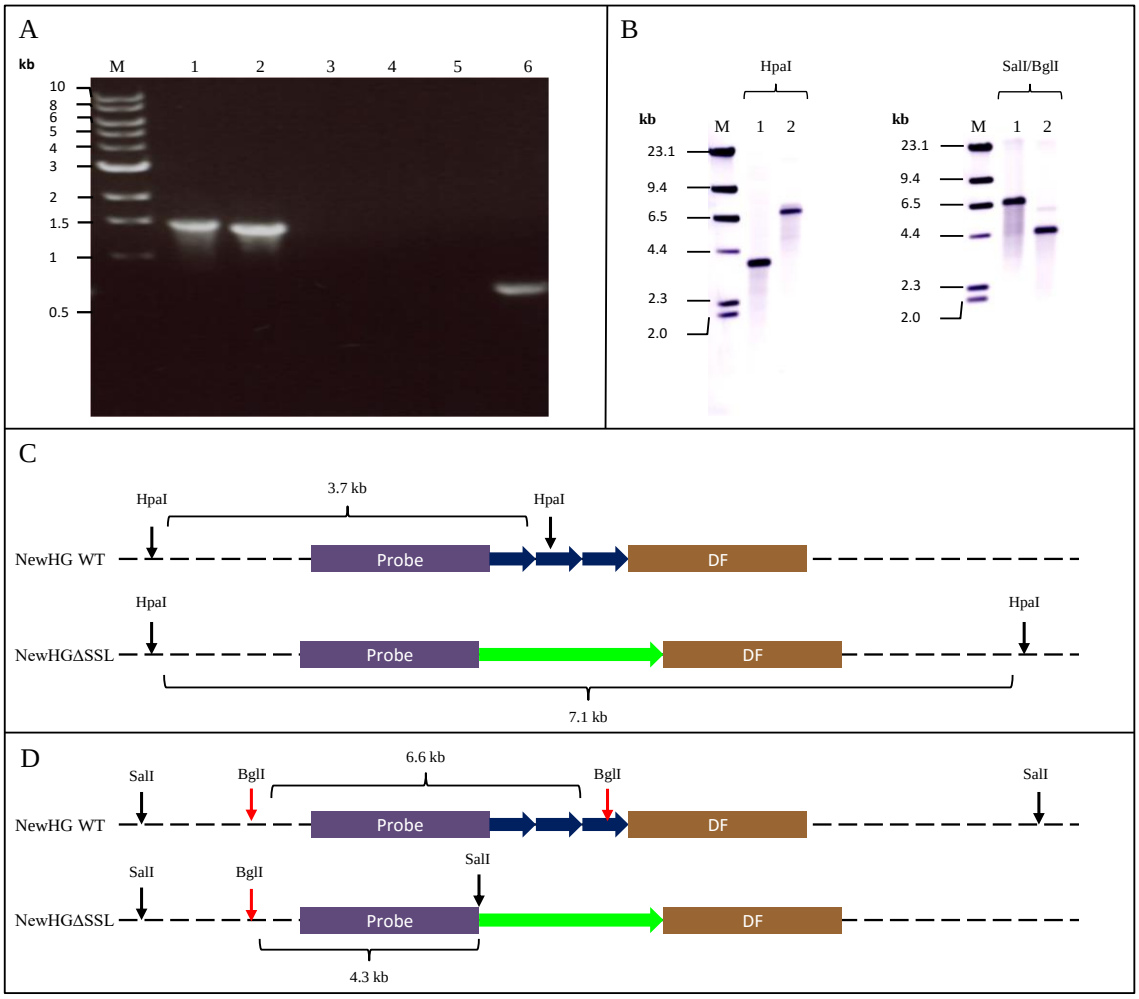

Figure 3.25 Confirmation of deletion of the SSL triplet from *S. aureus* NewHG.

DNA fragments were separated by 1% (w/v) agarose gel electrophoresis. Standards (M) of sizes shown are in each panel.

A. PCR confirmation of SSL deletion. **Lane 1**. NewHGΔSSL gDNA amplified with Kan-F' & Kan-R', **Lane 2**.NewHGΔSSL gDNA amplified with isdA-F' & isdA-R', **Lane 3-5**. NewHGΔSSL gDNA amplified with ssl12-F' & ssl12-R'; ssl13-F' & ssl13-R'; ssl14-F' & ssl14-R', respectively **Lane 6**. NewHG gDNA amplified with ssl12-F' & ssl12-R'. **B**. Southern hybridisation confirmation of SSL deletion. **HpaI lane 1**. NewHG genomic DNA cut with HpaI and probed with the UF fragment (expected product size 3.7 kb), **HpaI lane 2**. NewHGΔSSL genomic DNA cut with HpaI and probed with the UF fragment (expected product size 7.1 kb), **SalI/BglI lane 1**. NewHG genomic DNA cut with SalI/BglI and probed with the UF fragment (expected product size 6.6 kb), **SalI/BglI lane 2,** NewHGΔSSL genomic DNA cut with SalI/BglI and probed with the UF fragment (expected product size 4.3 kb). **C**. HpaI restriction digestion shown diagrammatically. **D**. SalI/BglI restriction digestion shown diagrammatically.

3.2.5.13 Growth characteristics of NewHGΔSSL

Before comparison of virulence of the SSL mutant strain with the wild-type strain, it was essential to know that growth rate in standard conditions of growth was not affected by the SSL deletion. A growth curve in BHI was carried-out to compare growth of NewHG and NewHGΔSSSL (Figure 3.26A). Growth was also compared in foetal bovine serum (Figure 3.26B). Growth of NewHGΔSSL was comparable to NewHG in both media.

3.2.5.14 Zebrafish model of systemic infection analysis of NewHGΔSSL

In order to determine the role of SSL12, 13 & 14 in pathogenicity, the zebrafish embryo model of systemic infection was used (Prajsnar *et al*., 2008). This work was done in collaboration with Alex Williams (for methodology see Chapter 2.23). Thirty zebrafish embryos of strain LWT, at 1 day old, were injected with ~1,500 CFU NewHG or 1,500 NewHGΔSSL. Health of the fish was monitored over 4 days and dead fish were tallied. After four days the remaining fish were killed. No attenuation in zebrafish killing was seen in the NewHGΔSSL strain ($p > 0.05$; Figure 3.27). Many of the VFs of *S. aureus* are human specific or have stronger or weaker effects depending on the animal host. Therefore, there being no attenuation in the zebrafish model did not rule out SSL12, 13 & 14 as potentially important VFs.

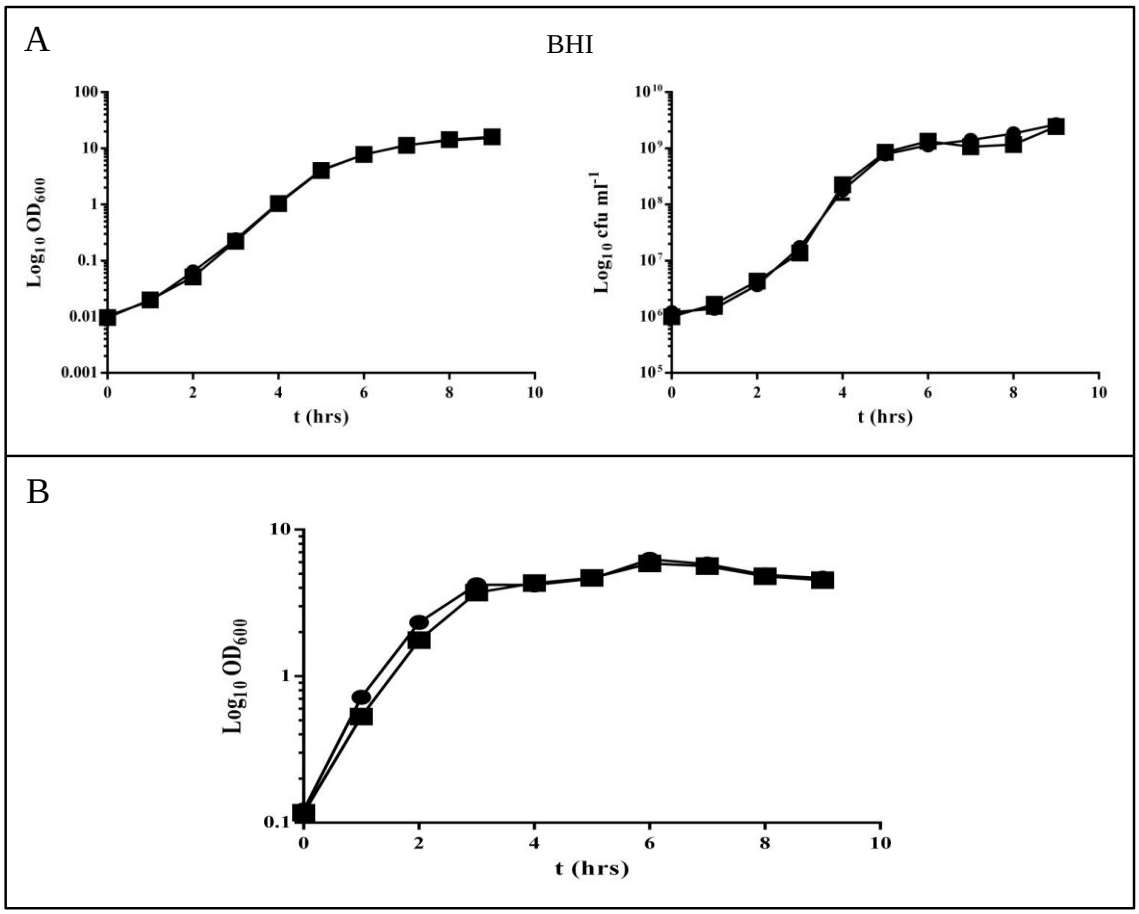

Figure 3.26 Role of SSL12, 13 & 14 in *S. aureus* growth.

● = NewHG, ■ = NewHGΔSSL

A CFU and OD_{600} measured hourly over 9 h show comparable growth between NewHG and NewHGΔSSL when grown in BHI.

B OD_{600} measured hourly over 9 h show comparable growth between NewHG and NewHGΔSSL when grown in FBS.

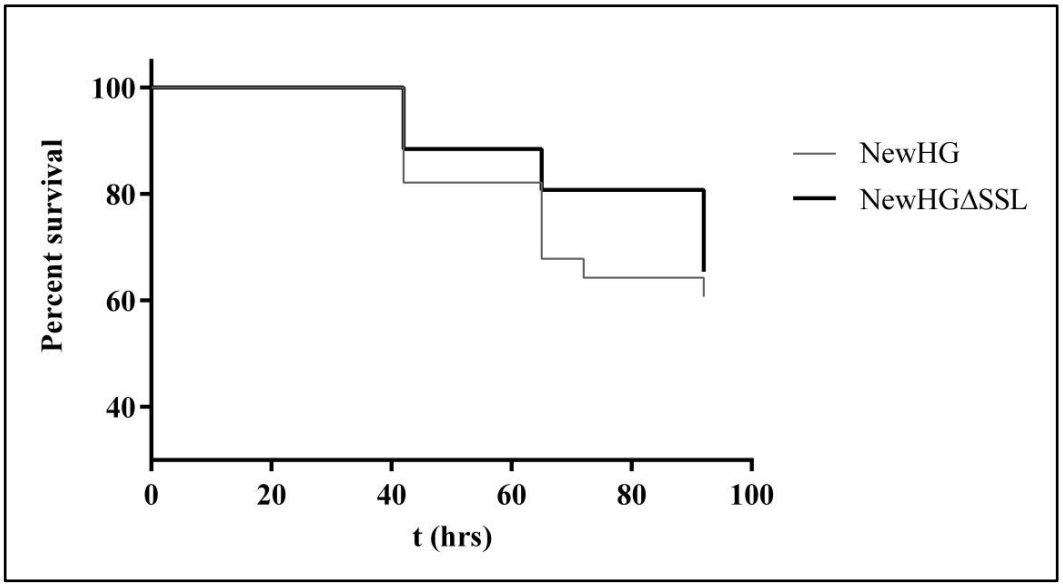

Figure 3.27 Role of the SSL triplet in pathogenesis in the zebrafish embryo model.

NewHGΔSSL shows no attenuation in the zebrafish model of systemic infection p=0.6114.

3.2.5.15 Analysis of growth of NewHGΔSSL in whole human blood

Human blood is rich with antimicrobial proteins, immune cells and is poor in available nutrients. Therefore it provides an ideal medium for the analysis of potential virulence factors. Growth of the NewHGΔSSL was assessed in whole human blood treated with sodium citrate to prevent clotting. Blood collection was done at The Royal Hallamshire Hospital, Sheffield (Chapter 2.1.3.1.1). Full details of the assay are given in Chapter 2.20. The method of Lancefield (1957) was modified for use with *S. aureus*. Approximately 1000 CFU of NewHG and NewHGΔSSL were used as inoculum per ml of blood. The CFU was measured immediately and the samples were incubated at 37^{o}C with gentle agitation for 3 h. CFU was then measured and wild type and mutant growth compared. Difference in growth was calculated as the growth of NewHGΔSSL relative to the wild-type (i.e. wild-type growth was set at 100% and mutant growth was compared with this). There is a small, but significant difference between NewHG and NewHGΔSSL (Figure 3.28).

3.2.5.16 Analysis of growth of NewHGΔSSL in human plasma

To determine whether the growth difference between NewHG and NewHGΔSSL seen in Figure 3.28 were due to non-cellular factors, the whole blood assay was repeated using human platelet rich plasma (PRP). PRP preparation method is given in section 2.1.3.1.2. The exact protocol was that used in 3.2.5.15, except plasma was exchanged for blood. No significant difference in growth was found between mutant and wild-type (Figure 3.29). This suggests that the SSLs interact with the cellular component of human blood, aiding survival of *S. aureus* in blood.

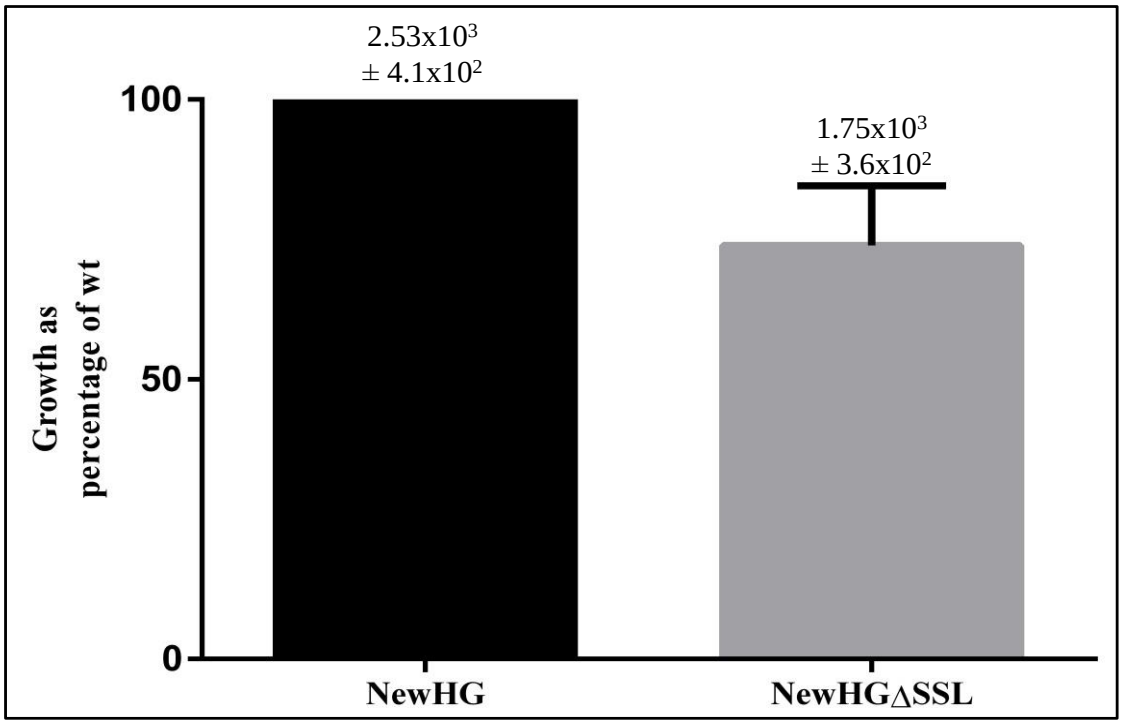

Figure 3.28 Analysis of the role of the SSL triplet in growth in human blood.

NewHG grows significantly better than NewHGΔSSL in whole human blood, $p < 0.05$.

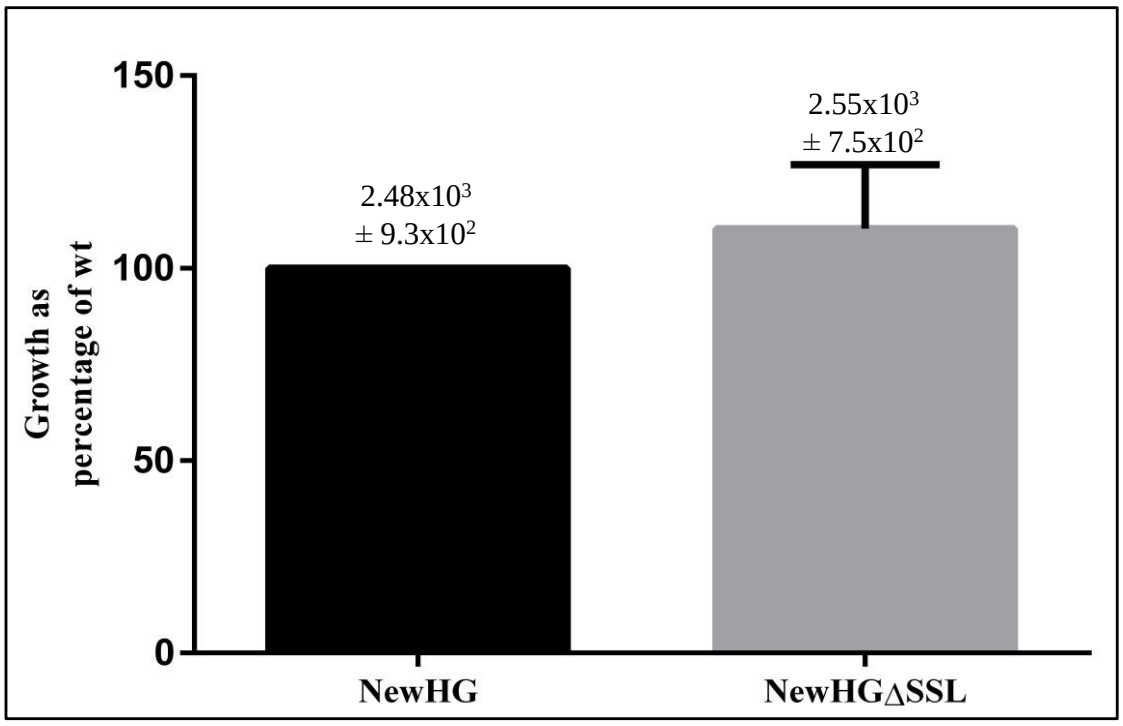

Figure 3.29 Analysis of the role of the SSL triplet in growth in human plasma.

Growth of NewHG and NewHGΔSSL was comparable in human plasma, $p > 0.05$.

3.2.5.17 Complementation of the SSL triplet with pGM073 plasmid system

To determine if the SSL triplet was responsible for the growth phenotype in human blood, NewHGΔSSL was genetically complemented using the pGM073 complementation system. The pGM073 plasmid was constructed by Gareth McVicker from the plasmid pKasbar, by addition of the genes *ezrA* and *PSmOrange*. This plasmid has an *attP* site allowing recognition by the phage integrase enzyme. Lysogenic bacteriophage DNA integrates into the *S. aureus* genome via its *attP* site and the bacterial genome encoded *attB* site, mediated by the integrase enzyme. In *S. aureus* the *attB* recognition site is located at the gene for glycerol ester hydrolase (*geh*) and incorporation of phage DNA leads to loss of lipase activity (Lee & Iandolo, 1986). The pGM073 plasmid encodes an *attP* site, allowing integration of the plasmid at lipase in the presence of integrase. Primers tripF and tripR (containing ApaI and BbvCI restriction sites, respectively) were designed to amplify the SSL triplet and up and downstream control elements (Chapter 2.12.1.1).

The SSL triplet and up and downstream control elements were amplified and ligated into pGM073 (Figure 3.30A). Primers and plasmid were cut with ApaI and BbvCI and ligated (Chapter 2.12.2 and Chapter 2.12.4, respectively). Successful construction was confirmed by purification of the plasmid from *E. coli* and digestion with ApaI and BbvCI and analysis by 1% (w/v) electrophoresis (Figure 3.30B). Cutting the plasmid with these enzymes removes the *ezrA* and *PSmOrange* genes. Ligation gives the plasmid pJC001, the pKasbar plasmid with the SSL triplet inserted. Plasmid DNA was sequenced by GATC Biotech, using primers Tset1F, Tset1R & Tset2F, Tset2R & Tset3F, Tset3R & Tset4F, Tset4R, to confirm that the correct sequence of the triplet was inserted (Appendix 3.6). The plasmid was then used to transform an *S. aureus* RN4220 strain containing the pYL112Δ19 plasmid. This plasmid encodes the integrase enzyme required for *geh* integration (Figure 3.31).

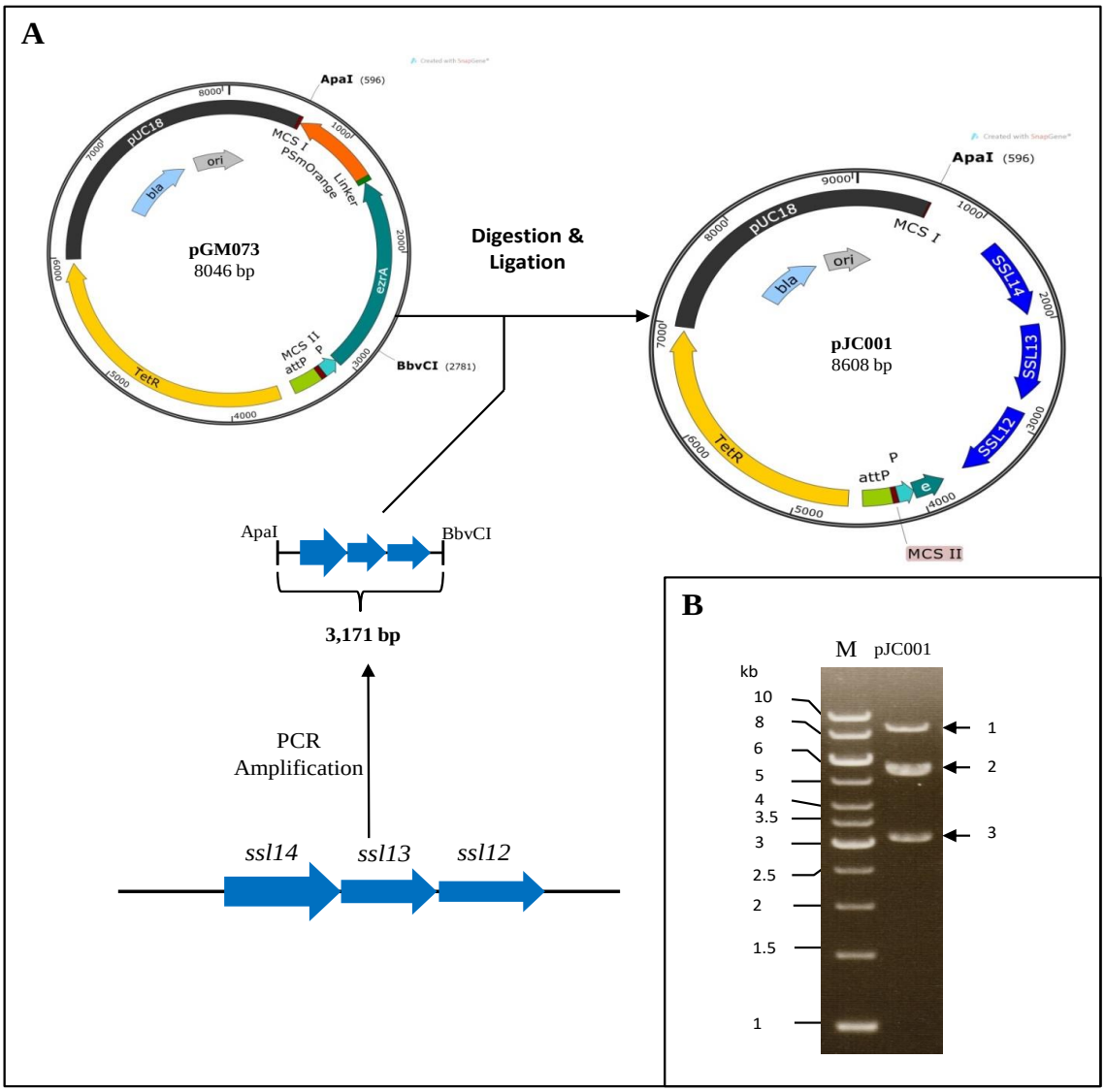

Figure 3.30 Construction of the complementation plasmid pJC001.

A. The SSL triplet with up and downstream control elements was amplified using primers with ApaI and BbvCI restriction sites designed into them, giving a PCR product of 3,171 bp. The pGM073 and amplified triplet were then digested with ApaI and BbvCI and purified. Digestion of the plasmid removes the *PSmOrange* and *ezrA* genes, reducing the plasmid size to 5,437bp. The triplet was then ligated into the digested pGM073 plasmid to give the 8,608 bp plasmid pJC001.

B. DNA fragments were separated by 1% (w/v) agarose gel electrophoresis. Standards (M) of sizes shown.

Bands corresponding in size to the undigested or partially digested plasmid (**1**; 8,608 bp), digested plasmid (**2**; 5,864 bp) and insert (**3**; 3,171 bp) are indicated.

3.2.5.18 Integration of pJC001 into *S. aureus* RN4220

Integration of pJC001 into RN4220 is shown diagrammatically in Figure 3.31. Integration of the pJC001 plasmid into *geh* results in loss of lipase activity. Lipase activity was compared with RN4220 to confirm insertion of pJC001 (Figure 3.32A). The pJC001 plasmid was transferred from the RN4220 genome to NewHG and NewHGΔSSL by bacteriophage transduction (Chapter 2.10.3), allowing integration into the genome by homologous recombination. The pKasbar backbone was also transduced into NewHG and NewHGΔSSL to give control strains for the integration of DNA at *geh*. PCR was carried out to confirm the successful integration of pJC001 or pKasbar into NewHGΔSSL and the wild-type. Three sets of primers were used to determine correct insertion: Tset1F and Tset1R, which amplify a section of the SSL triplet in wild-type or complemented strain DNA, or nothing in the mutant DNA; KanF and KanR, amplify the Kan^R cassette in the mutant, but nothing in the wild-type and pGM-F and pGM-R, amplify the insertion site on the pKasbar plasmid to confirm the integration of pKasbar and not pJC001. The primer combination pGM-F and Tset1R were also used to amplify the pJC001 plasmid from outside of the insert to within the insert, demonstrating the presence of pJC001 and not pKasbar (primer sequences given in Chapter 2.12.1.1). Amplification products of expected sizes were found for all genetically complemented strains (Figure 3.32B).

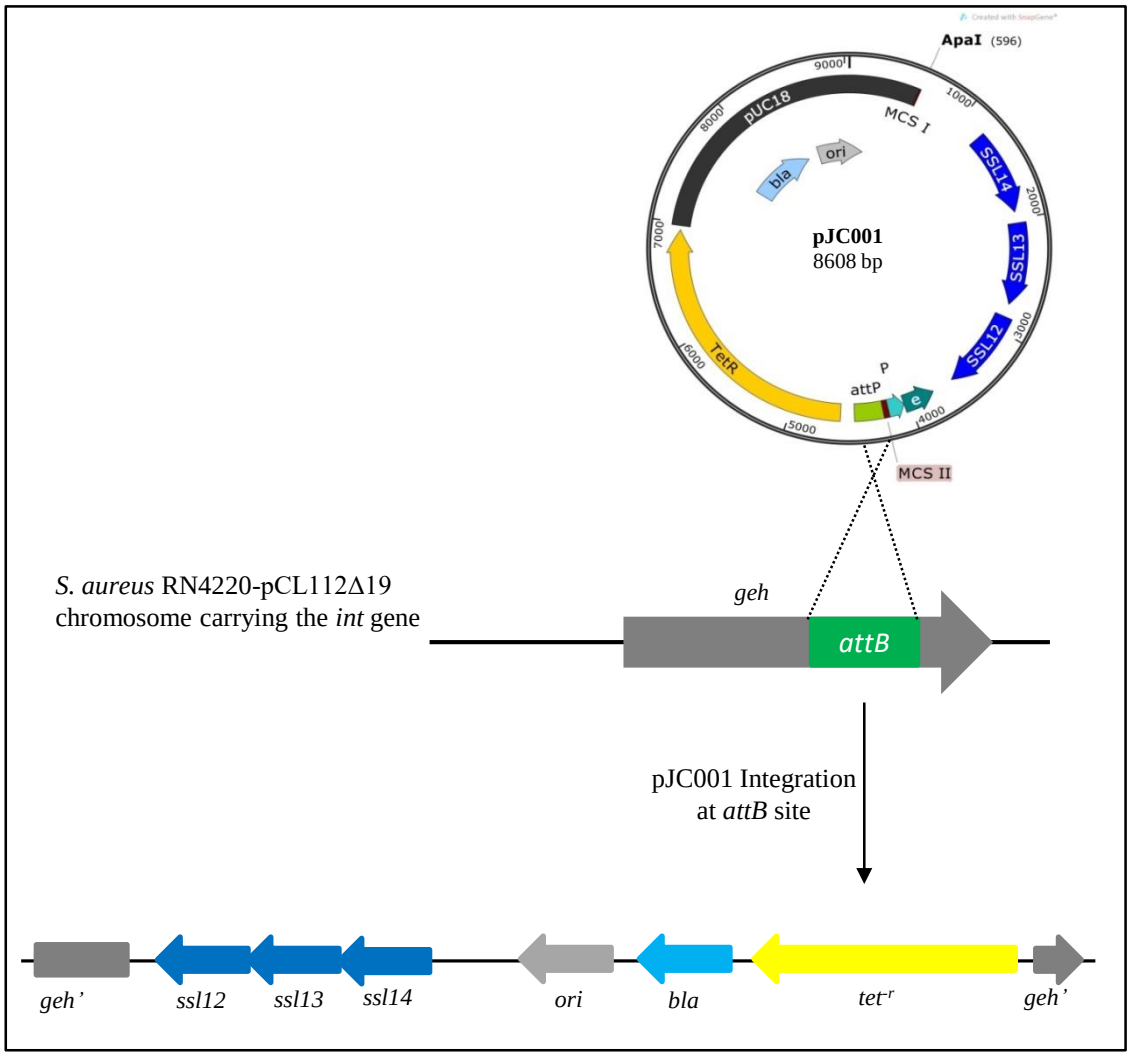

Figure 3.31 Site specific integration of pJC001 at the *geh* gene of *S. aureus* RN4220.

The pJC001 plasmid was transformed into RN4220 carrying the integrase gene within a separate plasmid. The integrase mediates site specific recombination between the plasmid encoded *attP* site and the *attB* site within the *geh* gene of RN4220. This leads to integration of the entire plasmid into *geh*, disrupting lipase activity.

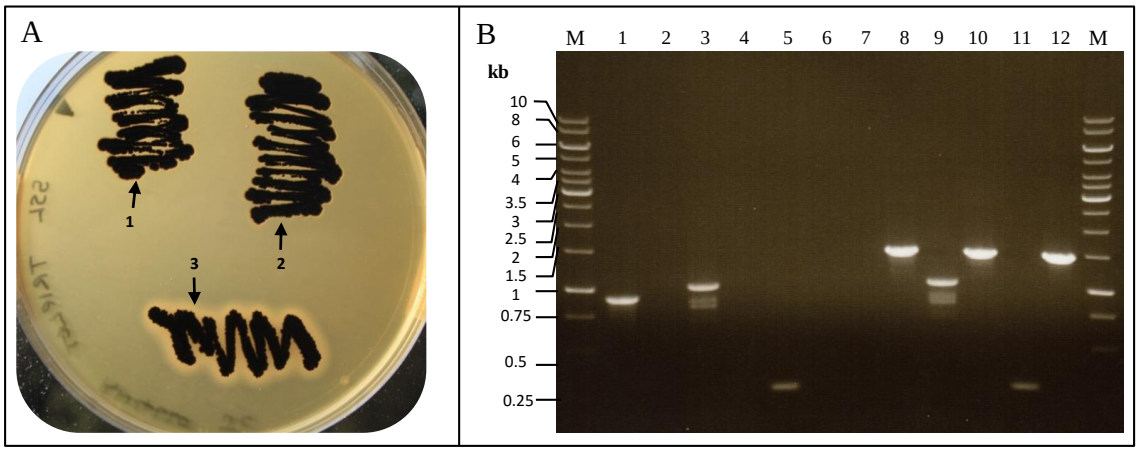

Figure 3.32 Confirming pJC001 integration into RN4220 by analysis of *geh* activity and confirmation of pJC001 & pKasbar transduction into the wild-type strains, SH-*pabA* and JE2-*pabA* by PCR.

A 1 RN4220 disruption of *geh* by pJC001, 2 RN4220 disruption of *geh* by pJC001, 3 RN4220 wild-type Geh activity.

B DNA fragments were separated by 1% (w/v) agarose gel electrophoresis. Standards (M) of sizes shown.

PCR confirmation of pJC001 or pKasbar integration into NewHG and NewHGΔSSL. All bands are of expected sizes.

Lane 1: NewHG gDNA amplified with Tset1F and Tset1R.

Lane 2: NewHG gDNA amplified with KanF and KanR.

Lane 3: NewHG+pJC001 gDNA amplified with pGM-F and Tset1R.

Lane 4: NewHG+pJC001 gDNA amplified with KanF and KanR.

Lane 5: NewHG+pKasbar gDNA amplified with pGM-F and pGM-R.

Lane 6: NewHG+pKasbar gDNA amplified with KanF and KanR.

Lane 7: NewHGΔSSL gDNA amplified with Tset1F and Tset1R.

Lane 8: NewHGΔSSL gDNA amplified with KanF and KanR.

Lane 9: NewHGΔSSL+pJC001 gDNA amplified with pGM-F and Tset1R.

Lane 10: NewHGΔSSL+pJC001 gDNA amplified with KanF and KanR.

Lane 11: NewHGΔSSL+pKasbar gDNA amplified with pGM-F and pGM-R.

Lane 12: NewHGΔSSL+pKasbar gDNA amplified with KanF and KanR.

3.2.5.19 Whole blood growth is restored in the complemented strain

The whole human blood assay was repeated as in 3.2.5.15. The growth of the complemented mutant is restored to equivalence with the wild-type. However, growth of the complemented mutant was not significantly different from NewHGΔSSL, $p = 0.17$. Insertion of the pKasbar vector does not alter the NewHGΔSSL phenotype (Figure 3.33).

3.2.5.20 Do the SSLs affect neutrophil phagocytosis of *S. aureus* NewHG?

The neutrophil phagocytic index was calculated for NewHG and NewHGΔSSL to measure variation in engulfment by neutrophils of the mutant strain in comparison to the wild-type (Sano *et al*., 2003). The method used is given in Chapter 2.19. Neutrophils were mixed with *S. aureus* in triplicate at a required MOI and phagocytosis by neutrophils was allowed over 30 min. Cytospins were prepared for each replicate and total neutrophils (a count > 300 per cytospin required for reliable results), total neutrophils with engulfed bacteria and total number of ingested bacteria were counted by light microscopy. The experiment was repeated three times and the mean value of each was used to compare the phagocytic indices of NewHG and NewHGΔSSL (Figure 3.34). No significant difference in neutrophil phagocytosis activity was observed, $p > 0.05$.

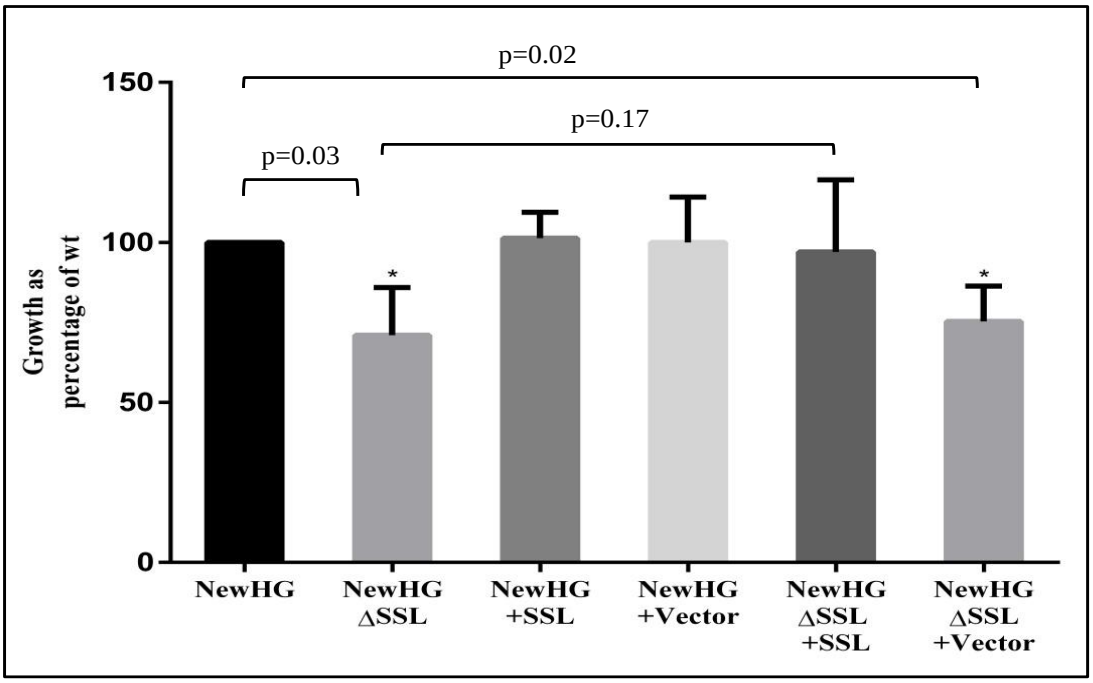

Figure 3.33 Genetic complementation of the NewHGΔSSL phenotype in human blood.

Only NewHGΔSSL and NewHGΔSSL+Vector are significantly different compared with the wild-type, $p < 0.05$.

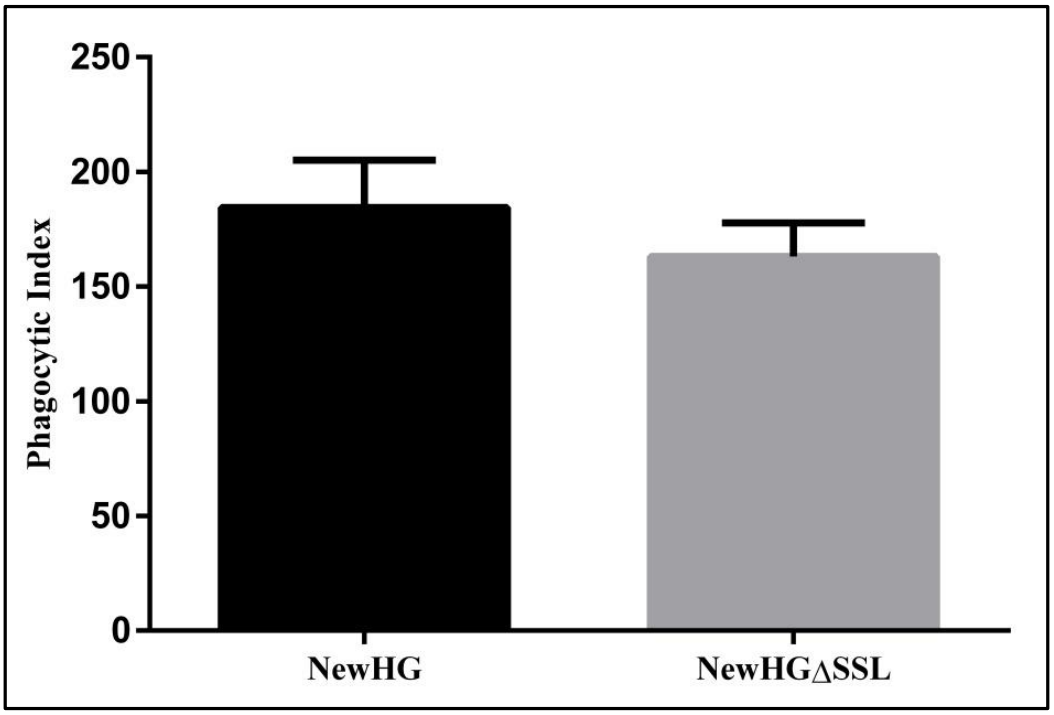

Figure 3.34 Analysis of the role of SSLs in phagocytosis of *S. aureus* by neutrophils.

No significant difference in phagocytic index was seen between NewHG and NewHGΔSSL, $p > 0.05$.

3.2.5.21 Analysis of neutrophil integrity in response to NewHG and NewHGΔSSL supernatant

The vital dye To-Pro-3 indicates neutrophil necrosis, as it enters neutrophils that have lost membrane integrity, emitting fluorescence upon DNA binding. This can be measured by flow cytometry to show the membrane integrity of a sample of neutrophils. NewHG and NewHGΔSSL supernatants were prepared as per Chapter 2.18.2. Supernatants were diluted with fresh RPMI-1640 + FBS and prepared on the day of use. Flow cytometry was done as in section 3.2.2. Neutrophils were incubated in neat, 1in5 and 1in10 supernatant dilutions and at 1 h or 3 h time points the level of To-Pro-3 activity was measured. To-Pro-3 activity was comparable between neutrophils incubated with NewHG or NewHGΔSSL supernatant (Figure 3.35A). The activity was high for both strains, likely as a result of LukAB/GH activity at these dilutions. The following dilutions were prepared: 1in50, 1in100, 1in500 and 1in1000. These dilutions were added to neutrophils with the aim of removing the LukAB/GH effect by diluting it out, thereby allowing any difference to be measured at the edge of supernatant toxicity to neutrophils. Furthermore, a 30min time point was used to replace the 3 h time point. The neutrophil necrotic phenotype of *S. aureus* was lost and the mutant and wild-type had comparable To-Pro-3 activity at all dilutions (Figure 3.35B). Clearly any neutrophil killing effect will be difficult if not impossible to resolve using this method, as LukAB/GH activity is so high. Deletion of the SSL triplet from a Δ*lukAB/GH*, may allow resolution of neutrophil killing activity by flow cytometry analysis.

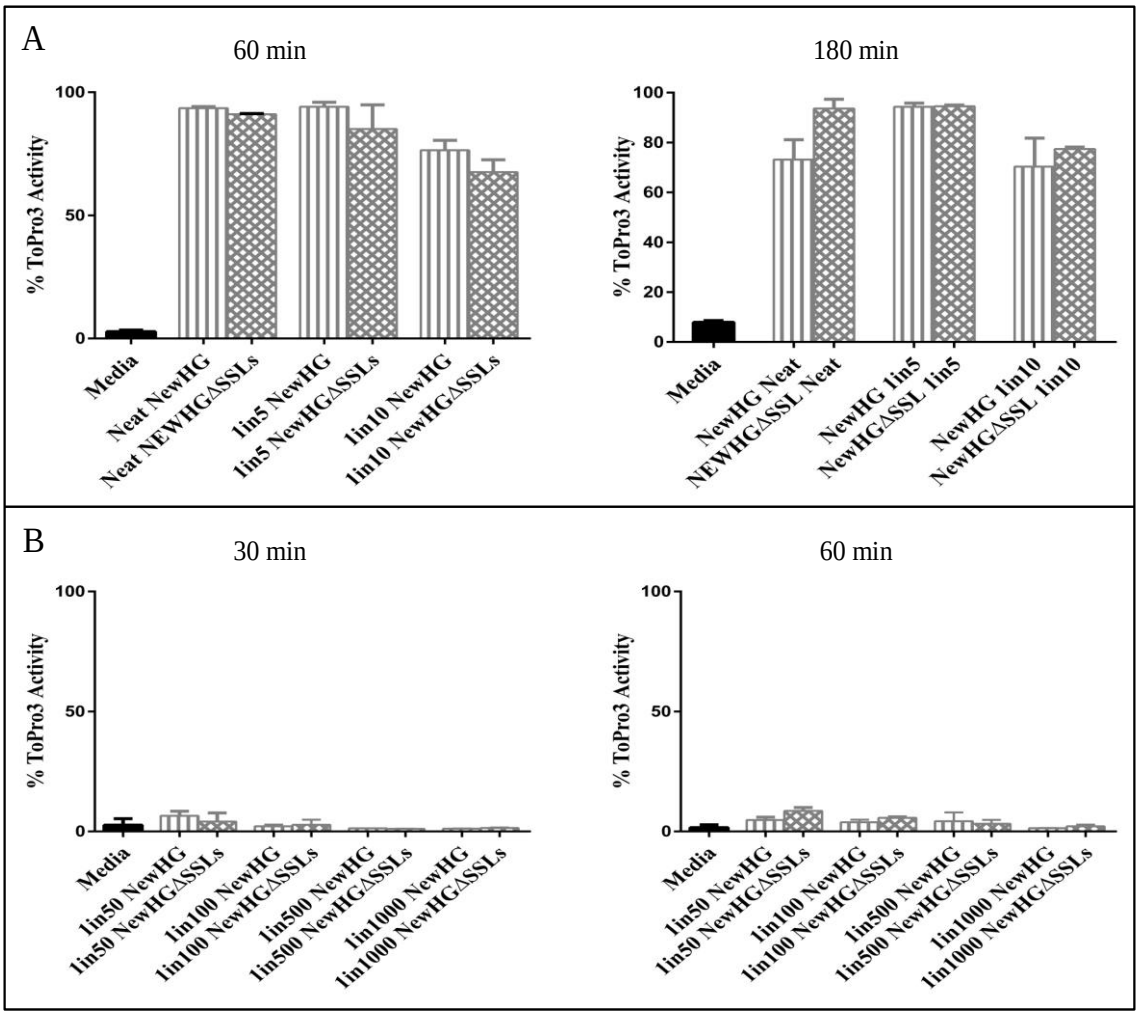

Figure 3.35 Analysis of the role of SSLs in neutrophil necrosis.

A. To-Pro-3 activity of neutrophils after 60 min and 180 min incubation with neat NewHG or NewHGΔSSL supernatant or supernatant diluted 1 in 5 or 1 in 10. To-Pro-3 activity is comparable for neutrophils incubated with supernatant from either wild-type or mutant cultures, irrespective of dilution or length of incubation, $p > 0.05$.

B. To-Pro-3 activity of neutrophils after 30 min and 60 min incubation with NewHG or NewHGΔSSL supernatant diluted 1 in 50, 1 in 100, 1 in 500 or 1 in 1000. To-Pro-3 activity is comparable for neutrophils incubated with supernatant from either wild-type or mutant cultures, irrespective of dilution or length of incubation, $p > 0.05$.

3.3 Discussion

The identification of LukAB as a cytotoxin with a potent necrotic effect on human neutrophils (Dumont *et al*., 2011; Ventura *et al*., 2010), allowed for rapid confirmation that the neutrophil necrosis phenotype associated with SAF was that of LukAB. Since publication by Dumont *et al*. and Ventura *et al*., studies to further characterise LukAB have established that it is an important virulence determinant of *S. aureus*.

As discussed in Chapter 1, two-component leukotoxins consist of an S and F subunit. One subunit binds to the host cell surface promoting dimerisation with the other component leading to surface pore formation. Unlike other *S. aureus* two-component leukotoxins, LukAB forms a heterodimer in solution and not on the surface of its target cell. This is a requirement based on surface exposed hydrophobic regions, hidden by dimerisation (Badarau *et al*., 2015; DuMont *et al*., 2014). Neutrophil cytotoxicity is dependent on binding of the heterodimer to the CD11b receptor on neutrophils, mediated by a specific glutamic acid residue (DuMont *et al*., 2013a, 2014). Although LukAB can induce necrosis of neutrophils extracellularly, it has a greater lytic capacity intracellularly (DuMont *et al*., 2013b). The activity of LukAB has been shown to be concentration dependent (Badarau *et al*., 2015), which suggests that the increased LukAB activity associated with engulfed *S. aureus* is the results of higher concentration due to the closed intracellular environment. However, human monocytes are only killed extracellularly by LukAB (Melehani *et al*., 2015). Similarly to the related two-component leukotoxin PVL, in addition to pore formation on the surface of neutrophils, LukAB promotes production of neutrophil extracellular traps (NETs; Malachowa *et al*., 2013; Pilsczek *et al*., 2010). Whether this is more beneficial to host or pathogen is as yet unclear.

In addition to LukAB, the cytotoxicity against human neutrophils of other toxins has been identified and added to the characterised *S. aureus* armoury relatively recently. The PVL toxin has come to prominence, due to recognition of its association with community-acquired MRSA (Foster, 2005). Its role as a potent human/rabbit neutrophil cytotoxin has since been determined (Holzinger *et al*., 2012; Loffler *et al*., 2010). The phenol soluble modulins (PSMs) activate and attract neutrophils and are able to lyse them extracellularly or intracellularly. They were discovered in 1999 in *S. epidermidis*

(Mehlin *et al*., 1999), but were not recognised in *S. aureus* until 2007 (Wang *et al*., 2007). The recent identification of these novel toxins presented the possibility that other novel virulence determinants remain to be found.

The bioinformatics approach used in this work did not identify any novel toxins amongst the hypothetical protein sequences of *S. aureus*. Four putative SSL immune evasion proteins were found amongst the hypothetical protein sequences of *S. aureus*. However, three of the four were the previously recognised SSLs, SSL12, SSL13 and SSL14 and work was ongoing by another group on the remaining SSL (putative SSL15). The incorrect annotation of these protein sequences, and others found in this work (SCIN and FLIPr), highlighted the errors associated with database annotation and the care required when interpreting bioinformatics data.

The SSL proteins have structural similarity to superantigens, but do not overstimulate T-cells, due to loss of the major histocompatibility binding site (Al-Shangiti *et al*., 2004; Hermans *et al*., 2012). Of the 15 SSLs, those with a known function in *S. aureus* virulence all have a role in immune evasion (Table 3.6). The functions of SSL12, 13 & 14 were not known and it was decided to attempt to identify the role of these proteins in *S. aureus* virulence. SSL12, 13 & 14 proteins could only be purified in a soluble form in the presence of a solubilising agent (urea or guanidine). Attempts to remove the solubilising agent, while retaining protein solubility failed to produce an adequate quantity of protein for analysis. Therefore, an isogenic SSL12, 13 & 14 mutant was made to characterise the role of the SSLs in *S. aureus* pathogenicity.

Species specificity is seen for several *S. aureus* virulence determinants (including SSL10, see Table 3.6). For example, the plasminogen activator staphylokinase (Sak) shows specificity to human, dog and baboon plasminogen, but cannot activate horse, mouse, cow, sheep, pig or rabbit plasminogen (Gladysheva *et al*., 2003). The chemotaxis inhibitory protein (CHIPS), discovered in 2004, inhibits neutrophil migration to the site of infection in response to formylated peptides and complement protein C5a. CHIPS is 30-fold more effective at blocking human neutrophil migration than mouse neutrophil migration (de Haas, 2004). The superantigen SEA, structurally similar to SSLs, stimulates human T-cells 1000 times more effectively than mouse T-cells (Dohlsten *et al*., 1993). This species specificity provides a potential explanation for

Table 3.6 Known functions of the SSL proteins.

Protein Name	Function	Reference
SSL1	The structure of SSL1 has been determined, which will likely aid identification of SSL1 function.	(Dutta *et al*., 2014)
SSL2	Unknown function	-
SSL3	SSL3 inhibits secretion of the proinflammatory cytokine TNF-α by macrophages, neutrophils and monocytes by binding to TLR2intracellularly, blocking activation by *S. aureus* cell wall components.	(Yokoyama *et al*., 2012; Bardoel *et al*., 2012)
SSL4	SSL4 binds to sialated glycoproteins on the surface of neutrophils, macrophages and monocytes, promoting uptake of the SSL protein. The role of SSL4 once internalised is unknown.	(Hermans *et al*., 2012)
SSL5	SSL5 binds to the collagen receptor GPVI and the GPIbα glycoprotein on the surface of platelets leading to their activation and aggregation.	(Hu *et al*., 2011; De Haas *et al*., 2009)
	Reduces wound healing and causes thromboembolism in a murine cut-tail bleeding model.	(Armstrong *et al*., 2012)
	Inhibits matrix metalloproteinase 9 of human neutrophils, a protease required for basement membrane degradation during transmigration of neutrophils from the bloodstream to the site of infection.	(Itoh *et al*., 2010a)
	SSL5 inhibits neutrophil rolling by binding to P-selectin glycoprotein ligand (PSGL-1) blocking binding to P-selectin. This was shown under static conditions and when exposed to the shearing forces of a flow chamber, to mimic the forces applied within blood vessels.	(Bestebroer *et al*., 2007)
SSL6	SSL6 binds the host surface receptor CD47. This receptor has a role in self-recognition, and is important for preventing activated macrophages from phagocytosing early haemapoietic cells. SSL6 may interfere with this process promoting autoimmune damage at the site of infection.	(Fevre *et al*., 2014)
SSL7	Binds complement protein C5, preventing its cleavage to the chemoattractant C5a. Has an anti-inflammatory effect in a murine inflammation model.	(Bestebroer *et al*., 2010; Langley *et al*., 2005)
	Binds to the surface of monocytes and a subpopulation of B-cells, via a specific, as yet unidentified receptor, and is found in vesicles within dendritic cells.	(Al-Shangiti *et al*., 2004)
	SSL7 binds to IgA blocking recognition of IgA bound *S. aureus* by leukocytes.	(Langley *et al*., 2005)
SSL8	SSL8 binds the host wound repair protein tenascin-C, slowing wound repair by fibroblasts.	(Itoh *et al*., 2013a)
SSL9	Binds to the surface of monocytes, via a specific, as yet unidentified receptor, and is found in large vesicles within dendritic cells.	(Al-Shangiti *et al*., 2004)
SSL10	Binds to the phospholipid phosphatidylserine expressed on apoptotic cells, which may interfere with their clearance. Phosphatidylserine is also found on the surface of activated platelets, which may also be a target of SSL10.	(Itoh *et al*., 2012)
	SSL10 binds IgG, but shows preferential binding to prothrombin over IgG. Binding to prothrombin prevents its cleavage to thrombin and reduces the non-proteolytic activation of prothrombin by *S. aureus* coagulase, thereby acting as an anticoagulant.	(Itoh *et al*., 2013b)
	SSL10 binds specifically to human and non-human primate IgG via the constant region, blocking phagocytosis of *S. aureus* by neutrophils and complement activation via the classical (IgG-dependent) pathway.	(Patel*et al*., 2010)
SSL11	Binds neutrophils, monocytes via sialated glycoproteins. SSL11 also binds to IgA via the same sialic acid moiety as that of glycoproteins bound by SSL11 on the surface monocytes and neutrophils, thereby preventing IgA binding to neutrophils. Similarly to SSL5, SSL11 binds to PSGL-1. Labelled SSL11 has also been shown to be internalised by neutrophils.	(Chung *et al*., 2007)
SSL12	Unknown function	-
SSL13	Unknown function	-
SSL14	Unknown function	-
SSL15	Unconfirmed SSL	-

why no difference in pathogenicity was seen between the SSL mutant and the wild-type in the zebrafish model of systemic infection.

A subtle reduced growth phenotype of the SSL mutant was seen in human blood, but not in human plasma. This suggested that the SSLs interact with the cellular component of human blood. Comparison of engulfment of the SSL mutant and wild-type was carried out and no difference was found. Based on the known functions of SSLs (Table 3.6) it was hypothesised that the effect would relate to immune evasion, rather than toxicity. However, toxicity to human neutrophils was assessed, but the results were clouded by the potent toxicity of other *S. aureus* components.

The role of SSL12, 13 and 14 in human blood, may be the result of only one protein of the triplet or a combination of them. Potential roles include uptake by host cells and intracellular modification of cell activity, as with SSL3 and potentially SSL4 and SSL11 (Table 3.6). The proteins may block specific receptors on immune cells, or disrupt the binding of opsonins to the bacterial surface. The effect may well be unrelated to immune evasion, presenting possibilities such as stress tolerance, nutrient acquisition and nutrient synthesis.

The bioinformatics analysis used in this chapter was limited to certain classes of virulence determinants. Methods exist, such as those discussed in Chapter 1 (STM, IVET, SCOTS) that allow for analysis of a broader range of virulence determinants. However, this chapter has also highlighted the potential human specificity of three *S. aureus* virulence determinants. For this reason, a broader approach, in conditions mimicking an important human host environment, is the focus of Chapter 4.

CHAPTER 4

IDENTIFICATION OF *S. AUREUS* COMPONENTS INVOLVED IN THE INTERACTION WITH HUMAN BLOOD

4.1 Introduction

A common approach towards understanding those bacterial components involved in the interaction with their environment is through the use of mutational analysis. Allelic replacement is used to mutate the gene of interest and the resulting phenotype is then compared to the parental strain. The mutant phenotype indicates the function of the protein encoded by the gene (Beasley *et al*., 2011; Bubeck Wardenburg *et al*., 2008; Giraudo *et al*., 1996; Palmqvist *et al*., 2002). Although this is a useful methodology, it is time consuming and laborious when applied to the full gene complement of a species. Transposons are a powerful molecular tool allowing for functional analysis of multiple genes within a single screen. Class II transposons, such as the mariner Tn, have terminal inverted repeats, flanking a transposase gene and genes for other functions including antibiotic resistance. The transposase mediates excision of the Tn by interaction with the inverted repeats, the transposon circularises and inserts into a random site in its host DNA (Hamer *et al*., 2001; Hayes, 2003). The standard procedure for transposon mutagenesis is delivery of a plasmid encoding the transposon into the species of interest. Transposition events mediated either by a self-encoded transposase, or a transposase encoded on a separate plasmid, then take place as the bacteria grows in media with two antibiotics (resistance to which is encoded by the transposon and the plasmid respectively) and the plasmid is then removed by growth in the absence of the plasmid resistance encoded antibiotic, at a temperature non-permissive to plasmid replication. The bacteria in the culture should possess a transposon stably inserted somewhere in their chromosome. The phenotype of the bacteria is then screened using a chosen condition or conditions. Identification of the transposon insertion point in the chromosome allows determination of the gene function. The list of biological processes assessed with this approach includes, identification of genes involved in virulence factor regulation (Shaw *et al*., 2006), starvation survival response in *Listeria monocytogenes* (Herbert & Foster, 2001), haem toxicity (Wakeman *et al*., 2012) and regulation of β-lactam resistance genes (Zscheck & Murray, 1993). Although less time-consuming and expensive than the individual knockout of all genes in a species, the identification of Tn

insertion sites is time-consuming and expensive (Chaudhuri *et al*., 2009) and advances have been made to address this.

A bacterium with a Tn insertion within an essential gene will not grow. This allows Tn mutagenesis to be used for identification of the essential gene complement within a species of bacteria (Chaudhuri *et al*., 2009); important as essential genes may provide novel targets for new therapeutics or vaccines. *In vitro* transposition into large regions of *Haemophilus influenzae* and *Streptococcus pneumoniae* DNA has been used in a genetic fingerprinting method to assess essential genes in these species (Akerley *et al*., 1998; Lampe *et al*., 1996). Both of these naturally competent species are transformed with Tn inserted DNA, which can replace the native DNA by homologous recombination (Figure 4.1A). Primers recognising the Tn and chromosomal sections along the *in vitro* DNA are used to "fingerprint" the DNA as sections containing essential genes will be highlighted as missing bands in electrophoresis gels i.e. a chromosomal primer with an essential gene downstream of its binding site will show a pattern of PCR products as follows: larger sized bands from transposons inserted downstream of the essential gene and smaller bands from Tn inserts upstream of the essential gene; however, bands in the middle of the gel will not be present, as Tn insertion into the essential gene abolishes the viability of the bacterium and it is not represented in the library (Akerley *et al*., 1998; Figure 4.1B).

Modification of the transposon by introduction of a T7 promoter was used by Chaudhuri *et al*., 2009 to provide rapid identification of essential genes in *S. aureus*. A mutant library was constructed and genomic DNA was digested with a specific restriction enzyme, giving short fragments with/without a Tn insertion present. Transposon mediated differential hybridisation was then used to rapidly identify essential genes. Transcription from the T7 promoter was induced and the RNA fragments, bounded by the length of the digested fragment were hybridised to a microarray of *S. aureus* genes. Those spots on the microarray that are "off" (i.e. unbound by RNA) are not downstream of a Tn insertion, suggesting that they are within essential genes (Chaudhuri *et al*., 2009). Signature-tagged mutagenesis (STM) developed by Hensel *et al*. (1995) uses transposons modified with a unique sequence tag, primarily for *in vivo* studies. The methodology is discussed in detail in Chapter 1. Briefly, strains with a sequence-tagged Tn insert are mixed, giving a large heterogeneous pool of strains, which is then used in

an animal model. At the endpoint of the model, bacteria are collected and the surviving Tn insert strains are analysed by PCR of their unique sequence-tag, followed by Southern hybridisation to identify the strain. Those tags not present at the end of the infection are likely inserted into genes important for the infection model being used. Their importance to different stages of infection can also be assessed by taking bacterial samples over the course of the infection. Not only is this beneficial for measuring the genetic requirements of a species in the changing conditions of a living host, the same pool can also be used to look at different genetic requirements in different infection types within the same host species (Coulter *et al*., 1998; Mei *et al*., 1997). STM studies by Brown *et al*. (2000) & Coulter *et al*. (1998) have highlighted the importance of nutrient acquisition and biosynthetic pathways involved in amino acid, purine and tetrahydrofolate production in *Aspergillus fumigatus* and *S. aureus*, respectively. This is not surprising considering that although the mammalian host is nutrient rich, many nutrients are sequestered as a means of inhibiting pathogen growth (Prentice *et al*., 2007).

An ordered transposon library, in which all Tn insertion sites have been characterised is a valuable resource for the analysis of gene function. Screens can be done in multiple conditions and PCR and sequencing is not required, as the Tn insertion site is known for each strain in the library. Producing an ordered Tn library is a demanding and expensive undertaking, however it has been done in two *S. aureus* strain backgrounds, Newman (Bae *et al*., 2004) and the community-acquired MRSA strain USA300 JE2 (Fey *et al*., 2013). Both groups used the same method to make their libraries (shown diagrammatically in Figure 4.2). The Mariner based *bursa aurealis* Tn, encoding an erythromycin/lincomycin (ery/lin) resistance cassette, was used to make the Nebraska Transposon Mutagenesis Library (NTML) in the CA-MRSA USA300 JE2 strain background. Strain JE2 is identical to the clinical strain isolated in the Los Angeles County Jail LAC, except that it has been cured of plasmids. The library consists of 1,952 ery/lin resistant strains each with a Tn inserted in the coding sequence (CDS) of a non-essential gene. Each strain has undergone Sanger sequencing out from the transposon and the resulting sequence aligned with *S. aureus* strain FPR3757 chromosomal DNA by blastn, allowing identification of 1,952 genes disrupted by Tn insertion. Mannitol utilisation, pigment formation, protease activity and haemolysis were all assessed using the library upon its completion (Fey *et al*., 2013). The JE2

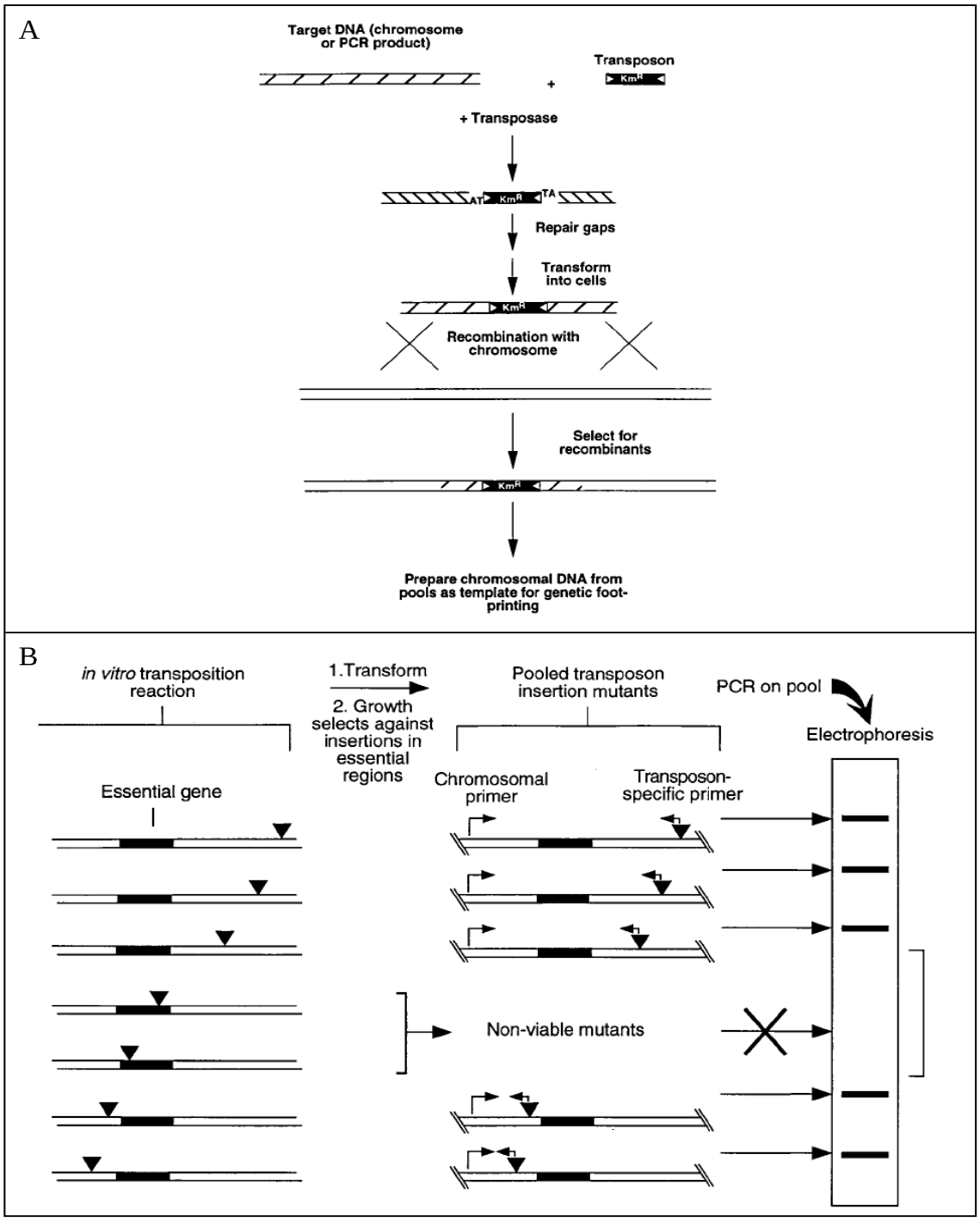

Figure 4.1 Identification of essential genes by genetic fingerprinting.

A. DNA that has been subjected to *in vitro* transposition is transformed into competent bacteria, where homologous recombination replaces native DNA for Tn inserted DNA.
B. After growth and extraction of chromosomal DNA, PCR is used to determine the locations of putative essential genes.
Adapted from Akerley *et al*. (1998).

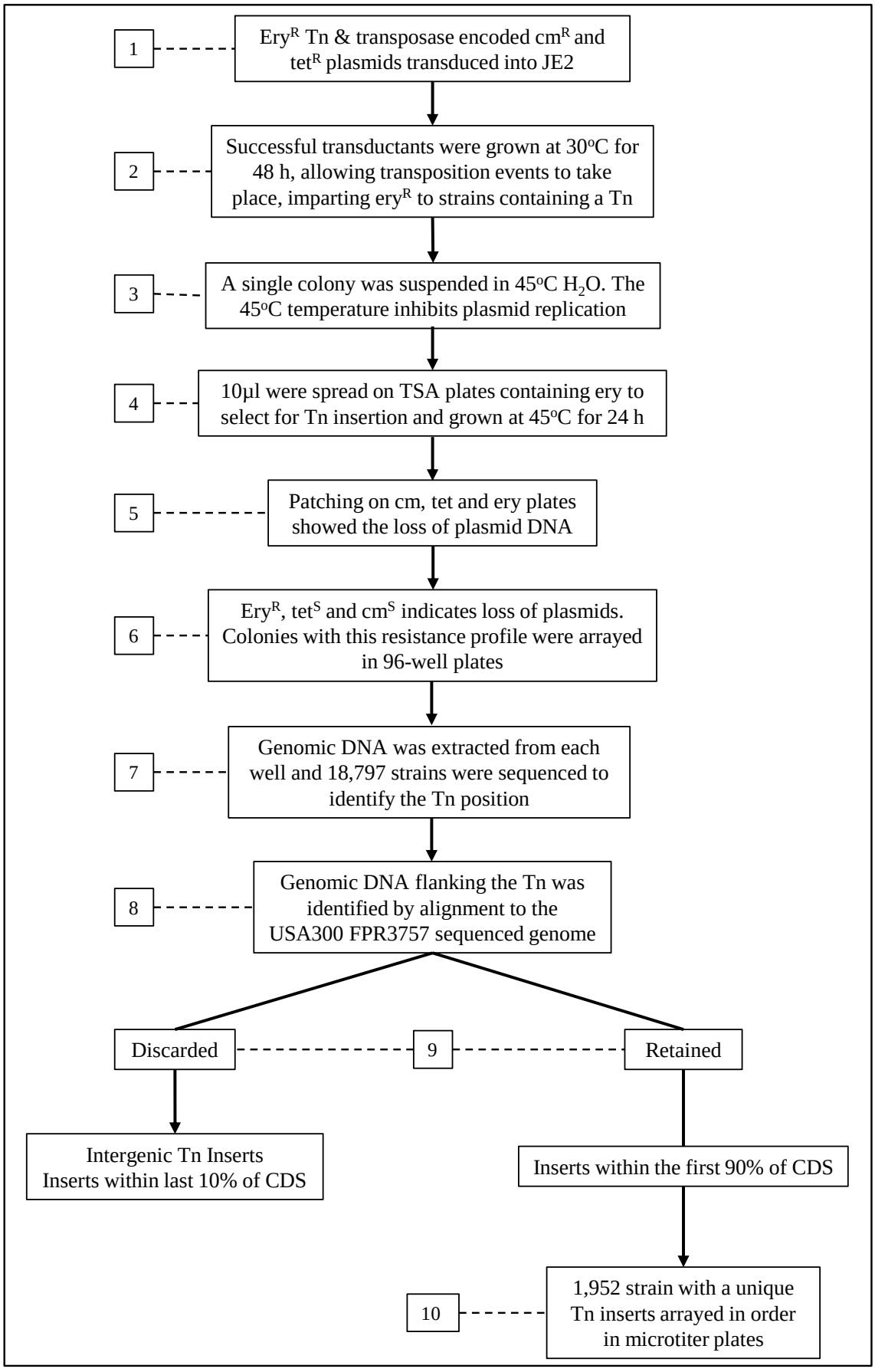
1
Ery^R Tn & transposase encoded cm^R and tet^R plasmids transduced into JE2
2
Successful transductants were grown at 30^{o}C for 48 h, allowing transposition events to take place, imparting ery^R to strains containing a Tn
3
A single colony was suspended in 45^{o}C H_2O. The 45^{o}C temperature inhibits plasmid replication
4
10µl were spread on TSA plates containing ery to select for Tn insertion and grown at 45^{o}C for 24 h
5
Patching on cm, tet and ery plates showed the loss of plasmid DNA
6
Ery^R, tet^S and cm^S indicates loss of plasmids. Colonies with this resistance profile were arrayed in 96-well plates
7
Genomic DNA was extracted from each well and 18,797 strains were sequenced to identify the Tn position
8
Genomic DNA flanking the Tn was identified by alignment to the USA300 FPR3757 sequenced genome
Discarded
9
Retained
Intergenic Tn Inserts
Inserts within last 10% of CDS
Inserts within the first 90% of CDS
10
1,952 strain with a unique Tn inserts arrayed in order in microtiter plates

Figure 4.2 Construction of the NTML shown diagrammatically.

Step 1: The pBursa plasmid containing the transposon sequence and chloramphenicol resistance cassette was transduced into JE2, which was also transduced with pFA545, which contains the transposase gene and tetracycline resistance. **Step 2**: Transductants were grown at 30^{o}C on solid media for 48 h, allowing tranposition events to occur. **Step 3**: A single colony was suspended in 45^{o}C in H_2O immediately heating the bacteria to the non-permissive temperature. **Step4**: Bacteria were spread on erythromycin plates to select for Tn insertion and grown at the non-permissive temperature to promote loss of the plasmids. **Step 5**: Colonies were patched on to tetracycline, chloramphenicol and erythromycin plates. **Step 6**: Those bacteria that were ery^{R}, but tet^{S} and cm^{S} had lost the plasmid and had a Tn insert and were arrayed in 96-well plates. **Step 7**: Genomic DNA was extracted and sequenced out from the Tn into the neighbouring genomic DNA for each well of the 96-well plates. **Step 8**: Sequencing results were aligned with *S. aureus* USA300 FPR3757 genomic DNA to determine Tn insertion site. **Step 9**: Strain were discarded or retained depending on the Tn insertion position. **Step 10**: The 1,952 were arrayed in order in microtitre plates.

Based on Bae *et al*. (2004) & Fey *et al*. (2013).

library is freely available to registered *S. aureus* researchers and a website has been produced to accompany the library, which includes information on the insertion site of each Tn and files for the visual inspection of Tn insertion sites using the GView genome browser.

The aim of this chapter was to screen the NTML with the aim of identifying genes associated with *S. aureus* virulence. Growth and haemolysis phenotypes were assessed on citrated human blood agar. Growth on bovine serum agar was also assessed, as it was a readily available and inexpensive alternative to human serum. Haemolysis was measured using 5% (v/v) sheep blood with Columbia agar base, a standard method for measuring haemolytic activity in *S. aureus* (Chow *et al*., 1983; Vítkova & Votava, 2005). The immune components of blood are immobilised in blood agar, so *S. aureus* will not be directly challenged by immune cells or proteins during screening. However, CA-MRSA strains are responsible for the majority of skin and soft tissue infections and 20% of bacteraemias in the USA and the ability to grow in blood is necessary to establish bacteraemia and systemic infections (Malachowa & DeLeo, 2011). Haemolysins and other toxins have been shown to be upregulated in transcription studies of *S. aureus* grown in liquid blood, which apart from their anti-immune function, have a likely role in liberation of nutrients. Iron acquisition proteins and other metal ion transport systems and amino acid metabolism genes are up and down-regulated in blood (Malachowa *et al*., 2011). The Malachowa study and the studies by Brown *et al*., 2000 and Coulter *et al*., 1998 mentioned above, suggest that the ability to cause blood-borne infection is not simply a matter of immune evasion, but one of survival and growth by nutrient acquisition and biosynthesis.

4.2 Results

4.2.1 Bioinformatic analysis of the NTML hypothetical protein sequences

4.2.1.1 Identification of novel virulence determinants in the NTML by BLAST search of the VF database

It was not guaranteed that the screen of the NTML would provide targets for further study. Therefore, the hypothetical protein sequences, containing secretory signal sequences, of the NTML were subjected to the same bioinformatics analysis as used in

Chapter 3 for *S. aureus* 8325. The purpose of the bioinformatics was to provide alternative targets, should the screen fail to produce any interesting results and to highlight any strains that are of particular interest in the screen results. Furthermore, attempts could be made to characterise the genes while the screening process was ongoing. Also, following on from the analysis of the previous strain (Chapter 3), it was hypothesised that the analysis of JE2 sequences would identify virulence determinants not found in *S. aureus* 8325, due to the genetic background differences and the high virulence of the JE2 strain (Francis *et al*., 2005).

A homology search was done against the virulence factor (VF) database created in Chapter 3. This database was constructed in Chapter 3 in order to identify potential VFs amongst the sequences annotated as hypothetical sequences in the *S. aureus* 8325 genome. This same approach was applied to the sequences amongst the 1,952 NTML strains that are annotated as hypothetical or unknown function proteins and that contain a signal sequence (the method is shown diagrammatically in Figure 4.3). Signal sequence encoding protein sequences were extracted from the full list of 1,952 NTML sequences using SignalP 3.0 (Bendtsen *et al*., 2004). 44 of the NTML protein sequences were annotated as hypothetical proteins and contained an N-terminal signal sequence. The 44 sequences were used to BLAST the VF database created in Chapter 3.2.3.5. The query returned 4 alignments. The protein ID of the 4 hypothetical protein sequences were then used to query the NCBI Protein database in order to acquire information on the sequence. The returned webpage allows a search for identical proteins within the database. Two of the hypothetical proteins were SSL proteins identified in Chapter 3 and two were staphylococcal complement inhibitor (SCIN) proteins (Table 4.1). This demonstrated that these 4 protein sequences were incorrectly annotated in the NTML.

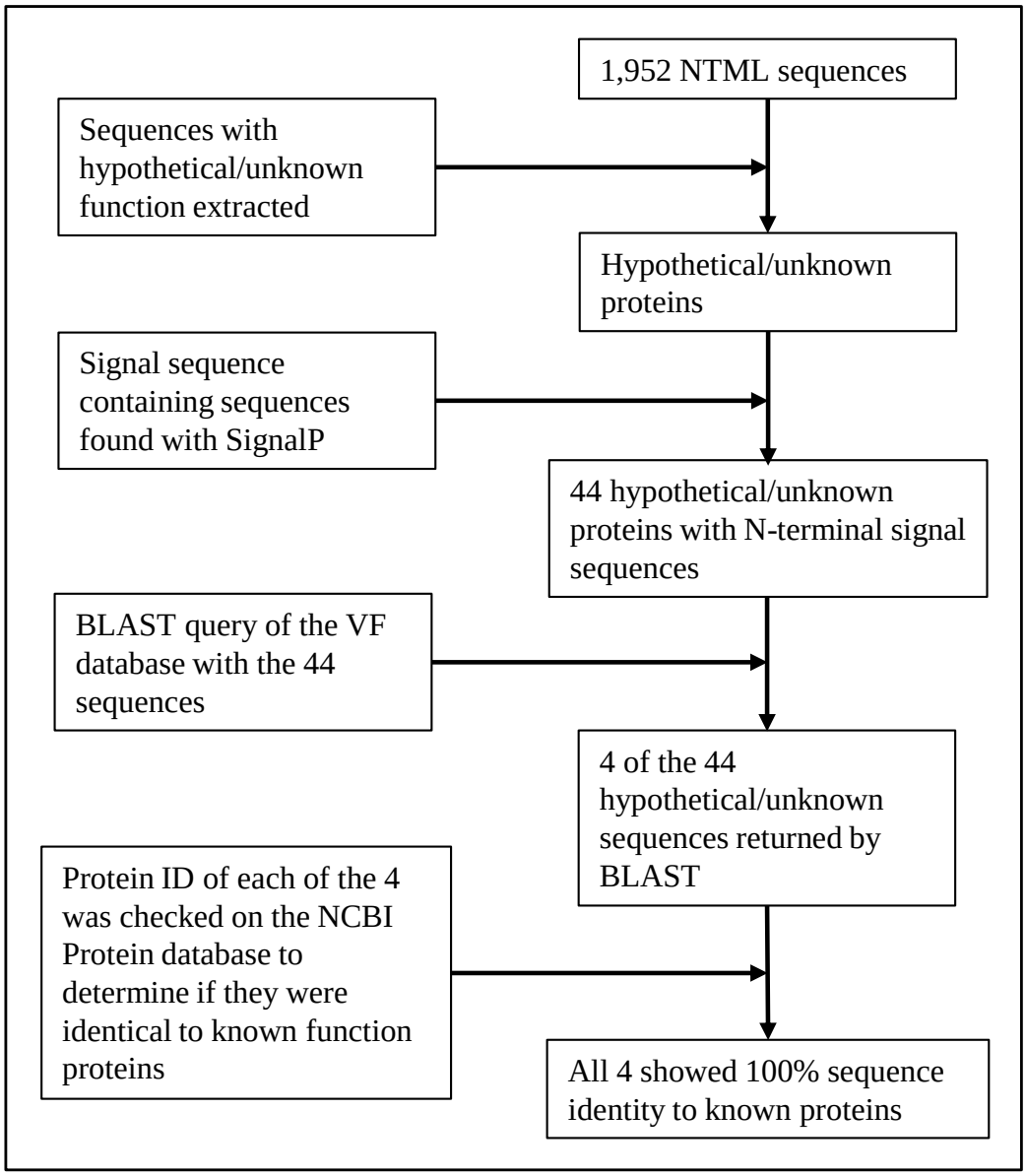

Figure 4.3 BLAST query of the VF database with the 44 NTML sequences, shown diagrammatically.

The hypothetical proteins that aligned with the VF database were incorrectly annotated as hypothetical proteins.

Table 4.1 Identification of novel potential virulence factors in the NTML by BLAST search.

The protein ID and the identity assigned by the NTML are given in the Column 1 and Column 2, respectively. The most common sequence that the query aligned to in the BLAST analysis is shown in Column 3. The number of BLAST hits is shown in Column 4. Column 5 shows the actual identity of the NTML protein sequence. Column 6 provides a reference for each of the proteins.

Query ID	NTML Identity	Aligned to in the VF Database	Number of Hits	Confirmed Identity	Reference
SAUSA300_1919	Hypothetical protein	SCIN	1	SCIN-A	Garcia *et al*., 2012
SAUSA300_1056	Hypothetical protein	SCIN	1	SCIN-B	
SAUSA300_1060	Hypothetical protein	Exotoxin/SSLs	77	SSL13	Patel *et al*., 2010
SAUSA300_1061	Hypothetical protein	Exotoxin/SSLs	63	SSL14	

4.2.1.2 Identification of novel virulence determinants in the NTML by BLAST search of the non-redundant database

The homology search in the previous section did not highlight any new potential virulence factors. Therefore it was decided to repeat the search using the non-redundant bacterial sequence database that was constructed in Chapter 3.2.3.8. The method employed was exactly that shown in Figure 4.3, but the non-redundant bacterial database was searched, rather than the VF database.

The non-redundant database constructed in Chapter 3 was aimed to contain representatives from all varieties of VF. To do this, all known bacterial protein sequences with known-function annotation were used in constructing the database, which was then clustered to 90% identity to remove redundant and similar sequences (Figure 4.4A). The database contains many non-VF sequences, but contains high VF diversity. BLAST was used to query the 44 hypothetical sequences from the NTML (section 4.2.1.1) against the non-redundant database and those that hit against database sequences annotated as virulence factors were retained (Figure 4.4B; Table 4.2). Again the two SSLs and two SCIN proteins were found. Additionally the Eap, Emp and SasF proteins were annotated as hypothetical protein sequences in the NTML.

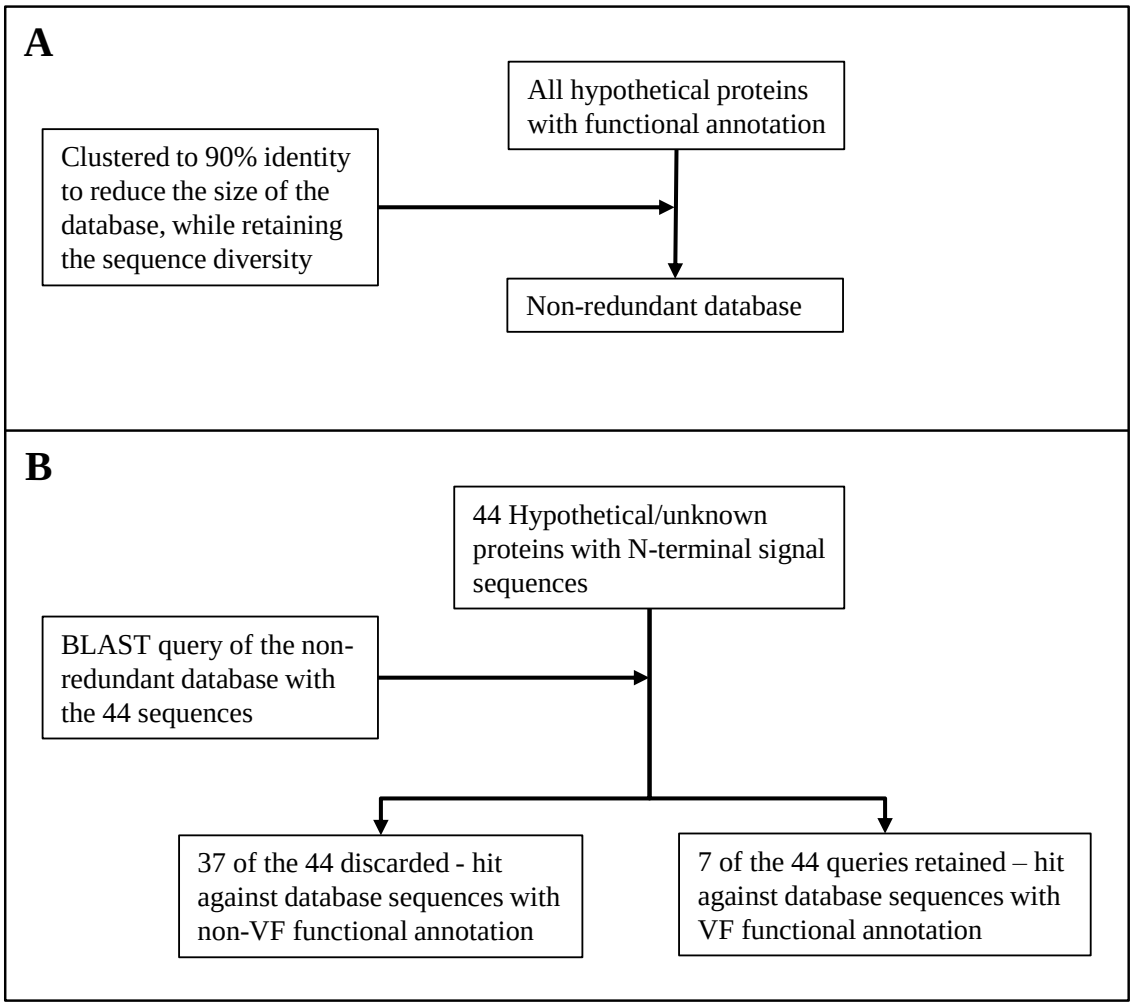

Figure 4.4 Construction and BLAST search of the non-redundant database, shown diagrammatically.

A. Construction of the non-redundant database

B. BLAST query of the non-redundant database.

Table 4.2 Identification of novel potential virulence factors in the NTML by BLAST search.

The protein ID and the identity assigned by the NTML are given in the Column 1 and Column 2, respectively. The most common sequence that the queries aligned to in the BLAST analysis are shown in Column 3. The number of BLAST hits is shown in Column 4. Column 5 shows the actual identity of the NTML protein sequence. Colum 6 provides a reference for each of the proteins.

Query ID	NTML Identity	Aligned to in the VF Database	Number of Hits	Confirmed Identity	Reference
SAUSA300_1919	Hypothetical protein	SCIN	12	Staphylococcal complement inhibitor A (SCIN-A)	(Garcia *et al*., 2012)
SAUSA300_1056	Hypothetical protein	SCIN	11	Staphylococcal complement inhibitor B (SCIN-B)	
SAUSA300_1060	Hypothetical protein	Exotoxin/SSLs	16	Staphylococcal superantigen-like protein 13 (SSL13)	(Patel *et al*., 2010)
SAUSA300_1061	Hypothetical protein	Exotoxin/SSLs	16	Staphylococcal superantigen-like protein 14 (SSL14)	
SAUSA300_0775	Hypothetical protein	Coagulase	20	Extracellular Matrix Binding Protein (Emp)	(Johnson, Cockayne, & Morrissey, 2008)
SAUSA300_0883	Hypothetical protein	Map Protein	48	Extracellular Adherence Protein (Eap)	(Haggar *et al*., 2003)
SAUSA300_2581	Hypothetical protein	Cell Wall Anchor Protein	13	Surface associated protein (SasF)	(Kwiecinski, Jin, & Josefsson, 2014)

4.2.2 Preparation for the NTML library screen

4.2.2.1 Deconvolution of the NTML library

The Nebraska Transposon Mutagenesis Library (NTML) was received from Dr Kenneth Bayles, University of Nebraska Medical Centre. Only 1,920 of the 1,952 strains were received in 5 x 384-well microtitre plates. The remaining 32 were not supplied, as the Tn inserts were close to the 3' ends of these genes and may not completely disrupt gene function. However, these genes were available on request if required. For screening and for long-term propagation the library needed to be deconvoluted into 96-well plates, and into individual strain stocks for long-term usage (Figure 4.5A). Deconvolution to 96-well plates was required for screening purposes, as the screen is an agar based screen and the strains will be transferred to agar using a 96-pin replicator (Boekel Industries). Although 384-pin replicators are available, the ability to resolve differences in haemolysis and growth between such closely inoculated strains would be difficult if not impossible. The 1,920 strains were also added to separate bead stocks to allow easy access to individual strains within the library. Spare copies of the library were also made for future screening experiments and storage. Strains were transferred from the 384-well plate to 96-well plates using the 96-pin replicator (for details of the library, including identity of strains in each well of the plate, see Appendix 4.1). As the strains were transferred they were also used to inoculate BHI agar plates to determine if any obvious contaminants were present (e.g. fungal growth). This screen was also used to highlight any pitfalls associated with the screening method. Example plate images from the contamination screen are shown in Figure 4.5B; all plate images are included in Appendix 4.2. No obvious contaminants were found to be present when grown on BHI.

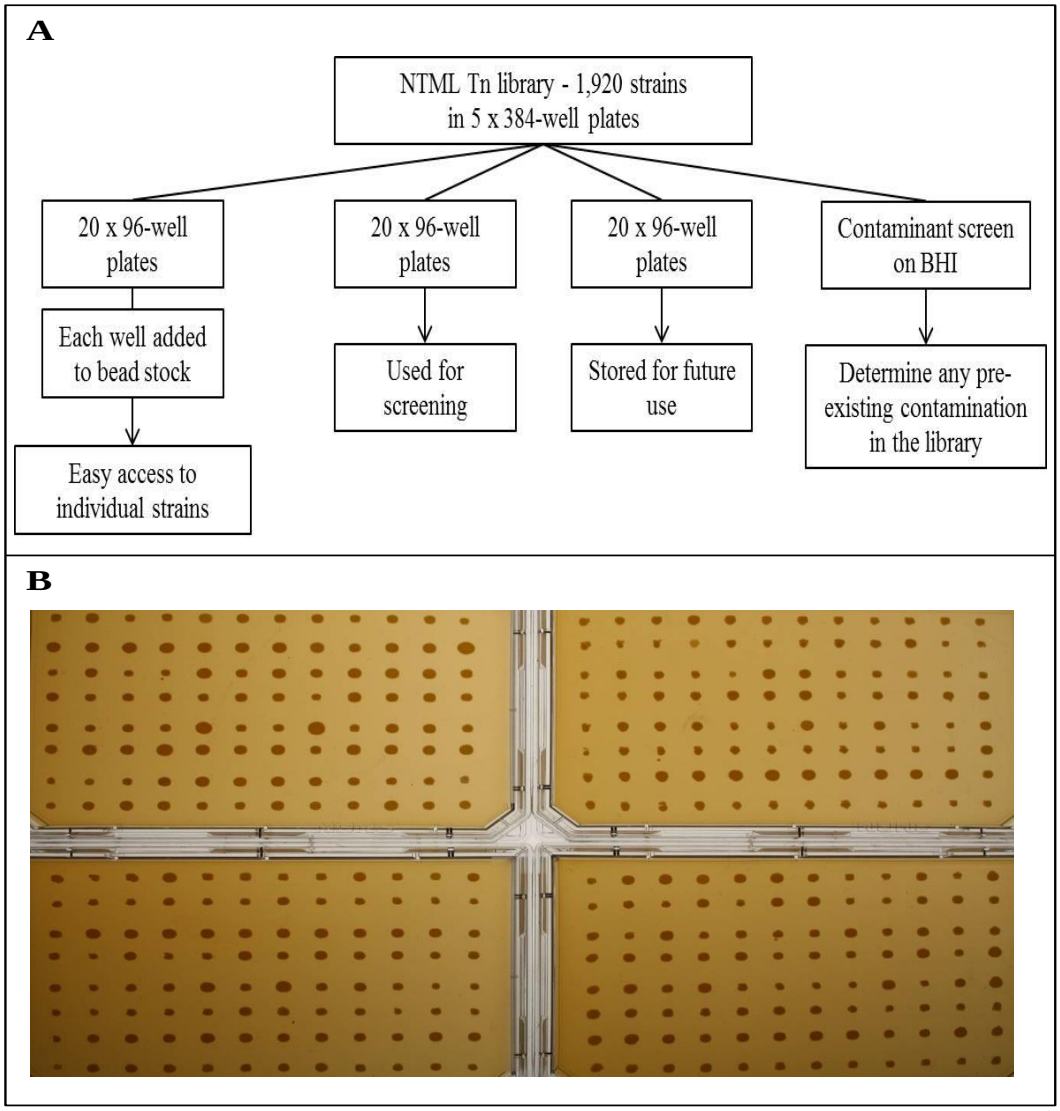

Figure 4.5 Deconvolution of the NTML.

A Diagram showing the deconvolution of the NTML strains, transferred from 384-well format to 96-well format, separation of the library into bead stocks and the contaminant screen.

B Example plates from the contaminant screen of the NTML, carried out during deconvolution of the library. By appearance there were no obvious contaminants found in the library, as each pin-inoculation had the appearance of *S. aureus*.

4.2.2.2 Determining suitable media for the NTML screen

Defining suitable concentrations of human blood and bovine serum was required before screening. As discussed in section 4.1 the plan was to screen the library on human blood agar, in which the only nutrient source is human blood, bovine serum agar, in which serum provides the nutrients and 5% (v/v) sheep blood with Columbia agar base, the Columbia agar providing a rich nutrient source. Small scale experiments using the wild-type, JE2, were performed to determine suitable blood and serum concentrations for the screen. Initial experiments were carried-out using standard Petri dishes (Figure 4.6). The method of preparation of human blood agar, sheep blood agar and bovine serum agar is given in Chapter 2.1.3. No growth was seen at 5, 10 and 20% (v/v) serum agar concentrations after 24 h (Figure 4.6A). Barely visible growth was seen on 20% (v/v) human blood agar after 24h and no growth was seen at the lower concentrations tested (Figure 4.6B; the poor growth on 20% (v/v) human blood could not be visualised by photography). Using 5 or 10% (v/v) sheep blood plus Columbia agar made no difference to the quality of haemolytic plates (Figure 4.6C).

The aim was to screen the library by applying the inoculum from a 96-well plate to rectangular OmniTray agar plates (Nunc) using a 96-pin replicator (Boekel Industries). Therefore, it was decided that further experiments to determine the correct serum and blood concentration would be done using the replicator and OmniTrays, thereby mimicking the conditions of the screen. The incubation period was also increased to 48 h and growth in aerobic and anaerobic conditions was assessed. A 96-well microtitre plate containing JE2 in each well was prepared. This was used to inoculate 30% (v/v) and 50% (v/v) human blood agar plates, which were then incubated under aerobic or anaerobic conditions for 48 h. Anaerobic growth was performed in anaerobic chambers using Anaerogen sachets (Thermo Scientific). Growth of JE2 on 30% (v/v) human blood in aerobic conditions was visible, but poor in comparison to growth under anaerobic conditions for 48 h (Figure 4.7A 1&2 respectively). Growth on 50% (v/v) human blood, in either aerobic or anaerobic conditions, was more apparent than growth on 30% (v/v) human blood grown anaerobically (Figure 4.7B).

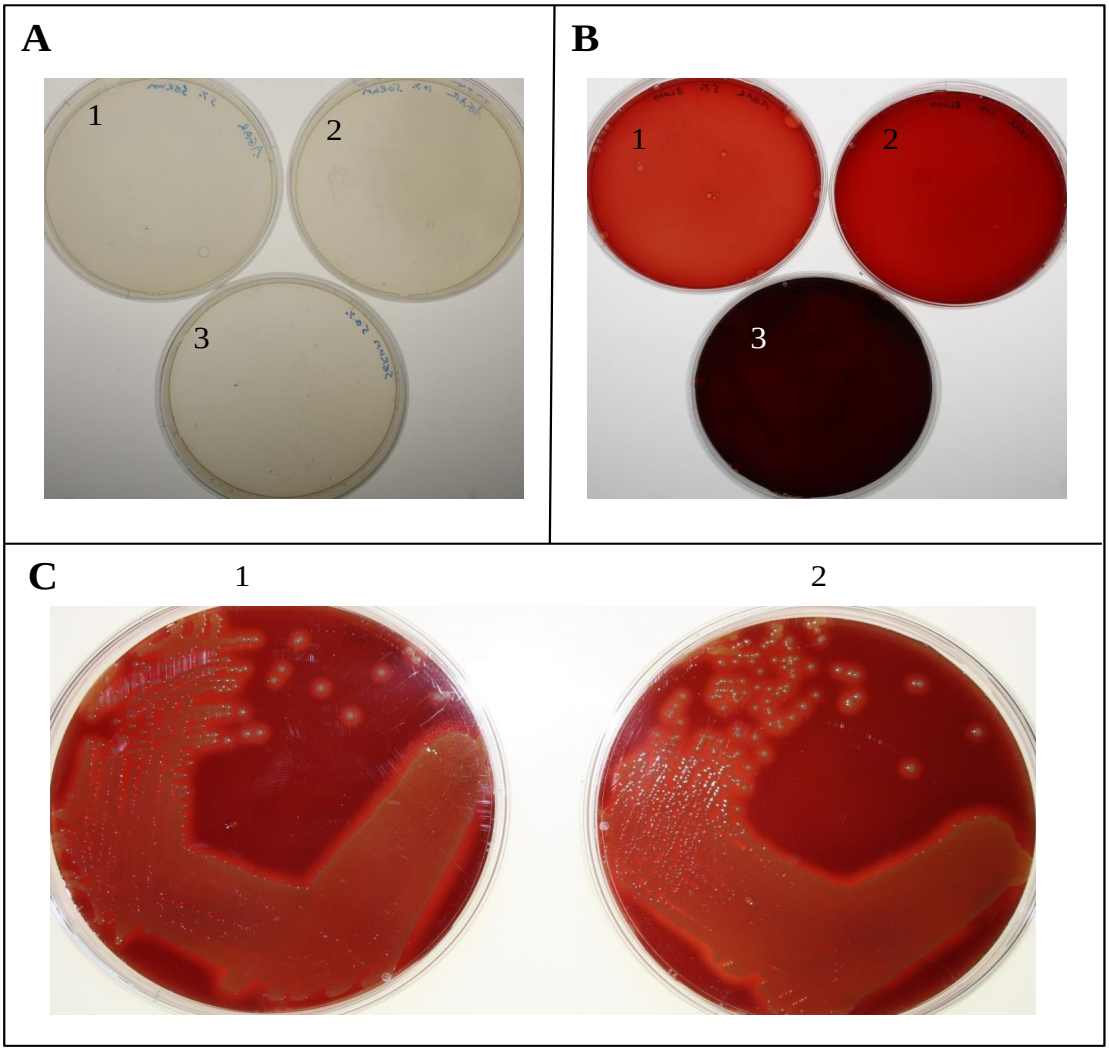

Figure 4.6 Determination of the correct blood/serum concentrations to be used for the NTML screen.

A1, **A2** and **A3** show 5% (v/v), 10% (v/v) and 20% (v/v) bovine serum agar plates respectively. No growth was seen after 24 h incubation at 37^{o}C.

B1, **B2** and **B3** show 5% (v/v), 10% (v/v) and 20% (v/v) human blood agar plates respectively. A small amount of growth was seen on 20% plates (could not be visualised on the photograph), and no growth was seen on 5 and 10% (v/v) human blood agar after 24 h incubation at 37^{o}C.

C1 and **C2** show 5% (v/v) and 10% (v/v) sheep blood with Columbia agar respectively, incubated at 37^{o}C for 24 h followed by 6 h at 4^{o}C. Both give healthy colonies with clear halos of haemolysis.

Growth on 30% (v/v) human blood in anaerobic conditions was deemed suitable for the screen, as the growth is clear and this concentration minimises the requirement for blood donors. Growth on bovine serum at 50% (v/v) was clear, as was growth and haemolysis using 5% (v/v) sheep blood plus Columbia agar (Figure 4.7C 1&2 respectively). However, it was decided to reduce the incubation period for sheep blood plates, as haemolysis was nearly complete across the whole plate after 24 h growth at 37^{o}C and 6 h at 4^{o}C (Figure 4.7C2). The large black spots seen on human blood plates are the result of clotting due to slow collection from donors. The blood collection procedure is outlined in Chapter 2.1.3.1.1. Only blood that was quickly collected and aliquoted into Falcon tubes containing anticoagulant within 5 min of collection would be used for the screen.

4.2.3 Screening the NTML library

4.2.3.1 Preliminary screen

A preliminary screen of the library was done on BHI +ery/lin, to confirm the presence of the Tn, which encodes an ery/lin^{R} cassette (Example plate images are shown in Figure 4.8, see Appendix 4.3 for all plate images). Bacteria from the wells of each 96-well plate of the library were transferred to solid media using a 96-pin replicator (Boekel Industries). Growth was seen for all wells of the NTML 96-well plates except for well G5 on the final plate, corresponding to the strain with the NARSA ID NE1901 (see arrow Figure 4.8). When tested for contaminants in section 4.2.2.1, this strain grew poorly compared to all other strains. The growth seen during the contaminant screen was either a contaminant, or NE1901 had such poor growth due to a growth defect resulting from Tn insertion that it did not grow enough to carry-over to the 96-well plates. The gene disrupted in NE1901 codes for the enzyme acetyl-CoA acetyltransferase (thiolase). Analysis of the Kegg and Biocyc databases revealed that this enzyme has roles in metabolism of fatty acids, butanoate, propanoate and pyruvate and in the catabolism of specific amino acids. Therefore, poor growth of this strain is potentially the result of diminished energy production. Any growth or lack of growth from this strain was not considered when analysing the screen results.

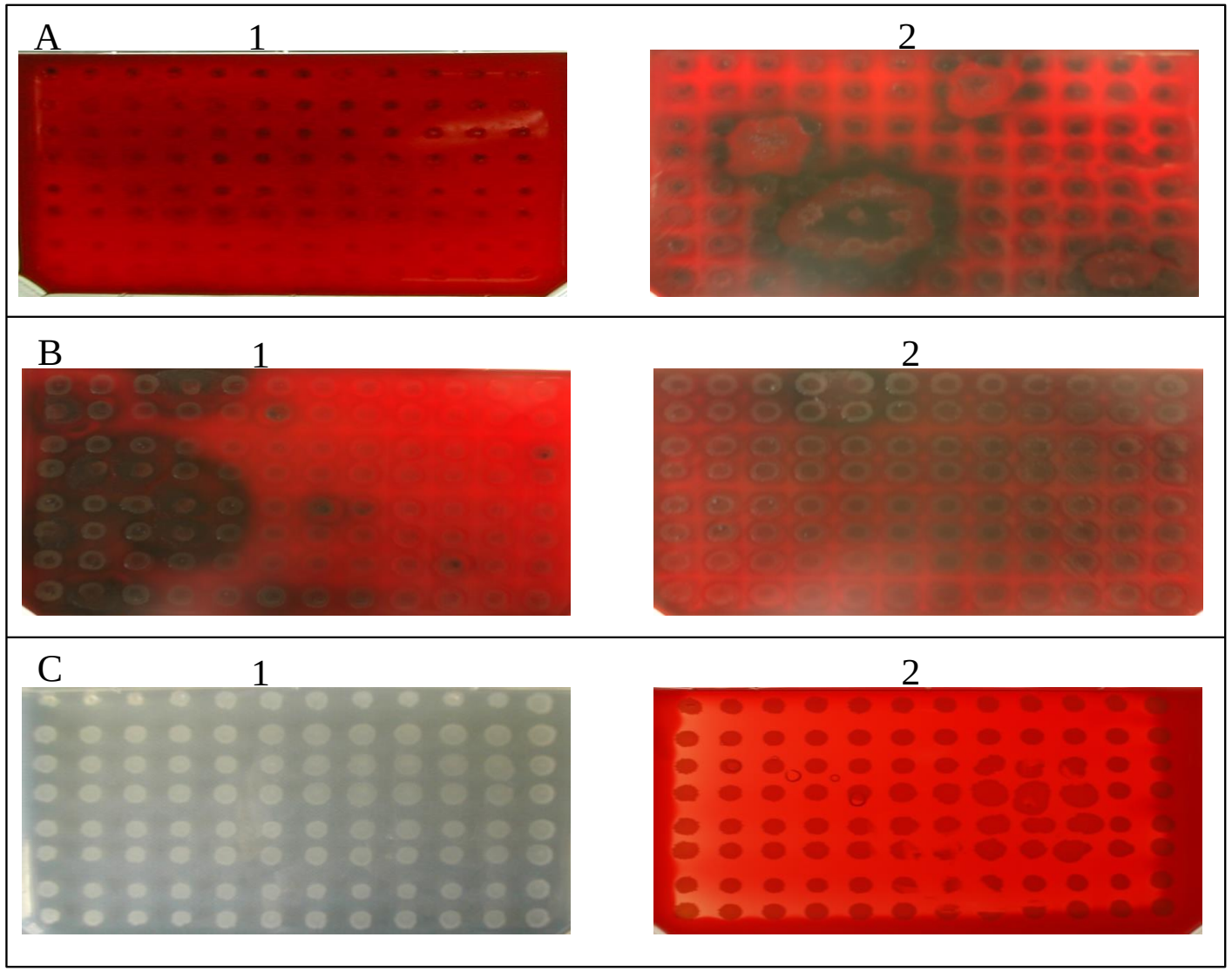

Figure 4.7 Establishment of conditions required for the NTML screen.

All plates were incubated at 37°C for 48 h unless stated.

A1 JE2 grown aerobically on 30% (v/v) human blood agar.

A2 JE2 grown anaerobically on 30% (v/v) human blood agar.

B1 JE2 grown aerobically on 50% (v/v) human blood agar.

B2 JE2 grown anaerobically on 50% (v/v) human blood agar.

C1 JE2 grown aerobically on 50% (v/v) bovine serum agar.

C2 JE2 grown aerobically on 5% (v/v) sheep blood + Columbia agar, for 24 h.

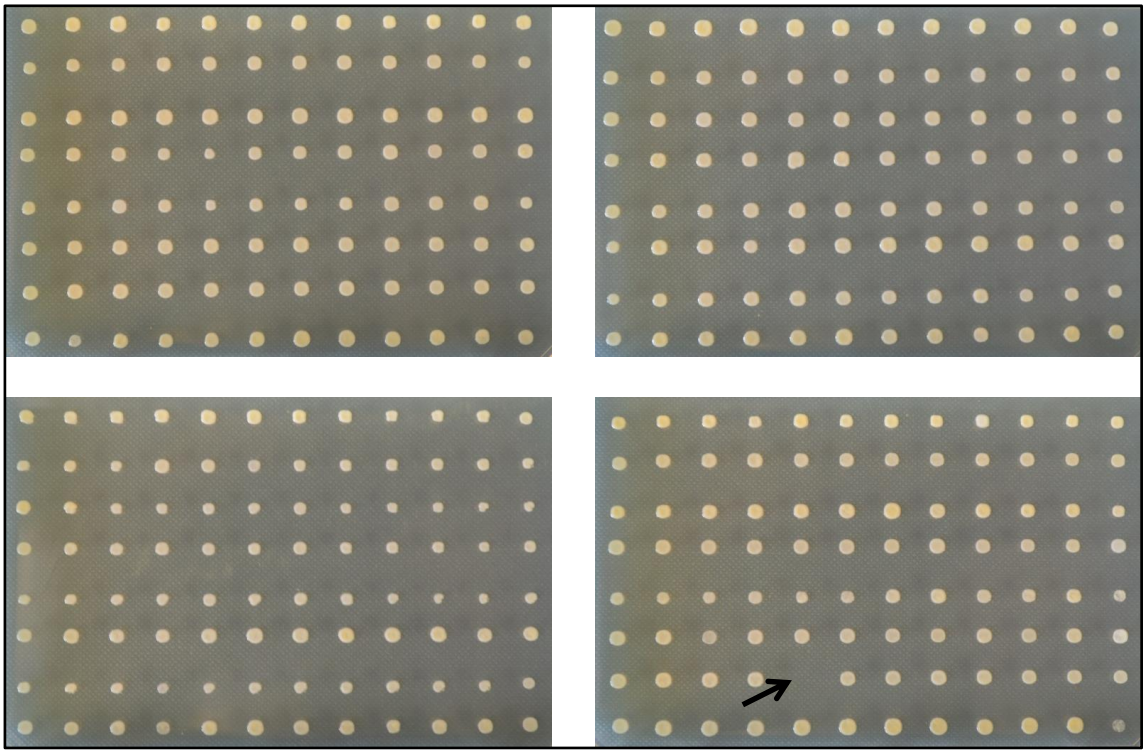

Figure 4.8 Example plates from the preliminary screen for resistance to ery/lin.

Arrow indicates no growth for well G5 on plate 5D, corresponding to the strain NE1901.

Growth was seen for all NTML strains other than NE1901.

4.2.3.2 Screening of the NTML library on human blood, bovine serum and sheep blood + Columbia agar

The NTML was screened on 30% (v/v) human blood, 50% (v/v) bovine serum and 5% (v/v) sheep blood + Columbia agar base. Before implementing the screen, it was decided strains would be selected visually based on alterations in growth, colony morphology and, where possible, haemolysis, in all media conditions. Altered phenotypes were judged based on the surrounding strains on the plate.

The full screening procedure is given in Chapter 2.22. A 96-pin replicator was used to inoculate the library on to each screen condition. Sheep blood + Columbia agar plates were incubated for 16 h at 37^{o}C then chilled at 4^{o}C for 4 h to allow for β-haemolysis (Figure 4.9). 50% (v/v) bovine serum agar plates were incubated at 37^{o}C for 48 h aerobically (Figure 4.10). 30% (v/v) human blood agar plates were incubated at 37^{o}C for 48 h anaerobically (Figure 4.11). Figures 4.10-4.12 show example plate images for each screen condition; all plate images are given in Appendices 4.4, 4.5 & 4.6.

4.2.4 Confirmation of the NTML screen results

4.2.4.1 Repeat screening of altered phenotype strains

Of the 1,920 strains screened, 100 had an altered phenotype on one or more of the growth conditions, when compared to their nearest neighbours on the plate. Of the 100, 72 had an altered phenotype on human blood only or human blood plus one or both of the other conditions. To confirm the phenotype, each of the 100 strains was patched back on to the three conditions to see if the phenotype was retained (Figure 4.12). Sixty eight of the patched strains retained the phenotype observed in the screen. However, the primary goal of the screen was to find strains whose growth is altered when grown on human blood. The other conditions were used to give an indication why the growth is altered, for example low haemolysis on sheep blood may indicate that this strain cannot liberate nutrients from red blood cells, or good growth on serum but poor growth on blood may indicate an inhibitory component in human blood. Therefore, only those that retained their phenotype on human blood alone, or human blood and one or both of the other conditions were taken forward for further analysis. This gave 46 strains of interest resulting from the screen and patching confirmation (Table 4.3).

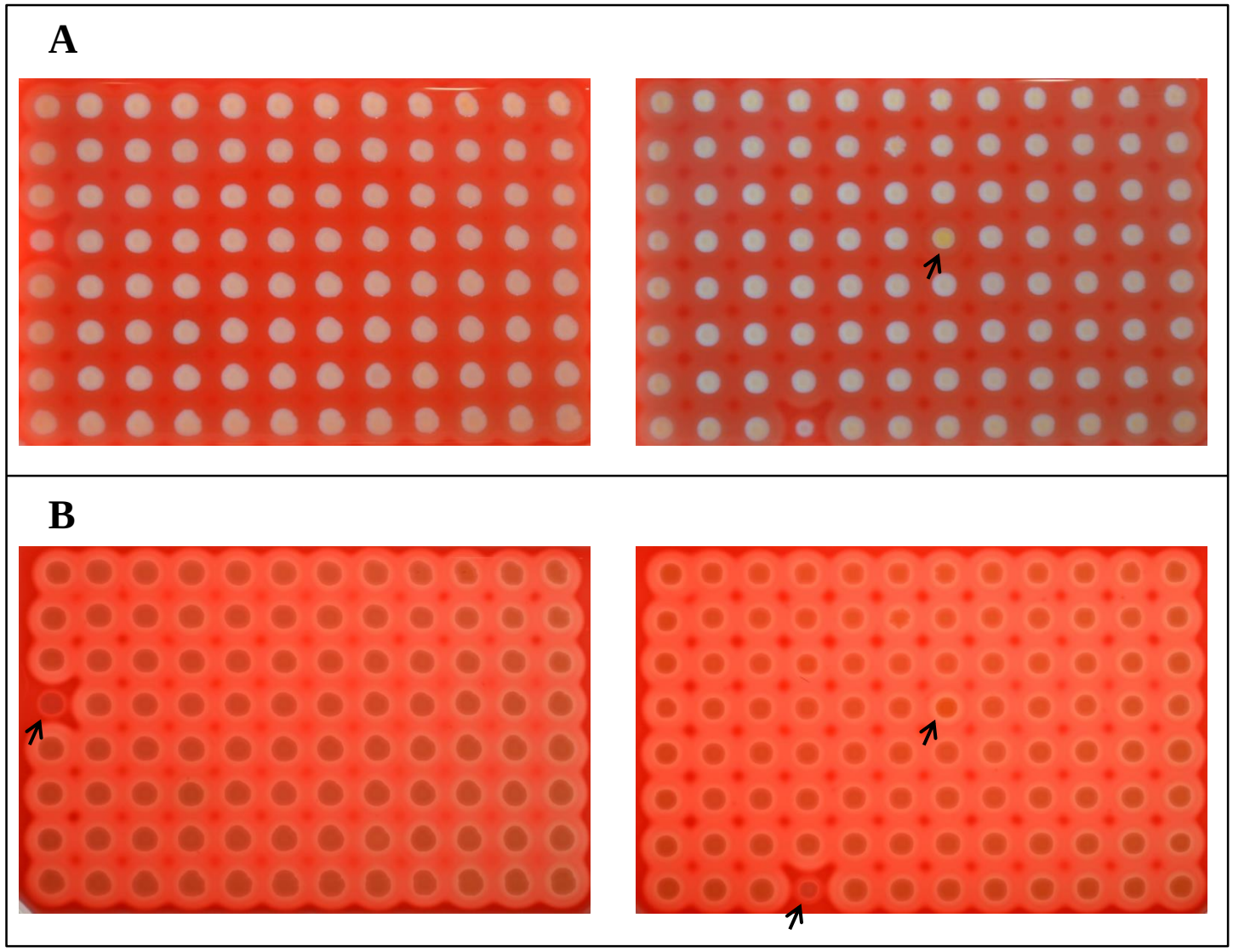

Figure 4.9 Identification of mutants with altered growth, morphology or haemolysis on sheep blood + Columbia agar.

Arrows indicate example strains of interest.

A Strains with altered morphology were selected for further study.

B Strains with increased or reduced haemolysis were selected for further study.

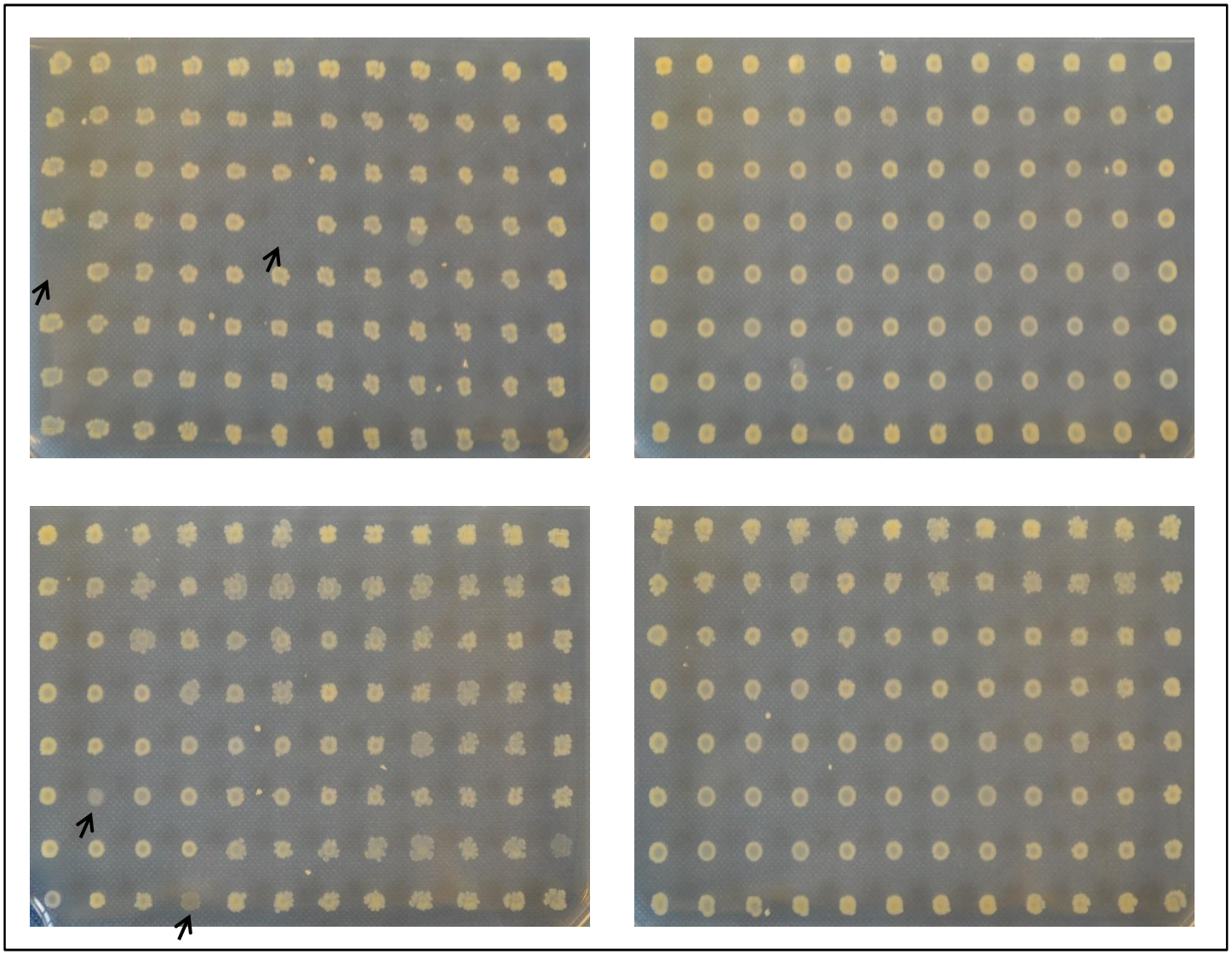

Figure 4.10 Identification of mutants with altered growth or morphology on bovine serum agar.

Arrows indicate example strains of interest.

Strains showing no growth, reduced growth or altered pigmentation or morphology were selected for further study

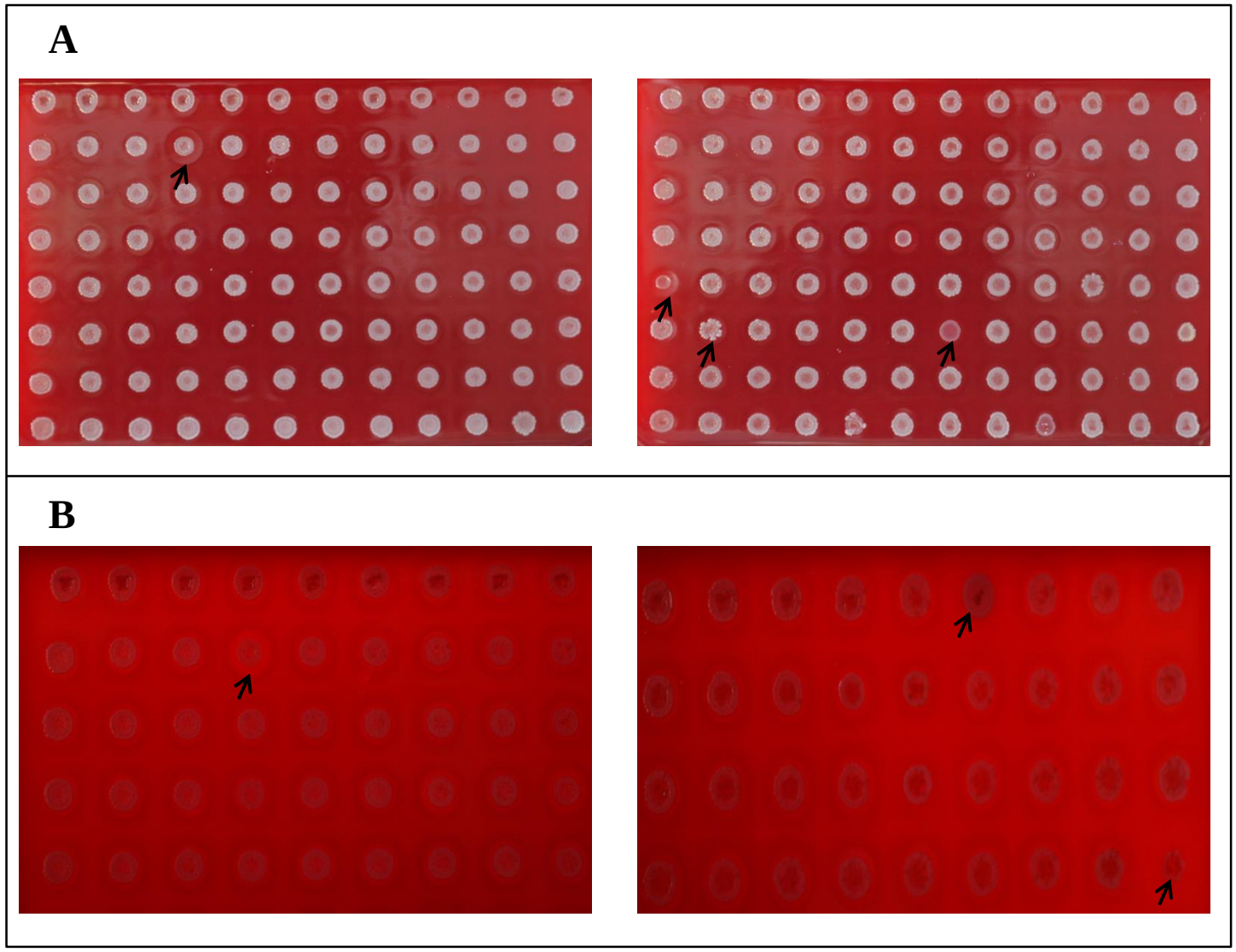

Figure 4.11 Identification of mutants with altered growth, morphology or haemolysis on human blood agar.

Arrows indicate example strains of interest.

A Strains with reduced growth and altered morphology were chosen for further study.

B Haemolysis was difficult to see on human blood agar plates, due to the high concentration of blood. However, strains showing a clear difference in haemolysis were selected.

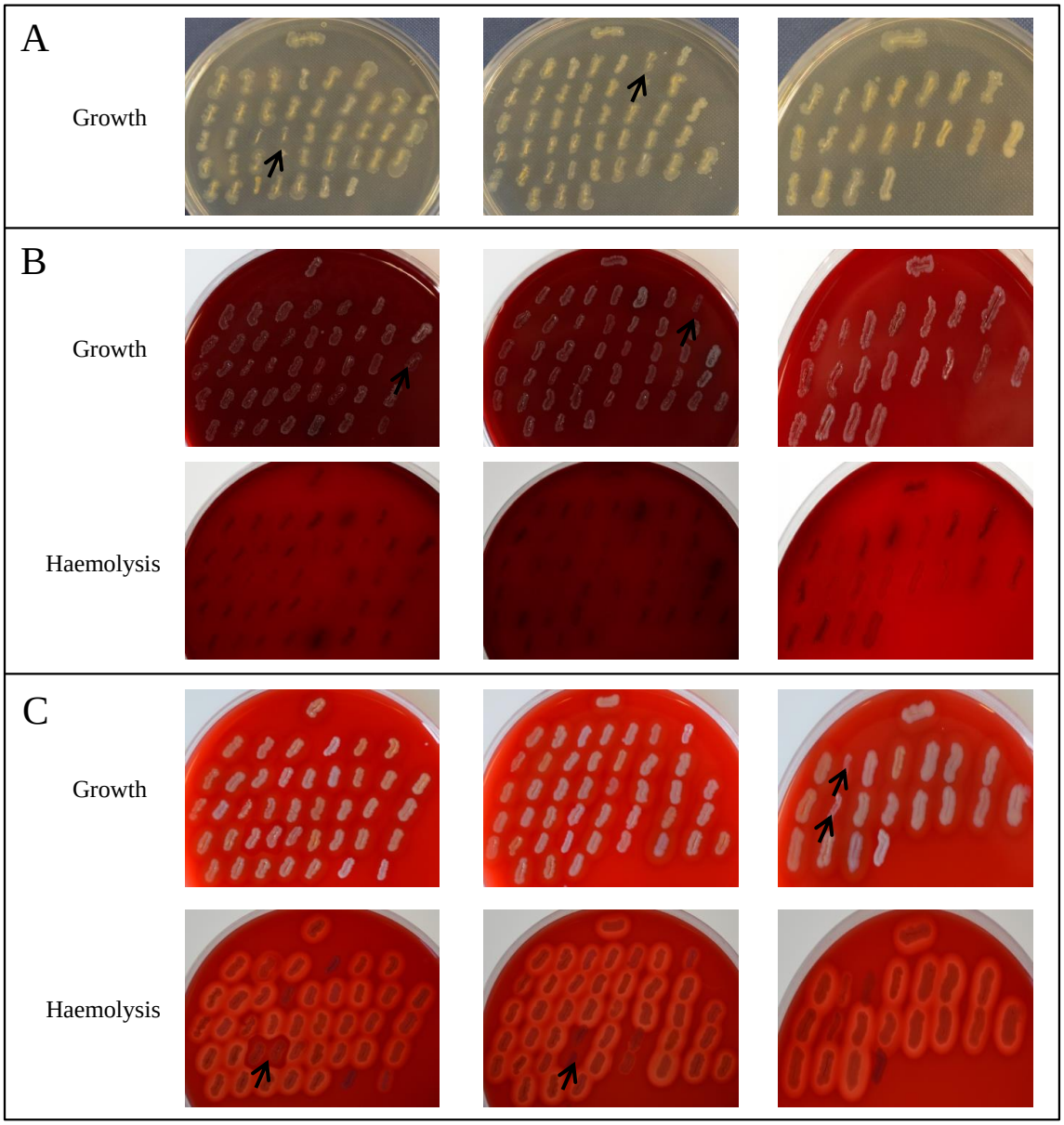

Figure 4.12 Repeat screening for mutant phenotypes.

JE2 strain is patched at the 12 o'clock position on each plate.

Arrows indicate example strains that retained their mutant phenotype

A Bovine serum.

B Human blood.

C Sheep blood + Columbia agar.

68 of the strains retained their phenotype when patched back on to their corresponding screen condition.

Table 4.3 Strains identified as having an altered phenotype on human blood agar. ------ = No altered phenotype found.

NARSA Strain ID	Gene ID	Gene Name	Description	SH1000 identity (%)	Screen Conditions		
					30% Human Blood Agar	5% Sheep Blood + Columbia Agar	50% Bovine Serum Agar
NE27	SAUSA300_1895	*nos*	nitric oxide synthase oxygenase	100	Slightly reduced growth	------	------
NE92	SAUSA300_0963	*qoxA*	quinol oxidase, subunit II	99	Reduced growth. No haemolysis	------	------
NE95	SAUSA300_1989	*agrB*	accessory gene regulator protein B	100	No haemolysis. Opaque pigmentation	No haemolysis	------
NE229	SAUSA300_1119	-	hypothetical protein	100	Reduced growth and haemolysis	Highly reduced haemolysis	------
NE427	SAUSA300_1801	*fumC*	fumarate hydratase class II	100	No haemolysis. Opaque pigmentation	------	------
NE460	SAUSA300_0955	*atl*	autolysin	99	Opaque pigmentation	------	------
NE522	SAUSA300_1889	*purB*	adenylosuccinate lyase	100	Reduced growth	Reduced haemolysis and growth	Highly reduced growth
NE529	SAUSA300_0017	*purA*	adenylosuccinate synthetase	100	Reduced growth	Increased haemolysis	Highly reduced growth
NE547	SAUSA300_1306	*odhA*	2-oxoglutarate dehydrogenase E1 component	100	Reduced growth	------	------
NE552	SAUSA300_2408	*nikD*	oligopeptide ABC transporter ATP-binding protein	100	Slightly reduced growth	------	------
NE573	SAUSA300_1713	*ribBA*	riboflavin biosynthesis protein	100	Slightly reduced growth	------	White opaque pigmentation
NE594	SAUSA300_1641	*gltA*	citrate synthase II	100	Slightly reduced growth	------	------
NE635	SAUSA300_1714	*ribE*	riboflavin synthase subunit alpha	100	Reduced growth	------	------
NE821	SAUSA300_0698	*pabA*	para-aminobenzoate synthase, glutamine amidotransferase, component II	100	Reduced growth	------	------
NE857	SAUSA300_2346	*nirB*	nitrite reductase [NAD(P)H], large subunit	100	Opaque pigmentation	------	------
NE873	SAUSA300_1991	*agrC*	accessory gene regulator protein C	99	No haemolysis. Opaque pigmentation	No haemolysis	------
NE884	SAUSA300_2409	*nikC*	oligopeptide ABC transporter permease	100	Reduced haemolysis and slightly reduced growth	------	------
NE896	SAUSA300_0903	-	hypothetical protein	100	No haemolysis	------	------
NE912	SAUSA300_0752	*clpP*	ATP-dependent Clp protease proteolytic subunit	100	Reduced growth	Reduced haemolysis and growth	Reduced growth. White opaque pigmentation
NE945	SAUSA300_0188	*brnQ*	branched-chain amino acid transport system II carrier protein	100	Highly reduced haemolysis. Opaque pigmentation	------	------
NE1048	SAUSA300_1092	*pyrP*	uracil permease		No haemolysis	------	Slightly reduced growth
NE1063	SAUSA300_0699	*pabB*	chorismate-binding domain-containing protein	100	Increased haemolysis and reduced growth	------	------
NE1236	SAUSA300_0338	-	glyoxalase family protein	100	Increased haemolysis	------	------

Table 4.3 continued

NARSA Strain ID	Gene ID	Gene Name	Description	SH1000 identity (%)	Screen Conditions		
					30% Human Blood Agar	5% Sheep Blood + Columbia Agar	50% Bovine Serum Agar
NE1253	SAUSA300_0193	*murQ*	*N*-acetylmuramic acid-6-phosphate etherase	100	Increased haemolysis	------	------
NE1260	SAUSA300_1731	*pckA*	phosphoenolpyruvate carboxykinase	100	Increased haemolysis	------	------
NE1267	SAUSA300_0391	-	hypothetical protein	100	Increased haemolysis	Increased haemolysis	------
NE1296	SAUSA300_0690	*saeS*	sensor histidine kinase	100	No haemolysis	Highly reduced haemolysis	------
NE1299	SAUSA300_0905	-	hypothetical protein	100	Increased haemolysis	------	------
NE1304	SAUSA300_2326	*araC*	transcription regulatory protein	100	No haemolysis	------	------
NE1315	SAUSA300_0899	*mecA*	adaptor protein	100	Increased haemolysis	------	------
NE1354	SAUSA300_1058	*hla*	alpha-hemolysin	100	No haemolysis	Highly reduced haemolysis	------
NE1391	SAUSA300_1305	*odhB*	dihydrolipoamide succinyltransferase	100	Reduced growth	Highly increased haemolysis	------
NE1404	SAUSA300_1605	*mreC*	rod shape-determining protein	100	Highly reduced haemolysis. Opaque pigmentation	------	------
NE1434	SAUSA300_1016	*ctaB*	protoheme IX farnesyltransferase	99	No haemolysis. Reduced growth	------	------
NE1509	SAUSA300_0630	*abcA*	ABC transporter ATP-binding protein	100	Reduced haemolysis. Opaque pigmentation	------	------
NE1532	SAUSA300_1992	*agrA*	accessory gene regulator protein A	100	No haemolysis. Opaque pigmentation	None haemolysis	------
NE1536	SAUSA300_0791	*gcvH*	glycine cleavage system protein H	100	Reduced growth	Increased haemolysis	------
NE1543	SAUSA300_0961	*qoxC*	quinol oxidase, subunit III	100	No haemolysis. Slightly reduced growth	------	------
NE1604	SAUSA300_2407	*nikE*	oligopeptide ABC transporter ATP-binding protein	100	Slightly reduced growth	------	------
NE1610	SAUSA300_0996	*lpdA*	dihydrolipoamide dehydrogenase	99	Highly reduced growth	Reduced growth and reduced haemolysis	Reduced growth
NE1622	SAUSA300_0691	*saeR*	DNA-binding response regulator	100	No haemolysis	Highly reduced haemolysis	------
NE1659	SAUSA300_0195	-	transcriptional regulator	100	Highly increased haemolysis	Highly increased haemolysis	------
NE1751	SAUSA300_0979	-	hypothetical protein	100	Highly reduced growth	------	Slightly reduced growth
NE1770	SAUSA300_1139	*sucD*	succinyl-CoA synthetase subunit alpha	100	Highly reduced growth	Reduced growth	------
NE1775	SAUSA300_0320	*lipA*	triacylglycerol lipase	99	Highly increased haemolysis. Slightly reduced growth	Increased haemolysis	------
NE1908	SAUSA300_1911	-	ABC transporter ATP-binding protein	100	None haemolysis. Opaque pigmentation	No haemolysis	White opaque pigmentation

4.2.4.2 Transduction of Tn inserts into JE2 and SH1000

Each of the 46 Tn inserts were transduced back into JE2 and into SH1000. This was done in the JE2 background to establish that the mutant phenotype was associated with the Tn insertion. Strains of choice would also be studied in SH1000 to demonstrate the effect of the mutations in an independent genetic background (see Chapter 5). SH1000 was chosen, as it is a common laboratory *S. aureus* strain (Horsburgh *et al.*, 2002). Furthermore, when grown on human blood agar aerobically and anaerobically it had similar growth and haemolysis characteristics to JE2 (Figure 4.13).

The Tn inserts were transduced back into JE2 to show that the phenotype is linked to the Tn insertion, and not the result of non-linked genome changes. The transduction procedure is shown diagrammatically in Figure 4.14. A total of 92 transductions were carried out (i.e. each of the 46 Tn inserts transduced into JE2 and each of the 46 transduced into SH1000) and 33 of the 46 Tn transductions in each background gave colonies for both strains (JE2 and SH1000). For the transduction method see Chapter 2.10.3. Although repeated attempts were made, the remaining 15 Tn inserts could not be transduced into either background.

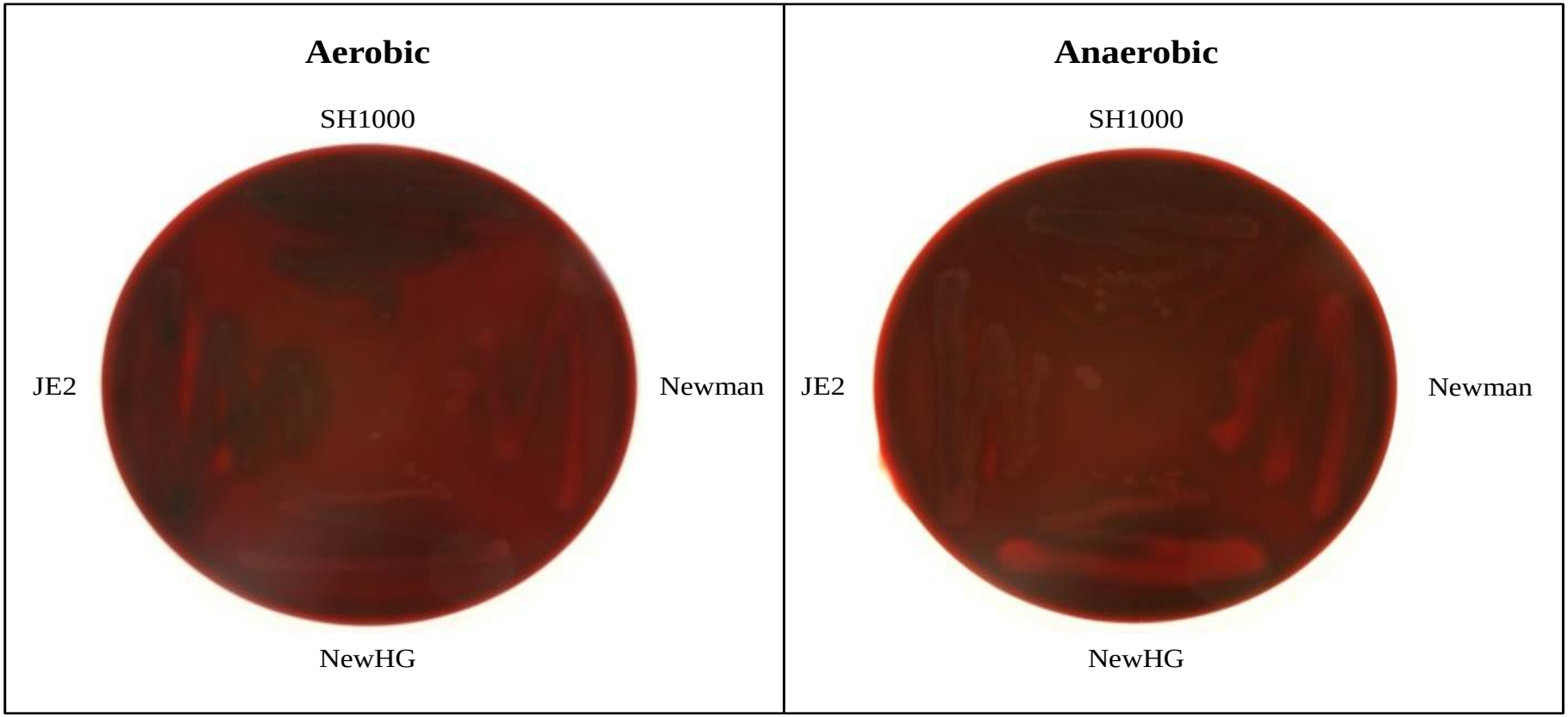

Figure 4.13 Growth and haemolysis of different strains of *S. aureus* on human blood agar.

Again haemolysis was difficult to visualise on 30% (v/v) human blood agar. However, strains NewHG and Newman appear to have higher haemolytic activity on human blood than JE2 and SH1000.

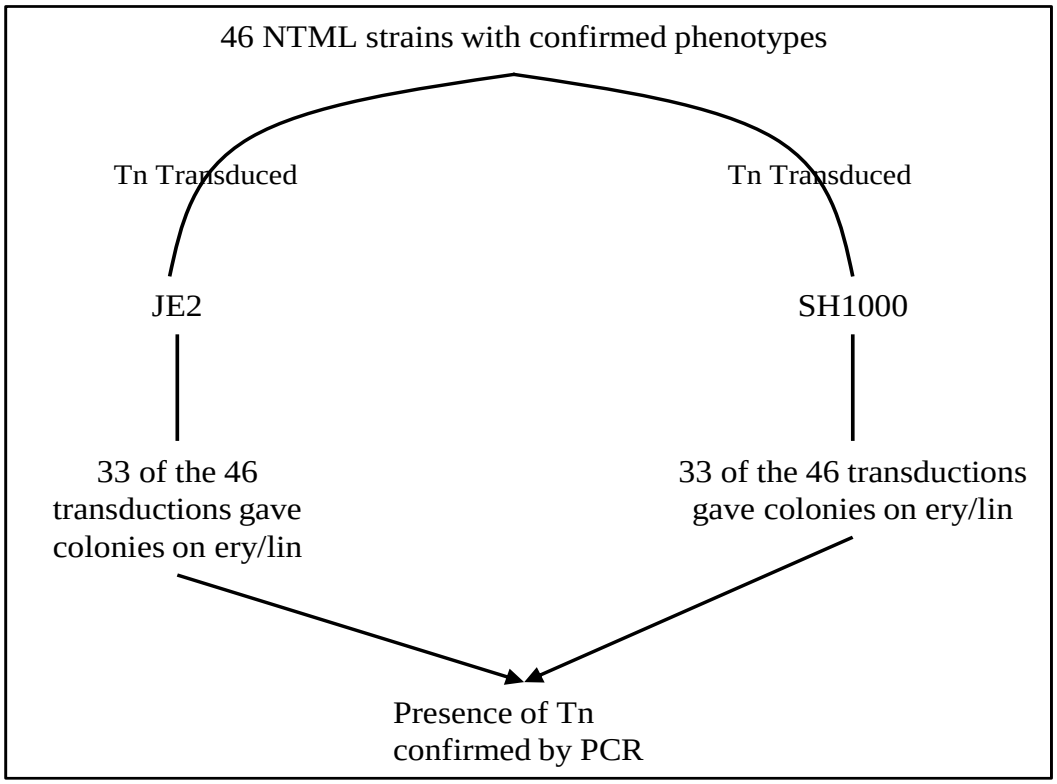

Figure 4.14 Diagram of the transduction of the Tn from the 46 NTML screen results into SH1000 and JE2.

Attempts were made to transduce all 46 Tn insertions into SH1000 and JE2. Only 33 of the 46 transductions gave colonies on ery/lin for both strain backgrounds. Colonies were checked for the presence of the Tn by PCR.

4.2.4.2.1 Confirmation of successful transduction

The NTML database provides the exact insertion site for every Tn in the library. 33 sets of primers were designed against the *S. aureus* USA300 FPR3757 genome, 400bp upstream and 400bp downstream of the insertion sites given in the database (for primer sequences see Chapter 2.12.1.1). If the Tn was present in any of the transduction colonies, then the primers would amplify the full transposon giving a PCR product of ~4kb. If the transduction failed, the transposon would not be present and only a small region of 800bp maximum size would be amplified (Figure 4.15). The PCR products were assessed by 1% (w/v) gel electrophoresis (Chapter 2.12.5), which showed that 31 of the 33 strains that gave colonies after transduction were successful transductants (Figure 4.16; Table 4.4).

4.2.4.3 Is the JE2 phenotype linked to the Tn insertion?

Strains were streaked on different media to confirm that the phenotype is linked to the Tn insertion. As all 31 strains were originally selected on human blood, they were tested on 30% (v/v) human blood agar to confirm the phenotype (an example plate is given in Figure 4.17 A1, all plates for all conditions in Figure 4.17 are given in Appendix 4.7 a, b, c & d). As seen in the screen results (Figure 4.11) and when growing the wild-type strains (Figure 4.13), disparity in haemolysis was particularly difficult to observe on human blood plates containing 30% (v/v) blood. This was no different when the 31 strains were grown as single colonies on 30% (v/v) blood. Therefore, it was decided that only variations in growth would be assessed on these plates (Figure 4.17 A1). Additionally, rabbit blood agar was inoculated with the 31 transductant strains to determine any difference in growth between human blood and rabbit blood (Figure 4.17 A2). To assess haemolysis, the strains were grown on Columbia agar containing 5% (v/v) sheep blood or 5% (v/v) human blood (Figure 4.17 B1 and B2 respectively). The resulting growth and haemolysis phenotypes are shown in Table 4.5.

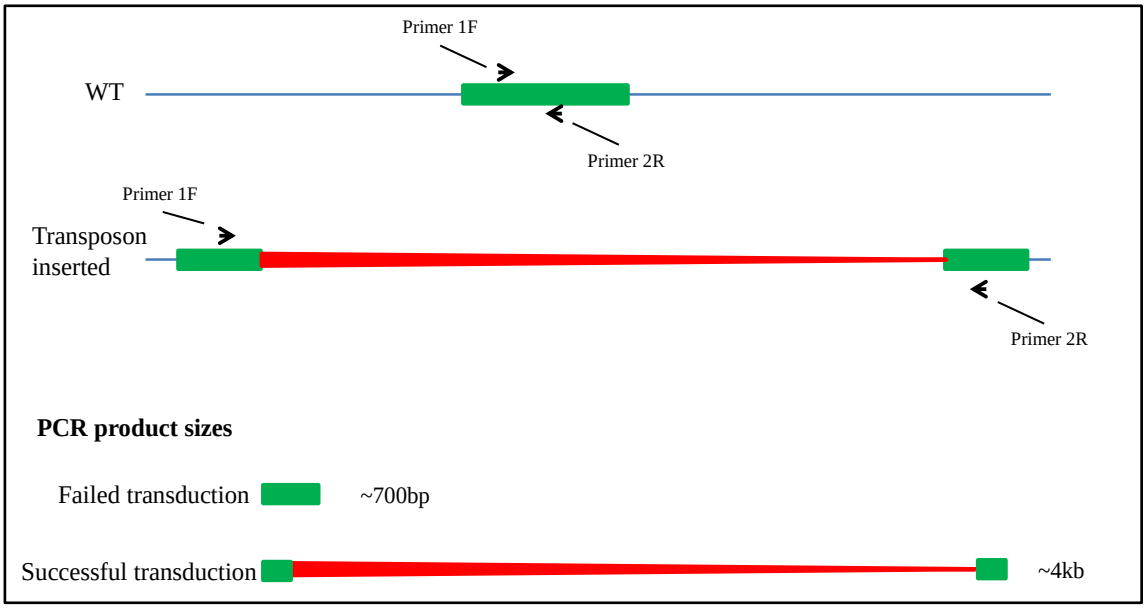

Figure 4.15 Diagram showing how primers were designed to confirm Tn insertion by transduction.

Successful transductions have the Tn inserted between the primer sites and so the full Tn will amplify. Failed transductions will not have the Tn present, so the short region containing the insertion site will be amplified.

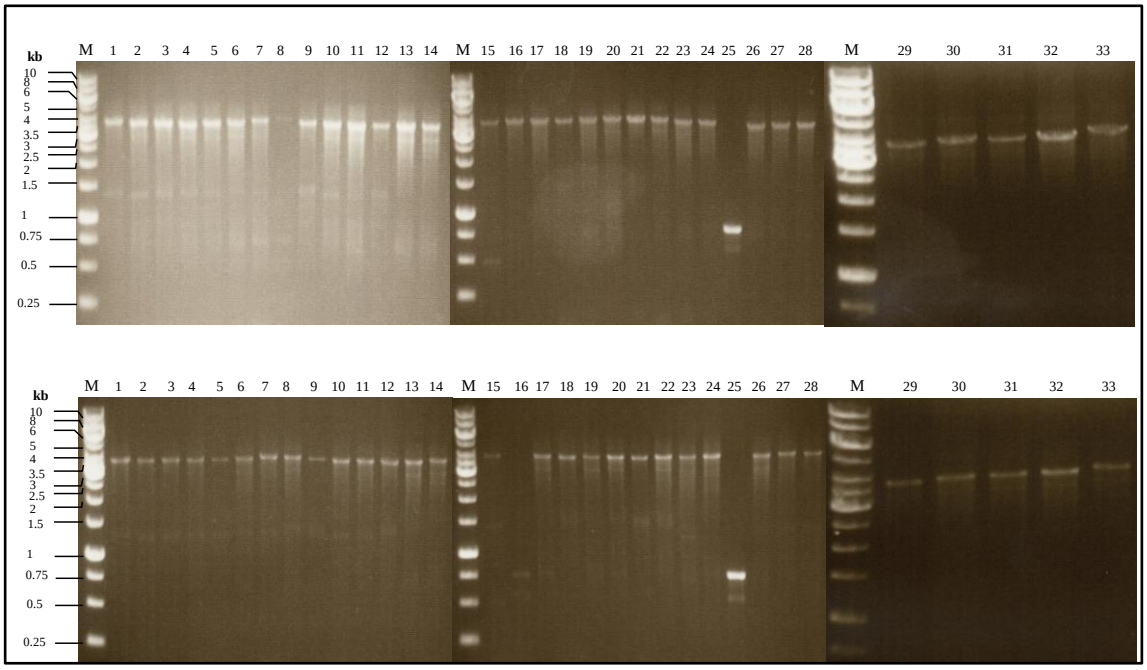

Figure 4.16 Demonstration of Tn insertion site in transductants.

DNA fragments were separated by 1% (w/v) agarose gel electrophoresis. Standards (M) of sizes shown are in each panel.

The top row gels are the SH1000 PCR products. Lane 25 shows a PCR product corresponding to the size of the insertion site without the Tn insert. The bottom row gels are JE2 PCR products. Lanes 16 and 25 show PCR products of sizes corresponding to failed transductions. The first gel on both rows appears to show a lot of weak bands. These are the result of non-specific binding at the 56^{o}C annealing temperature used for the PCR. Increasing the temperature for the PCRs removes the faint bands. From the above images 31 of the 33 transductions that gave colonies on ery/lin containing solid media have the Tn inserted in the gene corresponding to the library strain.

Table 4.4 Transduction of Tn inserts from isolated NTML mutants into the JE2 and SH1000 strain background.

NARSA Strain ID	Gene ID	Gene Name	Gene name	Transductant Strain Designations – JE2	Transductant Strain Designations – SH1000
NE27	SAUSA300_1895	*nos*	nitric oxide synthase oxygenase	JE2-*nos*	SH-*nos*
NE92	SAUSA300_0963	*qoxA*	quinol oxidase, subunit II	JE2-*qoxA*	SH-*qoxA*
NE95	SAUSA300_1989	*agrB*	accessory gene regulator protein B	JE2-*agrB*	SH-*agrB*
NE229	SAUSA300_1119	-	hypothetical protein	JE2-229	SH-229
NE460	SAUSA300_0955	*atl*	autolysin	JE2-*atl*	SH-*atl*
NE522	SAUSA300_1889	*purB*	adenylosuccinate lyase	JE2-*purB*	SH-*purB*
NE529	SAUSA300_0017	*purA*	adenylosuccinate synthetase	JE2-*purA*	SH-*purA*
NE573	SAUSA300_1713	*ribBA*	riboflavin biosynthesis protein	JE2-*ribBA*	SH-*ribBA*
NE594	SAUSA300_1641	*gltA*	citrate synthase	JE2-*gltA*	SH-*gltA*
NE635	SAUSA300_1714	*ribE*	riboflavin synthase subunit alpha	JE2-*ribE*	SH-*ribE*
NE821	SAUSA300_0698	*pabA*	para-aminobenzoate synthase, glutamine amidotransferase, component II	JE2-*pabA*	SH-*pabA*
NE873	SAUSA300_1991	*agrC*	accessory gene regulator protein C	JE2-*agrC*	SH-*agrC*
NE896	SAUSA300_0903	-	hypothetical protein	JE2-896	SH-896
NE912	SAUSA300_0752	*clpP*	ATP-dependent Clp protease proteolytic subunit	JE2-*clpP*	SH-*clpP*
NE1048	SAUSA300_1092	*pyrP*	uracil permease	JE2-*pyrP*	SH-*pyrP*

Table 4.4 continued

NARSA Strain ID	Gene ID	Gene Name	Gene name	Transductant Strain Designations – JE2	Transductant Strain Designations – SH1000
NE1253	SAUSA300_0193	*murQ*	*N*-acetylmuramic acid-6-phosphate etherase	JE2-*murQ*	SH-*murQ*
NE1267	SAUSA300_0391	-	hypothetical protein	JE2-1267	SH-1267
NE1296	SAUSA300_0690	*saeS*	sensor histidine kinase	JE2-*saeS*	SH-*saeS*
NE1299	SAUSA300_0905	-	hypothetical protein	JE2-1299	SH-1299
NE1304	SAUSA300_2326	*araC*	transcription regulatory protein	JE2-*araC*	SH-*araC*
NE1315	SAUSA300_0899	*mecA*	adaptor protein	JE2-*mecA*	SH-*mecA*
NE1354	SAUSA300_1058	*hla*	alpha-hemolysin	JE2-*hla*	SH-*hla*
NE1391	SAUSA300_1305	*odhB*	dihydrolipoamide succinyltransferase	JE2-*odhB*	SH-*odhB*
NE1434	SAUSA300_1016	*ctaB*	protoheme IX farnesyltransferase	JE2-*ctaB*	SH-*ctaB*
NE1509	SAUSA300_0630	*abcA*	ABC transporter ATP-binding protein	JE2-*abcA*	SH-*abcA*
NE1532	SAUSA300_1992	*agrA*	accessory gene regulator protein A	JE2-*agrA*	SH-*agrA*
NE1536	SAUSA300_0791	*gcvH*	glycine cleavage system protein H	JE2-*gcvH*	SH-*gcvH*
NE1604	SAUSA300_2407	*nikE*	oligopeptide ABC transporter ATP-binding protein	JE2-*nikE*	SH-*nikE*
NE1622	SAUSA300_0691	*saeR*	DNA-binding response regulator	JE2-*saeR*	SH-*saeR*
NE1775	SAUSA300_0320	*lipA*	triacylglycerol lipase	JE2-*lipA*	SH-*lipA*
NE1908	SAUSA300_1911	-	ABC transporter ATP-binding protein	JE2-1908	SH-1908

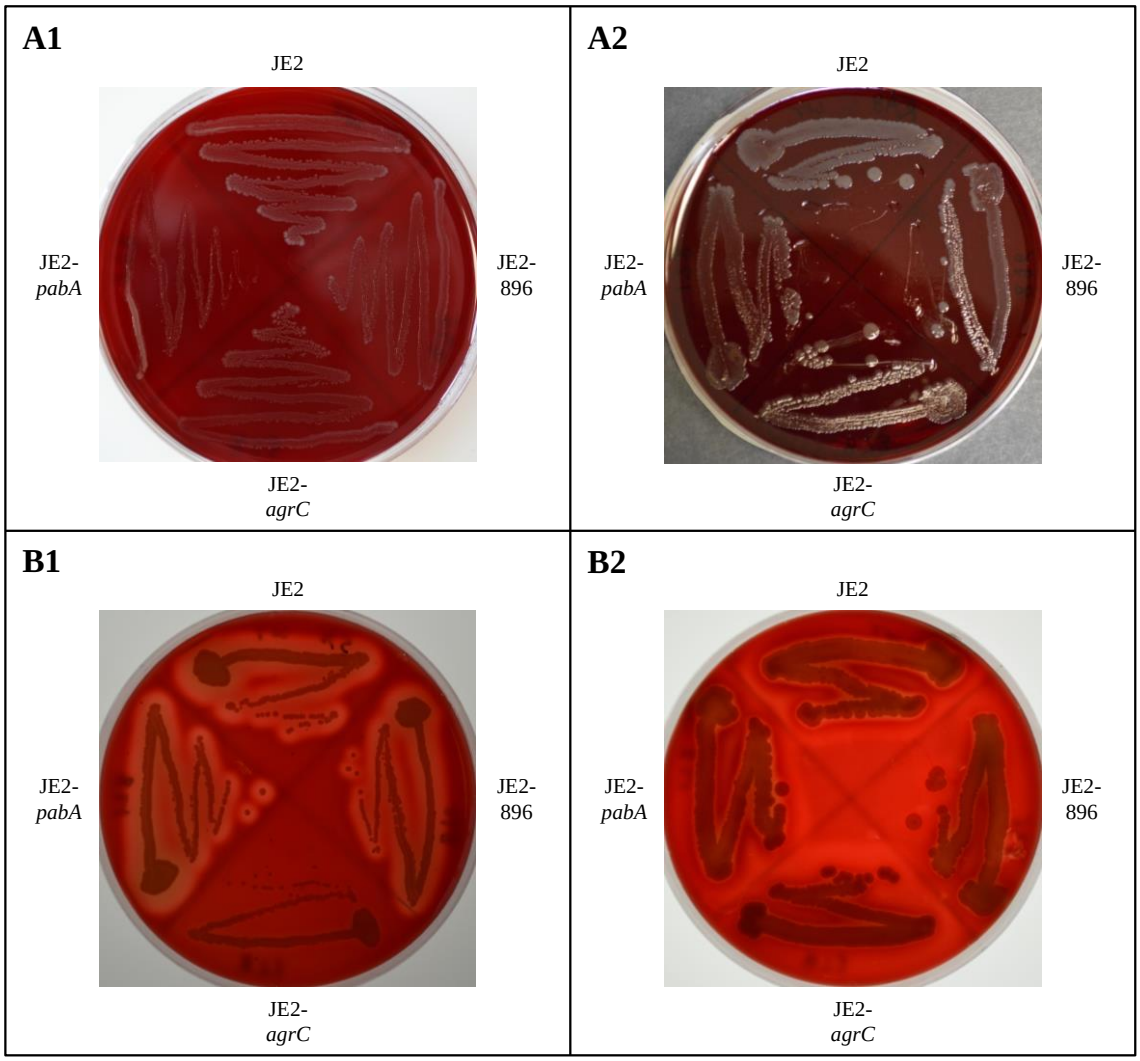

Figure 4.17 Phenotype of transductants on blood agar plates.

A1. Growth phenotypes on 30% (v/v) human blood agar.

A2. Growth phenotypes on 30% (v/v) rabbit blood agar.

B1. Haemolysis on 5% sheep blood + Columbia agar.

B2. Haemolysis on 5% human blood + Columbia agar.

Table 4.5 Identification of strains with altered phenotype post-transduction. ------ = no difference to the wild-type.

Category	NARSA Strain ID	Strain Name	Growth Phenotype		Haemolysis Phenotype	
			Human Blood	Rabbit Blood	5% Human Blood + Columbia Agar	5% Sheep Blood + Columbia Agar
A1	NE522	JE2-*purB*	Reduced Growth	Reduced Growth	Increased Haemolysis	Reduced Haemolysis
	NE529	JE2-*purA*	Reduced Growth	Reduced Growth	Increased Haemolysis	Slightly Increased Haemolysis
	NE821	JE2-*pabA*	Highly Reduced Growth	Slightly Reduced Growth	------	------
A2	NE460	JE2-*atl*	Opaque Colony	Opaque Colony	Increased Haemolysis	------
	NE1253	JE2-*murQ*	------	------	Increased Haemolysis	Increased Haemolysis
	NE1304	JE2-*araC*	------	------	Reduced Haemolysis	------
	NE1315	JE2-*mecA*	------	------	Reduced Haemolysis	Slightly Reduced Haemolysis
	NE1391	JE2-*odhB*	Slightly Reduced Growth	Slightly Reduced Growth	Increased Haemolysis	Increased Haemolysis
	NE1775	JE2-*lipA*	Slightly Reduced Growth	------	Increased Haemolysis	------
B	NE95	JE2-*agrB*	------	------	------	Reduced Haemolysis
	NE873	JE2-*agrC*	------	------	Slightly Reduced	No Haemolysis
	NE1296	JE2-*saeS*	------	------	------	No Haemolysis
	NE1354	JE2-*hla*	------	------	------	No Haemolysis
	NE1532	JE2-*agrA*	------	------	Reduced Haemolysis	No Haemolysis
	NE1622	JE2-*saeR*	------	------	------	No Haemolysis

Category A1 in Table 4.5 shows all strains that gave a clear growth phenotype when grown on human blood agar. Category A2 shows those strains that gave a clear haemolysis phenotype on 5% (v/v) human blood plus Columbia agar. Some strains in category A2 gave a growth phenotype, however, this was only slight when compared with the growth defect of category A1 strains. Category B strains are those strains that gave a clear phenotype, but are the in-built controls within the screen. When screening on human blood, it was expected that virulence gene regulator proteins and toxins such as α-haemolysin would be found amongst the positive results. The strains in category B provided confidence in the screen results, but their role in pathogenicity is well characterised and they were not taken forward for further study.

4.2.5 Species specificity of JE2-*pabA* phenotype

Interestingly the *pabA* mutant strain, JE2-*pabA*, showed highly reduced growth on human blood, but only a subtle reduction in growth was seen when grown on rabbit blood (Figure 4.17). Furthermore, when screening the NTML, strain NE821 (the NTML *pabA* mutant) showed highly reduced growth on human blood and normal growth on bovine serum. This suggested that the phenotype was specific to human blood, or the blood of a subset of species. Growth of JE2-*pabA* was compared to that of JE2 on 30% (v/v) sheep blood agar and 30% (v/v) horse blood agar (Figure 4.18 A & B, respectively). Growth of JE2-*pabA* was comparable to JE2 on sheep blood and only slightly reduced on horse blood. This demonstrated that the *pabA* phenotype is strain specific.

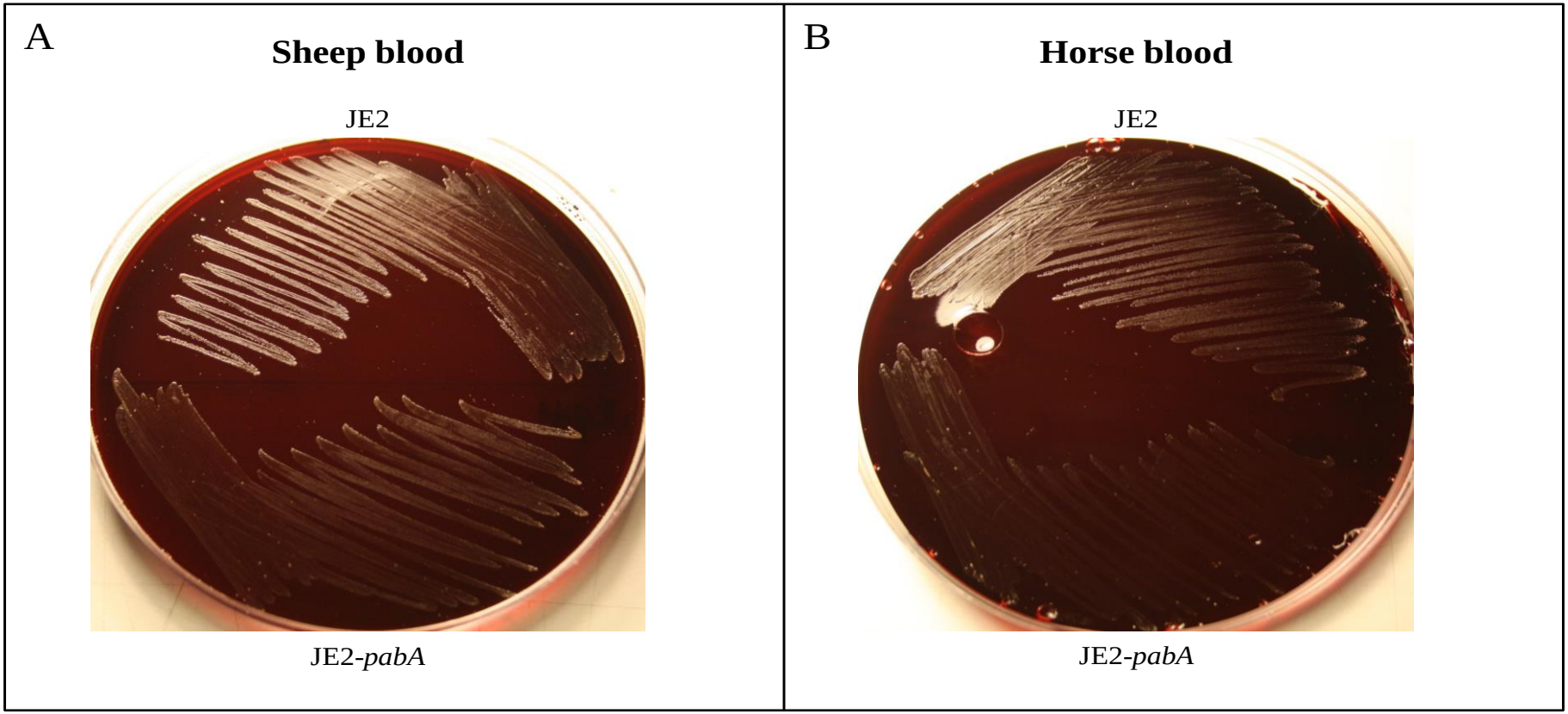

Figure 4.18 Growth analysis of JE2-*pabA* on sheep and horse blood agar.

A. Growth phenotypes on 30% (v/v) sheep blood agar.

B. Growth phenotypes on 30% (v/v) horse blood agar.

Plates were incubated for 48 h at 37^{o}C.

4.2.6 Bioinformatic analysis of the 9 strains of interest

The IDs of the disrupted genes in the nine strains of interest were used for bioinformatic analysis in order to obtain known information for these genes. The method used is shown diagrammatically in Figure 4.19. Sequence features including protein description, function and gene/protein length were confirmed using the Uniprot and NCBI Protein databases. The Kegg (linked to from Uniprot) and Biocyc databases were searched to give the known pathways that each gene has a role in. Information for each strain is given in Table 4.6. Atl and MurQ are involved in peptidoglycan degradation and recycling, both have roles in muropeptide turnover and recycling. PurA and PurB catalyse steps in the *de novo* purine biosynthesis pathway. PabA catalyses a step in tetrahydrofolate metabolism. The OdhB protein has a role in energy production via the tricarboxylic acid cycle (TCA). LipA is a lipase with a role in the triacylglycerol degradation pathway. All 9 genes were present in all *S. aureus* strains currently sequenced and all genes, apart from *lipA*, have homologous genes in other *Staphylococcus sp*.

Tn insertion site for each gene was obtained from the NARSA website, which is the companion website of the NTML. The website hosts the free genome viewer, GView (Petkau *et al*., 2010), which was used to identify the genome position and flanking genes for each of the nine NTML results. Genome position, flanking genes and Tn insertion sites are displayed in Figure 4.20 A-I. Analysis of the flanking genes suggested that eight of the nine genes may be part of an operon Figure 4.20 A-H. It was essential to confirm this, as if the genes had to be complemented in future work, then the entire operon would have to be used to complement the strain, due to potential polar effects. The operonic structure for *pabA*, *murQ*, *araC* and *odhB* (Figure 4.20 D, E, F & H respectively) has been further verified by transcriptomics (Broeke-Smits *et al*., 2010).

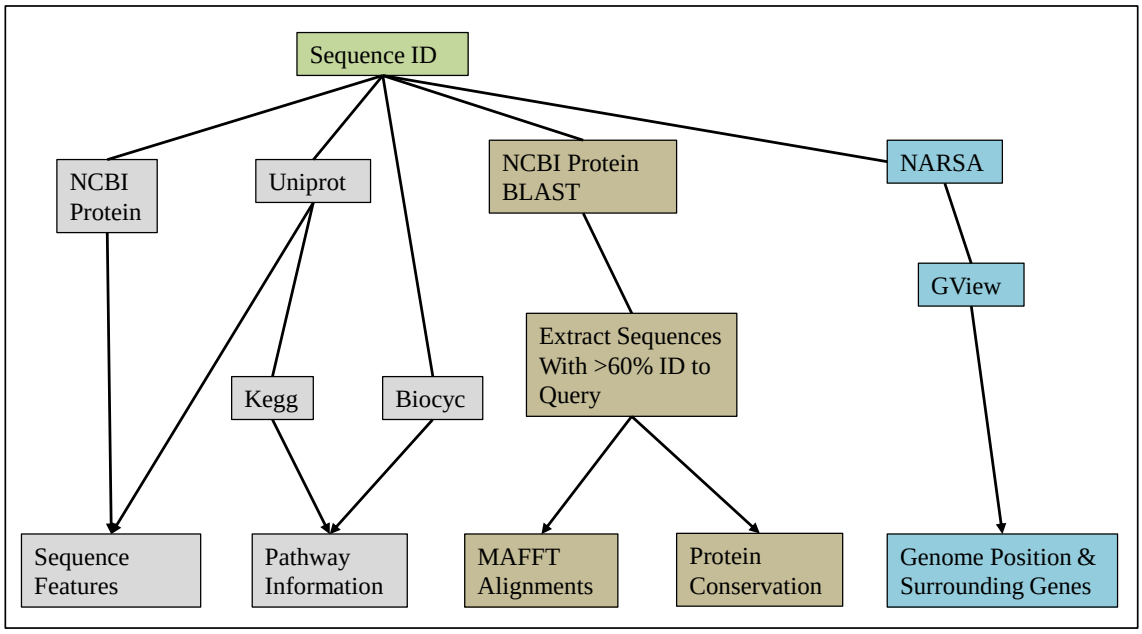

Figure 4.19 Diagram of the methods employed to acquire information on each of the nine Tn inserted genes.

NCBI Protein and Uniprot were used to confirm sequence features. Pathway information was obtained from the Kegg and Biocyc databases. NCBI protein BLAST was used to assess level of conservation of each gene. Genome position, Tn insertion site and surrounding gene information was found on the NARSA website accompanying the NTML.

Table 4.6 Sequence features, function and pathway information for the nine NTML Tn inserted genes.

NARSA Strain ID	Protein ID	Protein Length (aa)	Gene Length (bp)	Description	Gene Name	Function	Pathway
NE460	SAUSA300_0955	1256	3771	Autolysin	*atl*	Peptidoglycan degradation & recycling	Peptidoglycan metabolism
NE522	SAUSA300_1889	431	1296	Adenylosuccinate lyase	*purB*	Catalyses 2 steps in purine biosynthesis	Purine biosynthesis
NE529	SAUSA300_0017	427	1284	Adenylosuccinate synthetase	*purA*	Catalyses 1 step in purine biosynthesis	Purine biosynthesis
NE821	SAUSA300_0698	197	594	Paraaminobenzoate synthase, glutamine amidotransferase, component_II	*pabA*	Catalyses 1 step in the production of p-aminobenzoic acid from chorismate. Essential in tetrahydrofolate production	Folate biosynthesis pathway
NE1253	SAUSA300_0193	298	897	*N*-acetylmuramic acid-6-phosphate esterase*	*murQ*	Peptidoglycan degradation & recycling	Peptidoglycan metabolism
NE1304	SAUSA300_2326	701	2106	Transcription regulatory protein	*araC*	Contains HTH domain. A domain primarily observed in positive regulators of transcription	------
NE1315	SAUSA300_0899	239	720	Adaptor protein	*mecA*	Targets unfolded/aggregated proteins for ClpP degradation	------
NE1391	SAUSA300_1305	422	1269	Dihydrolipoamide succinyltransferase	*odhB*	Conversion of 2-oxoglutarate to succinyl-CoA and CO_2	Tricarboxylic acid cycle
NE1775	SAUSA300_0320	690	2073	Triacylglycerol lipase precursor	*lipA*	Converts triglycerides to diglycerides in fatty acid metabolism	Triacylglycerol degradation

* Annotated in the NTML library as a conserved hypothetical protein. Uniprot, BLAST and NCBI Protein give the description in the table.

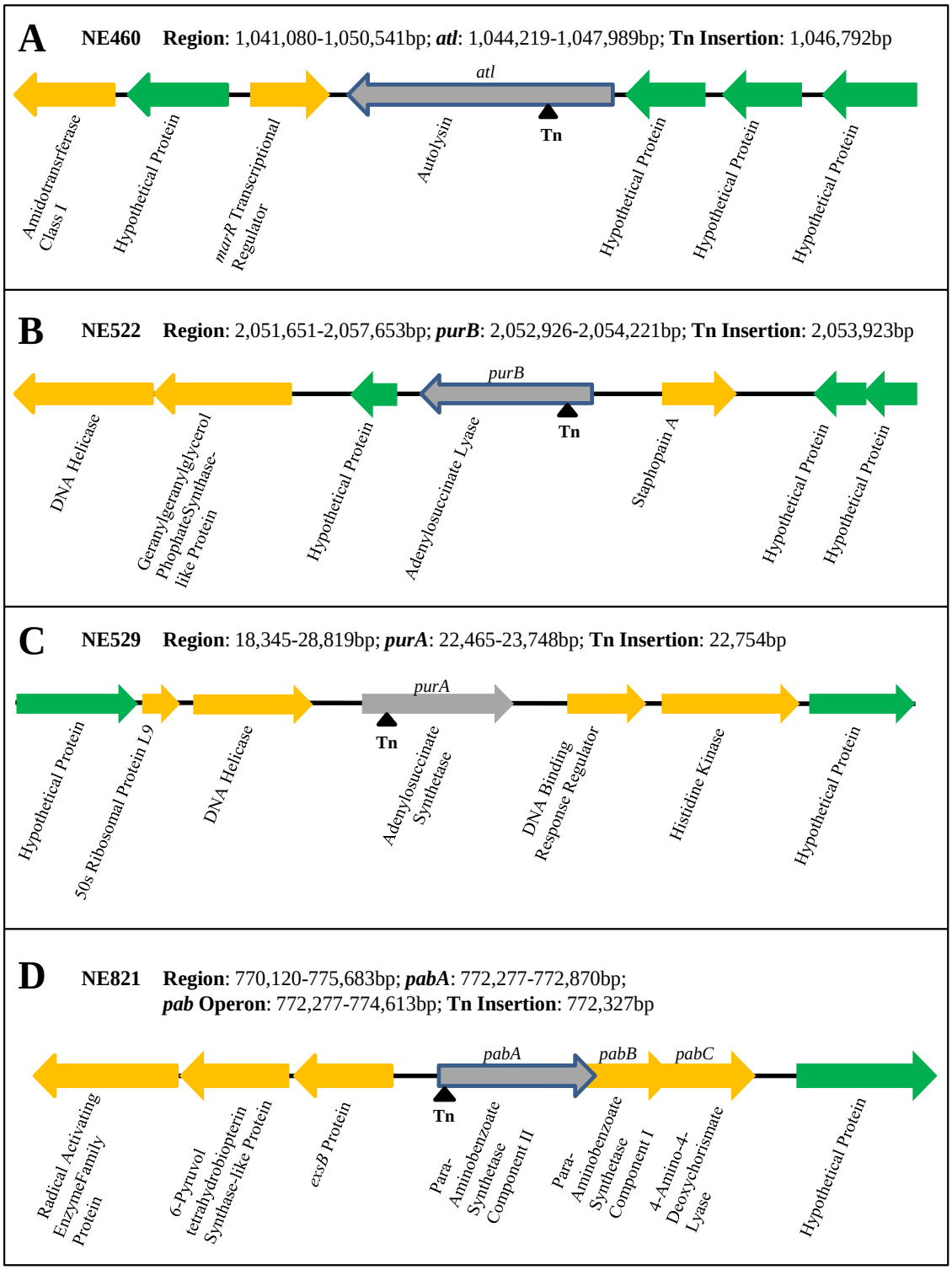
A
NE460 Region: 1,041,080-1,050,541bp; atl: 1,044,219-1,047,989bp; Tn Insertion: 1,046,792bp
atl
Tn
Amidotransrférase Class I
Hypothetical Protein
marR Transcriptional Regulator
Autolysin
Hypothetical Protein
Hypothetical Protein
Hypothetical Protein
B
NE522 Region: 2,051,651-2,057,653bp; purB: 2,052,926-2,054,221bp; Tn Insertion: 2,053,923bp
purB
Tn
DNA Helicase
GeranylgeranylglycerolPhphateSynthase-like Protein
Hypothetical Protein
Adenylosuccinate Lyase
Staphopain A
Hypothetical Protein
Hypothetical Protein
C
NE529 Region: 18,345-28,819bp; purA: 22,465-23,748bp; Tn Insertion: 22,754bp
purA
Tn
Hypothetical Protein
50s Ribosomal Protein L9
DNA Helicase
Adenylosuccinate Synthetase
DNA Binding Response Regulator
Histidine Kinase
Hypothetical Protein
D
NE821 Region: 770,120-775,683bp; pabA: 772,277-772,870bp;
pab Operon: 772,277-774,613bp; Tn Insertion: 772,327bp
pabA
pabB
pabC
Tn
Radical Activating EnzymeFamily Protein
6-Pyruvol tetrahydrobiopterin Synthase-like Protein
exsB Protein
Para-Aminobenzoate Synthetase Component II
Para-Aminobenzoate Synthetase Component I
4-Amino-4-Deoxychorismate Lyase
Hypothetical Protein

E **NE1253** **Region**: 219,419-231,736bp; ***murQ***: 225,019-225,915bp;
***mur* Operon**: 223,964-228,259; **Tn Insertion**: 225,272bp

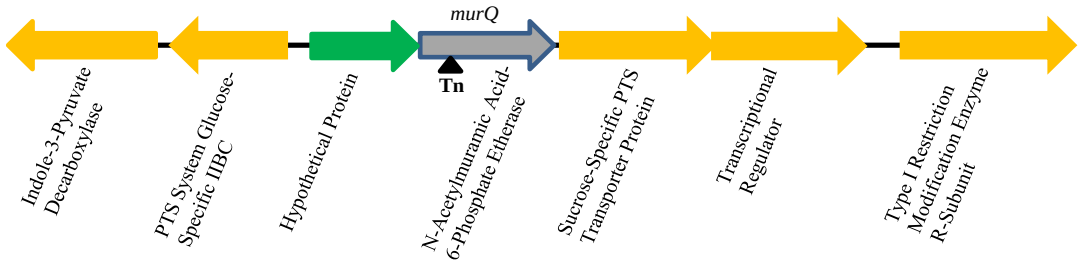

F **NE1304** **Region**: 2,496,801-2,506,227bp; ***araC***: 2,501,327-2,503,432bp;
***ara* Operon**: 2,501,327-2,503,925bp; **Tn Insertion**: 2,501,453bp

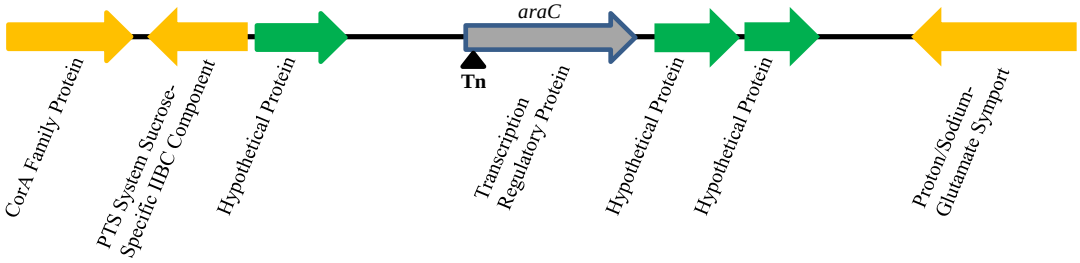

G **NE1315** **Region**: 984-763-991,417bp; ***mecA***: 987,736-988,455bp; **Tn Insertion**: 987,925bp

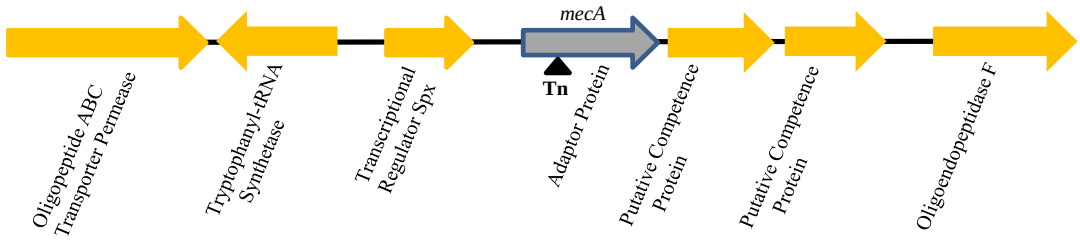

H **NE1391** **Region**: 1,433,301-1,442,269bp; ***odhB***: 1,435,894-1,437,162bp;
***odh* Operon**: 1,435,894-1,439,974bp; **Tn Insertion**: 1,436,724bp

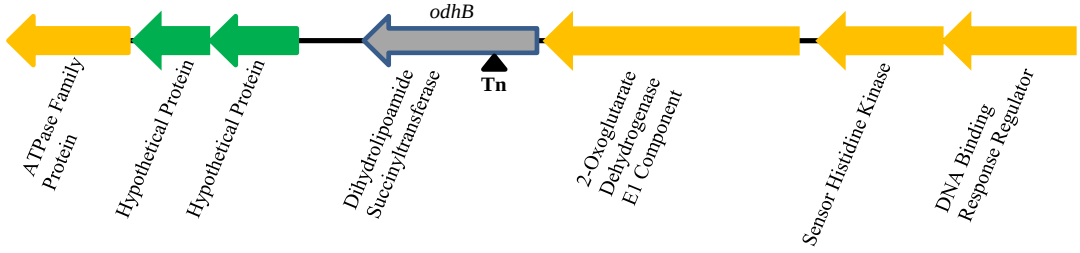

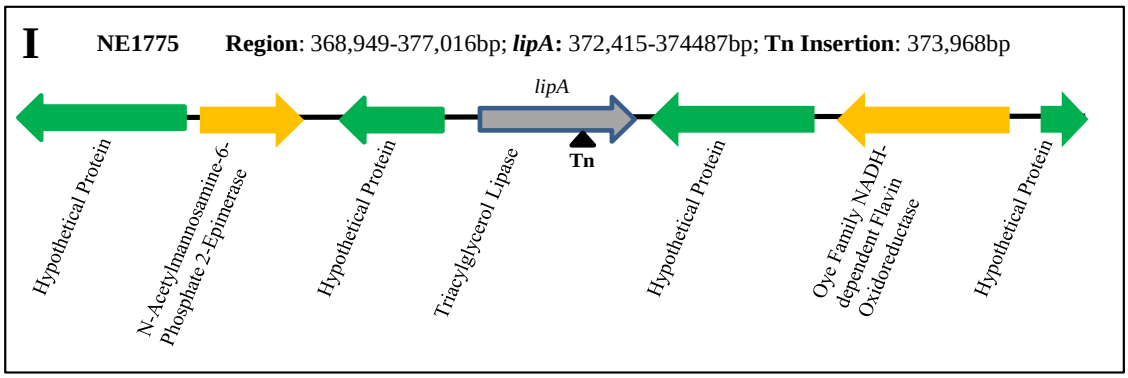

Figure 4.20 Tn insertion position and surrounding genes for each of the 9 genes of interest.

The Tn inserts within the first third of each gene except *lipA*, in which the Tn is inserted 75% into the gene sequence. The *pabA* gene (**D**) is in an operon with two downstream genes. There are four genes in the *murQ* operon (**E**), one upstream of *murQ*, and two downstream genes. The *araC* gene (**F**) is in an operon with a downstream hypothetical protein. The *odhB* gene (**H**) is transcribed from the promoter of the gene just upstream from it.

4.3 Discussion

The NTML provides a valuable resource for the *S. aureus* research community. It allows for rapid identification of genes important for *S. aureus* growth and survival in any environment that is testable in a laboratory setting. For *S. aureus* to cause severe diseases such as endocarditis and sepsis, it must be able to survive and replicate in human blood (Alonzo *et al*., 2012; Zheng *et al*., 2015). Survival and growth is not simply a matter of immune evasion, the bacteria needs to access available nutrients and synthesise the nutrients that are not freely available (Brown *et al*., 2000 & Coulter *et al*., 1998). Therefore, the importance of 1,920 of the NTML genes was assessed for growth using human blood as the sole nutrient source.

Before screening, the NTML hypothetical proteins were analysed bioinformatically to determine if any were homologous to known virulence factors. The sequence files and databases constructed in Chapter 3 were used for the analysis. Two of the four staphylococcal superantigen-like proteins found in Chapter 3 were found amongst the NTML hypothetical proteins. Similarly, several of the hypothetical proteins of the NTML proved to be genes with known functions (Table 4.2 & 4.3). Indeed one of the nine genes found above, to be subjected to further study, was annotated in the NTML as a hypothetical protein, and was in fact *N*-acetylmuramic acid-6-phosphate esterase (*murQ*; Table 4.6). No potential virulence factors, other than two of those found previously in Chapter 3, were found bioinformatically.

Screening the NTML returned 100 strains with an interesting phenotype, 72 of which had an altered growth or haemolysis phenotype on human blood. The 100 results included 30 genes annotated as transporters (1 sugar transporter, 1 Fe transporter, 12 ABC transporter permeases, 7 amino acid transporters and 9 genes simply annotated as transporters). Genes involved in biosynthetic pathways, including nucleotide, amino acid and cofactor biosynthesis had 19 representatives in the screen results. These results are in agreement with Brown *et al*. (2000) & Coulter *et al*. (1998), highlighting the importance of nutrient acquisition and biosynthesis for pathogen growth in human blood.

After confirming the phenotype of each of the 100, there were 46 strains remaining with an interesting phenotype on human blood. Repeated attempts to transduce the Tn from these strains into the SH1000 and JE2 strain backgrounds gave 31 strains of interest. Transduction of the Tn insert from the remaining 15 NTML strains was unsuccessful potentially due to inefficient phage lysis of these strains, or slow growth of the strains resulting in low phage titre. After repeated attempts, these strains were not concentrated on further, as 31 strains had given colonies in both backgrounds and their Tn insertions had been confirmed. After transduction, only 9 of the 31 strains retained the altered phenotype seen in the screen. This confirmed linkage of the phenotype to the transposon insertion for the 9 strains and suggested that the phenotype seen for the other 22 strains was the result of unlinked genomic events (e.g. point mutations in other regions of the genome). The following Tn disrupted genes are found in these 9 strains: autolysin (*atl*), adenylosuccinate lyase (*purB*), adenylosuccinate synthetase (*purA*), paraaminobenzoate synthase, glutamine amidotransferase, component_II (*pabA*), *N*-acetylmuramic acid-6-phosphate esterase (*murQ*), transcription regulatory protein (*araC*), adaptor protein (*mecA*), dihydrolipoamide succinyltransferase (*odhB*) and a triacylglycerol lipase precursor (*lipA*).

Two of the above genes are involved in peptidoglycan degradation and recycling (*atl* and *murQ*). Disruption of the *atl* gene produced a strain with an unusual opaque colony morphology on human and rabbit blood and increased haemolysis on human blood. The Atl protein is a large protein that is secreted and proteolytically cleaved extracellularly to give two active forms, an amidase (AM) and a glucosaminidase (GL; Bose *et al*., 2012). Both proteins have DNA binding activity, but their primary function is in peptidoglycan degradation (Grilo *et al*., 2014). AM cleaves the amide bond between *N*-acetylmuramic acid and the L-alanine of the crosslinking peptide in peptidoglycan. The GL protein cleaves the bond between *N*-acetyl-β-D-glucosamine and *N*-acetyl muramic acid. This activity is important for release of peptidoglycan from the surface of *S. aureus*, and for release of the daughter cell upon cell division (Bose *et al*., 2012; Foster, 1995). Loss of Atl activity results in formation of clusters of attached *S. aureus* cells. This may explain the unusual colony morphology seen in the screen. However, the increased haemolysis phenotype conflicts with the results of the study by Pasztor *et al*. (2010), which found that *atl* plays a role in secretion of proteins via "nonclassical protein secretion" and secretome analysis of an *atl* mutant strain found reduced levels of

α-haemolysin. Disruption of the *murQ* gene produced a strain with increased haemolysis on human blood agar. In *E. coli* and *Haemophilus influenzae*, hydrolysed peptidoglycan is internalised and degraded further by a series of enzymes. The MurQ enzyme converts MurNAc 6P to GlcNAc 6P by cleavage of an ether bond, which can then be used for glycolysis (Hadi *et al*., 2008; Hadi *et al*., 2013). It is unclear why disruption of this enzyme would produce an increased haemolysis phenotype.

The *araC* family of transcriptional regulators have roles in pathogenesis, sugar metabolism and response to stress. JE2-*araC* had a reduced haemolysis phenotype on human blood. The *araC* gene from JE2 is identical to the *araC* family gene *rsp* from *S. aureus* MW2. Deletion of this gene was found to radically alter the secreted protein profile of *S. aureus* MW2 (Lei *et al*., 2011). This secretion of different proteins in the *rsp*$^{-}$ background indicates that the reduced haemolysis phenotype seen for the *araC* strain may occur at the transcription, translation, protein-turnover or secretion level, thereby altering the amount of haemolytic proteins released by JE2-*araC*.

The *mecA* gene is related to *mecA* from *Bacillus subtilis*, which is involved in glycopeptide antibiotic resistance, including teicoplanin and vancomycin (Jousselin *et al*., 2013; Renzoni *et al*., 2009). JE2-*mecA* had a reduced haemolysis phenotype on human blood agar. The *mecA* gene is upregulated by the Spx protein, the gene for which is just upstream from *mecA* (Figure 4.20G). MecA is an adapter protein, which aids Clp chaperones in the delivery of proteins to the ClpP and ClpQ protease, which then proteolytically degrade them, allowing control of protein levels during normal growth and in response to a changing environment (Donegan *et al*., 2014). The observed reduced haemolysis phenotype for this strain may result from extended survival of regulators that downregulate haemolytic toxin production.

The *odhB* gene is a tricarboxylic acid cycle (TCA) enzyme, a system for aerobic respiration. TCA cycle mutants were not expected in the results on human blood, as the human blood plates were grown anaerobically. JE2-*odhB* showed increased haemolytic activity on human blood. OdhB is part of an enzyme complex of three proteins, well studied in *Bacillus subtilis*. The complex catalyses oxidative decarboxylation of 2-oxoglutarate to succinyl coenzyme A, in the TCA cycle (Carlsson & Hederstedt, 1989).

Triacylglycerol lipase proteins are required for resistance to fatty acids. JE2-*lipA* showed an increased haemolysis phenotype on human blood agar. Triglycerides are antimicrobial fatty acids secreted with other fatty acids from the sebaceous glands on skin. This cocktail of fatty acids is known as sebum. Lipases degrade the fatty acids allowing colonisation of the skin (Cadieux *et al*., 2014). Lipases likely have an important role in blood, as lipase mutants have reduced bacterial loads in the liver, kidney and spleen of mice.

The *purA* and *purB* genes are involved in the biosynthesis of purines and the mutants had reduced growth on human blood and bovine serum. Serum based analysis of an *E. coli* mutant library identified nucleotide biosynthesis as essential for growth of *E. coli* in serum (Samant *et al*., 2008). In the same study, *Salmonella enterica* and *Bacillus anthracis* nucleotide synthesis mutants could not grow in serum and the *B. anthracis* strain was highly attenuated in a murine infection model. McFarland & Stocker, 1987 found that 10^7 CFU of a *Salmonella dublin purA* mutant could not kill mice on intraperitoneal infection, whereas 10 CFU of the wild-type was found to be deadly. They also found that in *S. enteria* subspecies *enterica* serovar typhimurium, the lethal dose was $2.5x10^3$ for the wild-type in mice and a *purA* or *purB* mutant caused no death in mice infected with $2.5x10^7$. This attenuation was also seen in humans who voluntarily drank 10^8-10^{10} CFU of a *purA* mutant of *S. typhi* with no ill effects (Stocker, 1988). The results of the above studies tally with the findings of the NTML screen for the *purA* and *purB* mutants.

PabA, along with PabB and PabC produce 4-aminobenzoic acid (PABA) from chorismate and L-glutamine, a necessary step in the synthesis of folates (Neidhardt *et al*., 1996; Tran & Nichols, 1991; Wegkamp *et al*., 2007). The NTML *pabA* mutant showed an unusual altered phenotype in that it grew poorly on human blood, but had normal growth on bovine serum. Like the purine synthesis genes, the *pabA* gene has been shown to be attenuated in *S. typhi* (Brown & Stocker, 1987). The importance of folate for virulence has been known for many years. The sulphonamide antimicrobials are known to act on enzyme steps downstream of PABA (Proctor, 2008; Projan, 2002). Attempts have also been made to find antimicrobials using chorismate analogues in *E. coli*, which were found to competitively inhibit *pabB* activity (Payne *et al*., 2009; Ziebart *et al*., 2010).

Attempts to define the importance to pathogenicity of the 9 genes of interest and characterise those that have a demonstrable role in pathogenicity are the primary objectives of the next chapter.

CHAPTER 5

CHARACTERISATION OF THE ROLE OF GENES REQUIRED FOR GROWTH ON HUMAN BLOOD

5.1 Introduction

In addition to the armoury of toxins and immune evasion proteins that *S. aureus* and other pathogens possess, physiological dynamics is essential for their ability to cause disease. This may involve switching off, or severely reducing the activity of, aspects of metabolism in order to persist in the presence of antibiotics (Amato *et al*., 2014), upregulating proteins for the acquisition of nutrients sequestered by the host (Hammer & Skaar, 2012; Weinberg, 1974) and the upregulation of *de novo* biosynthetic pathways to produce essential products not readily available in the environment (Autret & Charbit, 2005; Heroven & Dersch, 2014; McFarland & Stocker, 1987; Shea *et al*., 2000). A review of the literature on antibiotics highlights the importance of metabolism to infection. The majority of antimicrobials function by disrupting essential metabolic processes, thereby killing the pathogen (bacteriocidal antibiotics) or inhibiting their growth (bacteriostatic antibiotics; Kohanski *et al*., 2010). Common antimicrobial targets include peptidoglycan synthesis (Labischinski, 1992), protein synthesis (Mast & Wohlleben, 2014), nucleic acid synthesis (Chernyshev *et al*., 2007; Hartmann *et al*., 1968; Rottman & Guarino, 1964) and synthesis of tetrahydrofolate (THF) by the sulphonamide PABA analogues (Brain *et al*., 2008) and the dihydrofolate reductase (DHFR) inhibitors (Laue *et al*., 2007; Proctor, 2008).

The THF synthesis inhibitors are of particular relevance to this chapter. THF is an important cofactor in many metabolic reactions, acting as a donor and acceptor of single carbon units (Figure 5.1). Serine is converted to glycine reversibly by the enzyme GlyA, using THF as methylene acceptor, in a process known as serine/glycine interconversion (Appling, 1991; Basset *et al*., 2004; Wegkamp *et al*., 2007; Figure 5.1A). Serine/glycine interconversion releases 5,10-methylene-THF, which can then be used in the biosynthesis of panothenate (vitamin $B_{5;}$ Figure 5.1B), which itself is a precursor of coenzyme A, a cofactor for many reactions in central metabolism (Ernst & Downs, 2015). 5,10-methylene-THF is also required for deoxythymidine triphosphate (dTTP) synthesis from deoxyuridine monophospate (dUMP) (Figure 5.1C). 5,10-methylene-

THF can be converted by MetF to 5-methyl-THF, a cofactor for the remethylation of L-homocysteine to methionine (Figure 5.1 D & E). THF is converted to 10-formyl-THF by the enzyme Fhs in the presence of ATP and formate. 10-formyl-THF is the formyl donor for the synthesis of fMet and purines (Friso & Choi, 2005; Harvey, 1973; Projan, 2002); Figure 5.1 F, G & H).

The apparent loss of THF synthesis, in the NTML strain NE821, due to disruption of the *pab* operon, resulted in a severe growth defect when grown on human blood agar. Characterising the phenotype associated with this strain is the main topic of this chapter. The phenotypes of two other strains isolated in the NTML screen (Chapter 4) involved in *de novo* purine biosynthesis are also examined.

5.2 Results

5.2.1 Effect of Tn insertion in the 9 strains isolated from the NTML

The importance of the nine mutations identified in Chapter 4 (Table 4.6) in pathogenicity was assessed using the zebrafish embryo model of systemic infection (Prajsnar *et al*., 2008). All zebrafish assays were done in collaboration with Dr Emma Johnson M.D. For the full zebrafish infection assay protocol, see Chapter 2.23. All 9 strains were first assayed in the USA300 JE2 background and those that were attenuated were then assayed in the SH1000 background to confirm that the phenotype is not strain specific. Thirty zebrafish embryos of strain LWT, at 1 day old, were injected with ~1,500 CFU *S. aureus* USA300 JE2, SH1000 or each of the 9 NTML mutants in the respective strain backgrounds. Survival of the fish was monitored over 4 days and then the remaining fish were culled (Figure 5.2). Previous analyses have shown that USA300 JE2 is more virulent than SH1000 in the zebrafish embryo model (data not shown). JE2 kills approximately 60-80% of the embryos, whereas SH1000 kills approximately 40-50% of embryos.

None of the NTML strains with a haemolysis phenotype in the JE2 background (Chapter 4, Table 4.5A2) were attenuated in the zebrafish embryo model of systemic infection, $p > 0.05$ (Figure 5.2A), as over a 4 day period an equivalent number of embryos to those infected with JE2 died. The 3 strains that showed a growth defect in the screen (Chapter 4, Table 4.5A1) were highly attenuated over the 4 day analysis $p <$

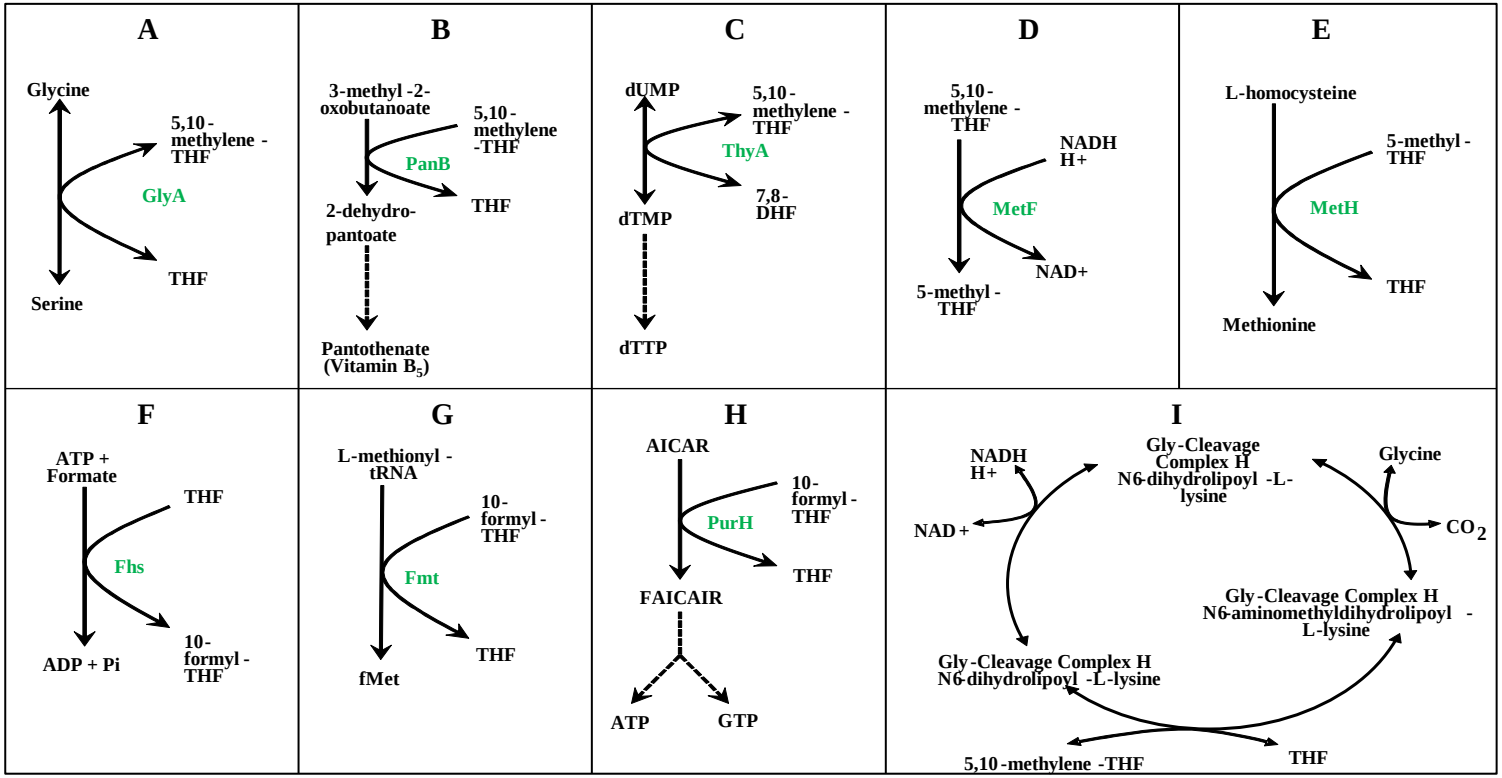

Figure 5.1 The roles of THF in *S. aureus* metabolism.

Dashed lines indicate that 1 or more steps are not shown. **A**. Serine/glycine interconversion. **B**. Vitamin B_5 biosynthesis. **C**. Synthesis of dTTP from dTMP. **D**. Conversion of 5,10-methylene-THF to 5-methyl-THF. **E**. Remethylation of L-homocysteine in the synthesis of methionine. **F**. 10-formyl-THF production from THF. **G**. Use of 10-formyl-THF to formylate L-methionine charged tRNA. **H**. 10-formyl-THF-dependent conversion of AICAIR to FAICAIR in the purine *de novo* biosynthesis pathway. **I**. Glycine cleavage pathway. Cleavage of glycine to CO2, ammonia and a methyl group. Abbreviations: AICAIR, 5-amino-1-(5-phospho-D-ribosyl)imidazole-4-carboxamide; FAICAIR, 5-formamido-1-(5-phospho-D-ribosyl)-imidazole-4-carboxamide.

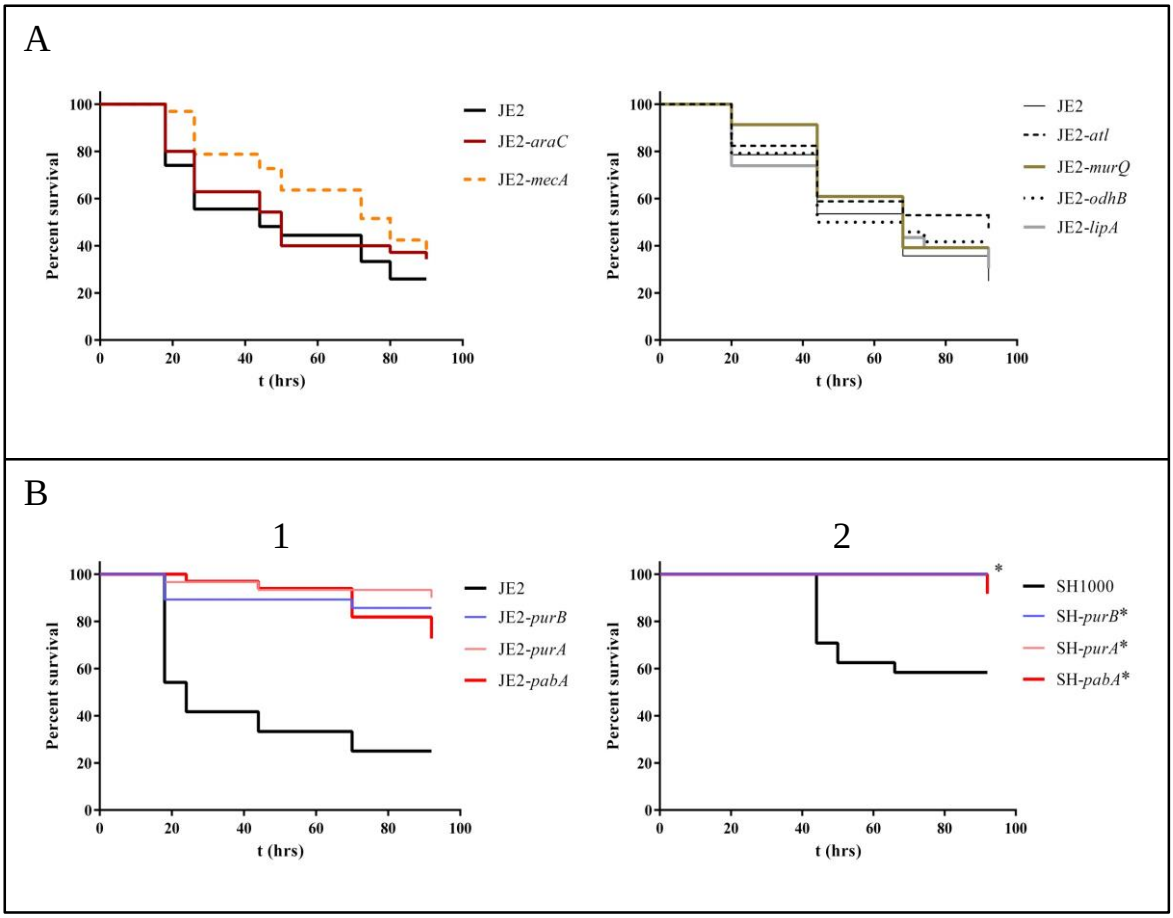

Figure 5.2 Role of the isolated NTML mutants in pathogenesis in the zebrafish embryo model.

*The data points overlap.

A Survival of embryos injected with strains JE2-*atl*, JE2-*murQ*, JE2-*araC*, JE2-*mecA*, JE2-*odhB* and JE2-*lipA* was not significantly different compared to embryos injected with JE2, $p > 0.05$.

B1 Survival of embryos injected with JE2-*purB*, JE2-*purA* and JE2-*pabA* was significantly improved compared to JE2, $p < 0.0001$.

B2 Survival of embryos injected with SH-*purB*, SH-*purA* and SH-*pabA* was significantly improved compared to SH1000, $p < 0.0001$.

0.0001, with >70% survival of embryos infected with the mutant strains in the JE2 background, compared to 25% survival of embryos infected with JE2; and for the SH1000 background, there was 90-100% embryo survival when injected with the mutant strains, compared to 60% survival of embryos injected with SH1000 (Figure 5.2 B1 & B2). The pathogenesis screen was used as a cut-off to define those strains that would be taken on for further analysis. The SH1000 background was used for the ensuing zebrafish infection experiments, as it is a well-established strain background for host-pathogen interaction studies using the zebrafish embryo model (McVicker *et al*., 2014; Prajsnar *et al*., 2012). As in Chapter 4 (Table 4.4) mutant strains in the SH1000 background are named SH- followed by the gene name.

5.2.2 Analysis of the role of *purA* and *purB* in *S. aureus* growth

Growth curves of JE2-*purB* and JE2-*purA* were carried out (see Chapter 2.8 for growth curve method). In the original screen, the NTML strains NE522 and NE529 had reduced growth on human blood agar and bovine serum agar. Their growth was comparable to the wild-type on 5% (v/v) sheep blood with the nutrient rich Columbia agar base. The results suggested that their growth was reduced by a nutrient limitation in bovine serum and human blood that was supplied in the nutrient rich Columbia agar. It was expected that growth of the strain would be comparable to the wild-type in BHI and poor in bovine or human serum. Growth characteristics of JE2-*purB* and JE2-*purA* matched expectations (Figure 5.3). Therefore, the *purA* and *purB* mutants likely have a nutrient requirement for growth.

5.2.3 Analysis of the *purA* and *purB* genes

Strain JE2-*purA* has a Tn inserted in the *purA* gene, which encodes adenylosuccinate synthetase that catalyses 1 step in the biosynthesis of ATP in the purine pathway (Figure 5.4). The *purB* gene, disrupted by a Tn insertion in strain JE2-*purB* encodes adenylosuccinate lyase, which has two roles in the purine biosynthesis pathway (Figure 5.4). Inosine monophosphate (IMP) in the purine pathway (Figure 5.4) is a branch-point leading to GTP synthesis, or ATP synthesis. PurB has a role in ATP synthesis after IMP branching in the pathway and a role before branching. Therefore, *purA* is likely essential for ATP synthesis only and *purB* is likely essential for both ATP and GTP

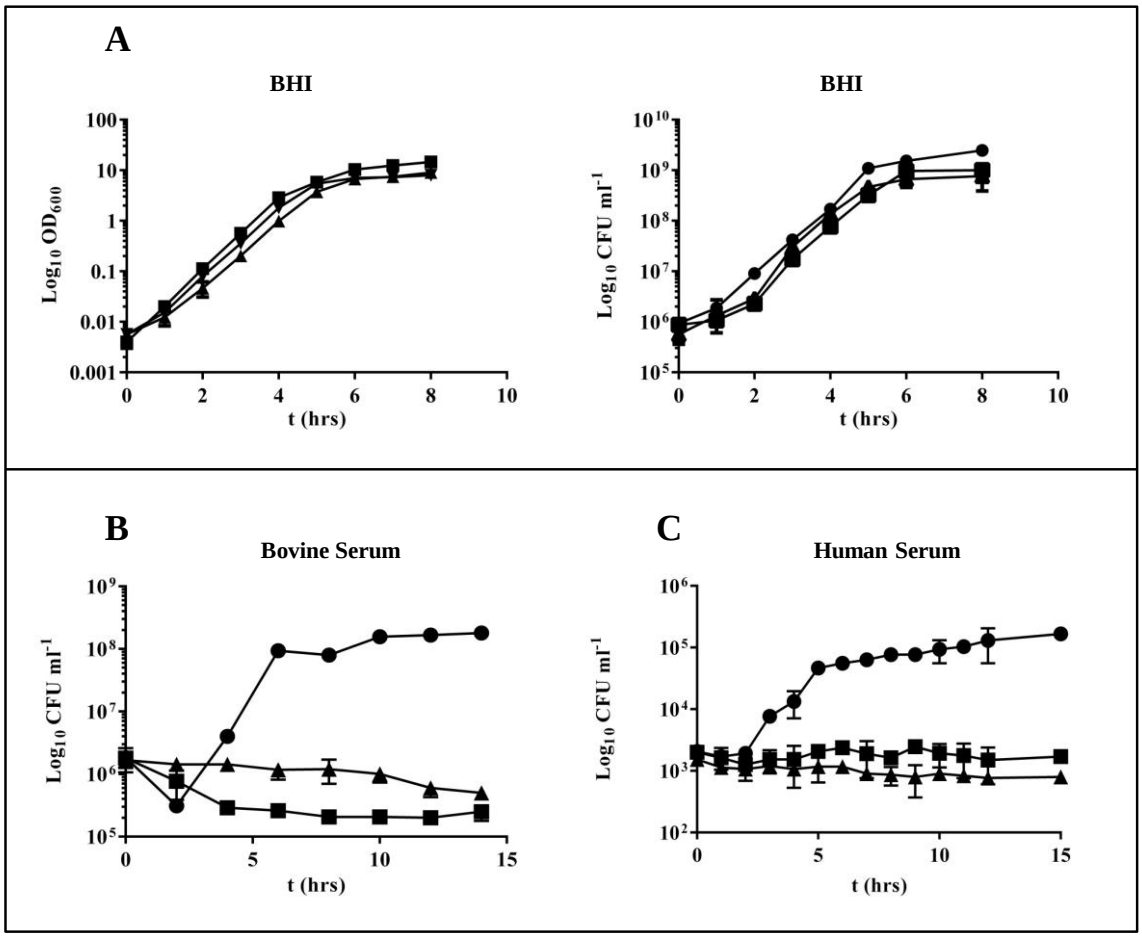

Figure 5.3 Role of *purA* and *purB* in *S. aureus* growth.

● = JE2, ■ = JE2-*purB*, ▲ = JE2-*purA*

A In BHI both strains have comparable growth to JE2 measured by optical density at 600nm (OD_{600}) or CFU.

B JE2-*purB* and JE2-*purA* show reduced growth in bovine serum relative to JE2.

C Growth in human serum is reduced for JE2-*purB* and JE2-*purA* relative to JE2.

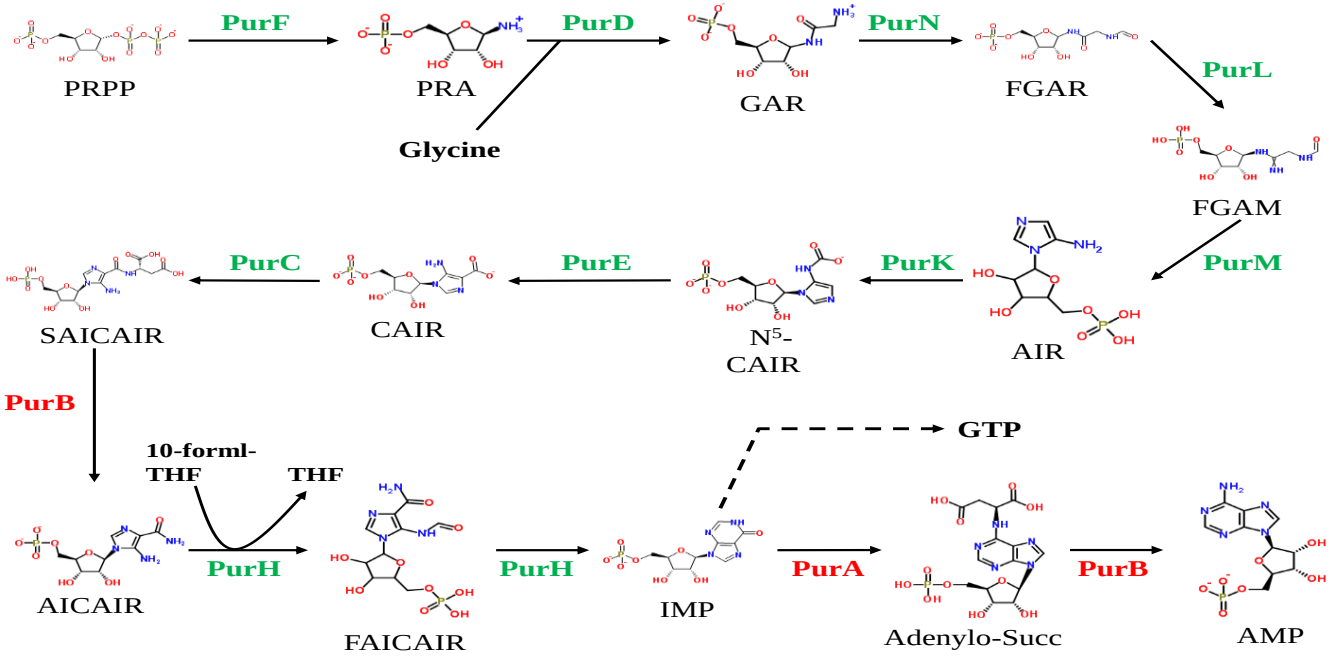

Figure 5.4 Purine *de novo* biosynthesis pathway.

The PurA and PurB enzymes are coloured red, all other enzymes are green. PurB has two roles in the pathway, one before IMP branching and one after branching leading to ATP synthesis. Abbreviations: PRPP, 5-phospho-α-D-ribose 1-diphosphate; PRA, 5-phospho-β-D-ribosylamine; GAR, N^1-(5-phospho-β-D-ribosyl)glycinamide; FGAR, N^2-formyl-N^1-(5-phospho-β-D-ribosyl)glycinamide; FGAM, 2-(formamido)-N^1-(5-phospho-β-D-ribosyl)acetamidine; AIR, 5-amino-1-(5-phospho-β-D-ribosyl)imidazole; N^5-CAIR, N^5-carboxyaminoimidazole ribonucleotide; CAIR, 5-amino-1-(5-phospho-D-ribosyl)imidazole-4-carboxylate; SAICAIR, 5'-phosphoribosyl-4-(*N*-succinocarboxamide)-5-aminoimidazole; AICAIR, 5-amino-1-(5-phospho-D-ribosyl)imidazole-4-carboxamide; FAICAIR, 5-formamido-1-(5-phospho-D-ribosyl)-imidazole-4-carboxamide; IMP, inosine monophosphate, Adenylo-succ, N^6-(1,2-dicarboxyethyl)-AMP; AMP, adenosine-monophosphate. Pathway information was acquired from the Kegg and Biocyc websites, and molecule images were obtained from ChemSpider.

synthesis. The *purA* and *purB* genes are at positions 22,465 bp and 2,054,221 bp on the JE2 genomes, respectively, whereas the other *pur* genes, encoding the enzymes shown in green in Figure 5.4, are in an operon at position 1,059,510 – 1,070,681 bp on the JE2 genome. The *pur* genes are in approximate positions on the SH1000 genome.

5.2.4 Analysis of bacterial population dynamics of *purA* & *purB* in the zebrafish embryo model of systemic infection

5.2.4.1 Growth of SH-*purB* and SH-*purA in vivo*

As SH-*purA* and SH-*purB* have an apparent growth defect in liquid culture, attenuation in the zebrafish model could be due to an inability to grow and divide. *In vivo* growth analysis was carried out to determine the growth of SH-*purB* and SH-*purA* over the course of infection. In order to track the growth of SH-*purA* and SH-*purB in vivo*, bacterial numbers, defined as CFU per embryo, were determined over 92 h, the standard time for a zebrafish embryo experiment. The full method used for determining bacterial numbers *in vivo* is given in Chapter 2.23.6. At 10-12 h time points, bacteria were harvested from all dead embryos and 6 live embryos. The bacterial numbers were then determined by serial dilution and compared to SH1000 (Figure 5.5). Growth of SH-*purA* and SH-*purB* was arrested in zebrafish embryos and their numbers slowly declined over the 92 h experiment. This suggested that attenuation of the *purA* and *purB* mutant strains was the result of an inability to grow within zebrafish embryos.

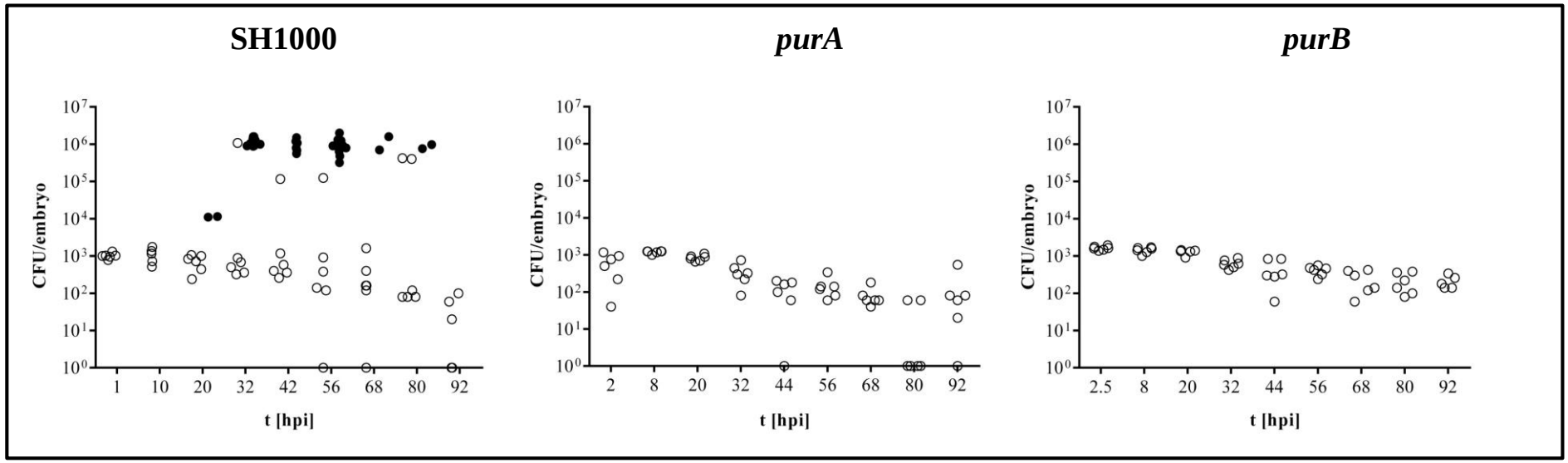

Figure 5.5 Proliferation of SH-*purA*, SH-*purB* and SH1000 within zebrafish embryos.

○ = live embryos, ● = dead embryos. Over the course of infection SH-*purA* and SH-*purB* were unable to multiply and bacterial numbers slowly declined, no embryo death was seen. At each time point 6 live embryo and any dead embryos were collected and CFU per embryo determined.

5.2.4.2 The effect of purines on SH-*purA* and SH-*purB in vivo*

Based on assessment of the purine biosynthesis pathway (Figure 5.4) it was hypothesised that SH-*purA* might be complemented *in vivo* with adenine, whereas SH-*purB* would require both adenine and guanine for *in vivo* complementation. Attempts were made to use adenine and guanine as they can be converted directly to AMP and GMP respectively (Houlberg & Jensen, 1983). In the zebrafish embryo model, upon injection with ~1,500 CFU bacteria, the embryos are incubated in E3 solution, pH7.4 (for E3 preparation see Chapter 2.5.6). In the complementation experiments, the aim was to dissolve guanine and adenine in the E3 solution allowing diffusion of the purines into the embryos. However, stock guanine (Sigma-Aldrich) is dissolved in 5M HCl and when added to E3 it precipitated. As inosine is the branch-point in the purine biosynthesis pathway (Figure 5.4) leading to ATP or GTP synthesis and is soluble in water, it was decided that inosine would be used as an alternative to guanine *in vivo*. SH-*purA* and SH-*purB* remained highly attenuated in embryos incubated in E3 + 300 µg ml^{-1} adenine (Figure 5.6). Addition of 400 µg ml^{-1} inosine and 300 µg ml^{-1} adenine to E3 solution did not restore the pathogenicity of SH-*purB in vivo* (Figure 5.7).

The reason why adenine and inosine did not restore SH-*purA* and SH-*purB* virulence *in vivo* was uncertain. It was considered that adenine and inosine may not be what is required by SH-*purA* and SH-*purB*, or that adenine and inosine (or adenine alone as both strains were thought to require adenine for growth) could not diffuse into embryos, to allow their use by the bacteria. If the latter possibility was the case, then an alternative method for assessing the importance of purines to the *purA* and *purB* mutants was required.

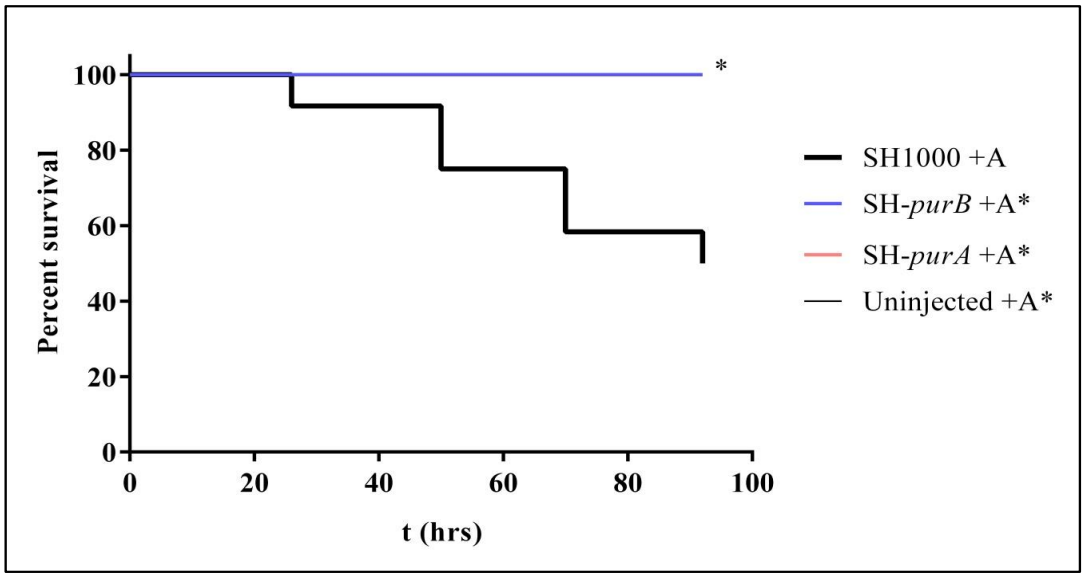

Figure 5.6 Effect of adenine on SH-*purA* and SH-*purB* virulence.

* Data points overlap.

Abbreviation: A, adenine 300 µg ml^{-1}. Addition of adenine to E3 solution did not restore virulence to SH-*purA* or SH-*purB* mutants, compared to SH1000, $p < 0.0001$.

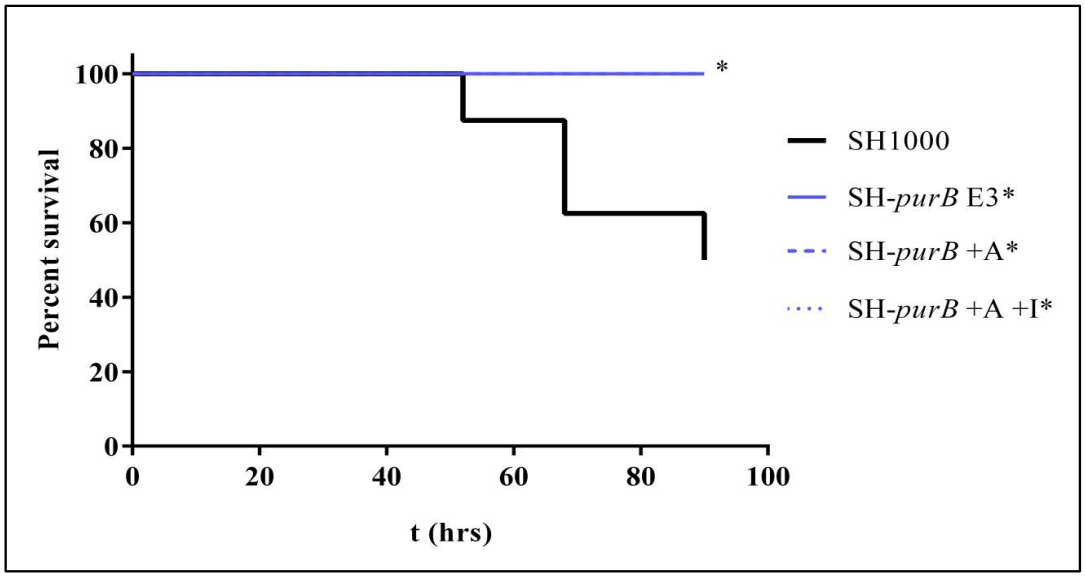

Figure 5.7 Effect of adenine and inosine on SH-*purB* virulence.

* Data points overlap.

Abbreviations: A, adenine 300 µg ml^{-1}; I, inosine 400 µg ml^{-1}. Addition of adenine and inosine to E3 solution did not restore virulence to SH-*purB* compared to SH1000, $p < 0.0001$.

5.2.4.3 The effect of purines on JE2-*purA* and JE2-*purB* growth

Chemically defined media (CDM) was used to determine the importance of adenine and guanine/inosine in restoring the ability of JE2-*purA* and JE2-*purB* to grow. Details on the preparation of CDM agar are given in Chapter 2.1.4. CDM contains adenine and guanine, allowing their removal to determine their importance to the *purA* and *purB* mutants. CDM agar was made with the following combinations of adenine (A) and guanine (G):

1. +A & +G
2. –A & –G
3. +A & –G
4. –A & +G

Based on the purine biosynthesis pathway (Figure 5.4) JE2-*purA* should only be able to grow on purine combinations 1 and 3 (i.e. in the presence of adenine). For the growth of JE2-*purB*, combination 1 would be the only purine combination that would support growth in this experiment (i.e. both adenine and guanine would be required). Figure 5.8 and Table 5.1 show that growth met expectations for both strains. JE2 was able to grow in all conditions tested. JE2-*purB* growth was comparable to JE2 on full CDM, but did not grow when adenine & guanine or either adenine or guanine was not added to CDM. JE2-*purA* growth was only seen in the presence of adenine. Aeration conditions did not affect the relative growth of the *purA* and *purB* mutants compared to JE2.

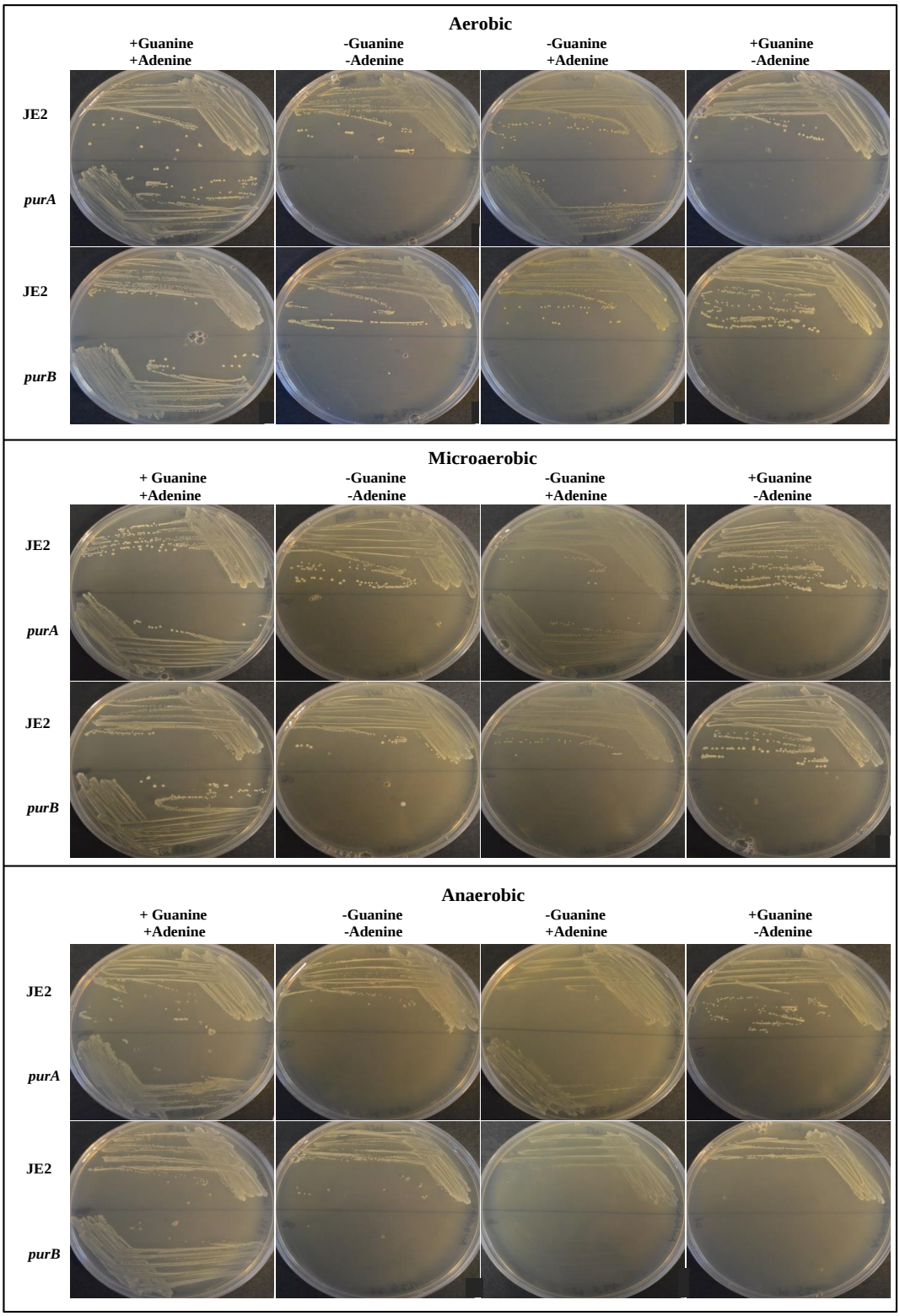

Figure 5.8 Role of adenine and guanine in the growth of JE2-*purA* and JE2-*purB* on solid media.

JE2 can grow in the absence of purines. JE2-*purA* requires addition of adenine for growth, whereas JE2-*purB* requires both adenine and guanine. Varying oxygen availability does not alter the results. Plates were incubated at 37^{o}C for 24 h.

Table 5.1 Growth analysis of JE2-*purA* and JE2-*purB* in the presence or absence of adenine and guanine.

Strain	Chemically Defined Media			
	+Adenine +Guanine	-Adenine -Guanine	+Adenine -Guanine	-Adenine +Guanine
Aerobic Growth				
JE2	+	+	+	+
purB	+	-	-	-
purA	+	-	+	-
Microaerobic Growth				
JE2	+	+	+	+
purB	+	-	-	-
purA	+	-	+	-
Anaerobic Growth				
JE2	+	+	+	+
purB	+	-	-	-
purA	+	-	+	-

+ = Growth
- = No Growth

CDM was also used to confirm that inosine could be used as a valid alternative to guanine. As above, CDM agar was prepared with different combinations of adenine (A), guanine (G) and inosine (I):

1. +I & –A & –G
2. +I & +A & –G
3. +I & –A & +G

Neither the *purA* mutant nor the *purB* mutant should be complemented by combination 1 or 3, as both require adenine. JE2-*purA* would be expected to grow on combination 2, as it only requires adenine. However, JE2-*purB* should only grow on combination 2, if inosine replaces the requirement for guanine. Figure 5.9 and Table 5.2 show the growth results for both strains. Both strains had comparable growth to JE2 on condition 2. This showed that inosine was able to replace the guanine requirement of JE2-*purB*.

The results of the CDM experiments tallied with the known pathway information for *S. aureus*. Therefore, it was determined that to go any further with these strains would only lead to confirmation of what is already known about the importance of purine biosynthesis to bacterial growth and pathogenicity (Baxter-Gabbard & Pattee, 1970; McFarland & Stocker, 1987; Stocker, 1988).

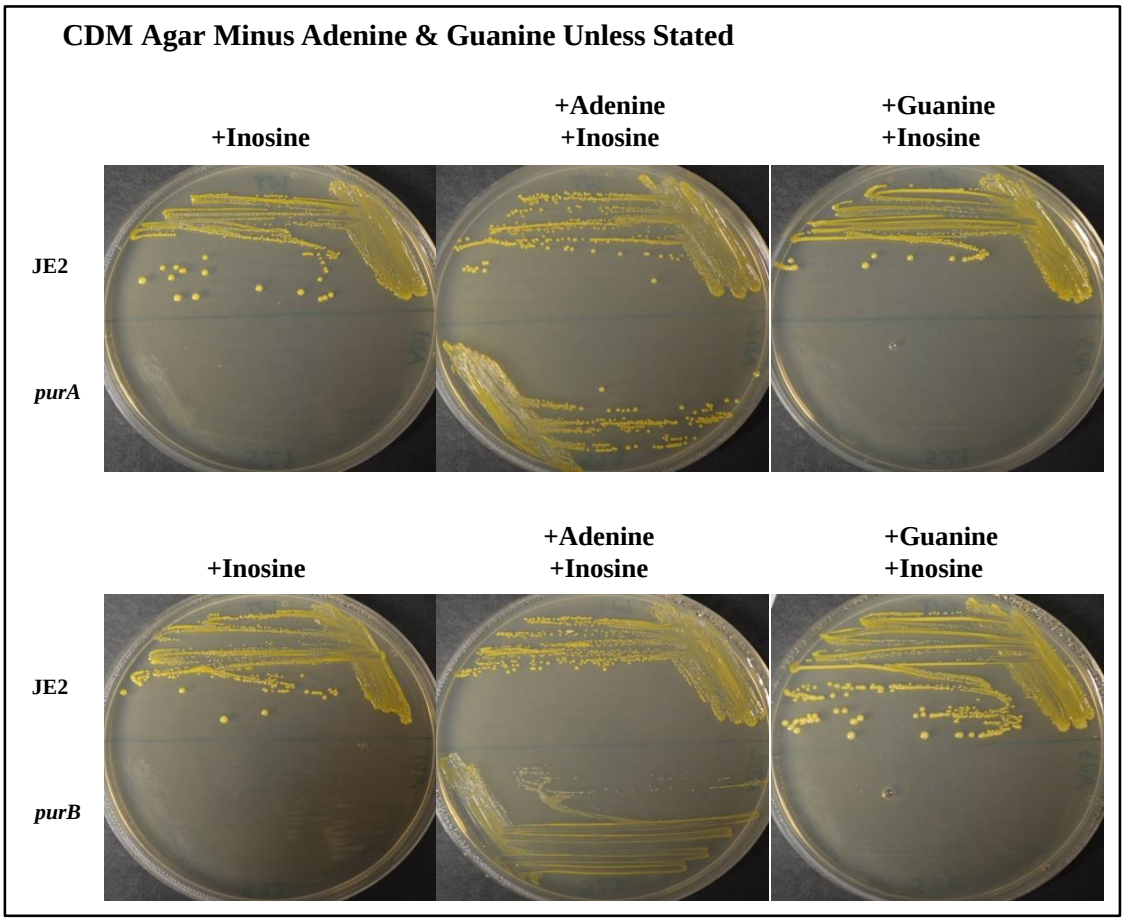

Figure 5.9 Role of adenine, guanine and inosine in the growth of JE2-*purA* and JE2-*purB* on solid media.

Inosine can be used to complement JE2-*purB* as an alternative to guanine. Inosine does not replace the requirement for adenine by both strains. Plates were incubated at 37^{o}C for 48 h.

Table 5.2 Growth analysis of JE2-*purA* and JE2-*purB* in the presence or absence of adenine and guanine, and in the presence of inosine.

Strain	Chemically Defined Media		
	-Adenine -Guanine +Inosine	+Adenine -Guanine +Inosine	-Adenine +Guanine +Inosine
Aerobic Growth			
JE2	+	+	+
purB	-	+	-
purA	-	+	-

5.2.5 Analysis of the role of *pabA*

5.2.5.1 Growth assays of JE2-*pabA*

Growth curves of JE2-*pabA* were carried out in order to confirm that growth of the *pabA* mutant on bovine serum (Sigma-Aldrich) was comparable to JE2, as seen in the initial screen of the NTML (Chapter 4). JE2-*pabA* growth was also assessed in human serum (Millipore) to determine if its growth remained comparable to JE2 using human serum as a nutrient source. See Chapter 2.8 for growth curve method. JE2-*pabA* showed comparable growth to JE2 in BHI, measured by OD_{600} and CFU, bovine serum and human serum, measured by CFU (Figure 5.10 A, B & C respectively).

In the original screen, the NTML strain NE821 showed reduced growth on human blood and normal growth on bovine serum. When JE2-*pabA* was inoculated on rabbit blood agar (Chapter 4, Figure 4.17A2), sheep blood agar and horse blood agar (Chapter 4, Figure 4.18A & B, respectively), only a slight reduction in growth or comparable growth to JE2 was seen. This disparity between blood from different species suggested the possibility that bovine serum was either richer in nutrients than human blood or richer in a specific nutrient required by NE821. Figure 5.10C demonstrates that this is not the case, as JE2-*pabA* growth was comparable to JE2 in human serum. If greater nutrient availability in bovine serum was the cause of the disparity in growth between human blood and bovine serum, then it would be expected that human serum would not sustain growth of JE2-*pabA* to the same level as JE2.

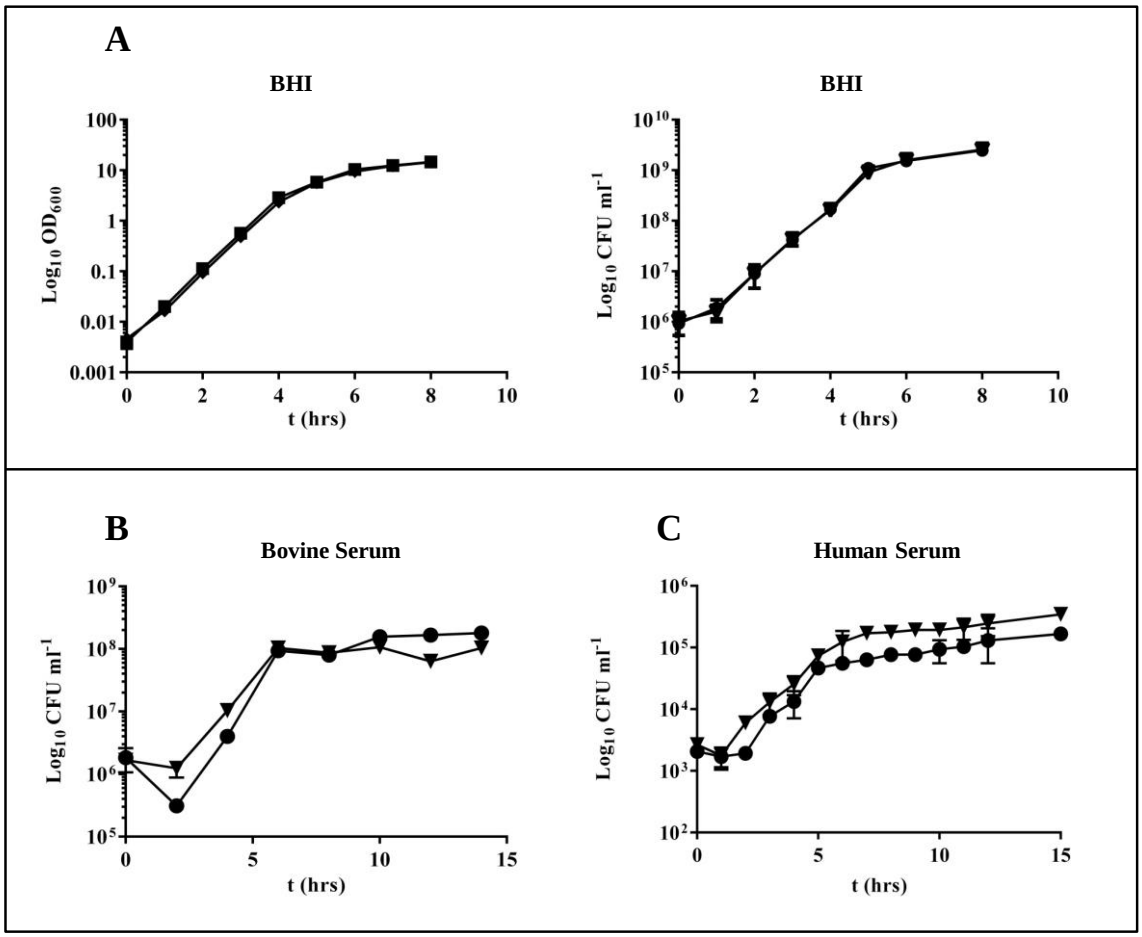

Figure 5.10 Role of *pabA* in *S. aureus* growth.

▼ = JE2-*pabA*, ● = JE2

A In BHI JE2-*pabA* shows comparable growth to JE2 measured by OD_{600} or CFU.

B JE2-*pabA* shows comparable growth to JE2 in bovine serum.

C JE2-*pabA* shows slightly better growth than JE2 in human serum. Confirming that growth was not reduced in JE2-*pabA* in human serum.

5.2.5.2 Why does NE821 grow poorly on blood, but not on serum?

It was hypothesised that nutrients are released from the cellular component of blood during preparation of serum, allowing JE2-*pabA* to grow on serum, but not human blood. Furthermore, this was thought to account for the comparable growth seen on animal blood, which was purchased from TCS Biosciences and may lyse in transit to the university releasing nutrients. The bovine serum and the human serum used in section 5.2.5.1 were prepared off-clot. After clotting of blood, the clot, including the clumped red blood cells, was harvested after centrifugation and the serum supernatant was carefully removed. The hypothesis was that the clotting process leads to lysis of blood cells, liberating cell contents that can be used as a nutrient source by JE2-*pabA* allowing growth on human or bovine serum. Blood was collected at The Royal Hallamshire Hospital and off-clot serum was made and plasma was prepared by centrifugation to minimise cell disruption (see Chapter 2.1.3.1.2 and Chapter 2.1.3.1.3 for preparation of plasma and serum respectively).

Using the serum and plasma prepared above, 50% (v/v) serum agar and 50% (v/v) plasma agar was made. 30% (v/v) human blood agar was also prepared, using blood from the same pooled blood donations. Growth of JE2-*pabA* was compared with JE2 on each medium in aerobic, microaerobic and anaerobic conditions. If nutrients leak from blood cells during serum preparation, then growth would be expected on human serum, but not on human plasma or human blood agar. Figure 5.11 shows that growth was seen on human serum and human plasma agar, but was highly reduced on human blood. This demonstrated that nutrients released from blood cells, during preparation of human serum, was not the cause of the growth disparity between JE2-*pabA* and JE2 when grown on human blood and human serum. The different aeration conditions did not alter the results.

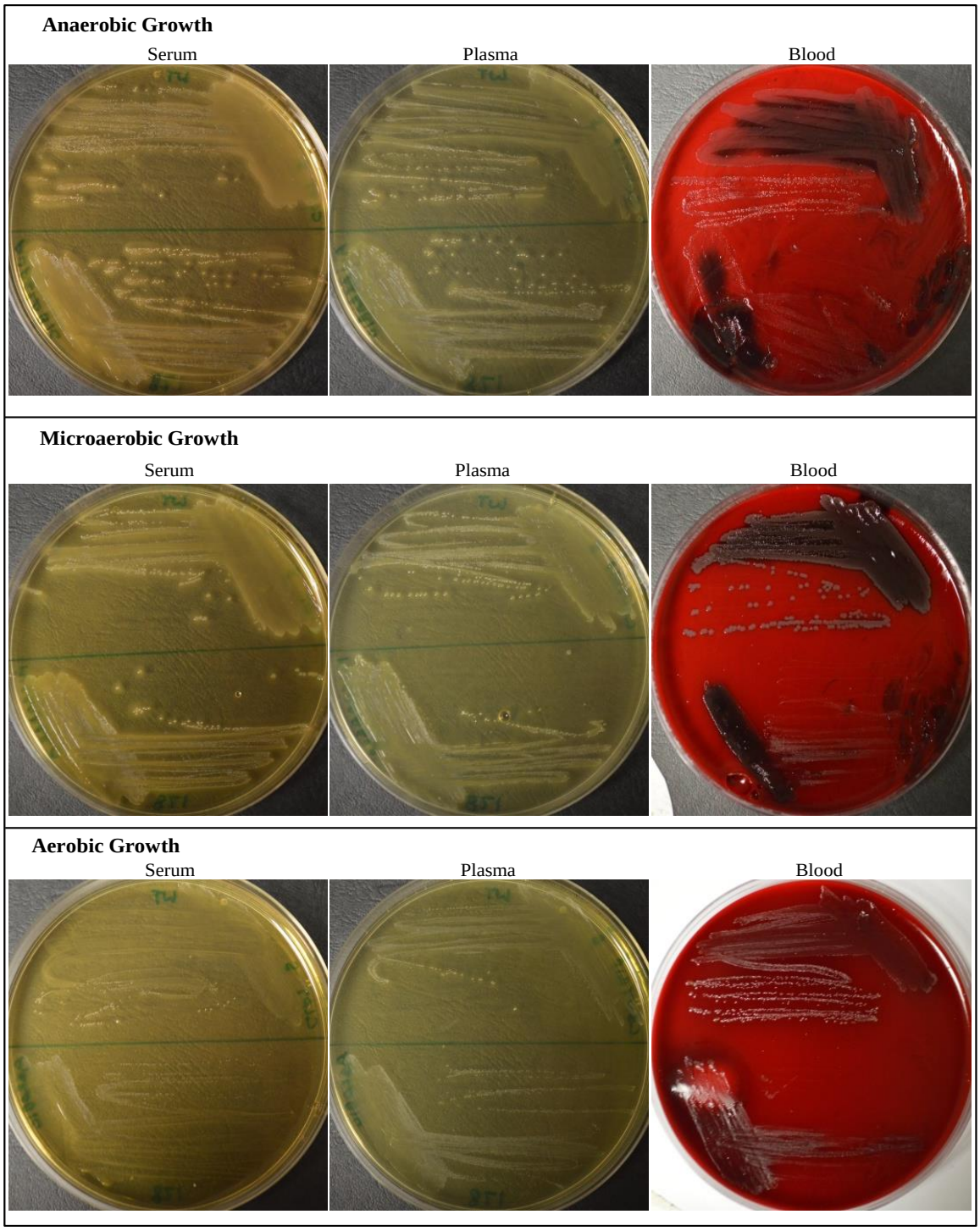

Figure 5.11 Growth of JE2-*pabA* on different human blood components.

JE2 is at the 12 o'clock position on all plates. JE2-*pabA* grows poorly on 30% (v/v) human blood agar relative to JE2. Growth of JE2-*pabA* on 50% (v/v) human plasma and 50% (v/v) human serum is equivalent to JE2. Plates were incubated at 37^{o}C for 24 h.

5.2.5.3 Serum concentration

It was unclear whether the JE2-*pabA* phenotype was caused by the relatively low serum concentration in human blood agar. In a normally hydrated blood donor, ~50% (v/v) of blood consists of plasma, with the remaining 50% (v/v) consisting primarily of red blood cells (RBCs), therefore, JE2-*pabA* is growing on only 15% (v/v) plasma when grown on 30% (v/v) blood agar. If JE2-*pabA* requires a limiting nutrient found in human serum or plasma, then the strain is receiving less of this nutrient when grown on 30% (v/v) blood agar, compared to when it is grown on 50% (v/v) serum or 50% (v/v) plasma agar. To determine whether this was the cause of the poor growth of this strain on 30% (v/v) human blood and comparable growth to JE2 on 50% (v/v) plasma, growth of JE2-*pabA* was compared with JE2 when grown on plasma agar increasing in concentration from 10% (v/v) to 50% (v/v) (Figure 5.12). At the lower concentrations of 10% (v/v) and 15% (v/v) (15% being the approximate plasma concentration in 30% (v/v) blood agar) growth of JE2-*pabA* was poor, but comparable to JE2 which also displayed poor growth at this concentration. It was therefore concluded that the reduced growth on human blood was not a result of lower serum levels in human blood agar.

5.2.6 Analysis of the *pab* operon

Strain NE821 has a Tn inserted in the *pabA* gene, the first member of a 3 gene operon with *pabB* and *pabC* (Chapter 4, Figure 4.20D). These 3 genes catalyse two steps in the folate pathway, to produce 4-aminobenzoic acid (PABA; Figure 5.13). PABA is essential for the synthesis of tetrahydrofolate (THF), a cofactor in many cellular reactions (Figure 5.1). Without the *pab* operon, *S. aureus* growth is severely inhibited on human blood agar (Figure 5.11).

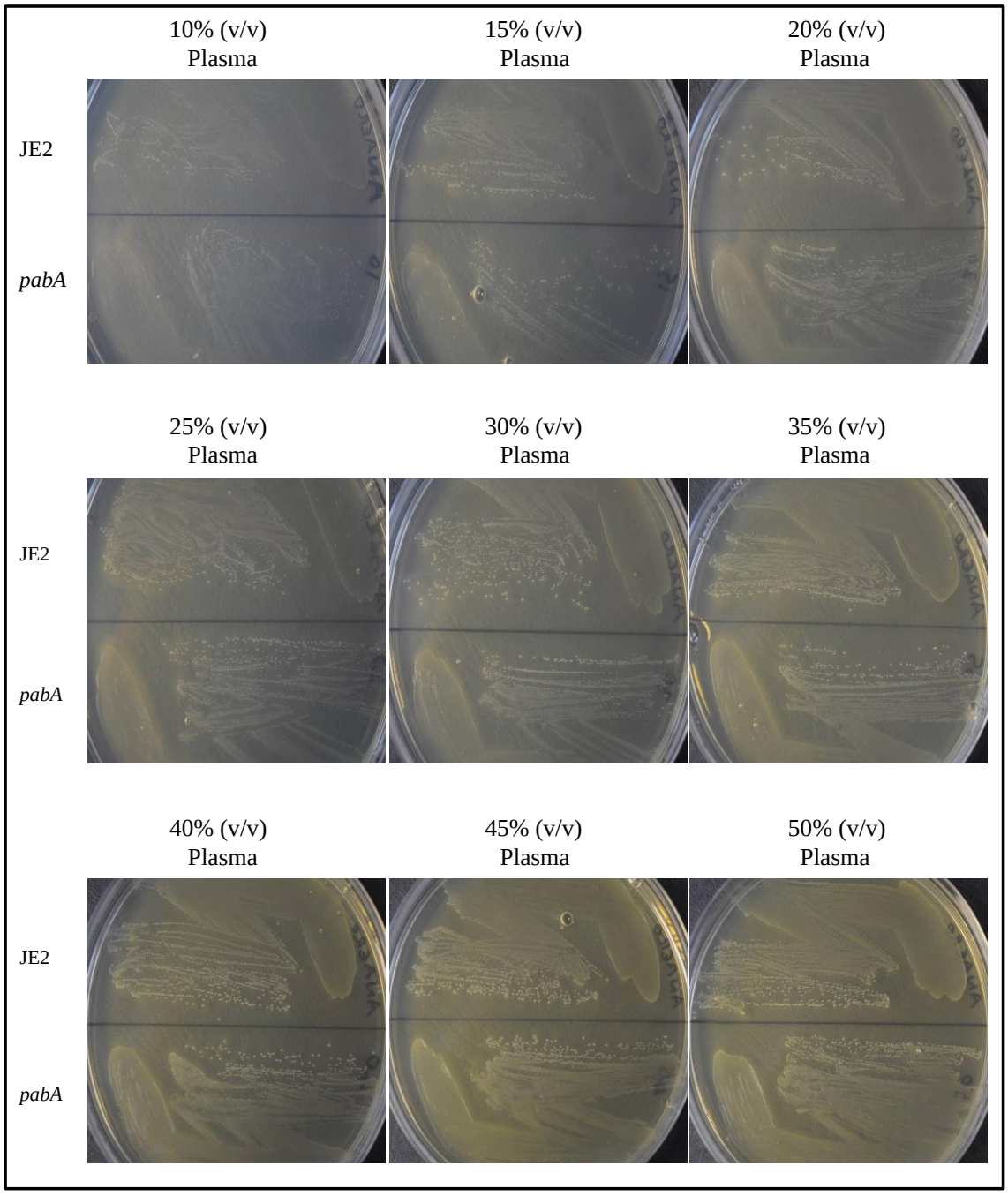

Figure 5.12 Growth of JE2-*pabA* on human plasma.

JE2-*pabA* growth was comparable to that of JE2 at all plasma concentrations. Plates were incubated at 37^{o}C for 48 h.

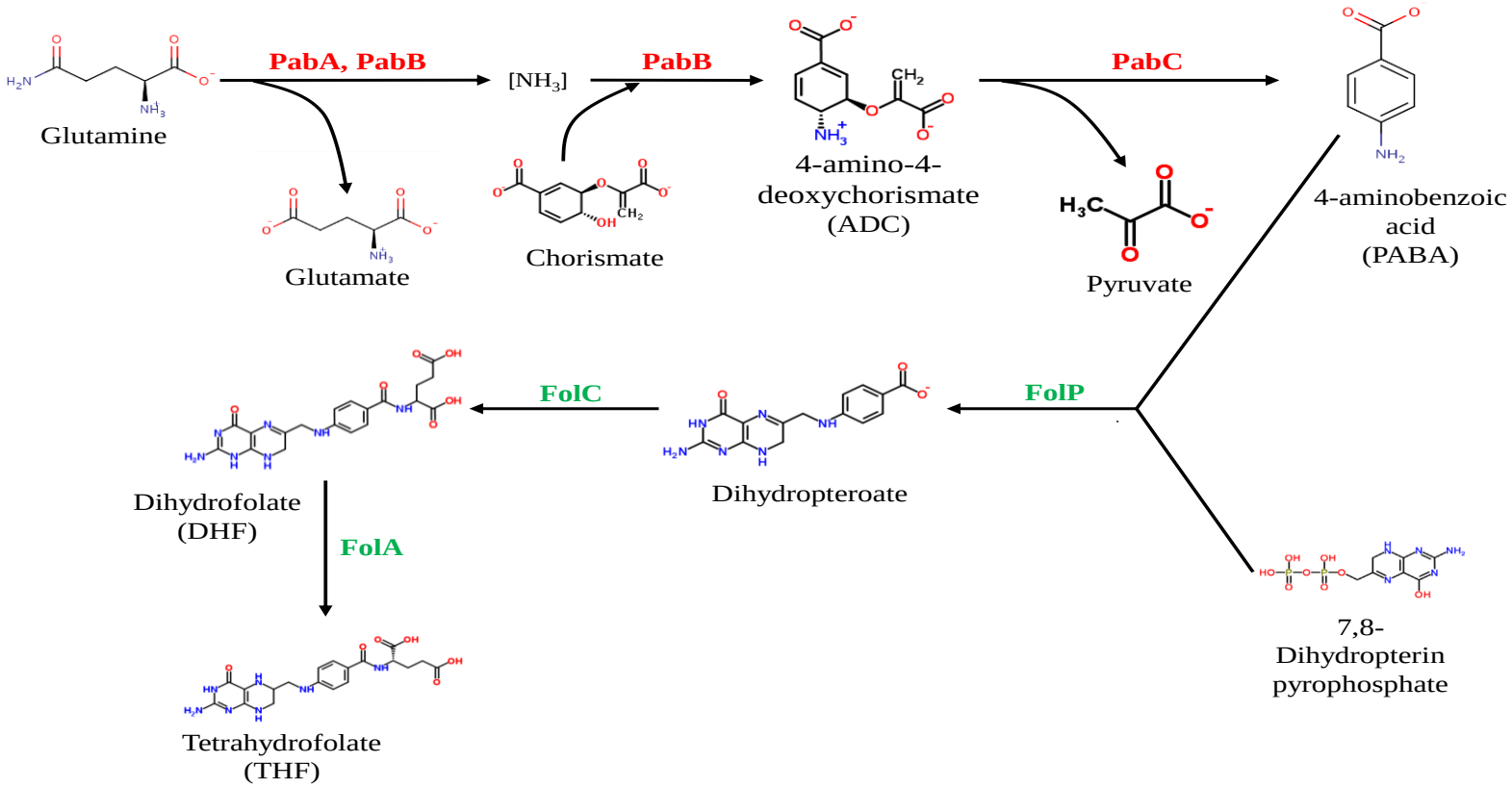

Figure 5.13 Folate biosynthesis pathway.

The *pab* operon encoded enzymes are shown in red; all other enzymes are shown in green. Pathway information was acquired from the Kegg and Biocyc websites. Molecule images were obtained from ChemSpider.

5.2.7 Preliminary analysis of the *pab* operon with the zebrafish embryo model of systemic infection

5.2.7.1 Analysis of SH-*pabB* and SH-*pabC* pathogenicity

To determine if the other members of the *pab* operon show reduced virulence in the zebrafish embryo model of systemic infection, the Tn inserts from NTML strains NE1063 and NE108 were transduced into *S. aureus* SH1000 to give SH-*pabB* and SH-*pabC* respectively. Transductions were carried out as in Chapter 2.10.3 and confirmed by analysis of PCR products on 1% (w/v) electrophoresis gels (data not shown). Both SH-*pabB* and SH-*pabC* were attenuated in the zebrafish model (Figure 5.14). Interestingly NE1063 (the *pabB* mutant) was shown to have reduced growth on human blood in the NTML screen, but was not successfully transduced into both JE2 and SH1000 backgrounds. NE108 (the *pabC* mutant) was not isolated in the original screen, but a re-examination of the original screen plates showed that it did appear to have slightly reduced growth, but not as reduced as the *pabA* or *pabB* mutant.

5.2.7.2 Growth of SH-*pabA in vivo*

In vivo growth analysis was carried out to determine the growth of SH-*pabA* in zebrafish embryos over the course of infection. Experiments were carried out as in section 5.2.4.1 (full details in Chapter 2.23.6). SH-*pabA* can grow in zebrafish embryos resulting in embryo death (Figure 5.15). However, the frequency in which this occurs is reduced compared to SH1000.

5.2.7.3 The effect of folic acid on SH-*pabA*

The enzymes of the *pab* operon catalyse synthesis of PABA, a precursor in THF synthesis (Figure 5.13). As folic acid can be converted to THF, catalysed by the Fol enzymes of *S. aureus* (Bailey, 2009), it was used in the zebrafish model to attempt to complement the *pabA* mutant (Figure 5.16). Folic acid did not alter the virulence of SH1000, or restore virulence to the *pabA* mutant (Figure 5.16 A & B respectively). As with *in vivo* addition of purines (section 5.2.4.2), it was uncertain whether folic acid could not diffuse into the embryos, or if it could not be used by SH-*pabA* to complement the disruption of the *pab* operon.

A

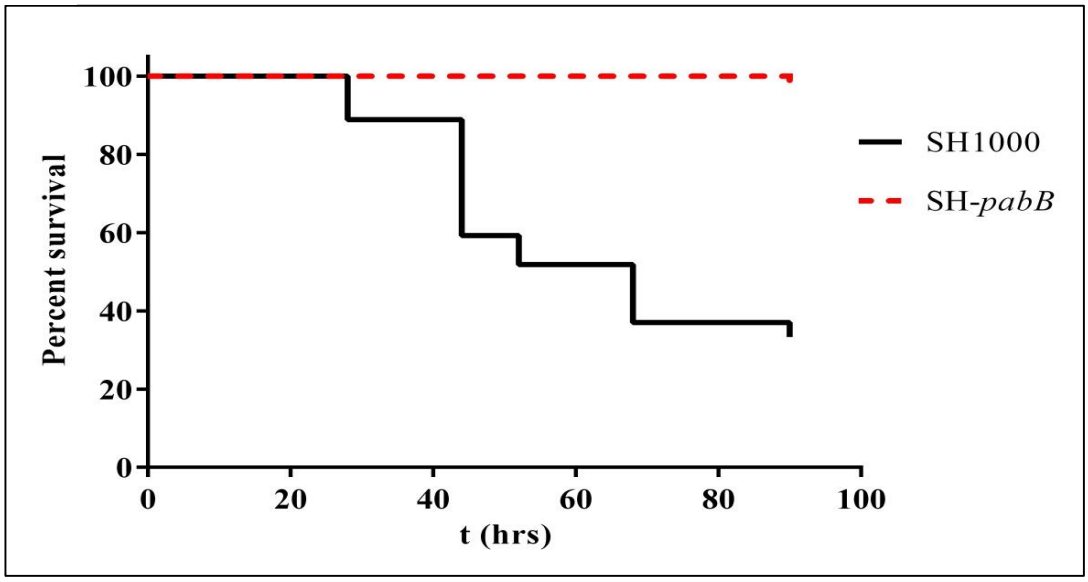

B

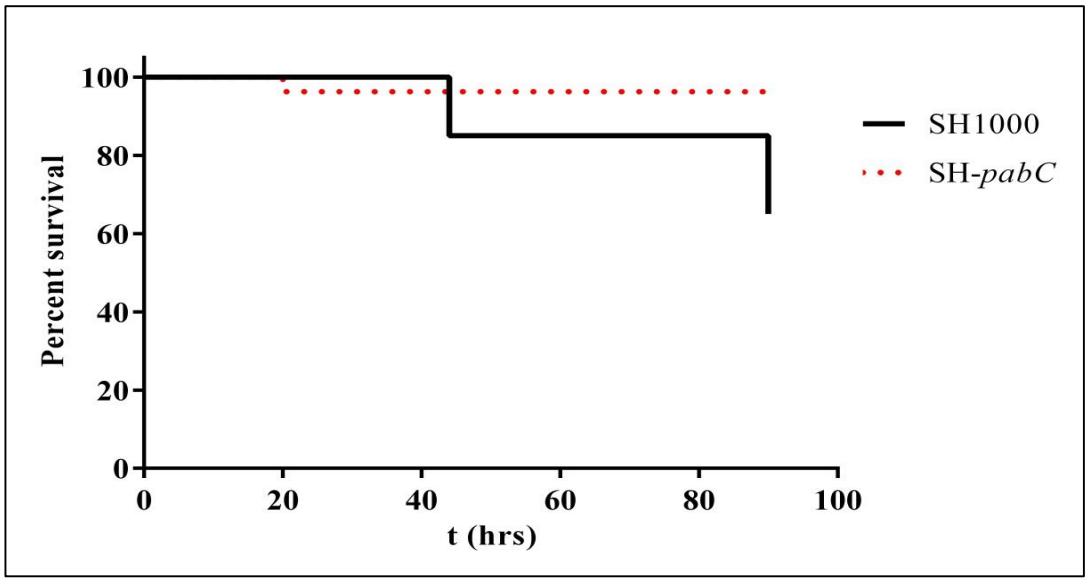

Figure 5.14 Role of *pabB* and *pabC* in virulence.

A. SH-*pabB* was attenuated in the zebrafish model, compared to SH1000, $p < 0.0001$.

B. SH-*pabC* was attenuated in the zebrafish model, compared to SH1000, $p < 0.01$.

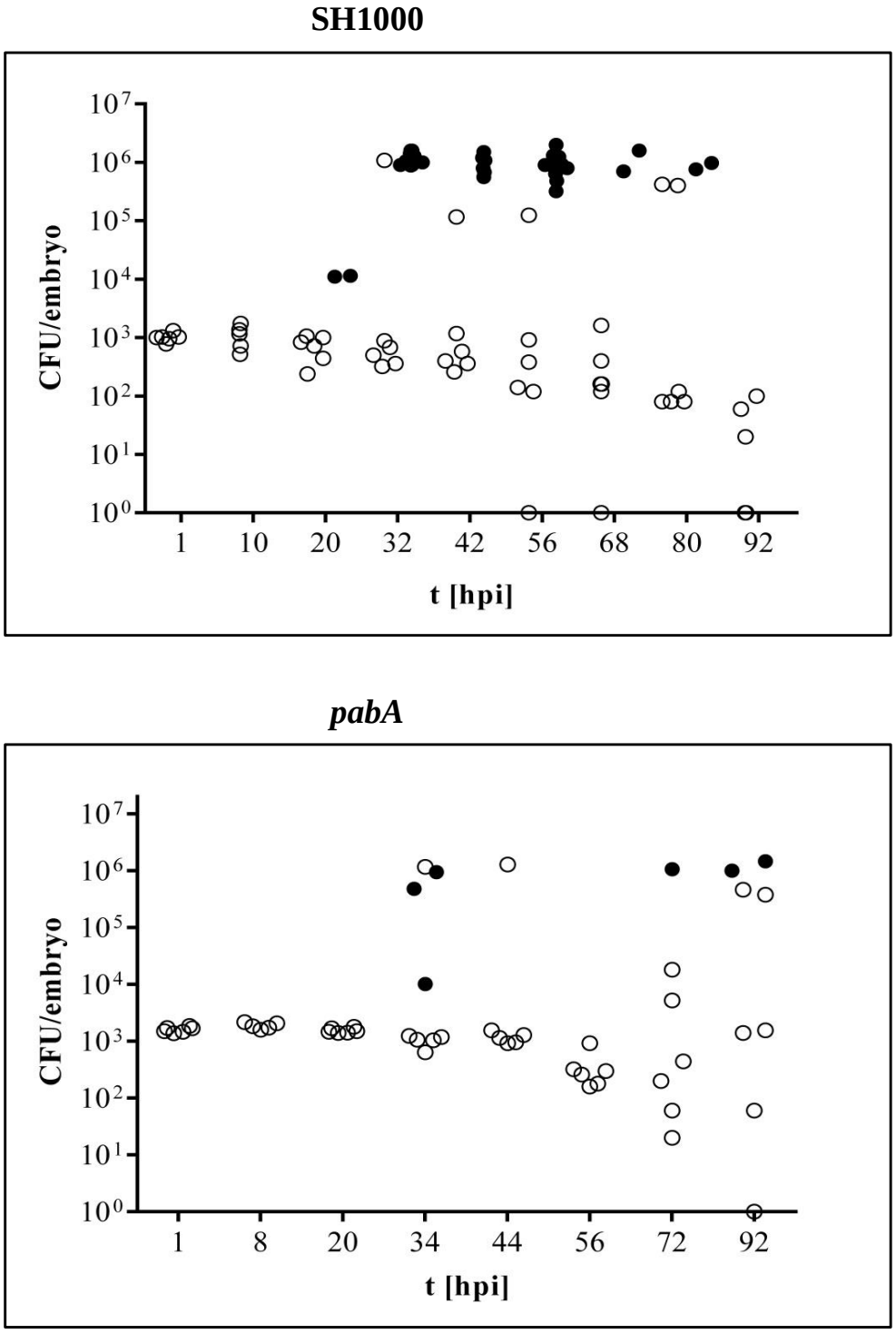

Figure 5.15 Proliferation of SH-*pabA* within zebrafish embryos.

○ = live embryos, ● = dead embryos.

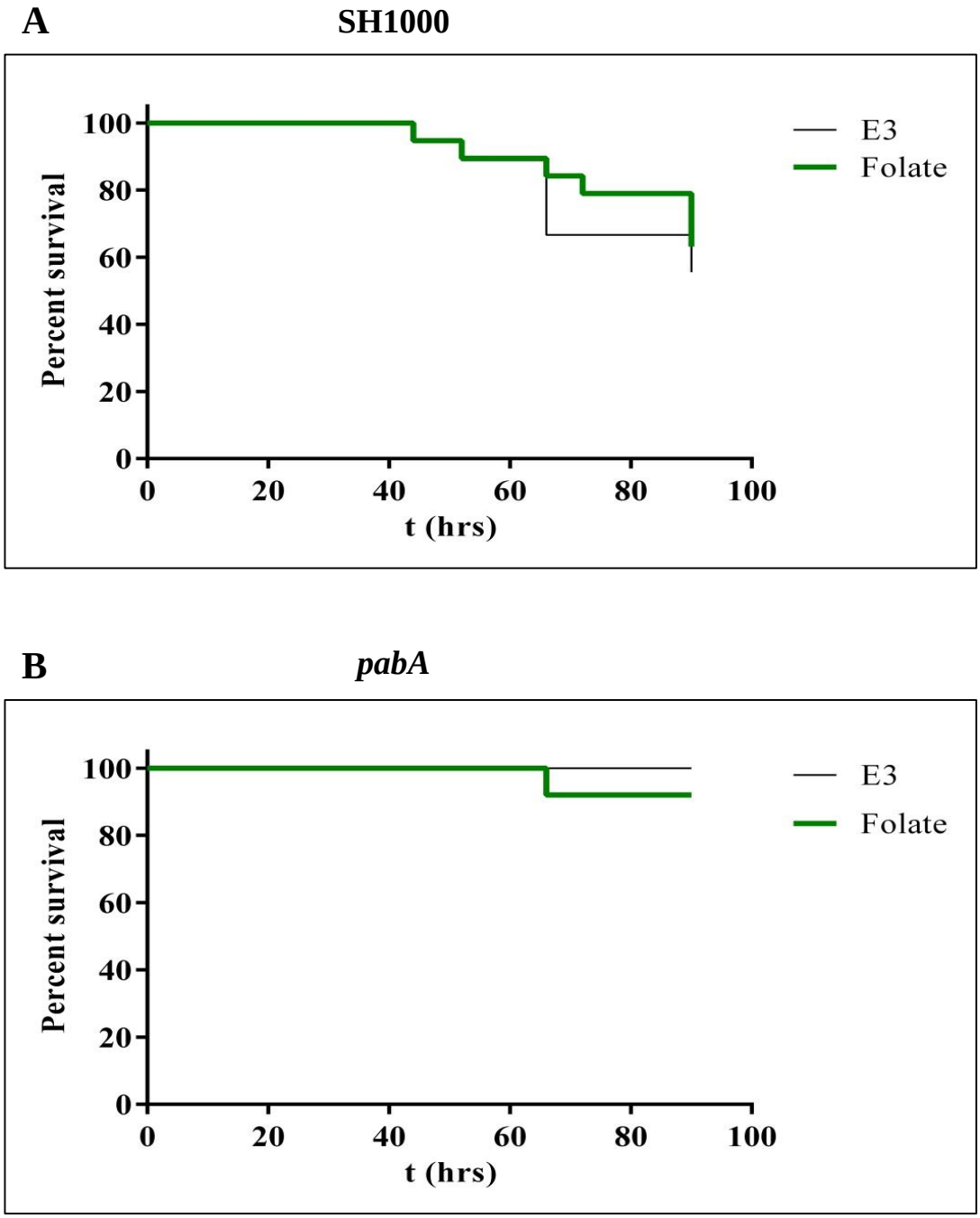

Figure 5.16 Effect of 50 µM folic acid on SH-*purB* virulence.

A. Survival of zebrafish embryos injected with ~1,500 CFU of SH1000 was not significantly altered by addition of 50 µM folic acid, $p > 0.05$.

B. Survival of zebrafish embryos injected with ~1,500 CFU of SH-*pabA* was not significantly altered by addition of 50 µM folic acid, $p > 0.05$.

5.2.7.4 The effect of inosine on SH-*pabA in vivo*

Analysis of the purine *de novo* biosynthesis pathway showed that 10-formyl-THF is a cofactor in the conversion of AICAIR to FAICAIR by the purine pathway enzyme PurH (Figure 5.4). PurH activity occurs earlier in the pathway than the IMP branch point leading to GTP and ATP production. Therefore, it was hypothesised that incubation of zebrafish embryos injected with ~1,500 CFU of SH-*pabA* in E3 solution plus inosine may restore pathogenicity (Figure 5.17). Analysis of the *purA* and *purB* mutants demonstrated that adenine could not complement in the zebrafish embryo model, but it was still a possibility that inosine could diffuse into the embryos and be used by the bacteria. However, addition of inosine did not restore virulence to SH-*pabA* (Figure 5.17). Again it was uncertain whether inosine did not diffuse into the embryos or whether it was unable to phenotypically complement the *pabA* mutation.

5.2.8 Analysis of *pabA* on CDM agar

Although it was not possible to complement the *purA* and *purB* mutants *in vivo* with purines, the CDM and screen results (Figure 5.8 and Chapter 4, Table 4.5, respectively) for these two strains suggested that purines are not freely available in zebrafish embryos and on human blood agar. Disruption of *pabA* blocks synthesis of THF, which has a role in the conversion of AICAIR to FAICAIR in the *de novo* purine biosynthesis pathway. Therefore, it was hypothesised that the lack of available purines in blood and zebrafish embryos explains the poor growth of the *pabA* mutant on blood and attenuation in the zebrafish model. However, this does not explain why JE2-*pabA* grows on human serum or plasma. It was hypothesised that the bioavailability of purines may be increased in serum and plasma and would be investigated further if purines were found to be a requirement for growth on CDM and complemented JE2-*pabA* growth on human blood.

5.2.8.1 Growth of JE2-*pabA* on CDM agar

The synthesis of deoxythymidine monophosphate (dTMP) requires either exogenous thymidine or the THF-dependent conversion of dUMP to dTMP (Figure 5.1C). As CDM does not contain pyrimidines, it was necessary to confirm that CDM is a viable means of assessing growth requirements of JE2-*pabA*, by determining whether the

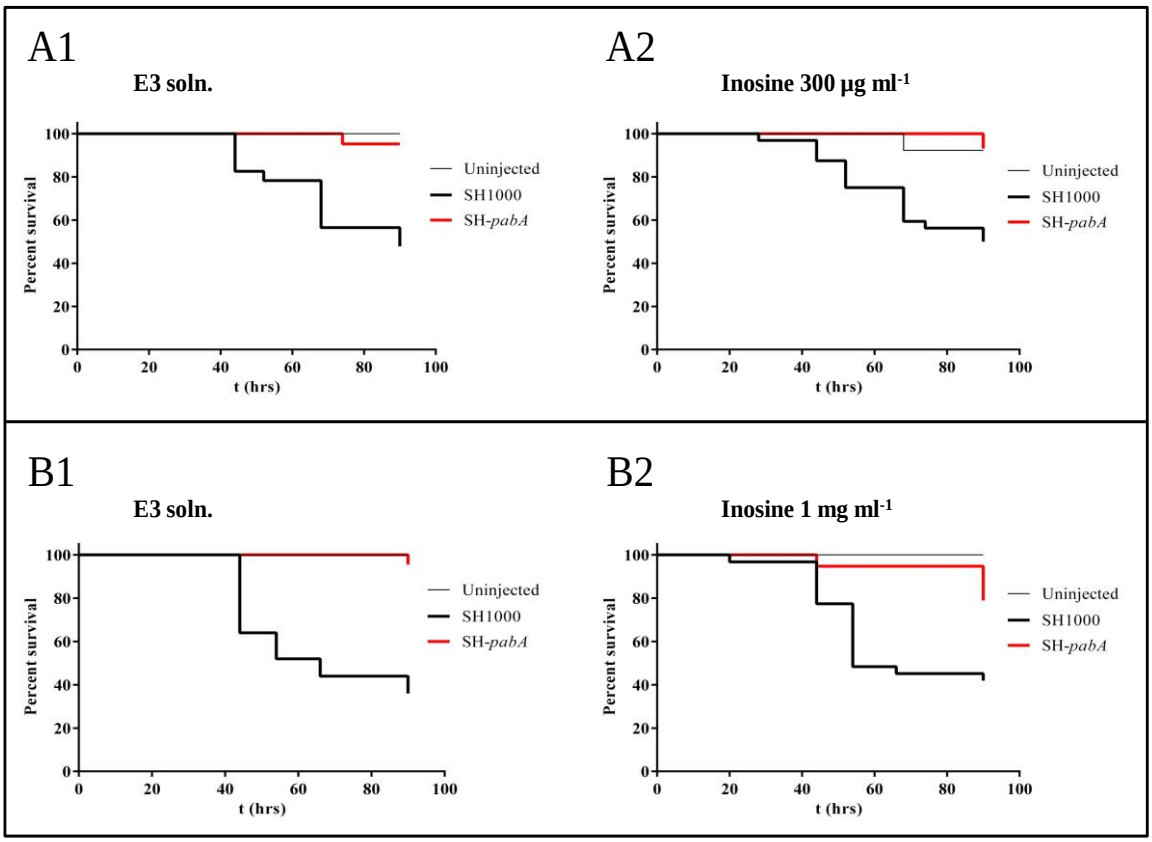

Figure 5.17 Effect of inosine on SH-*pabA* virulence.

A1. Embryos incubated in E3 soln. were injected with ~1,500 CFU of SH-*pabA* or SH1000. SH-*pabA* was attenuated compared to SH1000, $p < 0.0001$. **A2**. Embryos incubated in E3 soln. plus 300 µg ml^{-1} inosine were infected with ~1,500 CFU SH-*pabA* or SH1000. SH-*pabA* remained attenuated compared to SH1000, $p = 0.0001$.

B1. Embryos incubated in E3 soln. were infected with ~1,500 CFU of SH-*pabA* or SH1000. SH-*pabA* was attenuated compared to SH1000, $p < 0.0001$. **B2**. Embryos incubated in E3 soln. plus 1 mg ml^{-1} inosine were infected with ~1,500 CFU SH-*pabA* or SH1000. SH-*pabA* remained attenuated compared to SH1000, $p = 0.0002$.

strain has equivalent growth to JE2 on CDM. Growth of JE2-*pabA* was comparable to JE2 on CDM agar (Figure 5.18). Addition of folic acid to the agar did not enhance growth of either JE2-*pabA* or JE2. CDM agar was incubated in aerobic, microaerobic and anaerobic conditions, to determine the role of oxygenation conditions in the JE2-*pabA* growth phenotype.

5.2.8.2 Role of purine availability in growth of JE2-*pabA*

Growth of JE2-*pabA* and JE2 were compared on CDM agar with or without adenine and guanine (Figure 5.19). If low purine availability in the zebrafish embryo model and on human blood agar was the cause of the JE2-*pabA* phenotype, it was expected that lack of purines in CDM would mimic this. However, growth of JE2-*pabA* in the absence of purines, or an individual purine, was comparable to JE2.

THF has a role in the synthesis of dTMP, methionine, vitamin B_5, purines and the interconversion of serine/glycine (Figure 5.1). The absence of nucleobases was shown to have no impact on JE2-*pabA* growth relative to JE2 (Figure 5.19). Therefore, it was hypothesised that if the *pabA* mutant phenotype is the result of a nutritional deficiency then assessment of the role of glycine, serine, vitamin B_5 and methionine on CDM should highlight this. As 5,10-methylene-THF is produced by conversion of serine to glycine (Figure 5.1A) and is required directly for pantothenate synthesis (Figure 5.1B) and indirectly for methionine biosynthesis (Figure 5.1D & E) it was hypothesised that serine/glycine interconversion would be the most active of the THF-dependent reactions. Therefore, the role of glycine and serine was assessed first on CDM agar.

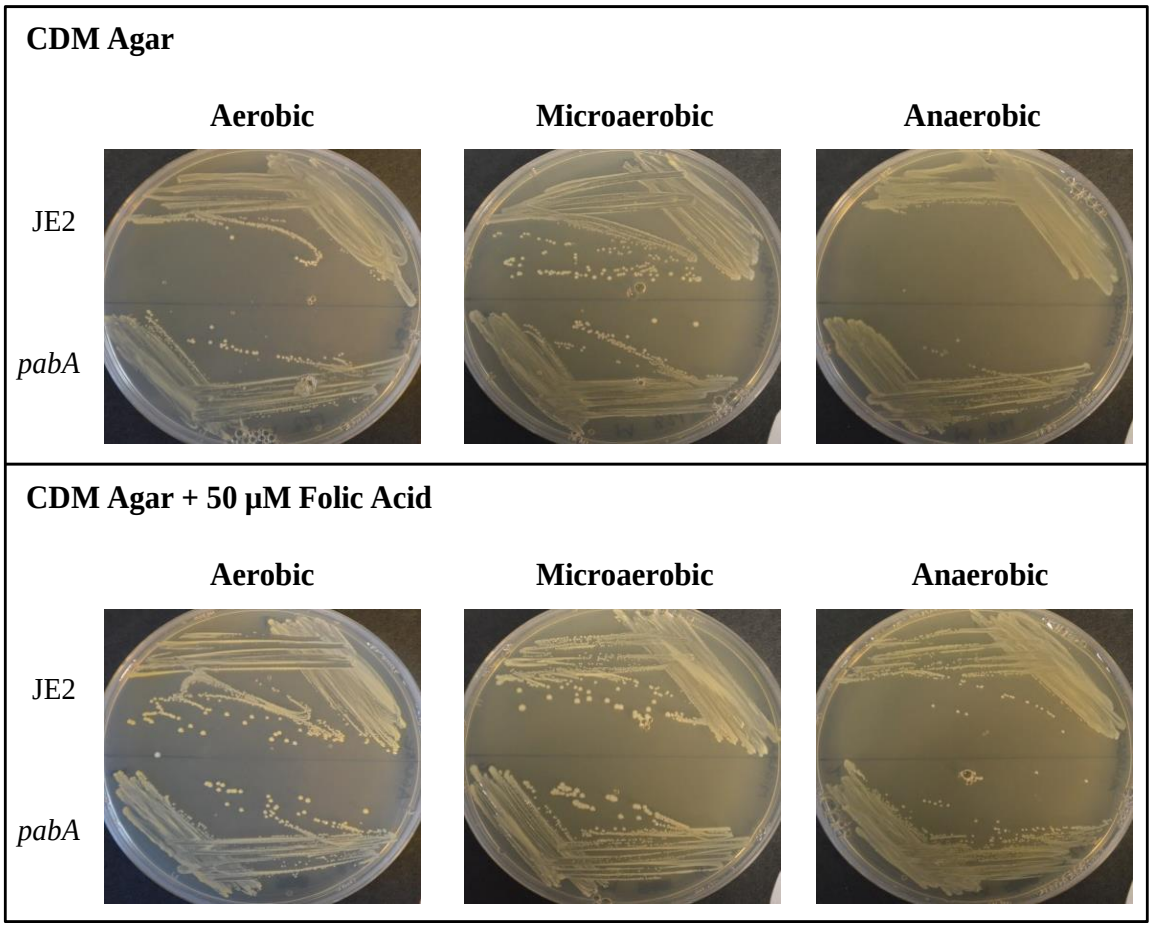

Figure 5.18 Growth of JE2-*pabA* on CDM agar.

Growth of JE2-*pabA* after 48 h incubation at 37^{o}C was equivalent to JE2 in all conditions. Addition of folic acid did not enhance the growth of either strain.

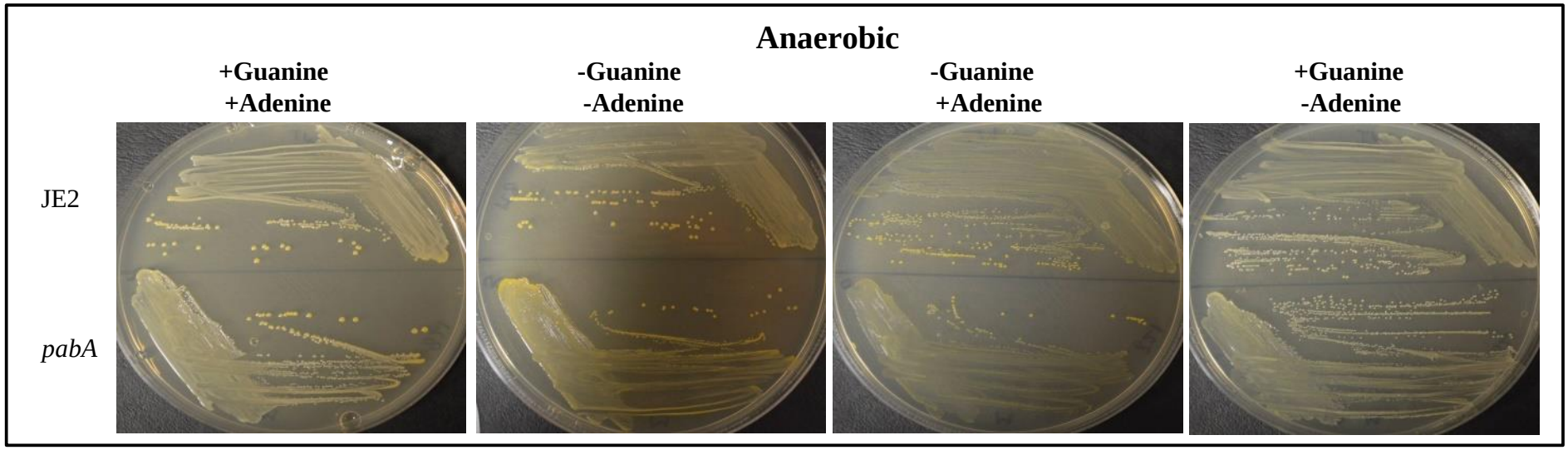

Figure 5.19 Role of purines in the growth of JE2-*pabA* and JE2.

Presence of purines in CDM did not alter the growth of JE2-*pabA*. Plates were incubated at 37^{o}C for 48 h.

5.2.8.3 The effect of glycine, serine & folic acid on JE2-*pabA* growth

JE2-*pabA* growth was compared to JE2 on CDM plus or minus glycine and serine. CDM was prepared without purines, as it was shown in section 5.2.8.2 that purines are not essential for comparable growth of JE2-*pabA* to JE2. Folic acid was used to determine if it could complement the *pabA* mutant *in vitro*. Results are shown in Figure 5.20 and Table 5.3. In the absence of serine, growth of JE2 was not affected, but growth of JE2-*pabA* was poor, suggesting that serine is important to the *pabA* mutant. In the absence of glycine, JE2 growth was poor, but JE2-*pabA* growth was very poor. This suggests that glycine is important for both strains. In the absence of serine and glycine both JE2 and the *pabA* mutant showed very poor growth with no apparent difference between them. However, in the presence of glycine, serine and folic acid growth of the *pabA* mutant appeared to be slightly reduced compared to JE2. Addition of folic acid did not restore JE2-*pabA* growth to that of JE2.

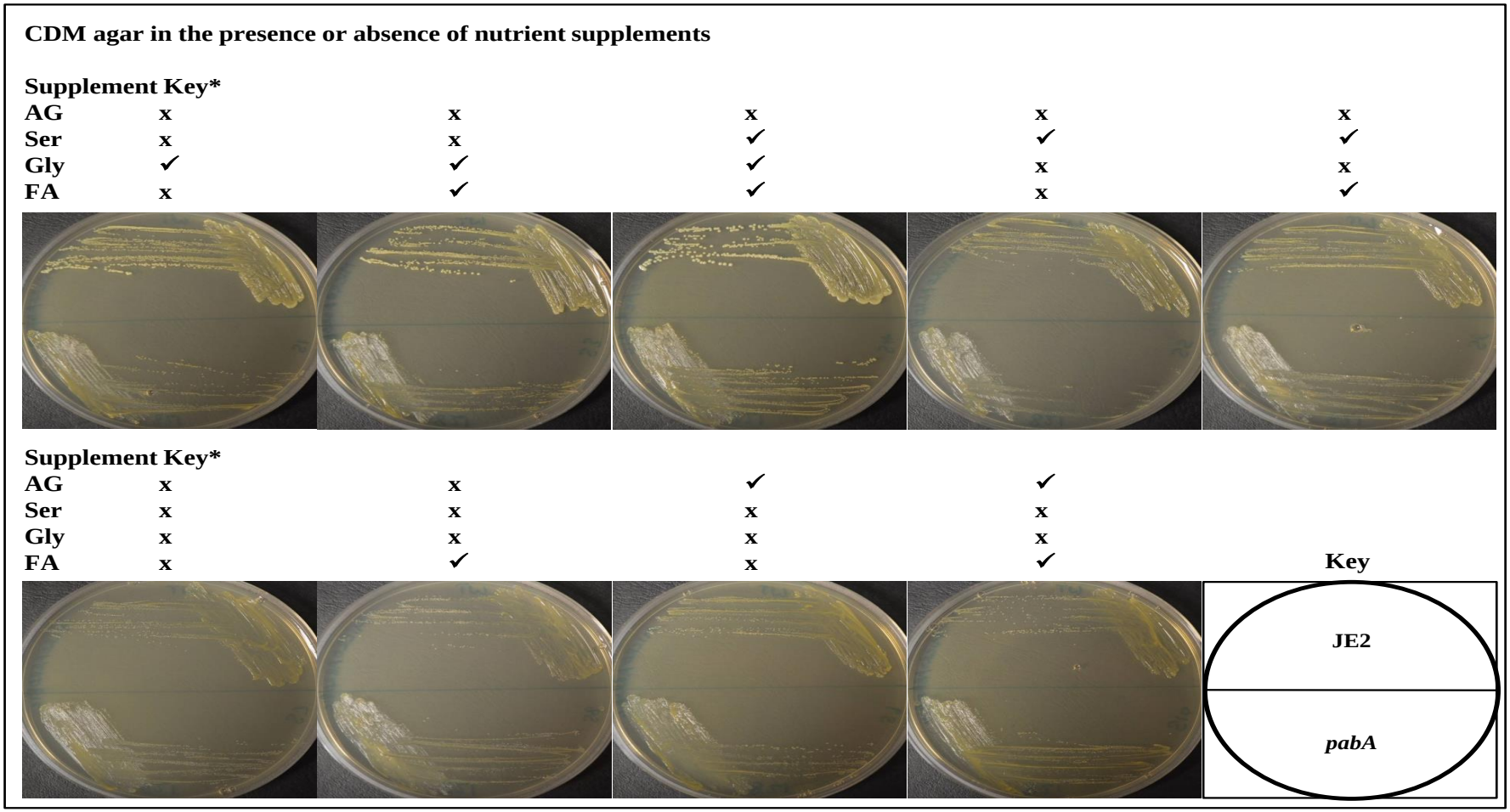

Figure 5.20 Role of glycine, serine, folic acid and purines (AG) in the growth of JE2-*pabA* and JE2.
x indicates absence of supplement; ✓ indicates presence of supplement, corresponding to the supplement key
Plates were incubated at 37^{o}C for 48 h.
* AG = adenine & guanine, Ser = serine, Gly = glycine, FA = folic acid.

Table 5.3 Analysis of the role of glycine, serine, folic acid and purines (AG) in the growth of JE2-*pabA* and JE2.

Strain	Key	Nutrient supplements								
	Adenine & Guanine	**x**	**x**	**x**	**x**	**x**	**x**	**x**	✓	✓
	Serine	**x**	**x**	✓	✓	✓	**x**	**x**	**x**	**x**
	Glycine	✓	✓	✓	**x**	**x**	**x**	**x**	**x**	**x**
	Folic Acid	**x**	✓	✓	**x**	✓	**x**	✓	**x**	✓
JE2		++++	++++	++++	++	++	+	+	+	+
pabA		++	++	+++	+	+	+	+	+	+

+ Very poor growth
++ Poor growth
+++ Slightly reduced growth
++++ Normal growth
✓ indicates addition of supplement, corresponding to the key
x indicates absence of supplement, corresponding to the key

5.2.8.4 The effect of 4-aminobenzoic acid (PABA) on growth of JE2-*pabA*

Folic acid did not restore the growth of JE2-*pabA* to the level of JE2 in the absence of serine/glycine. Therefore, folic acid does not complement *in vitro* and could not be used as a positive control for complementation in further experiments. Hamilton-Miller, (1988) reported that folic acid, folinic acid, THF and DHF did not inhibit trimethoprim activity in *S. aureus*, whereas folinic acid, THF and DHF, but not folic acid, did inhibit trimethoprim activity in enterococci. Trimethoprim is an antifolate antibiotic that inhibits the DHFR enzyme (FolA in Figure 5.13) in THF synthesis downstream of PABA synthesis (Proctor, 2008). It has been reported that *E. coli* and *Salmonella sp.* are unable to transport folates into the cytoplasm, which is common to strains that can synthesise THF (Neidhardt *et al*., 1996; Tran & Nichols, 1991). However, 4-aminobenzoate (PABA) has been used to complement a *pabA* mutant strain of *E. coli*, at 5 ng ml^{-1} (Tran & Nichols, 1991). PABA concentrations up to 200 µg ml^{-1} have been used to determine the efficacy of folate inhibitors in *S. aureus* USA300 (Phetsang *et al*., 2013). Therefore 50 µg ml^{-1} PABA was used as an alternative to folic acid in the complementation of JE2-*pabA* (Figure 5.21; Table 5.4).

In the absence of serine and glycine, PABA slightly improves the growth of both JE2-*pabA* and the parent. Addition of serine did not alter the very poor growth of both strains. The presence of glycine in the absence of serine restored JE2 growth, but JE2-*pabA* growth was slightly reduced compared to JE2. This reduction in growth was complemented by PABA or serine. This suggested that PABA can be used to complement the *pabA* mutation. Serine does have a role, as the growth of JE2-*pabA* was slightly reduced in its absence and restored to JE2 levels when serine was added. The importance of glycine to both strains was clear, as both strains grew very poorly in its absence. Whether glycine has an increased importance to the *pabA* mutant relative to JE2 was not resolved in this experiment. The slight reduction in growth of the *pabA* mutant in CDM containing all components barring purines (Figure 5.20) was not seen in this experiment.

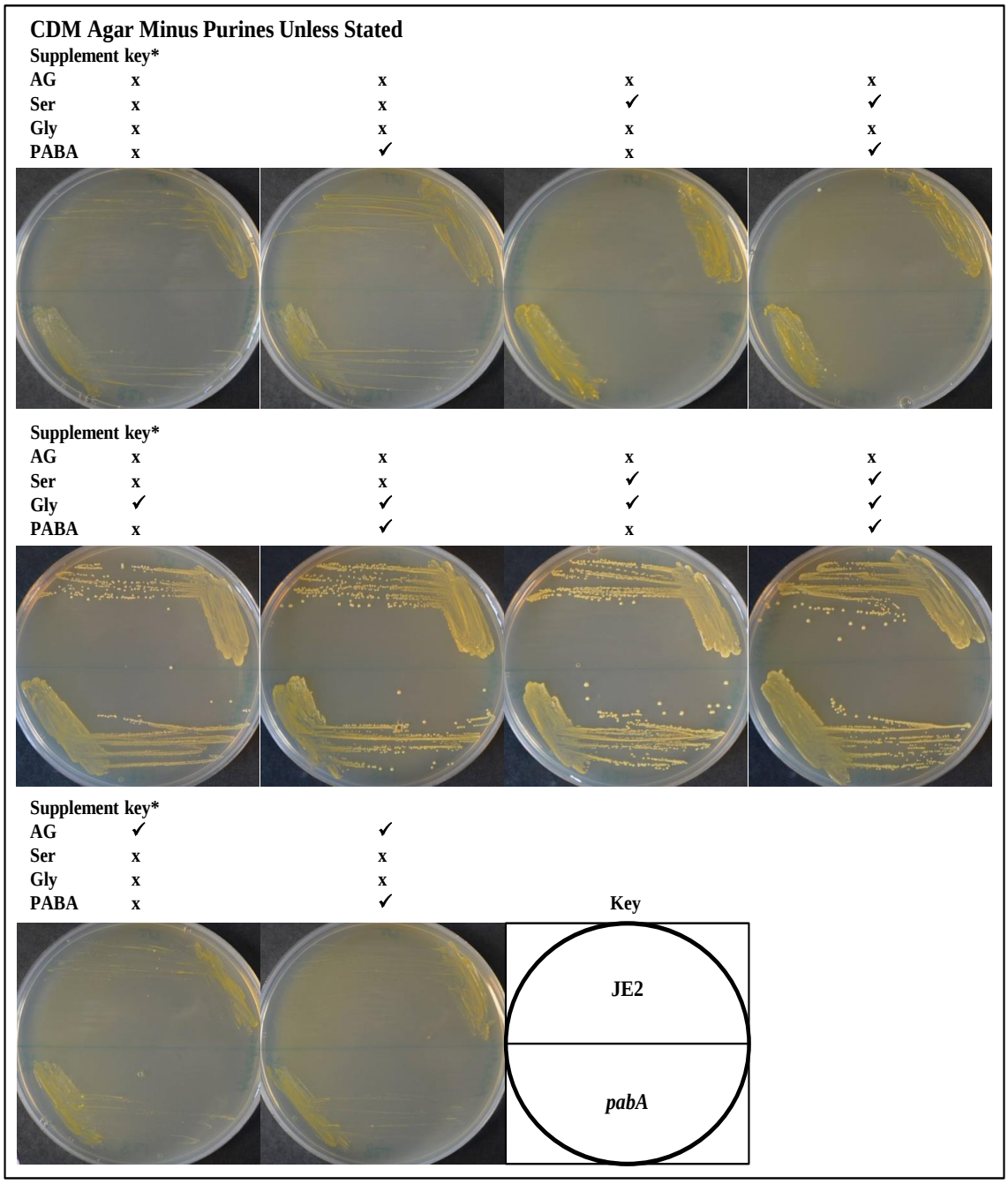

Figure 5.21 Role of glycine, serine, PABA and purines (AG) in the growth of JE2-*pabA* and JE2.

x indicates absence of supplement; ✓ indicates presence of supplement, corresponding to the supplement key

Plates were incubated at 37^{o}C for 48 h.

* AG = adenine & guanine, Ser = serine, Gly = glycine.

Table 5.4 Analysis of the role of glycine, serine, PABA and purines (AG) in the growth of JE2-*pabA* and JE2.

Strain	Key	Nutrient supplements									
	Adenine & Guanine	**x**	**x**	**x**	**x**	**x**	**x**	**x**	**x**	✓	✓
	Serine	**x**	**x**	✓	✓	**x**	**x**	✓	✓	**x**	**x**
	Glycine	**x**	**x**	**x**	**x**	✓	✓	✓	✓	**x**	**x**
	PABA	**x**	✓	**x**	✓	**x**	✓	**x**	✓	**x**	✓
JE2		+	~+	+	+	++++	++++	++++	++++	+	+
pabA		+	~+	+	+	+++	++++	++++	++++	+	+

+ Very poor growth
~+ Very poor, but slightly better than previous condition
++ Poor growth
+++ Slightly reduced growth
++++ Normal growth
✓ indicates addition of supplement, corresponding to the key
x indicates absence of supplement, corresponding to the key

5.2.8.5 Role of PABA, serine and glycine in SH-*pabA* pathogenicity

CDM concentrations of glycine, serine and 7 μg ml^{-1} PABA were assessed in the zebrafish embryo model of systemic infection using SH-*pabA*. A lower concentration of PABA was used for the embryo model to minimise the influence of ethanol (used as the PABA diluent), as the CDM PABA concentration (50 μg ml^{-1}) was found to be toxic to the embryos (data not shown). When infected embryos were incubated in E3 solution SH-*pabA* remained attenuated (Figure 5.22A). Addition of CDM concentrations of glycine, serine and 7 μg ml^{-1} PABA restored the virulence of the *pabA* mutant (Figure 5.22B).

5.2.8.6 The role of glycine and serine in the growth of JE2-*pabA*

To determine the relative importance of glycine and serine to the growth of JE2-*pabA*, different concentrations of these two amino acids were added to CDM. A hypothesis was developed based on serine/glycine interconversion shown in Figure 5.1A, shown diagrammatically in Figure 5.23. Glycine can be produced from threonine by threonine aldolase, however, the primary endogenous source of glycine is via THF-dependent serine conversion by the enzyme GlyA (Aller *et al*., 2015; Liu *et al*., 2015). As glycine is an important component of *S. aureus* peptidoglycan (Maidhof *et al*., 1991; Zhou & Cegelski, 2012), is required for biosynthesis of purines (Cheng *et al*., 1990) and is required as an amino acid in proteins, cutting off the primary source of endogenous glycine creates a need for exogenous glycine. The requirement for serine is less certain, as serine can be synthesised by JE2-*pabA*. This synthesis is subject to end product inhibition of the enzyme D-3-phosphoglycerate dehydrogenase (Ponce-de-Leon & Pizer, 1972). The hypothesis was that in JE2, conversion from serine provides a pool of glycine. Serine is important for the synthesis of other amino acids (Denk & Böck, 1987; Lane & Kirschner, 1983), the synthesis of phosphatidylserine and sphingolipids (Inuzuka *et al*., 2005) and for its role as an amino acid in proteins. Therefore, if the bacteria have to respond to a sudden need for lipids or certain amino acids, then glycine from the hypothetical glycine pool (shown in red in Figure 5.23) can be quickly converted to serine by GlyA and THF, bypassing the end product inhibition that slows the biosynthesis of serine. If the hypothesis was correct, then JE2-*pabA* would not have

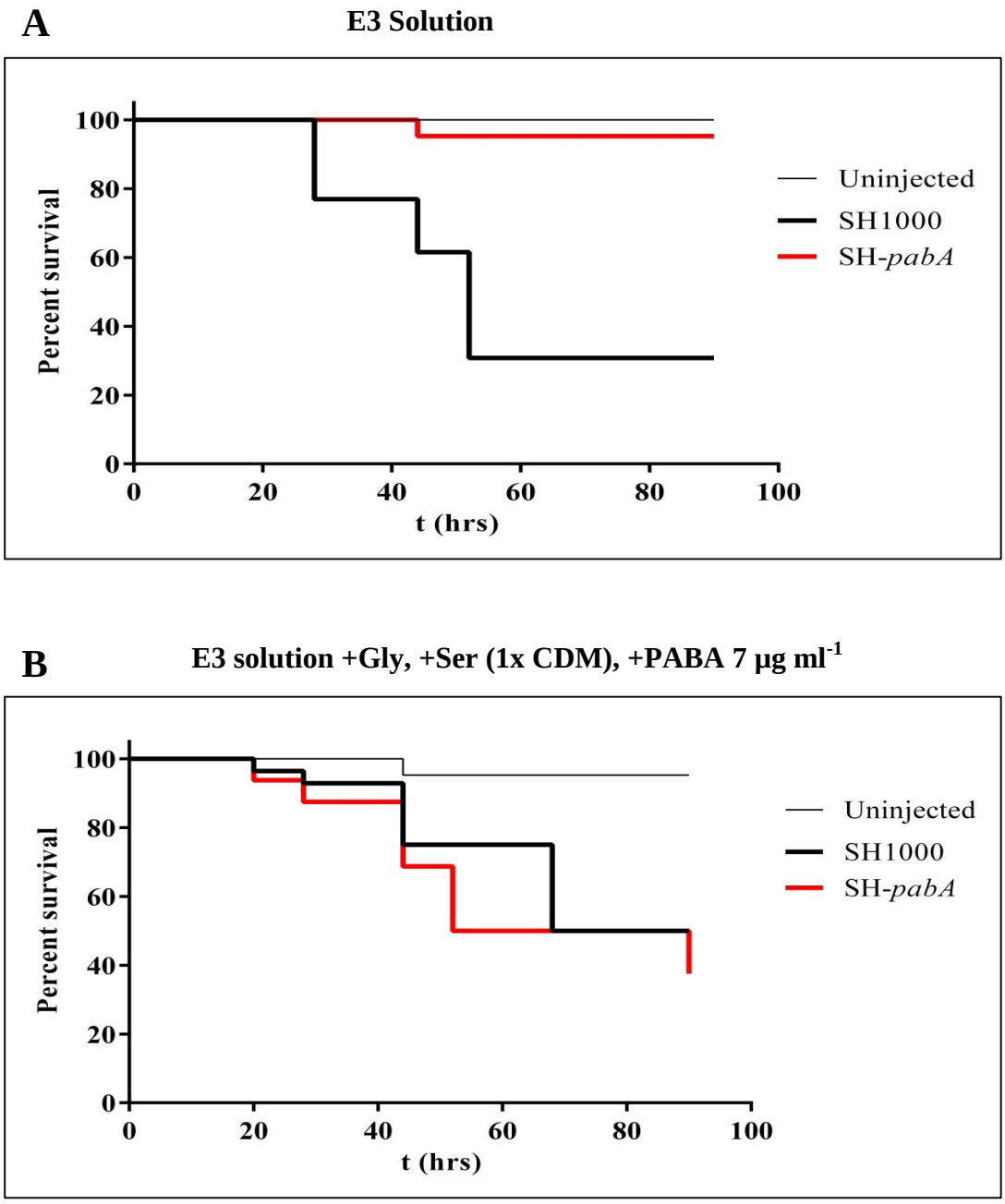

Figure 5.22 Effect of glycine, serine and PABA on SH-*pabA* virulence.

A. SH-*pabA* pathogenesis was attenuated compared to SH1000 in embryos incubated in E3 solution, $p < 0.0001$.

B. Pathogenesis was restored to SH-*pabA* in embryos incubates in E3 solution +1x CDM concentrations of glycine and serine and 7 µg ml^{-1} PABA compared to SH-*pabA* incubated in E3 solution $p < 0.0001$.

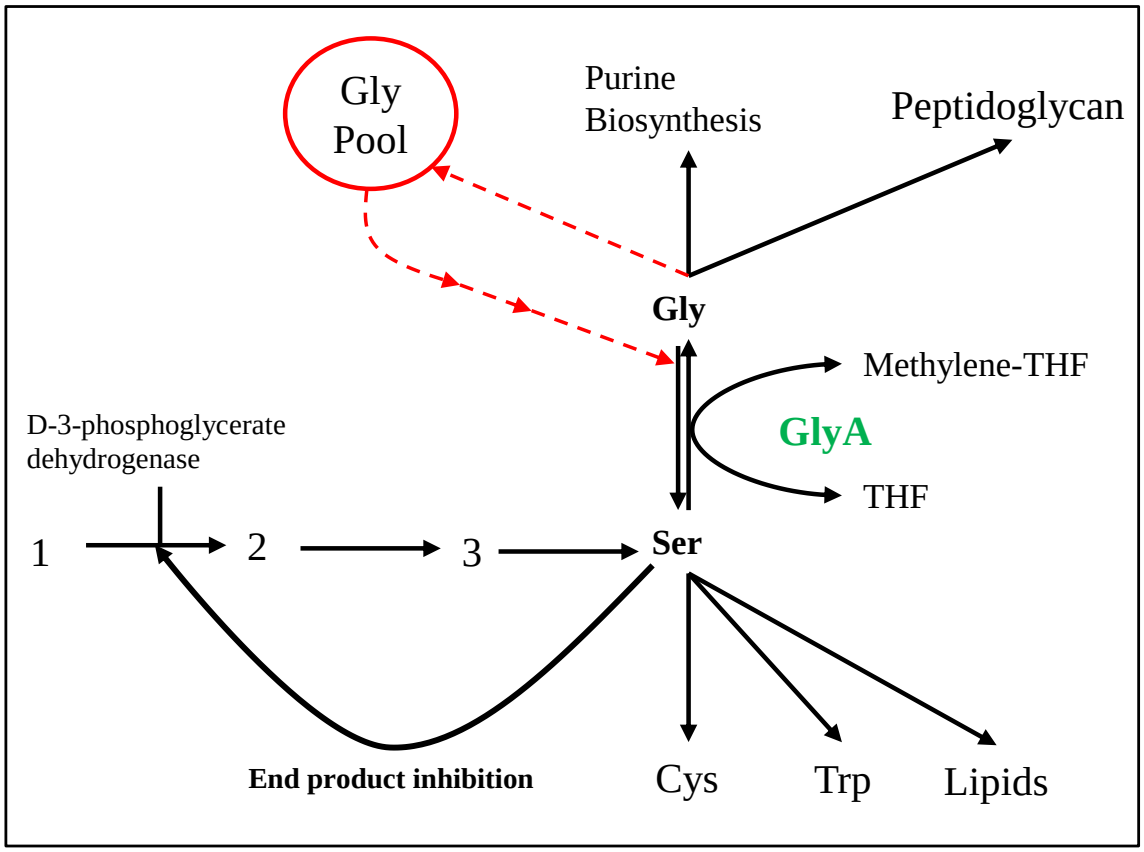

Figure 5.23 Diagrammatic representation of serine/glycine interconversion.

Hypothetical aspects of the diagram are shown in red.

access to this serine/glycine pool and may require an excess of one over the other in order to respond to the changing needs of the bacteria during growth.

Figure 5.24 and Table 5.5 show that excess serine in the absence of glycine resulted in poor growth of both strains. When glycine was added, JE2 growth was restored and JE2-*pabA* growth was only partially restored. In the presence of excess glycine, in the presence or absence of serine JE2 growth was completely restored, but growth of JE2-*pabA* was poor. This suggested that addition of excess glycine had a negative impact on the *pabA* mutant. Where differences in growth could be resolved, PABA restored the growth of JE2-*pabA* to that of JE2.

High concentrations of glycine have been associated with cell wall damage, lysis and accumulation of cell wall synthesis intermediates including nucleotides involved in cell wall synthesis in *S. aureus* (Parisi & Suling, 1968; Strominger & Birge, 1965). Bacteria avoid the toxic effects of glycine using the glycine cleavage system, which degrades glycine to CO_2, NH_4^+ and a methylene group (Tezuka & Ohnishi, 2014). As THF is required for this process (Figure 5.1I), it is likely that the *pabA* mutant would be more susceptible to the effects of high glycine concentration than the wild-type. Furthermore, in the absence of serine/glycine interconversion, toxic levels of glycine cannot be converted to serine. As blood glycine levels have been shown to be 5x less than the standard CDM glycine concentration (shown to be non-toxic to *S. aureus*; De Vries *et al*., 1948), glycine toxicity on human blood agar was ruled out as a potential cause of the JE2-*pabA* phenotype. Based on these results the hypothesis shown in Figure 5.23 was reasoned to be invalid, as low glycine concentrations need to be maintained to avoid glycine toxicity.

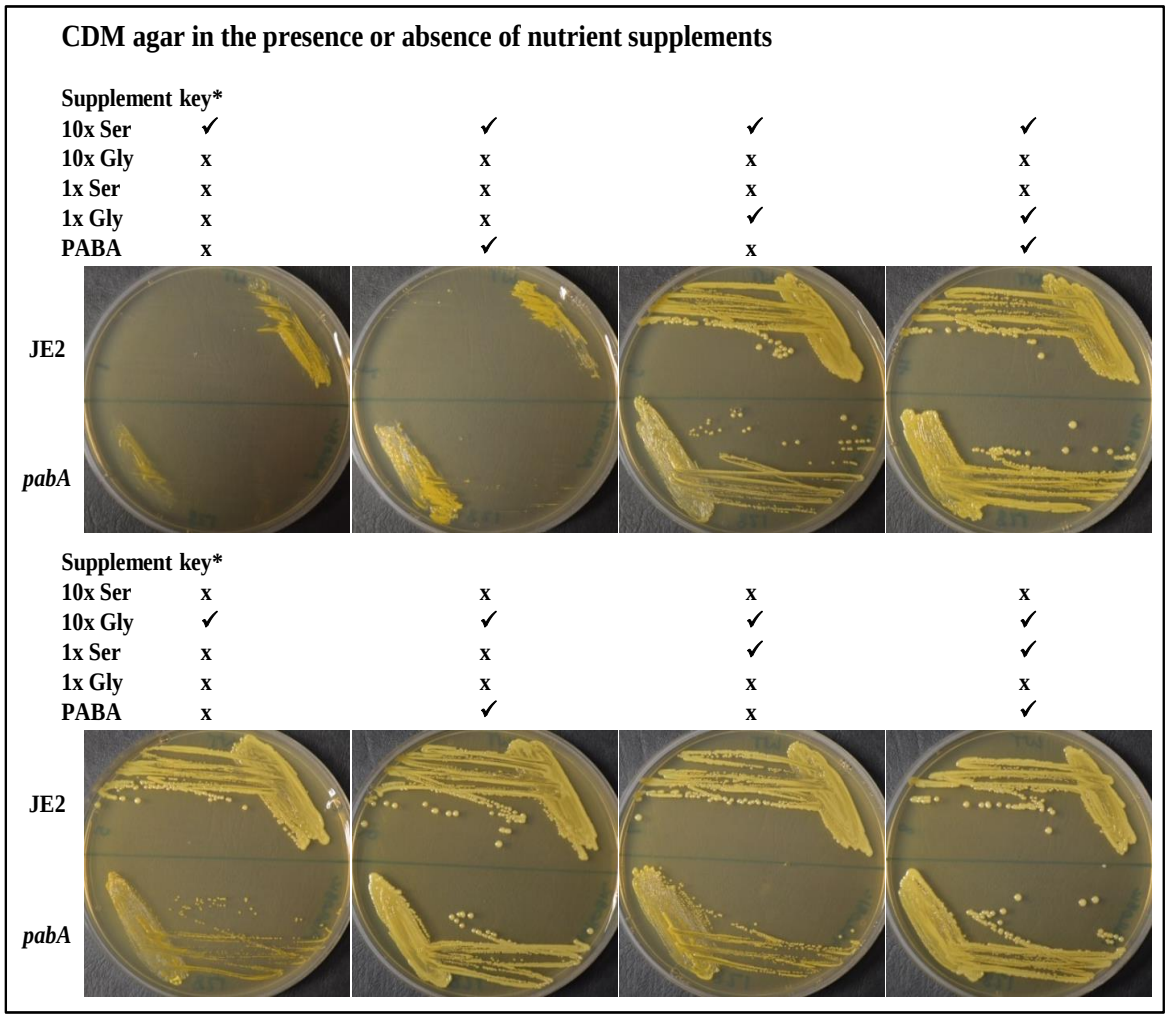

Figure 5.24 Role of 10x CDM concentration of glycine or serine, and 1x CDM concentration of glycine and serine in the growth of JE2-*pabA* and JE2.

x indicates absence of supplement; ✓ indicates presence of supplement, corresponding to the supplement key

Plates were incubated at 37^{o}C for 48 h.

* 10x Ser = 1 mg ml^{-1} serine, 10x Gly = 1 mg ml^{-1} glycine, 1x Ser = 100 µg ml^{-1} Ser, 1x Gly = 100 µg ml^{-1} glycine.

Table 5.5 Analysis of the role of 10x CDM concentration of glycine or serine, and 1x CDM concentration of glycine and serine in the growth of JE2-*pabA* and JE2.

Strain	Key*	Nutrient supplements							
	10x Ser	✓	✓	✓	✓	x	x	x	x
	10x Gly	x	x	x	x	✓	✓	✓	✓
	1x Ser	x	x	x	x	x	x	✓	✓
	1x Gly	x	x	✓	✓	x	x	x	x
	PABA	x	✓	x	✓	x	✓	x	✓
JE2		+	+	++++	++++	++++	++++	++++	++++
pabA		+	+	+++	++++	++	++++	++	++++

+ Very poor growth
++ Poor growth
+++ Slightly reduced growth
++++ Normal growth
✓ indicates addition of supplement, corresponding to the key
x indicates absence of supplement, corresponding to the key

* 10x Ser = 1 mg ml^{-1} serine, 10x Gly = 1 mg ml^{-1} glycine, 1x Ser = 100 µg ml^{-1} Ser, 1x Gly = 100 µg ml^{-1} glycine.

5.2.8.7 Role of GlyA in virulence

Serine/glycine interconversion is catalysed by the enzyme GlyA. To determine the importance of serine/glycine interconversion the transposon insertion from the NTML *glyA* mutant strain NE213 was transduced into SH1000 to give SH-*glyA*. Transduction was confirmed by PCR and analysis of PCR products on 1% (w/v) electrophoresis gel (data not shown). For transduction, PCR and electrophoresis methods see Chapter 2.10.3, Chapter 2.12.1.2 and Chapter 2.12.5, respectively. SH-*glyA* was then assessed *in vivo* using the zebrafish embryo model of systemic infection (Figure 5.25). Disruption of *glyA* did not result in loss of virulence. This suggested that loss of serine/glycine interconversion due to loss of THF is not responsible for the JE2-*pabA* or the SH-*pabA* virulence phenotype in the zebrafish model. It was hypothesised that loss of serine/glycine interconversion may still relate to the JE2-*pabA* and SH-*pabA* phenotype, but the full effect (i.e. loss of virulence and poor growth on blood) may be due to the cumulative effect of the loss of all reactions requiring THF.

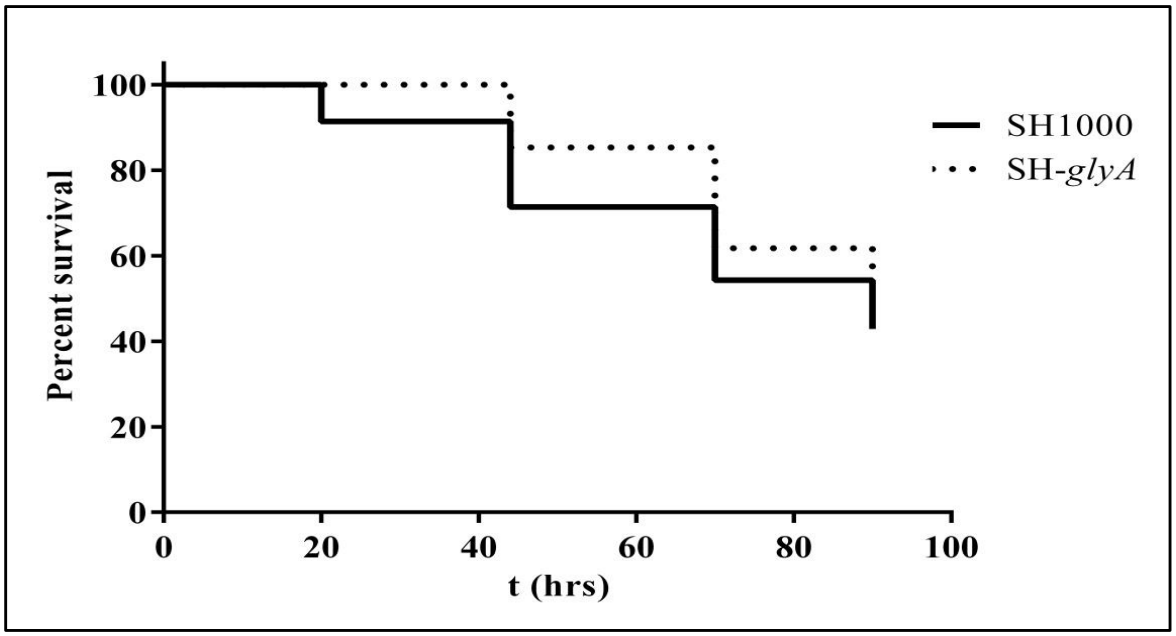

Figure 5.25 Role of *glyA* in *S. aureus* pathogenesis in the zebrafish embryo model.

SH-*glyA* was not attenuated in the zebrafish embryo model compared to SH1000, $p > 0.05$.

5.2.8.8 The role of serine, glycine, methionine & $VitB_5$ on growth of JE2-*pabA*

Table 5.1 shows that THF is involved in synthesis of methionine, $VitB_5$ and glycine/serine interconversion. It was hypothesised that the JE2-*pabA* phenotype was the result of growth defects caused by the cumulative effect of the loss of these functions. The importance of serine, glycine, $VitB_5$ and methionine to JE2-*pabA* growth was assessed in CDM (Figure 5.26; Table 5.6). In the absence of methionine growth of JE2 and the *pabA* mutant was very poor, therefore, no conclusion was drawn on the importance of methionine to JE2-*pabA*. The growth of JE2-*pabA* in the absence of $VitB_5$ or glycine was slightly reduced relative to JE2. However, growth of JE2-*pabA* when all components were added to CDM was also slightly reduced relative to JE2. Only serine showed a clear effect when removed from CDM, resulting in JE2-*pabA* growing poorly in comparison to the growth of JE2.

This suggested two things: firstly $VitB_5$ and glycine may not be required by JE2-*pabA* for comparable growth to JE2, as their removal from CDM did not affect the relative growth of JE2-*pabA* to JE2 when compared to the addition of glycine and $VitB_5$. Secondly that something not present in CDM is required by JE2-*pabA* as it shows slightly reduced growth in the presence of all CDM components, barring purines. Purines were found to not be required for comparable growth of JE2-*pabA* to JE2 (Figure 5.19), therefore, they were not added to CDM. The lack of purines in the CDM may be responsible for the reduced growth of JE2-*pabA* in the CDM used for this experiment. Alternatively, THF has a role in conversion of dUMP to dTTP, via dTMP (Figure 5.1C). CDM does not contain any pyrimidines, which suggested that this may be the cause of the reduced growth of JE2-*pabA* compared to JE2 in CDM.

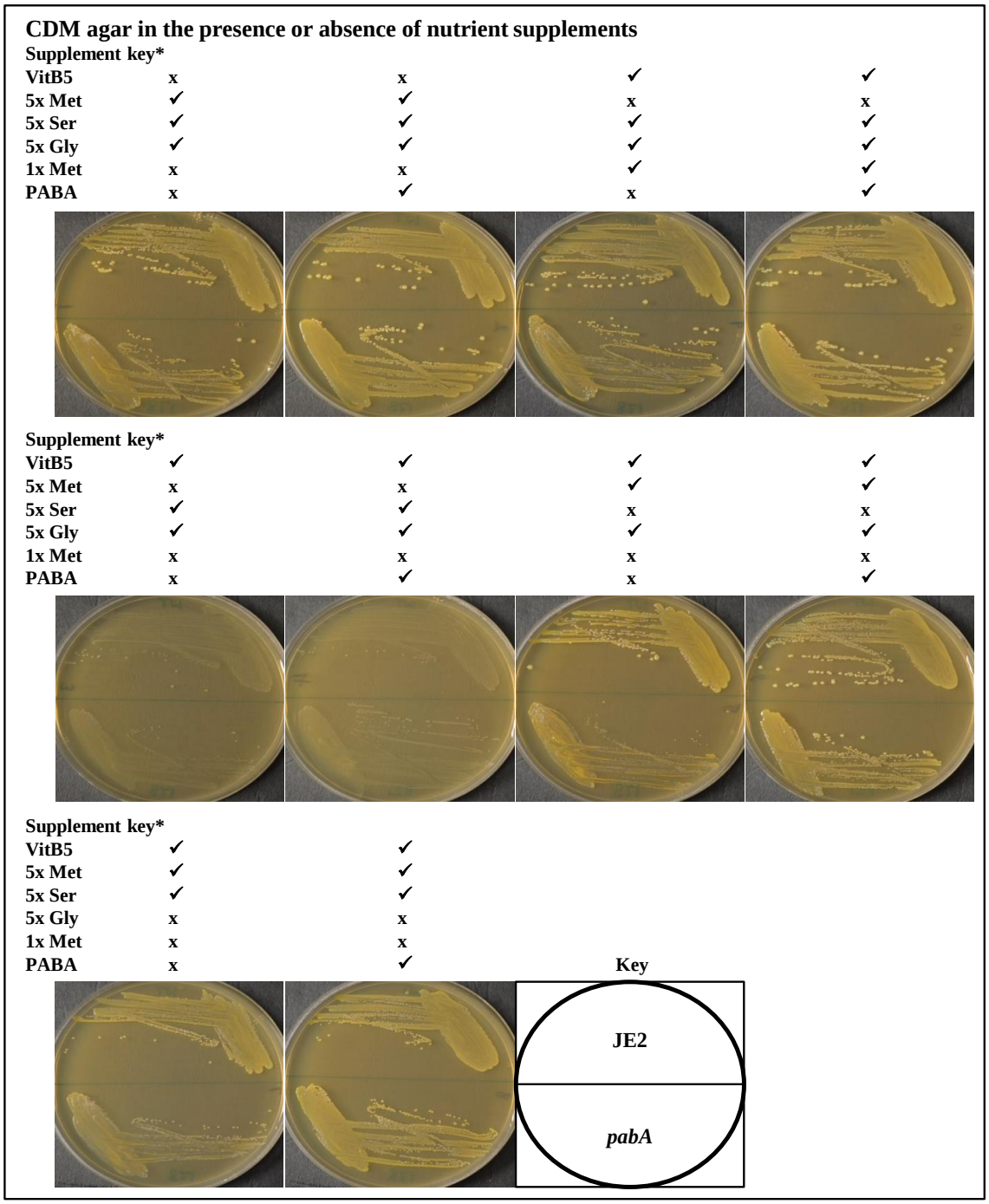

Figure 5.26 Role of glycine, serine, vitamin B_5 and methionine in the growth of JE2-*pabA* and JE2.

x indicates absence of supplement; ✓ indicates presence of supplement, corresponding to the supplement key.

Plates were incubated at 37^{o}C for 48 h.

* $VitB_5$ = 400 ng ml^{-1} vitamin B_5, 5x Met = 500 µg ml^{-1} methionine, 5x Ser = 500 µg ml^{-1} serine, 5x Gly = 500 µg ml^{-1} glycine, 1x Met = 100 µg ml^{-1} methionine.

Table 5.6 Analysis of the role of glycine, serine, vitamin B_5 and methionine in the growth of JE2-*pabA* and JE2.

Strain	Key*	Nutrient supplements									
	$VitB_5$	**x**	**x**	✓	✓	✓	✓	✓	✓	✓	✓
	5x Met	✓	✓	**x**	**x**	**x**	**x**	✓	✓	✓	✓
	5x Ser	✓	✓	✓	✓	✓	✓	**x**	**x**	✓	✓
	5x Gly	✓	✓	✓	✓	✓	✓	✓	✓	**x**	**x**
	1x Met	**x**	**x**	✓	✓	**x**	**x**	**x**	**x**	**x**	**x**
	PABA	**x**	✓	**x**	✓	**x**	✓	**x**	✓	**x**	✓
JE2		++++	++++	++++	++++	+	+	++++	+++	+++	+++
pabA		+++	++++	+++	++++	+	+	++	+++	++	+++

+ Very poor growth
++ Poor growth
+++ Slightly reduced growth
++++ Normal growth
✓ indicates addition of supplement, corresponding to the key
x indicates absence of supplement, corresponding to the key

* $VitB_5$ = 400 ng ml^{-1} vitamin B_5, 5x Met = 500 µg ml^{-1} methionine, 5x Ser = 500 µg ml^{-1} serine, 5x Gly = 500 µg ml^{-1} glycine, 1x Met = 100 µg ml^{-1} methionine.

5.2.8.9 The effect of methionine & thymine on JE2-*pabA* growth

S. aureus uses THF as a cofactor in the synthesis of the pyrimidine biosynthesis pathway intermediate deoxythymidine monophosphate (dTMP; Figure 5.1C) and in the synthesis of the amino acid methionine (Figure 5.1E). As CDM does not contain pyrimidines and the role of methionine in the JE2-*pabA* phenotype was not resolved in the previous experiment (Figure 5.26), their impact on JE2-*pabA* growth was investigated in CDM. To assess the effect of methionine on JE2-*pabA* growth, low levels of methionine were added to determine if JE2-*pabA* had a greater methionine requirement than JE2 (i.e. to determine if growth of JE2 was restored at a lower concentration to the *pabA* mutant). The nucleobase thymine was also used to determine if it could restore growth of JE2-*pabA* to that of JE2 (i.e. to see if the absence of pyrimidines was the missing factor in CDM). Figure 5.27 and Table 5.7 show that the requirement for methionine of both strains was equivalent. Furthermore, in the presence of thymine growth of JE2-*pabA* remained slightly reduced compared to JE2.

5.2.8.10 Role of serine, glycine, methionine & $VitB_5$ in SH-*pabA* pathogenicity

The role of serine, glycine, methionine and $VitB_5$ in the pathogenicity of SH-*pabA* was assessed using the zebrafish embryo model of systemic infection. Embryos were injected with ~1,500 CFU of SH1000 or SH-*pabA* and incubated in E3 solution +glycine, serine, methionine and $VitB_5$. Infected embryos incubated in E3 +PABA and E3 only were used as positive and negative controls, respectively. Experiments were repeated using 100 µg ml^{-1}, 1 mg ml^{-1} or 2 mg ml^{-1} of the amino acids, and 290 ng ml^{-1}, 2.9 µg ml^{-1} or 5.8 µg ml^{-1} $VitB_5$ (equivalent to 1x, 10x and 20x CDM concentrations; Figure 5.28), as higher levels may be required for complementation in the zebrafish model. SH-*pabA* was attenuated when embryos were incubated in E3. Addition of PABA to E3 restored virulence to SH-*pabA*. Addition of glycine, serine, methionine and $VitB_5$ to E3, at all concentrations tested, did not restore virulence to SH-*pabA*. It remains uncertain as to whether glycine, serine, methionine and $VitB_5$ have a role in SH-*pabA* pathogenicity, as the bacteria may not have access to the nutrients from within the embryos. The experiments did confirm that PABA can restore virulence of SH-*pabA* *in vivo*.

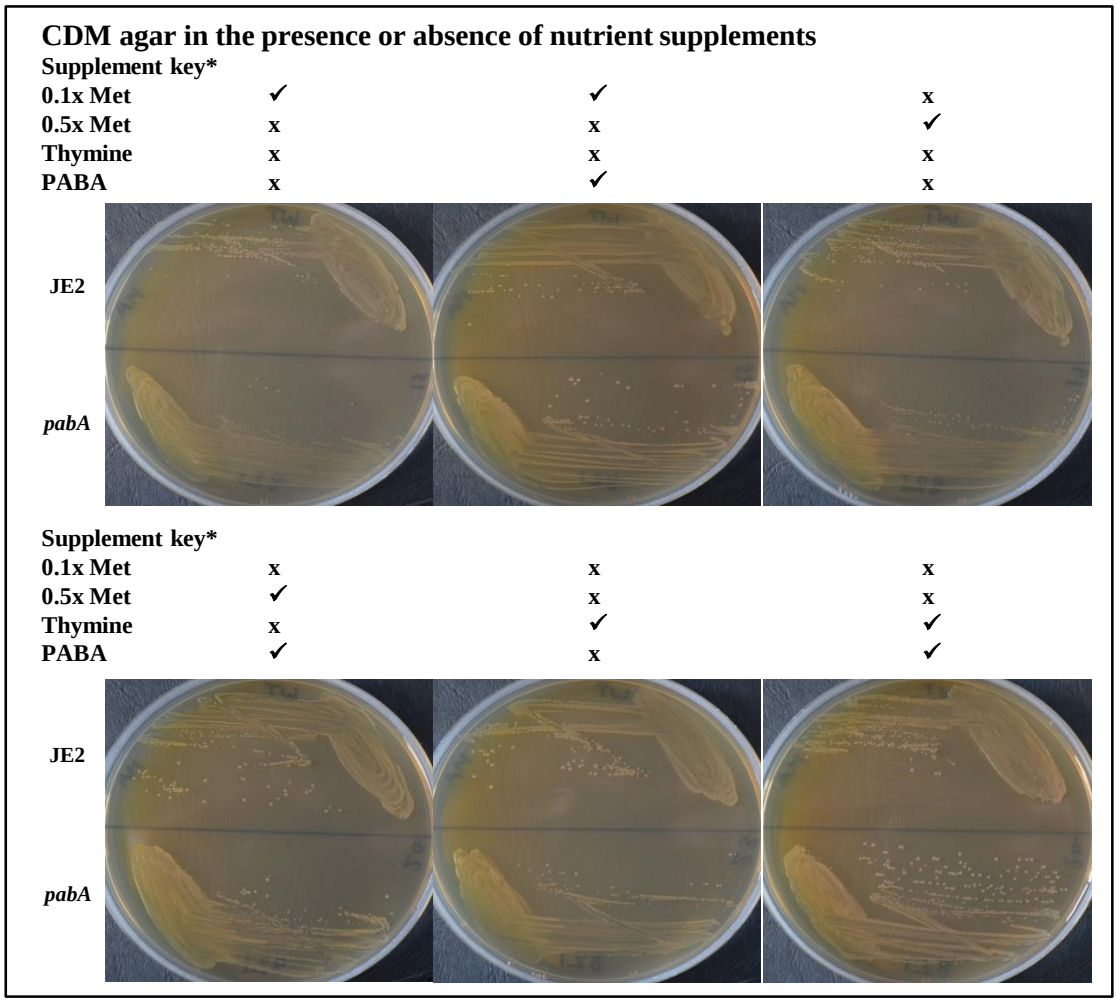

Figure 5.27 Role of methionine and thymine in the growth of JE2-*pabA* and JE2.

x indicates absence of supplement; ✓ indicates presence of supplement, corresponding to the supplement key.

Plates were incubated at 37^{o}C for 48 h.

* 0.1x Met = 10 µg ml^{-1} methionine, 0.5x Met = 50 µg ml^{-1} methionine, Thymine = 40 µg ml^{-1} thymine.

Table 5.7 Analysis of the role of methionine and thymine in the growth of JE2-*pabA* and JE2.

Strain	Key*	Nutrient supplements					
	0.1x Met	✓	✓	x	x	x	x
	0.5x Met	x	x	✓	✓	x	x
	Thymine	x	x	x	x	✓	✓
	PABA	x	✓	x	✓	x	✓
JE2		+	++	++	++	++++	++++
pabA		+	++	++	++	+++	++++

+ Very poor growth
++ Poor growth
+++ Slightly reduced growth
++++ Normal growth
✓ indicates addition of supplement, corresponding to the key
x indicates absence of supplement, corresponding to the key

* 0.1x Met = 10 µg ml^{-1} methionine, 0.5x Met = 50 µg ml^{-1} methionine, Thymine = 40 µg ml^{-1} thymine.

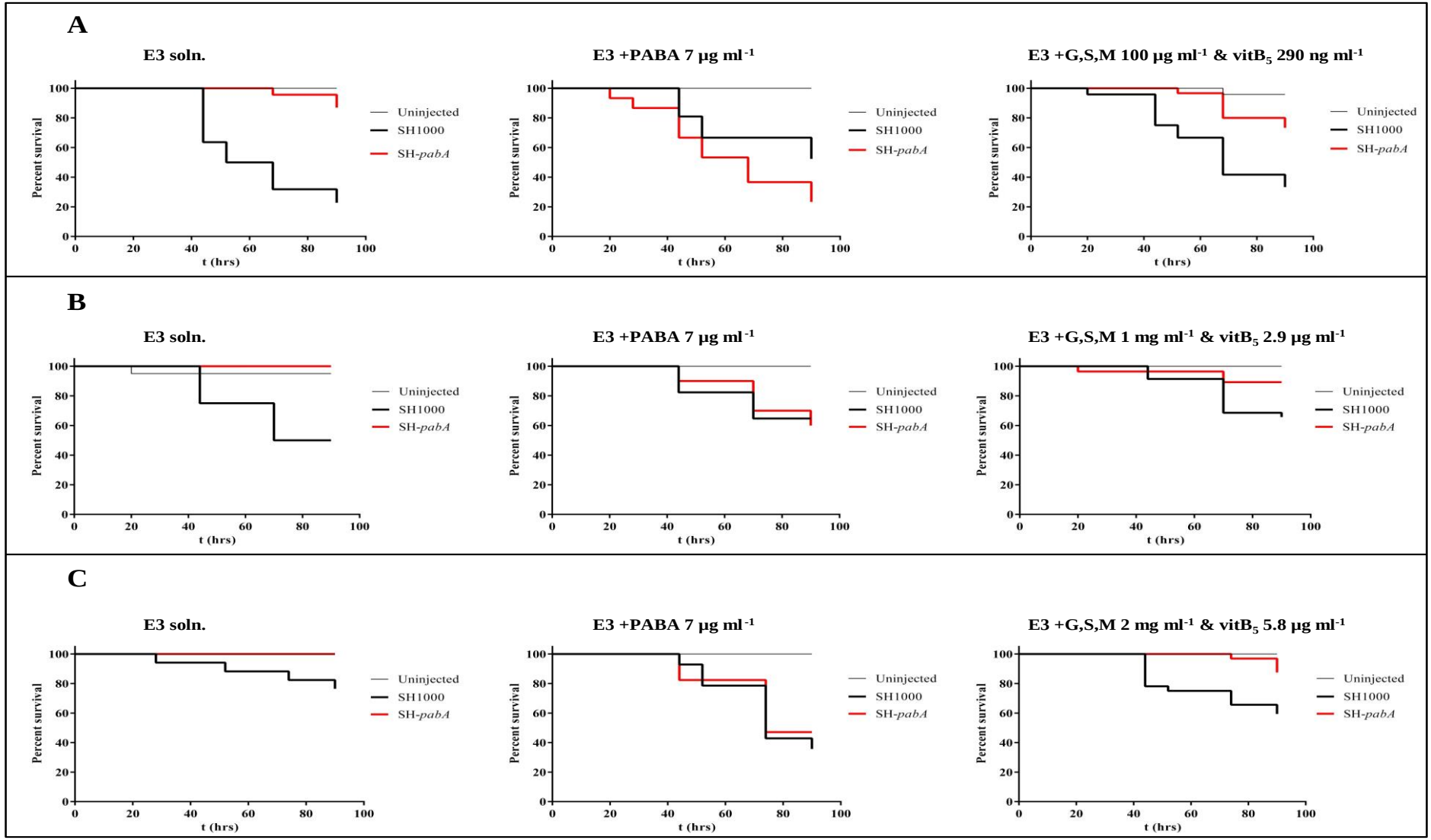
A
E3 soln.
E3 +PABA 7 µg ml-1
E3 +G,S,M 100 µg ml-1 & vitB5 290 ng ml-1
B
E3 soln.
E3 +PABA 7 µg ml-1
E3 +G,S,M 1 mg ml-1 & vitB5 2.9 µg ml-1
C
E3 soln.
E3 +PABA 7 µg ml-1
E3 +G,S,M 2 mg ml-1 & vitB5 5.8 µg ml-1
Percent survival
t (hrs)
Uninjected
SH1000
SH-pabA

Figure 5.28 Effect of addition of glycine, serine, methionine and vitamin B_5 on SH-*pabA* virulence.

Survival of zebrafish embryos was assessed upon injection of embryos with 1,500 CFU SH-*pabA* or SH1000 and incubation in E3 soln. plus 100 µg ml^{-1}, 1 mg ml^{-1} or 2 mg ml^{-1} of the amino acids, and 290 ng ml^{-1}, 2.9 µg ml^{-1} or 5.8 µg ml^{-1} $VitB_5$ (**A**, **B** and **C**, respectively). Incubation in E3 soln. and incubation in E3 soln. plus 7 µg ml^{-1} PABA were used as negative and positive controls respectively. Incubation in the presence of glycine, serine, methionine and $VitB_5$ did not restore SH-*pabA* virulence compared to the SH1000 control, $p < 0.0001$.

5.2.8.11 PABA complementation is associated with the *pab* operon

It is possible that addition of PABA improves the growth of SH-*pabA* in a way that is unrelated to the *pab* operon, allowing enough growth within embryos to restore killing. To confirm that the effect of PABA was associated with the *pab* operon, attempts were made to complement *S. aureus* NewHGΔ*pheP*Δ*saeR*, which is highly attenuated in the zebrafish embryo model of systemic infection (Figure 5.29). This strain remained highly attenuated in the presence of PABA.

5.2.9 Liquid CDM growth analysis of *pabA*

Analysis of the relative growth of JE2-*pabA* on CDM agar is subjective and subtle differences in growth are difficult to resolve. This difficulty was thought to explain slight variation in previous experiments, in which growth between JE2 and the *pabA* mutant is comparable on CDM with or without purines (Figure 5.19), or the *pabA* mutant shows slightly reduced growth compared with JE2 in CDM without purines (Figure 5.26). The results on CDM agar highlighted the possibility that the phenotype (particularly the phenotype on human blood) is not related to a nutrient deficiency on blood, but rather an inhibitory effect, as the differences seen between JE2-*pabA* and JE2 on CDM were slight, relative to the growth differences between the two strains on blood. However, phenotypic complementation by cross-feeding, caused by PABA diffusion, has been shown between pab^+ and pab^- strains on agar (Huang & Pittard, 1967), allowing the growth of *pabA* and *pabB* mutants of *E. coli* on minimal media agar. This effect may well have diminished any growth difference between strains on CDM agar. It was thought essential to first confirm or deny that a nutrient deficiency was the cause of the JE2-*pabA* phenotype.

A series of experiments were designed to determine if the results of the CDM agar analysis of the JE2-*pabA* phenotype remained the same in liquid CDM culture. All combinations of glycine, serine and $VitB_5$ were to be assessed in the presence of adenine and guanine (Table 5.8), after confirmation that purines are required for comparable growth of JE2-*pabA* to JE2.

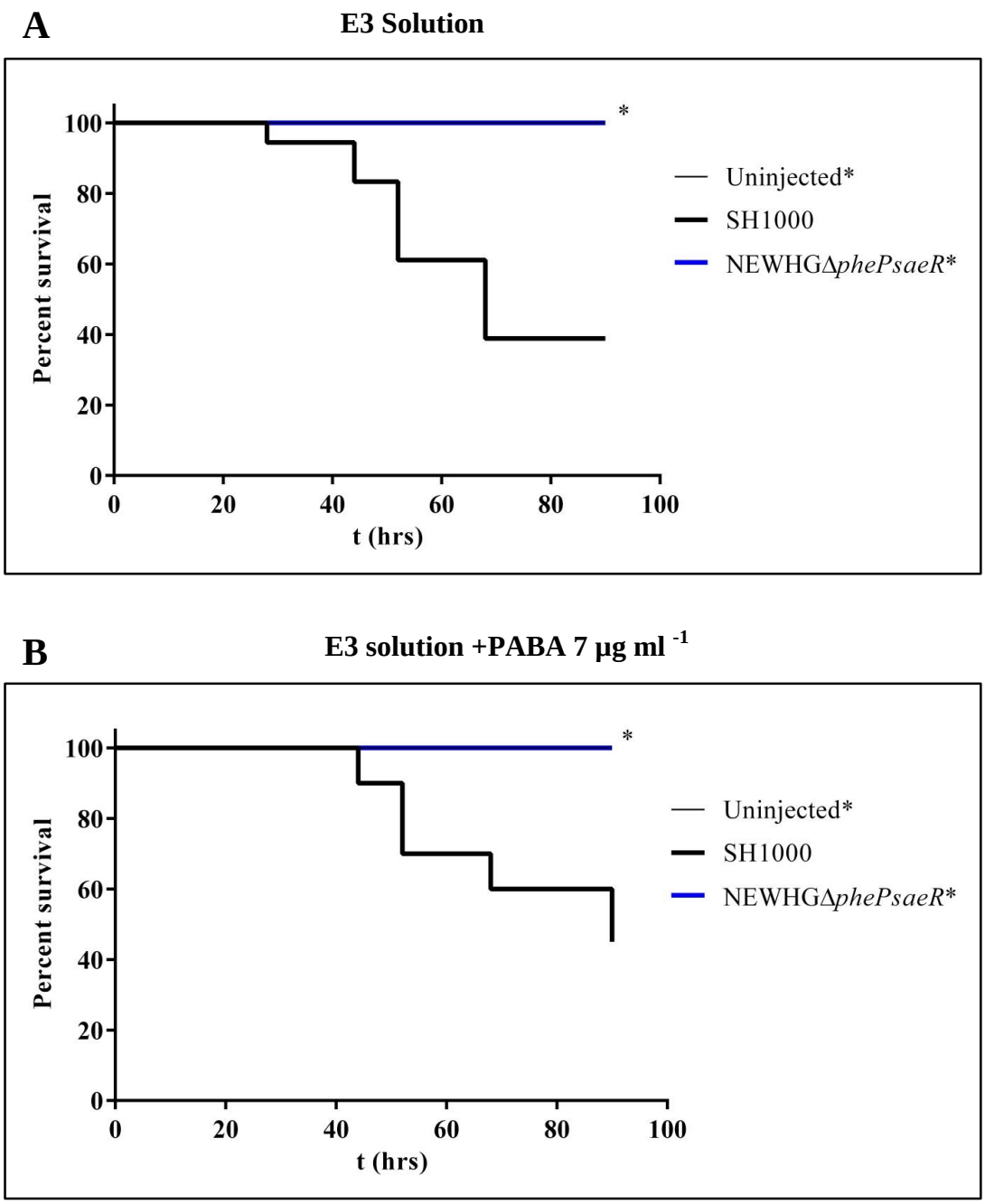

Figure 5.29 Effect of addition of PABA on NewHGΔ*phePΔsaeR* pathogenesis.

* Data points overlap.

A. *S. aureus* NewHGΔ*phePΔsaeR* is highly attenuated.

B. Addition of PABA does not complement *S. aureus* NewHGΔ*phePΔsaeR* and it remains highly attenuated.

Table 5.8 Experimental plan for the liquid CDM analysis of glycine, serine and $VitB_5$.

	Chemically Defined Media Plus Adenine & Guanine							
	Expt. 1	**Expt. 2**	**Expt. 3**	**Expt. 4**	**Expt. 5**	**Expt. 6**	**Expt. 7**	**Expt. 8**
$VitB_5$	x	✓	x	x	✓	✓	x	✓
Serine	x	x	✓	x	✓	x	✓	✓
Glycine	x	x	x	✓	x	✓	✓	✓

✓ indicates addition
x indicates absence

5.2.9.1 Are purines required for full growth of JE2-*pabA* in CDM?

To determine if purines were the missing components of CDM required by JE2-*pabA* for comparable growth to JE2, growth curves were carried out in CDM minus purines, CDM (i.e. with guanine and adenine added) and CDM plus inosine (Figure 5.30). For growth curve method and liquid CDM preparation see Chapter 2.8 and 2.1.4, respectively. In CDM minus purines the growth rate and maximum optical density at 600nm (OD_{600}) of JE2-*pabA* was reduced compared to JE2. Addition of purines restored the growth of JE2-*pabA* to that of JE2.

5.2.9.2 Liquid CDM growth experiments

To analyse growth of JE2-*pabA* in CDM with all combinations of purines, glycine, serine and $VitB_5$, would require growth in 15 different conditions for both strains, with and without PABA in triplicate. Therefore, it was decided to carry out a series of individual growth experiments to determine the role of glycine, serine and $VitB_5$ in CDM plus purines. The experiments would indicate whether glycine, serine or $VitB_5$ would complement the JE2-*pabA* phenotype. The analysis shows that serine and glycine are a requirement of JE2-*pabA* for comparable growth to JE2 and that $VitB_5$ has a negative impact on JE2-*pabA* growth (Figure 5.31). The full growth curve method is given in section 2.8.

Growth in CDM without glycine, serine and $VitB_5$ resulted in a 10 h lag phase for both strains (Figure 5.31A). The growth rate of JE2-*pabA* was reduced, but both strains reached a similar maximum OD_{600} of 3. Addition of $VitB_5$ did not reduce the 10 h lag phase and the growth rate of JE2-*pabA* remained less than that of JE2. Furthermore, the *pabA* mutant reached an OD_{600} of 1.76, whereas the maximum OD_{600} of JE2 was 3 (Figure 5.31B). This suggested that $VitB_5$ may be inhibitory to JE2-*pabA* growth rather than a requirement. Addition of glycine was beneficial to the growth of both strains; reducing the lag phase to 3-5 h and increasing their growth rate (Figure 5.31C). Furthermore, although the growth rate of JE2-*pabA* was still reduced in comparison to JE2, the time required for the *pabA* mutant to reach the same max OD_{600} of 4 was reduced when grown in the presence of glycine. This suggested that glycine may be a requirement for comparable growth of JE2-*pabA* to JE2. Addition of serine and $VitB_5$ restored the growth of JE2-*pabA* to a comparable level of growth to JE2 (Figure 5.31D).

A **CDM –Adenine & -Guanine**

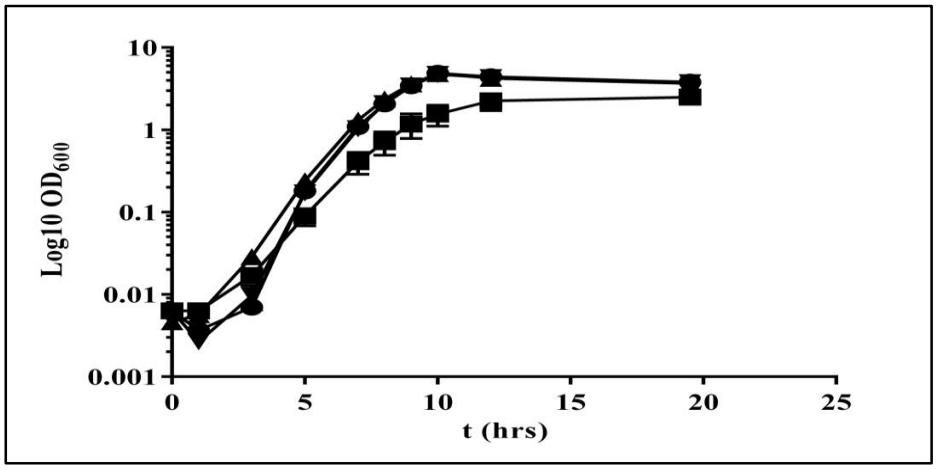

B **CDM +Adenine 20 µg ml $^{-1}$ & +Guanine 20 µg ml $^{-1}$**

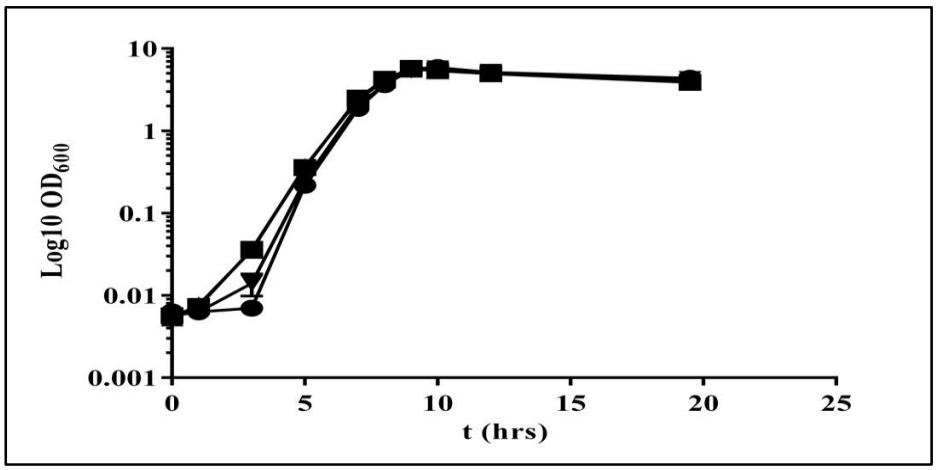

C **CDM –Adenine & -Guanine, +Inosine 20 µg ml $^{-1}$**

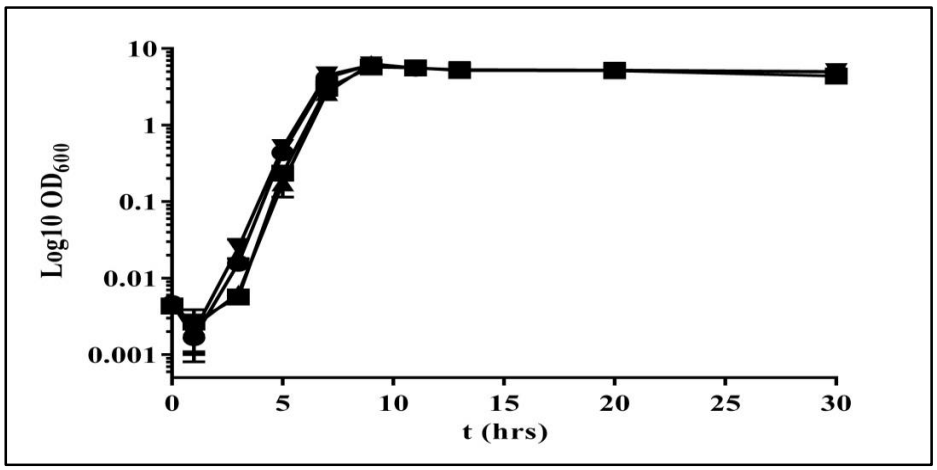

Figure 5.30 Importance of purines to JE2-*pabA* growth.

● = JE2, ■ = JE2-*pabA*, ▼ = JE2 +PABA, ▲ = JE2-*pabA*+PABA.

Purines are required by JE2-*pabA* to restore comparable growth to JE2.

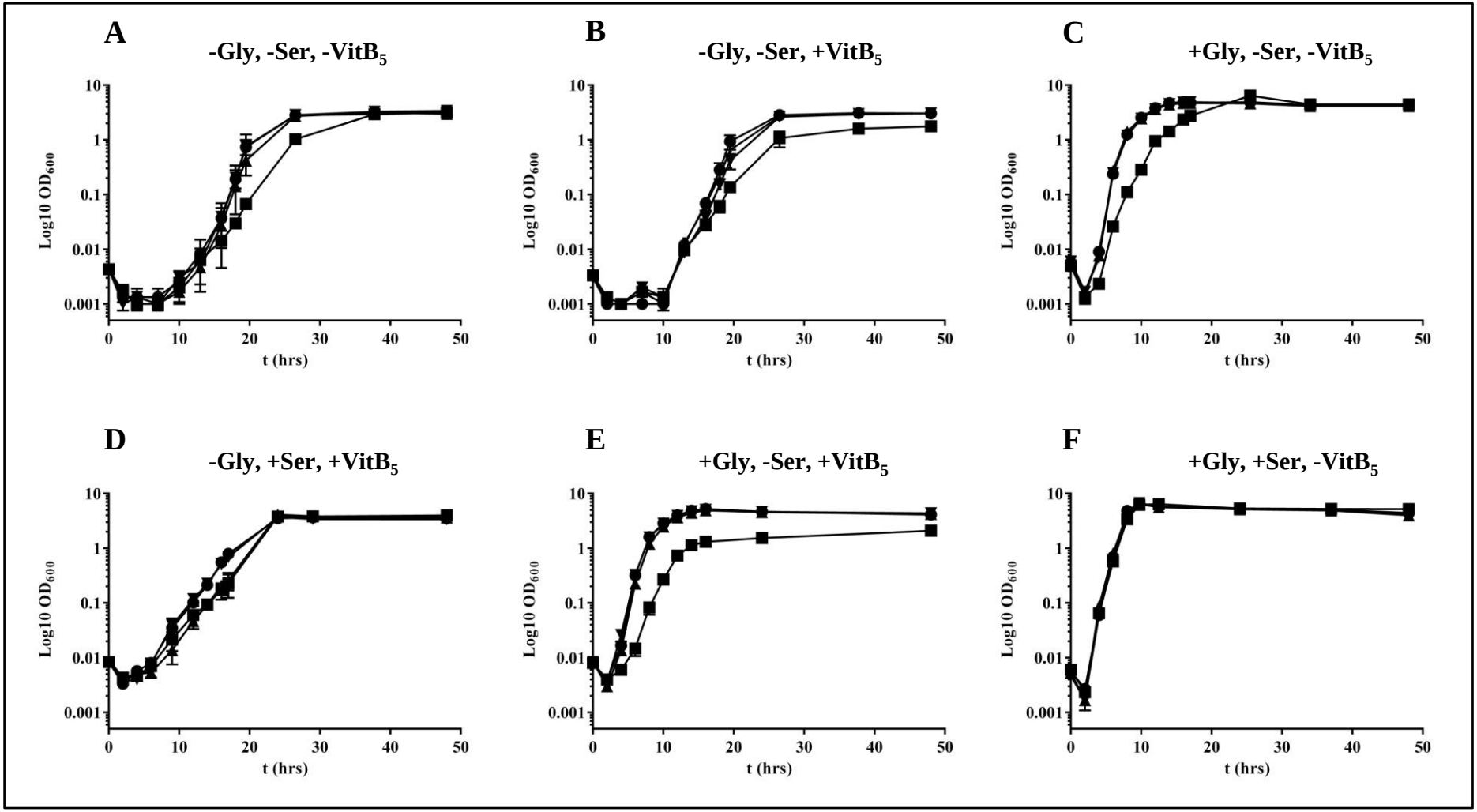

● = USA300 JE2, ■ = JE2-*pabA*, ▼ = USA300 JE2 +PABA, ▲ = JE2-*pabA*+PABA.

Figure 5.31 Liquid CDM analysis of JE2-*pabA* growth.

A. CDM minus serine, glycine and $VitB_5$

B. CDM minus serine and glycine

C. CDM minus serine and $VitB_5$

D. CDM minus glycine

E. CDM minus serine

F. CDM minus $VitB_5$

However, when glycine and $VitB_5$ were added to CDM the $VitB_5$ appeared to have a negative effect on JE2-*pabA* growth compared to when just glycine was added (Figure5.31E & Figure 5.31C, respectively). This again suggested a negative effect of $VitB_5$ on the growth of JE2-*pabA*. Addition of glycine and serine in the absence of $VitB_5$ gave comparable growth of JE2-*pabA* to JE2 (Figure 5.31F).

5.2.9.3 Analysis of the relative importance of serine, glycine and purines to JE2-*pabA* growth

Two experiments were carried out to determine the relative importance of glycine, serine and purines to the growth of JE2-*pabA*. In both experiments, JE2 and the *pabA* mutant were grown in base CDM (CDM minus purines, glycine and serine) in the presence or absence of PABA ($VitB_5$ was no longer used in CDM preparations, due to its potentially negative impact on JE2-*pabA*). In experiment 1 growth was assessed in base CDM and base CDM plus glycine, serine or purines (Figure 5.32 A-D). In experiment 2 growth of both strains was assessed in base CDM plus all two or more member combinations of glycine, serine and purines (Figure 5.32 E-H).

In experiment 1, no improvement in growth of JE2-*pabA* could be seen relative to JE2. Growth was improved for both strains by serine or glycine addition to base CDM, but the relative difference in growth remained the same (Figure 5.32 C & D).

In experiment 2, the addition of two of the additives in any combination did not improve the growth rate of JE2-*pabA* relative to JE2, but the same max OD_{600} was reached (Figure 5.32E, F, G). The growth rate of JE2-*pabA* was improved relative to JE2 only in the presence of purines, glycine and serine. However, the growth rate of JE2-*pabA* was still not fully restored.

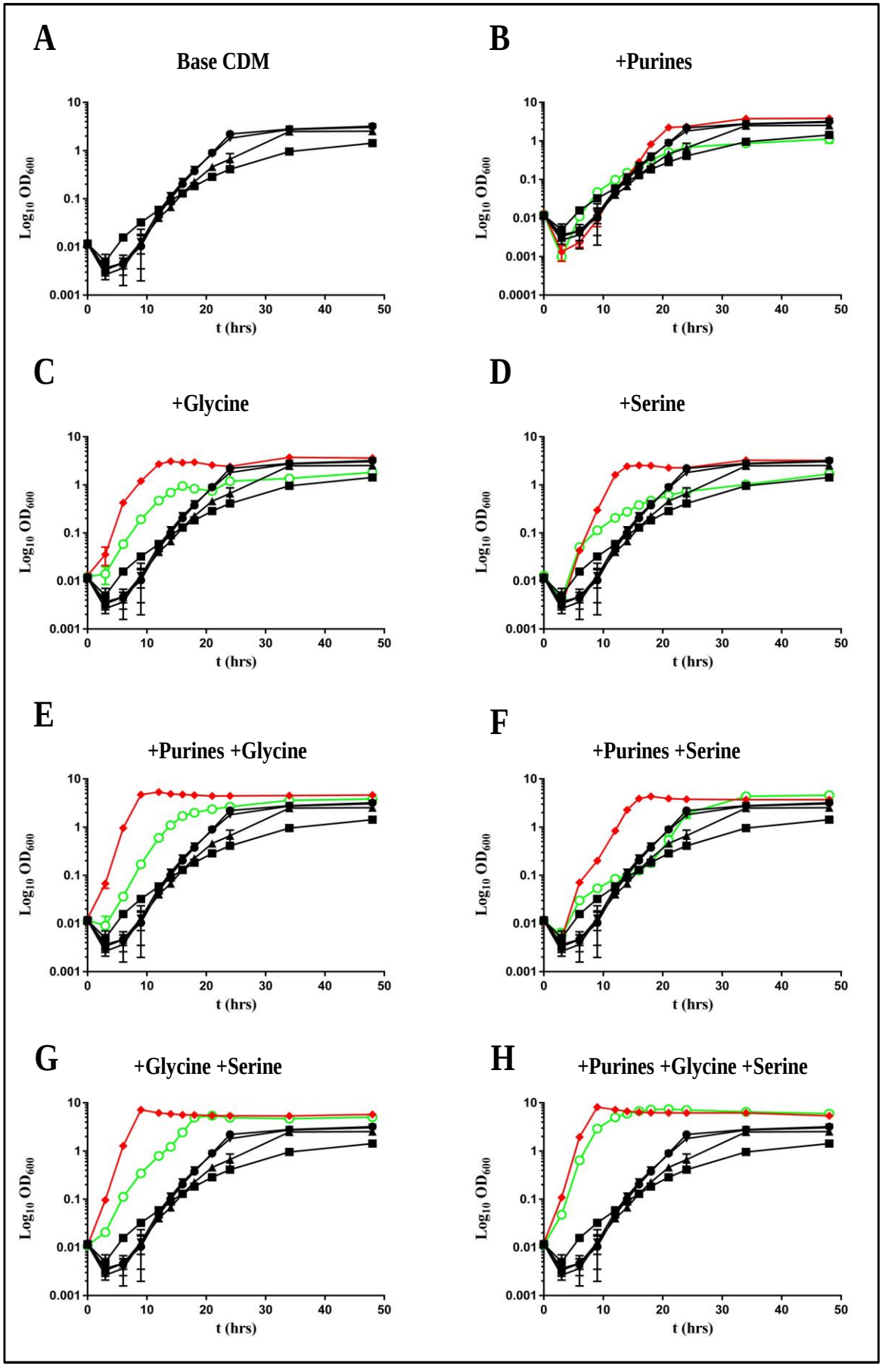
A
Base CDM
B
+Purines
C
+Glycine
D
+Serine
E
+Purines +Glycine
F
+Purines +Serine
G
+Glycine +Serine
H
+Purines +Glycine +Serine
Log10 OD600
t (hrs)

Figure 5.32 Analysis of the JE2-*pabA* phenotype in liquid CDM.

● = JE2, ■ = JE2-*pabA*, ▼ = JE2 +PABA, ▲ = JE2-*pabA*+PABA, ♦ = JE2 +additive labelled above graph, ○ = JE2-*pabA* +additive labelled above graph.

Growth of JE2-*pabA* was compared with JE2 in CDM base with all combinations of glycine, serine and purines. Addition of all 3 components to the CDM base restored the growth of JE2-*pabA* to a comparable level to JE2.

5.2.9.4 Analysis of trimethoprim activity in the presence of $VitB_5$

Trimethoprim (TMP) is an antifolate antimicrobial that inhibits DHFR, the enzyme that converts DHF to THF downstream of PABA synthesis (Proctor, 2008). It was thought that addition of TMP to JE2 would lead to JE2-*pabA*-like growth of the wild-type, due to loss of THF. Therefore, as $VitB_5$ appeared to inhibit the growth of JE2-*pabA* it was hypothesised that TMP activity would be enhanced in the presence of $VitB_5$ as JE2 would be inhibited by both TMP and the *pabA* phenotype associated impact of $VitB_5$ on growth.

TMP MIC experiments were carried out from 1000 - 0 µg ml^{-1}, as in Chapter 2.17, in base CDM, which did not contain purines, glycine, serine or $VitB_5$. The MIC experiment was repeated using 290ng ml^{-1} $VitB_5$, 580 ng ml^{-1} $VitB_5$ and 1.45 µg ml^{-1} $VitB_5$ (equivalent to 1x, 2x and 5x CDM concentrations, respectively). A baseline growth was determined, by growth of JE2 alongside MIC experiments in the absence of TMP. Increase in JE2 OD_{600} was determined as TMP levels were decreased. This increase was compared for MIC experiments with or without $VitB_5$. The presence of higher levels of $VitB_5$ did not alter the recovery of JE2 to the baseline OD_{600} as the TMP concentration was reduced (Figure 5.33). This suggested that $VitB_5$ has no impact on TMP activity against JE2.

290 ng ml $^{-1}$ VitB$_5$

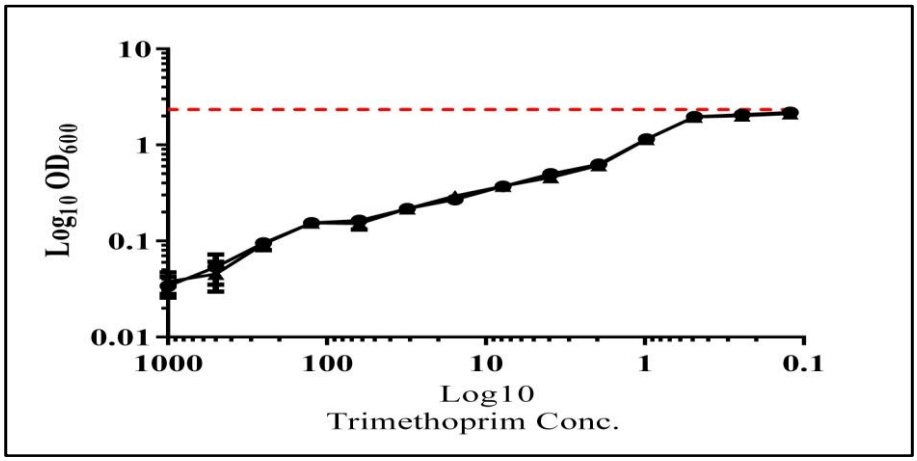

580 ng ml $^{-1}$ VitB$_5$

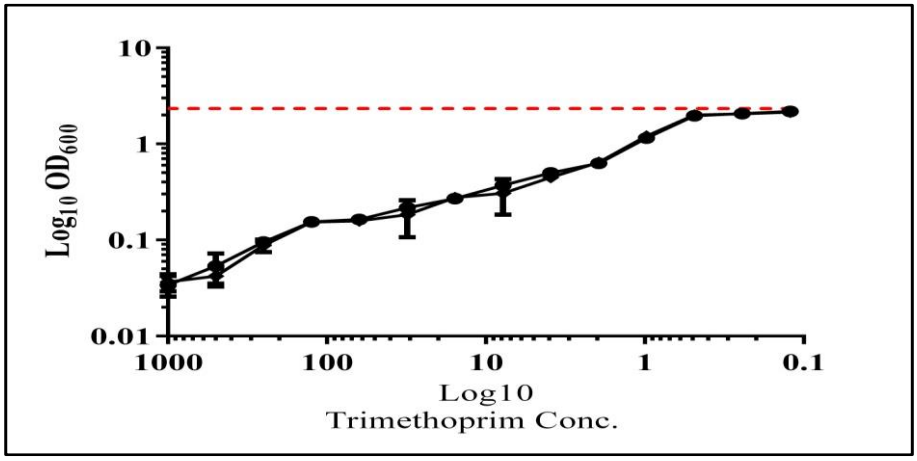

1.45 µg ml $^{-1}$ VitB$_5$

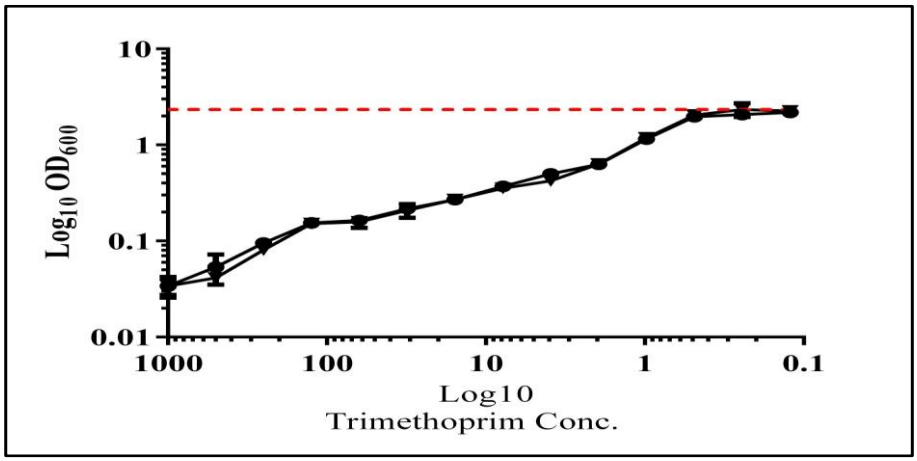

Figure 5.33 Analysis of the effect of VitB$_5$ concentration on trimethoprim activity.

Dashed red line indicates baseline growth without TMP. ● = MIC in base CDM. ▼ = MIC in base CDM +VitB$_5$. Addition of VitB$_5$ at any concentration tested had no effect on the growth of JE2 exposed to TMP.

5.2.10 Effect of inosine on SH-*pabA* *in vivo*

An unsuccessful attempt was made above to restore virulence to SH-*pabA* using serine, glycine, methionine and $VitB_5$ in the zebrafish embryo model of systemic infection (Figure 5.28). The liquid CDM analysis showed that purines are a growth requirement of JE2-*pabA*. Therefore, the zebrafish embryo assay was used with the addition of inosine (Figure 5.34). Two concentrations of inosine were used, 150 µg ml^{-1} and 1 mg ml^{-1} (Figure 5.34 A & B respectively). SH-*pabA* remained attenuated at both concentrations compared to SH1000, $p < 0.0001$.

5.2.11 Role of *pabA* in growth on human blood

5.2.11.1 Analysis of JE2-*pabA* growth on human blood plus purines, glycine or serine

A conclusion of the CDM experiments was that glycine, serine and purines were required in combination to enhance the growth of JE2-*pabA* to that of JE2. To confirm that a lack of purines, glycine and serine was the cause of the JE2-*pabA* phenotype, their effects on the growth of the *pabA* mutant was compared to JE2 on 30% (v/v) human blood agar (Figure 5.35). Neither purines, nor serine nor glycine restored the growth of JE2-*pabA* on human blood agar in any combination. Addition of 50 µg ml^{-1} PABA did restore the growth of the *pabA* mutant. Additionally chocolate agar was made by heating human blood to 70^{o}C or 80^{o}C. Lysis and release of nutrients caused by heating did not restore comparable growth of JE2-*pabA* to JE2.

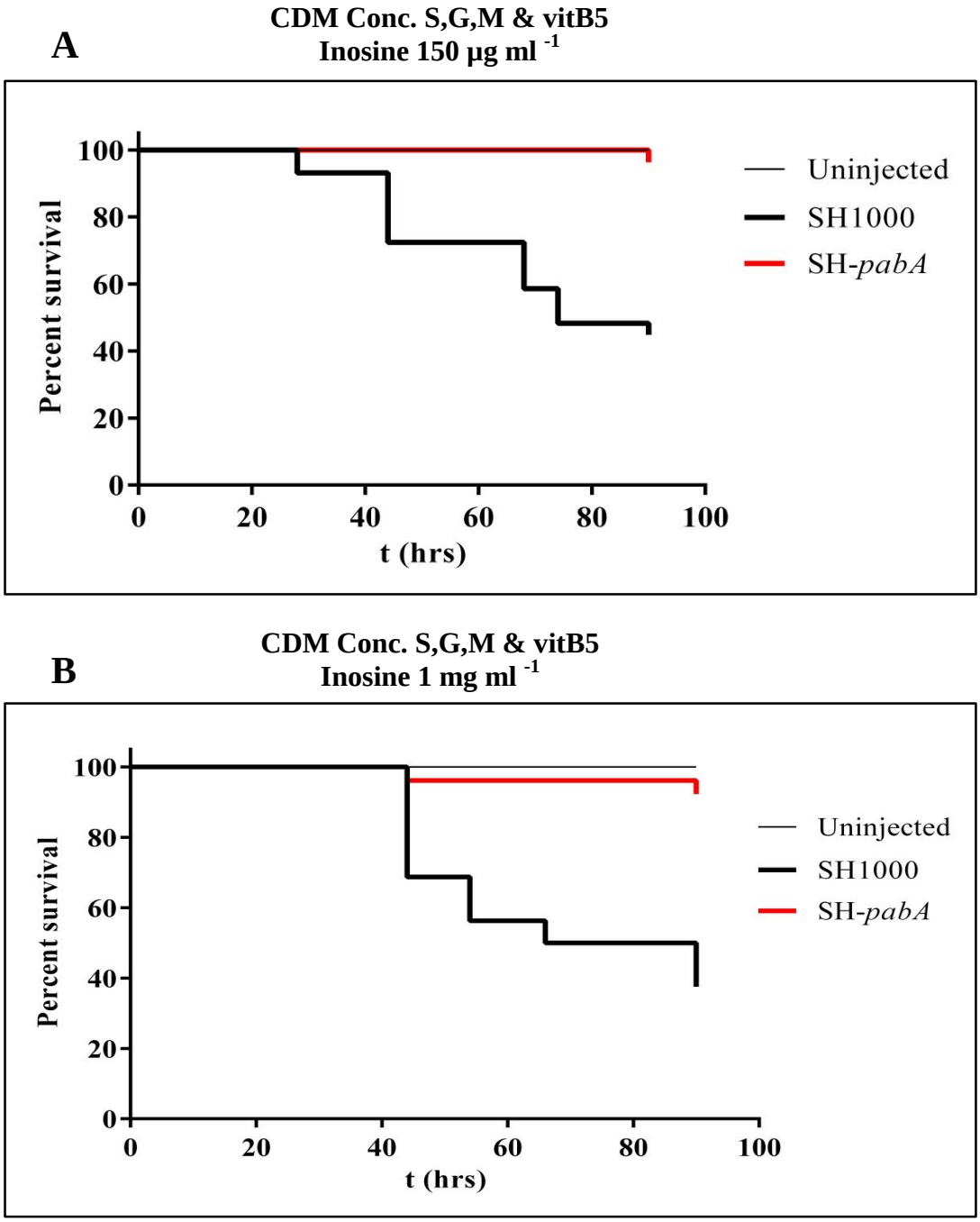

Figure 5.34 Effect of inosine on SH-*pabA* virulence.

A. 150 µg ml^{-1} inosine with 1x CDM concentration of serine, glycine, methionine and $VitB_5$ did not restore SH-*pabA* pathogenicity, $p < 0.0001$.

B. 1 mg ml^{-1} inosine with 1x CDM concentration of serine, glycine, methionine and $VitB_5$ did not restore SH-*pabA* pathogenicity, $p < 0.0001$.

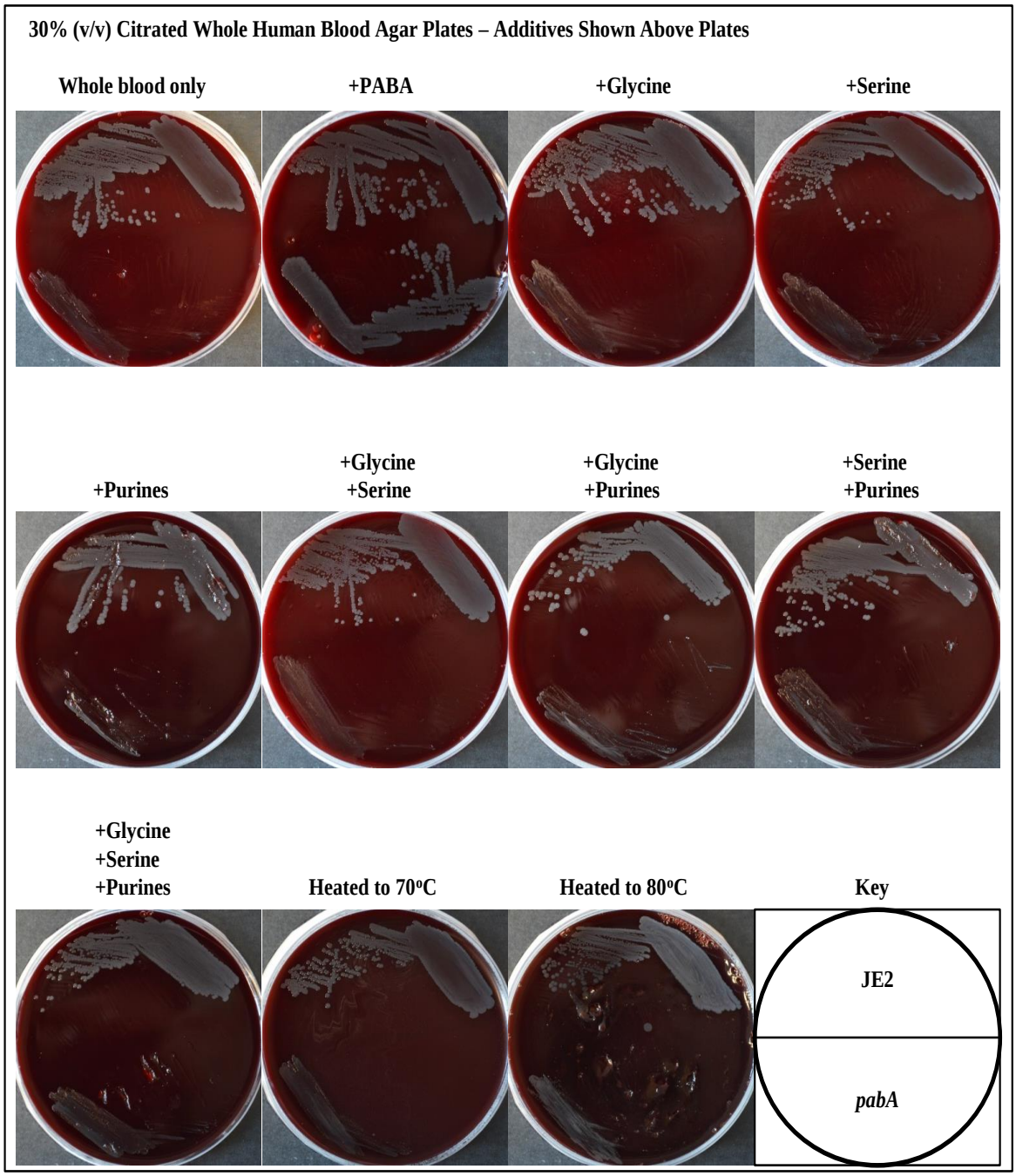

Figure 5.35 Analysis of the growth of JE2-*pabA* on human blood with various supplements.

30% (v/v) human blood agar was supplemented with all combinations of glycine, serine and purines to determine their role in JE2-*pabA* growth. 30% (v/v) human blood agar was also heated to release nutrients and PABA was added as a positive control.
Plates were incubated at 37^{o}C for 48 h.

5.2.11.2 Analysis of JE2-*pabA* growth on human blood plus methionine, $VitB_5$ or thymine

To confirm that the JE2-*pabA* phenotype was not the result of a lack of any of the CDM components assessed above, the effect of addition of methionine, $VitB_5$ and thymine was assessed on 30% (v/v) human blood agar (Figure 5.36). Neither methionine nor $VitB_5$ restored the growth of JE2-*pabA*. However, thymine at a concentration equivalent to that of purines in CDM (40 µg ml^{-1}) did partially restore JE2-*pabA* growth on human blood. This suggested that increased pyrimidine synthesis may be required on blood, or that thymine is an antagonist of a factor that is inhibitory to the *pabA* mutant in human blood.

5.2.12 Is the JE2-*pabA* phenotype on human blood the result of inhibition?

Plasma extracted from RBC disrupted blood was used to assess inhibition of JE2-*pabA*. Blood from the same donation was pooled and separated into 2 aliquots. One aliquot was vortexed hard for 3min then plasma was extracted from both blood aliquots (for the plasma preparation method see Chapter 2.1.3.1.2). Figure 5.37A shows straw coloured plasma from non-vortexed blood on the left (NV plasma), and red coloured plasma from vortexed blood on the right (V plasma). The red colouration demonstrated lysis of RBCs. Plasma agar was prepared using NV and V plasma as shown in Table 5.9. Growth of JE2-*pabA* and JE2 was compared on each plasma agar ratio (Figure 5.37B). Growth of JE2-*pabA* was comparable to JE2 on 50% (v/v) NV plasma. Addition of just 5% (v/v) V plasma resulted in highly reduced growth of the JE2-*pabA* mutant compared to JE2. This suggested that the JE2-*pabA* phenotype was the result of growth inhibition by an unidentified component of blood.

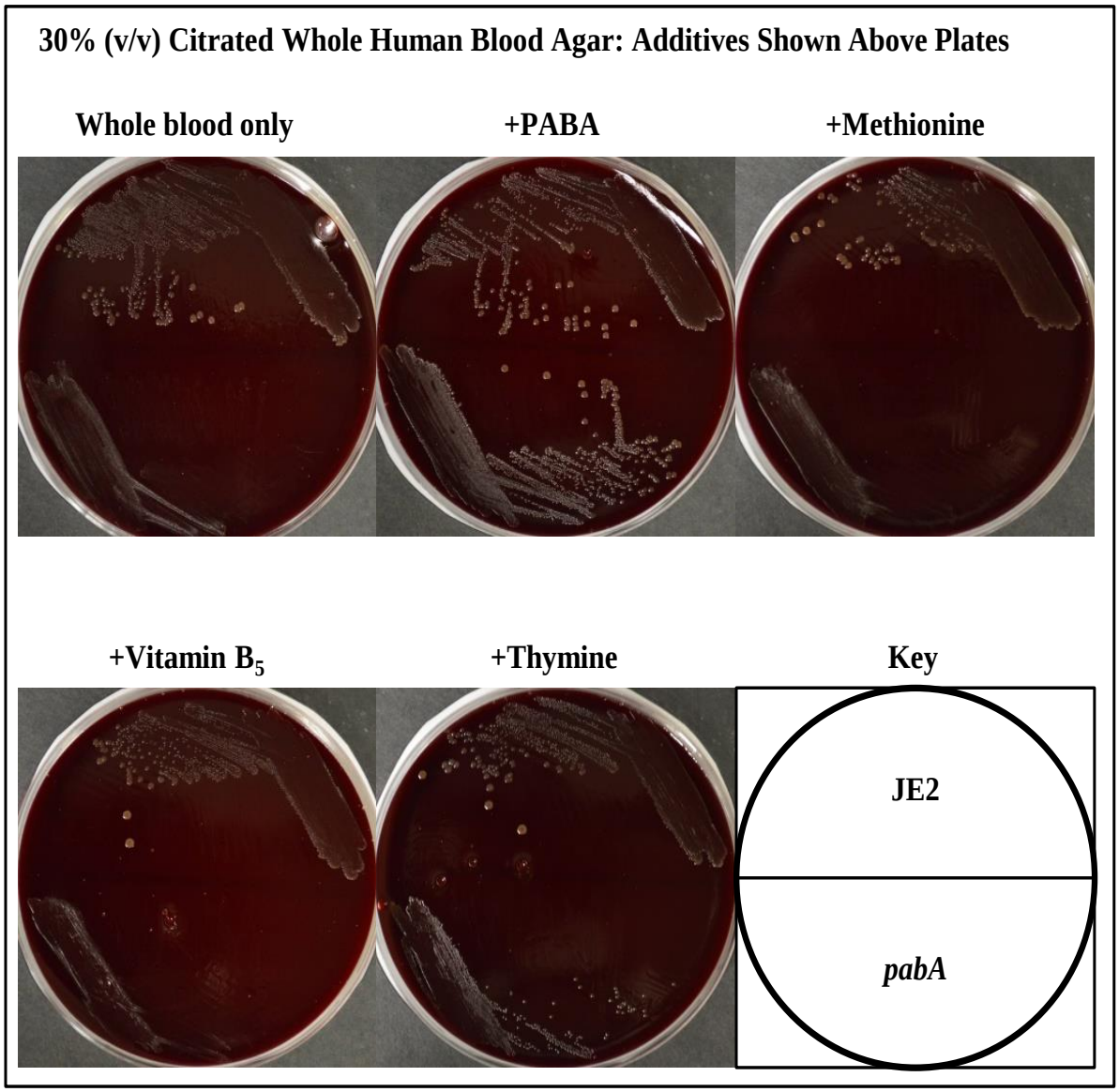

Figure 5.36 Analysis of methionine, VitB_5 and thymine on JE2-*pabA* growth on human blood.

Neither methionine nor VitB_5 complemented JE2-*pabA* on human blood. 40 µg ml^{-1} thymine (equivalent to the total purine concentration in CDM) partially complemented JE2-*pabA* growth. Plates were incubated at 37^{o}C for 48 h.

Table 5.9 Composition of vortexed and non-vortexed plasma agar plates (by volume).

Non-vortexed (NV) Plasma (%)	Vortexed (V) Plasma (%)	2x Agar (%)
50	0	50
45	5	50
37.5	12.5	50
25	25	50
12.5	37.5	50
5	45	50
0	50	50

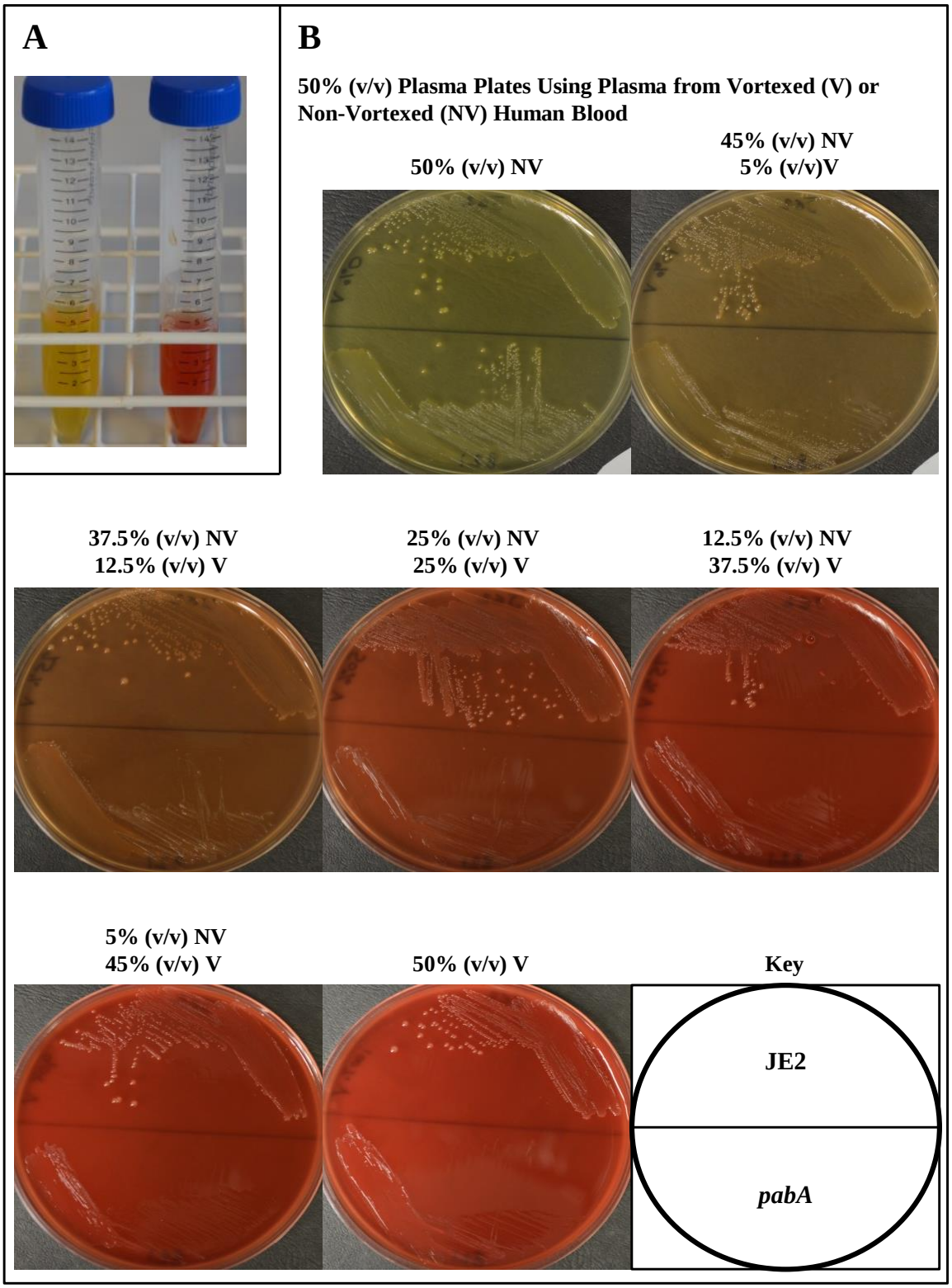

Figure 5.37 Inhibition of JE2-*pabA* by plasma from vortexed blood.

A. Straw coloured plasma from non-vortexed (NV) blood shown in the left tube. Red plasma from vortexed (V) blood shown in the right tube.

B. Growth of JE2-*pabA* was comparable to JE2 on 50% (v/v) NV plasma, but increasing the ratio of V to NV plasma immediately inhibited JE2-*pabA* growth.

Plates were incubated at 37^{o}C for 48 h.

5.2.13 Genetic complementation of the *pab* operon

5.2.13.1 Construction of the lipase integration plasmid pJC002

The pGM073 plasmid was constructed by Gareth McVicker by insertion of the *ezrA* and *PSmOrange* genes into the pKasbar plasmid. Lysogenic bacteriophage DNA integrates into the *S. aureus* genome via its *attP* site and the bacterial genome encoded *attB* site, mediated by the integrase enzyme. In *S. aureus* the *attB* recognition site is located at the gene for glycerol ester hydrolase (*geh*) and incorporation of phage DNA leads to loss of lipase activity (Lee & Iandolo, 1986). The pGM073 plasmid encodes an *attP* site, allowing integration of the plasmid at lipase in the presence of integrase. Primers pab-F and pab-R were designed to amplify the *pab* operon and up and downstream control elements (for all primers and primer design method see Chapter 2.12.1.1). The primers were designed with an ApaI restriction site in the pab-F primer and an XhoI site in the pab-R primer. Primers and plasmid were cut with ApaI and XhoI and ligated (Chapter 2.12.2 and Chapter 2.12.4, respectively). Cutting the plasmid with these enzymes removes the *ezrA* and *PSmOrange* genes. Ligation gives the plasmid pJC002, the pKasbar plasmid with the *pab* operon inserted (Figure 5.38A). The plasmid construct was then used to transform *Escherichia coli* strain Top10 (see Chapter 2.9.1.2 for transformation method). Successful construction was confirmed by purification of the plasmid from *E. coli* and digestion with ApaI and XhoI and analysis by 1% (w/v) electrophoresis. Bands corresponding in size to the plasmid and insert are indicated (Figure 5.38B). Plasmid DNA was sequenced by GATC Biotech, using primers pab1F, pab1R & pab2F, pab2R & pab3F, pab3R & pab4F, pab4R, to confirm that the correct sequence of the *pab* operon was inserted (for sequence data see Appendix 5.1).

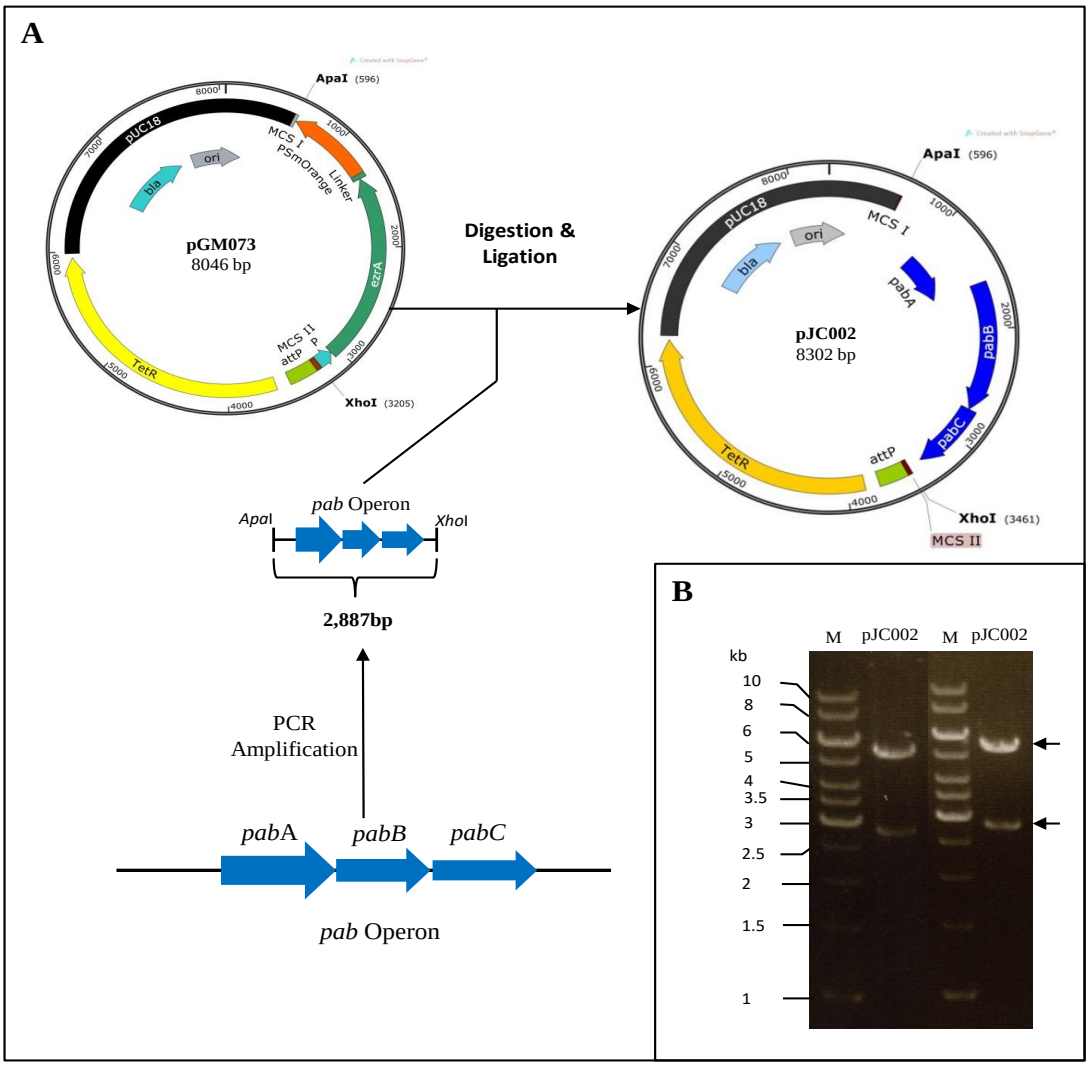

Figure 5.38 Construction of the complementation plasmid pJC002.

A. The *pab* operon with up and downstream control elements was amplified using primers with ApaI and XhoI restriction sites designed into them, giving a PCR product of 2,887bp. The pGM073 and amplified *pab* operon were then digested with ApaI and XhoI and purified. Digestion of the plasmid removes the *PSmOrange* and *ezrA* genes, reducing the plasmid size to 5,437bp. The *pab* operon was then ligated into the digested pGM073 plasmid to give pJC002.

B. DNA fragments were separated by 1% (w/v) agarose gel electrophoresis. Standards (M) of sizes shown are in each panel.

5.2.13.2 Integration of pJC002 into *S. aureus* RN4220

Integration of pJC002 into RN4220 is shown diagrammatically in Figure 5.39. The pJC002 was transformed into *S. aureus* RN4220 containing the pYL112Δ19 plasmid (Chapter 2.9.2.2). This plasmid encodes the integrase enzyme required for site-specific integration at *geh*. Integration of the pJC002 plasmid into *geh* results in loss of lipase activity. Lipase activity was compared with RN4220 to confirm insertion of pJC002 (Figure 5.40A). The pJC002 plasmid was transferred from the RN4220 genome to JE2-*pabA*, SH-*pabA*, JE2 and SH1000 by bacteriophage transduction (Chapter 2.10.3), allowing integration into the genome by homologous recombination. The pKasbar backbone was also transduced into JE2-*pabA*, SH-*pabA*, JE2 and SH1000 to give control strains for the integration of DNA at *geh*. PCR was carried out to confirm the successful integration of pJC002 or pKasbar into JE2-*pabA*, SH-*pabA* and the wild-type strains. Three sets of primers were used to determine correct insertion: NE821F and NE821R, which amplify the NE821 Tn insertion site, giving a fragment of the *pabA* gene from wild-type DNA, or the full Tn from *pabA* mutant DNA; pGM-F and pab1R, which amplify within pJC002 from outside the insertion site, to within the *pab* operon, confirming insertion of the pJC002 plasmid and pGM-F and pGM-R, which amplify within pKasbar from either side of the *pab* operon insertion site to confirm the integration of pKasbar and not pJC002 (primer sequences given in Chapter 2.12.1.1). Amplification products of expected sizes were found for all genetically complemented strains (Figure 5.40B).

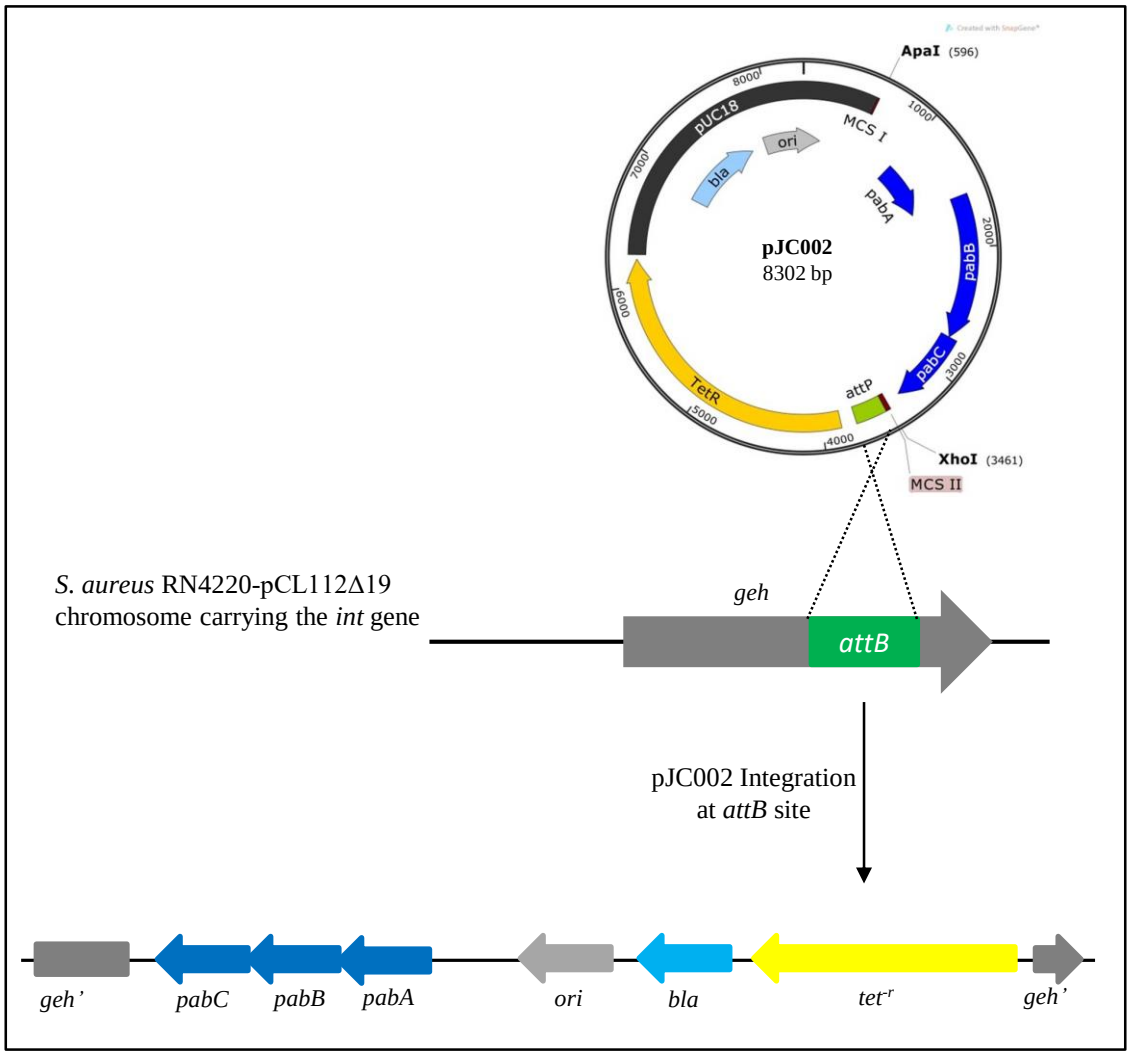

Figure 5.39 Site specific integration of pJC002 at the *geh* gene of *S. aureus* RN4220.

The pJC002 plasmid was transformed into RN4220 carrying the integrase gene within a separate plasmid. The integrase mediates site specific recombination between the plasmid encoded *attP* site and the *attB* site within the *geh* gene of RN4220. This leads to integration of the entire plasmid into *geh*, disrupting lipase activity.

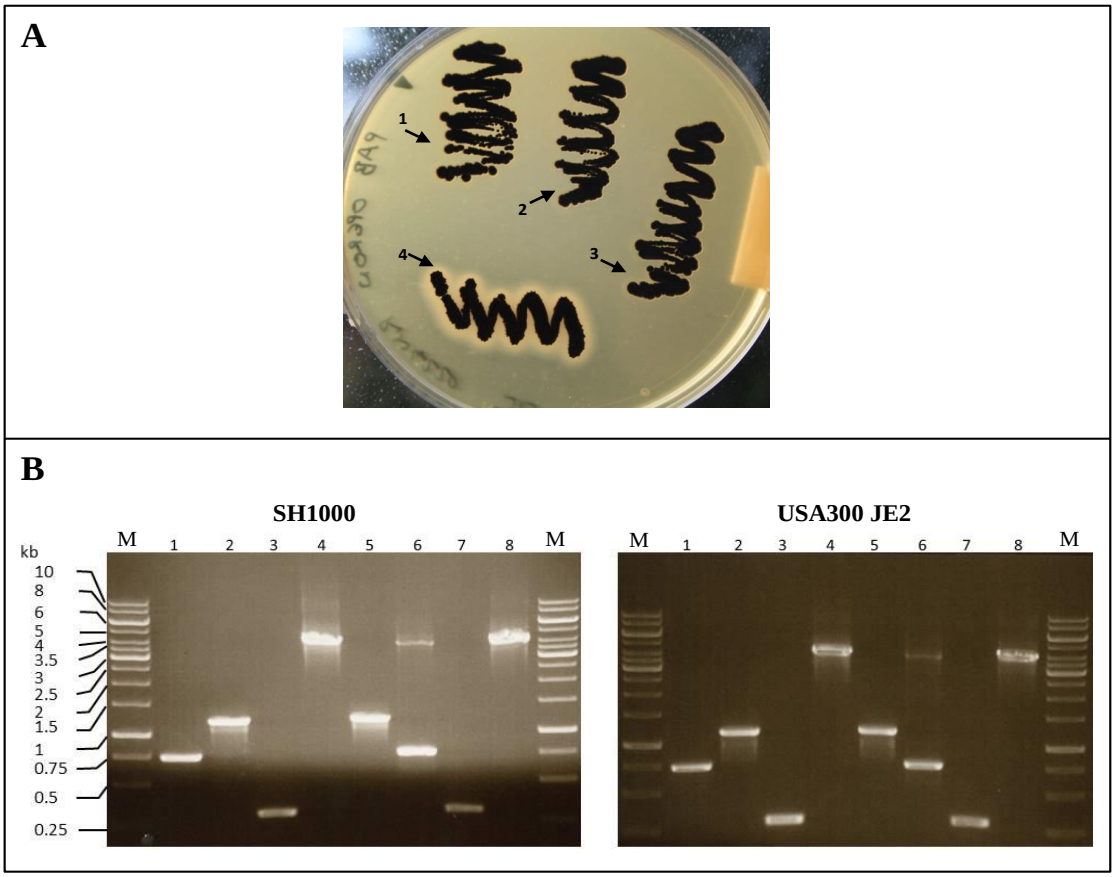

Figure 5.40 Confirming pJC002 integration into RN4220 by analysis of *geh* activity and confirmation of pJC002 & pKasbar transduction into the wild-type strains, SH-*pabA* and JE2-*pabA* by PCR.

A. Arrows 1, 2 and 3 show loss of lipase activity from RN4220, due to disruption of *geh* caused by integration of pJC002. Arrow 4 shows RN4220 lipase activity.
B. DNA fragments were separated by 1% (w/v) agarose gel electrophoresis. Standards (M) of sizes shown are in each panel.

PCR confirmation of pJC002 or pKasbar integration into JE2-*pabA*, SH-*pabA*, JE2 and SH1000. All bands are of expected sizes.
Lane 1: SH1000 or JE2 gDNA amplified with NE821F and NE821R.
Lane 2: SH1000+pJC002 or JE2+pJC002 gDNA amplified with pGM-F and pab1R.
Lane 3: SH1000+pKasbar or JE2+pKasbar gDNA amplified with pGM-F and pGM-R.
Lane 4: SH-*pabA* or JE2-*pabA* gDNA amplified with NE821F and NE821R.
Lane 5: (SH-*pabA* or JE2-*pabA*)+pJC002 gDNA amplified with pGM-F and pab1R.
Lane 6: (SH-*pabA* or JE2-*pabA*)+pJC002 gDNA amplified with NE821F and NE821R.
Lane 7: (SH-*pabA* or JE2-*pabA*)+pKasbar gDNA amplified with pGM-F and pGM-R.
Lane 8: (SH-*pabA* or JE2-*pabA*)+pKasbar gDNA amplified with NE821F and NE821R.

5.2.13.3 Analysis of the genetically complemented JE2-*pabA in vitro*

The growth of genetically complemented JE2-*pabA* was assessed on 30% (v/v) human blood agar (Figure 5.41). JE2-*pabA* showed highly reduced growth on human blood. Insertion of the pJC002 at lipase restored the growth of JE2-*pabA* on human blood, whereas insertion of pKasbar at lipase did not alter the reduced growth phenotype. Insertion of pJC002 or pKasbar at lipase did not alter the growth of JE2.

5.2.13.4 Analysis of the genetically complemented SH-*pabA in vivo*

The pathogenicity of the genetically complemented SH-*pabA* strains was assessed using the zebrafish embryo model of systemic infection. Approximately 1,500 CFU of each strain was injected into zebrafish embryos, which were then incubated in E3 solution for four days. SH-*pabA* was highly attenuated, as was SH-*pabA*+pKasbar (Figure 5.42). Integration of the *pab* operon encoding pJC002 plasmid restored the virulence of SH-*pabA* to that of SH1000.

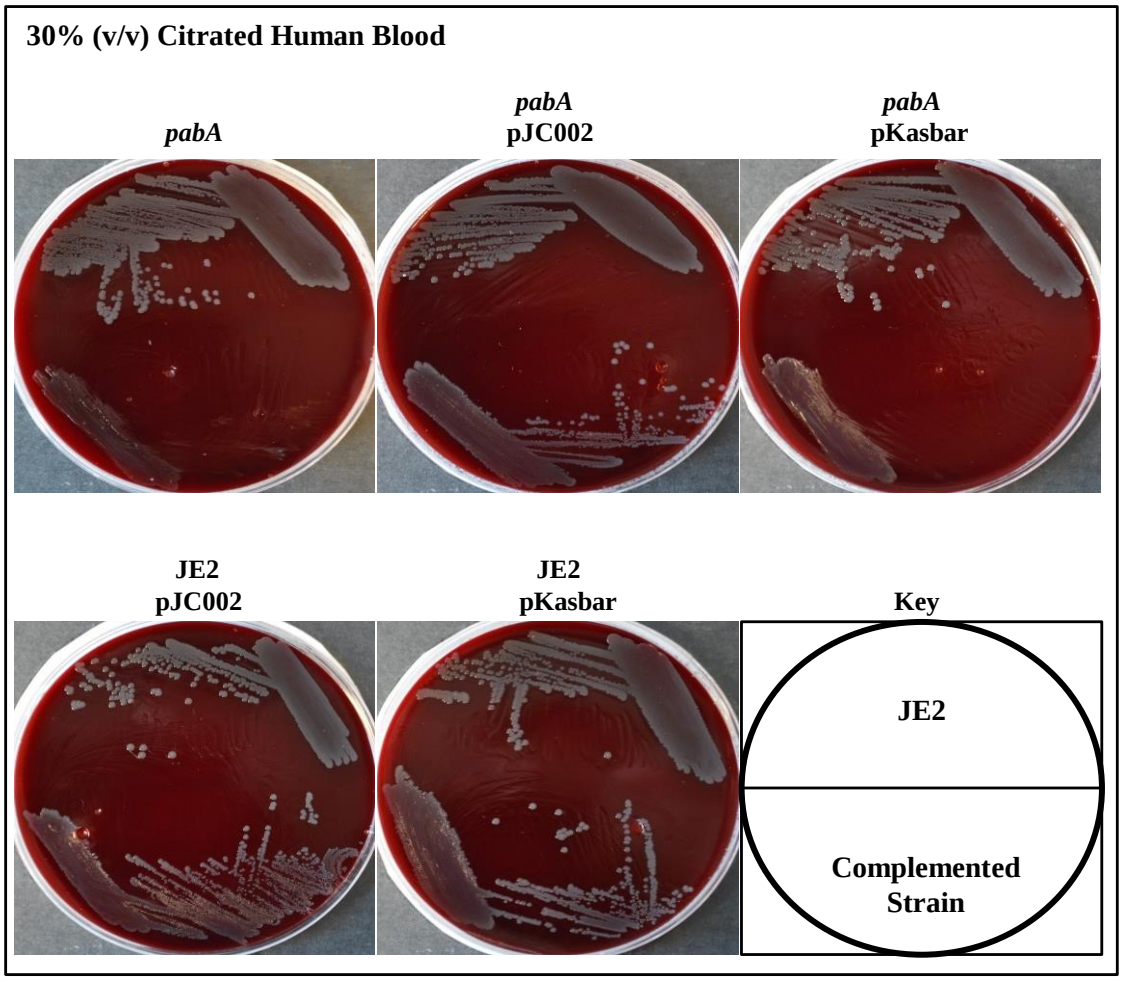

Figure 5.41 Growth of genetically complemented strains on 30% (v/v) human blood agar.

Insertion of pJC002 into JE2-*pabA* restored growth to that of JE2 on human blood. Insertion of pKasbar did not alter the JE2-*pabA* phenotype on human blood. Insertion of pJC002 or pKasbar into JE2 did not alter the growth of the wild-type. Plates were incubated at 37^{o}C for 48 h.

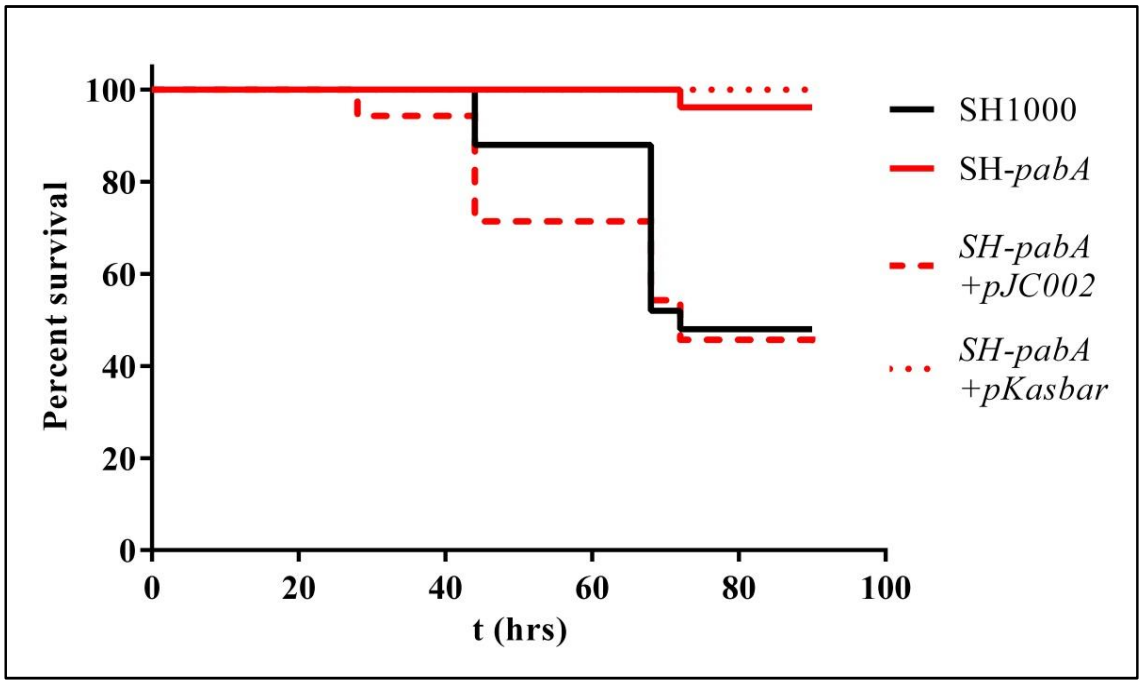

Figure 5.42 *In vivo* analysis of the genetically complemented strains.

Insertion of pJC002 carrying the *pab* operon restored the virulence of SH-*pabA* to that of SH1000, $p > 0.05$. SH-*pabA*+pKasbar remained attenuated compared to SH1000, $p < 0.0001$.

5.2.14 Effect of thymidine on SH-*pabA* virulence

The effect of thymidine on SH-*pabA* pathogenicity was assessed using the zebrafish embryo model of systemic infection. As thymine was found to partially complement the JE2-*pabA* phenotype on human blood agar (Figure 5.36) attempts were made to assess its role in pathogenicity. Initial attempts to replicate thymine complementation *in vivo* were frustrated by an inability to dissolve thymine in E3 solution. E3 has an ideal pH of 7.4 for zebrafish embryos. Thymine dissolves in 1M NaOH or in E3 at pH 12 and adjusting the pH of E3 solution plus thymine toward pH 7.4 lead to thymine precipitation well above pH 7.4. Analysis of the pyrimidine biosynthesis pathways on the Kegg and Biocyc databases suggested that thymidine may provide an alternative to thymine (Figure 5.43). *S. aureus* conversion of dUMP to dTMP is THF-dependent (Chatterjee *et al*., 2008); however, there is an alternative means of producing dTMP, known as nucleotide salvage (Neidhardt *et al*., 1996; Zander *et al*., 2010). This is dependent on the conversion of thymine to thymidine by the enzyme pyrimidine-nucleoside phosphorylase (Pdp), which can then be converted to dTMP by thymidine kinase (Tdk). Thymidine dissolved at a much lower pH and remained in solution in pH 7.4 E3 solution.

A high thymidine concentration of 800 µg ml^{-1}, equivalent to 20x the total purine concentration of CDM, was used. Initially an effect was seen (data not shown), but this was not reproducible. Therefore, thymidine does not complement the virulence phenotype of SH-*pabA* in the zebrafish embryo model. Thymidine has since been shown to complement on whole human blood agar, which suggests that the inability of thymidine complementation *in vivo*, was the result of its poor diffusion into the zebrafish embryos.

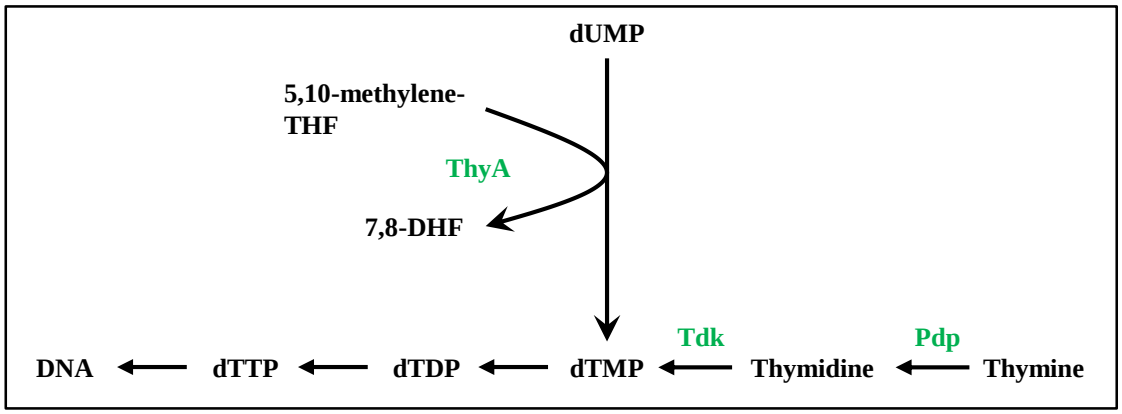

Figure 5.43 Thymidine monophosphate biosynthesis in *S. aureus*.

Conversion of dUMP to dTMP by ThyA (shown in green) is THF-dependent. Thymine can be converted to dTMP via thymidine by the sequential activity of the Pdp and Tdk enzymes (shown in green). Pathway information acquired from the Biocyc and Kegg databases.

5.2.15 The effect of homogenised RBCs on JE2-*pabA* growth

Red blood cells (RBCs) are a by-product of leukocyte preparations carried out at The Royal Hallamshire Hosptital. Plasma and clotting factors are removed and the majority of white blood cells are separated from the RBCs, providing a source of primarily RBCs. The RBC preparation procedure is given in Chapter 2.18.1. The RBCs are normally discarded, but were frozen at -20^{o}C for use in this study. After thawing, the RBCs were vortexed hard for 3 min. Freezing the RBCs was expected to cause lysis, but vortexing was still carried out. An equal volume of PPP was added, to give an RBC concentration equivalent to blood. After centrifugation there was no clear demarcation between RBCs and PPP. This was likely due to complete lysis of the RBCs from freezing resulting in RBC fragments that were too small to pellet at the centrifugation speed used and the release of all haemoglobin from the RBCs. The top 50% of the centrifuged RBC, PPP mixture was collected to give the RBC homogenate.

Growth of JE2-*pabA* was assessed on 30% (v/v) RBC homogenate agar (Figure 5.44). Growth of JE2-*pabA* was inhibited on RBC homogenate agar. 50 µg ml^{-1} PABA completely restored growth of JE2-*pabA* and increasing the thymine concentration to 400 µg ml^{-1}, 10x the concentration that gave partial complementation in 30% (v/v) human blood agar (Figure 5.36), gave comparable growth to JE2 on RBC homogenate agar.

The absence of thymine from CDM, which supports comparable growth of JE2-*pabA* to JE2, demonstrates that it is not an essential supplement for JE2-*pabA* growth. Figure 5.43 shows that JE2 can synthesise dTMP from dUMP using ThyA and THF. The lack of THF in the *pabA* mutant means that dTMP can only be synthesised from thymidine by the enzyme Tdk. A low level of thymidine partially restored growth of JE2-*pabA*, whereas a higher level restored growth to that of JE2. This suggests that in CDM the *pabA* mutant can survive via the nucleotide salvage pathway, but cannot in blood. One possible explanation is that a component of blood competitively inhibits the Tdk enzyme, allowing partial complementation with low levels of thymidine and complete complementation at a higher concentration. Another possibility is that growth in human blood creates an increased demand for dTMP, which cannot be met by the THF deficient *pabA* mutant.

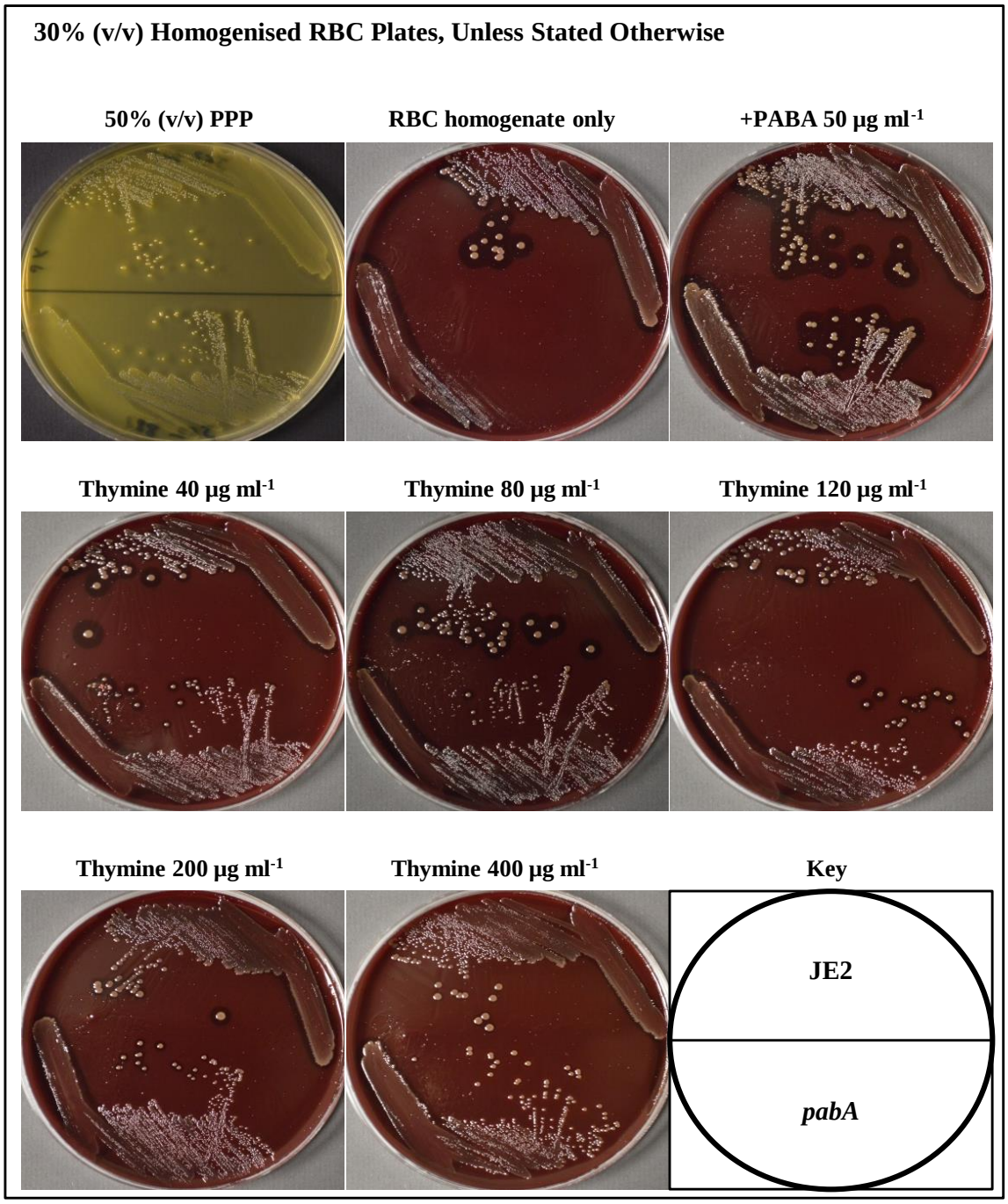

Figure 5.44 Analysis of the effect of RBC homogenate and thymine on the growth of JE2-*pabA*.

RBC homogenate inhibits JE2-*pabA* growth. Increasing thymine concentration restores growth of JE2-*pabA* to equivalence with JE2. Plates were incubated at 37^{o}C for 48 h.

5.2.16 Analysis of JE2-*pabA* inhibition by blood

5.2.16.1 The effect of platelets on JE2-*pabA* growth

The plasma produced up until this point was produced by a relatively high speed centrifugation of blood. At this speed, platelets would be removed from the resulting plasma, giving platelet poor plasma (PPP). A lower speed centrifugation procedure was used to produce plasma with a higher platelet concentration, platelet rich plasma (PRP; for PPP and PRP preparation see Chapter 2.1.3.1.2). Growth of JE2-*pabA* was compared to JE2 on PPP and PRP and PRP+PABA (Figure 5.45). JE2-*pabA* growth was comparable to JE2 in all conditions, which suggested that platelets are not the inhibitory factor in human blood.

5.2.16.2 The effect of Fe^{2+} conc. on JE2-*pabA* growth

Fe^{2+} was added to 30% (v/v) RBC homogenate agar to assess its role in inhibition of JE2-*pabA*. It was hypothesised that the poor growth of JE2-*pabA* on human blood may result from an inability to respond to a greater demand for dTMP, due to DNA damage caused by haem toxicity. The *S. aureus* iron regulated surface determinant system (Isd system) extracts haem from haemoglobin and transports it across the cell wall and membrane into the cytosol. The haem can be used intact or degraded to give free Fe (Anzaldi & Skaar, 2010; Hammer & Skaar, 2011). The Fur protein negatively regulates the *isd* genes when Fe levels are high, by binding to a consensus sequence (the Fur box) upstream of the *isd* operons inhibiting transcription. When Fe levels are low, Fur binding is alleviated and *isd* transcription can take place (Cassat & Skaar, 2012; Skaar, Gaspar, & Schneewind, 2004). It was hypothesised that addition of high levels of Fe to RBC homogenate agar would switch off the Isd system preventing acquisition of haem, thereby preventing haem toxicity (Figure 5.46). Addition of ammonium ferrous sulphate (AFS) at 6 µg ml^{-1}, 12 µg ml^{-1}, 30 µg ml^{-1} and 60 µg ml^{-1} (equivalent to 1x, 2x, 5x and 10x CDM concentration) did not alter the JE2-*pabA* growth phenotype.

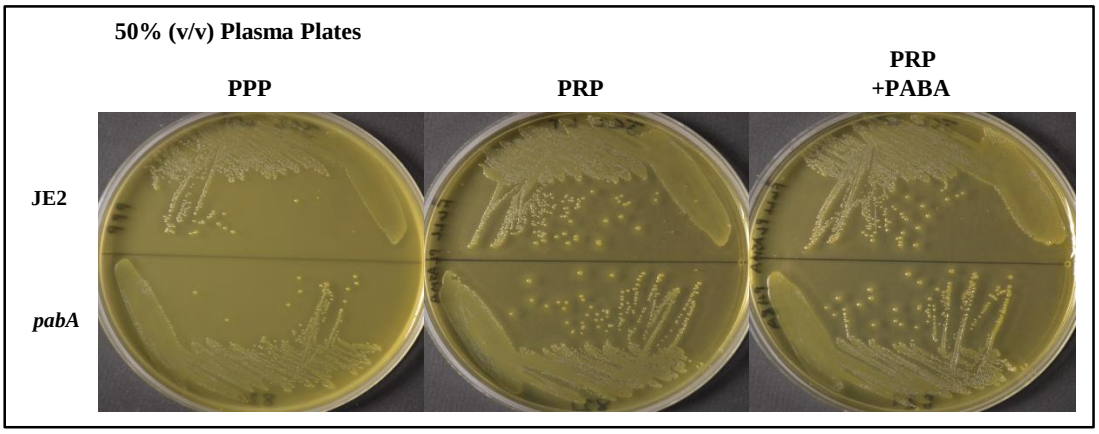

Figure 5.45 Analysis of the effect of clotting factors on JE2-*pabA* growth.

Abbreviations: PPP, platelet poor plasma; PRP, platelet rich plasma (normal levels of clotting factors). The presence of clotting factors does not inhibit the growth of JE2-*pabA*. Plates were incubated at 37^{o}C for 48 h.

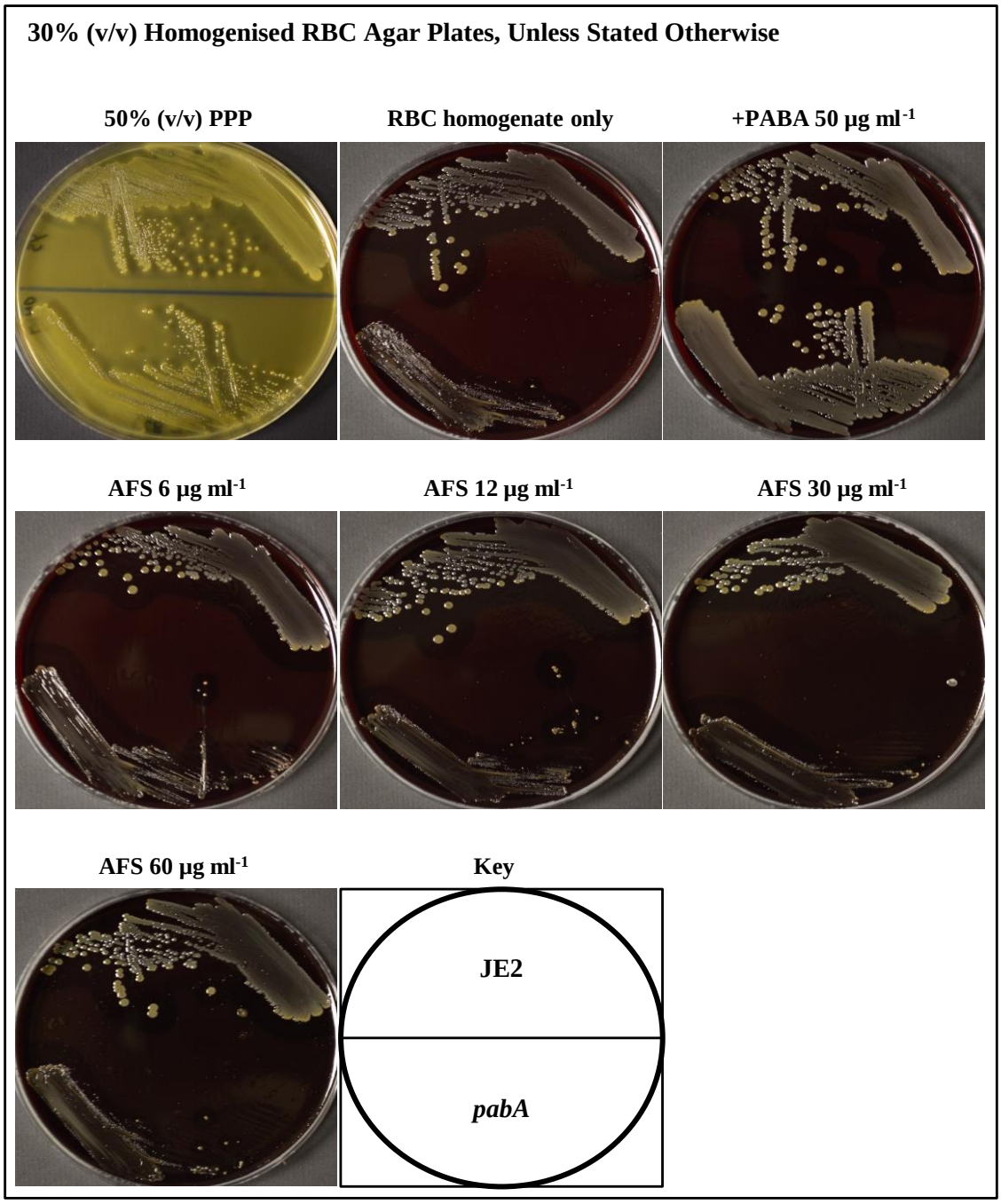

Figure 5.46 Analysis of Fe concentration on the growth of JE2-*pabA* on RBC homogenate.

The presence of Fe^{2+} in the form of Ammonium ferrous sulphate at 1x, 2x, 5x and 10x CDM concentration does not alter the inhibition of JE2-*pabA*. Plates were incubated at 37^{o}C for 48 h.

5.2.16.3 The effect of bovine haemin on JE2-*pabA* growth

Growth of JE2-*pabA* was assessed on 50% (v/v) plasma agar with addition of haemin. Haemin is a chlorinated form of haem used in laboratory analysis of haem toxicity. Bovine haemin has been demonstrated to cause haem toxicity in *S. aureus* strains at concentrations as low as 3 µg ml^{-1} (Nitzan *et al*., 1987). *S. aureus* Newman *srtA*$^{-}$ was found to be more resistant to haemin, which was thought to be due to the role of SrtA in binding IsdABC & H to the *S. aureus* surface (Torres *et al*., 2007). It was hypothesised that if increased susceptibility to haem toxicity is the cause of the JE2-*pabA* phenotype then addition of haemin to plasma would replicate the JE2-*pabA* phenotype seen on human blood. Growth of JE2-*pabA* was found to be no different to JE2 on 50% (v/v) plasma agar with or without haemin (Figure 5.47). Unexpectedly both strains grew at the highest concentration (20 µg ml^{-1}).

5.2.16.4 The effect of bovine haemoglobin on JE2-*pabA* growth

Growth of JE2-*pabA* was assessed on 50% (v/v) human plasma agar supplemented with bovine haemoglobin. *S. aureus* is able to grow utilising haemoglobin as its only Fe source at as low a concentration as 5 µg ml^{-1} (Pishchany *et al*., 2010). It was hypothesised that if increased susceptibility to haem toxicity is the cause of the JE2-*pabA* phenotype then addition of bovine haemoglobin to plasma would replicate the JE2-*pabA* phenotype seen on human blood. Figure 5.48 shows that growth of JE2-*pabA* was not altered by bovine haemoglobin. The use of bovine haemin in section 5.2.16.3 and the use of bovine haemoglobin above did not completely rule out the possibility that the JE2-*pabA* phenotype is the result of haem toxicity. Pishchany *et al*., (2010) showed that *S. aureus* has evolved specificity for human haemoglobin over murine haemoglobin. This specificity may result in poor acquisition of bovine haem minimising the effects of haem toxicity. However, if haem toxicity is not the cause of the JE2-*pabA* and SH-*pabA* phenotype, then the possibility that the cause is a Tdk inhibitory compound in human blood remains, as does the possibility that there is a greater demand for pyrimidines when growing on human blood.

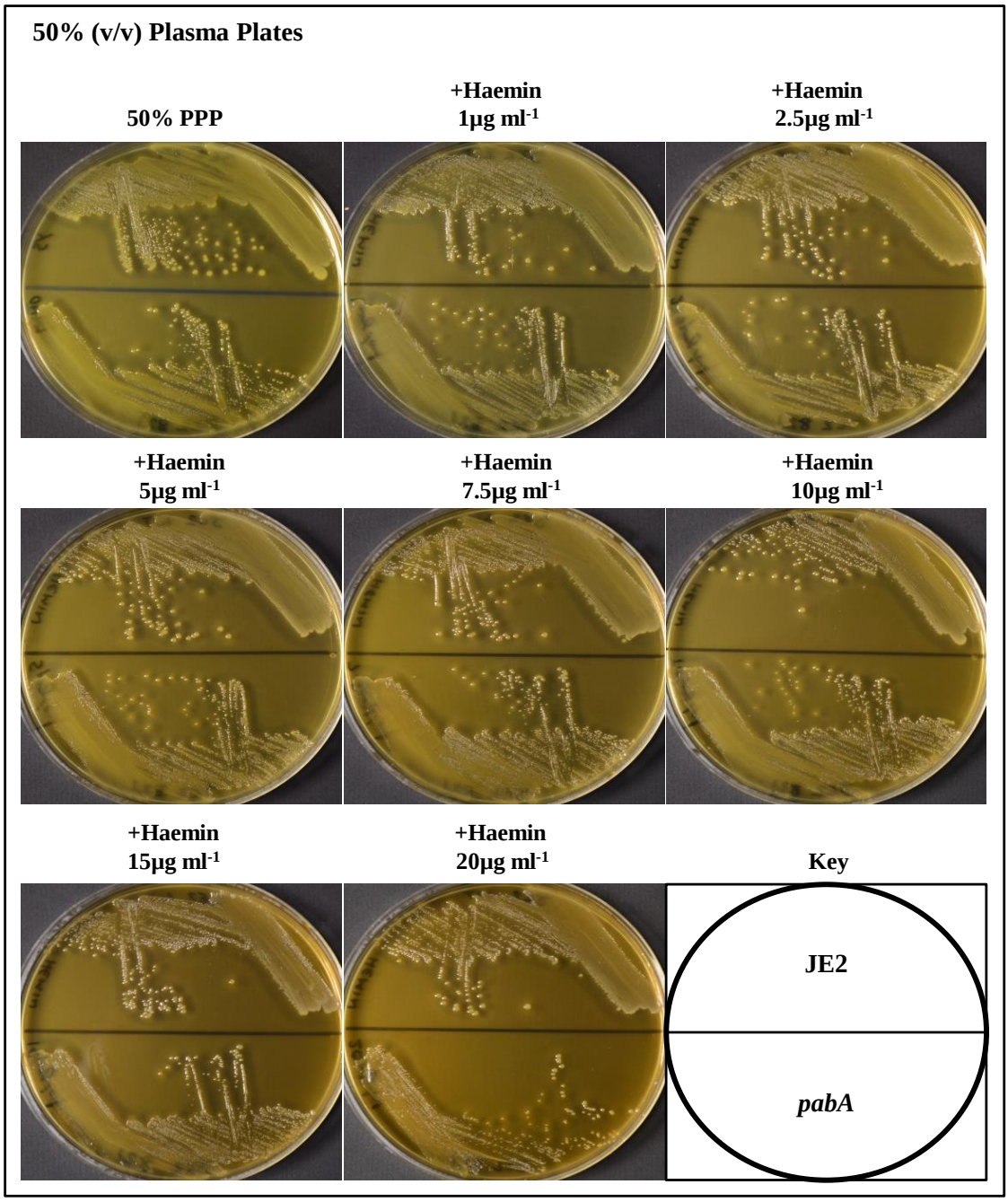

Figure 5.47 Analysis of the effect of bovine haemin on the JE2-*pabA* growth phenotype.

Increasing concentrations of bovine haemin does not inhibit growth of JE2-*pabA* on 50% (v/v) human plasma. Plates were incubated at 37^{o}C for 48 h.

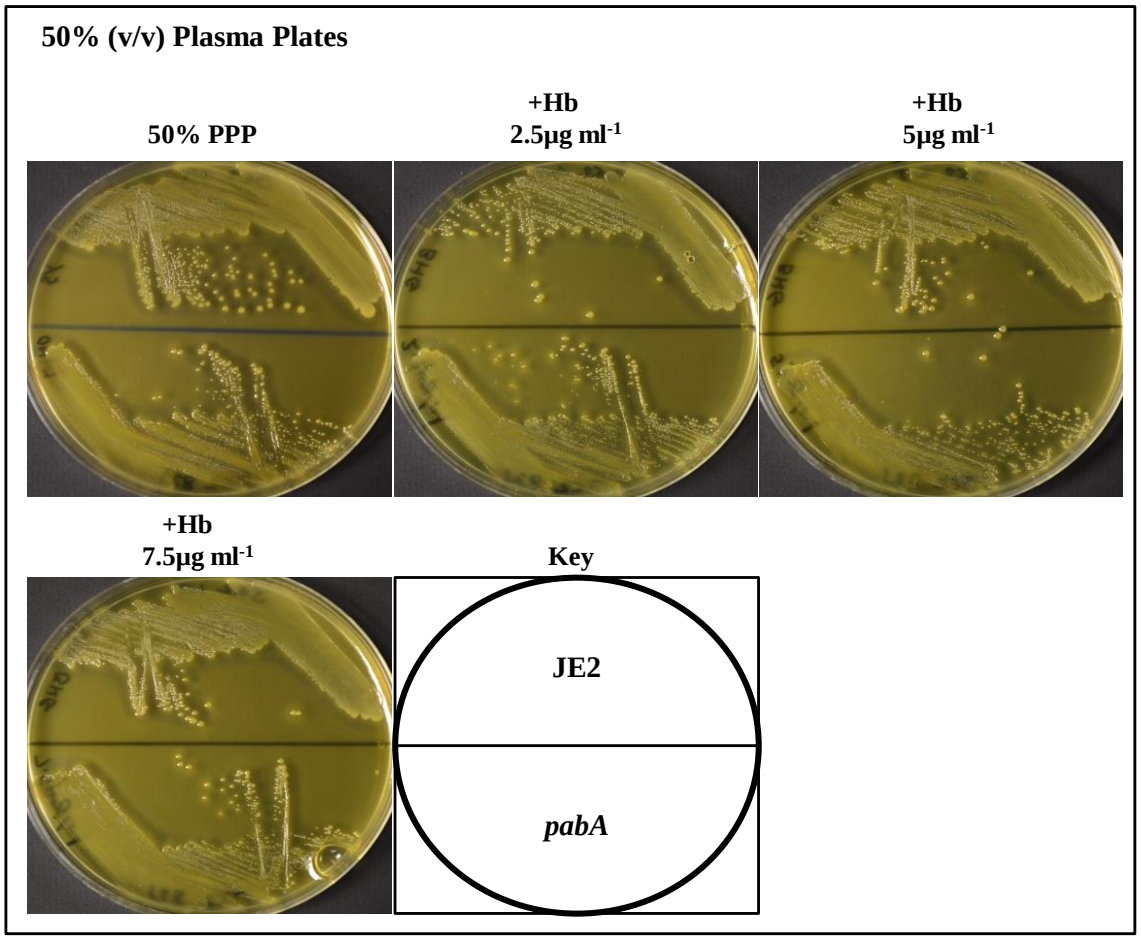

Figure 5.48 Analysis of the effect of bovine haemoglobin on the JE2-*pabA* growth phenotype.

Increasing bovine haemoglobin concentration did not alter the growth of JE2-*pabA* on 50% (v/v) human plasma. Plates were incubated at 37^{o}C for 48 h.

5.3 Discussion

Nine strains, each with a separate gene disrupted by Tn insertion, were identified by screening the NTML on human blood agar (see Chapter 4). Characterising the phenotype caused by the loss of each of the nine genes was not a realistic possibility in the timeframe given for the analysis. Therefore, the zebrafish embryo model of systemic infection was employed to identify those strains whose phenotype resulted in reduced pathogenesis in this model. Of the nine, two strains with Tn disrupted genes involved in *de novo* purine biosynthesis and one strain with a Tn disrupted gene required for synthesis of folates were highly attenuated in the zebrafish embryo model. The phenotype of these three strains was then characterised.

5.3.1 Analysis of *purA* & *purB*

Analysis of the purine pathway mutants JE2-*purA*, SH-*purA*, JE2-*purB* and SH-*purB* followed the scheme of the flow diagram shown in Figure 5.49. When screened on bovine serum agar, human blood agar and sheep blood plus Columbia agar base, NE529 and NE522 had reduced growth on human blood agar and bovine serum agar, but grew normally on sheep blood with the nutrient rich Columbia agar base. The phenotype was confirmed for the transduced strains, JE2-*purA* and JE2-*purB*, by growth curves in BHI and human or bovine serum. The ability to grow in nutrient rich media suggested that the *purA* and *purB* disrupted strains had a nutrient requirement missing from serum and blood. Analysis of the *de novo* purine biosynthesis pathway suggested that both strains could not synthesise AMP and the *purB* mutant had an additional requirement for GMP.

The requirement for purines was not confirmed in the zebrafish model. This was likely the result of poor uptake of adenine and inosine to allow their use by the *purA* or *purB* mutant strains. However, since both strains required adenine, poor uptake could only be assumed for adenine. CDM analysis confirmed that the purine requirement of both strains matched the known roles of the *purA* and *purB* genes in *S. aureus* (Baxter-Gabbard & Pattee, 1970). The analysis also suggested that purine availability in zebrafish embryos and in human blood is low. As the role of *purA* and *purB* in the *de novo* biosynthesis of purines by *S. aureus* is well characterised (Baxter-Gabbard & Pattee, 1970) and their importance to pathogenesis has been documented by other

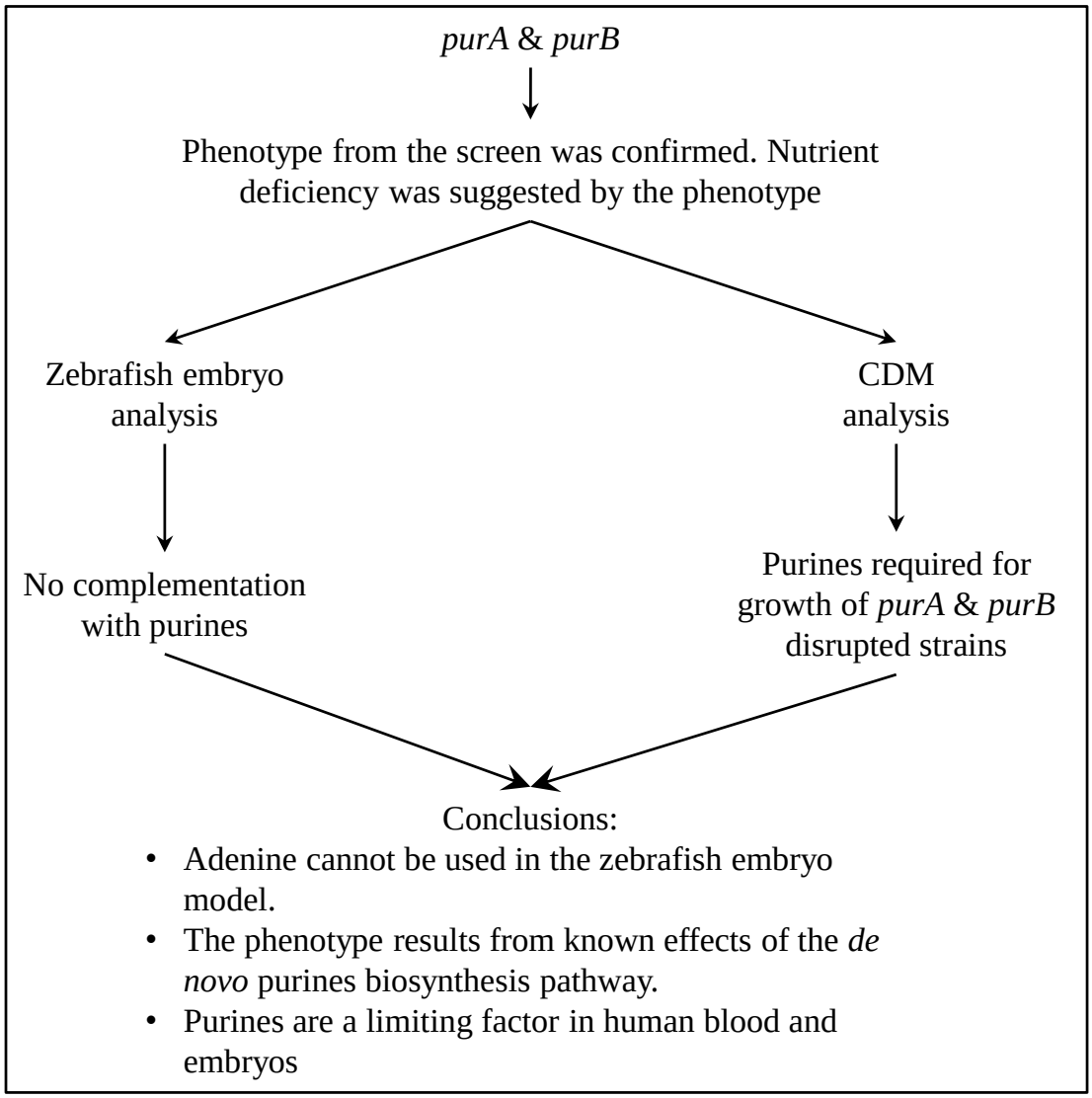

Figure 5.49 Diagram of the analysis of the *purA* and *purB* genes.

groups (McFarland & Stocker, 1987; Stocker, 1988) it was decided to centre all further effort on the folate pathway mutants JE2-*pabA* and SH-*pabA*.

5.3.2 Analysis of *pabA*

Analysis of the role of *pabA* followed the scheme of the flow diagram shown in Figure 5.50. In the NTML screen (Chapter 4), strain NE821 showed an unusual phenotype, growing poorly on blood, but normally on bovine serum. The phenotype was confirmed above and shown to not be related to the different aeration conditions used in the screen, the low serum concentration in blood agar, or nutrient release during serum preparation. The phenotype was also found to be restricted to human blood when growth was assessed on 30% (v/v) horse, rabbit and sheep blood agar. The phenotype was thought to be the result of either inhibition by a human blood component or a nutrient that is more available in serum or plasma than in blood. The role of THF in the biosynthesis of some amino acids, nucleic acids and vitamins made it likely that the latter possibility was correct.

The importance of purines, glycine, serine, vitamin B_5, methionine and thymine in the growth and pathogenicity of JE2-*pabA* and SH-*pabA* was determined. Agar based and liquid CDM experiments were carried out and only glycine, serine and purines were found to complement the *pabA* mutant. However, in the absence of these components the difference in growth between the *pabA* mutant and JE2 was slight, relative to the difference seen on human blood agar. Furthermore, no combination of purines, glycine or serine restored JE2-*pabA* growth on human blood or restored virulence to SH-*pabA* in the zebrafish embryo model. Thymine was found to partially restore growth of JE2-*pabA* on human blood at a concentration equivalent to the purine concentration in CDM. The CDM and whole human blood complementation results suggested that the *pabA* mutant phenotype was the result of inhibition in human blood and that this inhibition was antagonised by thymine, or that growth in human blood creates a greater demand for dTMP.

Analysis of the inhibition of the *pabA* mutant demonstrated that the putative inhibitory factor was associated with the RBC component of blood and was likely to be found inside RBCs. Thymine or thymidine at high concentrations, relative to CDM purine

concentration, was found to complement on RBC homogenate agar. In the biosynthesis of dTTP, *S. aureus* converts dUMP to dTMP in a folate-dependent reaction. In the absence of folate, *S. aureus* depends on the nucleotide salvage pathway, in which the enzyme Pdp converts thymine to thymidine, which can then be converted to dTMP by thymidine kinase (Tdk; Figure 5.43). Complementation therefore suggested that conversion of thymidine to dTMP was possible in serum and plasma, but not in human blood and potentially that something in RBCs may competitively inhibit Tdk, leading to a requirement for a high thymidine or thymine concentration to overcome the inhibition.

This did not explain how JE2-*pabA* could grow in chemically defined media, which does not contain thymine or thymidine. Wegkamp *et al*., (2007) demonstrated that trace amounts of PABA, folate, glycine, serine or nucleobases in CDM minus glycine, serine and nucleobases were able to sustain reduced but consistent growth of a *pab* operon deletion strain of *Lactococcus lactis*. Fresh inoculation of *L. lactis pabA* into spent CDM minus glycine, serine and nucleobases with added glucose (i.e. CDM minus glycine, serine and nucleobases that has sustained the growth of *L. lactis pabA* to its maximum OD, filtered and supplemented with glucose) resulted in no growth of the *pab* operon mutant. Furthermore, the growth could be restored by addition of PABA. This suggested that trace amounts of PABA may have resulted in JE2-*pabA* growth in CDM.

One possible explanation for CDM growth of the *pabA* mutant, but its lack of growth in human blood, was the presence of the *thyX* gene in *S. aureus*. ThyX allows for flavin-dependent, folate-independent conversion of dUMP to dTMP (Myllykallio *et al*., 2002). If ThyX could be found amongst the *S. aureus* protein sequences, then it would suggest that ThyX conversion of dUMP to dTMP was possible in serum, plasma and CDM, but ThyX activity was inhibited in blood. The *thyX* gene is not commonly found in strains possessing the folate-dependent method of dTMP synthesis and there are no ThyX proteins reported on the Uniprot database for any *S. aureus* strains. Furthermore, a search of all USA300 protein sequences against the Pfam database found no protein containing a thy1 domain (the domain associated with the ThyX protein). Therefore, the presence of a *thyX* gene in the *pabA* mutant was ruled out.

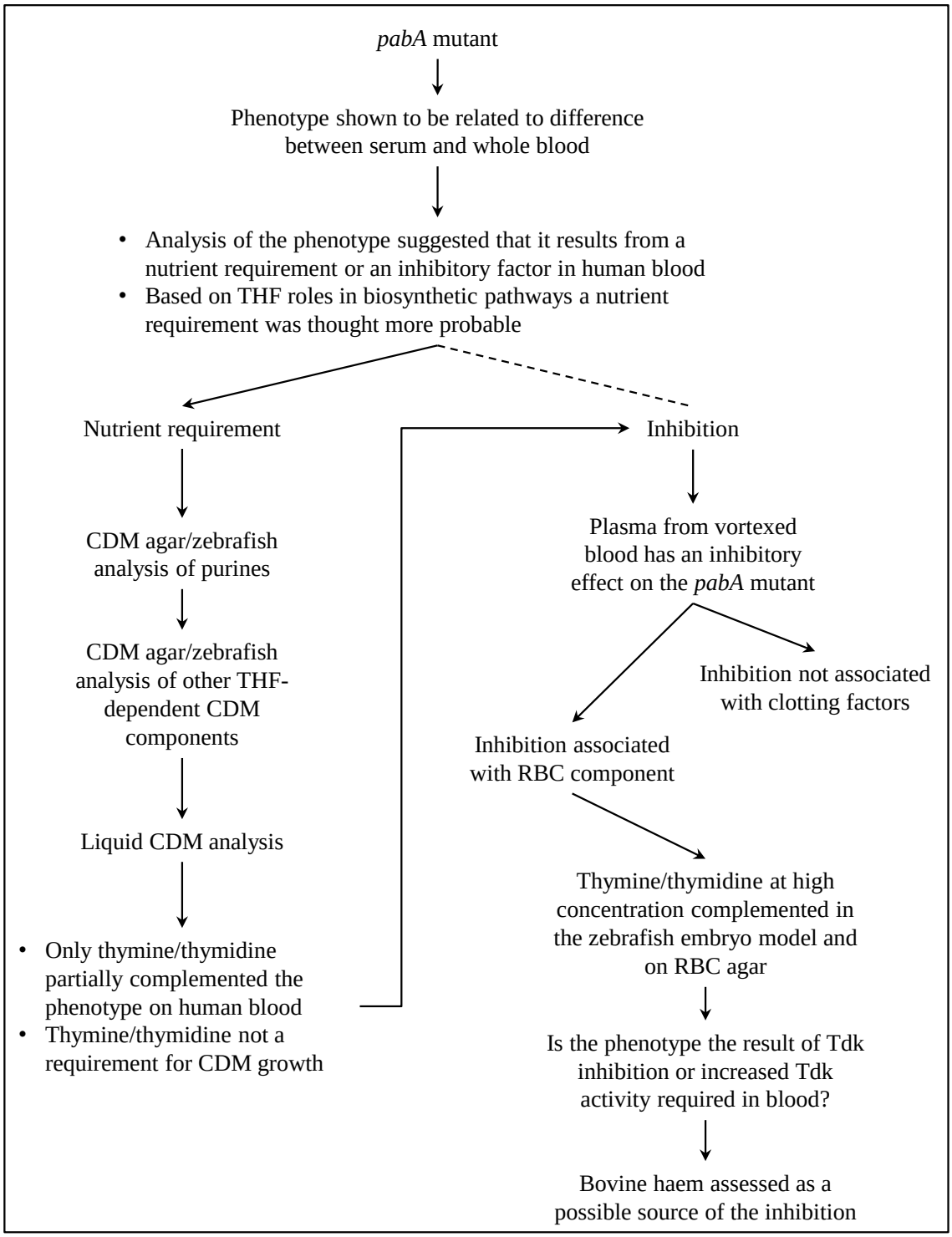

Figure 5.50 Analysis of *pabA* shown diagrammatically.

Another possible explanation could be that the requirement for dTTP could be supplied by some other less effective means, which is enough to allow growth of JE2-*pabA* in CDM. When growing on human blood however, JE2-*pabA* may be more susceptible to haem toxicity or some other effect that results in increased demand for dTMP. Acquisition of haem primarily from host haemoglobin is a requirement for the pathogenicity of *S. aureus*, which uses haem as a cofactor in many reactions (Hammer & Skaar, 2011; Torres *et al*., 2006). Haem can be toxic at high levels leading to protein, lipid and DNA damage (Anzaldi & Skaar, 2010; Stauff *et al*., 2008). DNA damage caused by haem toxicity may result in a greater requirement for dTMP, which JE2-*pabA* cannot respond to in the absence of THF or thymine.

Neither addition of increased Fe concentrations to downregulate haem acquisition in *S. aureus*, nor addition of bovine haemin or bovine haemoglobin altered the JE2-*pabA* phenotype. At the completion of the above analysis it remained possible that haem was the inhibitory factor, as *S. aureus* has been shown to favour acquisition of human haem as opposed to haem from other mammals (Pishchany *et al*., 2010). The lack of inhibition of JE2-*pabA* on rabbit, sheep and horse blood agar supports this possibility (Chapter 4). It also remained possible that something else in human blood drives a greater need for pyrimidines resulting in a requirement for exogenous thymine or thymidine or that something in blood interacts with the Tdk protein competitively inhibiting its function, which would also result in a greater requirement for thymine or thymidine.

5.3.3 The ongoing analysis of *pabA*

Dr Emma Johnson has followed up the above analysis, attempting to identify the cause of the JE2-*pabA* phenotype. Human haem was found to have no effect on the growth of JE2-*pabA* when added to human plasma agar and thymidine was found to complement JE2-*pabA* on 30% (v/v) human blood agar.

Interestingly, growth of a *tdk*, *pabA* double mutant of *S. aureus* USA300 JE2 could not be restored by either thymine or thymidine on human blood agar. This demonstrates that the thymine and thymidine added to blood is being used by the *pabA* mutant to produce dTMP. It does not answer the question as to whether the requirement for high levels of

thymine or thymidine is to prevent competitive inhibition of Tdk or to complement an increased requirement for pyrimidines in human blood.

5.3.4 Future work

It is essential to genetically complement the *tdk* gene in the *pabA*/*tdk* mutant, thereby proving that the *tdk* gene is required for thymidine complementation. Complementing the *pabA*/*tdk* double mutant and the *pabA* mutant with the product of Tdk activity (deoxythymidine monophosphate; dTMP) would also demonstrate the importance of Tdk activity to the *pabA* mutant.

To determine whether Tdk is able to function in plasma, but is inhibited in human blood, Tdk inhibitors could be employed. The enzyme dihydrofolate reductase (DHFR) reduces DHF to THF in the THF biosynthesis pathway. The antifolate trimethoprim binds to bacterial DHFR with 10^5 times greater affinity than it binds to vertebrate DHFR (Hawser *et al*., 2006). Loss of DHFR activity leads to loss of THF and THF-dependent functions, including folate-dependent synthesis of dTMP by thymidylate synthase (ThyA), as seen in the *pabA* mutant. Thymidine has been shown to reduce the potency of trimethoprim (Proctor, 2008), by allowing THF-independent conversion of thymidine to dTMP by Tdk. Tdk inhibitors have been used to restore the potency of trimethoprim in the presence of thymidine (Zander *et al*., 2010). Therefore, Tdk inhibition of the *pabA* mutant using a Tdk inhibitor may replicate the *pabA* mutant phenotype, seen on blood, on plasma. This would demonstrate that the phenotype on blood is the result of Tdk inhibition. If the phenotype is not replicated, then this would suggest that there is a greater need for dTMP when growing on human blood.

An interesting experiment would be to compare the resistance of the wild-type and *pabA* mutant to trimethoprim. Long-term patient treatment with trimethoprim can result in small colony variant (SCV) strains of *S. aureus*, collected from many sites in the body including blood (Besier *et al*., 2008), all of which result from SNP changes in the *thyA* gene, producing slow growing trimethoprim resistant strains (Garcia *et al*., 2013). If the *pabA* mutant is found to be resistant to trimethoprim in CDM in the absence of serine, glycine and nucleic acids, this would suggest that *pabA* mutants resistant to trimethoprim are not commonly found in patients because of their inability to grow in

blood (i.e. they are resistant to trimethoprim, but they lack the ability to grow in blood and are therefore not found as resistant SCVs associated with patients). Also, it would suggest that the activity of sulphonamide drugs is the result of inhibition of THF coupled with the inhibition of Tdk in blood. It would be expected that the wild-type would be resistant to THF-inhibiting antimicrobials in rich media and susceptible to them on blood, where synthesis of dTMP is limited by the suspected inhibitor of Tdk and trimethoprim inhibition of THF-dependent synthesis of dTMP. If high thymidine concentration then restores wild-type growth on blood in the presence of trimethoprim, as it does with the *pabA* mutant, then this would suggest a role for Tdk inhibition by blood in the activity of antifolate antibiotics.

As wild-type *S. aureus* can make dTMP via the THF-dependent route, Tdk inhibition has no evolutionary benefit unless natural inhibitors of THF biosynthesis exist, or if there are other pathogens that rely solely on nucleotide salvage for their dTMP. The genome of the human pathogen *Ureaplasma urealyticum* does not carry the genes required for *de novo* synthesis of dTMP and relies on Tdk activity for dTTP synthesis (Kosinska *et al*., 2005). Furthermore, a potent inhibitor of DHFR known as 10-formyl folic acid has been found in rat livers, which is thought to have a role in regulating folate levels (d' Urso-Scott *et al*., 1974). Whether this or other folate regulators would recognise bacterial DHFR is uncertain. However, the existence of vertebrate DHFR regulation and pathogens reliant on Tdk activity does offer potential reasons for the evolution of Tdk inhibition.

CHAPTER 6

GENERAL DISCUSSION

6.1 Introduction

The goal at the outset of this work was to identify and characterise a putative toxin that showed a dramatic necrotic effect on human neutrophils. Two independent publications allowed rapid identification of LukAB/GH as the putative toxin (Dumont *et al*., 2011; Ventura *et al*., 2010). Two methods were then employed to identify novel or uncharacterised virulence factors (VFs) required by *S. aureus* for pathogenesis. A bioinformatics approach was first used (Chapter 3), followed by screening of an ordered Tn mutagenesis library on human blood (Chapter 4). The genes isolated in the NTML screen were then characterised (Chapter 5).

6.2 What is a virulence factor?

When discussing virulence factors (VF), the standard texts focus primarily on adhesion & invasion proteins, toxins, immune evasion, biofilm and iron acquisition proteins (Atlas, 1997; Madigan, 2000; Prescott, 1999; Wu *et al*., 2008). Much less attention is given to essential metabolic functions and factors that allow the pathogen to respond to the host environment, which are key to *S. aureus* pathogenicity. Components essential for growth in any environment, such as cell wall synthesis, DNA replication, transcription and translation proteins cannot be classed as VFs, as they are required for growth not just during infection. A more meaningful definition would be factors that are non-essential for growth *in vitro*, but are essential for growth in the host. The purine and folate biosynthesis enzymes which were the subject of Chapter 5 are clearly required for growth in human blood. To categorise the purine pathway enzymes as VFs would likely be invalid, as full growth of the *purA* and *purB* mutants could only be supported in rich media, and are likely a requirement in all environments faced by *S. aureus* outside the laboratory. There is some justification for labelling the folate pathway enzyme PabA a VF, as growth was normal in a variety of conditions (i.e. serum, plasma, CDM and rich media) and only exhibited reduced growth in human blood. This demonstrated that PABA synthesis was not essential for growth in all environments and that *pabA* is required for the virulence of *S. aureus*. Although PabA does not have a direct role in

virulence, such as adhesion, tissue damage or immune evasion, it does meet the definition of a VF.

6.2.1 VFs are a bacterium's response to its environment

The versatility of *S. aureus* in its ability to respond to the hostile and nutritionally dynamic environment of the host is what makes it such an effective pathogen. A primary purpose of infection is the acquisition of nutrients; virulence determinants are produced to enable this acquisition. During the early stage of a *S. aureus* infection adhesins and immune evasion proteins are expressed, often regulated by the *saeRS* two-component sensor regulator system (Geiger *et al*., 2008; Giraudo *et al*., 1996). This allows colonisation of the infection site, while protecting the bacteria from host defences. At this stage of infection the bacteria will be using the available nutrients and synthesising those nutrients that are sequestered by the host, such as purines. As the bacterial load at the site of infection increases, nutrient availability decreases. *S. aureus* constitutively secretes the octapeptide AIP, at a high bacterial load it reaches a threshold level resulting in activation of the AgrAC two-component sensor regulator system, which leads to expression of RNAIII (Chien *et al*., 1999; Wang *et al*., 2014). RNAIII promotes downregulation of adhesins allowing migration from the site of infection to other areas in the body and upregulation of exoenzymes promoting tissue damage. Toxins such as haemolysins and PSMs are also positively regulated by the *agr* system to combat leukocytes and liberate nutrients from non-immune cells (Cheung *et al*., 2011; Chien *et al*., 1999; Wang *et al*., 2014). The *agr* system is normally repressed in the early stages of infection by CodY. However, if the nutrient levels are too low to support growth before the AIP threshold is reached, CodY derepresses *agr* allowing expression of exoenzymes and toxins for nutrient acquisition (Pohl *et al*., 2009). This response to reduced nutrients is not unique to *S. aureus*, for instance toxin expression in the pathogen *Clostridium difficile* is upregulated by the TdcR protein, due to CodY derepression, in the absence of a readily useable carbon source (Bouillaut *et al*., 2014; Dineen *et al*., 2010).

6.3 Success of *S. aureus* as a pathogen

As well as disease, the success of a pathogen is also mediated by its ability to move between hosts and survive in the environment. *S. aureus* produces several proteins that allow it to do this. These factors cannot be classed as virulence factors, but their role is important for successful pathogenesis. The IsdA protein binds fibrinogen, fibronectin and is involved in nasal colonisation, allowing adhesion to squamous nasal epithelial cells, and has been shown to be important for colonisation of cotton rats (Clarke *et al*., 2006; Clarke *et al*., 2004). As discussed in Chapter 1 & Chapter 5 the Isd system is controlled by the negative regulator Fur, leading to repression of the *isd* genes in high iron concentrations. The results of Clarke *et al*. (2004, 2006) suggest that the anterior nares of the human host are iron limited, leading to expression of IsdA to allow colonisation. This demonstrates adaptation by *S. aureus* to its environment allowing an appropriate response upon recognition of the appropriate signals. Although colonisation of the nares primarily leads to asymptomatic infection, *S. aureus* is an opportunistic pathogen, and nasal colonisation has been shown to increase the likelihood of invasive infections (Von Eiff *et al*., 2001).

The KatA and AhpC enzymes contribute to *S. aureus* survival in aerobic environments such as the nares and resistance to desiccation (Cosgrove *et al*., 2007). The aerobic environment of the nares leads to endogenous H_2O_2 production that can damage bacterial DNA. The iron regulated PerR protein responds to the low iron levels in the nares, promoting expression of the H_2O_2 scavengers KatA and AhpC (Horsburgh *et al*., 2001). Furthermore, the intermittently dry environment of the nares can lead to desiccation of *S. aureus*. ClpX and the regulatory protein SigB have also been shown by Tn library screening to be required for desiccation survival (Chaibenjawong & Foster, 2011). The ability to survive desiccation is not only important for survival in the nares, but also allows survival outside the host and has been implicated in the spread of *S. aureus* infection in the hospital environment (Farrington *et al*., 1992; Rountree, 1963).

6.4 The bioinformatics toolbox

Bioinformatics tools can be used to mine the vast amount of sequence data found on biological sequence databases, allowing for a comprehensive analysis of the VFs of

pathogens. The purpose of my bioinformatics study was to identify a component of interest relatively quickly, which could then be assessed in the laboratory. The bioinformatics of Chapter 3 broached only the standard definition of a VF (i.e. components directly involved in virulence, such as toxins, adhesins and immune evasion proteins). The methodology was similar to that used by Barh & Kumar (2009) to search for essential genes in *Neisseria gonorrhoeae* by blastp and blastx search of the *N. gonorrhoeae* protein sequences against the Database of Essential Genes (DEG).

No novel VFs were found amongst the protein sequences of *S. aureus*, but that is not to say that there was no novel VFs to find. The methodology allowed for a relatively rapid analysis of the *S. aureus* genome, to identify targets that were potentially important virulence determinants. Certain aspects of the bioinformatics were employed to speed up the process, which likely reduced the sensitivity of the analysis. Limiting the hypothetical protein and database sequences to those containing N-terminal signal sequences improved the specificity, but likely had an impact on the sensitivity of the method. For instance, GAPDH is a metabolic protein that catalyses one step in glycolysis in the cytoplasm. It possesses no signal sequence, but is also found on the surface of *S. aureus* and other pathogens and has a role in plasmin binding (Modun & Williams, 1999; Taylor & Heinrichs, 2002). Therefore, this metabolic protein, absent of a recognisable signal sequence, could have a direct role in pathogenicity through tissue invasion. Similar VFs, possessing no signal sequence, would not have been found in the analysis.

The analysis highlighted the level of incorrect/outdated annotation of the sequence databases. The 3 target proteins that were characterised in Chapter 3 (SSL12, SSL13 and SSL14) were annotated as hypothetical proteins, but were in fact previously recognised SSLs. Little was known about the function of these SSLs, therefore the bioinformatics succeeded in isolating 3 targets for laboratory analysis. If this had not been the case, other approaches could have been used to isolate proteins of interest. Molecular mimicry is a common tactic employed by bacteria to subvert host functions during infection (Doxey & McConkey, 2013; Stebbins & Galán, 2001). Mimicry is either at the structural level or protein sequence level. Blastp comparison of the *S. aureus* protein sequences against all human protein sequences may reveal mimicry

strategies employed by *S. aureus* that benefit the pathogen during infection. This may identify novel VFs or indicate the function of VFs that have already been identified.

6.5 Strain libraries as tools for virulence studies

The results of the SSL characterisation suggested that they may be important for survival in human blood. However, the evidence for this was a relatively weak assay and no further support for a role in human blood could be found. It was decided to screen the NTML on human blood agar as an alternative method of identifying genes required for pathogenicity. Human blood agar was considered an ideal medium for assessing virulence, as survival in human blood is essential for *S. aureus* diseases such as septicaemia and endocarditis. Another benefit of analysing growth on human blood was that it had the potential to identify types of VF that were not likely to be found using the bioinformatics strategy employed in Chapter 3, such as metabolic proteins that are essential for growth on human blood, but not in other media.

The merits and disadvantages of *in vivo* analysis of strain libraries (IVET & STM) or *in vivo* analysis of transcription (SCOTS) are discussed in Chapter 1. Arguably these methods are the most effective for the analysis of proteins important for virulence, as they rely on analysis of bacterial gene expression, or requirement, in the host environment over the course of infection, rather than *in vitro*. In reference to this work, the primary disadvantage discussed in Chapter 1 is the clonal expansion of *S. aureus* in the host leading to loss of many viable strains from the *in vivo* assay results (McVicker *et al*., 2014; Prajsnar *et al*., 2012). Screening the NTML on human blood agar was considered a rapid alternative to these methods, allowing identification of genes essential for survival of *S. aureus* in a close approximation of a key host environment.

6.6 What is known about virulence determinants *in vivo*?

Identification of VFs is an important step in understanding the interactions between host and pathogen that lead to disease. Virulence factors and their known functions were discussed in detail in Chapter 1. Clearly, much of what is known about the mechanism of VFs is from *in vitro* analyses (Abraham & Jefferson, 2012; Higgins *et al*., 2006). The use of isogenic VF mutants verifies the requirement of a specific VF for disease, but

does not address what the protein does in the host, which has to be inferred from *in vitro* data. IsdA has multiple functions as an adhesin (Clarke *et al*., 2004), haem acquisition protein (Torres *et al*., 2010) and is important for immune evasion of secreted immune factors on the skin surface (Clarke *et al*., 2007). What is it used for *in vivo*? If IsdA has multiple functions, which function is the most essential for virulence? Is the function of IsdA dependent on the site of infection, demonstrating the adaptability of *S. aureus* to its host? These are interesting questions that are not broached by simple identification of VFs.

As an academic question it is interesting to know how a particular protein functions while in the host environment, where host proteins may interact with it blocking or enhancing its function. If academic curiosity towards these difficult problems leads to a greater understanding of the behaviour of VFs *in vivo*, this will have utilitarian benefits allowing for targeted drug design. A need rapidly becoming pressing, due to the evolution of resistance to many of the antibiotics used to treat important infections.

6.7 Future directions

This study used an *in silico* homology screen and a Tn mutant library screen on human blood to identify proteins important for the virulence of *S. aureus*. Proteins from a family with roles in immune evasion and nutrient biosynthesis proteins were found. Several methods could be employed to expand on this work. Comparison of *S. aureus* genomes to identify genes required for virulence cannot provide a complete understanding of why one strain is more virulent than another, as many *S. aureus* proteins have no designated function and slight sequence variations between strains may account for enhanced activity of individual proteins (Olivas *et al*., 2012). However, the genomes of subgroups of *S. aureus* associated with specific outbreaks or diseases could be compared to highlight subtle genomic differences, such as single nucleotide polymorphisms (SNPs) in order to determine their impact on virulence.

The Nebraska Tn mutagenesis library (NTML) is a valuable resource for the analysis of virulence determinants. The role of each of the 1,920 strains in pathogenicity could be assessed using the zebrafish embryo model of systemic infection. This work has highlighted the specificity of *S. aureus* virulence determinants, having an effect only on

human or a specific subset of species. Therefore, this specificity would likely lead to false negative results using the zebrafish model. This could be overcome using *ex vivo* human material. Multiple affects towards human cell lines could be assessed for each Tn disrupted gene, for example superantigenic activity towards B and T-cells, leukocyte apoptosis, necrosis, activation and phagocytosis.

It is by a combinatorial approach that a more comprehensive understanding of the role of individual virulence factors can be established. This in turn will identify components towards which novel control regimes can be directed to combat such an important human pathogen.

REFERENCES

Abraham, N. M., & Jefferson, K. K. (2012). *Staphylococcus aureus* clumping factor B mediates biofilm formation in the absence of calcium. *Microbiology (Reading, England)*, **158**(**Pt 6**): 1504–1512.

Akerley, B. J., Rubin, E. J., Camilli, A., Lampe, D. J., Robertson, H. M., & Mekalanos, J. J. (1998). Systematic identification of essential genes by *in vitro* mariner mutagenesis. *Proceedings of the National Academy of Sciences*, **95**(**15**): 8927–8932.

Aller, K., Adamberg, K., Reile, I., Timarova, V., Peebo, K., & Vilu, R. (2015). Excess of threonine compared to serine promotes threonine aldolase activity in *Lactococcus lactis* IL1403. *Microbiology (Reading, England)*. **161**(**Pt 5**): 1073-80.

Alonzo, F., Benson, M. A., Chen, J., Novick, R. P., Shopsin, B., & Torres, V. J. (2012). *Staphylococcus aureus* leucocidin ED contributes to systemic infection by targeting neutrophils and promoting bacterial growth *in vivo*. *Molecular Microbiology*, **83**(**2**): 423–435.

Alonzo III, F., Kozhaya, L., Rawlings, S. A., Reyes-Robles, T., DuMont, A. L., Myszka, D. G., Landau, N. R., Unutmaz, D., & Torres, V. J. (2012). CCR5 is a receptor for *Staphylococcus aureus* leukotoxin ED. *Nature*, **493**(**7430**): 51–55.

Al-Shangiti, A. M., Naylor, C. E., Nair, S. P., Briggs, D. C., Henderson, B., & Chain, B. M. (2004). Structural Relationships and Cellular Tropism of Staphylococcal Superantigen-Like Proteins. *Infection and Immunity*, **72**(**7**): 4261–4270.

Altschul, S. F., Gish, W., Miller, W., Myers, E. W., & Lipman, D. J. (1990). Basic local alignment search tool. *J Mol Biol*, **215**(**3**): 403–10.

Amagai, M., Yamaguchi, T., Hanakawa, Y., Nishifuji, K., Sugai, M., & Stanley, J. R. (2002). Staphylococcal exfoliative toxin B specifically cleaves desmoglein 1. *The Journal of Investigative Dermatology*, **118**(**5**): 845–850.

Amato, S. M., Fazen, C. H., Henry, T. C., Mok, W. W. K., Orman, M. A., Sandvik, E. L., Volzing, K. G., & Brynildsen, M. P. (2014). The role of metabolism in bacterial persistence. *Frontiers in Microbiology*, **5**: 70.

Angelichio, M. J., & Camilli, A. (2002). *In Vivo* Expression Technology. *Infection and Immunity*, **70**(**12**): 6518–6523.

Anzaldi, L. L., & Skaar, E. P. (2010). Overcoming the heme paradox: heme toxicity and tolerance in bacterial pathogens. *Infection and Immunity*, **78**(**12**): 4977–4989.

Appling, D. R. (1991). Compartmentation of folate-mediated one-carbon metabolism in eukaryotes. *The FASEB Journal*, **5**(**12**): 2645–2651.

Arcus, V. L., Langley, R., Proft, T., Fraser, J. D., & Baker, E. N. (2002). The Three-dimensional structure of a superantigen-like protein, SET3, from a pathogenicity island of the *Staphylococcus aureus* genome. *J Biol Chem*, **277**(**35**): 32274–81.

Argudín, M. Á., Mendoza, M. C., & Rodicio, M. R. (2010). Food poisoning and *Staphylococcus aureus* enterotoxins. *Toxins*, **2**(**7**): 1751–1773.

Armstrong, P. C. J., Hu, H., Rivera, J., Rigby, S., Chen, Y.-C., Howden, B. P., Gardiner, E., & Peter, K. (2012). Staphylococcal superantigen-like protein 5 induces thrombotic and bleeding complications *in vivo*: inhibition by an anti-SSL5 antibody and the glycan Bimosiamose. *Journal of thrombosis and haemostasis: JTH*, **10**(**12**): 2607–2609.

Arvidson, S., & Tegmark, K. (2001). Regulation of virulence determinants in *Staphylococcus aureus*. *International journal of medical microbiology: IJMM*, **291**(**2**): 159–170.

Askarian, F., van Sorge, N. M., Sangvik, M., Beasley, F. C., Henriksen, J. R., Sollid, J. U. E., van Strijp, J. A. G., Nizet, V., & Johannessen, M. (2014). A *Staphylococcus*

aureus TIR Domain Protein Virulence Factor Blocks TLR2-Mediated NF-κB Signaling. *Journal of Innate Immunity*. **6**(**4**): 485-98.

Atkins, K. L., Burman, J. D., Chamberlain, E. S., Cooper, J. E., Poutrel, B., Bagby, S., Jenkins, A. T. A., Feil, E. J., & van den Elsen, J. M. H. (2008). *S. aureus* IgG-binding proteins SpA and Sbi: host specificity and mechanisms of immune complex formation. *Molecular Immunology*, **45**(**6**): 1600–1611.

Atlas, R. M. (1997). *Principles of Microbiology*. McGraw-Hill Higher Education.

Autret, N., & Charbit, A. (2005). Lessons from signature-tagged mutagenesis on the infectious mechanisms of pathogenic bacteria. *FEMS Microbiology Reviews*, **29**(**4**): 703–717.

Baba, T., Takeuchi, F., Kuroda, M., Yuzawa, H., Aoki, K., Oguchi, A., Nagai, Y., Iwama, N., Asano, K., Naimi, T., Kuroda, H., Cui, L., Yamamoto, K., & Hiramatsu, K. (2002). Genome and virulence determinants of high virulence community-acquired MRSA. *Lancet (London, England)*, **359**(**9320**): 1819–1827.

Badarau, A., Rouha, H., Malafa, S., Logan, D. T., Håkansson, M., Stulik, L., Dolezilkova, I., Teubenbacher, A., Gross, K., Maierhofer, B., Weber, S., Jägerhofer, M., Hoffman, D., & Nagy, E. (2015). Structure-Function Analysis of Heterodimer Formation, Oligomerization, and Receptor Binding of the *Staphylococcus aureus* Bi-component Toxin LukGH. *The Journal of Biological Chemistry*, **290**(**1**): 142–156.

Bae, T., Banger, A. K., Wallace, A., Glass, E. M., Aslund, F., Schneewind, O., & Missiakas, D. M. (2004). *Staphylococcus aureus* virulence genes identified by *bursa aurealis* mutagenesis and nematode killing. *Proceedings of the National Academy of Sciences of the United States of America*, **101**(**33**): 12312–12317.

Bailey, L. B. (2009). *Folate in Health and Disease, Second Edition*. CRC Press.

Baltes, N., & Gerlach, G. F. (2004). Identification of Genes Transcribed by Actinobacillus pleuropneumoniae in Necrotic Porcine Lung Tissue by Using Selective Capture of Transcribed Sequences. *Infection and Immunity*, **72**(**11**): 6711–6716.

Bardoel, B. W., Vos, R., Bouman, T., Aerts, P. C., Bestebroer, J., Huizinga, E. G., Brondijk, T. H. C., van Strijp, J. A. G., & de Haas, C. J. C. (2012). Evasion of Toll-like receptor 2 activation by staphylococcal superantigen-like protein 3. *Journal of Molecular Medicine*, **90**(**10**): 1109–1120.

Barh, D., & Kumar, A. (2009). *In silico* identification of candidate drug and vaccine targets from various pathways in *Neisseria gonorrhoeae*. *In silico biology*, **9**(**4**): 225–231.

Barrio, M. B., Rainard, P., & Prévost, G. (2006). LukM/LukF'-PV is the most active *Staphylococcus aureus* leukotoxin on bovine neutrophils. *Microbes and Infection / Institut Pasteur*, **8**(**8**): 2068–2074.

Bartlett, A. H., & Hulten, K. G. (2010). *Staphylococcus aureus* pathogenesis: secretion systems, adhesins, and invasins. *The Pediatric Infectious Disease Journal*, **29**(**9**): 860–861.

Basset, G. J., Quinlivan, E. P., Ravanel, S., Rébeillé, F., Nichols, B. P., Shinozaki, K., Seki, M., Adams-Phillips, L. C., Giovannoni, J. J., Gregory, J. F., & others. (2004). Folate synthesis in plants: the *p*-aminobenzoate branch is initiated by a bifunctional PabA-PabB protein that is targeted to plastids. *Proceedings of the National Academy of Sciences of the United States of America*, **101**(**6**): 1496–1501.

Baxter-Gabbard, K. L., & Pattee, P. A. (1970). Purine biosynthesis in *Staphylococcus aureus*. *Archiv für Mikrobiologie*, **71**(**1**): 40–48.

Beasley, F. C., Marolda, C. L., Cheung, J., Buac, S., & Heinrichs, D. E. (2011). *Staphylococcus aureus* transporters Hts, Sir, and Sst capture iron liberated from human

transferrin by Staphyloferrin A, Staphyloferrin B, and catecholamine stress hormones, respectively, and contribute to virulence. *Infection and Immunity*, **79**(**6**): 2345–2355.

Bendtsen, J. D., Nielsen, H., von Heijne, G., & Brunak, S. (2004). Improved prediction of signal peptides: SignalP 3.0. *Journal of Molecular Biology*, **340**(**4**): 783–795.

Bennion, B. J., & Daggett, V. (2003). The molecular basis for the chemical denaturation of proteins by urea. *Proc Natl Acad Sci U S A*, **100**(**9**): 5142–7.

Benson, M. A., Lilo, S., Nygaard, T., Voyich, J. M., & Torres, V. J. (2012). Rot and SaeRS Cooperate To Activate Expression of the Staphylococcal Superantigen-Like Exoproteins. *Journal of Bacteriology*, **194**(**16**): 4355–4365.

Benson, M. A., Lilo, S., Wasserman, G. A., Thoendel, M., Smith, A., Horswill, A. R., Fraser, J., Novick, R. P., Shopsin, B., & Torres, V. J. (2011). *Staphylococcus aureus* regulates the expression and production of the staphylococcal superantigen-like secreted proteins in a Rot-dependent manner. *Molecular Microbiology*, **81**(**3**): 659–675.

Berends, E. T. M., Horswill, A. R., Haste, N. M., Monestier, M., Nizet, V., & von Köckritz-Blickwede, M. (2010). Nuclease expression by *Staphylococcus aureus* facilitates escape from neutrophil extracellular traps. *Journal of Innate Immunity*, **2**(**6**): 576–586.

Berube, B. J., Sampedro, G. R., Otto, M., & Bubeck Wardenburg, J. (2014). The psmα locus regulates production of *Staphylococcus aureus* alpha-toxin during infection. *Infection and Immunity*, **82**(**8**): 3350–3358.

Besier, S., Zander, J., Siegel, E., Saum, S. H., Hunfeld, K.-P., Ehrhart, A., Brade, V., & Wichelhaus, T. A. (2008). Thymidine-Dependent *Staphylococcus aureus* Small-Colony Variants: Human Pathogens That Are Relevant Not Only in Cases of Cystic Fibrosis Lung Disease. *Journal of Clinical Microbiology*, **46**(**11**): 3829–3832.

Bestebroer, J., Aerts, P. C., Rooijakkers, S. H. M., Pandey, M. K., Köhl, J., Van Strijp, J. A. G., & De Haas, C. J. C. (2010). Functional basis for complement evasion by staphylococcal superantigen-like 7: SSL7 inhibits C5a generation. *Cellular Microbiology*, **12**(**10**): 1506–1516.

Bestebroer, J., Poppelier, M. J., Ulfman, L. H., Lenting, P. J., Denis, C. V., van Kessel, K. P., van Strijp, J. A., & de Haas, C. J. (2007). Staphylococcal superantigen-like 5 binds PSGL-1 and inhibits P-selectin-mediated neutrophil rolling. *Blood*, **109**(**7**): 2936–43.

Bestebroer, J., van Kessel, K. P., Azouagh, H., Walenkamp, A. M., Boer, I. G., Romijn, R. A., van Strijp, J. A., & de Haas, C. J. (2009). Staphylococcal SSL5 inhibits leukocyte activation by chemokines and anaphylatoxins. *Blood*, **113**(**2**): 328–37.

Bischoff, M., Dunman, P., Kormanec, J., Macapagal, D., Murphy, E., Mounts, W., Berger-Bächi, B., & Projan, S. (2004). Microarray-based analysis of the *Staphylococcus aureus* sigmaB regulon. *Journal of Bacteriology*, **186**(**13**): 4085–4099.

Bjerketorp, J., Jacobsson, K., & Frykberg, L. (2004). The von Willebrand factor-binding protein (vWbp) of *Staphylococcus aureus* is a coagulase. *FEMS microbiology letters*, **234**(**2**): 309–314.

Boles, B. R., & Horswill, A. R. (2008). *agr*-Mediated Dispersal of *Staphylococcus aureus* Biofilms. *PLoS Pathogens*, **4**(**4**): e1000052.

Bose, J. L., Lehman, M. K., Fey, P. D., & Bayles, K. W. (2012). Contribution of the *Staphylococcus aureus* Atl AM and GL Murein Hydrolase Activities in Cell Division, Autolysis, and Biofilm Formation. (H. Ton-That, Ed.)*PLoS ONE*, **7**(**7**): e42244.

Bouillaut, L., Dubois, T., Sonenshein, A. L., & Dupuy, B. (2014). Integration of metabolism and virulence in *Clostridium difficile*. *Research in Microbiology*. **166**(**4**): 375-83.

Brain, R. A., Ramirez, A. J., Fulton, B. A., Chambliss, C. K., & Brooks, B. W. (2008). Herbicidal Effects of Sulfamethoxazole in *Lemna gibba* : Using *p* -Aminobenzoic Acid As a Biomarker of Effect. *Environmental Science & Technology*, **42**(**23**): 8965–8970.

Broeke-Smits, N. J. P. ten, Pronk, T. E., Jongerius, I., Bruning, O., Wittink, F. R., Breit, T. M., van Strijp, J. A. G., Fluit, A. C., & Boel, C. H. E. (2010). Operon structure of *Staphylococcus aureus*. *Nucleic Acids Research*, **38**(**10**): 3263–3274.

Bronner, S., Monteil, H., & Prévost, G. (2004). Regulation of virulence determinants in *Staphylococcus aureus*: complexity and applications. *FEMS Microbiology Reviews*, **28**(**2**): 183–200.

Brown, J. S., Aufauvre-Brown, A., Brown, J., Jennings, J. M., Arst, H., & Holden, D. W. (2000). Signature-tagged and directed mutagenesis identify PABA synthetase as essential for *Aspergillus fumigatus* pathogenicity. *Molecular microbiology*, **36**(**6**): 1371–1380.

Brown, R. F., & Stocker, B. A. (1987). *Salmonella typhi* 205aTy, a strain with two attenuating auxotrophic characters, for use in laboratory teaching. *Infection and immunity*, **55**(**4**): 892–898.

Bubeck Wardenburg, J., Palazzolo-Ballance, A. M., Otto, M., Schneewind, O., & DeLeo, F. R. (2008). Panton-Valentine leukocidin is not a virulence determinant in murine models of community-associated methicillin-resistant *Staphylococcus aureus* disease. *J Infect Dis*, **198**(**8**): 1166–70.

Buermans, H. P. J., & Dunnen, J. T. den. (2014). Next generation sequencing technology: Advances and applications. *Biochimica et Biophysica Acta (BBA) - Molecular Basis of Disease*, **1842**(**10**): 1932–1941.

Bukowski, M., Wladyka, B., & Dubin, G. (2010). Exfoliative Toxins of *Staphylococcus aureus*. *Toxins*, **2**(**5**): 1148–1165.

Burks, C., Fickett, J. W., Goad, W. B., Kanehisa, M., Lewitter, F. I., Rindone, W. P., Swindell, C. D., Tung, C.-S., & Bilofsky, H. S. (1985). CABIOS REVIEW The GenBank nucleic acid sequence database. *Computer applications in the biosciences: CABIOS*, **1**(**4**): 225–233.

Burman, J. D., Leung, E., Atkins, K. L., O'Seaghdha, M. N., Lango, L., Bernadó, P., Bagby, S., Svergun, D. I., Foster, T. J., Isenman, D. E., & van den Elsen, J. M. H. (2008). Interaction of human complement with Sbi, a staphylococcal immunoglobulin-binding protein: indications of a novel mechanism of complement evasion by *Staphylococcus aureus*. *The Journal of Biological Chemistry*, **283**(**25**): 17579–17593.

Burrack, L. S., & Higgins, D. E. (2007). Genomic approaches to understanding bacterial virulence. *Current Opinion in Microbiology*, **10**(**1**): 4–9.

Cadieux, B., Vijayakumaran, V., Bernards, M. A., McGavin, M. J., & Heinrichs, D. E. (2014). Role of Lipase from Community-Associated Methicillin-Resistant *Staphylococcus aureus* Strain USA300 in Hydrolyzing Triglycerides into Growth-Inhibitory Free Fatty Acids. *Journal of Bacteriology*, **196**(**23**): 4044–4056.

Camacho, C., Coulouris, G., Avagyan, V., Ma, N., Papadopoulos, J., Bealer, K., & Madden, T. L. (2009). BLAST+: architecture and applications. *BMC bioinformatics*, **10**: 421.

Carlsson, P., & Hederstedt, L. (1989). Genetic characterization of Bacillus subtilis *odhA* and *odhB*, encoding 2-oxoglutarate dehydrogenase and dihydrolipoamide transsuccinylase, respectively. *Journal of bacteriology*, **171**(**7**): 3667–3672.

Casey, A. L., Lambert, P. A., & Elliott, T. S. J. (2007). Staphylococci. *International Journal of Antimicrobial Agents*, **29 Suppl 3**: S23–32.

Cassat, J. E., & Skaar, E. P. (2012). Metal ion acquisition in *Staphylococcus aureus*: overcoming nutritional immunity. *Seminars in immunopathology*, **34**(**2**): 215–235.

Chaibenjawong, P., & Foster, S. J. (2011). Desiccation tolerance in *Staphylococcus aureus*. *Archives of Microbiology*, **193**(**2**): 125–135.

Chatterjee, I., Kriegeskorte, A., Fischer, A., Deiwick, S., Theimann, N., Proctor, R. A., Peters, G., Herrmann, M., & Kahl, B. C. (2008). *In Vivo* Mutations of Thymidylate Synthase (Encoded by *thyA*) Are Responsible for Thymidine Dependency in Clinical Small-Colony Variants of *Staphylococcus aureus*. *Journal of Bacteriology*, **190**(**3**): 834–842.

Chaudhuri, R. R., Allen, A. G., Owen, P. J., Shalom, G., Stone, K., Harrison, M., Burgis, T. A., Lockyer, M., Garcia-Lara, J., Foster, S. J., Pleasance, S. J., Peters, S. E., Maskell, D. J., & Charles, I. G. (2009). Comprehensive identification of essential *Staphylococcus aureus* genes using Transposon-Mediated Differential Hybridisation (TMDH). *BMC genomics*, **10**: 291.

Chavakis, T., Preissner, K. T., & Herrmann, M. (2007). The anti-inflammatory activities of *Staphylococcus aureus*. *Trends in immunology*, **28**(**9**): 408–418.

Cheng, A. G., Missiakas, D., & Schneewind, O. (2014). The giant protein Ebh is a determinant of *Staphylococcus aureus* cell size and complement resistance. *Journal of Bacteriology*, **196**(**5**): 971–981.

Cheng, Y. S., Shen, Y., Rudolph, J., Stern, M., Stubbe, J., Flannigan, K. A., & Smith, J. M. (1990). Glycinamide ribonucleotide synthetase from *Escherichia coli*: cloning, overproduction, sequencing, isolation, and characterization. *Biochemistry*, **29**(**1**): 218–227.

Chernyshev, A., Fleischmann, T., & Kohen, A. (2007). Thymidyl biosynthesis enzymes as antibiotic targets. *Applied Microbiology and Biotechnology*, **74**(**2**): 282–289.

Cheung, A. L., Bayer, A. S., Zhang, G., Gresham, H., & Xiong, Y.-Q. (2004). Regulation of virulence determinants *in vitro* and *in vivo* in *Staphylococcus aureus*. *FEMS Immunology & Medical Microbiology*, **40**(**1**): 1–9.

Cheung, A. L., Nishina, K. A., Trotonda, M. P., & Tamber, S. (2008). The SarA protein family of *Staphylococcus aureus*. *The International Journal of Biochemistry & Cell Biology*, **40**(**3**): 355–361.

Cheung, G. Y. C., Wang, R., Khan, B. A., Sturdevant, D. E., & Otto, M. (2011). Role of the Accessory Gene Regulator *agr* in Community-Associated Methicillin-Resistant *Staphylococcus aureus* Pathogenesis. *Infection and Immunity*, **79**(**5**): 1927–1935.

Chien, Y., Manna, A. C., Projan, S. J., & Cheung, A. L. (1999). SarA, a global regulator of virulence determinants in *Staphylococcus aureus*, binds to a conserved motif essential for sar-dependent gene regulation. *The Journal of Biological Chemistry*, **274**(**52**): 37169–37176.

Chow, A. W., Gribble, M. J., & Bartlett, K. H. (1983). Characterization of the hemolytic activity of *Staphylococcus aureus* strains associated with toxic shock syndrome. *Journal of Clinical Microbiology*, **17**(**3**): 524–528.

Chung, M. C., Wines, B. D., Baker, H., Langley, R. J., Baker, E. N., & Fraser, J. D. (2007). The crystal structure of staphylococcal superantigen-like protein 11 in complex with sialyl Lewis X reveals the mechanism for cell binding and immune inhibition. *Mol Microbiol*, **66**(**6**): 1342–55.

Claassen, M., Nouwen, J., Fang, Y., Ott, A., Verbrugh, H., Hofman, A., van Belkum, A., & Uitterlinden, A. (2005). *Staphylococcus aureus* nasal carriage is not associated with

known polymorphism in the Vitamin D receptor gene. *FEMS Immunol Med Microbiol*, **43**(**2**): 173–6.

Clarke, S. R., Andre, G., Walsh, E. J., Dufrene, Y. F., Foster, T. J., & Foster, S. J. (2009). Iron-Regulated Surface Determinant Protein A Mediates Adhesion of *Staphylococcus aureus* to Human Corneocyte Envelope Proteins. *Infection and Immunity*, **77**(**6**): 2408–2416.

Clarke, S. R., Brummell, K. J., Horsburgh, M. J., McDowell, P. W., Mohamad, S. A. S., Stapleton, M. R., Acevedo, J., Read, R. C., Day, N. P., Peacock, S. J., & others. (2006). Identification of *in vivo*–expressed antigens of *Staphylococcus aureus* and their use in vaccinations for protection against nasal carriage. *Journal of Infectious Diseases*, **193**(**8**): 1098–1108.

Clarke, S. R., Mohamed, R., Bian, L., Routh, A. F., Kokai-Kun, J. F., Mond, J. J., Tarkowski, A., & Foster, S. J. (2007). The *Staphylococcus aureus* surface protein IsdA mediates resistance to innate defenses of human skin. *Cell Host Microbe*, **1**(**3**): 199–212.

Clarke, S. R., Wiltshire, M. D., & Foster, S. J. (2004). IsdA of *Staphylococcus aureus* is a broad spectrum, iron-regulated adhesin. *Molecular Microbiology*, **51**(**5**): 1509–1519.

Clement, S., Vaudaux, P., Francois, P., Schrenzel, J., Huggler, E., Kampf, S., Chaponnier, C., Lew, D., & Lacroix, J.-S. (2005). Evidence of an intracellular reservoir in the nasal mucosa of patients with recurrent *Staphylococcus aureus* rhinosinusitis. *The Journal of Infectious Diseases*, **192**(**6**): 1023–1028.

Coates, R., Moran, J., & Horsburgh, M. J. (2014). Staphylococci: colonizers and pathogens of human skin. *Future Microbiology*, **9**(**1**): 75–91.

Cooper, M. D., & Herrin, B. R. (2010). How did our complex immune system evolve? *Nature Reviews. Immunology*, **10**(**1**): 2–3.

Corrigan, R. M., Miajlovic, H., & Foster, T. J. (2009). Surface proteins that promote adherence of *Staphylococcus aureus* to human desquamated nasal epithelial cells. *BMC Microbiology*, **9**(**1**): 22.

Corrigan, R. M., Rigby, D., Handley, P., & Foster, T. J. (2007). The role of *Staphylococcus aureus* surface protein SasG in adherence and biofilm formation. *Microbiology (Reading, England)*, **153**(**Pt 8**): 2435–2446.

Cosgrove, K., Coutts, G., Jonsson, I.-M., Tarkowski, A., Kokai-Kun, J. F., Mond, J. J., & Foster, S. J. (2007). Catalase (KatA) and Alkyl Hydroperoxide Reductase (AhpC) Have Compensatory Roles in Peroxide Stress Resistance and Are Required for Survival, Persistence, and Nasal Colonization in *Staphylococcus aureus*. *Journal of Bacteriology*, **189**(**3**): 1025–1035.

Coulter, S. N., Schwan, W. R., Ng, E. Y., Langhorne, M. H., Ritchie, H. D., Westbrock-Wadman, S., Hufnagle, W. O., Folger, K. R., Bayer, A. S., & Stover, C. K. (1998). *Staphylococcus aureus* genetic loci impacting growth and survival in multiple infection environments. *Molecular Microbiology*, **30**(**2**): 393–404.

Craven, R. R., Gao, X., Allen, I. C., Gris, D., Bubeck Wardenburg, J., McElvania-Tekippe, E., Ting, J. P., & Duncan, J. A. (2009). *Staphylococcus aureus* alpha-hemolysin activates the NLRP3-inflammasome in human and mouse monocytic cells. *PloS One*, **4**(**10**): e7446.

Cross, A. S. (2008). What is a virulence factor? *Critical Care*, **12**(**6**): 196.

Dalla Serra, M., Coraiola, M., Viero, G., Comai, M., Potrich, C., Ferreras, M., Baba-Moussa, L., Colin, D. A., Menestrina, G., Bhakdi, S., & Prévost, G. (2005). *Staphylococcus aureus* bicomponent gamma-hemolysins, HlgA, HlgB, and HlgC, can

form mixed pores containing all components. *Journal of Chemical Information and Modeling*, **45**(**6**): 1539–1545.

Darwin, A. J. (2005). Genome-wide screens to identify genes of human pathogenic *Yersinia* species that are expressed during host infection. *Current issues in molecular biology*, **7**(**2**): 135.

de Haas, C. J. C. (2004). Chemotaxis Inhibitory Protein of *Staphylococcus aureus*, a Bacterial Antiinflammatory Agent. *Journal of Experimental Medicine*, **199**(**5**): 687–695.

de Haas, C. J. C., Weeterings, C., Vughs, M. M., De Groot, P. G., Van Strijp, J. A., & Lisman, T. (2009). Staphylococcal superantigen-like 5 activates platelets and supports platelet adhesion under flow conditions, which involves glycoprotein Ibα and $\alpha_{IIb}\beta_3$. *Journal of Thrombosis and Haemostasis*, **7**(**11**): 1867–1874.

Dellabona, P., Peccoud, J., Kappler, J., Marrack, P., Benoist, C., & Mathis, D. (1990). Superantigens interact with MHC class II molecules outside of the antigen groove. *Cell*, **62**(**6**): 1115–1121.

Denk, D., & Böck, A. (1987). L-cysteine biosynthesis in *Escherichia coli*: nucleotide sequence and expression of the serine acetyltransferase (*cysE*) gene from the wild-type and a cysteine-excreting mutant. *Journal of General Microbiology*, **133**(**3**): 515–525.

Devos, D., & Valencia, A. (2001). Intrinsic errors in genome annotation. *Trends in genetics: TIG*, **17**(**8**): 429–431.

De Vries, A., Alexander, B., & Quamo, Y. (1948). Studies on amino acid metabolism. II. Blood glycine and total amino acids in various pathological conditions, with observations on the effects of intravenously administered glycine. *Journal of Clinical Investigation*, **27**(**5**): 655.

Dineen, S. S., McBride, S. M., & Sonenshein, A. L. (2010). Integration of Metabolism and Virulence by *Clostridium difficile* CodY. *Journal of Bacteriology*, **192**(**20**): 5350–5362.

Dockrell, D. H., Marriott, H. M., Prince, L. R., Ridger, V. C., Ince, P. G., Hellewell, P. G., & Whyte, M. K. B. (2003). Alveolar macrophage apoptosis contributes to pneumococcal clearance in a resolving model of pulmonary infection. *Journal of Immunology (Baltimore, Md.: 1950)*, **171**(**10**): 5380–5388.

Dohlsten, M., Björklund, M., Sundstedt, A., Hedlund, G., Samson, D., & Kalland, T. (1993). Immunopharmacology of the superantigen staphylococcal enterotoxin A in T-cell receptor V beta 3 transgenic mice. *Immunology*, **79**(**4**): 520.

Donegan, N. P., Marvin, J. S., & Cheung, A. L. (2014). Role of Adaptor TrfA and ClpPC in Controlling Levels of SsrA-Tagged Proteins and Antitoxins in *Staphylococcus aureus*. *Journal of Bacteriology*, **196**(**23**): 4140–4151.

Doxey, A. C., & McConkey, B. J. (2013). Prediction of molecular mimicry candidates in human pathogenic bacteria. *Virulence*, **4**(**6**): 453–466.

Dumont, A. L., Nygaard, T. K., Watkins, R. L., Smith, A., Kozhaya, L., Kreiswirth, B. N., Shopsin, B., Unutmaz, D., Voyich, J. M., & Torres, V. J. (2011). Characterization of a new cytotoxin that contributes to *Staphylococcus aureus* pathogenesis. *Mol Microbiol*, **79**(**3**): 814–25.

DuMont, A. L., Yoong, P., Day, C. J., Alonzo, F., McDonald, W. H., Jennings, M. P., & Torres, V. J. (2013)a. *Staphylococcus aureus* LukAB cytotoxin kills human neutrophils by targeting the CD11b subunit of the integrin Mac-1. *Proceedings of the National Academy of Sciences of the United States of America*, **110**(**26**): 10794–10799.

DuMont, A. L., Yoong, P., Liu, X., Day, C. J., Chumbler, N. M., James, D. B. A., Alonzo, F., Bode, N. J., Lacy, D. B., Jennings, M. P., & Torres, V. J. (2014). Identification of

a Crucial Residue Required for *Staphylococcus aureus* LukAB Cytotoxicity and Receptor Recognition. *Infection and Immunity*, **82**(**3**): 1268–1276.

DuMont, A. L., Yoong, P., Surewaard, B. G. J., Benson, M. A., Nijland, R., van Strijp, J. A. G., & Torres, V. J. (2013)b. *Staphylococcus aureus* Elaborates Leukocidin AB To Mediate Escape from within Human Neutrophils. *Infection and Immunity*, **81**(**5**): 1830–1841.

d'Urso-Scott, M., Uhoch, J., & Bertino, J. R. (1974). Formation of 10-formylfolic acid, a potent inhibitor of dihydrofolate reductase, in rat liver slices incubated with folic acid. *Proceedings of the National Academy of Sciences*, **71**(**7**): 2736–2739.

Duthie, E. S., & Lorenz, L. L. (1952). Staphylococcal coagulase; mode of action and antigenicity. *Journal of General Microbiology*, **6**(**1-2**): 95–107.

Dutta, D., Dutta, A., Bhattacharjee, A., Basak, A., & Das, A. K. (2014). Cloning, expression, crystallization and preliminary X-ray diffraction studies of staphylococcal superantigen-like protein 1 (SSL1). *Acta Crystallographica Section F Structural Biology Communications*, **70**(**5**): 600–603.

Edwards, A. M., Potter, U., Meenan, N. A. G., Potts, J. R., & Massey, R. C. (2011). *Staphylococcus aureus* keratinocyte invasion is dependent upon multiple high-affinity fibronectin-binding repeats within FnBPA. *PloS One*, **6**(**4**): e18899.

Ellis, M., Serreli, A., Colque-Navarro, P., Hedstrom, U., Chacko, A., Siemkowicz, E., & Möllby, R. (2003). Role of staphylococcal enterotoxin A in a fatal case of endocarditis. *Journal of Medical Microbiology*, **52**(**Pt 2**): 109–112.

Ernst, D. C., & Downs, D. M. (2015). The *stm4195* gene product (PanS) transports Coenzyme A precursors in *Salmonella enterica*. *Journal of Bacteriology*, **197**(**8**) 1368-77.

Falugi, F., Kim, H. K., Missiakas, D. M., & Schneewind, O. (2013). Role of protein A in the evasion of host adaptive immune responses by *Staphylococcus aureus*. *mBio*, **4**(**5**): e00575–13.

Farrington, M., Brenwald, N., Haines, D., & Walpole, E. (1992). Resistance to desiccation and skin fatty acids in outbreak strains of methicillin-resistant *Staphylococcus aureus*. *Journal of medical microbiology*, **36**(**1**): 56–60.

Fechter, P., Caldelari, I., Lioliou, E., & Romby, P. (2014). Novel aspects of RNA regulation in *Staphylococcus aureus*. *FEBS Letters*, **588**(**15**): 2523–2529.

Federhen, S. (2012). The NCBI Taxonomy database. *Nucleic Acids Research*, **40**(**Database issue**): D136-143.

Fedtke, I. (2004). Bacterial evasion of innate host defenses--the *Staphylococcus aureus* lesson. *International Journal of Medical Microbiology*, **294**(**2-3**): 189–194.

Fevre, C., Bestebroer, J., Mebius, M. M., de Haas, C. J. C., van Strijp, J. A. G., Fitzgerald, J. R., & Haas, P.-J. A. (2014). *Staphylococcus aureus* proteins SSL6 and SElX interact with neutrophil receptors as identified using secretome phage display: Bacterial protein-cell interaction by phage display. *Cellular Microbiology*, **16**(**11**): 1646–1665.

Fey, P. D., Endres, J. L., Yajjala, V. K., Widhelm, T. J., Boissy, R. J., Bose, J. L., & Bayles, K. W. (2013). A genetic resource for rapid and comprehensive phenotype screening of nonessential *Staphylococcus aureus* genes. *MBio*, **4**(**1**): e00537–12.

Finn, R. D., Bateman, A., Clements, J., Coggill, P., Eberhardt, R. Y., Eddy, S. R., Heger, A., Hetherington, K., Holm, L., Mistry, J., Sonnhammer, E. L. L., Tate, J., & Punta, M. (2014). Pfam: the protein families database. *Nucleic Acids Research*, **42**(**Database issue**): D222–230.

Fitzgerald, J. R., Reid, S. D., Ruotsalainen, E., Tripp, T. J., Liu, M., Cole, R., Kuusela, P., Schlievert, P. M., Jarvinen, A., & Musser, J. M. (2003). Genome diversification in

Staphylococcus aureus: Molecular evolution of a highly variable chromosomal region encoding the Staphylococcal exotoxin-like family of proteins. *Infect Immun*, **71**(**5**): 2827–38.

Fleischmann, R. D., Adams, M. D., White, O., Clayton, R. A., Kirkness, E. F., Kerlavage, A. R., Bult, C. J., Tomb, J. F., Dougherty, B. A., & Merrick, J. M. (1995). Whole-genome random sequencing and assembly of *Haemophilus influenzae* Rd. *Science (New York, N.Y.)*, **269**(**5223**): 496–512.

Flock, J. I., Fröman, G., Jönsson, K., Guss, B., Signäs, C., Nilsson, B., Raucci, G., Höök, M., Wadström, T., & Lindberg, M. (1987). Cloning and expression of the gene for a fibronectin-binding protein from *Staphylococcus aureus*. *The EMBO journal*, **6**(**8**): 2351.

Foster, S. J. (1995). Molecular characterization and functional analysis of the major autolysin of *Staphylococcus aureus* 8325/4. *Journal of bacteriology*, **177**(**19**): 5723–5725.

Foster, T. J. (2005). Immune evasion by staphylococci. *Nat Rev Microbiol*, **3**(**12**): 948–58.

Foster, T. J., & Höök, M. (1998). Surface protein adhesins of *Staphylococcus aureus*. *Trends in Microbiology*, **6**(**12**): 484–488.

Francis, J. S., Doherty, M. C., Lopatin, U., Johnston, C. P., Sinha, G., Ross, T., Cai, M., Hansel, N. N., Perl, T., Ticehurst, J. R., Carroll, K., Thomas, D. L., Nuermberger, E., & Bartlett, J. G. (2005). Severe community-onset pneumonia in healthy adults caused by methicillin-resistant *Staphylococcus aureus* carrying the Panton-Valentine leukocidin genes. *Clinical Infectious Diseases: An Official Publication of the Infectious Diseases Society of America*, **40**(**1**): 100–107.

François, P., Scherl, A., Hochstrasser, D., & Schrenzel, J. (2010). Proteomic approaches to study *Staphylococcus aureus* pathogenesis. *Journal of Proteomics*, **73**(**4**): 701–708.

Friso, S., & Choi, S.-W. (2005). Gene-nutrient interactions in one-carbon metabolism. *Current drug metabolism*, **6**(**1**): 37–46.

Gaca, A. O., Colomer-Winter, C., & Lemos, J. A. (2015). Many Means to a Common End: the Intricacies of (p)ppGpp Metabolism and Its Control of Bacterial Homeostasis. (W. Margolin, Ed.)*Journal of Bacteriology*, **197**(**7**): 1146–1156.

Garcia, B. L., Summers, B. J., Lin, Z., Ramyar, K. X., Ricklin, D., Kamath, D. V., Fu, Z.-Q., Lambris, J. D., & Geisbrecht, B. V. (2012). Diversity in the C3b [corrected] contact residues and tertiary structures of the staphylococcal complement inhibitor (SCIN) protein family. *The Journal of Biological Chemistry*, **287**(**1**): 628–640.

Garcia, L. G., Lemaire, S., Kahl, B. C., Becker, K., Proctor, R. A., Denis, O., Tulkens, P. M., & Van Bambeke, F. (2013). Antibiotic activity against small-colony variants of *Staphylococcus aureus*: review of *in vitro*, animal and clinical data. *Journal of Antimicrobial Chemotherapy*, **68**(**7**): 1455–1464.

Geiger, T., Goerke, C., Mainiero, M., Kraus, D., & Wolz, C. (2008). The virulence regulator Sae of *Staphylococcus aureus*: promoter activities and response to phagocytosis-related signals. *Journal of Bacteriology*, **190**(**10**): 3419–3428.

Geisinger, E., Adhikari, R. P., Jin, R., Ross, H. F., & Novick, R. P. (2006). Inhibition of *rot* translation by RNAIII, a key feature of *agr* function. *Molecular Microbiology*, **61**(**4**): 1038–1048.

Gemmell, C. G. (1986). Coagulase-negative staphylococci. *Journal of Medical Microbiology*, **22**(**4**): 285–295.

Geoghegan, J. A., Corrigan, R. M., Gruszka, D. T., Speziale, P., O'Gara, J. P., Potts, J. R., & Foster, T. J. (2010). Role of surface protein SasG in biofilm formation by *Staphylococcus aureus*. *Journal of Bacteriology*, **192**(**21**): 5663–5673.

George, E. A., & Muir, T. W. (2007). Molecular Mechanisms of *agr* Quorum Sensing in Virulent Staphylococci. *ChemBioChem*, **8**(**8**): 847–855.

Giese, B., Glowinski, F., Paprotka, K., Dittmann, S., Steiner, T., Sinha, B., & Fraunholz, M. J. (2011). Expression of δ-toxin by *Staphylococcus aureus* mediates escape from phago-endosomes of human epithelial and endothelial cells in the presence of β-toxin. *Cellular Microbiology*, **13**(**2**): 316–329.

Gill, S. R., Fouts, D. E., Archer, G. L., Mongodin, E. F., DeBoy, R. T., Ravel, J., Paulsen, I. T., Kolonay, J. F., Brinkac, L., Beanan, M., Dodson, R. J., Daugherty, S. C., Madupu, R., Angiuoli, S. V., Durkin, A. S., Haft, D. H., Vamathevan, J., Khouri, H., Utterback, T., Lee, C., et al. (2005). Insights on Evolution of Virulence and Resistance from the Complete Genome Analysis of an Early Methicillin-Resistant *Staphylococcus aureus* Strain and a Biofilm-Producing Methicillin-Resistant *Staphylococcus epidermidis* Strain. *Journal of Bacteriology*, **187**(**7**): 2426–2438.

Giraudo, A. T., Rampone, H., Calzolari, A., & Nagel, R. (1996). Phenotypic characterization and virulence of a *sae- agr-* mutant of *Staphylococcus aureus*. *Canadian Journal of Microbiology*, **42**(**2**): 120–123.

Gladysheva, I. P., Turner, R. B., Sazonova, I. Y., Liu, L., & Reed, G. L. (2003). Coevolutionary patterns in plasminogen activation. *Proceedings of the National Academy of Sciences of the United States of America*, **100**(**16**): 9168–9172.

Goerke, C., Fluckiger, U., Steinhuber, A., Bisanzio, V., Ulrich, M., Bischoff, M., Patti, J. M., & Wolz, C. (2005). Role of *Staphylococcus aureus* Global Regulators *sae* and sigmaB in Virulence Gene Expression during Device-Related Infection. *Infection and Immunity*, **73**(**6**): 3415–3421.

Golovanov, A. P., Hautbergue, G. M., Wilson, S. A., & Lian, L. Y. (2004). A simple method for improving protein solubility and long-term stability. *J Am Chem Soc*, **126**(**29**): 8933–9.

Gouaux, J. E., Braha, O., Hobaugh, M. R., Song, L., Cheley, S., Shustak, C., & Bayley, H. (1994). Subunit stoichiometry of staphylococcal alpha-hemolysin in crystals and on membranes: a heptameric transmembrane pore. *Proceedings of the National Academy of Sciences of the United States of America*, **91**(**26**): 12828–12831.

Graham, J. E., & Clark-Curtiss, J. E. (1999). Identification of *Mycobacterium tuberculosis* RNAs synthesized in response to phagocytosis by human macrophages by selective capture of transcribed sequences (SCOTS). *Proceedings of the National Academy of Sciences*, **96**(**20**): 11554–11559.

Grilo, I. R., Ludovice, A. M., Tomasz, A., de Lencastre, H., & Sobral, R. G. (2014). The glucosaminidase domain of Atl - the major *Staphylococcus aureus* autolysin - has DNA-binding activity. *MicrobiologyOpen*, **3**(**2**): 247–256.

Hadi, T., Dahl, U., Mayer, C., & Tanner, M. E. (2008). Mechanistic Studies on *N* -Acetylmuramic Acid 6-Phosphate Hydrolase (MurQ): An Etherase Involved in Peptidoglycan Recycling. *Biochemistry*, **47**(**44**): 11547–11558.

Hadi, T., Hazra, S., Tanner, M. E., & Blanchard, J. S. (2013). Structure of MurNAc 6-Phosphate Hydrolase (MurQ) from *Haemophilus influenzae* with a Bound Inhibitor. *Biochemistry*, **52**(**51**): 9358–9366.

Haggar, A., Ehrnfelt, C., Holgersson, J., & Flock, J.-I. (2004). The extracellular adherence protein from *Staphylococcus aureus* inhibits neutrophil binding to endothelial cells. *Infection and Immunity*, **72**(**10**): 6164–6167.

Haggar, A., Hussain, M., Lönnies, H., Herrmann, M., Norrby-Teglund, A., & Flock, J.-I. (2003). Extracellular adherence protein from *Staphylococcus aureus* enhances internalization into eukaryotic cells. *Infection and Immunity*, **71**(**5**): 2310–2317.

Hair, P. S., Foley, C. K., Krishna, N. K., Nyalwidhe, J. O., Geoghegan, J. A., Foster, T. J., & Cunnion, K. M. (2013). Complement regulator C4BP binds to *Staphylococcus aureus* surface proteins SdrE and Bbp inhibiting bacterial opsonization and killing. *Results in Immunology*, **3**: 114–121.**Hair, P. S., Ward, M. D., Semmes, O. J., Foster, T. J., & Cunnion, K. M.** (2008). *Staphylococcus aureus* clumping factor A binds to complement regulator factor I and increases factor I cleavage of C3b. *The Journal of Infectious Diseases*, **198**(**1**): 125–133.

Hamer, L., DeZwaan, T. M., Montenegro-Chamorro, M. V., Frank, S. A., & Hamer, J. E. (2001). Recent advances in large-scale transposon mutagenesis. *Current Opinion in Chemical Biology*, **5**(**1**): 67–73.

Hamilton-Miller, J. M. T. (1988). Reversal of activity of trimethoprim against gram-positive cocci by thymidine, thymine and "folates." *Journal of Antimicrobial Chemotherapy*, **22**(**1**): 35–39.

Hammer, N. D., & Skaar, E. P. (2011). Molecular mechanisms of *Staphylococcus aureus* iron acquisition. *Annual Review of Microbiology*, **65**: 129–147.

Hammer, N. D., & Skaar, E. P. (2012). The impact of metal sequestration on *Staphylococcus aureus* metabolism. *Current Opinion in Microbiology*, **15**(**1**): 10–14.

Hanakawa, Y., Schechter, N. M., Lin, C., Garza, L., Li, H., Yamaguchi, T., Fudaba, Y., Nishifuji, K., Sugai, M., Amagai, M., & Stanley, J. R. (2002). Molecular mechanisms of blister formation in bullous impetigo and staphylococcal scalded skin syndrome. *The Journal of Clinical Investigation*, **110**(**1**): 53–60.

Hartford, O., Francois, P., Vaudaux, P., & Foster, T. J. (1997). The dipeptide repeat region of the fibrinogen-binding protein (clumping factor) is required for functional expression of the fibrinogen-binding domain on the *Staphylococcus aureus* cell surface. *Molecular Microbiology*, **25**(**6**): 1065–1076.

Hartmann, G., Behr, W., Beissner, K.-A., Honikel, K., & Sippel, A. (1968). Antibiotics as inhibitors of nucleic acid and protein synthesis. *Angewandte Chemie International Edition in English*, **7**(**9**): 693–701.

Hart, M. E., Smeltzer, M. S., & Iandolo, J. J. (1993). The extracellular protein regulator (*xpr*) affects exoprotein and *agr* mRNA levels in *Staphylococcus aureus*. *Journal of bacteriology*, **175**(**24**): 7875–7879.

Hart, M. E., Tsang, L. H., Deck, J., Daily, S. T., Jones, R. C., Liu, H., Hu, H., Hart, M. J., & Smeltzer, M. S. (2013). Hyaluronidase expression and biofilm involvement in *Staphylococcus aureus* UAMS-1 and its *sarA*, *agr* and *sarA agr* regulatory mutants. *Microbiology*, **159**(**Pt 4**): 782–791.

Harvey, R. J. (1973). Growth and Initiation of Protein Synthesis in *Escherichia coli* in the Presence of Trimethoprim. *Journal of Bacteriology*, **114**(**1**): 309–322.

Hawser, S., Lociuro, S., & Islam, K. (2006). Dihydrofolate reductase inhibitors as antibacterial agents. *Biochemical Pharmacology*, **71**(**7**): 941–948.

Hayes, F. (2003). Transposon-based strategies for microbial functional genomics and proteomics. *Annual Review of Genetics*, **37**(**1**): 3–29.

Hecker, M., Becher, D., Fuchs, S., & Engelmann, S. (2010). A proteomic view of cell physiology and virulence of *Staphylococcus aureus*. *International journal of medical microbiology: IJMM*, **300**(**2-3**): 76–87.

Heilmann, C., Hartleib, J., Hussain, M. S., & Peters, G. (2005). The Multifunctional *Staphylococcus aureus* Autolysin Aaa Mediates Adherence to Immobilized Fibrinogen and Fibronectin. *Infection and Immunity*, **73**(**8**): 4793–4802.

He, J., Wang, G., Xu, R., Feng, J., Wang, J., Su, H., & Song, H. (2008). Refolding of a staphylokinase variant y1-Sak by reverse dilution. *Applied Biochemistry and Biotechnology*, **151**(**1**): 29–41.

Hempel, K., Pané-Farré, J., Otto, A., Sievers, S., Hecker, M., & Becher, D. (2010). Quantitative Cell Surface Proteome Profiling for SigB-Dependent Protein Expression in the Human Pathogen *Staphylococcus aureus* via Biotinylation Approach. *Journal of Proteome Research*, **9**(**3**): 1579–1590.

Hensel, M., Shea, J. E., Gleeson, C., Jones, M. D., Dalton, E., & Holden, D. W. (1995). Simultaneous identification of bacterial virulence genes by negative selection. *Science (New York, N.Y.)*, **269**(**5222**): 400–403.

Herbert, K. C., & Foster, S. J. (2001). Starvation survival in *Listeria monocytogenes*: characterization of the response and the role of known and novel components. *Microbiology (Reading, England)*, **147**(**Pt 8**): 2275–2284.

Herbert, S., Bera, A., Nerz, C., Kraus, D., Peschel, A., Goerke, C., Meehl, M., Cheung, A., & Götz, F. (2007). Molecular Basis of Resistance to Muramidase and Cationic Antimicrobial Peptide Activity of Lysozyme in Staphylococci. *PLoS Pathogens*, **3**(**7**): e102.

Hermans, S. J., Baker, H. M., Sequeira, R. P., Langley, R. J., Baker, E. N., & Fraser, J. D. (2012). Structural and functional properties of staphylococcal superantigen-like protein 4. *Infection and Immunity*, **80**(**11**): 4004–4013.

Heroven, A. K., & Dersch, P. (2014). Coregulation of host-adapted metabolism and virulence by pathogenic yersiniae. *Frontiers in Cellular and Infection Microbiology*, **4**: 146.

Hienz, S. A., Schennings, T., Heimdahl, A., & Flock, J. I. (1996). Collagen binding of *Staphylococcus aureus* is a virulence factor in experimental endocarditis. *The Journal of Infectious Diseases*, **174**(**1**): 83–88.

Higgins, J., Loughman, A., van Kessel, K. P. M., van Strijp, J. A. G., & Foster, T. J. (2006). Clumping factor A of *Staphylococcus aureus* inhibits phagocytosis by human polymorphonuclear leucocytes. *FEMS microbiology letters*, **258**(**2**): 290–296.

Hirschhausen, N., Schlesier, T., Schmidt, M. A., Götz, F., Peters, G., & Heilmann, C. (2010). A novel staphylococcal internalization mechanism involves the major autolysin Atl and heat shock cognate protein Hsc70 as host cell receptor: Atl-mediated staphylococcal internalization. *Cellular Microbiology*, **12**(**12**): 1746–1764.

Holden, M. T., Feil, E. J., Lindsay, J. A., Peacock, S. J., Day, N. P., Enright, M. C., Foster, T. J., Moore, C. E., Hurst, L., Atkin, R., & others. (2004). Complete genomes of two clinical *Staphylococcus aureus* strains: evidence for the rapid evolution of virulence and drug resistance. *Proceedings of the National Academy of Sciences of the United States of America*, **101**(**26**): 9786–9791.

Holtfreter, S., Nguyen, T. T., Wertheim, H., Steil, L., Kusch, H., Truong, Q. P., Engelmann, S., Hecker, M., Volker, U., van Belkum, A., & Broker, B. M. (2009). Human immune proteome in experimental colonization with *Staphylococcus aureus*. *Clin Vaccine Immunol*, **16**(**11**): 1607–14.

Holzinger, D., Gieldon, L., Mysore, V., Nippe, N., Taxman, D. J., Duncan, J. A., Broglie, P. M., Marketon, K., Austermann, J., Vogl, T., Foell, D., Niemann, S., Peters, G., Roth, J., & Löffler, B. (2012). *Staphylococcus aureus* Panton-Valentine leukocidin

induces an inflammatory response in human phagocytes via the NLRP3 inflammasome. *Journal of Leukocyte Biology*, **92**(**5**): 1069–1081.

Horsburgh, M. J., Aish, J. L., White, I. J., Shaw, L., Lithgow, J. K., & Foster, S. J. (2002). sigmaB modulates virulence determinant expression and stress resistance: characterization of a functional *rsbU* strain derived from *Staphylococcus aureus* 8325-4. *Journal of Bacteriology*, **184**(**19**): 5457–5467.

Horsburgh, M. J., Ingham, E., & Foster, S. J. (2001). In *Staphylococcus aureus*, Fur Is an Interactive Regulator with PerR, Contributes to Virulence, and Is Necessary for Oxidative Stress Resistance through Positive Regulation of Catalase and Iron Homeostasis. *Journal of Bacteriology*, **183**(**2**): 468–475.

Houlberg, U., & Jensen, K. F. (1983). Role of hypoxanthine and guanine in regulation of *Salmonella typhimurium pur* gene expression. *Journal of Bacteriology*, **153**(**2**): 837–845.

Huang, M., & Pittard, J. (1967). Genetic analysis of mutant strains of *Escherichia coli* requiring p-aminobenzoic acid for growth. *Journal of Bacteriology*, **93**(**6**): 1938–1942.

Hu, C., Xiong, N., Zhang, Y., Rayner, S., & Chen, S. (2012). Functional characterization of lipase in the pathogenesis of *Staphylococcus aureus*. *Biochemical and Biophysical Research Communications*, **419**(**4**): 617–620.

Huesca, M., Peralta, R., Sauder, D. N., Simor, A. E., & McGavin, M. J. (2002). Adhesion and virulence properties of epidemic Canadian methicillin-resistant *Staphylococcus aureus* strain 1: identification of novel adhesion functions associated with plasmin-sensitive surface protein. *Journal of Infectious Diseases*, **185**(**9**): 1285–1296.

Hu, H., Armstrong, P. C. J., Khalil, E., Chen, Y.-C., Straub, A., Li, M., Soosairajah, J., Hagemeyer, C. E., Bassler, N., Huang, D., Ahrens, I., Krippner, G., Gardiner, E., & Peter, K. (2011). GPVI and GPIbα Mediate Staphylococcal Superantigen-Like Protein 5 (SSL5) Induced Platelet Activation and Direct toward Glycans as Potential Inhibitors. (H. Tse, Ed.)*PLoS ONE*, **6**(**4**): e19190.

Hussain, M., Becker, K., von Eiff, C., Schrenzel, J., Peters, G., & Herrmann, M. (2001). Identification and Characterization of a Novel 38.5-Kilodalton Cell Surface Protein of *Staphylococcus aureus* with Extended-Spectrum Binding Activity for Extracellular Matrix and Plasma Proteins. *Journal of Bacteriology*, **183**(**23**): 6778–6786.

Hussain, M., Hastings, J. G. M., & White, P. J. (1991). A chemically defined medium for slime production by coagulase-negative staphylococci. *Journal of medical microbiology*, **34**(**3**): 143–147.

Hussain, M., Schäfer, D., Juuti, K. M., Peters, G., Haslinger-Löffler, B., Kuusela, P. I., & Sinha, B. (2009). Expression of Pls (plasmin sensitive) in *Staphylococcus aureus* negative for *pls* reduces adherence and cellular invasion and acts by steric hindrance. *The Journal of Infectious Diseases*, **200**(**1**): 107–117.

Iandolo, J. J. (1989). Genetic analysis of extracellular toxins of *Staphylococcus aureus*. *Annual Review of Microbiology*, **43**: 375–402.

Ibberson, C. B., Jones, C. L., Singh, S., Wise, M. C., Hart, M. E., Zurawski, D. V., & Horswill, A. R. (2014). *Staphylococcus aureus* hyaluronidase is a CodY-regulated virulence factor. *Infection and Immunity*, **82**(**10**): 4253–4264.

Ikuo, M., Kaito, C., & Sekimizu, K. (2010). The *cvfC* operon of *Staphylococcus aureus* contributes to virulence via expression of the *thyA* gene. *Microbial Pathogenesis*, **49**(**1-2**): 1–7.

Ingavale, S. S., Van Wamel, W., & Cheung, A. L. (2003). Characterization of RAT, an autolysis regulator in *Staphylococcus aureus*: Autolysis regulator in *S. aureus*. *Molecular Microbiology*, **48**(**6**): 1451–1466.

Inuzuka, M., Hayakawa, M., & Ingi, T. (2005). Serinc, an activity-regulated protein family, incorporates serine into membrane lipid synthesis. *The Journal of Biological Chemistry*, **280**(**42**): 35776–35783.

Itoh, S., Hamada, E., Kamoshida, G., Takeshita, K., Oku, T., & Tsuji, T. (2010)a. Staphylococcal superantigen-like protein 5 inhibits matrix metalloproteinase 9 from human neutrophils. *Infection and Immunity*, **78**(**7**): 3298–3305.

Itoh, S., Hamada, E., Kamoshida, G., Yokoyama, R., Takii, T., Onozaki, K., & Tsuji, T. (2010)b. Staphylococcal superantigen-like protein 10 (SSL10) binds to human immunoglobulin G (IgG) and inhibits complement activation via the classical pathway. *Mol Immunol*, **47**(**4**): 932–8.

Itoh, S., Yamaoka, N., Kamoshida, G., Takii, T., Tsuji, T., Hayashi, H., & Onozaki, K. (2013)a. Staphylococcal superantigen-like protein 8 (SSL8) binds to tenascin C and inhibits tenascin C-fibronectin interaction and cell motility of keratinocytes. *Biochemical and Biophysical Research Communications*, **433**(**1**): 127–132.

Itoh, S., Yokoyama, R., Kamoshida, G., Fujiwara, T., Okada, H., Takii, T., Tsuji, T., Fujii, S., Hashizume, H., & Onozaki, K. (2013)b. Staphylococcal superantigen-like protein 10 (SSL10) inhibits blood coagulation by binding to prothrombin and factor Xa via their γ-carboxyglutamic acid (Gla) domain. *The Journal of Biological Chemistry*, **288**(**30**): 21569–21580.

Itoh, S., Yokoyama, R., Murase, C., Takii, T., Tsuji, T., & Onozaki, K. (2012). Staphylococcal superantigen-like protein 10 binds to phosphatidylserine and apoptotic cells. *Microbiology and Immunology*, **56**(**6**): 363–371.

Iwasaki, A., & Medzhitov, R. (2010). Regulation of adaptive immunity by the innate immune system. *Science (New York, N.Y.)*, **327**(**5963**): 291–295.

Janeway, C. (2001). *Immunobiology Five*. Garland Pub.

Ji, G., Beavis, R. C., & Novick, R. P. (1995). Cell density control of staphylococcal virulence mediated by an octapeptide pheromone. *Proceedings of the National Academy of Sciences of the United States of America*, **92**(**26**): 12055–12059.

Jin, F., Matsushita, O., Katayama, S., Jin, S., Matsushita, C., Minami, J., & Okabe, A. (1996). Purification, characterization, and primary structure of *Clostridium perfringens* lambda-toxin, a thermolysin-like metalloprotease. *Infection and Immunity*, **64**(**1**): 230–237.

Jin, T., Bokarewa, M., Foster, T., Mitchell, J., Higgins, J., & Tarkowski, A. (2004). *Staphylococcus aureus* resists human defensins by production of staphylokinase, a novel bacterial evasion mechanism. *Journal of Immunology (Baltimore, Md.: 1950)*, **172**(**2**): 1169–1176.

Johnson, M., Cockayne, A., & Morrissey, J. A. (2008). Iron-regulated biofilm formation in *Staphylococcus aureus* Newman requires *ica* and the secreted protein Emp. *Infection and Immunity*, **76**(**4**): 1756–1765.

Johnson, M., Sengupta, M., Purves, J., Tarrant, E., Williams, P. H., Cockayne, A., Muthaiyan, A., Stephenson, R., Ledala, N., Wilkinson, B. J., Jayaswal, R. K., & Morrissey, J. A. (2011). Fur is required for the activation of virulence gene expression through the induction of the *sae* regulatory system in *Staphylococcus aureus*. *International journal of medical microbiology: IJMM*, **301**(**1**): 44–52.

Joo, H.-S., Chan, J. L., Cheung, G. Y. C., & Otto, M. (2010). Subinhibitory concentrations of protein synthesis-inhibiting antibiotics promote increased expression of the *agr* virulence regulator and production of phenol-soluble modulin cytolysins in community-associated methicillin-resistant *Staphylococcus aureus*. *Antimicrobial Agents and Chemotherapy*, **54**(**11**): 4942–4944.

Joo, H.-S., & Otto, M. (2015). Mechanisms of resistance to antimicrobial peptides in staphylococci. *Biochimica et Biophysica Acta*. S0005-2736(**15**)00049-8.

Josefsson, E., Juuti, K., Bokarewa, M., & Kuusela, P. (2005). The surface protein Pls of methicillin-resistant *Staphylococcus aureus* is a virulence factor in septic arthritis. *Infection and Immunity*, **73**(**5**): 2812–2817.

Jousselin, A., Kelley, W. L., Barras, C., Lew, D. P., & Renzoni, A. (2013). The *Staphylococcus aureus* Thiol/Oxidative Stress Global Regulator Spx Controls *trfA*, a Gene Implicated in Cell Wall Antibiotic Resistance. *Antimicrobial Agents and Chemotherapy*, **57**(**7**): 3283–3292.

Kaito, C., Kurokawa, K., Matsumoto, Y., Terao, Y., Kawabata, S., Hamada, S., & Sekimizu, K. (2005). Silkworm pathogenic bacteria infection model for identification of novel virulence genes. *Molecular Microbiology*, **56**(**4**): 934–944.

Kinkel, T. L., Roux, C. M., Dunman, P. M., & Fang, F. C. (2013). The *Staphylococcus aureus* SrrAB Two-Component System Promotes Resistance to Nitrosative Stress and Hypoxia. *mBio*, **4**(**6**): e00696–13.

Kloos, W. E., & Bannerman, T. L. (1994). Update on clinical significance of coagulase-negative staphylococci. *Clinical Microbiology Reviews*, **7**(**1**): 117–140.

Koboldt, D. C., Steinberg, K. M., Larson, D. E., Wilson, R. K., & Mardis, E. (2013). The Next-Generation Sequencing Revolution and Its Impact on Genomics. *Cell*, **155**(**1**): 27–38.

Koch, T. K., Reuter, M., Barthel, D., Böhm, S., van den Elsen, J., Kraiczy, P., Zipfel, P. F., & Skerka, C. (2012). *Staphylococcus aureus* proteins Sbi and Efb recruit human plasmin to degrade complement C3 and C3b. *PloS One*, **7**(**10**): e47638.

Kohanski, M. A., Dwyer, D. J., & Collins, J. J. (2010). How antibiotics kill bacteria: from targets to networks. *Nature Reviews Microbiology*, **8**(**6**): 423–435.

Kolar, S. L., Ibarra, J. A., Rivera, F. E., Mootz, J. M., Davenport, J. E., Stevens, S. M., Horswill, A. R., & Shaw, L. N. (2013). Extracellular proteases are key mediators of *Staphylococcus aureus* virulence via the global modulation of virulence-determinant stability. *MicrobiologyOpen*, **2**(**1**): 18–34.

Kosinska, U., Carnrot, C., Eriksson, S., Wang, L., & Eklund, H. (2005). Structure of the substrate complex of thymidine kinase from Ureaplasma urealyticum and investigations of possible drug targets for the enzyme. *FEBS Journal*, **272**(**24**): 6365–6372.

Koskinen, P., Törönen, P., Nokso-Koivisto, J., & Holm, L. (2015). PANNZER: high-throughput functional annotation of uncharacterized proteins in an error-prone environment. *Bioinformatics (Oxford, England)*, **31**(**10**): 1544–1552.

Kraus, D., Herbert, S., Kristian, S. A., Khosravi, A., Nizet, V., Götz, F., & Peschel, A. (2008). The GraRS regulatory system controls *Staphylococcus aureus* susceptibility to antimicrobial host defenses. *BMC microbiology*, **8**: 85.

Kreiswirth, B. N., Löfdahl, S., Betley, M. J., O'Reilly, M., Schlievert, P. M., Bergdoll, M. S., & Novick, R. P. (1983). The toxic shock syndrome exotoxin structural gene is not detectably transmitted by a prophage. *Nature*, **305**(**5936**): 709–712.

Kretschmer, D., Gleske, A.-K., Rautenberg, M., Wang, R., Köberle, M., Bohn, E., Schöneberg, T., Rabiet, M.-J., Boulay, F., Klebanoff, S. J., van Kessel, K. A., van

Strijp, J. A., Otto, M., & Peschel, A. (2010). Human formyl peptide receptor 2 senses highly pathogenic *Staphylococcus aureus*. *Cell Host & Microbe*, **7**(**6**): 463–473.

Kretschmer, D., Nikola, N., Dürr, M., Otto, M., & Peschel, A. (2012). The Virulence Regulator Agr Controls the Staphylococcal Capacity to Activate Human Neutrophils via the Formyl Peptide Receptor 2. *Journal of Innate Immunity*, **4**(**2**): 201–212.

Kuroda, M., Ito, R., Tanaka, Y., Yao, M., Matoba, K., Saito, S., Tanaka, I., & Ohta, T. (2008). *Staphylococcus aureus* surface protein SasG contributes to intercellular autoaggregation of *Staphylococcus aureus*. *Biochemical and Biophysical Research Communications*, **377**(**4**): 1102–1106.

Kwiecinski, J., Jin, T., & Josefsson, E. (2014). Surface proteins of *Staphylococcus aureus* play an important role in experimental skin infection. *APMIS: acta pathologica, microbiologica, et immunologica Scandinavica*, **122**(**12**): 1240–1250.

Kwieciński, J., Josefsson, E., Mitchell, J., Higgins, J., Magnusson, M., Foster, T., Jin, T., & Bokarewa, M. (2010). Activation of plasminogen by staphylokinase reduces the severity of *Staphylococcus aureus* systemic infection. *The Journal of Infectious Diseases*, **202**(**7**): 1041–1049.

Laarman, A. J., Ruyken, M., Malone, C. L., van Strijp, J. A. G., Horswill, A. R., & Rooijakkers, S. H. M. (2011). *Staphylococcus aureus* metalloprotease aureolysin cleaves complement C3 to mediate immune evasion. *Journal of Immunology (Baltimore, Md.: 1950)*, **186**(**11**): 6445–6453.

Labischinski, H. (1992). Consequences of the interaction of beta-lactam antibiotics with penicillin binding proteins from sensitive and resistant *Staphylococcus aureus* strains. *Medical Microbiology and Immunology*, **181**(**5**): 241–265.

Ladhani, S. (2003). Understanding the mechanism of action of the exfoliative toxins of *Staphylococcus aureus*. *FEMS Immunology & Medical Microbiology*, **39**(**2**): 181–189.

Lampe, D. J., Churchill, M. E., & Robertson, H. M. (1996). A purified mariner transposase is sufficient to mediate transposition *in vitro*. *The EMBO journal*, **15**(**19**): 5470.

Lancefield, R. C. (1957). Differentiation of group A streptococci with a common R antigen into three serological types, with special reference to the bactericidal test. *The Journal of Experimental Medicine*, **106**(**4**): 525–544.

Lane, A. N., & Kirschner, K. (1983). The mechanism of binding of L-serine to tryptophan synthase from *Escherichia coli*. *European journal of biochemistry / FEBS*, **129**(**3**): 561–570.

Langley, R., Wines, B., Willoughby, N., Basu, I., Proft, T., & Fraser, J. D. (2005). The staphylococcal superantigen-like protein 7 binds IgA and complement C5 and inhibits IgA-Fc alpha RI binding and serum killing of bacteria. *J Immunol*, **174**(**5**): 2926–33.

Laue, H., Weiss, L., Bernardi, A., Hawser, S., Lociuro, S., & Islam, K. (2007). *In vitro* activity of the novel diaminopyrimidine, iclaprim, in combination with folate inhibitors and other antimicrobials with different mechanisms of action. *Journal of Antimicrobial Chemotherapy*, **60**(**6**): 1391–1394.

Lee, C. Y., & Iandolo, J. J. (1986). Integration of staphylococcal phage L54a occurs by site-specific recombination: structural analysis of the attachment sites. *Proceedings of the National Academy of Sciences of the United States of America*, **83**(**15**): 5474–5478.

Lee, L. Y., Liang, X., Hook, M., & Brown, E. L. (2004). Identification and characterization of the C3 binding domain of the *Staphylococcus aureus* extracellular fibrinogen-binding protein (Efb). *J Biol Chem*, **279**(**49**): 50710–6.

Lei, M. G., Cue, D., Roux, C. M., Dunman, P. M., & Lee, C. Y. (2011). Rsp Inhibits Attachment and Biofilm Formation by Repressing *fnbA* in *Staphylococcus aureus* MW2. *Journal of Bacteriology*, **193**(**19**): 5231–5241.

Liang, X., Zheng, L., Landwehr, C., Lunsford, D., Holmes, D., & Ji, Y. (2005). Global Regulation of Gene Expression by ArlRS, a Two-Component Signal Transduction Regulatory System of *Staphylococcus aureus*. *Journal of Bacteriology*, **187**(**15**): 5486–5492.

Liew, A. T. F., Theis, T., Jensen, S. O., Garcia-Lara, J., Foster, S. J., Firth, N., Lewis, P. J., & Harry, E. J. (2011). A simple plasmid-based system that allows rapid generation of tightly controlled gene expression in *Staphylococcus aureus*. *Microbiology (Reading, England)*, **157**(**Pt 3**): 666–676.

Lina, G., Bohach, G. A., Nair, S. P., Hiramatsu, K., Jouvin-Marche, E., Mariuzza, R., & International Nomenclature Committee for Staphylococcal Superantigens. (2004). Standard nomenclature for the superantigens expressed by Staphylococcus. *The Journal of Infectious Diseases*, **189**(**12**): 2334–2336.

Liu, G. Y., Essex, A., Buchanan, J. T., Datta, V., Hoffman, H. M., Bastian, J. F., Fierer, J., & Nizet, V. (2005). *Staphylococcus aureus* golden pigment impairs neutrophil killing and promotes virulence through its antioxidant activity. *J Exp Med*, **202**(**2**): 209–15.

Liu, G., Zhang, M., Chen, X., Zhang, W., Ding, W., & Zhang, Q. (2015). Evolution of threonine aldolases, a diverse family involved in the second pathway of glycine biosynthesis. *Journal of Molecular Evolution*, **80**(**2**): 102–107.

Li, W., Jaroszewski, L., & Godzik, A. (2001). Clustering of highly homologous sequences to reduce the size of large protein databases. *Bioinformatics (Oxford, England)*, **17**(**3**): 282–283.

Li, Y., Karlin, A., Loike, J. D., & Silverstein, S. C. (2002). A critical concentration of neutrophils is required for effective bacterial killing in suspension. *Proc Natl Acad Sci U S A*, **99**(**12**): 8289–94.

Loffler, B., Hussain, M., Grundmeier, M., Bruck, M., Holzinger, D., Varga, G., Roth, J., Kahl, B. C., Proctor, R. A., & Peters, G. (2010). *Staphylococcus aureus* panton-valentine leukocidin is a very potent cytotoxic factor for human neutrophils. *PLoS Pathog*, **6**(**1**): e1000715.

Longauerova, A. (2006). Coagulase negative staphylococci and their participation in pathogenesis of human infections. *Bratislavské Lekárske Listy*, **107**(**11-12**): 448–452.

Lowy, F. D. (1998). *Staphylococcus aureus* infections. *N Engl J Med*, **339**(**8**): 520–32.

Luong, T. T., Dunman, P. M., Murphy, E., Projan, S. J., & Lee, C. Y. (2006). Transcription Profiling of the *mgrA* Regulon in *Staphylococcus aureus*. *Journal of Bacteriology*, **188**(**5**): 1899–1910.

Madigan, M. T. (2000). *Brock Biology of Microorganisms*. Prentice Hall.

Mahan, M. J., Slauch, J. M., & Mekalanos, J. J. (1993). Selection of bacterial virulence genes that are specifically induced in host tissues. *Science (New York, N.Y.)*, **259**(**5095**): 686–688.

Maidhof, H., Reinicke, B., Blümel, P., Berger-Bächi, B., & Labischinski, H. (1991). *femA*, which encodes a factor essential for expression of methicillin resistance, affects glycine content of peptidoglycan in methicillin-resistant and methicillin-susceptible *Staphylococcus aureus* strains. *Journal of Bacteriology*, **173**(**11**): 3507–3513.

Mainiero, M., Goerke, C., Geiger, T., Gonser, C., Herbert, S., & Wolz, C. (2010). Differential Target Gene Activation by the *Staphylococcus aureus* Two-Component System *saeRS*. *Journal of Bacteriology*, **192**(**3**): 613–623.

Malachowa, N., & DeLeo, F. R. (2011). *Staphylococcus aureus* survival in human blood. *Virulence*, **2**(**6**): 567–569.

Malachowa, N., Kobayashi, S. D., Freedman, B., Dorward, D. W., & DeLeo, F. R. (2013). *Staphylococcus aureus* Leukotoxin GH Promotes Formation of Neutrophil Extracellular Traps. *The Journal of Immunology*, **191**(**12**): 6022–6029.

Malachowa, N., Whitney, A. R., Kobayashi, S. D., Sturdevant, D. E., Kennedy, A. D., Braughton, K. R., Shabb, D. W., Diep, B. A., Chambers, H. F., Otto, M., & DeLeo, F. R. (2011). Global changes in *Staphylococcus aureus* gene expression in human blood. *PloS One*, **6**(**4**): e18617.

Manders, S. M. (1998). Toxin-mediated streptococcal and staphylococcal disease. *Journal of the American Academy of Dermatology*, **39**(**3**): 383–398.

Mani, N., Tobin, P., & Jayaswal, R. K. (1993). Isolation and characterization of autolysis-defective mutants of *Staphylococcus aureus* created by Tn*917-lacZ* mutagenesis. *Journal of Bacteriology*, **175**(**5**): 1493–1499.

Manna, A. C., & Cheung, A. L. (2003). *sarU*, a *sarA* Homolog, Is Repressed by SarT and Regulates Virulence Genes in *Staphylococcus aureus*. *Infection and Immunity*, **71**(**1**): 343–353.

Manna, A. C., Ingavale, S. S., Maloney, M., van Wamel, W., & Cheung, A. L. (2004). Identification of *sarV* (SA2062), a new transcriptional regulator, is repressed by SarA and MgrA (SA0641) and involved in the regulation of autolysis in *Staphylococcus aureus*. *Journal of Bacteriology*, **186**(**16**): 5267–5280.

Marchler-Bauer, A., Derbyshire, M. K., Gonzales, N. R., Lu, S., Chitsaz, F., Geer, L. Y., Geer, R. C., He, J., Gwadz, M., Hurwitz, D. I., Lanczycki, C. J., Lu, F., Marchler, G. H., Song, J. S., Thanki, N., Wang, Z., Yamashita, R. A., Zhang, D., Zheng, C., & Bryant, S. H. (2015). CDD: NCBI's conserved domain database. *Nucleic Acids Research*, **43**(**Database issue**): D222–226.

Mast, Y., & Wohlleben, W. (2014). Streptogramins – Two are better than one! *International Journal of Medical Microbiology*, **304**(**1**): 44–50.

Mazmanian, S. K., Skaar, E. P., Gaspar, A. H., Humayun, M., Gornicki, P., Jelenska, J., Joachmiak, A., Missiakas, D. M., & Schneewind, O. (2003). Passage of heme-iron across the envelope of *Staphylococcus aureus*. *Science (New York, N.Y.)*, **299**(**5608**): 906–909.

McFarland, W. C., & Stocker, B. A. (1987). Effect of different purine auxotrophic mutations on mouse-virulence of a Vi-positive strain of *Salmonella dublin* and of two strains of *Salmonella typhimurium*. *Microbial Pathogenesis*, **3**(**2**): 129–141.

McVicker, G., Prajsnar, T. K., Williams, A., Wagner, N. L., Boots, M., Renshaw, S. A., & Foster, S. J. (2014). Clonal expansion during *Staphylococcus aureus* infection dynamics reveals the effect of antibiotic intervention. *PLoS pathogens*, **10**(**2**): e1003959.

Medzhitov, R., Preston-Hurlburt, P., & Janeway, C. A. (1997). A human homologue of the *Drosophila* Toll protein signals activation of adaptive immunity. *Nature*, **388**(**6640**): 394–397.

Mehlin, C., Headley, C. M., & Klebanoff, S. J. (1999). An inflammatory polypeptide complex from *Staphylococcus epidermidis*: isolation and characterization. *The Journal of Experimental Medicine*, **189**(**6**): 907–918.

Mei, J. M., Nourbakhsh, F., Ford, C. W., & Holden, D. W. (1997). Identification of *Staphylococcus aureus* virulence genes in a murine model of bacteraemia using signature-tagged mutagenesis. *Molecular Microbiology*, **26**(**2**): 399–407.

Mekontso-Dessap, A., Honore, S., Kirsch, M., Plonquet, A., Fernandez, E., Touqui, L., Farcet, J. P., Soussy, C. J., Loisance, D., & Delclaux, C. (2005). Blood neutrophil bactericidal activity against methicillin-resistant and methicillin-sensitive *Staphylococcus aureus* during cardiac surgery. *Shock*, **24**(**2**): 109–13.

Melehani, J. H., James, D. B. A., DuMont, A. L., Torres, V. J., & Duncan, J. A. (2015). *Staphylococcus aureus* Leukocidin A/B (LukAB) Kills Human Monocytes via Host NLRP3 and ASC when Extracellular, but Not Intracellular. (L. S. Miller, Ed.)*PLOS Pathogens*, **11**(**6**): e1004970.

Miles, A. A., Misra, S. S., & Irwin, J. O. (1938). The estimation of the bactericidal power of the blood. *The Journal of Hygiene*, **38**(**6**): 732–749.

Modun, B., & Williams, P. (1999). The Staphylococcal Transferrin-Binding Protein Is a Cell Wall Glyceraldehyde-3-Phosphate Dehydrogenase. *Infection and Immunity*, **67**(**3**): 1086–1092.

Mölkänen, T., Tyynelä, J., Helin, J., Kalkkinen, N., & Kuusela, P. (2002). Enhanced activation of bound plasminogen on *Staphylococcus aureus* by staphylokinase. *FEBS letters*, **517**(**1-3**): 72–78.

Montgomery, C. P., Boyle-Vavra, S., Roux, A., Ebine, K., Sonenshein, A. L., & Daum, R. S. (2012). CodY Deletion Enhances *In Vivo* Virulence of Community-Associated Methicillin-Resistant *Staphylococcus aureus* Clone USA300. (S. M. Payne, Ed.)*Infection and Immunity*, **80**(**7**): 2382–2389.

Mootz, J. M., Benson, M. A., Heim, C. E., Crosby, H. A., Kavanaugh, J. S., Dunman, P. M., Kielian, T., Torres, V. J., & Horswill, A. R. (2015). Rot is a key regulator of *Staphylococcus aureus* biofilm formation. *Molecular Microbiology*. **96**(**2**): 388-404.

Morey, M., Fernández-Marmiesse, A., Castiñeiras, D., Fraga, J. M., Couce, M. L., & Cocho, J. A. (2013). A glimpse into past, present, and future DNA sequencing. *Molecular Genetics and Metabolism*, Special Issue: Diagnosis, **110**(**1–2**): 3–24.

Mulcahy, M. E., Geoghegan, J. A., Monk, I. R., O'Keeffe, K. M., Walsh, E. J., Foster, T. J., & McLoughlin, R. M. (2012). Nasal Colonisation by *Staphylococcus aureus* Depends upon Clumping Factor B Binding to the Squamous Epithelial Cell Envelope Protein Loricrin. (A. Peschel, Ed.)*PLoS Pathogens*, **8**(**12**): e1003092.

Murray, R. J. (2005). Recognition and management of *Staphylococcus aureus* toxin-mediated disease. *Internal Medicine Journal*, **35 Suppl 2**: S106–119.

Myllykallio, H., Lipowski, G., Leduc, D., Filee, J., Forterre, P., & Liebl, U. (2002). An alternative flavin-dependent mechanism for thymidylate synthesis. *Science*, **297**(**5578**): 105–107.

Nakamura, Y., Oscherwitz, J., Cease, K. B., Chan, S. M., Muñoz-Planillo, R., Hasegawa, M., Villaruz, A. E., Cheung, G. Y. C., McGavin, M. J., Travers, J. B., Otto, M., Inohara, N., & Núñez, G. (2013). *Staphylococcus* δ-toxin induces allergic skin disease by activating mast cells. *Nature*, **503**(**7476**): 397–401.

Neidhardt, F., C., Curtiss III, R., Ingraham, J. L., & Lin, E. C, C. (1996). *Escherichia Coli and Salmonella: Cellular and Molecular Biology*. ASM Press.

Nitzan, D. Y., Ladan, H., & Malik, Z. (1987). Growth-inhibitory effect of hemin on staphylococci. *Current Microbiology*, **14**(**5**): 279–284.

Nizet, V. (2007). Understanding how leading bacterial pathogens subvert innate immunity to reveal novel therapeutic targets. *Journal of Allergy and Clinical Immunology*, **120**(**1**): 13–22.

Novick, R. P. (1991). Genetic systems in staphylococci. *Methods in Enzymology*, **204**: 587–636.

Novick, R. P. (2003)a. Autoinduction and signal transduction in the regulation of staphylococcal virulence: Regulation of *staphylococcus* virulence. *Molecular Microbiology*, **48**(**6**): 1429–1449.

Novick, R. P. (2003)b. Mobile genetic elements and bacterial toxinoses: the superantigen-encoding pathogenicity islands of *Staphylococcus aureus*. *Plasmid*, **49**(**2**): 93–105.

Novick, R. P., Ross, H. F., Projan, S. J., Kornblum, J., Kreiswirth, B., & Moghazeh, S. (1993). Synthesis of staphylococcal virulence factors is controlled by a regulatory RNA molecule. *The EMBO journal*, **12**(**10**): 3967–3975.

Nusslein-Volhard, C., & Dahm, R. (Eds.). (2002). *Zebrafish* (1 edition.). Oxford: OUP Oxford.

O'Brien, L. M., Walsh, E. J., Massey, R. C., Peacock, S. J., & Foster, T. J. (2002). *Staphylococcus aureus* clumping factor B (ClfB) promotes adherence to human type I cytokeratin 10: implications for nasal colonization. *Cellular microbiology*, **4**(**11**): 759–770.

O'Callaghan, D., Maskell, D., Liew, F. Y., Easmon, C. S., & Dougan, G. (1988). Characterization of aromatic-and purine-dependent *Salmonella typhimurium*: attention, persistence, and ability to induce protective immunity in BALB/c mice. *Infection and immunity*, **56**(**2**): 419–423.

Ogston, A. (1881). Report upon Micro-Organisms in Surgical Diseases. *Br Med J*, **1**(**1054**): 369.b2–375.

Ohbayashi, T., Irie, A., Murakami, Y., Nowak, M., Potempa, J., Nishimura, Y., Shinohara, M., & Imamura, T. (2011). Degradation of fibrinogen and collagen by staphopains, cysteine proteases released from *Staphylococcus aureus*. *Microbiology (Reading, England)*, **157**(**Pt 3**): 786–792.

Olivas, A. D., Shogan, B. D., Valuckaite, V., Zaborin, A., Belogortseva, N., Musch, M., Meyer, F., Trimble, W. L., An, G., Gilbert, J., Zaborina, O., & Alverdy, J. C. (2012). Intestinal tissues induce an SNP mutation in *Pseudomonas aeruginosa* that enhances its virulence: possible role in anastomotic leak. *PloS One*, **7**(**8**): e44326.

Oliver, D. R., Brown, B. L., & Clewell, D. B. (1977). Characterization of plasmids determining hemolysin and bacteriocin production in *Streptococcus faecalis* 5952. *Journal of Bacteriology*, **130**(**2**): 948–950.

Olivier, A. C., Lemaire, S., Van Bambeke, F., Tulkens, P. M., & Oldfield, E. (2009). Role of *rsbU* and staphyloxanthin in phagocytosis and intracellular growth of *Staphylococcus aureus* in human macrophages and endothelial cells. *The Journal of Infectious Diseases*, **200**(**9**): 1367–1370.

Ortega, E., Abriouel, H., Lucas, R., & Gálvez, A. (2010). Multiple roles of *Staphylococcus aureus* enterotoxins: pathogenicity, superantigenic activity, and correlation to antibiotic resistance. *Toxins*, **2**(**8**): 2117–2131.

Osbourn, A. E., Barber, C. E., & Daniels, M. J. (1987). Identification of plant-induced genes of the bacterial pathogen *Xanthomonas campestris* pathovar *campestris* using a promoter-probe plasmid. *The EMBO journal*, **6**(**1**): 23–28.

Palmqvist, N., Foster, T., Tarkowski, A., & Josefsson, E. (2002). Protein A is a virulence factor in *Staphylococcus aureus* arthritis and septic death. *Microbial Pathogenesis*, **33**(**5**): 239–249.

Pandelia, M.-E., Nitschke, W., Infossi, P., Giudici-Orticoni, M.-T., Bill, E., & Lubitz, W. (2011). Characterization of a unique [FeS] cluster in the electron transfer chain of the oxygen tolerant [NiFe] hydrogenase from *Aquifex aeolicus*. *Proceedings of the National Academy of Sciences of the United States of America*, **108**(**15**): 6097–6102.

Pantrangi, M., Singh, V. K., Wolz, C., & Shukla, S. K. (2010). Staphylococcal superantigen-like genes, *ssl5* and *ssl8*, are positively regulated by Sae and negatively by Agr in the Newman strain. *FEMS Microbiol Lett*, **308**(**2**): 175–84.

Papakyriacou, H., Vaz, D., Simor, A., Louie, M., & McGavin, M. J. (2000). Molecular analysis of the accessory gene regulator (*agr*) locus and balance of virulence factor expression in epidemic methicillin-resistant *Staphylococcus aureus*. *The Journal of Infectious Diseases*, **181**(**3**): 990–1000.

Parcina, M., Wendt, C., Goetz, F., Zawatzky, R., Zähringer, U., Heeg, K., & Bekeredjian-Ding, I. (2008). *Staphylococcus aureus*-induced plasmacytoid dendritic cell activation is based on an IgG-mediated memory response. *Journal of Immunology (Baltimore, Md.: 1950)*, **181**(**6**): 3823–3833.

Parisi, J. T., & Suling, W. J. (1968). Antibiotic resistance of glycine-resistant variants of *Staphylococcus aureus*. *Canadian Journal of Microbiology*, **14**(**7**): 811–812.

Pasztor, L., Ziebandt, A.-K., Nega, M., Schlag, M., Haase, S., Franz-Wachtel, M., Madlung, J., Nordheim, A., Heinrichs, D. E., & Gotz, F. (2010). Staphylococcal Major Autolysin (Atl) Is Involved in Excretion of Cytoplasmic Proteins. *Journal of Biological Chemistry*, **285**(**47**): 36794–36803.

Patel, D., Wines, B. D., Langley, R. J., & Fraser, J. D. (2010). Specificity of staphylococcal superantigen-like protein 10 toward the human IgG1 Fc domain. *J Immunol*, **184**(**11**): 6283–92.

Payne, R. J., Bulloch, E. M. M., Toscano, M. M., Jones, M. A., Kerbarh, O., & Abell, C. (2009). Synthesis and evaluation of 2,5-dihydrochorismate analogues as inhibitors of the chorismate-utilising enzymes. *Organic & Biomolecular Chemistry*, **7**(**11**): 2421.

Peschel, A., Otto, M., Jack, R. W., Kalbacher, H., Jung, G., & Götz, F. (1999). Inactivation of the *dlt* operon in *Staphylococcus aureus* confers sensitivity to defensins, protegrins, and other antimicrobial peptides. *The Journal of Biological Chemistry*, **274**(**13**): 8405–8410.

Petkau, A., Stuart-Edwards, M., Stothard, P., & Van Domselaar, G. (2010). Interactive microbial genome visualization with GView. *Bioinformatics (Oxford, England)*, **26**(**24**): 3125–3126.

Phetsang, W., Chaturongakul, S., & Jiarpinitnun, C. (2013). Electron-withdrawing substituted benzenesulfonamides against the predominant community-associated methicillin-resistant *Staphylococcus aureus* strain USA300. *Monatshefte für Chemie - Chemical Monthly*, **144**(**4**): 461–471.

Piette, A., & Verschraegen, G. (2009). Role of coagulase-negative staphylococci in human disease. *Veterinary Microbiology*, **134**(**1-2**): 45–54.

Pilsczek, F. H., Salina, D., Poon, K. K. H., Fahey, C., Yipp, B. G., Sibley, C. D., Robbins, S. M., Green, F. H. Y., Surette, M. G., Sugai, M., Bowden, M. G., Hussain, M., Zhang, K., & Kubes, P. (2010). A novel mechanism of rapid nuclear neutrophil extracellular trap formation in response to *Staphylococcus aureus*. *Journal of Immunology (Baltimore, Md.: 1950)*, **185**(**12**): 7413–7425.

Pishchany, G., McCoy, A. L., Torres, V. J., Krause, J. C., Crowe, J. E., Fabry, M. E., & Skaar, E. P. (2010). Specificity for human hemoglobin enhances *Staphylococcus aureus* infection. *Cell Host & Microbe*, **8**(**6**): 544–550.

Pohl, K., Francois, P., Stenz, L., Schlink, F., Geiger, T., Herbert, S., Goerke, C., Schrenzel, J., & Wolz, C. (2009). CodY in *Staphylococcus aureus*: a Regulatory Link between Metabolism and Virulence Gene Expression. *Journal of Bacteriology*, **191**(**9**): 2953–2963.

Ponce-de-Leon, M. M., & Pizer, L. I. (1972). Serine biosynthesis and its regulation in *Bacillus subtilis*. *Journal of Bacteriology*, **110**(**3**): 895–904.

Popowicz, G. M., Dubin, G., Stec-Niemczyk, J., Czarny, A., Dubin, A., Potempa, J., & Holak, T. A. (2006). Functional and structural characterization of Spl proteases from *Staphylococcus aureus*. *Journal of Molecular Biology*, **358**(**1**): 270–279.

Powers, M. E., Kim, H. K., Wang, Y., & Bubeck Wardenburg, J. (2012). ADAM10 mediates vascular injury induced by *Staphylococcus aureus* α-hemolysin. *The Journal of Infectious Diseases*, **206**(**3**): 352–356.

Pragman, A. A., Yarwood, J. M., Tripp, T. J., & Schlievert, P. M. (2004). Characterization of Virulence Factor Regulation by SrrAB, a Two-Component System in *Staphylococcus aureus*. *Journal of Bacteriology*, **186**(**8**): 2430–2438.

Prajsnar, T. K., Cunliffe, V. T., Foster, S. J., & Renshaw, S. A. (2008). A novel vertebrate model of *Staphylococcus aureus* infection reveals phagocyte-dependent resistance of zebrafish to non-host specialized pathogens. *Cell Microbiol*, **10**(**11**): 2312–25.

Prajsnar, T. K., Hamilton, R., Garcia-Lara, J., McVicker, G., Williams, A., Boots, M., Foster, S. J., & Renshaw, S. A. (2012). A privileged intraphagocyte niche is responsible for disseminated infection of *Staphylococcus aureus* in a zebrafish model. *Cellular Microbiology*, **14**(**10**): 1600–1619.

Prat, C., Haas, P.-J., Bestebroer, J., de Haas, C. J. C., van Strijp, J. A. G., & van Kessel, K. P. M. (2009). A homolog of formyl peptide receptor-like 1 (FPRL1) inhibitor from *Staphylococcus aureus* (FPRL1 inhibitory protein) that inhibits FPRL1 and FPR. *Journal of Immunology (Baltimore, Md.: 1950)*, **183**(**10**): 6569–6578.

Prentice, A. M., Ghattas, H., & Cox, S. E. (2007). Host-pathogen interactions: can micronutrients tip the balance? *The Journal of Nutrition*, **137**(**5**): 1334–1337.

Prescott, L. M. (1999). *Microbiology*. WCB/McGraw-Hill.

Prince, L. R., Graham, K. J., Connolly, J., Anwar, S., Ridley, R., Sabroe, I., Foster, S. J., & Whyte, M. K. B. (2012). *Staphylococcus aureus* induces eosinophil cell death mediated by α-hemolysin. *PloS One*, **7**(**2**): e31506.

Proctor, R. A. (2008). Role of Folate Antagonists in the Treatment of Methicillin-Resistant *Staphylococcus aureus* Infection. *Clinical Infectious Diseases*, **46**(**4**): 584–593.

Projan, S. J. (2002). New (and not so new) antibacterial targets–from where and when will the novel drugs come? *Current opinion in pharmacology*, **2**(**5**): 513–522.

Quinn, F. D., Newman, G. W., & King, C. H. (1997). In search of virulence factors of human bacterial disease. *Trends in Microbiology*, **5**(**1**): 20–26.

Rainard, P., Corrales, J.-C., Barrio, M. B., Cochard, T., & Poutrel, B. (2003). Leucotoxic activities of *Staphylococcus aureus* strains isolated from cows, ewes, and goats with mastitis: importance of LukM/LukF'-PV leukotoxin. *Clinical and Diagnostic Laboratory Immunology*, **10**(**2**): 272–277.

Rasigade, J.-P., Trouillet-Assant, S., Ferry, T., Diep, B. A., Sapin, A., Lhoste, Y., Ranfaing, J., Badiou, C., Benito, Y., Bes, M., Couzon, F., Tigaud, S., Lina, G., Etienne, J., Vandenesch, F., & Laurent, F. (2013). PSMs of hypervirulent *Staphylococcus aureus* act as intracellular toxins that kill infected osteoblasts. *PloS One*, **8**(**5**): e63176.

Reddick, L. E., & Alto, N. M. (2014). Bacteria Fighting Back: How Pathogens Target and Subvert the Host Innate Immune System. *Molecular Cell*, **54**(**2**): 321–328.

Rediers, H., Rainey, P. B., Vanderleyden, J., & De Mot, R. (2005). Unraveling the Secret Lives of Bacteria: Use of *In Vivo* Expression Technology and Differential Fluorescence Induction Promoter Traps as Tools for Exploring Niche-Specific Gene Expression. *Microbiology and Molecular Biology Reviews*, **69**(**2**): 217–261.

Reed, S. B., Wesson, C. A., Liou, L. E., Trumble, W. R., Schlievert, P. M., Bohach, G. A., & Bayles, K. W. (2001). Molecular characterization of a novel *Staphylococcus aureus* serine protease operon. *Infection and Immunity*, **69**(**3**): 1521–1527.

Renzoni, A., Kelley, W. L., Barras, C., Monod, A., Huggler, E., François, P., Schrenzel, J., Studer, R., Vaudaux, P., & Lew, D. P. (2009). Identification by genomic and genetic analysis of two new genes playing a key role in intermediate glycopeptide resistance in *Staphylococcus aureus*. *Antimicrobial Agents and Chemotherapy*, **53**(**3**): 903–911.

Reyes-Robles, T., Alonzo, F., Kozhaya, L., Lacy, D. B., Unutmaz, D., & Torres, V. J. (2013). *Staphylococcus aureus* leukotoxin ED targets the chemokine receptors CXCR1 and CXCR2 to kill leukocytes and promote infection. *Cell Host & Microbe*, **14**(**4**): 453–459.

Rhem, M. N., Lech, E. M., Patti, J. M., McDevitt, D., Höök, M., Jones, D. B., & Wilhelmus, K. R. (2000). The collagen-binding adhesin is a virulence factor in *Staphylococcus aureus* keratitis. *Infection and Immunity*, **68**(**6**): 3776–3779.

Ricklin, D., Ricklin-Lichtsteiner, S. K., Markiewski, M. M., Geisbrecht, B. V., & Lambris, J. D. (2008). Cutting edge: members of the *Staphylococcus aureus* extracellular fibrinogen-binding protein family inhibit the interaction of C3d with complement receptor 2. *Journal of Immunology (Baltimore, Md.: 1950)*, **181**(**11**): 7463–7467.

Rigby, K. M., & DeLeo, F. R. (2012). Neutrophils in innate host defense against *Staphylococcus aureus* infections. *Seminars in Immunopathology*, **34**(**2**): 237–259.

Rogolsky, M. (1979). Nonenteric toxins of *Staphylococcus aureus*. *Microbiological Reviews*, **43**(**3**): 320–360.

Rollof, J., Braconier, J. H., Söderström, C., & Nilsson-Ehle, P. (1988). Interference of *Staphylococcus aureus* lipase with human granulocyte function. *European Journal of Clinical Microbiology & Infectious Diseases: Official Publication of the European Society of Clinical Microbiology*, **7**(**4**): 505–510.

Rooijakkers, S. H. M., Ruyken, M., van Roon, J., van Kessel, K. P. M., van Strijp, J. A. G., & van Wamel, W. J. B. (2006). Early expression of SCIN and CHIPS drives instant immune evasion by *Staphylococcus aureus*. *Cellular Microbiology*, **8**(**8**): 1282–1293.

Rottman, F., & Guarino, A. J. (1964). The inhibition of purine biosynthesis *de novo* in *Bacillus subtilis* by cordycepin. *Biochimica Et Biophysica Acta*, **80**: 640–647.

Rountree, P. M. (1963). The effect of desiccation on the viability of *Staphylococcus aureus*. *Journal of Hygiene*, **61**(**03**): 265–272.

Said-Salim, B., Dunman, P. M., McAleese, F. M., Macapagal, D., Murphy, E., McNamara, P. J., Arvidson, S., Foster, T. J., Projan, S. J., & Kreiswirth, B. N. (2003). Global Regulation of *Staphylococcus aureus* Genes by Rot. *Journal of Bacteriology*, **185**(**2**): 610–619.

Salzberg, S. L., Delcher, A. L., Kasif, S., & White, O. (1998). Microbial gene identification using interpolated Markov models. *Nucleic Acids Research*, **26**(**2**): 544–548.

Samant, S., Lee, H., Ghassemi, M., Chen, J., Cook, J. L., Mankin, A. S., & Neyfakh, A. A. (2008). Nucleotide biosynthesis is critical for growth of bacteria in human blood. *PLoS pathogens*, **4**(**2**): e37.

Sambrook, J., & Russell, D. W. (2001). *Molecular Cloning: A Laboratory Manual*. Cold Spring Harbor Laboratory Press.

Sano, H., Hsu, D. K., Apgar, J. R., Yu, L., Sharma, B. B., Kuwabara, I., Izui, S., & Liu, F.-T. (2003). Critical role of galectin-3 in phagocytosis by macrophages. *The Journal of Clinical Investigation*, **112**(**3**): 389–397.

Schaffer, A. C., Solinga, R. M., Cocchiaro, J., Portoles, M., Kiser, K. B., Risley, A., Randall, S. M., Valtulina, V., Speziale, P., Walsh, E., Foster, T., & Lee, J. C. (2006). Immunization with *Staphylococcus aureus* clumping factor B, a major determinant in nasal carriage, reduces nasal colonization in a murine model. *Infection and Immunity*, **74**(**4**): 2145–2153.

Schelin, J., Wallin-Carlquist, N., Cohn, M. T., Lindqvist, R., Barker, G. C., & Rådström, P. (2011). The formation of *Staphylococcus aureus* enterotoxin in food environments and advances in risk assessment. *Virulence*, **2**(**6**): 580–592.

Schilcher, K., Andreoni, F., Uchiyama, S., Ogawa, T., Schuepbach, R. A., & Zinkernagel, A. S. (2014). Increased neutrophil extracellular trap-mediated *Staphylococcus aureus* clearance through inhibition of nuclease activity by clindamycin and immunoglobulin. *The Journal of Infectious Diseases*, **210**(**3**): 473–482.

Shanks, R. M. Q., Meehl, M. A., Brothers, K. M., Martinez, R. M., Donegan, N. P., Graber, M. L., Cheung, A. L., & O'Toole, G. A. (2008). Genetic evidence for an alternative citrate-dependent biofilm formation pathway in *Staphylococcus aureus* that is dependent on fibronectin binding proteins and the GraRS two-component regulatory system. *Infection and Immunity*, **76**(**6**): 2469–2477.

Shannon, O., & Flock, J.-I. (2004). Extracellular fibrinogen binding protein, Efb, from *Staphylococcus aureus* binds to platelets and inhibits platelet aggregation. *Thrombosis and Haemostasis*. **91**(**4**): 779-89.

Shannon, O., Uekötter, A., & Flock, J.-I. (2005). Extracellular fibrinogen binding protein, Efb, from *Staphylococcus aureus* as an antiplatelet agent *in vivo*. *Thrombosis and Haemostasis*, **93**(**5**): 927–931.

Shaw, L., Golonka, E., Potempa, J., & Foster, S. J. (2004). The role and regulation of the extracellular proteases of *Staphylococcus aureus*. *Microbiology (Reading, England)*, **150**(**Pt 1**): 217–228.

Shaw, L. N., Aish, J., Davenport, J. E., Brown, M. C., Lithgow, J. K., Simmonite, K., Crossley, H., Travis, J., Potempa, J., & Foster, S. J. (2006). Investigations into sigmaB-modulated regulatory pathways governing extracellular virulence determinant production in *Staphylococcus aureus*. *Journal of Bacteriology*, **188**(**17**): 6070–6080.

Shea, J. E., Santangelo, J. D., & Feldman, R. G. (2000). Signature-tagged mutagenesis in the identification of virulence genes in pathogens. *Current opinion in microbiology*, **3**(**5**): 451–458.

Sibbald, M. J. J. B., Ziebandt, A. K., Engelmann, S., Hecker, M., de Jong, A., Harmsen, H. J. M., Raangs, G. C., Stokroos, I., Arends, J. P., Dubois, J. Y. F., & van Dijl, J. M. (2006). Mapping the pathways to staphylococcal pathogenesis by comparative secretomics. *Microbiology and molecular biology reviews: MMBR*, **70**(**3**): 755–788.

Siboo, I. R., Chambers, H. F., & Sullam, P. M. (2005). Role of SraP, a Serine-Rich Surface Protein of *Staphylococcus aureus*, in binding to human platelets. *Infection and Immunity*, **73**(**4**): 2273–2280.

Sivashankari, S., & Shanmughavel, P. (2006). Functional annotation of hypothetical proteins – A review. *Bioinformation*, **1**(**8**): 335–338.

Skaar, E. P., Gaspar, A. H., & Schneewind, O. (2004). IsdG and IsdI, heme-degrading enzymes in the cytoplasm of *Staphylococcus aureus*. *The Journal of Biological Chemistry*, **279**(**1**): 436–443.

Smith, H. (1998). What happens to bacterial pathogens *in vivo*? *Trends in microbiology*, **6**(**6**): 239–243.

Smyth, D. S., Meaney, W. J., Hartigan, P. J., & Smyth, C. J. (2007). Occurrence of *ssl* genes in isolates of *Staphylococcus aureus* from animal infection. *J Med Microbiol*, **56**(**Pt 3**): 418–25.

Spaan, A. N., Surewaard, B. G. J., Nijland, R., & van Strijp, J. A. G. (2013). Neutrophils Versus *Staphylococcus aureus* : A Biological Tug of War. *Annual Review of Microbiology*, **67**(**1**): 629–650.

Stauff, D. L., Bagaley, D., Torres, V. J., Joyce, R., Anderson, K. L., Kuechenmeister, L., Dunman, P. M., & Skaar, E. P. (2008). *Staphylococcus aureus* HrtA Is an ATPase Required for Protection against Heme Toxicity and Prevention of a Transcriptional Heme Stress Response. *Journal of Bacteriology*, **190**(**10**): 3588–3596.

Stebbins, C. E., & Galán, J. E. (2001). Structural mimicry in bacterial virulence. *Nature*, **412**(**6848**): 701–705.

Stenz, L., Francois, P., Whiteson, K., Wolz, C., Linder, P., & Schrenzel, J. (2011). The CodY pleiotropic repressor controls virulence in gram-positive pathogens: CodY in pathogenic gram-positive pathogens. *FEMS Immunology & Medical Microbiology*, **62**(**2**): 123–139.

Stocker, B. A. (1988). Auxotrophic *Salmonella typhi* as live vaccine. *Vaccine*, **6**(**2**): 141–145.

Strominger, J. L., & Birge, C. H. (1965). Nucleotide accumulation induced in *staphylococcus aureus* by glycine. *Journal of Bacteriology*, **89**: 1124–1127.

Studier, F. W., & Moffatt, B. A. (1986). Use of bacteriophage T7 RNA polymerase to direct selective high-level expression of cloned genes. *Journal of Molecular Biology*, **189**(**1**): 113–130.

Sugawara-Tomita, N., Tomita, T., & Kamio, Y. (2002). Stochastic assembly of two-component staphylococcal gamma-hemolysin into heteroheptameric transmembrane pores with alternate subunit arrangements in ratios of 3:4 and 4:3. *Journal of Bacteriology*, **184**(**17**): 4747–4756.

Sun, F., Li, C., Jeong, D., Sohn, C., He, C., & Bae, T. (2010). In the *Staphylococcus aureus* Two-Component System *sae*, the Response Regulator SaeR Binds to a Direct Repeat Sequence and DNA Binding Requires Phosphorylation by the Sensor Kinase SaeS. *Journal of Bacteriology*, **192**(**8**): 2111–2127.

Suzek, B. E., Ermolaeva, M. D., Schreiber, M., & Salzberg, S. L. (2001). A probabilistic method for identifying start codons in bacterial genomes. *Bioinformatics (Oxford, England)*, **17**(**12**): 1123–1130.

Tajima, A., Iwase, T., Shinji, H., Seki, K., & Mizunoe, Y. (2009). Inhibition of endothelial interleukin-8 production and neutrophil transmigration by *Staphylococcus aureus* beta-hemolysin. *Infection and Immunity*, **77**(**1**): 327–334.

Tang, C. M., Hood, D. W., & Moxon, E. R. (1998). Microbial genome sequencing and pathogenesis. *Current Opinion in Microbiology*, **1**(**1**): 12–16.

Taylor, J. M., & Heinrichs, D. E. (2002). Transferrin binding in *Staphylococcus aureus*: involvement of a cell wall-anchored protein. *Molecular Microbiology*, **43**(**6**): 1603–1614.

Tezuka, T., & Ohnishi, Y. (2014). Two Glycine Riboswitches Activate the Glycine Cleavage System Essential for Glycine Detoxification in *Streptomyces griseus*. *Journal of Bacteriology*, **196**(**7**): 1369–1376.

Thoendel, M., Kavanaugh, J. S., Flack, C. E., & Horswill, A. R. (2011). Peptide Signaling in the Staphylococci. *Chemical Reviews*, **111**(**1**): 117–151.

Torres, V. J., Attia, A. S., Mason, W. J., Hood, M. I., Corbin, B. D., Beasley, F. C., Anderson, K. L., Stauff, D. L., McDonald, W. H., Zimmerman, L. J., Friedman, D.

B., Heinrichs, D. E., Dunman, P. M., & Skaar, E. P. (2010). *Staphylococcus aureus* Fur Regulates the Expression of Virulence Factors That Contribute to the Pathogenesis of Pneumonia. *Infection and Immunity*, **78**(**4**): 1618–1628.

Torres, V. J., Pishchany, G., Humayun, M., Schneewind, O., & Skaar, E. P. (2006). *Staphylococcus aureus* IsdB is a hemoglobin receptor required for heme iron utilization. *Journal of Bacteriology*, **188**(**24**): 8421–8429.

Torres, V. J., Stauff, D. L., Pishchany, G., Bezbradica, J. S., Gordy, L. E., Iturregui, J., Anderson, K. L., Dunman, P. M., Joyce, S., & Skaar, E. P. (2007). A *Staphylococcus aureus* regulatory system that responds to host heme and modulates virulence. *Cell Host & Microbe*, **1**(**2**): 109–119.

Tran, P. V., & Nichols, B. P. (1991). Expression of *Escherichia coli pabA*. *Journal of bacteriology*, **173**(**12**): 3680–3687.

Tseng, C. W., Kyme, P., Low, J., Rocha, M. A., Alsabeh, R., Miller, L. G., Otto, M., Arditi, M., Diep, B. A., Nizet, V., Doherty, T. M., Beenhouwer, D. O., & Liu, G. Y. (2009). *Staphylococcus aureus* Panton-Valentine leukocidin contributes to inflammation and muscle tissue injury. *PLoS One*, **4**(**7**): e6387.

Tuchscherr, L., Bischoff, M., Lattar, S. M., Llana, M. N., Pförtner, H., Niemann, S., Geraci, J., Van de Vyver, H., Fraunholz, M. J., Cheung, A. L., & others. (2015). Sigma Factor SigB Is Crucial to Mediate *Staphylococcus aureus* Adaptation during Chronic Infections. *PLoS pathogens*, **11**(**4**):e1004870.

Ulrich, M., Bastian, M., Cramton, S. E., Ziegler, K., Pragman, A. A., Bragonzi, A., Memmi, G., Wolz, C., Schlievert, P. M., Cheung, A., & Döring, G. (2007). The staphylococcal respiratory response regulator SrrAB induces *ica* gene transcription and polysaccharide intercellular adhesin expression, protecting *Staphylococcus aureus* from neutrophil killing under anaerobic growth conditions. *Molecular Microbiology*, **65**(**5**): 1276–1287.

Vandenesch, F., Lina, G., & Henry, T. (2012). *Staphylococcus aureus* hemolysins, bi-component leukocidins, and cytolytic peptides: a redundant arsenal of membrane-damaging virulence factors? *Frontiers in Cellular and Infection Microbiology*, **2**: 12.

van Dijk, E. L., Auger, H., Jaszczyszyn, Y., & Thermes, C. (2014). Ten years of next-generation sequencing technology. *Trends in Genetics*, **30**(**9**): 418–426.

Van Hooijdonk, C. A., Glade, C. P., & Van Erp, P. E. (1994). TO-PRO-3 iodide: a novel HeNe laser-excitable DNA stain as an alternative for propidium iodide in multiparameter flow cytometry. *Cytometry*, **17**(**2**): 185–9.

van Kessel, K. P. M., Bestebroer, J., & van Strijp, J. A. G. (2014). Neutrophil-Mediated Phagocytosis of *Staphylococcus aureus*. *Frontiers in Immunology*, **5**: 467.

Vazquez, V., Liang, X., Horndahl, J. K., Ganesh, V. K., Smeds, E., Foster, T. J., & Hook, M. (2011). Fibrinogen is a ligand for the *Staphylococcus aureus* microbial surface components recognizing adhesive matrix molecules (MSCRAMM) bone sialoprotein-binding protein (Bbp). *The Journal of Biological Chemistry*, **286**(**34**): 29797–29805.

Ventura, C. L., Malachowa, N., Hammer, C. H., Nardone, G. A., Robinson, M. A., Kobayashi, S. D., & DeLeo, F. R. (2010). Identification of a novel *Staphylococcus aureus* two-component leukotoxin using cell surface proteomics. *PLoS One*, **5**(**7**): e11634.

Visai, L., Yanagisawa, N., Josefsson, E., Tarkowski, A., Pezzali, I., Rooijakkers, S. H., Foster, T. J., & Speziale, P. (2009). Immune evasion by *Staphylococcus aureus* conferred by iron-regulated surface determinant protein IsdH. *Microbiology*, **155**(**Pt 3**): 667–79.

Visschedyk, D. D., Perieteanu, A. A., Turgeon, Z. J., Fieldhouse, R. J., Dawson, J. F., & Merrill, A. R. (2010). Photox, a Novel Actin-targeting Mono-ADP-ribosyltransferase from *Photorhabdus luminescens*. *Journal of Biological Chemistry*, **285**(**18**): 13525–13534.

Vítkova, A., & Votava, M. (2005). Inhibition of hemolytic activity of *Staphylococcus aureus* 3-hemolysin by an exosubstance produced by some *Enterococcus faecalis* strains. *Epidemiologie, Mikrobiologie, Imunologie: Casopis Spolecnosti Pro Epidemiologii a Mikrobiologii Ceské Lékarské Spolecnosti J.E. Purkyne*, **54**(**1**): 11–15.

Von Eiff, C., Becker, K., Machka, K., Stammer, H., & Peters, G. (2001). Nasal carriage as a source of *Staphylococcus aureus* bacteremia. *New England Journal of Medicine*, **344**(**1**): 11–16.

von Eiff, C., Peters, G., & Heilmann, C. (2002). Pathogenesis of infections due to coagulase-negative staphylococci. *The Lancet infectious diseases*, **2**(**11**): 677–685.

Voyich, J. M., Otto, M., Mathema, B., Braughton, K. R., Whitney, A. R., Welty, D., Long, R. D., Dorward, D. W., Gardner, D. J., Lina, G., Kreiswirth, B. N., & DeLeo, F. R. (2006). Is Panton-Valentine leukocidin the major virulence determinant in community-associated methicillin-resistant *Staphylococcus aureus* disease? *J Infect Dis*, **194**(**12**): 1761–70.

Voyich, J. M., Vuong, C., DeWald, M., Nygaard, T. K., Kocianova, S., Griffith, S., Jones, J., Iverson, C., Sturdevant, D. E., Braughton, K. R., Whitney, A. R., Otto, M., & DeLeo, F. R. (2009). The SaeR/S Gene Regulatory System Is Essential for Innate Immune Evasion by *Staphylococcus aureus*. *The Journal of Infectious Diseases*, **199**(**11**): 1698–1706.

Wakeman, C. A., Hammer, N. D., Stauff, D. L., Attia, A. S., Anzaldi, L. L., Dikalov, S. I., Calcutt, M. W., & Skaar, E. P. (2012). Menaquinone biosynthesis potentiates haem toxicity in *Staphylococcus aureus*: Menaquinone production potentiates haem toxicity. *Molecular Microbiology*, **86**(**6**): 1376–1392.

Walev, I., Weller, U., Strauch, S., Foster, T., & Bhakdi, S. (1996). Selective killing of human monocytes and cytokine release provoked by sphingomyelinase (beta-toxin) of *Staphylococcus aureus*. *Infection and Immunity*, **64**(**8**): 2974–2979.

Walker, J. N., Crosby, H. A., Spaulding, A. R., Salgado-Pabón, W., Malone, C. L., Rosenthal, C. B., Schlievert, P. M., Boyd, J. M., & Horswill, A. R. (2013). The *Staphylococcus aureus* ArlRS two-component system is a novel regulator of agglutination and pathogenesis. *PLoS pathogens*, **9**(**12**): e1003819.

Walport, M. J. (2001)a. Complement. First of two parts. *The New England Journal of Medicine*, **344**(**14**): 1058–1066.

Walport, M. J. (2001)b. Complement. Second of two parts. *The New England Journal of Medicine*, **344**(**15**): 1140–1144.

Wang, L., Quan, C., Xiong, W., Qu, X., Fan, S., & Hu, W. (2014)a. New insight into transmembrane topology of *Staphylococcus aureus* histidine kinase AgrC. *Biochimica Et Biophysica Acta*, **1838**(**3**): 988–993.

Wang, R., Braughton, K. R., Kretschmer, D., Bach, T. H., Queck, S. Y., Li, M., Kennedy, A. D., Dorward, D. W., Klebanoff, S. J., Peschel, A., DeLeo, F. R., & Otto, M. (2007). Identification of novel cytolytic peptides as key virulence determinants for community-associated MRSA. *Nat Med*, **13**(**12**): 1510–4.

Wang, Y., Yi, L., Wang, S., Lu, C., & Ding, C. (2014)b. Selective capture of transcribed sequences in the functional gene analysis of microbial pathogens. *Applied Microbiology and Biotechnology*, **98**(**24**): 9983–9992.

Wann, E. R., Gurusiddappa, S., & Höök, M. (2000). The Fibronectin-binding MSCRAMM FnbpA of *Staphylococcus aureus* Is a Bifunctional Protein That Also Binds to Fibrinogen. *Journal of Biological Chemistry*, **275**(**18**): 13863–13871.

Wegkamp, A., van Oorschot, W., de Vos, W. M., & Smid, E. J. (2007). Characterization of the Role of para-Aminobenzoic Acid Biosynthesis in Folate Production by *Lactococcus lactis*. *Applied and Environmental Microbiology*, **73**(**8**): 2673–2681.

Weidenmaier, C., Peschel, A., Kempf, V. A. J., Lucindo, N., Yeaman, M. R., & Bayer, A. S. (2005). DltABCD- and MprF-mediated cell envelope modifications of *Staphylococcus aureus* confer resistance to platelet microbicidal proteins and contribute to virulence in a rabbit endocarditis model. *Infection and Immunity*, **73**(**12**): 8033–8038.

Weinberg, E. D. (1974). Iron and susceptibility to infectious disease. *Science (New York, N.Y.)*, **184**(**4140**): 952–956.

Weinstock, G. M. (2000). Genomics and bacterial pathogenesis. *Emerging infectious diseases*, **6**(**5**): 496.

Wertheim, H. F., Vos, M. C., Ott, A., van Belkum, A., Voss, A., Kluytmans, J. A., van Keulen, P. H., Vandenbroucke-Grauls, C. M., Meester, M. H., & Verbrugh, H. A. (2004). Risk and outcome of nosocomial *Staphylococcus aureus* bacteraemia in nasal carriers versus non-carriers. *Lancet*, **364**(**9435**): 703–5.

Williams, R. J., Ward, J. M., Henderson, B., Poole, S., O'Hara, B. P., Wilson, M., & Nair, S. P. (2000). Identification of a novel gene cluster encoding staphylococcal exotoxin-like proteins: characterization of the prototypic gene and its protein product, SET1. *Infect Immun*, **68**(**8**): 4407–15.

Wu, H.-J., Wang, A. H.-J., & Jennings, M. P. (2008). Discovery of virulence factors of pathogenic bacteria. *Current Opinion in Chemical Biology*, **12**(**1**): 93–101.

Yang, Y.-H., Jiang, Y.-L., Zhang, J., Wang, L., Bai, X.-H., Zhang, S.-J., Ren, Y.-M., Li, N., Zhang, Y.-H., Zhang, Z., Gong, Q., Mei, Y., Xue, T., Zhang, J.-R., Chen, Y., & Zhou, C.-Z. (2014). Structural insights into SraP-mediated *Staphylococcus aureus* adhesion to host cells. *PLoS pathogens*, **10**(**6**): e1004169.

Yarwood, J. M., McCormick, J. K., & Schlievert, P. M. (2001). Identification of a novel two-component regulatory system that acts in global regulation of virulence factors of *Staphylococcus aureus*. *Journal of Bacteriology*, **183**(**4**): 1113–1123.

Yokoyama, R., Itoh, S., Kamoshida, G., Takii, T., Fujii, S., Tsuji, T., & Onozaki, K. (2012). Staphylococcal Superantigen-Like Protein 3 Binds to the Toll-Like Receptor 2 Extracellular Domain and Inhibits Cytokine Production Induced by *Staphylococcus aureus*, Cell Wall Component, or Lipopeptides in Murine Macrophages. *Infection and Immunity*, **80**(**8**): 2816–2825.

Ythier, M., Resch, G., Waridel, P., Panchaud, A., Gfeller, A., Majcherczyk, P., Quadroni, M., & Moreillon, P. (2012). Proteomic and Transcriptomic Profiling of *Staphylococcus aureus* Surface LPXTG-proteins: Correlation with *agr* Genotypes and Adherence Phenotypes. *Molecular & Cellular Proteomics*, **11**(**11**): 1123–1139.

Zander, J., Hartenfeller, M., Hähnke, V., Proschak, E., Besier, S., Wichelhaus, T. A., & Schneider, G. (2010). Multistep Virtual Screening for Rapid and Efficient Identification of Non-Nucleoside Bacterial Thymidine Kinase Inhibitors. *Chemistry – A European Journal*, **16**(**31**): 9630–9637.

Zheng, B., Jiang, S., Xu, Z., Xiao, Y., & Li, L. (2015). Severe infective endocarditis with systemic embolism due to community associated methicillin-resistant *Staphylococcus aureus* ST630. *The Brazilian Journal of Infectious Diseases: An Official Publication of the Brazilian Society of Infectious Diseases*, **19**(**1**): 85–89.

Zhou, X., & Cegelski, L. (2012). Nutrient-dependent structural changes in *S. aureus* peptidoglycan revealed by solid-state NMR spectroscopy. *Biochemistry*, **51**(**41**): 8143–8153.

Ziebart, K. T., Dixon, S. M., Avila, B., El-Badri, M. H., Guggenheim, K. G., Kurth, M. J., & Toney, M. D. (2010). Targeting Multiple Chorismate-Utilizing Enzymes with a Single Inhibitor: Validation of a Three-Stage Design. *Journal of Medicinal Chemistry*, **53**(**9**): 3718–3729.

Zscheck, K. K., & Murray, B. E. (1993). Genes involved in the regulation of beta-lactamase production in enterococci and staphylococci. *Antimicrobial Agents and Chemotherapy*, **37**(**9**): 1966–1970.

APPENDICES

All appendices are available online at the following URL:

https://figshare.com/s/b7732afdd4cff98046b9

Chapter 3

3.1

a. Redundancy removal program.
b. Formatting program for redundancy removal program.
Explanatory note.

3.2

a. Blasting program.
b. Parsing program.
Explanatory note.

3.3

Sequence trimming program for SignalP input.

3.4

Program to remove sequences from FASTA files based on gene ID.
Program for removal of historical headers.
Program for removal of short and long FASTA sequences.
Explanatory note.

3.5

Sequencing data for pET21d inserts for SSL12, 13 and 14.

3.6

Sequencing data for pJC001 insert of the SSL triplet.

Chapter 4

4.1

NTML library information.

4.2

NTML contamination screen images.
Explanatory note.

4.3

NTML images for screen on BHI plus erythromycin and lincomycin.
Explanatory note.

4.4

NTML images for screen on sheep blood plus Columbia base.
Explanatory note.

4.5

NTML images for screen on bovine serum.
Explanatory note.

4.6

NTML images for screen on human blood.
Explanatory note.

4.7

a. Images of 31 transductants screened on human blood.
b. Images of 31 transductants screened on rabbit blood.
c. Images of 31 transductants screened on sheep blood plus Columbia base.
d. Images of 31 transductants screened on human blood plus Columbia base.

Chapter 5

5.1

Sequencing data for pJC002 insert of the *pab* operon.